

In vitro Recapitulation of the Polymicrobial Communities Associated with Cystic Fibrosis Airway Infections



Thomas James O'Brien, Churchill College

March, 2021

This thesis is submitted for the degree of Doctor of Philosophy

For my family

This thesis is the result of my own work and includes nothing which is the outcome of work done in collaboration except as declared in the Preface and specified in the text. It is not substantially the same as any that I have submitted, or, is being concurrently submitted for a degree or diploma or other qualification at the University of Cambridge or any other University or similar institution except as declared in the Preface and specified in the text. I further state that no substantial part of my thesis has already been submitted, or, is being concurrently submitted for any such degree, diploma or other qualification at the University of Cambridge or any other University or similar institution except as declared in the Preface and specified in the text. It does not exceed the prescribed word limit for the Biology Degree Committee.

Acknowledgements

First and foremost, I am grateful to my supervisor, Dr. Martin Welch for his insight, advice and continued support throughout my PhD studies and professional development. I would also like to thank all members of the Welch and Salmond labs, past and present, for all they have done throughout my time in Cambridge and the many happy memories. I would like to particularly acknowledge Wendy Figueroa-Chavez for her help with the analysis of WGS data and countless helpful discussions. I would also like to thank Larson Grimm for providing the AHL biosensor strains, Dr. Christopher Randall for providing the pETLsy plasmid (and for giving me the initial confidence to undertake this PhD) and Professor Andres Floto for providing the *Candida albicans* and great insight into the project. I would like to acknowledge Dr. Freya Harrison and Dr. Marwa Hassan for help with the *ex vivo* porcine lung experiments and for their hospitality during my time in Warwick. Finally, I would like to thank Ellen, my family and all members of the Churchill College MCR (particularly the 207 residents). You have all made the last few years of my studies truly amazing and without your love and encouragement this work would not have been possible.

Thomas James O'Brien

In vitro recapitulation of the polymicrobial communities associated with cystic fibrosis airway infections

Abstract

The airways of persons with cystic fibrosis (CF) are prone to lifelong colonisation with dense microbial ecosystems comprised of a diverse combination of bacteria and fungi. The role of interspecies interactions in modulating changes in gene expression and the metabolism of individual members of a polymicrobial community, compared with growth as an axenic population, is becoming increasingly apparent within the field of medical microbiology. In part, these poorly understood interactions explain why, regardless of intense research efforts, therapeutic treatments designed to clear such chronic airway infections often fail within the clinical setting. The paucity of existing *in vitro* and *in vivo* models used to study CF-associated infections greatly hinders research into the behaviours of polymicrobial communities. Species that coexist within the same *in situ* environment often outcompete one another when grown as a mixed population using traditional culture methods. The work presented in this dissertation redresses these problems. I describe the development and characterisation of a novel *in vitro* continuous-flow culture model. This experimental system permits the stable co-cultivation of distinctly different microbial species commonly-associated with CF airway infections; species that ordinarily readily outcompete one another in existing models. I demonstrate that the metabolic state and mutation rates of species cultured within the model remain stable for extended periods of time. Furthermore, I show that antimicrobial compounds display decreased efficacy against their target organism when grown as part of a polymicrobial community. I also show that different combinations of microbial species display different biofilm-forming potential. This work provides the basis of future research efforts aimed at the *in vitro* recapitulation of an entire polymicrobial community directly derived from persons with CF. Ultimately, this will help to bridge the bench-to-bedside gap for the development of more efficacious airway infection management regimens.

Table of Contents

Acknowledgements.....	1
Abstract.....	2
Abbreviations	6
1. Introduction	7
1.1 Cystic Fibrosis (CF)	7
1.2 CF Airway Associated Infections	9
1.3 Polymicrobial Infections	17
1.4 <i>Pseudomonas aeruginosa</i> (PA)	17
1.5 Biofilms	22
1.6 CF Infection Models.....	26
1.6.1 A need for polymicrobial infection models	26
1.6.2 Existing models.....	27
1.7 Aims of the Current Work.....	28
1.8 Experimental Approach	31
1.8.1 Continuous-flow Culture	32
1.8.2 Artificial Sputum Medium	33
2. Materials and Methods.....	34
2.1 Strains	34
2.2 Growth media and solutions	34
2.3 Growth conditions	41
2.3.1 Continuous-flow culture model.....	41
2.3.2 Batch culture conditions	45
2.4 Calibration of flowrates	44
2.5 CFU mL ⁻¹ enumeration	47
2.6 Quantitative real-time PCR (RT-PCR).....	47
2.7 Determination of mutation rates.....	56
2.7.1 Continuous-flow mutation rates.....	56
2.7.2 Batch culture mutation rates.....	57
2.8 Pyocyanin quantification	59
2.9 Siderophore quantification	59
2.10 QS signal molecule quantification	59
2.11 External perturbation of steady-state microbial populations	60
2.11.1 Introduction of PA to steady-state SA-CA co-cultures	60
2.11.2 Minimum inhibitory concentrations in ASM.....	60
2.11.3 Antimicrobial perturbation of steady-state cultures	61
2.11.4 Antimicrobial susceptibility of isolates from perturbed steady-state communities.....	61

2.11.5 Whole genome sequencing	61
2.12 Biofilm assays.....	62
2.12.1 Batch culture	62
2.12.2 Microtiter plate continuous-flow	63
2.12.3 Culture-vessel biofilm growth	65
2.13 Culturing patient derived sputum samples	66
2.13.1 Sample collection	66
2.13.2 Model inoculation and incubation	66
2.13.3 Sample collection and gDNA extraction	69
2.13.4 Sample library preparation and sequencing	69
2.13.5 Data analysis	74
2.13.6 ASM supplementation	74
2.14 Statistical analysis	74
3. <i>In vitro</i> Maintenance of Polymicrobial co-cultures.....	78
3.1 Introductory Comments	78
3.2 Mono-species growth of PA	78
3.3 Mixed species co-culture (PA-SA)	80
3.4 Mixed species co-culture (PA-CA)	82
3.5 Mixed species co-culture (SA-CA)	88
3.6 Triple species co-culture	94
3.7 Conclusions	97
4. Characterisation of Cultures.....	100
4.1 Introductory Comments	100
4.2 Metabolic state of continuous-flow culture	100
4.3 Estimation of mutation rates	102
4.4 Pyocyanin quantification	107
4.5 Siderophores quantification	110
4.6 QS molecules quantification	116
4.7 pH.....	121
4.8 Conclusions	123
5. Perturbation of Steady-state Microbial Communities	126
5.1 Introduction of PA to SA-CA co-culture	126
5.2 Antimicrobial treatment of single-species and mixed-species populations	132
5.2.1 Introductory comments.....	132
5.2.2 MIC of antimicrobials in ASM	133
5.2.3 Treatment with colistin	135
5.2.4 Treatment with fusidic acid.....	141

5.2.5 Treatment with fluconazole	147
5.2.6 Conclusions	151
5.3 Antimicrobial resistance vs tolerance	154
5.3.1 Resistance profiles of isolates	154
5.3.2 Whole genome sequencing of resistant isolates	159
5.4 Conclusions	161
6. Polymicrobial Biofilms	165
6.1 Introductory Comments	165
6.2 Batch culture polymicrobial biofilms	166
6.3 Continuous-flow polymicrobial biofilms	173
6.4 Biofilms grown within the continuous-flow model	179
6.4.1 Agar associated biofilms	179
6.4.2 EVPL associated biofilms	182
6.4.3 Comparison between agar and EVPL biofilms	183
6.5 Conclusions	183
7. Growth of patient derived polymicrobial populations	185
7.1 Introductory comments	185
7.2 Growth of CF-sputum Samples in ASM	185
7.3 Flowrate optimisation	187
7.4 Supplementation of ASM	200
7.5 Further ASM supplementation	217
7.6 Conclusions	230
8. Discussion	232
8.1 Maintenance and characterisation of polymicrobial co-cultures	232
8.2 External perturbation of steady-state microbial populations	235
8.3 Formation of polymicrobial biofilms in ASM	238
8.4 <i>In vitro</i> cultivation of patient-derived polymicrobial communities	242
8.5 Benefits and limitations of the continuous-flow model	248
9. Final Conclusions	249
10. References	251
11. Appendices	280
12. Publications	295

Abbreviations

Agr	Accessory gene regulator
AHL	Acyl-homoserine lactone
AMR	Antimicrobial resistance
APE	Acute pulmonary exacerbation
ASM	Artificial sputum medium
BHL	<i>N</i> -butanoyl-L-homoserine lactone
BiGGY-A	BiGGY agar/ Nickerson's Medium
BSA	Bovine serum albumin
CA	<i>Candida albicans</i>
CAS	Chrome azurol S
CF	Cystic fibrosis
CFTR	Cystic fibrosis transmembrane conductance regulator
CFU	Colony forming units
Cip^r	Ciprofloxacin resistant isolate
CV	Crystal violet
EPS	Extracellular polysaccharide
EUCAST	European Committee on Antimicrobial Susceptibility Testing
EVPL	<i>Ex vivo</i> porcine lung tissue
FBS	Foetal bovine serum
GlcNAc	<i>N</i> -acetylglucosamine
ITS	18S rRNA internal transcribed spacer region
LB	Lysogeny broth
LMICs	Lower-middle income countries
MIC	Minimum inhibitory concentration
MSA	Mannitol salt agar
NGS	Next generation sequencing
OD_{600 nm}	Optical density (600 nm)
OdDHL	<i>N</i> -(3-Oxododecanoyl)-L-homoserine lactone
OM	Outer membrane
OTU	Operational taxonomic unit
PA	<i>Pseudomonas aeruginosa</i>
PBS	Phosphate buffered saline
PCoA	Principal coordinate(s) analysis
PIA	<i>Pseudomonas</i> isolation agar
PQS	2-heptyl-3-hydroxy-4-quinolone
Q	Flowrate
QS	Quorum sensing
Rif^r	Rifampicin resistant isolate
R_t	Retention time
RT-PCR	Real-time polymerase chain reaction
SA	<i>Staphylococcus aureus</i>
WGS	Whole genome sequencing
XTT	2,3-bis-(2-Methoxy-4-nitro-5-sulfophenyl)-2H-tetrazolium-5-carboxanilide
μ	Mutation rate

1. Introduction

1.1 Cystic Fibrosis (CF)

Cystic fibrosis (CF) is the most common life-limiting genetic disorder within the Caucasian population, estimated to affect 70,000 people worldwide (Cystic Fibrosis Foundation, www.cff.org). However, improved new-born screening and carrier testing programs have recently identified an emerging change in CF epidemiology within developing and lower-middle income countries (LMICs) as more individuals of non-European descent are being identified to have the disease (Bell et al., 2020). As current genetic tests for CF are largely based on the more common Caucasian-specific mutation databases, it is likely that the global number of persons with CF is underrepresented in the above estimates.

The 1980s saw a surge in our understanding of the molecular and genetic causes underpinning the pathophysiology of CF. First in 1983, when Quinton demonstrated chloride impermeability in sweat glands as the cause of raised sweat electrolytes in CF patients (Quinton, 1983), advancing the basic understanding of defective electrolyte transport across membranes. Then the concerted efforts of three research groups in 1989 identified CF as an autosomal recessive disorder caused by mutations in the cystic fibrosis transmembrane conductance regulator (CFTR) gene (Kerem et al., 1989, Riordan et al., 1989, Rommens et al., 1989). The *CFTR* gene is found on the long arm of chromosome 7 and to date the CF Genetic Analysis Consortium have identified over 1800 mutations known to cause CF (www.genet.sickkids.on.20ca/cftr/). The most common *CFTR* mutation, accounting for over 70% of CF cases within the Caucasian population, is caused by the deletion of 3 nucleotides, resulting in the in-frame deletion of a phenylalanine residue at position 508 in the CFTR protein, termed phe508del (Bobadilla et al., 2002). The phe508del mutation causes a trafficking defect, as abnormally folded CFTR fails to be targeted for insertion into the plasma membrane and the misfolded protein is subsequently degraded by the proteasome (Ward et al., 1995). A group of 15-20 less common mutations comprise a further 15% of the CF alleles seen in Caucasians, with varying degrees of disease severity pertaining to the amount of CFTR correctly localised in the plasma membrane (Boyle and De Boeck, 2013, Fraser-Pitt and O'Neil, 2015). *Figure 1.1.* summarises the different classes of *CFTR* mutations for reference.

CFTR is a member of the ABC transporter class of ion channel proteins and is responsible for the transport of chloride ions across the apical membrane of epithelial cells in tissues of the: airways, intestine, pancreas, kidneys, sweat glands and male reproductive tract (Boucher, 2002, Chambers et al., 2007, Elborn, 2016, Hwang and Kirk, 2013, Lubamba et al., 2012, Ratjen et al., 2015). The CFTR protein is also responsible for additional cellular functions,

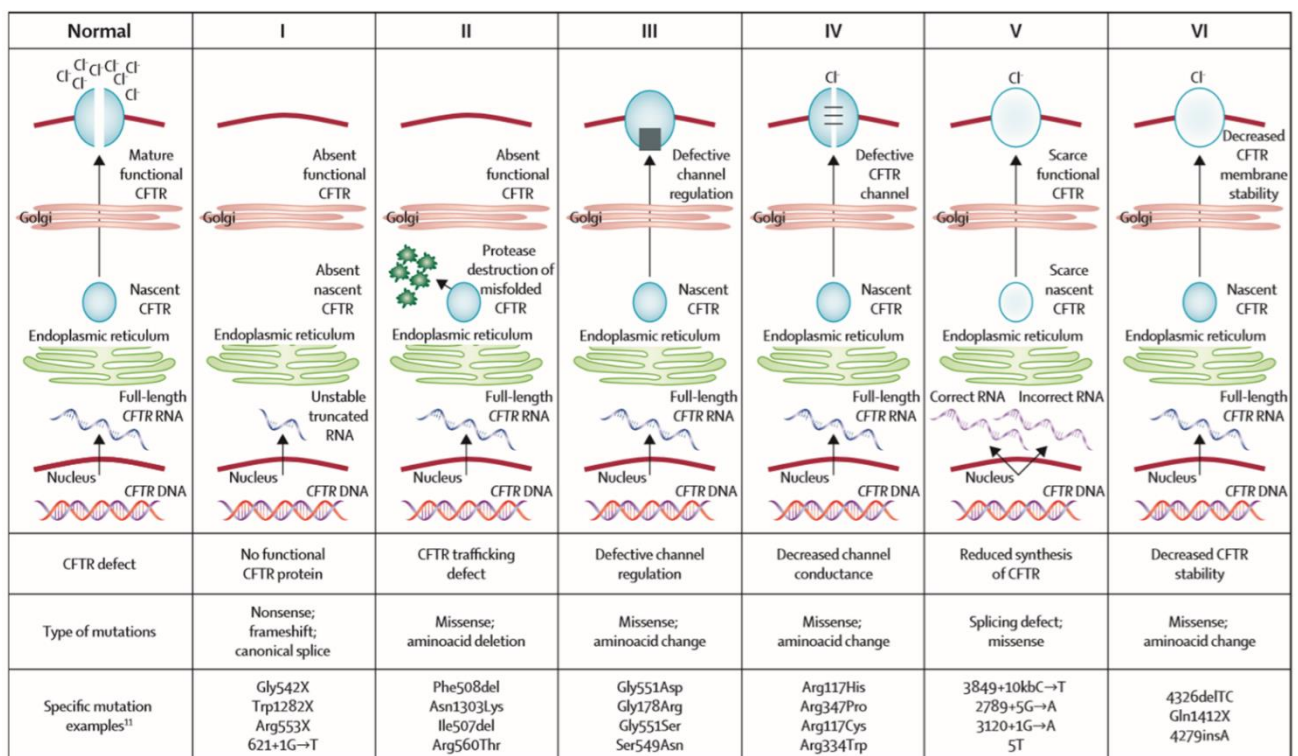


Figure 1.1. Classes of CFTR mutations and examples of their genetic causes.

Mutations within the *CFTR* gene can be divided into six distinct classes. Class I mutations result in no protein production. Class II mutations cause a trafficking defect and retention of misfolded protein at the endoplasmic reticulum, followed by proteasomal degradation. Class III mutations affect regulation of the CFTR channel and impair channel opening. Class IV mutations cause a decrease in ion conduction across the membrane. Class V mutations cause a significant decrease in gene transcription, and/or protein translation and synthesis. Class VI mutations reduce CFTR stability within the plasma membrane. Figure reproduced from (Boyle and De Boeck, 2013) by permission of Elsevier.

such as the secretion of bicarbonate to regulate the pH of airway surface liquid and hydration of mucins and airway secretions through inhibition of the epithelial sodium channel (ENaC) (Chmiel and Davis, 2003, Gentsch and Mall, 2018, Mall et al., 2004, Pezzulo et al., 2012). CF is characterised as a multiorgan disease, but perhaps the most striking manifestation of dysfunctional CFTR activity is the overproduction of nutrient-rich, mucilaginous sputum within the airways. This accumulates within the lumen of the bronchioles and blocks the airways to generate a highly heterogenous environment with steep oxygen gradients and a lowered pH (Boucher, 2002, Tate et al., 2002, Worlitzsch et al., 2002).

Common modern CF management techniques, such as high calorie diets, pancreatic enzyme replacement therapy, airway clearance techniques and the use of bronchodilators have all helped to improve the longevity and welfare of CF patients in recent decades (Bell et al., 2020). Further advancements in potentiator and corrective therapies that help to improve correct CFTR function, e.g. ivacaftor and lumacaftor, are showing additional positive impacts on clinical outcomes for patients with the more common CF mutations (Ratjen et al., 2017, Wainwright et al., 2015). However, approximately 90% of CF patients still succumb to respiratory failure brought on by a sustained immune response and airway scarring caused by chronic microbial infection of the airways (*Figure 1.2.*) (Carmody et al., 2013, Carmody et al., 2015, Chmiel and Davis, 2003, Elborn, 2016, Lammertyn et al., 2017, Lubamba et al., 2012, Lyczak et al., 2002, Rajan and Saiman, 2002, Rogers et al., 2010b, Rogers et al., 2010a, Sibley et al., 2006). Therefore, effective management of the microbiota associated with the CF airways remains the most important therapeutic strategy for improving the health and prognosis of all persons with CF. This is particularly true when considering the emergence of CF in LMICs, where access to CFTR corrective therapies remain limited and the multifaceted genetic causes of CF makes the development of a 'catch-all' corrective therapy unlikely (Cutting, 2010). An in-depth understanding of the CF-associated microbiome and how this changes over the course of a patient's life is therefore necessary to identify novel drug targets and develop improved therapeutic treatment regimens to manage such airway infections.

1.2 CF Airway Associated Infections

1.2.1 Predisposition for Airway Infections

Chronic obstruction of the airways through the overproduction of sputum generates a unique and heterogenous environment that is rich in mucins, amino acids and nitrates (Ghio et al., 2013, Grasemann et al., 1998, Jones et al., 2000, Palmer et al., 2007). As such, the airways of CF patients are prone to lifelong microbial colonisation, with the viscous lung secretions thought to provide a protective environment that shields the microbiota from effective

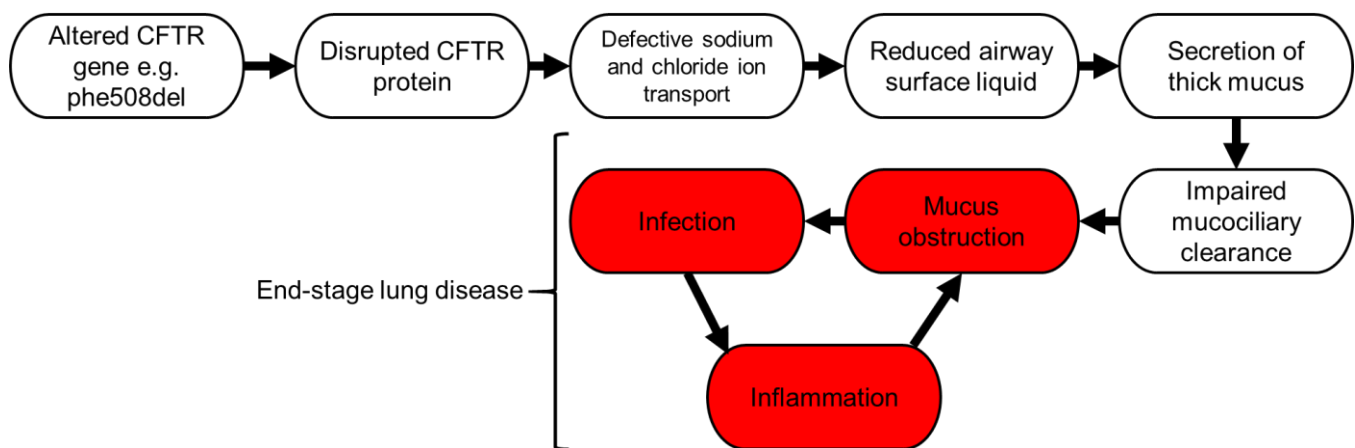


Figure 1.2. Schematic flow-diagram demonstrating disease progression and pathophysiology of CF airway associated infections.

Disruption of CFTR activity causes an imbalance of sodium and chloride ion transport within the airways, leading to the accumulation of thick airway secretions that cannot be cleared *via* the mucociliary escalator. The end-stages of lung disease are characterised by a positive feedback loop of chronic microbial infection triggering a sustained immunological response and scarring of the airways, causing a severe decline in pulmonary function (red boxes). Figure adapted from (Lubamba *et al.*, 2012) by permission of Elsevier.

antimicrobial treatment or immune clearance (Knowles and Boucher, 2002). Furthermore, CF gene modifiers, such as *MBL2* (encoding mannose-binding lectin), have been correlated within an alteration in a host's immune response or susceptibility to microbial infection, further predisposing CF patients to these persistent and ultimately fatal infections (Carlsson et al., 2005).

1.2.2 Culture-based analysis of CF airway associated microbiota

Traditionally, culture-based examination of expectorated sputum, bronchioalveolar lavage (BAL) or nasopharyngeal swab samples has been used to identify the causative agents of chronic CF airway infection (Burns and Rolain, 2014). In line with Koch's postulates, a relatively small number of easily culturable species were thought to be the cause of such infections (Govan and Nelson, 1993). Species such as *Staphylococcus aureus* (SA) and *Haemophilus influenzae* were identified as being prevalent among infant and adolescent patients (Greenberg and Stutman, 1991). This is often followed by invasion and subsequent domination of the airway microbiota by *Pseudomonas aeruginosa* (PA) (Høiby et al., 1987), alongside the occasional co-infection by other 'keystone' respiratory pathogens, such as *Burkholderia cepacia* complex and *Stenotrophomonas maltophilia* (Bittar and Rolain, 2010, Hauser et al., 2011, Lipuma, 2010, Sajjan et al., 2001, Valenza et al., 2008).

1.2.3 Culture-independent analysis of CF airway-associated microbiota

More recently, advances in next generation sequencing technologies (NGS) have permitted the widespread uptake of culture-independent molecular profiling approaches, for example sequencing of the hypervariable 16S rRNA and fungal ribosomal internal transcribed spacer (ITS) regions, to capture the true diversity of species present within metagenomic samples (Rogers et al., 2009, Rogers et al., 2010a). This has enabled the identification of fastidious and 'unculturable' microbial species, missed using traditional microbiological investigative techniques (Mahboubi et al., 2016).

The culture-independent analysis of CF-derived samples revealed a dynamic polymicrobial community of unprecedented species diversity, comprised of both bacteria and fungi (Ahmed et al., 2019, Boutin et al., 2015, Carmody et al., 2013, Carmody et al., 2015, Hogan et al., 2016, Jorth et al., 2019, Rogers et al., 2010b, Rogers et al., 2010a, Sibley et al., 2008, Zhao et al., 2012). This should perhaps be unsurprising, given the heterogenous nature of the airway environment, which affords an array of biochemically and spatially distinct habitat niches to support the diversification and evolution of separate microbial communities.

Longitudinal studies and sampling of the CF airway associated microbiota at different stages of a patient's life or during altered disease states have been performed in an attempt to decipher how these complex communities evolve and contribute towards a decline in lung function. Earlier studies suggested that fermentative aerobic species, such as SA and *H. influenzae*, initially colonise and dominate the airways (Conrad et al., 2013, Rogers et al., 2005, Tunney et al., 2008). However, more recent investigation into the microbiota of CF infants suggests that *Streptococcus* spp. dominate the airways, alongside a mixture of anaerobic and aerobic species, such as: *Veillonella*, *Prevotella*, *Granulicatella*, *Neisseria* and *Haemophilus* (Ahmed et al., 2019, Field et al., 2010, Frayman et al., 2017b, Frayman et al., 2017a, Sibley et al., 2008). The total bacterial load within the airways is thought to remain constant over the course of a patient's life and by age 20, 60-70% of CF patients show intermittent PA colonisation (Folkesson et al., 2012, Stressmann et al., 2011). The establishment of chronic PA infections (defined as a person testing positive with PA in more than 50% of the explored points of sampling (Proesmans et al., 2006)) later in life is correlated with a decrease in species diversity and a decline in pulmonary function, with the earlier acquisition of PA being associated with a more rapid deterioration of health and worsened patient prognosis (Cox et al., 2010, Emerson et al., 2002, Klepac-Ceraj et al., 2010, Valenza et al., 2008, Zhao et al., 2012). Species of *Aspergillus* and *Candida* are the most common fungal members of the polymicrobial community associated with the CF airways, with their presence being identified in up to 50% of CF patients (Chotirmall et al., 2010, Garczewska et al., 2016, Pihet et al., 2009, Valenza et al., 2008).

1.2.4 Variable microbiotas exist between persons with CF

Existing literature surrounding the true diversity of the CF-associated microbiome has recently been challenged by the work of Jorth *et al.* Through direct sampling of the lavage fluid of CF children, the authors suggest that, to a degree, the airway microbiota in previous reports arises through sample contamination within the oral cavity and further contamination during sample processing (Jorth et al., 2019). This notwithstanding, a core population of 'non-conventional pathogens' such as *Veillonella*, *Prevotella* and *Staphylococcus* spp. still exists alongside the 'traditional CF pathogens', e.g. PA. This affirms that CF-associated infections are indeed polymicrobial in nature.

A myriad of environmental, genetic and stochastic variables contributes towards conflicting hypotheses and a lack of cohesive knowledge surrounding the adaptive and evolutionary events occurring within the CF airways over time (Ahmed et al., 2018, Charlson et al., 2011, Cuthbertson et al., 2014, Prevaes et al., 2017, Renwick et al., 2014, Salter et al., 2014).

Primarily, the onset of a decline in lung function is met with prompt clinical intervention in the form of aggressive antimicrobial treatment (Stanojevic et al., 2017). Such therapies aim to reduce the microbial load of a principal pathogen, usually PA, but they also indiscriminately target other members of the population, thereby perturbing the entire polymicrobial community present. Furthermore, the practical limitations of sample collection often prevent detailed, temporally-resolved analysis of the biochemical and community-wide ecological changes that accompany such community perturbation. Therefore, little is known about the natural evolutionary trajectory of communities associated with CF airway infection or the true extent to which current therapeutic interventions impact upon this.

1.3 Polymicrobial Infections

1.3.1 Interspecies interactions

With the CF airways harbouring dense and varied microbial ecosystems, it could be hypothesised a complex web of interspecies interactions exists between members of the community. Species may 'communicate', advertently or inadvertently, through the recognition of cell surface proteins, receptors or other cell wall components and through the secretion/uptake of extracellular small metabolites, such as antimicrobial compounds or quorum sensing (QS) molecules. Such interspecies interactions may be antagonistic or synergistic in nature, causing changes in gene expression that subsequently impact upon the metabolic potential and activity of the microbiome (Antonic et al., 2013, Armbruster et al., 2010, Armbruster et al., 2016, Baldan et al., 2014, Barnabie and Whiteley, 2015, Beaume et al., 2015, Briaud et al., 2019, Conrad et al., 2013, Dalton et al., 2011, Diggle et al., 2007, Elias and Banin, 2012, Fugère et al., 2014, Hotterbeekx et al., 2017, Hibbing et al., 2010, Ibberson et al., 2017, Ibberson and Whiteley, 2020, Korgaonkar et al., 2013, Leekha et al., 2011, Mastropaolo et al., 2005, Peters et al., 2012a, Quinn et al., 2014, Rogers et al., 2010b, Rogers et al., 2009, Rogers et al., 2010a, Vega et al., 2013, Weimer et al., 2010). It is important to note that the direct recognition or uptake of extracellularly secreted compounds may not be the only stimuli that impact upon the community, as changes to the surrounding biochemical environment, e.g. an alteration in the pH of airway secretions, will be felt by all species.

A succession of different microbial populations is associated with the CF airways over the course of a patient's life, yet it remains unclear how new environmental species and strain variants, such as those which might originate from the oral cavity or nasopharynx, interact with the pre-existing microbiota. It is also unclear which airway-associated species can be considered as 'beneficial' commensals, helping to prevent chronic colonisation of the airways by classical pathogens. Similarly, it is unclear which species may promote colonisation by

pathogenic organisms, for example through the production of public goods or alteration of the airway environment to favour colonisation by certain species (Bjornson et al., 1982, Conrad et al., 2013, Kirketerp-Møller et al., 2008). To address these types of question, it will be essential to study entire patient-derived polymicrobial communities in order to unravel the impact of less abundant ('rare') and typically avirulent species on the wider community.

1.3.2 Species co-cultivation alters gene expression

Striking differences have been observed in the gene expression profiles of species cultured axenically or as mixed population co-cultures. Comparisons of the core essential genome of SA cultured using *in vitro* and *in vivo* infection models have identified an approximate 25% difference in the expression of genes required for growth as an axenic population compared to the genes expressed during co-culture with PA (Ibberson et al., 2017). Such alterations will cause variations in metabolism and the expression of virulence determinants by a microorganism, thereby causing deviations from the behaviours observed when studying a species in isolation. Indeed, recent transcriptomic studies on co-cultures of clinical SA and PA isolates revealed that PA isolates specifically cause the differential dysregulation of >200 genes, some of which are linked to virulence, antimicrobial resistance and even central metabolism in SA (Briaud et al., 2019).

1.3.3 Stable and disturbed disease states

The CF airway-associated microbiome is thought to exist in either a stable or disturbed state, with little known about the factors contributing towards a transition between the two (Conrad et al., 2013). Efforts made in trying to identify net changes in the composition of a CF community prior to and during periods of severe lung function decline, termed acute pulmonary exacerbations (APEs) (Stenbit and Flume, 2011), yielded little in the way of interesting observations (Zhao et al., 2012). Conrad *et al.* (2013) therefore proposed the intriguing notion that the species responsible for triggering such episodes of extreme immunological response and scarring of the patient airways are present in both the stable and disturbed airway associated microbiomes. Instead, they argue that it is changes in the metabolic activity of key species, e.g. PA, caused by the presence or altered activity of other members of the community, that contributes towards a worsening of patient prognosis and the onset of APEs (Gjødtsbøl et al., 2006). Therefore, species typically considered avirulent may play a role in the transition towards a more aggressive disease state.

1.3.4 Modulation of microbial consortium and host environment

One clear example of how interspecies interactions may underpin changes within both the composition of a microbial population and impact upon the disease state of a host is provided by Korgaonkar *et al.* (2013). Using an *in vivo* co-infection model, PA was found to specifically detect *N*-acetylglucosamine (GlcNAc) shed from the walls of Gram-positive species through a putative two-component response regulator encoded by gene PA0601. This environmental cue was used to increase the production and secretion of pyocyanin (discussed further in Section 4.4) and elastase, an extracellular protease lytic against both prokaryotic and eukaryotic cells. Coinfection of a rat lung model with PA and Gram-positive bacteria also caused an increase in lung damage and enhanced virulence factor production compared to infecting the model with PA only. Furthermore, bacterial peptidoglycan has also been found to elicit changes in the behaviour of *Candida albicans* (CA) and *Bacillus subtilis* in *in vitro* models (Shah *et al.*, 2008, Xu *et al.*, 2008). In combination, these studies identify the ability of PA, and other members of a polymicrobial co-culture, to survey the ecological composition and chemical space of mixed species infections and the ability of microorganisms to utilise extracellular cues to drive changes in the expression of virulence-associated genes. Additional studies co-infecting murine models with PA and *B. cenocepacia* have identified an increase in virulence factor production and an enhancement of the host immune response compared to infection with axenic populations of either microorganism. (Bragonzi *et al.*, 2012, Chatteraj *et al.*, 2010). Taken together, these data indicate that interspecies interactions may play a vital role in triggering bouts of excessive immunological inflammation, leading towards the onset of APEs.

A novel Winogradsky-based CF model, termed WinCF, combining the use of chemical indicators and the culture-independent analysis of sputum samples obtained at the onset of APEs, was used to try and dissect how changes in a polymicrobial community directly contribute towards a worsened disease state (Quinn *et al.*, 2015). A 2-unit reduction in pH and a 30% increase in gas production caused by the increased growth of fermentative species was observed prior to the onset of exacerbations. A separate study, co-culturing PA and SA with a physiologically relevant CF phe508del airway epithelial cell line, further demonstrated PA's ability to modulate the metabolic activity of SA (Filkins *et al.*, 2015). With this study demonstrating that SA adopts a fermentative metabolic profile and undergoes significant phenotypic changes, such as small colony variant growth. Combined, these studies point towards a complex interplay between the polymicrobial composition of a community and the impact which interspecies interactions have upon altering the total metabolic output of the microbiome, leading towards a worsened disease state within patients.

1.3.5 Quorum sensing among species

The use of autoinducer QS molecules to regulate population density and coordinate community-wide changes in gene expression has been characterised in both Gram-positive and Gram-negative bacterial species. The regulatory networks of Gram-negative bacteria, e.g. PA, are primarily controlled by the environmental concentration of bacterially-derived *N*-acyl homoserine lactones (AHLs) (Papenfort and Bassler, 2016). The QS network in PA is among the most widely and extensively studied, primarily due to its link with the regulation of virulence factor production and importance in establishing infections and regulating biofilm formation in a number of *in vivo* and *in vitro* models (de Kievit, 2009, Rutherford and Bassler, 2012). A hierarchical two-tiered acyl-homoserine lactone (AHL)-based QS network is employed by PA, with the *rhIR* system subordinate to the *lasIR* system (Lee and Zhang, 2015). Autoinducer synthases for the production of *N*-(3-Oxododecanoyl)-L-homoserine lactone (OdDHL) and *N*-butanoyl-L-homoserine lactone (BHL) are encoded by *lasI* and *rhII*, respectively. Under traditional culture methods these signalling molecules accumulate in a culture in a cell-density dependent manner and, once a critical threshold concentration of each signal is attained, form a complex with their corresponding intracellular receptors (LasR and RhIR, respectively). This signal-receptor complex then activates (or, more rarely, also represses) the transcription of target genes (Schuster and Greenberg, 2006). PA also possess a non-AHL signalling molecule: 2-heptyl-3-hydroxy-4-quinolone (the *Pseudomonas* quinolone signal, PQS) which is able to further modulate expression of the *las* and *rhl* systems (Diggle et al., 2003, Diggle et al., 2006). Over 30 different PA virulence factors are known to be under QS control (Bjarnsholt and Givskov, 2007). Some, such as proteases and elastases, are linked with interspecies competition and the elimination of rival species, e.g. SA, from traditional batch co-cultures (Section 1.8.1) (Hotterbeekx et al., 2017, Mashburn et al., 2005).

Alternatively, Gram-positive species such as SA and *Streptococcus* spp., utilise post-translationally modified thiolactone peptides, termed accessory gene regulators (Agr), as QS signals (Le and Otto, 2015). QS-like signalling networks have even been described in fungi, with species such as CA utilising farnesol accumulation (discussed further in Section 3.4.1) as a signalling molecule for the coordination of cellular processes (Nickerson et al., 2006). To date little is known about what effects QS molecules produced by an individual member of a polymicrobial consortium have at the community-wide level. Yet a degree of molecular cross-recognition has been identified in certain species *in vitro* (Armbruster et al., 2010, Diggle et al., 2007). For example, autoinducer-2 (AI-2) is a universal QS molecule produced by many bacteria (Vendeville et al., 2005). Despite PA not producing AI-2, studies have demonstrated that the addition of exogenous AI-2 regulates PA biofilm formation and virulence factor production in a dose-dependent manner (Li et al., 2015). Given the array of virulence

associated genes under the regulatory control of QS networks (Rutherford and Bassler, 2012), it is likely that such indirect interspecies signalling events contribute towards the progression and pathogenesis of CF-associated infections and other polymicrobial infection scenarios.

1.3.6 Antimicrobial treatment

The majority of therapeutic antimicrobial strategies aim to eradicate or reduce the load of a principal pathogen from the site of infection. However, polymicrobial communities display an altered, and often refractory, response to the action of antimicrobials compared with the treatment of a species in isolation (Fodor et al., 2012, Lopes et al., 2012, Peters et al., 2012a). These observations can, in part, be attributed to failings in drug discovery efforts and currently-used treatment regimens aimed at the prevention and clearance of chronic infections from the airways of CF patients. For example, *in vitro* co-cultures of PA, SA and *S. maltophilia* were found to be less susceptible to the action of ciprofloxacin (a clinically-used antimicrobial belonging to the fluoroquinolone class of compounds) when compared with mono-species cultures (Magalhães et al., 2016). Increased doses of ciprofloxacin caused a reduction in the viability of PA but not the other species in the co-culture, leading to speculation that PA may exert a protective effect against antimicrobial action on the other species. An array of interspecies interactions, which may either enhance or reduce the susceptibility of species to therapeutic intervention or immune clearance, are likely to exist in the CF airways and cause a dramatically altered responses to therapeutic intervention.

Since the indiscriminatory action of some antimicrobial compounds may wipe out the more susceptible members of the commensal airway microbiota, such interventions may create opportunities for invasion of the niche by drug-resistant species or strain variants (Ciofu et al., 2013, Conrad et al., 2013). This could contribute to further complications in the future treatment and a decline in pulmonary function of the patient in the long-term. Therefore, there is a clear need to evaluate the action of antimicrobials on entire polymicrobial populations, not just a single target species.

1.4 *Pseudomonas aeruginosa* (PA)

1.4.1 Genome and general characteristics

PA is a Gram-negative bacillus, ranging from 1.5 – 5 µm in length. The organism is motile, primarily through the use of a single, polar flagellum (Palleroni, 2004). PA belongs to the Gammaproteobacteria class. Some members of this bacterial class are also known as the

'fluorescent pseudomonads' due to their ability to produce fluorescent pigments, such as the blue-green redox-active phenazine dye, pyocyanin, discussed further in *Section 4.4*.

The first PA genome sequenced was that of the common laboratory reference strain PAO1, isolated from a burn wound in 1955 (Holloway, 1955). With the PAO1 genome comprising of 6.3 million base pairs, predicted to encode 5570 open reading frames (ORFs) (Stover et al., 2000), the coding complexity of PA strains approach that of simple eukaryotic cells. Indeed, PA has over 1300 more ORFs than most species of *Escherichia coli* (Blattner et al., 1997). Importantly, these extra ORFs do not simply encode for higher numbers of the same types of genes, but rather, an increased number of distinct gene families, indicative of a large functional and metabolic potential (Stover et al., 2000).

1.4.2 Adaptive metabolic potential

The immense metabolic range and ecological diversity of PA is demonstrated by its ubiquitous presence within the environment, with PA frequently isolated from soil and aquatic environments (Kulasekara and Lory, 2004). PA is a well-known opportunistic pathogen, hardly ever infecting healthy individuals but a breach in host defence mechanisms provides PA with the opportunity to establish an infection. Approximately 6% of healthy individuals harbour PA within their oropharynx, but this number is thought to approach 50% in hospitalised patients (van Delden, 2004) as PA can colonise virtually all mucosal surfaces and invade tissues and the bloodstream. With almost one-tenth of its genomic repertoire (9.3% of ORFs) encoding transcriptional regulators or two-component systems (Kulasekara and Lory, 2004), PA can tightly regulate its metabolic activity in response to environmental stimuli (Palmer et al., 2007, Stover et al., 2000). These features likely contribute towards enabling PA to inhabit some of the broadest environmental niches of any known bacterial species.

1.4.3 CF airway infection

PA preferentially utilises aerobic and oxidative metabolic pathways, but can easily adapt to life in microaerophilic and anaerobic environments by using nitrate or nitrite as a terminal electron acceptor (Zannoni, 1989, Zumft, 2004). Mucus plugging and obstruction of the bronchiolar lumen leads to the formation of steep oxygen gradients with hypoxic and even anoxic regions in the CF airways (Worlitzsch et al., 2002). Therefore, the ability of PA to tolerate changes in environmental oxygen concentration is significant for the bacterium's ability to chronically colonise all parts of the CF airway microenvironment. Furthermore, PA has been demonstrated to grow to high cell densities ($>10^9$ CFU mL⁻¹) in the CF airways

through utilisation of its phosphatidylcholine catabolism pathways (Singh et al., 2000, Son et al., 2007, Storey et al., 1992). Phosphatidylcholine constitutes approximately 80% of the total lipids present in lung surfactant and is found in high abundance in the CF airways (Bernhard et al., 2001). The action of PA-produced lipases and phospholipase C cleaves phosphatidylcholine into a phosphorylcholine headgroup, one molecule of glycerol and two long-chain fatty acids (Son et al., 2007, Sun et al., 2014). These molecules are then fed into the choline, glycerol and β -oxidation degradation pathways. Five operons have been identified to be involved in the degradation of fatty acids, termed *fadBA*-operons, with three of these being dominant for the utilisation of medium- and long-chain fatty acids. Triple knock-out mutants lacking these fatty acid degradation operons show a severe reduction in fitness, but not virulence factor production, when grown *in vivo* (Sun et al., 2014). By contrast, *E. coli* possess only a single *fad* operon (Clark, 1981).

1.4.4 Virulence factors

As previously mentioned in *Section 1.3*, the establishment of chronic PA infection in the CF airways is significantly correlated with a reduction in species diversity and a progressive decline in patient lung function. In addition to a complex and adaptive metabolic network, the PA genome also encodes for an arsenal of virulence factors and determinants, such as: iron scavenging/sequestering molecules (termed siderophores, discussed further in *Section 4.5*); elastases; proteases; phospholipases; rhamnolipids; exotoxin A, S, T, U and Y; AprA, AprX and HasAP. See Ben Haj Khalifa *et al.* (2011), van Delden (2004) and Kung *et al.* (2010), for a detailed review of PA virulence factors, functions and their regulation.

The ability of PA to modulate its surrounding environment is further exemplified by the all four of the extracellular secretion systems described in Gram-negative bacteria (reviewed in depth by (Green and Mecsas, 2016)) being identified in the PA genome (Blevess et al., 2010). Primarily, PA utilises the Type II secretion system to secrete virulence factors, such as exotoxin A, into its local environment (Cianciotto, 2005). Exotoxin A is considered the most potent extracellular virulence factor produced by PA, causing the inactivation of eukaryotic elongation factor 2 and thereby arresting protein translation to cause cell death and tissue necrosis (Michalska and Wolf, 2015). Additionally, the Type III secretion system, sometimes referred to as the 'injectisome', uses a needle-like structure to directly deliver effector proteins such as exotoxin S, T, U and Y, directly into the cytoplasm of a target cell *via* contact-dependent mechanisms (Engel and Balachandran, 2009). It is important to note that PA can produce virulence factors harmful against both prokaryotic and eukaryotic cells. For instance, rhamnolipids, which are essentially biological detergents, have both antimicrobial and

haemolytic activity (Espinosa-Urgel, 2003, Jensen et al., 2007, Soberón-Chávez et al., 2005). The array of virulence determinants and secretion systems encoded by PA is summarised in *Figure 1.3* and these demonstrate the ability of this pathogen to directly influence the metabolic activity, composition and evolutionary trajectory of the CF airway-associated microbiome. Furthermore, some extracellular virulence factors secreted by PA also act upon host tissues and the surrounding CF-airway environment to cause irreversible tissue damage and a decline in pulmonary function (Dalton et al., 2011).

1.4.5 Antimicrobial resistance

Once established, PA infections of the CF airways are almost impossible to eradicate (Fodor et al., 2012, Pressler et al., 2011). The primary focus of research into CF-associated infections has therefore centred on understanding the growth of PA in this environment, in an attempt to identify novel targets for the attenuation of virulence or the reduction of a microbial loads *in situ* (Döring et al., 2004). Yet despite decades of research, PA remains on the World Health Organisations' list of "priority 1: critical pathogens" for the development of new antimicrobial compounds (Asokan et al., 2019). The prolonged overuse of antimicrobials and a lack of novel compound classes entering the drug discovery pipeline, has led to a worrying rise in antimicrobial resistance (AMR) among bacterial species, and an innovation gap in the development of novel antimicrobials to combat this (Renwick et al., 2016). Furthermore, aggressive antimicrobial treatment at the onset of APEs is common and almost certainly contributes towards the emergence of AMR isolates in the CF airways (Sousa and Pereira, 2014, Stressmann et al., 2012).

AMR may arise through several different mechanisms, including direct inactivation of an antimicrobial through enzyme modification/cleavage, modification of a compound's target and prevention of a compound from reaching its target either by sequestration, or a decrease in uptake or an increase in efflux (Pang et al., 2019, Poole, 2011). In clinical PA isolates, the most prevalent AMR defence mechanism observed is a reduction in outer membrane (OM) permeability (Li et al., 2012). The relatively narrow size of the major membrane porin, OprF, ensures reduced penetration of solutes across the OM (by around two orders of magnitude, compared with *E. coli* (Hancock and Brinkman, 2002, Nikaido, 2003)). Multidrug efflux (Mex) pumps further facilitate the export of a large range of molecules, including antimicrobials from the cell (Li and Nikaido, 2009). An increase in the expression of Mex-systems works in conjunction with a down-regulation of OM porins during chronic airway infections, contributing to the rapid emergence of AMR PA isolates amongst microbial communities associated with infection of the CF airways (Pang et al., 2019, Poole, 2011).

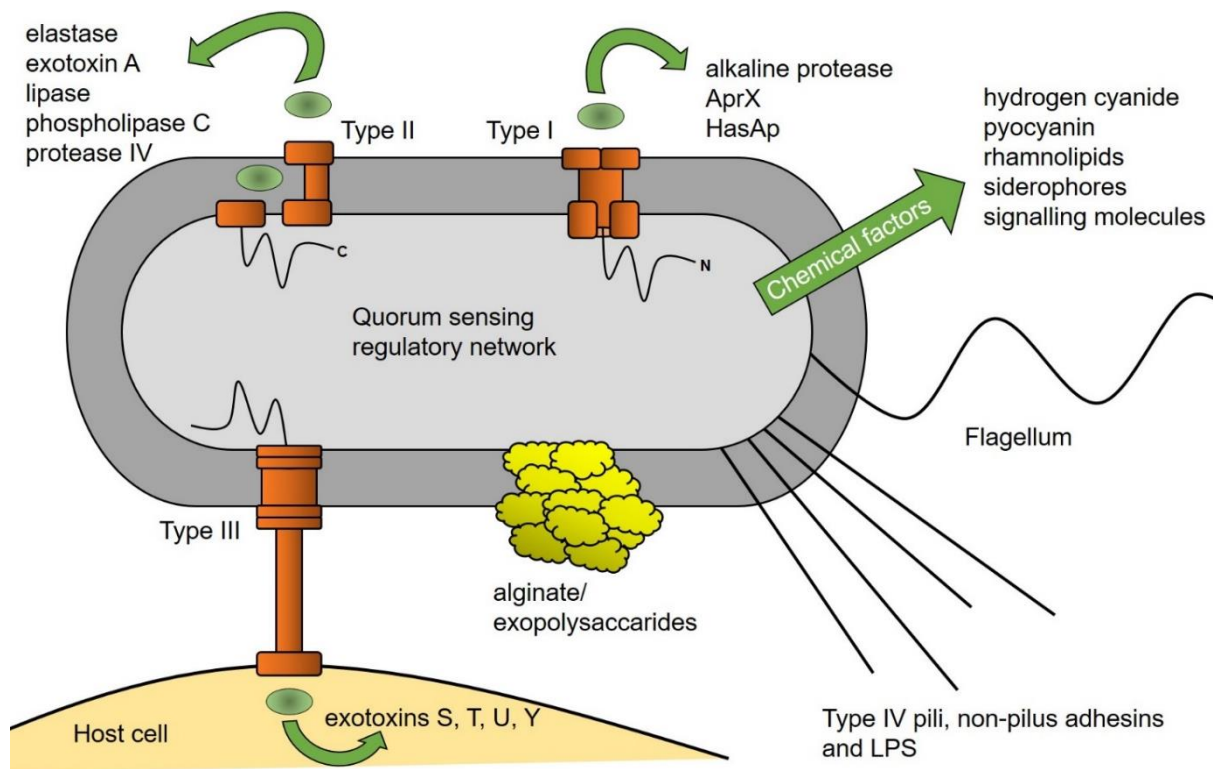


Figure 1.3. *Pseudomonas aeruginosa* virulence factors and secretion systems.

PA produces a large number of virulence factors. Some of these are cell-associated (flagellum, lipopolysaccharide (LPS), type IV pili, non-pilus adhesins) whereas others are secreted into the extracellular environment. Extracellular virulence factors are comprised of chemical agents (alginate/exopolysaccharides, hydrogen cyanide, pyocyanin, rhamnolipids, siderophores, signalling molecules) and proteins secreted *via* one of the three secretion systems. Type I substrates (alkaline protease, AprX, HasAP) have a C-terminal signal peptide. The periplasmic fusion protein interacts with the inner membrane ABC transporter and the outer membrane channel forming protein. Type II substrates (elastase, exotoxin A, lipase, phospholipase C, protease IV) have an N-terminal signal sequence, which is cleaved in the periplasm, where protein folding takes place. Transport then proceeds *via* a gated outer membrane channel protein. Type III effectors (exotoxins S, T, U and Y) are injected directly into the cytoplasm of a target host-cell *via* the secretion apparatus or 'injectisome'.

1.4.6 PA in the context of polymicrobial infections

To date, research into the role of PA as the primary pathogen of CF-associated infections has relied on studying the axenic growth of different strains using a variety of *in vitro* and *in vivo* models. Although such studies are beneficial in advancing a fundamental understanding of metabolic pathways, bacterial lifestyles and key virulence determinants, they do not accurately reflect the behaviour of PA when present as part of a polymicrobial community. Given the ability of PA to sense chemical and ecological changes in the environment, and its adaptive metabolic and virulence potential, I hypothesise that during co-culture, PA will adopt a distinctly different lifestyle when compared with mono-microbiological growth (O'Brien and Fothergill, 2017, Winstanley et al., 2016). Possible drug targets identified and validated using axenic growth models may be down-regulated, made redundant or even absent during co-culture and could, in part, explain some of the failings of modern efforts aimed at eradicating PA from the CF airway.

The dynamic and successive nature of CF-associated airway infections leads to changes in the composition of microbial species harboured by the lungs over the course of a patient's life. This will in turn impact upon the wealth of interspecies interactions and communication events occurring inside the airways, leading to modulations in behaviour and the evolutionary trajectory of PA and other key pathogens over time. Such changes that affect the evolution of the CF-airway associated microbiota may drive pathogens, or even typically avirulent species, towards a more persistent and multi-drug resistant lifestyle. Only by considering the presence of other species and their potential to perturb and influence the surrounding members of a polymicrobial community will it be possible to more accurately model and study the *in situ* behaviour of PA in the laboratory.

1.5 Biofilms

1.5.1 Historical perspective

Since the foundation of microbiology as scientific discipline, microbiologists have studied the growth of microorganisms in liquid culture (the “planktonic” growth state). The first published account of surface-associated bacteria was from Henrici in 1933, who noted that “It is quite evident for the most part bacteria are not free floating organisms, but grow upon submerged surfaces” (Henrici, 1933). In 1943, Zobell then showed that the fouling of submerged slides in seawater was caused by sessile marine bacteria (Zobell, 1943). Costerton was the first to formally coin the term biofilm in 1978 (Costerton et al., 1978), promptly followed by an exponential increase of research into this field, with over 5600 articles on biofilms published in 2019 alone (PubMed).

1.5.2 General characteristics

In recent years it has been made clear that the majority of microorganisms in nature and a disease setting reside as spatially-structured biofilm communities. With constant advances in the field of biofilm biology, what exactly constitutes a 'biofilm' is undergoing continual revision. However, a universally accepted basic biofilm definition is: a microbially-derived sessile community, irreversibly attached to a substratum, interface or each other which is encased within a matrix of self-produced extracellular polymeric substances (EPS, consisting of polysaccharides, protein and extracellular DNA), and exhibits an altered phenotype with respect to growth rate and gene transcription (Donlan, 2002).

Biofilms can form a highly diverse array of differentiated structures in the environment. Some biofilms simply consist of flat confluent communities, whereas others form complex mushroom-like towers, separated by fluid filled channels thought to deliver nutrients to the centre of the structure (Tolker-Nielsen and Molin, 2004). The high level of cellular coordination observed in the formation of biofilms, has led some to theorise that biofilm formation is a programmed developmental progress, similar to those seen within eukaryotic systems (Sauer, 2003, Stoodley et al., 2002). Others argue that these structures arise in response to a series of successive temporal events, reflecting the adaptation of individual members of a community to changes in the local microenvironment and nutrient availability, meaning biofilm formation could follow numerous pathways (Hentzer et al., 2005, Tolker-Nielsen and Molin, 2004).

1.5.3 Biofilms in infection

One crucial feature of microbial biofilms, and the reason for such intense research into this area, is their increased ability to bypass effective immune clearance and to avoid antimicrobial action (Leid et al., 2005). In fact, some bacterial biofilm communities have been determined to be 1000-times more resistant to antimicrobial treatment compared with their planktonic cell counterparts (Parsek, 2003). Over 60% of bacterial infections in the western world are believed to involve the formation of biofilms (Fux et al., 2005) and CF is no exception. In fact, the extensive formation of biofilms in the mucus obstructed airways is often cited as a key reason for the failings of therapeutic strategies aimed at eradicating chronic PA and other key pathogens from the airways of CF patients (Bjarnsholt et al., 2009, Folkesson et al., 2012, Elias and Banin, 2012, Høiby et al., 2010b, Leekha et al., 2011, Lopes et al., 2012, Mowat et al., 2011, Römling et al., 1994). As such, the inhalation of human deoxyribonuclease (rhDNases) such as dornase alfa and pulmozyme to aid in the degradation of extracellular DNA and mediate biofilm dispersal, is a common CF airway management treatment (Suri, 2005).

1.5.4 Biofilms and *Pseudomonas*

Alongside being the primary pathogen of late-stage CF airway infections, PA readily forms biofilms on numerous abiotic and biological interfaces, and so is frequently used as a model organism in the study of biofilm formation (Moreau-Marquis et al., 2008). The formation of PA biofilms is thought to follow five distinct developmental stages: reversible attachment, irreversible attachment, two stages of maturation and dispersal (*Figure 1.4*) (Maunder and Welch, 2017, Stoodley et al., 2002). However, the environment in which a biofilm grows is known to substantially alter the structure and developmental process of biofilm formation (Deretic et al., 1990, Høiby et al., 2010b).

PA is found to undergo striking phenotypic adaptations throughout the course of chronic CF airway infections. Isolates transition from a motile, non-mucoid lifestyle (associated with acute, early-stage infections) towards a non-motile, mucoid phenotype during late-stage chronic infection (Folkesson et al., 2012, Smith et al., 2006). The mucoid phenotype of PA is due to overproduction of alginate, a major polysaccharide component of the EPS matrix, enabling mucoid isolates to more readily form biofilms and display increased antimicrobial tolerance (Boyd and Chakrabarty, 1995, Franklin et al., 2011, Hentzer et al., 2001). Alginate overproduction is often caused by mutations in *mucA*, with over 80% of mucoid PA isolates recovered from late-stage CF airway infections containing mutations or insertions in the *mucABCD* gene cluster (Boucher et al., 1997, Pulcrano et al., 2012). *mucA* encodes for the anti-sigma factor MucA that binds and sequesters AlgU, an alternative sigma factor and positive regulator of alginate biosynthesis (Hershberger et al., 1995, Lizewski et al., 2004, Pulcrano et al., 2012). The loss of motility within mucoid phenotypes is accounted for by AlgU negatively regulating flagella production (Tart et al., 2005), highlighting a reciprocal relationship between motility and the establishment of chronic infection in the CF airways.

1.5.5 Evolution and adaptation within biofilms

The formation of DNA-damaging free-radicals and the bacterial ‘SOS’ response are the fundamental driving forces behind the emergence of mutations in microbial populations (Spiers et al., 2000). Microbial mutation, coupled with competition and the unique selection pressures of different niches in a heterogeneous environment, such as biofilms in the CF airways, cause the adaptive divergence of members of a polymicrobial community (Markussen et al., 2014, Schick and Kassen, 2018, Winstanley et al., 2016). Most of the research into biofilm formation has focused on a single species, such as PA, in isolation. These studies therefore neglect how the presence of other species influences the evolution and adaptation of polymicrobial biofilms (Dalton et al., 2011, Sands et al., 2013). As a result, little is known

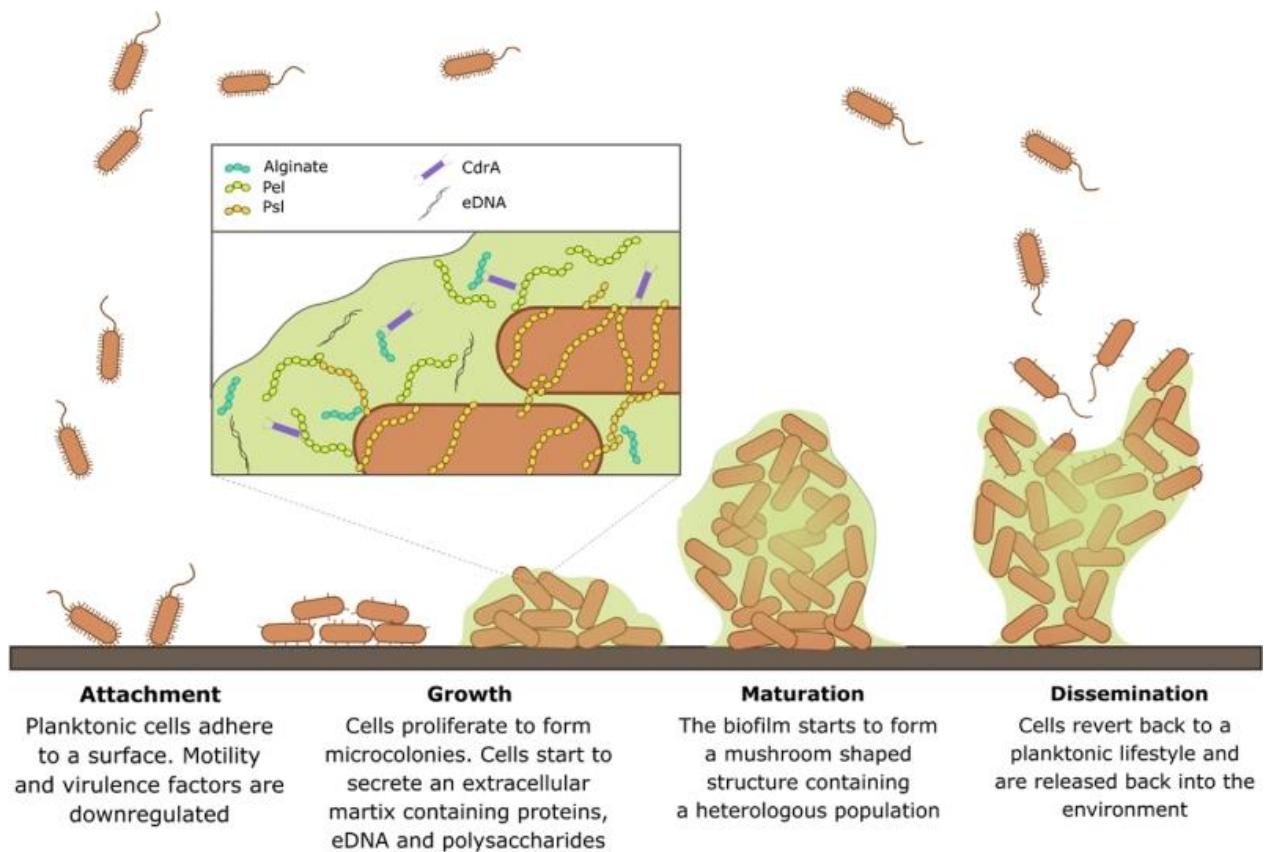


Figure 1.4. Biofilm development and life cycle.

Formation of model single-species PA biofilms begins when motile planktonic cells reversibly adhere to a surface. Cells proliferate and undergo phenotypic adaptation as microcolonies form and irreversibly adhere to the surface, motility apparatus is down-regulated and the production of extracellular polymeric substances is up-regulated to encase the biofilm community. Biofilms then undergo several maturation stages to form mushroom-like structures comprised of heterogenic microbial populations. In response to certain environmental conditions members of the population may revert to a motile phenotype and disseminated from the fixed biofilm structure to colonise new environmental niches. Figure reproduced from (Maunder and Welch, 2017) under CC BY 4.0.

about the formation, composition or structure of polymicrobial biofilm communities, especially in the context of CF. Whilst the transition towards a biofilm-centred, mucoid phenotype is commonly viewed as a global response to environmental stress (Davies et al., 2016), evidence is emerging to support that interspecies interactions within polymicrobial communities may play a crucial role in shaping biofilm formation, either positively or negatively (Bragonzi et al., 2012, Burmølle et al., 2006, Elias and Banin, 2012, C.J. et al., 2018, Hibbing et al., 2010, Lopes et al., 2012, Lopes et al., 2017, Makovcova et al., 2017, Wolcott et al., 2013, Woods et al., 2018). As an example, the co-culture of *Inquilinus limosus* with PA caused a reduction in the total biomass of the polymicrobial biofilm, whereas co-culturing *S. maltophilia* with PA caused an increase in the total biomass of the biofilm (Magalhães et al., 2016). Furthermore, ethanol produced by CA stimulates biofilm formation in PA (DeVault et al., 1990). Conversely, the protein SpA, secreted by SA, inhibits the formation of PA biofilms (Armbruster et al., 2016).

The production of exopolysaccharides plays a vital role in the spatial organisation of biofilms. The polysaccharide Pel, produced by PA, is required for close association of the bacterium with SA in biofilms, yet the polysaccharide Psl causes PA to grow as a single-species biofilm atop SA (Chew et al., 2014). What triggers changes in the production of factors key for biofilm formation, such as exopolysaccharides, in the CF airways are not yet clear, but the role of these factors in modulating biofilm formation is evident.

1.6 CF Infection Models

1.6.1 A need for polymicrobial infection models

A dynamic polymicrobial community is associated with the CF airways throughout the course of a patient's life (*Section 1.2*). Increasing evidence is indicating the emerging role interspecies interactions between members of a population may play in driving changes in the composition, evolutionary trajectory and transcriptional profile of the consortium (*Section 1.3*). Modulations in metabolic activity will not only impinge upon microbe-microbe interactions, but such alterations may trigger species, such as PA, to adopt a more pathogenic lifestyle. The subsequent increase in the expression of virulence factors will impact upon the surrounding host microenvironment and possibly also contribute towards tissue damage, a decline in pulmonary function and the onset of APEs. There is an essential need to consider the role of all species present in a polymicrobial population, not simply the principal pathogen of infection. Researchers are therefore being urged to move away from the study of axenic cultures in favour of more physiologically representative co-culture models to more accurately model natural infection events associated with the CF airways.

The development of physiologically-relevant laboratory models to permit the stable, long-term co-culture of species associated with the CF airways, or even an entire polymicrobial community derived from a CF patient's airways (i.e. from sputum or bronchoalveolar lavage samples) would be of enormous benefit to the respiratory research community. Such models would permit the real-time study of interspecies interactions and evolutionary events likely to occur *in situ* inside the airways, as well as allowing the capture of entire population dynamics in the face of external perturbation. Understanding what community-wide changes in population composition or gene expression occur amongst a polymicrobial community in response to antimicrobial treatment would enable a more informed understanding of why current strategies fail to eradicate chronic infections, adversely affect the commensal microbiota, or contribute towards the rise of AMR. Similarly, how a pre-established polymicrobial consortium responds to the introduction of new species or strain variants could also be assessed in such an experimental model. For example, how does a PA-negative polymicrobial community, associated with the early stages of airway infection, respond to the addition of PA? Such experiments could be used to model an initial infection event.

1.6.2 Existing models

Despite the clear need to consider the role of all species present in a polymicrobial infection setting, relatively little is known about what interspecies interactions and events are occurring in the CF airways. This is partly owing to the complexity of these populations, but it is the paucity of existing CF models that significantly hampers research efforts. Often laboratory models are insufficient at maintaining mixed species co-cultures for any length of time (O'Brien and Welch, 2019b). This is because the dominant CF pathogens rapidly outcompete other species in a co-culture and fastidious species simply do not grow. It is therefore difficult to discern what interspecies interactions occur between members of a CF-associated community and researchers are often forced to neglect the presence of unconventional and fastidious species.

The advantages and limitations of existing *in vivo*, *in vitro* and *in silico* CF models and the most feasible route for the development of a true polymicrobial model capable of recapitulating the entire CF associated microbiome in the laboratory setting have been recently reviewed in depth (O'Brien and Welch, 2019b). Therefore, these points will not be addressed further in this work. Instead, I direct the reader to the publications chapter of this document for further discussion and *Table 1* provides a summary of the key points raised for reference.

1.7 Aims of the Current Work

1.7.1 Development and Characterisation of an *in vitro* model to enable long-term co-culture of key CF-associated pathogens

Under traditional laboratory growth conditions, key CF associated pathogens, such as PA, rapidly outcompete and remove other microbial species present in a polymicrobial consortium. This limits the experimental analysis of interspecies interactions and population evolution. The primary aim of this work was to develop a physiologically-relevant and experimentally tractable model to enable the successful, long-term co-cultivation of key pathogens associated with CF airway infections. An *in vitro* continuous-flow co-culture model was designed, developed and characterised for this purpose. Using this model, the successful long-term co-culture of three distinct CF-associated pathogens, *P. aeruginosa* (PA), *S. aureus* (SA) and *C. albicans* (CA) could be maintained. *Section 1.8* details the rationale behind my choice of experimental approach.

1.7.2 Response of Polymicrobial Co-cultures to Therapeutic Intervention

Antimicrobial compounds are often developed and tested on axenic microbial populations to limit or eradicate the growth of a principal pathogen. As discussed previously (*Section 1.3*), microbial species display altered genetic and metabolic profiles when grown as part of a co-culture, meaning they may respond differently to antimicrobial treatment compared to what is expected from the study of axenic cultures. Due to species out-competition using traditional batch culture methods, previous work has relied heavily on studying the response of polymicrobial biofilms to antimicrobial agents. As predicted, these studies have found that polymicrobial biofilms display altered antimicrobial resistance profiles compared to single-species biofilms. My novel *in vitro* model, developed as the primary aim of this work (*Section 1.7.1*), provides an unparalleled opportunity to study how an actively-growing polymicrobial community differs in response to external perturbation following antimicrobial treatment. In this study, I compared the treatment of steady-state axenic and polymicrobial populations of PA, SA and CA with clinically-relevant antimicrobial compounds (colistin, fusidic acid and fluconazole) that specifically target each of the species present. However, in theory, any number/combination of antimicrobial compound classes or microbial species could be tested using the model.

Model Type	Advantages	Limitations
CF Mouse (<i>in vivo</i>)	<ul style="list-style-type: none"> • >14 models with different CFTR mutations in different genetic backgrounds available • Allows the immune response and host-pathogen interactions to be studied • Cheapest vertebrate CF model • Well characterised with large genetic manipulation toolbox available • Widely available 	<ul style="list-style-type: none"> • Knockout of the CFTR gene alone not sufficient to cause a disease phenotype; additional mutations are required which may have off-target effects • Does not develop spontaneous airway infections • Only suitable for acute infection studies; species are rapidly cleared from the airways unless immobilised within beads • Shares 78% CFTR homology with humans
CF Ferret (<i>in vivo</i>)	<ul style="list-style-type: none"> • Develop spontaneous polymicrobial airway infections with a similar species composition as humans • Allows the immune response and host-pathogen interactions to be studied • Shares 92% CFTR homology with humans 	<ul style="list-style-type: none"> • Only suitable for acute infection studies • Airway infections stimulate rapidly fatal immune responses; neonatal CF ferrets require prophylactic treatment with antibiotics to survive weaning
CF Pig (<i>in vivo</i>)	<ul style="list-style-type: none"> • Develop spontaneous polymicrobial airway infections with a similar species composition as adolescent CF patients • Allows the immune response and host-pathogen interactions to be studied • Spatial organisation of porcine and human airways share a remarkable degree of degree of homology with humans • Shares 91% CFTR homology with humans 	<ul style="list-style-type: none"> • Very costly to maintain • Requires highly specialised research facilities and technically demanding • Data does not exist on the long-term survival of model or how airway associated microbiota changes over time
Plant and Insect (<i>in vivo</i>)	<ul style="list-style-type: none"> • Low cost and minimal expertise/equipment required • Effective for high-throughput screening of mutant libraries • Limited similarities in innate immune response compared with vertebrate species 	<ul style="list-style-type: none"> • Limited range of CF associated species can establish an infection • Only suitable for acute infection studies (up to 48 hours) • Little physiological similarity to CF airways • Screening results should be viewed with caution as some hits may be missed, and false positives discovered
<i>In vitro</i>	<ul style="list-style-type: none"> • Low cost and minimal expertise/equipment required 	<ul style="list-style-type: none"> • No host cells/ immune system present (only useful for studying interspecies interactions and changes within microbial composition present)

	<ul style="list-style-type: none"> • Highly defined and experimentally tractable culture conditions • Lack of ethical concerns (experimentally perturbable) • Biochemically representative of CF airway environment • No time constraints (longitudinal/chronic studies possible) • Real-time and sensitive measurement of chemical and genetic changes within population possible • High-throughput 	<ul style="list-style-type: none"> • Lack of spatial organisation (although using an <i>ex vivo</i> porcine lung model or cell culture of an airway epithelial cell line, e.g. phe508del, could introduce this)
<i>In silico</i>	<ul style="list-style-type: none"> • Accurately predicts composition and metabolic activity of a polymicrobial community from published datasets • Able to identify very subtle changes in gene expression and metabolism that may be missed within experimental models • High-throughput • Cheap • No ethical concerns • Useful for informing future “wet-lab” validation and experimental research efforts 	<ul style="list-style-type: none"> • Relies on the quality of existing experimental data for accurate population modelling, therefore uncommon and fastidious species are poorly characterised and underrepresented within predictions (although this will improve as more experimental data is gathered)

Table 1.1. Overview of the key advantages and limitations of existing CF models.

Table provides a summary of the suitability of existing CF model types for the development of a long-term co-culture model that enables an entire polymicrobial community associated with CF airway infections to be recapitulated within the laboratory, as reviewed by O’Brien and Welch (2019b).

1.7.3 Analysis of Polymicrobial Biofilms in the Context of CF

As highlighted in *Section 1.5*, biofilms are implicated in the majority of chronic infection scenarios and their association with the CF microenvironment is no exception. Despite the importance of understanding biofilm behaviour and formation, relatively little is known about the formation of polymicrobial biofilms in the CF airways. I sought to compare biofilm formation in axenic and polymicrobial cultures of PA, SA and CA using a CF-relevant growth medium (artificial sputum medium, *Section 1.8.2*) in nutrient limited (batch) and continuous-flow culture conditions. Furthermore, I developed a method for reproducibly culturing biofilm populations upon removable pieces of solid substratum within the *in vitro* continuous-flow model and compared how two different substrata, agar chunks and porcine lung tissue sections, affect the composition of polymicrobial biofilms over time.

1.7.4 Growth of Patient Derived Polymicrobial Communities *in vitro*

Following the success of the aim described in *Section 1.7.1*, I aimed to refine the continuous-flow model's culture conditions to permit direct inoculation of the culture vessel with expectorated sputum samples collected from persons with CF. Through this I hoped to recapitulate the entire microbiota associated with CF airway infections, thereby enabling the study of patient-derived polymicrobial populations *in vitro*.

1.8 Experimental Approach

1.8.1 Continuous-flow culture

As summarised in (O'Brien and Welch, 2019b) the most feasible approach for the laboratory-based development of a polymicrobial community representative of those in the CF airways is through the development of an *in vitro* model. The inherent benefits and limitations of my *in vitro* co-culture model are discussed further in *Section 8.5*.

The inability of species to grow *per se*, or out-competition between members of a community are the most common reasons why existing experimental co-culture models fail. Some species have an extremely limited host range, thereby severely limiting the use of *in vivo* models to study polymicrobial communities. For example, *H. influenzae* is only able to infect human hosts (Pan et al., 2014). An *in vitro* model which closely mimics the nutritional and chemical environment of the CF airways is likely to be sufficient to permit the growth of such human-specific and fastidious species. Through inoculation of a model with an entire patient derived polymicrobial community, *i.e.* those contained within an expectorated sputum sample, auxotrophic strains and species reliant on the production of public goods produced by other

members of a community should still be cross-fed, allowing growth to be maintained within a culture vessel (Germerodt et al., 2016). Furthermore, the presence of animal-specific species and potential unwanted environmental “contaminants” are excluded when using a closed *in vitro* model system, allowing for interactions between members of the initial inoculum to be studied with confidence.

Competition between species in a community increases when the selection pressure for limited space and nutrients in an environmental niche mount. For example, PA and SA can be co-isolated from the airways of ~31% of CF patients (Hogan et al., 2016, Limoli et al., 2016, Wakeman et al., 2016, Zolin et al., 2019), yet attempts to co-culture these species together *in vitro* often result in the rapid killing and removal of SA from the co-culture (discussed further in Section 3). One limiting factor for the growth of all microbial species is likely to be iron availability (Zughaier and Cornelis, 2018). Studies of the essential PA genome during mono- and dual-species co-culture with SA under iron-limited conditions found that 5% of the total PA genome is differentially expressed (Mashburn et al., 2005). Interestingly, the genes associated with iron acquisition were down-regulated during co-culture, suggesting PA is able to outcompete SA and use the resulting cell lysate as a source of iron to support its own growth when environmental levels are limited (Barnabie and Whiteley, 2015, Nguyen et al., 2015, Nguyen and Oglesby-Sherrouse, 2016).

To date, the majority of existing *in vitro* co-culture models have attempted to grow mixed species consortia under batch culture conditions. A finite supply of nutrients is provided to support growth and space in the culture is limited. As the population grows the total cell density increases and nutrients become depleted (Wanner and Egli, 1990). This imposes a strong selection pressure on the community as it enters the stationary phase, causing species to aggressively compete with other members of the co-culture for the scant remaining resources. This underpins the killing and removal of some species by the more aggressive members of the population.

I hypothesised that though the use of a continuous-flow model, not unlike a small scale chemostat or microbial fermenter (see Section 2.3 for model details), it may be possible to maintain a long-term, stable co-culture of CF-associated pathogens *in vitro*. By providing a continual supply of fresh nutrients, competition for nutrients and space is likely to be reduced (Ziv et al., 2013). This continual provision of fresh nutrients may therefore enable mixed-species populations to be held at a stable carrying capacity inside the culture vessel for extended periods of time without entering the stationary phase of growth. My approach was intended to mimic the constant over-production of nutrient rich sputum in the CF airways alongside the periodic removal of “waste” sputum from the lungs by expectoration. The

abundance of nutrients in the CF airways may be the reason why co-cultures of species known to outcompete each other *in vitro* are commonly found together *in situ* in sputum samples. By altering the flowrate (Q) of my continuous-flow model, it should be possible to modulate the total carrying capacity of the culture vessel. Furthermore, altering Q may also allow for different phases of microbial growth, e.g. the stationary or exponential phase, to be experimentally studied.

1.8.2 Artificial Sputum Medium

Artificial sputum medium (ASM), or synthetic cystic fibrosis sputum, is a previously developed and chemically defined synthetic growth medium that captures the nutritional composition of CF airway secretions (Haley et al., 2012, Kirchner et al., 2012, Sousa et al., 2018, Sriramulu et al., 2005, Turner et al., 2015). Comparison of the essential genome of PA grown *in vitro* in ASM or in sputum derived from CF patients, established virtually no difference between the two (Turner et al., 2015). Furthermore, global transcription profiles of *P. aeruginosa* PA14 grown in ASM established that key genes associated with the growth of PA in the CF airways were expressed and that the transcriptional profile of PA was similar to that observed *in situ* (Fung et al., 2010). ASM also induces PA to exhibit significant phenotypic adaptations that closely resemble the behaviour of PA in sputum samples. For instance, PA grows as microcolonies closely associated with the mucin present in ASM (Sriramulu et al., 2005). In combination, these studies highlight the suitability of ASM as the ‘gold-standard’ synthetic medium for the growth of CF-associated species *in vitro* under physiologically-relevant conditions.

To the best of my knowledge, no study has yet attempt to grow an entire CF-associated microbial consortium in ASM. As all the essential nutrients and growth factors found in this environmental niche should be captured in ASM, the growth of all airway-associated species should be supported. An additional benefit of using a defined growth medium, is that the composition of ASM can be easily modified. Slightly altering the composition of ASM to include additional growth factors may help support the growth of some particularly fastidious species. Additionally, how variations in the availability of a particular nutrient component affects the population can be readily studied. As the composition of fresh ASM is known, subtle changes in the chemical composition of the culture medium can be characterised and directly attributed to microbial activity rather than to the confounding effects of non-controlled exogenous environmental factors.

2. Materials and Methods

2.1 Strains

All microbial strains used in this work are shown in *Table 2.1*. Strains were routinely cultured in lysogeny broth (LB) (Formedium) with vigorous aeration at 37°C overnight. Where necessary, cultures were supplemented with: 50 µg mL⁻¹ carbenicillin (to maintain pSB1057 in the *N*-(3-Oxododecanoyl)-L-homoserine lactone OdDHL biosensor strain and pET23Lys in lysostaphin expression strain); 10 µg mL⁻¹ tetracycline (to maintain pSB536 in the *N*-butanoyl-L-homoserine lactone BHL biosensor strain) or 20 µg mL⁻¹ tetracycline (to select for transposon-containing mutants in QS-associated genes obtained from the *Pseudomonas aeruginosa* PAO1 mutant library).

Candida albicans SC5314 was obtained from Prof. Andres Floto, Laboratory of Molecular Biology (Cambridge). *Escherichia coli* DH5α(pET23Lys) for the inducible expression and purification of recombinant lysostaphin was obtained from Dr Christopher Randall, University of Leeds.

2.2 Growth media and solutions

Unless otherwise stated, artificial sputum medium (ASM) was the growth medium employed in all experiments. To reduce media costs ASM was made using a modified version of the recipe published by Turner *et al.* (2015). Briefly, bovine maxillary mucin (£304 g⁻¹, Sigma) was replaced with 1.25 g L⁻¹ porcine stomach mucin type-II (£0.95 g⁻¹, Sigma) and salmon sperm DNA (£102 g⁻¹, Sigma) was replaced with 1.25 g L⁻¹ fish sperm DNA (£1.98 g⁻¹, Sigma) as described by Kirchner *et al.* (2012). A detailed protocol for preparing ASM can be found in *Appendix 2.1*.

All other growth media and solutions used within the current work are listed in *Table 2.2*.

Strain	Description	Reference
PAO1	<i>Pseudomonas aeruginosa</i> , spontaneous chloramphenicol-resistant derivative. Used worldwide as a laboratory reference strain (isolated Melbourne, 1954)	(Holloway, 1955)
ATCC 25923	<i>Staphylococcus aureus</i> Rosenbach (ATCC®25923D-5™), methicillin sensitive clinical isolate. Laboratory reference strain lacking recombinases and <i>mecA</i> (isolated Seattle, 1945)	(Treangen et al., 2014)
SC5314	<i>Candida albicans</i> , clinical isolate commonly used as a wild-type laboratory reference strain (isolated New York, 1980's)	(Gillum et al., 1984)
PAO1 $\Delta pqsA$ CTX- <i>lux::pqsA</i>	PQS biosensor strain. $\Delta pqsA$ mutant of PAO1 containing a <i>pqsA</i> promoter :: <i>luxCDABE</i> fusion integrated at a neutral site in the chromosome	(Fletcher et al., 2007)
JM109 (pSB1057)	OdDHL biosensor strain. <i>Escherichia coli</i> JM109 containing pSB1057	(Winson et al., 1998)
JM109 (pSB536)	BHL biosensor strain. <i>Escherichia coli</i> JM109 containing pSB536	(Winson et al., 1998)
DH5 α (pET23Lys)	<i>Escherichia coli</i> transformation strain containing pET23Lys, encoding lysostaphin gene from <i>Staphylococcus simulans</i> cloned into pET23B+ expression system for the overproduction of recombinant his-tagged lysostaphin	(Szweda et al., 2005)
Rosetta™ DE3 Competent Cells	<i>E. coli</i> BL21 <i>lacZY</i> derivatives optimized for the production of proteins from target genes cloned into pET vectors. Also encodes a T7 lysozyme to suppress basal expression of T7 RNA polymerase	Novagen
DE3(pET23Lys)	<i>E. coli</i> DE3 transformed with pET23Lys plasmid. Allows inducible production of His ₆ -tagged lysostaphin for 'in house' purification	Current work

Table 2.1 Microbial strains used in this study.

Media/ Solution	Composition (per litre unless otherwise stated)
Growth media	
Lysogeny Broth (LB)	20 g LB-broth Lennox (Formedium)
LB-agar	As for LB but with 15 g Bacto Agar
2xYT Broth	16 g Tryptone (Duchefa Biochemie) 10 g Yeast extract (Duchefa Biochemie) 5 g Sodium chloride (Fisher Scientific) pH 7.0
Pseudomonas Isolation Agar (PIA)	48.4 g Dehydrated pseudomonas isolation agar powder (Oxoid) 10 mL glycerol (Acros Organics) 200 mg Cetrimide (Sigma) 15 mg Sodium nalidixate (Alfa Aesar) [Final concentration (g L ⁻¹): bacto agar (11), peptone (16), casein hydrolysate (10) magnesium chloride (1.4), potassium sulfate (10), glycerol (1% v/v), cetrimide (0.2), sodium nalidixate (0.015). pH 7.1]
Mannitol Salt Agar (MSA, also known as Chapman's medium)	111 g Dehydrated mannitol salt agar powder (Oxoid) [Final concentration (g L ⁻¹): bacto agar (15), peptone (10), beef extract (1), sodium chloride (75), mannitol (10), phenol red (0.025). pH 7.4]
BiGGY agar (BiGGY-A, also known as Nickerson's medium)	45 g Dehydrated BiGGY agar powder (Oxoid) [Final concentration (g L ⁻¹): bacto agar (16), bismuth ammonium citrate (5), dextrose (10), glycine (10), sodium sulfite (3), yeast extract (1). pH 6.8] <i>N.B: media is not autoclaved, but boiled gently for 1 minute before pouring</i>
Glycerol stocks	700 µL overnight culture 300 µL 50% glycerol
PBS	10 x Phosphate Buffered Saline tablets (Oxoid)

	[Final concentration (g L ⁻¹): sodium chloride (8), potassium chloride (0.2), di-sodium hydrogen phosphate (1.15), potassium dihydrogen phosphate (0.2). pH 7.3]
Antibiotics	
Carbenicillin stock solution	20 mg mL ⁻¹ carbenicillin disodium salt (Melford) in ddH ₂ O. Filter sterilised through 0.22 µm membrane and stored at -20°C until use.
Chloramphenicol stock solution	20 mg mL ⁻¹ chloramphenicol (Sigma) in 95% ethanol. Stored at -20°C until use
Ciprofloxacin stock solution	20 mg mL ⁻¹ ciprofloxacin (Sigma) in 0.1 M HCl. Made fresh prior to each experiment.
Colistin stock solution	10 mg mL ⁻¹ colistin sulfate salt (Sigma) in ddH ₂ O and filter sterilised. Made fresh prior to each experiment.
Fluconazole stock solution	15 mg mL ⁻¹ fluconazole (Sigma) in 95% ethanol. Made fresh prior to each experiment.
Fusidic acid stock solution	10 mg mL ⁻¹ fusidic acid sodium salt (Sigma) in 95% ethanol. Made fresh prior to each experiment.
Gentamicin stock solution	20 mg mL ⁻¹ gentamicin sulfate (Melford) in ddH ₂ O. Stored at -20°C until use
Itraconazole stock solution	0.5 mg mL ⁻¹ itraconazole (Sigma) in dimethyl sulfoxide. Made fresh prior to each experiment
Rifampicin stock solution	20 mg mL ⁻¹ rifampicin (Sigma) in dimethyl sulfoxide. Made fresh prior to each experiment
Tetracycline stock solution	10 mg mL ⁻¹ tetracycline hydrochloride (Sigma) in ddH ₂ O. Stored at -20°C until use
Siderophore assays	
CAS stock solution	1.21 g L ⁻¹ Chrome azurol S (in ddH ₂ O)
Fe Stock Solution	1 mM FeCl ₃ (Sigma) 10 mM HCl
PIPES buffer	0.1 M PIPES (Sigma), pH 6.8
HDTMA solution	0.438 g hexadecyltrimethylammonium bromide ([CH ₃ (CH ₂) ₁₅](CH ₃) ₃ NBr, Acros Organics)
Shuttle solution	0.2 M 5-sulfosalicylic acid (Sigma)
CAS assay solution (100 mL)	50 mL HDTMA solution 1.5 mL Fe stock solution

	7.5 mL CAS stock solution 30 mL PIPES buffer (Store in dark above 25°C)
Quorum sensing molecules	
OdDHL stock solution	25 mM <i>N</i> -(3-Oxododecanoyl)-L-homoserine lactone (courtesy of David Spring, Dept. Chemistry, University of Cambridge) in DMSO
BHL stock solution	25 mM <i>N</i> -butanoyl-L-homoserine lactone (courtesy of David Spring, Dept. Chemistry, University of Cambridge) in DMSO
PQS stock solution	25 mM pseudomonas quinolone signal (2-heptyl-3-hydroxy-4-quinolone) (courtesy of David Spring, Dept. Chemistry, University Cambridge) in DMSO
Biofilm assays	
0.1% CV solution	1 g L ⁻¹ crystal violet (Sigma) in ddH ₂ O
30% Acetic acid	300 mL acetic acid (Sigma) 700 mL ddH ₂ O
XTT solution	4 mg 2,3-Bis-(2-Methoxy-4-Nitro-5-Sulfophenyl)-2H-Tetrazolium-5-Carboxanilide (Thermo Fisher) in 10 mL PBS. Solution filter sterilised (0.22 µm pore size) and stored in the dark at -80°C until use
Menadione solution	10 mM menadione sodium bisulfite (Sigma) in 100% acetone. Stored at -80°C until use
XTT-menadione solution	1 µL menadione solution 10 mL XTT solution (Use immediately)
DMEM/RPMI solution	500 mL Dulbecco's Modified Eagle Medium (DMEM, ThermoFisher) 500 mL Roswell Park Memorial Institute (RPMI) 1640 medium (ThermoFisher) 50 µg mL ⁻¹ ampicillin (Melford)
Protein purification	
Lysis buffer	50 mM Sodium dihydrogen phosphate (Fisher Scientific) 300 mM Sodium chloride 10 mM Imidazole (Sigma)

	pH 8.0 and stored at 4°C
Wash/ equilibration buffer	50 mM Sodium dihydrogen phosphate 300 mM Sodium chloride 20 mM Imidazole pH 8.0 and stored at 4°C
Elution buffer	50 mM Sodium dihydrogen phosphate 300 mM Sodium chloride 250 mM Imidazole pH 8.0 and stored at 4°C
Dialysis buffer	20 mM Tris-HCl (Sigma) (pH 7.5) 500 mM Sodium chloride
Sputum Sample Processing	
0.85% Saline solution	8.5 g L ⁻¹ Sodium chloride in ddH ₂ O
Sputasol	6.5 mM Dithiothreitol (DTT, Sigma) 128.3 mM Sodium chloride 2.7 mM Potassium chloride (Sigma) 7.9 mM Sodium dihydrogen phosphate 1.5 mM Potassium dihydrogen phosphate (Fisher Scientific) Filter sterilised (0.22 µm pore size) and stored at 4°C for up to one week.
SDS-PAGE	
1 x SDS running buffer	2.5 mM Tris base (Sigma) (pH 8.3) 19.2 mM glycine (Melford) 0.01% sodium dodecyl sulfate (SDS, Sigma)
Resolving gel (8%) (10 mL total)	4.7 mL ddH ₂ O 2.7 mL acrylamide (30%) 2.5 mL 1.5 M tris (pH 8.8) 50 µL SDS (20%) 100 µL ammonium persulfate (10%) 100 µL TEMED
Stacking gel (6%) (10 mL total)	2.7 mL ddH ₂ O 0.8 mL acrylamide (30%) 0.5 mL 1 M tris (pH 6.8) 20 µL SDS (20%) 40 µL Ammonium persulfate (10%)

	4 μ L TEMED
5 x Sample buffer	10% w/v SDS 0.2 M Tris-HCl (pH 6.) 20% Glycerol 10 mM β -mercaptoethanol 0.01% Bromophenol blue
Coomassie staining solution	45.4% methanol 4.6% acetic acid 0.1 % Coomassie Brilliant Blue R-250 (ThermoFisher)
Destaining solution	5% Methanol 7.5% Acetic acid

Table 2.2. Growth media and solutions.

List of all growth media and solutions used in the described experiments are listed in the table, apart from the formulation for ASM which can be found in *Appendix 2.1*.

2.3 Growth conditions

2.3.1 Continuous-flow culture model

A schematic diagram of the continuous-flow culture system is shown in *Figure 2.1*. The culture vessel consists of a 100 mL flask (Duran), fitted with an assembled 4-port HPLC GL80 screw cap (Duran). A 24-channel IPC ISM934C standard-speed digital peristaltic pump (Ismatec) was used to deliver sterile ASM from a media reservoir at a defined flowrate (Q) through 1.5 mm bore sterilin silicon tubing (Fisher Scientific) to the culture vessel. A different channel of the same pump was used to remove waste culture into a discard jar at the same flowrate. The entire culture system was maintained at 37°C and contents of the culture vessel kept homogenous *via* stirring (100 rpm) using a magnetic stir bar.

Overnight cultures were washed three times in PBS prior to inoculating the culture vessel. Pre-warmed ASM (100 mL) in the culture vessel was inoculated with the required combination of microbial species. Each species was introduced into the culture vessel to achieve a starting optical density (600 nm, $OD_{600\text{ nm}}$) of 0.05. The vessel was incubated for three hours prior to starting the flow of medium. For mono-species and co-culture experiments not containing CA, the $Q = 170\text{ }\mu\text{L min}^{-1}$. For co-culture experiments including CA, Q was decreased to $145\text{ }\mu\text{L min}^{-1}$. For all continuous-flow experiments, samples (1 mL volume) for cell enumeration and optical density measurements were withdrawn using a syringe fitted with a sterile 19-gauge needle (Terumo) inserted through the rubber septa in the HPLC ports.

When necessary, $OD_{600\text{ nm}}$ of a culture vessel was monitored by passing the removed waste culture through an in-line 6715 UV series spectrophotometer (Jenway) fitted with a continuous-flow cuvette, as demonstrated in *Figure 2.2*. When taking continuous $OD_{600\text{ nm}}$ measurements a bubble trap (obtained from Janus A. Haagensen, Biocentrum-DTU, Technical University of Denmark) was fitted before the spectrophotometer. Prior to inoculation, the model was primed by pumping sterile ASM from the media reservoir throughout the entire system to purge any air bubbles that might interfere with $OD_{600\text{ nm}}$ measurements.

As a 24-channel peristaltic pump was used to provide a continuous flowrate and each culture vessel has one input and one outlet line, the model can easily be multiplexed to study up to 12 different culture vessels in tandem. *Figure 2.3* demonstrates a representative image of five culture vessels grown concurrently on an 85 mm MULTISTIRRER6 multi-position magnetic stirrer (Velp Scientific). When measuring the optical density of multiple culture vessels, samples were removed from the HPLC ports (as described above) and $OD_{600\text{ nm}}$ measured using a BioSpectrometer Kinetic spectrophotometer (Eppendorf).

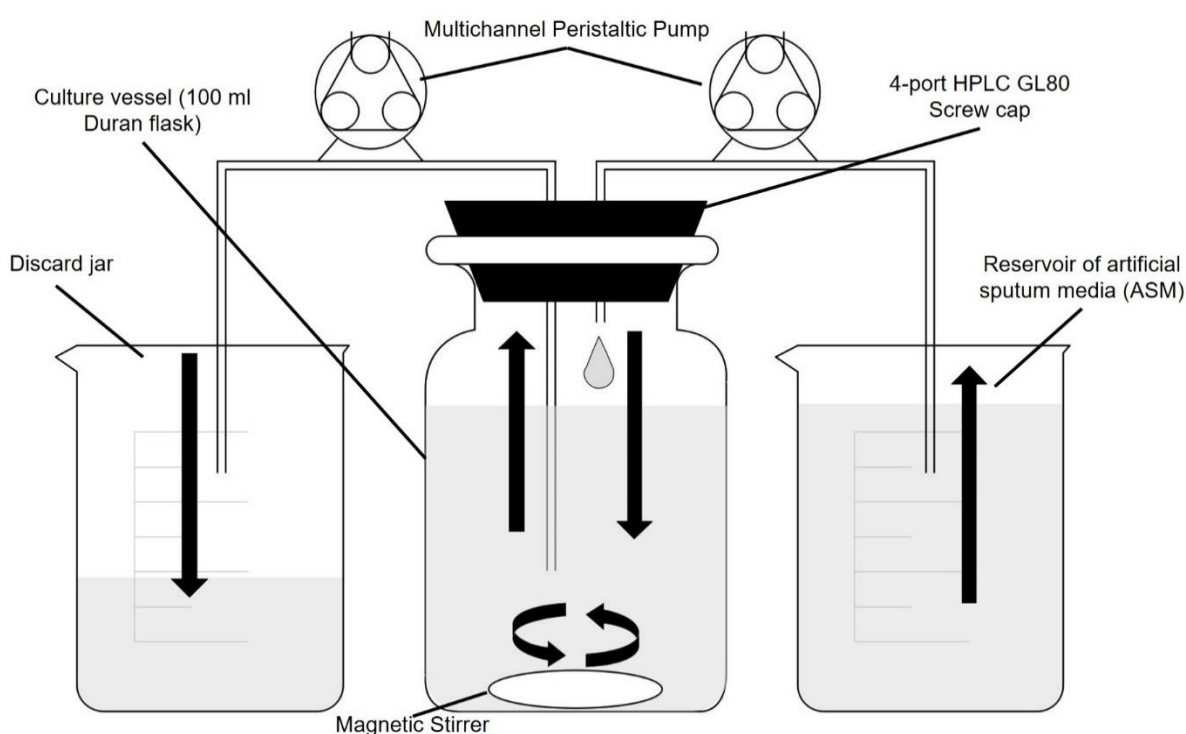


Figure 2.1 Schematic diagram of the *in vitro* continuous-flow culture system used in this study.

The main culture vessel (centre) is a 100 mL Duran bottle fitted with a 4-port HPLC GL80 screwcap lid, containing 4 sealable inlet/outlet ports. A multichannel peristaltic pump delivers fresh media (ASM) into the culture vessel from a reservoir, and also removes waste culture at the same rate of flow (Q). Arrows show the direction of flow. The culture vessel and media reservoirs are incubated at 37°C and the contents are kept homogenous through gentle stirring (100 rpm). If required, a bubble trap and in-line spectrophotometer fitted with a continuous-flow cuvette can be included in the setup prior to the discard jar (see *Figure 2.2*). The value for Q depends on the microbial species being cultured within the vessel.

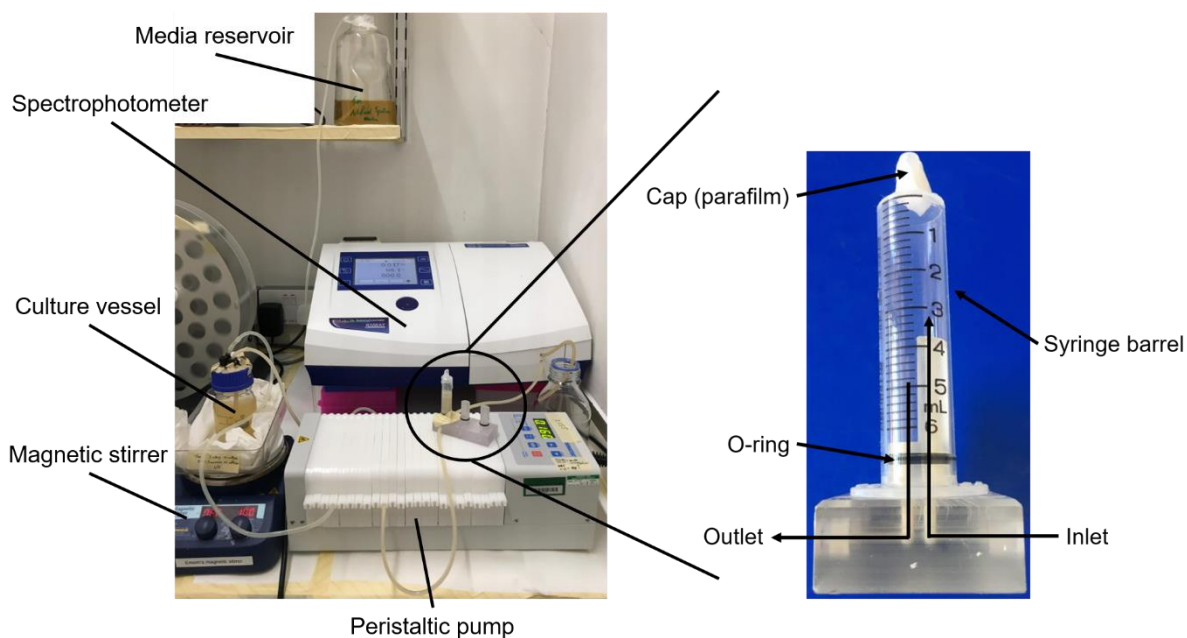


Figure 2.2 Model with in-line spectrophotometer and bubble trap.

A representative image of the continuous-flow model set up with an in-line spectrophotometer to take automated optical density (600 nm) measurements of the culture vessel. A bubble trap (right image) is included prior to the spectrophotometer to prevent bubbles from interfering with $OD_{600\text{ nm}}$ readings. The bubble trap is custom made from polycarbonate and has been constructed to fit a standard 5 ml syringe barre, with the O-ring providing an airtight seal for the system. The tip of the syringe is covered with either a syringe cap or parafilm. Prior to microbial inoculation, the entire culture system is filled with medium to purge air from the bubble trap. If any bubbles do enter the system, they rise to the top of the syringe barrel. As the outlet is lower than the inlet, air will not enter the system passed the trap.

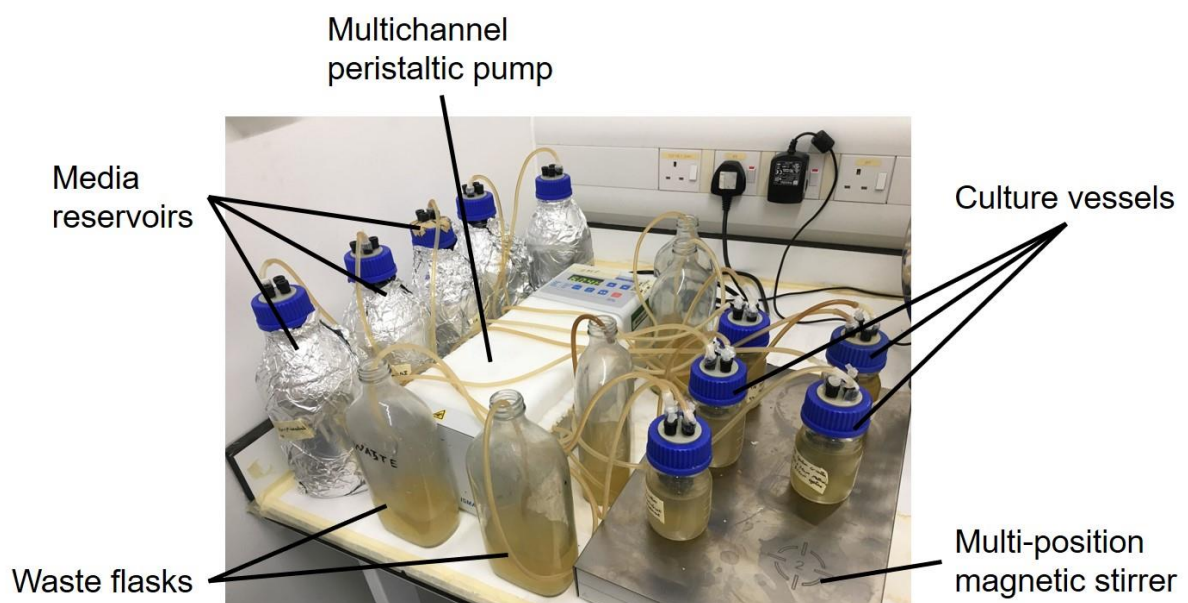


Figure 2.3 Multiplexing of continuous-flow model.

Representative image of the continuous-flow model multiplexed to study five separate culture vessels in tandem. A 24-channel peristaltic pump delivers fresh ASM from the media reservoirs (wrapped in aluminium foil, left side of image) to the culture vessels (right side of image) and removes waste culture at the same rate of flow to the discard jars (front of image). Culture vessel contents are kept homogenous *via* stirring (100 rpm) on a multi-position magnetic stirrer (Velp Scientific).

2.3.2 Batch culture conditions

For aerobic batch cultures, 250 mL Erlenmeyer flasks containing 100 mL pre-warmed ASM were inoculated with the indicated strain (washed three times in PBS, as in *Section 2.3.1*) to a starting OD_{600 nm} of 0.05. Flasks were incubated at 37°C in a water bath with 180 rpm shaking. Stirred batch cultures were set up as described for the continuous-flow experiments (*Section 2.3.1*), except $Q = 0 \mu\text{L min}^{-1}$. Samples (1 mL) were aseptically removed from the batch cultures for measurement of OD_{600 nm} (as described above) and viable cell counting (*Section 2.5*).

2.4 Calibration of flowrates

Prior to growing any microbial strains, the speed of the multichannel peristaltic pump was calibrated and Q within the culture vessel determined experimentally using *Equation 2.1*.

$$Q = \frac{V}{R_t}$$

Equation 2.1 Calculation of flowrate.

Q = flowrate, V = volume of culture vessel and R_t = residency time.

The volume (V) of the culture vessel (100 mL) is constant for all experiments. To determine residency time (R_t) the model was set up to include an in-line spectrophotometer (*Section 2.3.1*). ASM within the media reservoir was stained with Coomassie Brilliant Blue R-250 (ThermoFisher) to a final absorbance (465 nm) of 1.0. Displacement of unstained media within the culture vessel was followed by measuring Abs_{465 nm} every 5 min, with R_t taken as the time at which Abs_{465 nm} reaches an asymptote of 1.0.

Figure 2.4 demonstrates a representative example of how Q was determined for continuous-flow experiments using mono-species PA cultures and PA-SA co-cultures. The function for the non-linear regression model of this displacement curve is displayed on the figure. When solving with $y = 1.0$, R_t is determined to be 589 min, therefore $Q = 170 \mu\text{L min}^{-1}$.

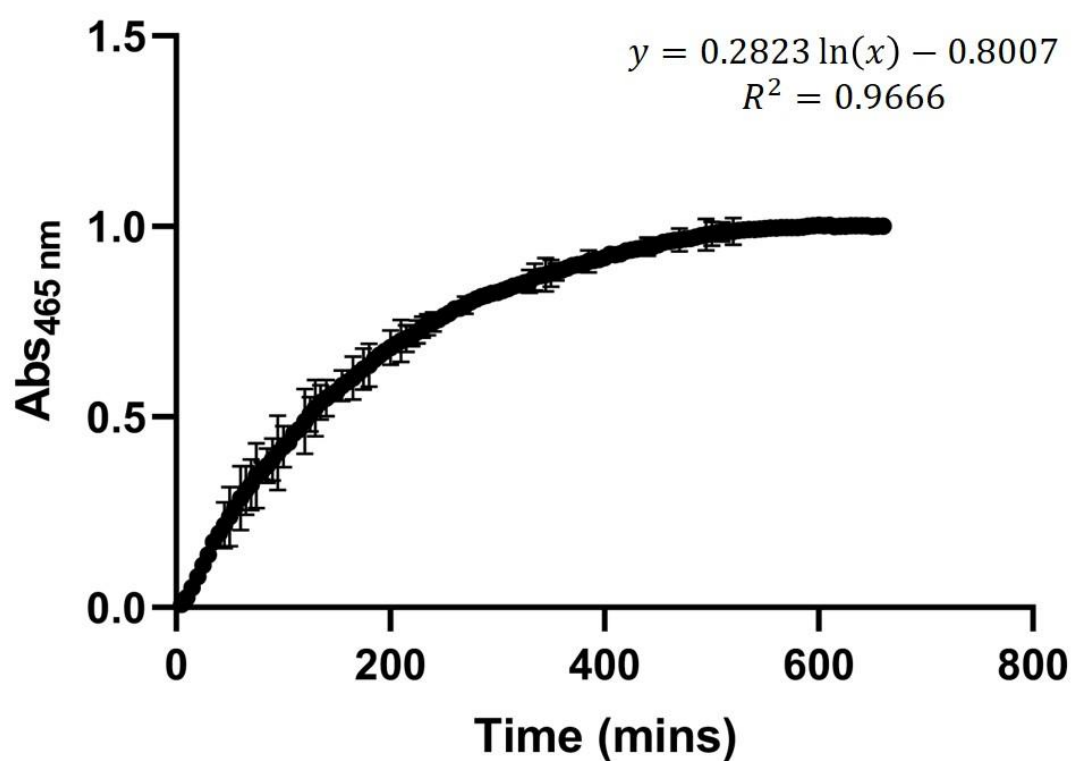


Figure 2.4 Determination of flow rate within culture vessel.

Representative displacement curve within the culture vessel (100 mL) when flow rate (Q) = $170 \mu\text{L min}^{-1}$. Absorbance (465 nm) of vessel contents was measured every 5 min using an in-line spectrophotometer and continuous-flow cuvette. Unstained ASM was displaced by media stained with Coomassie Brilliant Blue ($\text{Abs}_{465 \text{ nm}} 1.0$) from the reservoir tank. Data represented as the mean \pm standard deviation from three independent experiments, fitted with a non-linear regression model. Function of the curve and R^2 values are displayed and the residency time (R_t) is calculated as the value for x when $y = 1.0$.

2.5 CFU mL⁻¹ Enumeration

Colony forming units (CFU) per mL of culture were determined using the single plate-serial dilution spotting method, as described previously (Thomas et al., 2015). Serial dilutions were made in sterile PBS and 20 μ L of each dilution was spotted onto the appropriate selective agar. PA was isolated on pseudomonas isolation agar (PIA, Oxoid), SA was isolated on mannitol salt agar (MSA, Oxoid) and CA was isolated on BiGGY agar (Oxoid). During co-culture experiments involving CA, the agar plates used to isolate PA and SA were further supplemented with 5 μ g mL⁻¹ itraconazole to inhibit the growth of CA. All plates were incubated at 37°C. PIA and MSA plates were incubated overnight (16 hr) and BiGGY agar plates were incubated for 24 hr. CFU mL⁻¹ counts are averages taken from three technical repeats.

Axenic overnight cultures of PA, SA and CA were routinely grown and plated out for CFU mL⁻¹ enumeration on non-selective (LB-agar) and the appropriate selective agar. There was no significant difference between total CFU mL⁻¹ counts of microbial cultures between the selective and non-selective agar (*Figure 2.5*).

2.6 Quantitative real-time PCR (RT-PCR)

2.6.1 RNA extraction

Single species cultures of PA were grown in ASM under continuous-flow and batch culture conditions, as described in *Sections 2.3.1* and *2.3.2* respectively. Cells were harvested by removing 2 mL of the culture on ice, pelleting *via* centrifugation (13,000 x *g*, 1 min, 4°C) and immediately resuspending the pellet in 750 μ L of RNeasy Lysis Buffer (Qiagen). Culture/RNeasy Lysis Buffer mixtures were incubated at 4°C overnight and stored at -80°C until use.

Before extraction, samples were thawed on ice. Cells in the culture/RNeasy Lysis Buffer solution were sedimented by centrifugation (13,000 x *g*, 5 min, 4°C) and the supernatant carefully removed. Cells were resuspended in 1 mg mL⁻¹ lysozyme (Sigma) in DEPEC-treated water (Ambion) and incubated for 10 min at room temp with 50 rpm shaking. RNA was extracted using RNeasy Plus Mini Kit (Qiagen) following the manufacturers bacterial extraction protocol. RNA was eluted in 30 μ L DEPEC-treated water and stored at -80°C. RNA concentration was quantified using a Nanodrop ND-1000 Spectrophotometer (Labtech International), with an A260/A280 ratio of >1.8 and an A260/230 ratio of >2.0 considered acceptable purity. Final concentrations of RNA were between 1.1 and 2.4 mg mL⁻¹.

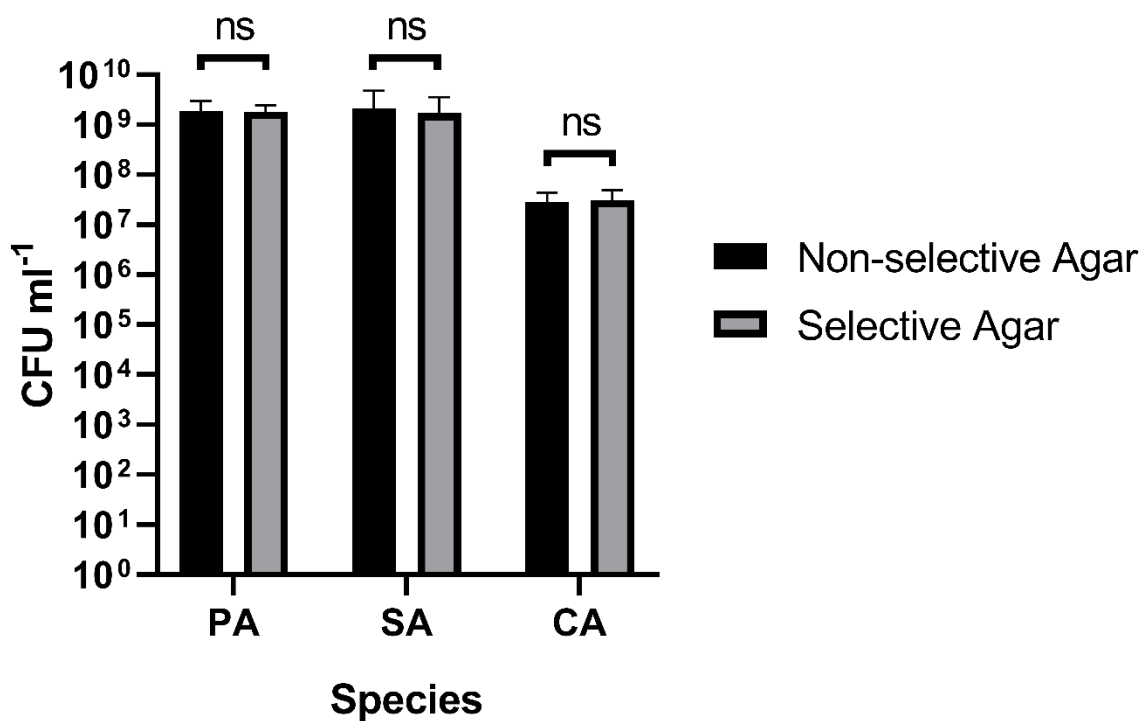


Figure 2.5 Comparison of total CFU mL⁻¹ counts between selective and non-selective agar.

Viable cell counts (CFU mL⁻¹) of overnight single-species cultures of *P. aeruginosa* PAO1 (PA), *S. aureus* 25923 (SA) and *C. albicans* SC5314 (CA) on non-selective (black bars) and selective (grey bars) agar plates. Data represented as mean \pm standard deviation from three independent experiments. $P > 0.05$ is considered not significantly different (ns).

2.6.3 cDNA synthesis

The cDNA synthesis was performed using a single step reaction using High-Capacity cDNA Reverse Transcription Kit (ThermoFisher) within a thermocycler and. The reaction mixture and cycling conditions for cDNA synthesis are shown in *Table 2.3*. RNA was removed by adding NaOH (20 μ L, 1 M) to each sample, incubating at 65°C for 30 min then cooling to 4°C and neutralising with HCl (20 μ L, 1 M). cDNA was purified using GeneJET PCR Purification Kit (ThermoFisher) following the manufacturer's instructions. Samples were stored at -20°C until use.

As a control cDNA samples and purified RNA (from *Section 2.6.2*) were used as templates for the amplification of the 16S rRNA housekeeping gene encoding for the 30S subunit (Clarridge, 2004, Kolbert and Persing, 1999, Woese, 1987) using the protocol described in detail within *Section 2.14.4*. A clear, single band corresponding to the correct size (1500 bp) of the 16S rRNA gene can be seen in the reactions using synthesised cDNA and genomic DNA (positive control) as templates only. As RNA cannot be amplified by Taq polymerase, no bands can be observed in the reaction utilising RNA as the template, indicating no DNA contamination of the RNA samples (*Figure 2.6*).

2.6.4 RT-PCR primer design

To determine the metabolic state of cells harvested in *Section 2.6.1*, four stationary phase-specific and four exponential-phase specific PA genes were selected from a previously published transcriptomic dataset (Mikkelsen et al., 2007). Primer-BLAST software (NCBI, www.ncbi.nlm.nih.gov/tools/primer-blast/) was used to identify suitable primer pairs with an approximate T_m of 58°C and yielding an amplicon product of 150 bp, compatible with SYBR Green RT-PCR conditions (*Table 2.4*). A validated primer pair for RT-PCR amplification of the PA 16S rRNA housekeeping gene was obtained from Dr. Shunsuke Numata (University of Cambridge, personal communication) and are included at the bottom of *Table 2.4*.

2.6.4 RT-PCR

RT-PCR amplification was carried out in MicroAmp Optical 96-well Reaction Plates (Applied Biosystems) sealed with MicroAmp Optical Adhesive Film (Applied Biosystems) using a 7300 Real-Time PCR System (Applied Biosystems). Reactions were carried out in 20 μ L total volumes, using Universal PowerUp SYBR Green Master Mix (Applied Biosystems), following the manufacturer's instructions and using ROX as a passive reference dye. The reaction

Reaction mixture		
Component	Volume/amount	Final concentration
Total RNA	10 µg	0.5 µg µL ⁻¹
10 x RT Buffer	2 µL	-
dNTP mix (100 mM)	0.8 µL	4 mM
MultiScribe Reverse Transcriptase	1 µL	2.5 U µL ⁻¹
Nuclease-free H ₂ O	3.2 µL	-
Total reaction volume	20 µL	
Thermocycler conditions		
Step	Temperature (°C)	Time (min)
1	25	10
2	37	120
3	85	5
4	4	∞

Table 2.3. Synthesis of cDNA.

Reaction mixture and thermocycling conditions for cDNA synthesis from purified RNA using High-Capacity cDNA Reverse Transcription Kit.

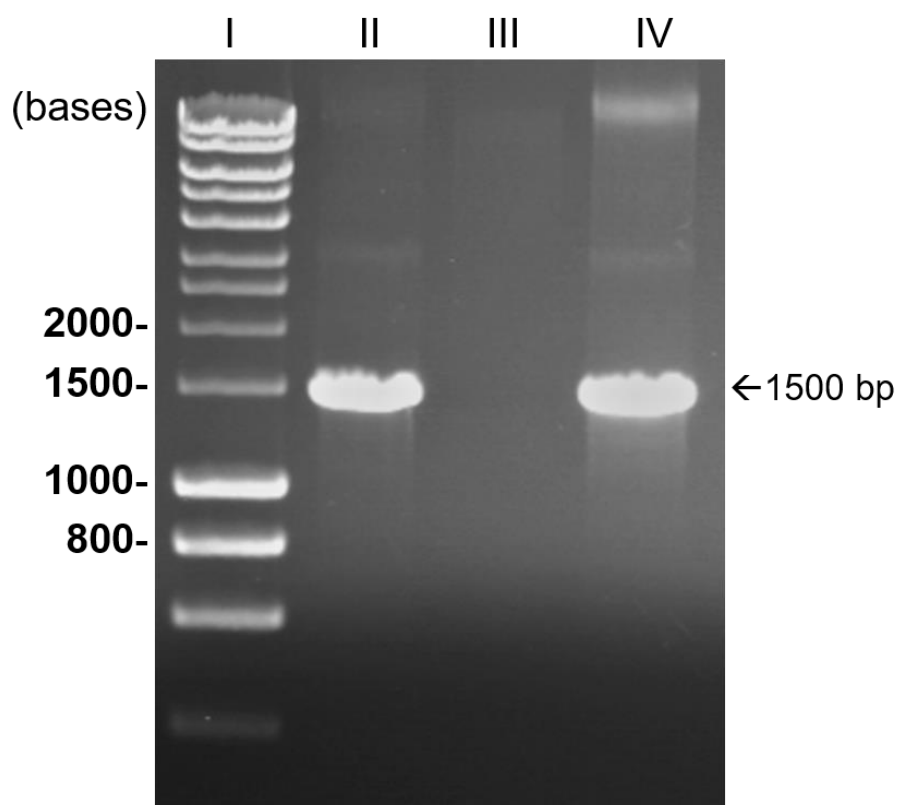


Figure 2.6 RNA and cDNA synthesis quality control.

PCR amplification of the 16S ribosomal RNA housekeeping using the conditions described in *Section 2.14.4*. Lane I: Hyperladder 1 kb DNA marker (Bioline). Lane II: PCR amplification using synthesised cDNA as the template. Lane III: PCR amplification using extracted RNA as the template. Lane IV: PCR amplification using PAO1 genomic DNA as the template (positive control). Bright bands of approximately 1500 bp, corresponding to the size of the 16S rRNA gene, can be seen for the positive control (lane IV) and when using cDNA as the template (lane II) indicating successful cDNA synthesis. The absence of a band in lane III indicates that extracted RNA does not contain any contaminating DNA.

Name	Target Gene	5' - 3' Sequence	Growth Phase
rpsM-F	<i>rpsM</i>	CGTCGCGAAATCAACATGAAC	<i>E</i>
rpsM-R		TTACTTGCGGATCGGCTTAC	
rplM-F	<i>rplM</i>	TACCACCACTCCGGCTTC	<i>E</i>
rplM-R		CACCTTCAGCTTGCGATACA	
rpoA-F	<i>rpoA</i>	GCACCGAAGTGGAAGTGTG	<i>E</i>
rpoA-R		CAGTGGCCTTGTCGTCTTTC	
sodB-F	<i>sodB</i>	AACACCTACGTGGTGAACCT	<i>E</i>
sodB-R		GCTCAGGCAGTTCCAGTAGA	
rmf-F	<i>rmf</i>	ACGGCATAACCGGTAAATCTC	<i>S</i>
rmf-R		GCTGGAGTTGATTGAGACGTT	
rsmA-F	<i>rsmA</i>	CCCTGATGGTAGGTGACGAC	<i>S</i>
rsmA-R		GGTTTGGCTCTTGATCTTTCTCT	
rpoS-F	<i>rpoS</i>	AAGCTCGACCACGAACCTT	<i>S</i>
rpoS-R		CGTATCCAGCAGGGTCTTGT	
sodM-F	<i>sodM</i>	CTTCGAGGCGTTCAAGGATG	<i>S</i>
sodM-R		ATCGGCGTATTGCCGTTC	
F-16SrRNA-Pa-RT	16S <i>rRNA</i>	ACACTGGAAGTGAAGACACG	<i>C</i>
R-16SrRNA-Pa-RT		AGACCTTCTTCACACACG	

Table 2.4 Primer pairs for RT-PCR analysis of metabolic state of axenic PA cultures.

Forward and reverse primers for a specific target gene are denoted by '-F' or '-R' respectively and growth phase indicates at what point within a typical growth curves these genes are expressed: (E) exponential phase, (S) stationary phase and (C) constitutively expressed.

Reaction mixture		
Component	Volume	Final Concentration
2 x PowerUp SYBR Green Master mix	10 μ L	
Forward Primer	1 μ L	2.5 nM
Reverse Primer	1 μ L	2.5 nM
cDNA Template	0.4 μ L	10 ng μ L ⁻¹
Nuclease-free water	7.6 μ L	
Thermocycler conditions		
Temperature (°C)	Time	No. Cycles
50	2 min	Hold
95	2 min	Hold
95	15 secs	40
60	2 min	
4	∞	Hold

Table 2.5 RT-PCR reaction mixture and conditions.

Reaction mixture (20 μ L total volume) and thermocycling conditions for RT-PCR of target genes using universal PowerUP SYBR Green Master Mix kit and a 7300 Real-Time PCR System.

mixture and cycle conditions used for all RT-PCR reactions is displayed in Table 2.5. RT-PCR of 16S rRNA housekeeping gene was performed for each cDNA sample tested on every 96-well reaction plate to normalise results (Section 2.6.5) and account for plate-to-plate variability between reactions. As a control, amplicon products were resolved on a 1.4% (w/v) agarose gel to check that a single band of approximately 150 bp in size was present, *Figure 2.7* shows a representative image of this.

2.6.5 Data analysis

Cycle threshold (C_t) values of cDNA samples obtained by RT-PCR were analysed through the comparative $\Delta\Delta C_t$ method (Giulietti et al., 2001). For each gene target, this method compares the C_t value of the test sample with the C_t value from a reference sample. In this work samples collected from the continuous-flow model (test sample) are compared with samples collected from batch culture (reference sample) at the same corresponding time points. For each target gene C_t values are normalised according to the C_t value of the constitutively expressed 16S rRNA housekeeping gene on the same reaction plate, as shown in *Equation 2.2*. Subsequently, the relative expression (RE) of normalised C_t values obtained from the continuous-flow test sample were compared with the corresponding C_t values obtained from the same target gene after the same length of incubation from the reference sample as shown in *Equation 2.3*.

$$\Delta C_t = C_t(\text{target gene}) - C_t(\text{housekeeping gene})$$

Equation 2.2. Normalisation of C_t values.

Where $C_t(\text{target gene})$ is the cycle threshold value for the gene of interest and $C_t(\text{housekeeping gene})$ is the cycle threshold value for the 16S rRNA housekeeping gene from the same RT-PCR reaction. ΔC_t is the normalised cycle threshold value for the gene of interest.

$$RE = 2^{-\Delta\Delta C_t} [\text{where } \Delta\Delta C_t = \Delta C_t(\text{test sample}) - \Delta C_t(\text{reference sample})]$$

Equation 2.3 Calculation of relative gene expression from normalised C_t values.

Where RE indicates relative gene expression, $\Delta C_t(\text{test sample})$ indicates normalised C_t value of the target gene from the continuous-flow model and $\Delta C_t(\text{reference sample})$ indicates normalised C_t value of the same target gene from the batch culture sample. Normalised C_t values are calculated using *Equation 2.2*.

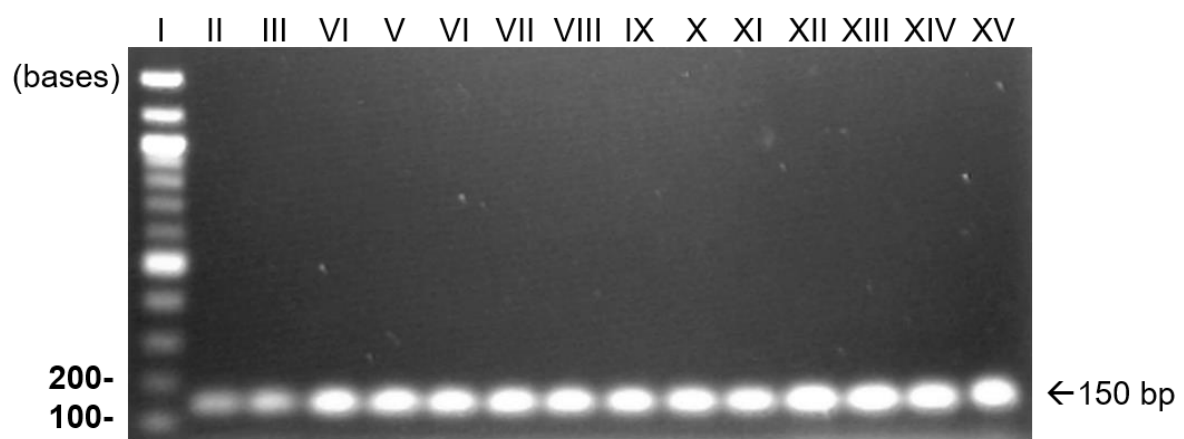


Figure 2.7 RT-PCR amplification products.

Representative image demonstrating amplification products from RT-PCR reactions, described in *Section 2.6.4*, resolved on a 1.4% w/v agarose gel. Lane I: Quick-load 100 bp DNA ladder (NEB). Lanes II – XV: RT-PCR amplification products. A single clear band of approximately 150 bp, corresponding to the predicted size of all RT-PCR products in this study, can be observed in every lane demonstrating that the reaction was successful and specific for the targeted gene of interest in each reaction.

2.7.1 Determination of mutation rates

The rate of mutation (μ) for single-species and co-cultures of PA and SA was inferred experimentally under batch culture and continuous-flow conditions. The emergence of spontaneous ciprofloxacin resistant (cip^r) or rifampicin resistant (rif^r) isolates within a population was used as a proxy to measure mutant accumulation (m) under the different experimental conditions. Then μ was calculated using the methods reviewed by Foster (2006).

In order to identify the emergence of cip^r and rif^r isolates, the minimum inhibitory concentration (MIC) of ciprofloxacin and rifampicin to inhibit the growth of PA and SA on PIA and MSA selective plates was determined. Overnight bacterial cultures were struck out onto selective plates supplemented with antimicrobials at a range of concentrations and the MIC was determined as the lowest concentration sufficient to inhibit the growth of single colonies (data not shown). Based on these data, in the subsequent mutation rate experiments, PIA plates were supplemented with 60 $\mu\text{g mL}^{-1}$ rifampicin or 0.12 $\mu\text{g mL}^{-1}$ ciprofloxacin and MSA plates were supplemented with 0.05 $\mu\text{g mL}^{-1}$ rifampicin or 0.6 $\mu\text{g mL}^{-1}$ ciprofloxacin.

2.7.2 Continuous-flow mutation rates

Mutation rates within a continuous-flow model can be determined by measuring mutant accumulation (Kubitschek and Gustafson, 1964, Novick and Szilard, 1950). As the population within the culture vessel is continually dividing (*Section 4.2*) μ can therefore be calculated using *Equation 2.4* (Drake, 1970).

$$\mu = \frac{1}{N\lambda} \frac{r_2 \text{ or } 3 - r_1}{t_2 \text{ or } 3 - t_1}$$

Equation 2.4 Calculation of mutation rates within a continuous-flow vessel.

Where μ indicates mutation rate (mutations per cell division), N is total cell count (CFU mL^{-1}) in the culture vessel, λ is the growth rate constant, r is the number of observed resistant isolates (CFU mL^{-1}) and t is time (hrs).

Initially, the growth rate constant (λ) associated with the exponential growth of PA or SA during mono-species or dual-species growth was determined. A stirred batch culture was inoculated and incubated as described in *Section 2.3.2*, and samples were removed hourly for CFU mL^{-1} enumeration and values for λ determined from the resulting growth curve.

Fresh bacterial cultures were inoculated into the continuous-flow culture vessel and incubated as described in *Section 2.3.1*. Total cell counts (N) for each culture condition were taken as an average of CFU mL⁻¹ counts onto selective plates without antibiotics every 24 hrs. The value for N did not change appreciably after 24 hrs of incubation (*Section 3*). The number of spontaneous antibiotic-resistant mutants (r) were measured by plating 15 x 100 µL culture aliquots onto selective agar plates supplemented with antibiotics (as described in *Section 2.7.1*) after 0, 24 and 96 hrs of incubation (t_1 , t_2 and t_3 respectively). Plates were incubated at 37°C for 24 hrs before counting, with one CFU assumed to be the progeny of a single resistant isolate.

2.7.2 Batch culture mutation rates

Mutation accumulation (m) within axenic and mixed microbial cultures under batch culture conditions were estimated experimentally using a modified version of the Luria-Delbrück fluctuation assay (Luria and Delbrück, 1943) and m calculated using the Jones median estimator, *Equation 2.5* (Jones et al., 1994). This method improves upon the original Lea-Coulson model which quantified the distribution of mutants within a bacterial population and identified this to be a Poisson distribution (Lea and Coulson, 1949). A value for μ can then be calculated using *Equation 2.6* (Armitage, 1952).

$$m = \frac{\left(\tilde{r}_{obs}/z\right) - \ln(2)}{\ln\left(\tilde{r}_{obs}/z\right) + \ln[\ln(2)]}$$

Equation 2.5 The Jones median estimator of mutation accumulation.

Where m is mutant accumulation, \tilde{r}_{obs} is median number of resistant isolates observed within a fluctuation assay and z is the dilution factor (fraction of the bacterial population plated within a fluctuation assay).

$$\mu = \frac{m \ln(2)}{N_t}$$

Equation 2.6 Calculation of mutation rate from estimates of mutant accumulation.

Where μ is mutation rate (mutations per cell division), m is mutation accumulation (calculated using *Equation 2.6*) and N_t is the final number of cells within a population.

To achieve precision whilst calculating m , fluctuation assays rely on mutant accumulation to be measured across a large number of parallel cultures (c) (Foster, 2006). Batch culture methods described in *Section 2.3.2* were not feasibly compatible with this approach and batch culture fluctuation assays were instead performed using a microtiter plate format. Overnight cultures were washed in PBS, then diluted to $OD_{600\text{ nm}} 0.05$ in fresh pre-warmed ASM. Normalised bacterial suspensions were used to inoculate 80 cultures in parallel (1 mL per well) within flat bottomed 24-well microtiter plates (Nunc). For mixed species cultures a 1:1 ratio of normalised cultures (500 μL of each) was inoculated within wells. Plates were sealed with Breathe-Easy gas permeable adhesive membranes (Sigma) and incubated for 24 hrs at 37°C with 100 rpm shaking. To ensure no cip^r or rif^r isolates were present within the starting cultures, aliquots (10 x 100 μL) were plated onto selective plates supplemented with antibiotics (as discussed in *Section 2.7.1*).

After incubation, $OD_{600\text{ nm}}$ of saturated cultures was measured using a FLUOstar Omega plate reader (BMG). Forty parallel cultures within $OD_{600\text{ nm}} 0.1$ of each other were chosen at random for plating ($c = 40$). If $c > 40$ there is little gain in precision when determining m (Jones et al., 1999, Rosche and Foster, 2000). Total cell number (N_t) within individual populations was determined by removing 100 μL of culture for CFU mL^{-1} enumeration and N_t was calculated as the average of CFU mL^{-1} counts across all parallel cultures. Variations in N_t between cultures selected for plating were not statistically significant (data not shown).

Cells in the remaining culture (900 μL) were sedimented by centrifugation (13,000 x g , 5 min, room temp) and pellets resuspended in 300 μL PBS. For single species cultures 3 x 100 μL aliquots were plated onto selective media supplemented with antibiotics and for co-cultures 3 x 50 μL aliquots were plated onto both types of selective media supplemented with antibiotics. Plates were incubated for 24 hrs and the total number cip^r and rif^r isolates (r) for each culture within a parallel series was calculated. Plates containing too many colonies to accurately count were truncated at 150 CFU mL^{-1} , previously reported to give little loss in precision (Asteris and Sarkar, 1996, Jones et al., 1999). The median number of resistant isolates across the 40 parallel cultures was taken as the value for \tilde{r}_{obs} . The dilution factor (z) is 0.9 and 0.45 for the single-species and co-culture fluctuation assays respectively, as 90% or 45% of the resuspended cell culture was plated onto each agar type to determine cip^r and rif^r .

2.8 Pyocyanin quantification

Pyocyanin quantification was performed following chloroform extraction of the pigment (Knight et al., 1979). Aliquots (10 mL volume) of culture were collected after 96 hrs growth and cells were pelleted by centrifugation ($4000 \times g$, 30 min, 4°C). The culture supernatants were filter sterilised ($0.22 \mu\text{m}$ pore size). Chloroform (4.5 mL) was added to 7.5 mL of the cell-free culture supernatant and the suspension was vigorously vortexed for 30 sec. The immiscible layers were separated by centrifugation ($4000 \times g$, 10 min, 4°C). An aliquot (3 mL volume) of the blue-green chloroform phase was removed and mixed with 1.5 mL 0.2 M HCl. The immiscible layers were then separated by further centrifugation and 1 mL of the rose-pink phase was transferred to a cuvette. Pyocyanin absorbance was measured at 520 nm using a BioSpectrometer Kinetic spectrophotometer (Eppendorf) and converted to concentration ($\mu\text{g mL}^{-1}$) by multiplying the $\text{Abs}_{520 \text{ nm}}$ value by 26.6.

2.9 Siderophore quantification

Siderophores in culture supernatants were quantified using the Chrome Azurol S (CAS) assay described by (Payne, 1994), with minor modifications to enable the assay to be performed in a 96 well microtiter plate format. Aliquots (1.5 mL volume) of culture supernatant were collected every 24 hrs throughout incubation and cells sedimented by centrifugation in a benchtop centrifuge ($15,000 \times g$, 5 min, 4°C). Supernatants were filter sterilised ($0.22 \mu\text{m}$ pore size), snap-frozen in liquid nitrogen and stored at -20°C . Samples were thawed on ice and 100 μL of supernatant was mixed with 100 μL CAS assay solution and 10 μL shuttle solution in a clear flat-bottomed 96-well plate (Nunc). Plates were incubated in the dark for 15 min at 30°C with 50 rpm shaking. Loss of blue colour was recorded by measuring $\text{Abs}_{630 \text{ nm}}$ in a FLUOstar Omega plate reader (BMG). For each set of samples, a medium only control was included for reference and a standard curve was constructed of deferoxamine mesylate salt (Sigma) dissolved in ASM. It should be noted that some culture supernatants (primarily batch culture supernatants) had to be diluted in ddH_2O so that the concentration of siderophores fell within the linear portion of the standard curve, this dilution factor was accounted for when normalising final concentrations.

2.10 QS signal molecule quantification

Aliquots (1.5 mL volume) of culture supernatant were collected every 24 hrs throughout incubation and cells sedimented by centrifugation in a benchtop centrifuge ($15,000 \times g$, 5 min, 20°C). Supernatants were then filter sterilised ($0.22 \mu\text{m}$ pore size), snap-frozen in liquid

nitrogen and stored at -20°C. OdDHL was detected using JM109(pSB1057). BHL was detected using JM109(pSB536). PQS was detected using PAO1 $\Delta pqsA$ CTX-*lux::pqsA*. Overnight starter cultures of the reporter strains were sub-cultured in LB supplemented with the appropriate antibiotics and grown to OD_{600 nm} = 1.0. Following this, aliquots (60 μ L volume) of the normalised cell culture were transferred to a sterile clear-bottomed black opaque 96-well plate (Greiner Bio-One) containing an equal volume of thawed culture supernatant. The plates were incubated at 30°C with shaking (100 rpm) for 3 hrs. Bioluminescence was recorded using a FLUOstar Omega plate reader (BMG). On each plate standard curves to calibrate the biosensor outputs were constructed using known concentrations of synthetic quorum sensing molecules dissolved in ASM. It should be noted that some culture supernatants (primarily batch culture supernatants) had to be diluted in ddH₂O so that the concentration of QS molecules fell within the linear portion of the standard curve, this dilution factor was accounted for when normalising final concentrations.

2.11 External perturbation of steady-state microbial populations

2.11.1 Introduction of PA to steady-state SA-CA co-cultures

Dual species co-cultures of *S. aureus* 25923 and *C. albicans* SC5314 were grown to a steady-state for 24 hrs under continuous-flow conditions (as described in *Section 2.3.1*). Routine overnight cultures of *P. aeruginosa* PAO1 were then washed three times in PBS and introduced into the culture vessel to final OD_{600 nm} 0.05, 0.1, 0.25 or 0.5. The culture vessel was then incubated under continuous-flow conditions, $Q = 145 \mu\text{L min}^{-1}$. Supernatant samples were aseptically removed from the culture vessel for OD_{600 nm} measurements or CFU enumeration as described in *Section 2.3.1* and *Section 2.5*, respectively.

2.11.2 Minimum inhibitory concentrations in ASM

Minimum inhibitory concentration (MIC) of colistin, fluconazole and fusidic acid against *P. aeruginosa* PAO1, *S. aureus* 25923 and *C. albicans* SC5314 in ASM were determined using the broth microdilution method described by the Clinical and Laboratory Standards Institute (CLSI, 2019). Briefly, stock solutions of the antimicrobials were freshly prepared prior to each experiment (*Table 2.2*). Serial 2-fold dilutions of the antimicrobials were prepared in fresh pre-warmed ASM in a 96-well microtiter plate (Nunc). Routine overnight cultures of the microbial strains were washed three times in sterile PBS and normalised cultures were inoculated into the wells to OD_{600 nm} 0.05 (final well volume 150 μ L). Plates were sealed with a gas permeable

Breathe-Easy membrane and incubated for 16 hrs at 37°C with 100 rpm shaking. The MIC was taken as the lowest antimicrobial concentration able to inhibit visible microbial growth.

2.11.3 Antimicrobial perturbation of steady-state cultures

Mono-species or triple-species cultures of *P. aeruginosa* PAO1, *S. aureus* 25923 and *C. albicans* SC5314 were grown to a steady-state for 24 hrs under continuous-flow conditions (as described in Section 2.3.1). Pre-established microbial cultures were then treated with the appropriate antimicrobial compound at a final concentration of 1 x, 2 x or 5 x MIC determined in Section 2.11.2 (Table 5.1). Cultures were incubated for 1 h under batch culture conditions, $Q = 0 \mu\text{L min}^{-1}$. An appropriate flowrate, $Q = 170 \mu\text{L min}^{-1}$ for PA and SA mono-species cultures and $Q = 145 \mu\text{L min}^{-1}$ for CA mono-species and triple-species cultures, was then applied to the culture vessel and the model incubated as standard for 48 hrs. Samples were aseptically removed from the culture vessel for OD_{600 nm} measurements and CFU enumeration as described in Section 2.3.1 and Section 2.5, respectively.

2.11.4 Antimicrobial susceptibility of isolates from perturbed steady-state communities

Four PA single colonies were randomly selected after 1, 8, 24 and 48 hrs incubation with different concentrations of colistin from PIA pates during CFU enumeration and four SA or CA isolates were randomly selected during CFU enumeration onto MSA or BiGGY-A plates after 3, 8, 24 and 48 hrs incubation with different concentrations of fusidic acid or fluconazole (as in Section 2.11.4). Isolates (48 of each species from mono-species cultures and 48 of each species from polymicrobial co-cultures) were routinely cultured in LB overnight and stored at -80°C. Strains were tested against increasing concentrations of colistin, fluconazole or fusidic acid in ASM in the 96-well microtiter plate format (as described in Section 2.11.2) and the MIC of each isolate was compared to that of the parental strain. Inhibition of growth was determined by eye and MICs were confirmed over three independent experiments using fresh ASM and antimicrobial stocks.

2.11.5 Whole genome sequencing

Eight PA isolates able to grow in the presence of 1 mg mL⁻¹ colistin were selected for whole genome sequencing (WGS) alongside the parental PAO1 strain. Two resistant isolates were selected from: the mono-species culture after 1 h exposure to 8 µg mL⁻¹ colistin (isolates A and B); the mono-species culture after 8 hrs exposure to colistin (isolates E and F); the polymicrobial co-culture after 1 h exposure to colistin (isolates C and D) and the polymicrobial

co-culture after 8 hrs exposure to colistin (isolates G and H). WGS of the isolates was performed by MicrobesNG (Birmingham, UK) using the Nextera XT library prep protocol v.05 (Illumina) on an Illumina MiSeq platform using 2 x 250 bp paired-end reads. The reads were adapter-trimmed using Trimmomatic v0.30 with a sliding window quality cut-off of Q15. Taxonomic classification of sequences and assessment of sequence contamination was performed using Kraken (Wood and Salzberg, 2014). The *de novo* assembly of contigs was performed using SPAdes v3.14.0 using the default parameter settings and the automated annotation of the resulting contigs was performed using Prokka v1.12. Variants were called using Snippy v2.5/Freebayes v0.9.21-7 (<https://github.com/tseemann/snippy>) with a minimum base quality of 20, read coverage of 10x and a 90% read concordance at a locus for a variant to be reported. Variants in the different isolates were compared against the progenitor strain (PAO1) to determine mutations arising during treatment with 8 $\mu\text{g mL}^{-1}$ colistin. Called variants were visually inspected by mapping the reads on the reference genome (accession number NC_002516) using the software Artemis (<http://sanger-pathogens.github.io/Artemis/Artemis/>).

2.12 Biofilm assays

The formation of single-species and polymicrobial biofilms within ASM over time under batch (Section 2.12.1) and continuous-flow (Sections 2.12.2 and 2.12.3) conditions was assayed using a range of methods. Crystal violet (CV) staining was used to quantify total biofilm biomass and the total metabolic activity and viability of biofilms was assayed using XTT (2,3-Bis-(2-Methoxy-4-Nitro-5-Sulfophenyl)-2H-Tetrazolium-5-Carboxanilide) staining. Actively respiring cells convert water-soluble XTT into an orange product *via* a formazan reaction which can be measured colorimetrically (Roslev and King, 1993). CFU mL^{-1} enumeration was also used to determine the ecological composition of both the biofilms and supernatant.

2.12.1 Batch culture biofilms

Biofilm growth under batch conditions was measured using a microtiter plate format. Overnight cultures were washed in PBS and resuspended to OD_{600 nm} 0.05 in fresh, pre-warmed ASM. Normalised cell suspensions were then transferred to the wells of a round bottomed 96-well microtiter plate (Nunc) to give a final volume of 150 μL per well. Equal volumes of normalised cell cultures of the individual species were inoculated during dual-species (75 μL each species) and triple-species co-culture (50 μL each species) experiments. Plates were sealed with a gas permeable Breathe-Easy membrane and incubated without the plate lid in a sealed box lined with damp tissue at 37°C with 100 rpm shaking. An average of four technical

replicates were recorded for each biological replicate and media only controls were included on every plate.

For CFU mL⁻¹ enumeration, 100 µL of the culture supernatant was removed and plated out as described in *Section 2.5*. Residual supernatant was carefully removed and loosely attached, planktonic bacteria removed by gently washing the wells three times with 200 µL sterile ddH₂O, taking care not to dislodge the attached biofilm. PBS (100 µL) was then added to the wells and biofilm disrupted by scraping with a pipette tip, vigorous pipetting and vortexing. The homogenised biofilm fraction was then plated onto selective plates as normal.

For both the CV and XTT assays, the culture supernatant was carefully aspirated and the attached biofilm carefully washed three times in 200 µL ddH₂O. For CV staining, 0.1% CV solution (120 µL) was added to each well and plates incubated for 15 min at room temperature. The dye was aspirated, the stained biofilm washed three times in ddH₂O and plates dried. Acetic acid (30%, 120 µL) was added to each well and the plate vortexed to solubilise the dye. Abs_{590 nm} was then measured in a FLUOstar Omega plate reader. For XTT staining, 120 µL of XTT-menadione solution was added to washed biofilm and plates incubated in the dark at 37°C for 2 hrs with 100 rpm shaking. Aliquots of the resulting yellow-orange solution (100 µL) were then transferred to the wells of a clean microtiter plate and Abs_{450 nm} measured in a FLUOstar plate reader. Readings for both assays were normalised by subtracting background absorbance measured in the culture-only wells.

2.12.2 Microtiter plate continuous-flow setup

A schematic diagram of the Kadouri drip-fed model (Merritt et al., 2005) used to study biofilm formation under continuous-flow conditions within a microtiter plate format is shown in *Figure 2.8*. The model consists of a flat bottomed 6-well culture dish (Nunc) fitted with a modified lid, constructed as part of this study. Holes (1.06 mm diameter) were bored into the lid at opposite ends of each well. Acetal resin standard tubing connectors (2.5 mm, Ismatec) were then fixed over the holes to act as spacers and securely hold the needle tips. A 2.54 cm 19-gauge needle was inserted through the inlet hole and a 3.81 cm 19-gauge needle through the outlet. Before use, the plate lid was UV irradiated overnight (needle side up) in a laminar flow hood. Overnight cultures were washed in PBS and normalised to OD_{600 nm} 0.05 in fresh, pre-warmed ASM. Each well was inoculated with 3 mL normalised culture, with equal volumes of each species inoculated during the co-culture experiments. Plates were incubated at 37°C with 100 rpm shaking and $Q = 55 \mu\text{L min}^{-1}$ (following the protocol of (Crusz et al., 2012)) was applied to the model after 1.5 hrs incubation.

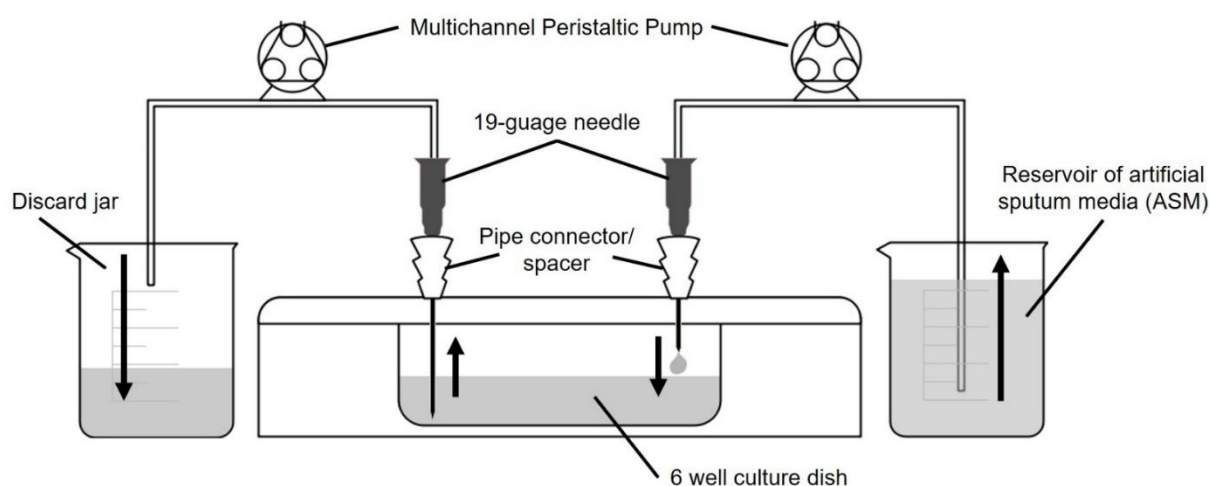


Figure 2.8 Schematic diagram of the microtiter continuous-flow biofilm model.

Bacterial cultures (3 mL) were cultured within the wells of a 6-well culture dish (centre). Two holes above each well were bored into the lid of the plate and standard sized pipe connectors for 2.5 mm diameter tubing were attached as spacers. A 2.54 cm 19-gauge needle was inserted into the inlet hole (right) and a 3.81 cm 19-gauge needle was inserted into the outlet hole (submerged within the media, left). A multichannel peristaltic pump delivers fresh media (ASM) into each well and removes waste culture at a flow rate of $60 \mu\text{L min}^{-1}$. Arrows show the direction of flow. The entire system was incubated at 37°C and the plate contents kept homogenous by shaking (100 rpm).

For CFU mL⁻¹ enumeration, 100 µL of the supernatant fraction was removed and plated out as described above. The remaining supernatant was discarded and the biofilm gently washed three times in 3 mL sterile ddH₂O. PBS (1 mL) was then added to each well and the biofilm disrupted using a sterile cell scraper (Greiner). Plates were vortexed to homogenise samples and the resulting biofilm fraction plated out as previously described.

For CV staining, 0.1% CV solution (3 mL) was added to each well and plates incubated for 15 min at room temp. The dye was then aspirated and the stained biofilm washed three times in ddH₂O and plates left to dry. Once dried, 30% acetic acid (3 mL) was added to each well and the plate vortexed. For XTT staining, 3 mL of XTT-menadione solution was added to the pre-washed biofilm and plates incubated as described in *Section 2.11.1*. Aliquots (150 µL) were transferred to the wells of a clean 96-well microtiter plate and absorbance at the appropriate wavelength measured as described in *Section 2.11.1*.

2.12.3 Culture-vessel biofilm growth

Biofilm formation within the continuous-flow culture vessel was measured on two types of solid substratum, agar chunks and *ex vivo* porcine lung tissue (EVPL) sections. To keep the substratum suspended in the culture media and prevent contact with the magnetic stir bar, bespoke cylindrical biofilm containers (25 mm diameter x 35 mm length) were constructed by hand for this study from stainless steel wire gauze (Fisher Scientific) (*Figure 2.9.A* and *2.9.B*). Containers were then suspended in the culture vessel *via* hanging from a piece of silicon tubing threaded through two of the unused HPLC ports (*Figure 2.9.C*).

Agar plates (2.5% w/v bacto agar in ddH₂O) were poured to a depth of 5 mm. Using sterile scalpel and forceps, cubes of approximately 5 mm x 5 mm were cut from the plate and transferred into the sterile biofilm container. Biofilm work using EVPL sections was performed in collaboration with Freya Harrison at the University of Warwick, using previously described methods (Harrison and Diggle, 2016). Briefly, fresh pig lungs were collected from the butchers (John Taylors, Coventry, UK) and processed within the hour. To remove surface contaminants, a heated palette knife was briefly tapped (< 1 s) on the area to be dissected. A sterile razor blade was used to excise the bronchiole and remove all alveolar tissue, a cleaned bronchiole can be seen in *Figure 2.10*. Bronchioles were washed in DMEM/RPMI solution (40 mL) and cut into 5 mm wide strips with sterile dissection scissors. The strips were washed in DMEM/RPMI and cut into 5 mm x 5 mm squares. EVPL sections were washed again in DMEM/RPMI, then transferred to a petri dish containing 40 mL ASM and irradiated in UV lightbox for 5 min before being aseptically transferred to the biofilm container. The culture

vessel was filled with ASM (100 mL) and the system warmed to 37°C before being inoculated and incubated as described in *Section 2.3.1*.

At the point of sampling, pieces of substratum were aseptically transferred to 500 µL PBS within 24-well microtiter plates. Loosely attached planktonic cells were removed from the substratum by swirling the plates. Samples were homogenised in 2 mL bead beating tubes, containing 1 mL PBS and 18 x 2.38 mm metal beads (Qiagen), using a FastPrep-24 5G benchtop homogeniser (MP Biomedicals) for 40 secs at 4 m s⁻¹. CFU mL⁻¹ counts were performed as described in *Section 2.3.1*, three separate substratum pieces were sampled per timepoint.

2.13 Culturing patient derived sputum samples

2.13.1 Sample collection

Spontaneously expectorated sputum samples from healthy CF outpatients were collected by clinical staff as part of routine monthly appointments at the Adult Cystic Fibrosis Centre (Cambridge Centre for Lung Infection, Royal Papworth Trust Hospital [with the ethical approval of the Hospital Research Tissue Bank T02449 (October 1st 2018)]). Samples were preferentially collected from patients believed to harbour a diverse airway-associated microbiota (as determined by clinical staff during previous appointments) and all samples were fully anonymised, with no patient data being collected. Samples were transported on ice and immediately processed upon arrival at the lab. Saliva and oral contaminants were removed by gently washing sputum in approximately five-times volume of 0.85% saline. An equal volume of sputasol was added to the sputum and the solution incubated at 37°C with gentle agitation until homogenous (approximately 30 min) (McClellan et al., 2010). Samples were stored as 1 mL aliquots with 10% glycerol at -80°C until use.

2.13.2 Model inoculation and incubation

The continuous-flow culture vessel was set up with 2.5% w/v agar chunks for solid substratum within the biofilm container, as described in *Section 2.12.3*. Sputum aliquots were thawed on ice and cell material sedimented *via* centrifugation (13,000 x g, 5 min, 4°C). Cell pellets were gently resuspended in 600 µL PBS. A 100 µL aliquot of the sample was removed and stored at -80°C to act as a t = 0 timepoint. The remaining culture was inoculated into the culture vessel and the model incubated for 24 hrs before applying Q.

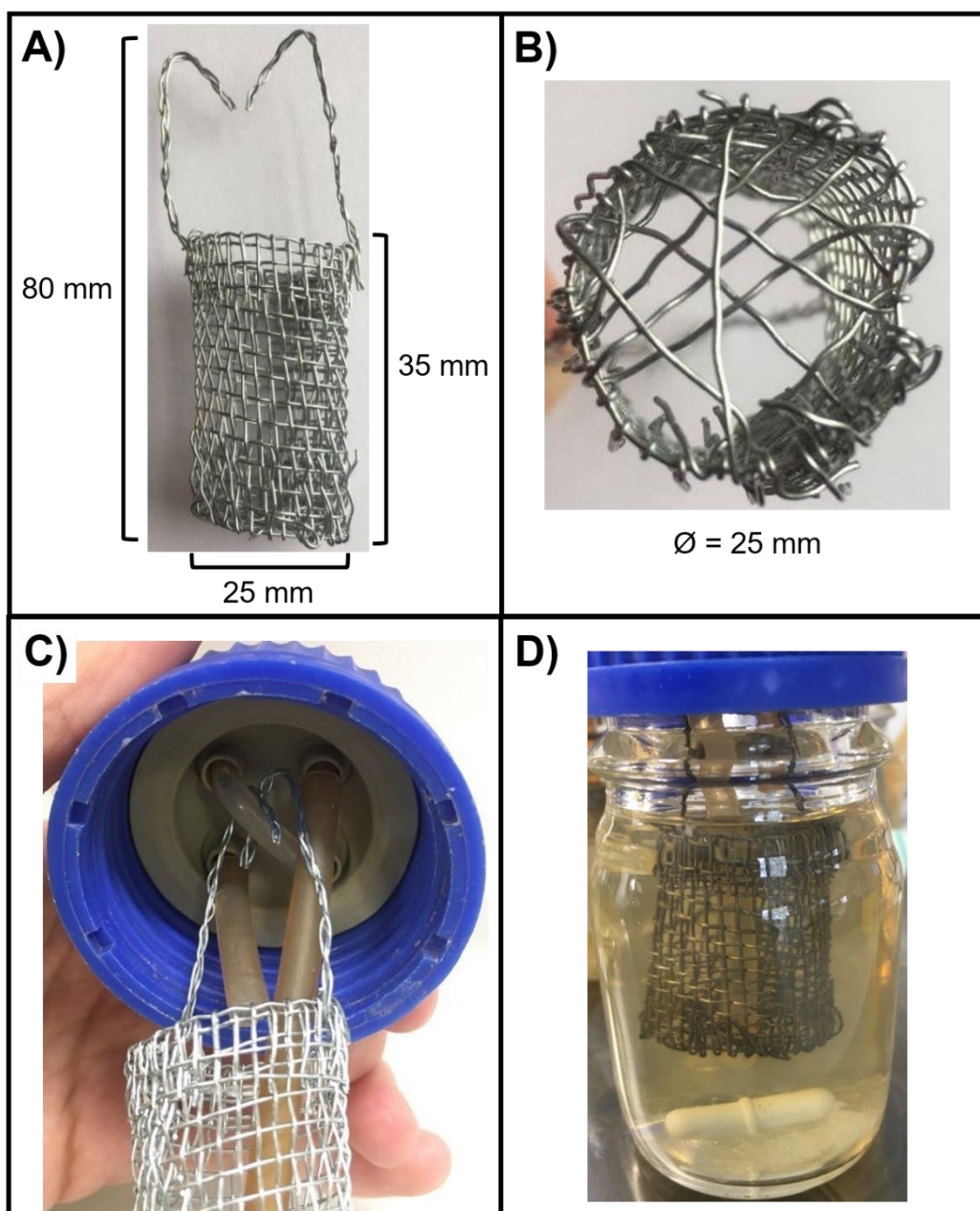


Figure 2.9 Container for culturing biofilms within the continuous-flow model.

Representative photographs of the biofilm container constructed from stainless steel gauze by hand for this study. Biofilm containers consisted of a cylinder, 35 mm in length and 25 mm in diameter (\emptyset), connected to 2 stainless steel arms (45 mm in length) that suspend the container from the HPLC screw-port lid. **(A)** Side view of the container with dimensions. **(B)** Bottom view of the container. Single strands of stainless-steel wire were threaded across the bottom of the container to form a mesh and prevent solid substratum from falling through. A small gap was also included for the outlet tube to be threaded through to allow the removal of culture media during incubation. **(C)** View of the 4-port HPLC screw cap lid. The bottom left port is the media inlet, the top right port is the media outlet and the two remaining ports are threaded with a single piece of rubber tubing (1.5 mm bore), which the arms from the container are fitted onto prior to autoclaving. **(D)** Biofilm container in use within a 100 mL Durant flask. Note that the container is completely submerged within the growth medium but is separated from the magnetic stir bar to prevent interference with the continual stirring of the culture vessel.



Figure 2.10 *Ex vivo* porcine bronchiole.

A single bronchiole excised from porcine lungs after cleaning and a single wash in DMEM/RPMI solution. All alveolar and vascular tissue was removed using a razor blade and dissection scissors. After cleaning bronchiole tissue was cut into 5 mm x 5 mm squares for use as solid substratum to promote biofilm growth within the continuous-flow culture vessel.

2.13.3 Sample collection and gDNA extraction

Supernatant samples were collected by aseptically removing 2 mL of culture from the vessel. Aliquots (1.5 mL) were centrifuged (13,000 x g, 5 min, room temp) and the pellet stored at -80°C for genomic DNA (gDNA) extraction. The remaining culture supernatant was used for CFU mL⁻¹ enumeration and OD_{600 nm} measurements. Three pieces of biofilm substratum were removed from the container per timepoint and transferred to 500 µL PBS in 24-well microtiter plates. Planktonic cells were removed by gently swirling the plates and the substratum pieces pooled in sterile 2 mL tubes, stored at -80°C.

Samples were thawed at room temperature and total gDNA was extracted using FastDNA SPIN kit for soil (MP Biomedicals). To ensure complete lysis and improve gDNA extraction from Gram-positive and Gram-negative species within the samples 100 µg mL⁻¹ recombinant lysostaphin (produced in-house for this work, see *Appendix 2.2*), 100 µg mL⁻¹ mutanolysin (Sigma) and 20 mg mL⁻¹ lysozyme (Sigma) were combined with the sodium phosphate buffer (at step 2 of the manufacturer's instructions) and samples incubated at 37°C with 180 rpm shaking for 30 min, as described by (Gill et al., 2016, Wada, 2001). Manufacturer's instructions were followed from step 2 onwards. The concentration and quality of DNA was assessed using a Nanodrop ND-1000 Spectrophotometer, and samples were stored at -20°C.

2.13.4 Sample library preparation and sequencing

Libraries for sequencing were prepared following the protocol described by Duarte *et al* (Duarte et al., 2017). Briefly, the full length bacterial 16S rRNA 30S ribosomal subunit encoding gene was PCR amplified using primers, 27F and U1492R (*Table 2.6*), and the reaction conditions described in *Table 2.7*. Amplification products were resolved on a 1.4% (w/v) agarose gel to check for the presence of a single clear band corresponding to the approximate size of the target gene (1522 base pairs). *Figure 2.11.A* shows a representative image of a successful amplification of the entire 16S rRNA gene. PCR products were cleaned up with GeneJet PCR Purification kit (ThermoFisher) and the V3 to V4 hypervariable region was then amplified from full length 16S rRNA gene using Illumina-compatible primers, MiSeq 16S rRNA-F and MiSeq 16S rRNA-R (*Table 2.6*), and the reaction conditions described in *Table 2.8*, as detailed by Illumina (Illumina, 2013). Samples with Illumina-adaptor overhangs were resolved on a 1.4% agarose gel and bands of approximately 460 base pairs were excised and DNA purified using GeneJet Gel Extraction kit (ThermoFisher). *Figure 2.11.B* demonstrates a representative image of the resulting PCR products separated *via* electrophoresis. Sample libraries were sent to the Cambridge DNA Sequencing Facility

Primer	5' - 3' Sequence	Reference
27F	AGAGTTTGATCMTGGCTCAG	(Weisburg et al., 1991)
U1492R	GGTTACCTTGTTACGACTT	(Weisburg et al., 1991)
MiSeq 16S rRNA-F	TCGTCGGCAGCGTCAGATGTGTATAAGAGACAG CCTACGGGNGGCWGCAG	(Illumina, 2013)
MiSeq 16S rRNA-R	GTCTCGTGGGCTCGGAGATGTGTATAAGAGACA GGACTACHVGGGTATCTAATCC	(Illumina, 2013)

Table 2.6 Primers for preparation of sequencing libraries.

Reaction Mixture		
Component	Volume/amount	Final Concentration
10 x Reaction buffer	5 μ L	1 x
dNTP mx (100 mM)	1 μ L	2 mM
Forward primer (27F)	1 μ L	2 μ M
Reverse primer (U1492R)	1 μ L	2 μ M
Genomic DNA	50 – 100 ng	1 – 2 ng μ L ⁻¹
Q5 High-Fidelity Polymerase	0.25 μ L	1.25 U μ L ⁻¹
Nuclease-free H ₂ O	Up to 50 μ L	
Thermocycler Conditions		
Temperature (°C)	Time	No. Cycles
94	4 min	1
94	1 min	30
48	30 secs	
72	1 min 30 secs	
72	7 min	1
4	∞	-

Table 2.7 PCR amplification of full 16S rRNA gene.

Reaction mixture (50 μ L total volume) and cycle conditions for PCR amplification of bacterial 16S rRNA encoding gene from genomic DNA samples.

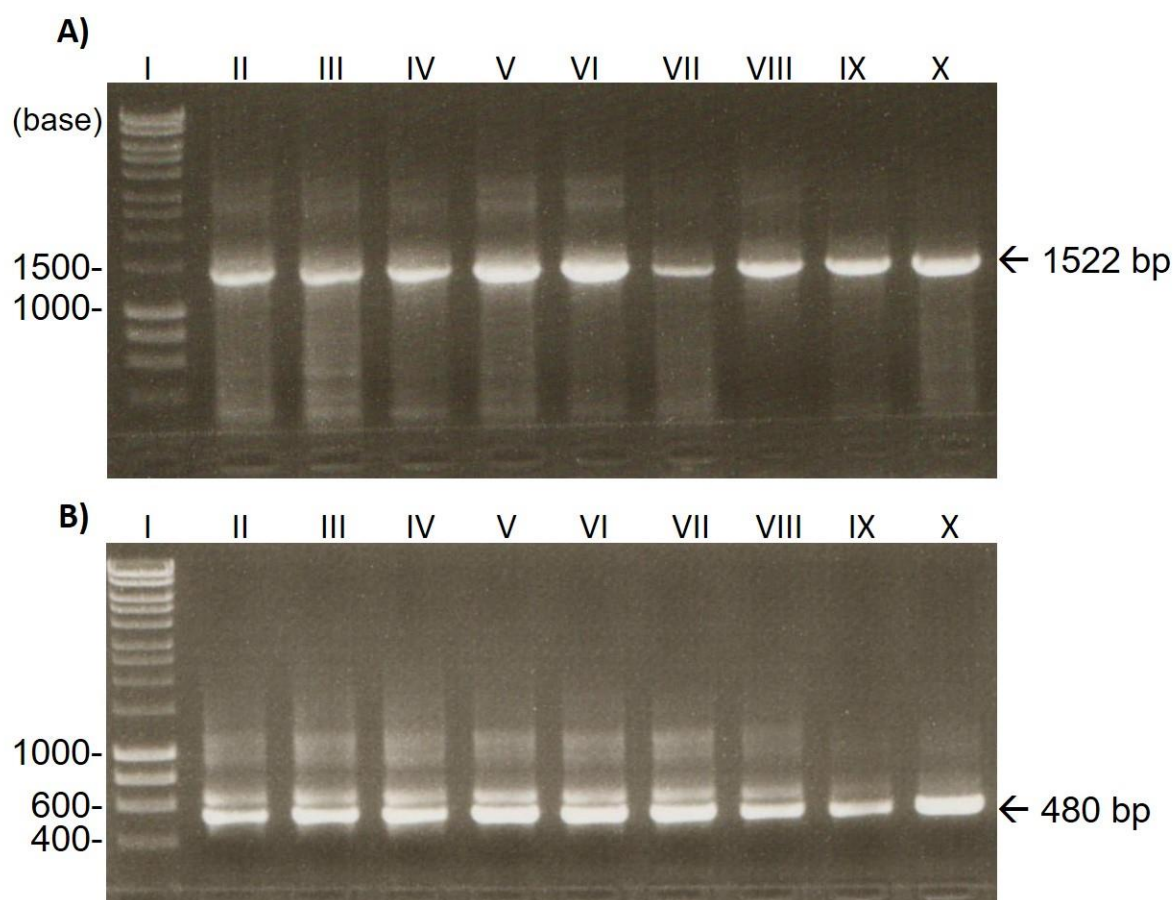


Figure 2.11 Preparation of sample libraries for sequencing.

Sample libraries for sequencing were prepared in two separate PCR amplification steps. For images (A) and (B), Lane I: Hyperladder 1kb DNA marker (Bioline). Lanes II-X: representative sample libraries prepared as part of the current work. **(A)** Amplification of full length 16S rRNA encoding gene from total extracted genomic DNA. A clear band of approximately 1522 bp, corresponding to the size of the full 16S rRNA gene, can be seen in all sample lanes. **(B)** Amplification of V3 – V4 hypervariable region with Illumina compatible primers from full length 16S rRNA amplicon generated in (A). A bright band of approximately 480 bp, corresponding to the size of the sequence libraries, alongside a band of approximately 600 bp and a smear at 1000 bp in size can be seen in most sample lanes. Bands of the correct size (~480 bp) were excised and the sample libraries purified using a GeneJet gel extraction kit (ThermoFisher).

Reaction Mixture		
Component	Volume/ amount	Final Concentration
10 x Reaction buffer	5 μ L	
dNTP mx (100 mM)	1 μ L	2 mM
Forward primer (27F)	1 μ L	2 μ M
Reverse primer (U1492R)	1 μ L	2 μ M
Template DNA	25 ng	1 ng μ l ⁻¹
Q5 High-Fidelity Polymerase	0.1 μ L	1 U μ L ⁻¹
Nuclease-free H ₂ O	Up to 25 μ L	
Thermocycler Conditions		
Temperature (°C)	Time	No. Cycles
95	4 min	1
95	30 secs	25
55	30 secs	
72	30 secs	
72	5 min	1
4	∞	-

Table 2.8 PCR amplification of full hypervariable V3/V4 region.

Reaction mixture (25 μ L total volume) and cycle conditions for PCR amplification of the V3 – V4 hypervariable region of the 16S rRNA gene with Illumina-compatible primers. Full 16S rRNA amplification products (*Table 2.7*) are used as template DNA.

(Department of Biochemistry, University of Cambridge) for high-throughput paired-end sequencing using an Illumina MiSeq instrument and 600-cycles with reagent kit v3 (Illumina).

2.13.5 Data analysis

Sequence reads were de-noised and analysed by following the Qiime2-Deblur pipeline (Amir et al., 2017, Bolyen et al., 2019) using the opensource bioinformatics software QIIME 2 2020.6.0 within a VirtualBox 64-bit Ubuntu operating system (Oracle VM VirtualBox). Commands used to filter and cluster sequences into operational taxonomic units (OTUs) and perform subsequent phylogenetic metric tests are described in detail in *Appendix 2.3*.

2.13.6 ASM supplementation

The composition of modified ASM used in the culture of patient derived sputum samples are described in *Table 2.9*. The standard protocol for making ASM was followed (*Appendix 2.1*), with media supplemented with the appropriate components before filter sterilisation. Culture vessels were inoculated and incubated as described in *Section 2.13.2*, with $Q = 55 \mu\text{L min}^{-1}$.

2.14 Statistical analysis

Unless otherwise stated, all data represent the mean \pm SD of three independent biological experiments. Results were analysed by one-way or two-way ANOVA, or Student's unpaired t-test using GraphPad Prism version 8.2.0, with $P < 0.05$ being considered statistically significant.

Name	Supplement composition [notes]
ASM + 40 μM FeSO_4	40 μM FeSO_4 [11.111 mL of $\text{FeSO}_4 \cdot 7\text{H}_2\text{O}$ stock (<i>Appendix 2.1</i>) within 1 L of ASM, Replaces 3.6 μM FeSO_4 in standard ASM]
ASM + 5 mM Met/Cys	5 mM Methionine 5 mM Cysteine [50 mL of Met and Cys amino acid stocks (<i>Appendix 2.1</i>) in 1 L ASM, replaces 633 μM methionine and 160 μM cysteine in standard ASM]
ASM + micronutrients	30 nM Ammonium molybdate tetrahydrate 4 μM Boric acid 300 nM Cobalt chloride 100 nM Cupric sulfate 800 nM Manganese chloride 100 nM Zinc sulfate [1 mL of 100x micronutrient stock (LaBauve and Wargo, 2012) diluted in 1 L standard ASM]
ASM + 1 mM KNO_3	1 mM KNO_3 [1mL of KNO_3 stock (<i>Appendix 2.1</i>) in 1 L ASM, replaces 348 μM KNO_3 in standard ASM]
ASM + desferrioxamine	50 mg L^{-1} Desferrioxamine mesylate salt (Sigma) [Powder dissolved directly in ASM]
ASM + NAM	1 mg L^{-1} N-Acetylmuramic acid (NAM or MurNAc) (Sigma) [Powder dissolved directly in ASM]
ASM + Sodium pyrophosphate	100 μM Disodium dihydrogen pyrophosphate (Sigma) [Powder dissolved directly in ASM]

ASM + vitamins	<p>5 µg ml⁻¹ Ascorbic acid [vitamin C] (Sigma)</p> <p>5 µg ml⁻¹ Biotin [vitamin B₇] (Sigma)</p> <p>5 µg ml⁻¹ Cyanocobalamin [vitamin B₁₂] (Sigma)</p> <p>5 µg ml⁻¹ Folic acid [vitamin B₉] (Sigma)</p> <p>5 µg ml⁻¹ α-lipoic acid (Sigma)</p> <p>5 µg ml⁻¹ Nicotinamide [vitamin B₃] (Sigma)</p> <p>5 µg ml⁻¹ Pantothenic acid [vitamin B₅] (Sigma)</p> <p>5 µg ml⁻¹ Pyridoxamine [vitamin B₆] (Sigma)</p> <p>5 µg ml⁻¹ Riboflavin [vitamin B₂] (Sigma)</p> <p>5 µg ml⁻¹ Thiamine [vitamin B₁] (Sigma)</p> <p>[Stock solutions made in ddH₂O kept in the dark at 4°C for up to 1 week before use]</p>
ASM + FBS (1%)	<p>1% Heat inactivated foetal bovine calf serum (FBS, Sigma)</p> <p>[Lot number: BCBZ5076]</p>
ASM + FBS (5%)	<p>5% Heat inactivated FBS</p> <p>[Lot number: BCBZ5076]</p>
ASM + FBS (10%)	<p>10% Heat inactivated FBS</p> <p>[Lot number: BCBZ5076]</p>
ASM + BSA	<p>2.5% Bovine serum albumin (BSA, FisherScientific)</p> <p>[25 g powder directly dissolved in 1 L standard ASM]</p>
ASM + Charcoal stripped FBS	<p>5% Charcoal stripped Heat inactivated FBS (FisherScientific)</p>
ASM + ≥ 30 kDa FBS	<p>50 mL heat inactivated FBS was centrifuged (4000 x g, 1 hr, 4°C) in a 30 kDa MWCO Vivaspın column (GE Healthcare) and retentate added to 1 L standard ASM</p> <p>[FBS lot number: BCBZ5076]</p>
ASM + 5 – 30 kDa FBS	<p>Permeate from 50 mL of ≥ 30 kDa FBS fraction (above) was centrifuged (4000 x g, 1 hr, 4°C) in a 30 kDa MWCO Vivaspın column (GE Healthcare) and retentate added to 1 L standard ASM</p> <p>[FBS lot number: BCBZ5076]</p>
ASM + ≤ 5 kDa FBS	<p>Permeate from 50 mL of 5 – 30 kDa FBS fraction (above) added to 1 L standard ASM</p> <p>[FBS lot number: BCBZ5076]</p>

ASM + hemin	100 mg L ⁻¹ Hemin from bovine (Sigma) [Lyophilised powder added directly to ASM]
ASM + hemoglobin	100 mg L ⁻¹ Hemoglobin from bovine blood (Sigma) [Lyophilised powder added directly to ASM]
ASM + micronutrients and 40 µM FeSO ₄	ASM + micronutrients prepared as described above, supplemented with 40 µM FeSO ₄
ASM + micronutrients, 40 µM FeSO ₄ and FBS	ASM + micronutrients and 40 µM FeSO ₄ prepared as described above, supplemented with 5% FBS [FBS lot number: BCBZ5076]

Table 2.9 Composition of supplemented ASM.

Standard ASM was prepared according to *Appendix 2.1*, with medium supplemented with the appropriate chemicals before filter sterilisation (0.22 µM pore size).

3. *In vitro* maintenance of polymicrobial co-cultures

3.1 Introductory comments

The work presented in this chapter describes the maintenance of stable co-cultures of commonly used laboratory reference strains in the continuous-flow culture model. These strains were chosen to represent the three major classes of microbial species associated with CF airway infections: *P. aeruginosa* (PA, Gram-negative bacteria), *S. aureus* (SA, Gram-positive bacteria) and *C. albicans* (CA, dimorphic fungi/yeast). I first confirmed that all three species could grow in ASM. Each species was inoculated into a flat-bottomed 96-well microtiter plate (Nunc) containing ASM. Plates were incubated at 37°C with 180 rpm shaking within a FLUOStar Omega plate reader and culture density ($OD_{600\text{ nm}}$) measured every 15 min. All species grew rapidly in ASM, achieving a final $OD_{600\text{ nm}}$ of >1.0 after 24 hrs (*Appendix 3.1*).

Media flowrate (Q) within the model was paramount to achieving successful co-cultures. If Q is too high, a washout of species within the culture vessel occurs. If Q is too low, the microbial density within the vessel becomes saturated and species begin to out-compete one another. To the best of my knowledge, this study is the first to attempt the co-culture of polymicrobial communities using a continuous-flow model. As such, a lot of time was spent optimising parameters such as the diameter of tubing, culture vessel size and values for Q . For the sake of brevity, only results using optimised conditions are reported. Speed of the peristaltic pump and Q were calibrated experimentally using the methods described in *Section 2.4* and *Figure 2.4* demonstrates a representative image of this. This work has been published in *Frontiers in Microbiology* (O'Brien and Welch, 2019a).

3.2 Mono-species growth of PA

Mono-species growth of PA under continuous-flow and batch culture conditions was followed by measuring $OD_{600\text{ nm}}$ (*Figure 3.1*). The laboratory reference strain PAO1 was inoculated into the culture vessel ($Q = 170\text{ }\mu\text{L min}^{-1}$) and $OD_{600\text{ nm}}$ measured every 30 min using an in-line spectrophotometer (as described in *Section 2.3.1*). $OD_{600\text{ nm}}$ of the culture increased linearly for the first 8 hrs of incubation, before reaching a plateau of $OD_{600\text{ nm}} \approx 0.4$ after 10 hrs of incubation. Turbidity of the culture remained consistent for the remainder of incubation, with no statistically significant changes in $OD_{600\text{ nm}}$ occurring after $T = 10$ hrs.

When PA was grown under stirred batch culture conditions ($Q = 0\text{ }\mu\text{L min}^{-1}$, *Section 2.3.2*) $OD_{600\text{ nm}}$ exceeded 0.4 after 8 hrs of incubation and a final $OD_{600\text{ nm}}$ of > 1.0 was reached. After 24 hrs of incubation $OD_{600\text{ nm}}$ measurements in the batch culture began to decrease,

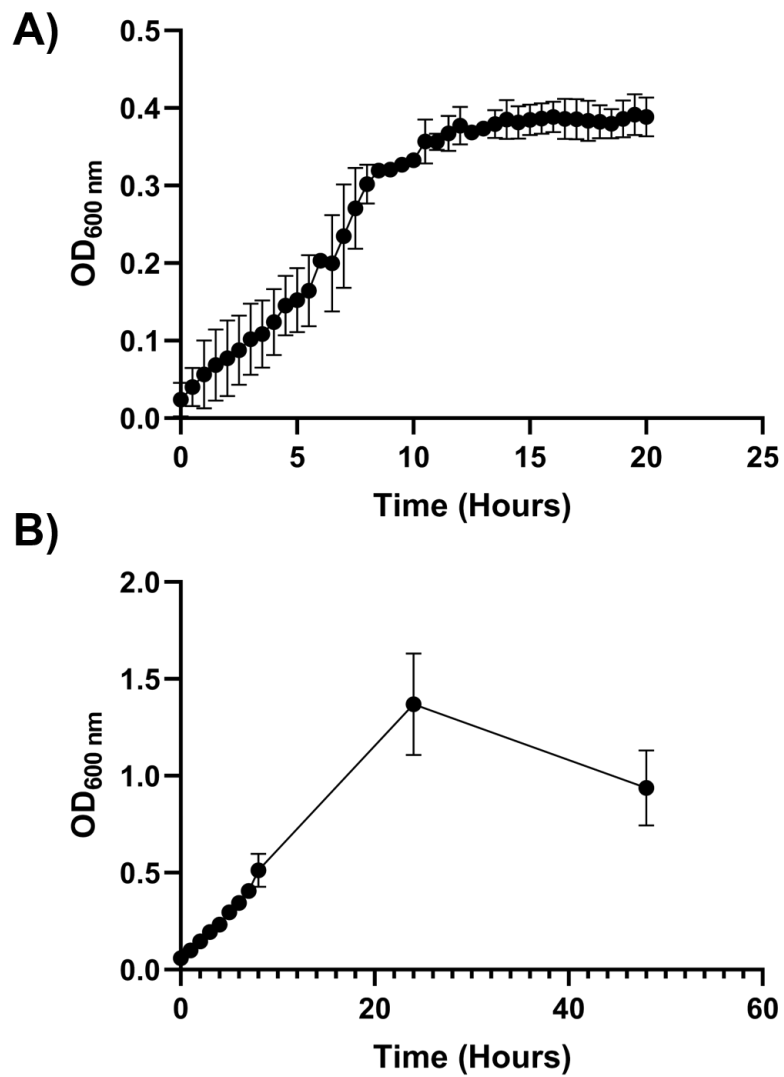


Figure 3.1 PA mono-species growth.

Growth of *P. aeruginosa* PAO1 in ASM in both batch and continuous-flow culture conditions. Growth is monitored by optical density (OD_{600 nm}) during **(A)** continuous-flow culture ($Q = 170 \mu\text{L min}^{-1}$); **(B)** batch culture ($Q = 0 \mu\text{L min}^{-1}$). Data represent the mean \pm standard deviation from three independent experiments.

suggesting the culture had entered the stationary phase of growth. Using the continuous-flow model, a mono-species PA culture can be maintained at a steady-state carrying capacity with OD_{600 nm} measurements kept well-below what is associated with entry into the stationary phase of growth in ASM.

3.3 Mixed-species co-culture (PA-SA)

3.3.1 Comments

SA is another species commonly associated with CF airway infections and can be isolated from over 50% of early adult CF patients (Jarry and Cheung, 2006). As mentioned in *Section 1.2*, PA often displaces SA over time to become the dominant pathogen of the CF airways. Some reports even suggest pre-colonisation of the airways with SA is a risk factor contributing towards the establishment of chronic PA infections (Cigana et al., 2018, Hoffman et al., 2006, Junge et al., 2016, Maselli et al., 2003). Despite the fact PA and SA can be co-isolated from the lungs of ~31% of CF patients (Hogan et al., 2016, Limoli et al., 2016, Wakeman et al., 2016, Zolin et al., 2019), previous attempts at co-culturing these species in *in vitro* and *in vivo* models have failed (Hotterbeekx et al., 2017). As discussed in *Section 1.4.4*, PA produces a wealth of extracellular virulence factors (van Delden, 2004), some of which are directly harmful to SA (e.g. pyocyanin, 4-hydroxy-2-alkylquinolone, 4-hydroxy-2-heptaquinolone-*N*-oxide, rhamnolipids, elastase and proteases) and prevent the long-term co-culture of these species being maintained within experimental models (Cardozo et al., 2013, DeLeon et al., 2014, Fugère et al., 2014, Hoffman et al., 2006, Hotterbeekx et al., 2017, Korgaonkar and Whiteley, 2011, Korgaonkar et al., 2013, Mashburn et al., 2005, Mitchell et al., 2010, Palmer et al., 2005). These interspecies interactions are not all one-sided, as mentioned in *Section 1.5.1*, SpA produced by SA is known to modulate the ability of PA to form biofilms (Armbruster et al., 2016). As no models yet exist which permit the successful long-term co-cultivation of PA and SA within the laboratory, research into how interspecies interaction may modulate gene expression and the evolutionary trajectory of these microorganisms in the CF microenvironment is severely hindered.

3.3.2 Batch culture

In accordance with existing reports, when PA and *S. aureus* 25923 are co-cultured in ASM under batch culture conditions, PA rapidly outcompetes SA in the culture vessel (*Figure 3.2*). During aerobic batch culture, no viable SA cells can be recovered from the flask after 96 hrs of incubation (*Figure 3.2.A*). Under stirred batch-culture conditions, PA also outcompetes

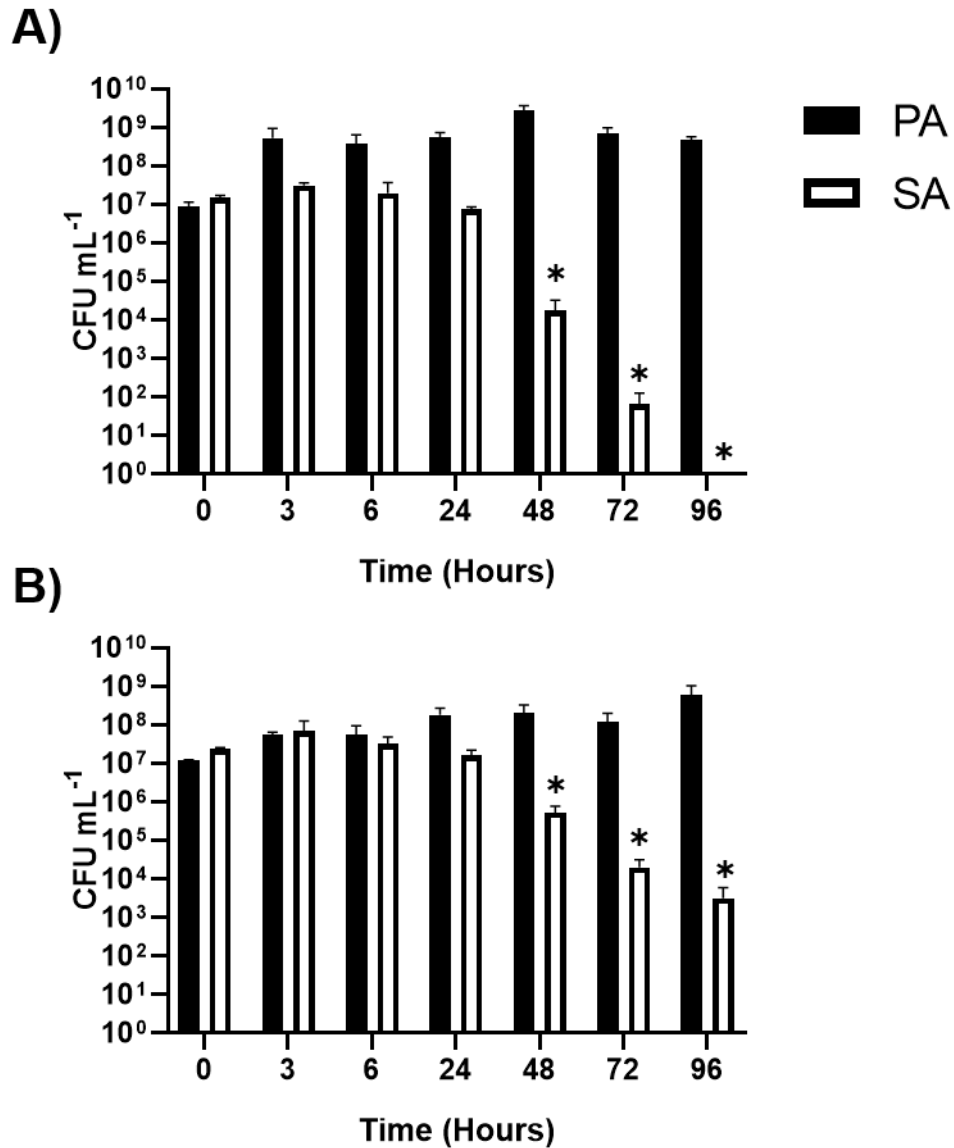


Figure 3.2 PA-SA co-culture grown in batch culture conditions.

Viable cell counts [colony forming units (CFUs) per mL] of *P. aeruginosa* PAO1 (PA, black bars) and *S. aureus* 25923 (SA, white bars) during co-culture in ASM in **(A)** aerobic batch culture and **(B)** stirred batch culture conditions. Data represented as mean \pm standard deviation from three independent experiments. Asterisks represent significant ($*P < 0.05$) differences in CFU mL⁻¹ counts in comparison with the data from the 24 hrs time point.

SA, albeit at a slower rate. Viable SA cells can still be recovered from the culture vessel after 96 hrs of incubation, but a significant 3 log-fold decrease in CFU mL⁻¹ counts is observed between T = 24 and T = 96 hrs (*Figure 3.2.B*).

3.3.3 Continuous-flow culture

Culturing PA and SA under continuous-flow conditions ($Q = 170 \mu\text{L min}^{-1}$) enabled both species to be readily maintained together as a co-culture (*Figure 3.3*). After 24 hrs of incubation bacterial populations established a stable, steady-state composition of approximately 10^7 SA CFU mL⁻¹ and 10^8 PA CFU mL⁻¹ in the culture vessel. There was no significant difference in viable cell counts for either species after T = 24 hrs ($P > 0.05$).

3.3.4 OD_{600 nm} Measurements

No significant difference ($P > 0.05$) in OD_{600 nm} measurements can be observed between the batch or continuous-flow culture vessels for the first 8 hrs of incubation (*Figure 3.4*). After 24 hrs of incubation OD_{600 nm} of the continuous-flow vessel is significantly lower than both the stirred batch ($P < 0.005$) and aerobic batch ($P < 0.0001$) co-cultures. A gradual but non-significant ($P > 0.9$) increase in OD_{600 nm} of the continuous-flow co-culture occurs between 24 hrs (OD_{600 nm} ≈ 1.4) and 96 hrs (OD_{600 nm} ≈ 1.6) of incubation. The optical density of the continuous-flow culture never reached peak OD_{600 nm} values observed in either batch culture populations. Turbidity of the aerobic co-culture begins to decrease after T = 24 hrs and the same trend is observed for the stirred batch culture vessel after T = 72 h. This suggests that both batch culture populations enter the stationary phase of growth, whereas populations cultured under continuous-flow conditions do not. Automated optical density measurements of the continuous-flow co-culture taken every 30 min using the in-line spectrophotometer are included in *Appendix 3.2*.

3.4 Mixed species co-culture (PA-CA)

3.4.1 Comments

Fungal species are also commonly associated with CF airway infections and more than 50% of CF patients test positive for colonisation with species of *Candida* or *Aspergillus* (Garczewska et al., 2016, Valenza et al., 2008). It is therefore essential that my model can support co-cultures of bacteria and fungi. The role of *C. albicans* (CA) as part of the polymicrobial communities associated with the CF airways is poorly characterised, but interspecies interactions between PA and CA have been reported. For instance, mixed

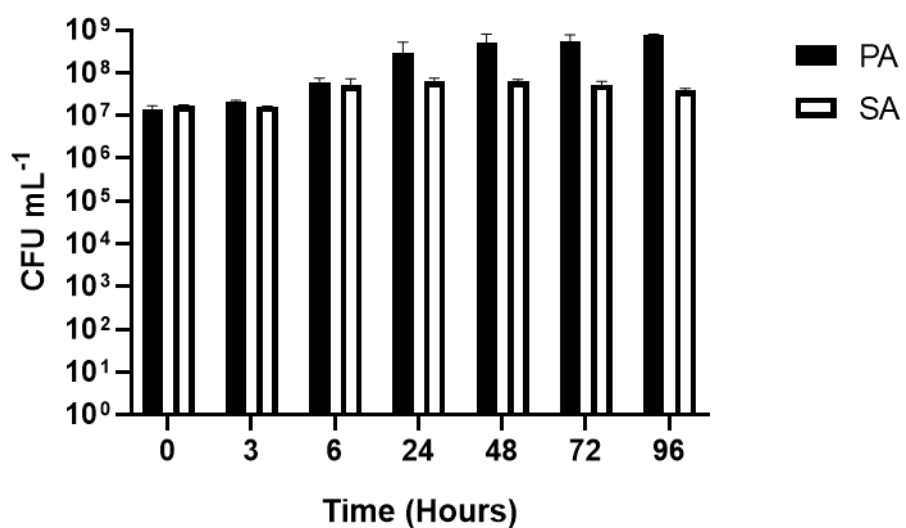


Figure 3.3 PA-SA co-culture grown under continuous-flow conditions.

Viable cell counts (CFU mL⁻¹) of *P. aeruginosa* PAO1 (PA, black bars) and *S. aureus* 25923 (SA, white bars) during co-culture in ASM in the continuous-flow model. Flowrate (Q) = 170 μ L min⁻¹. Data represented as mean \pm standard deviation from three independent experiments.

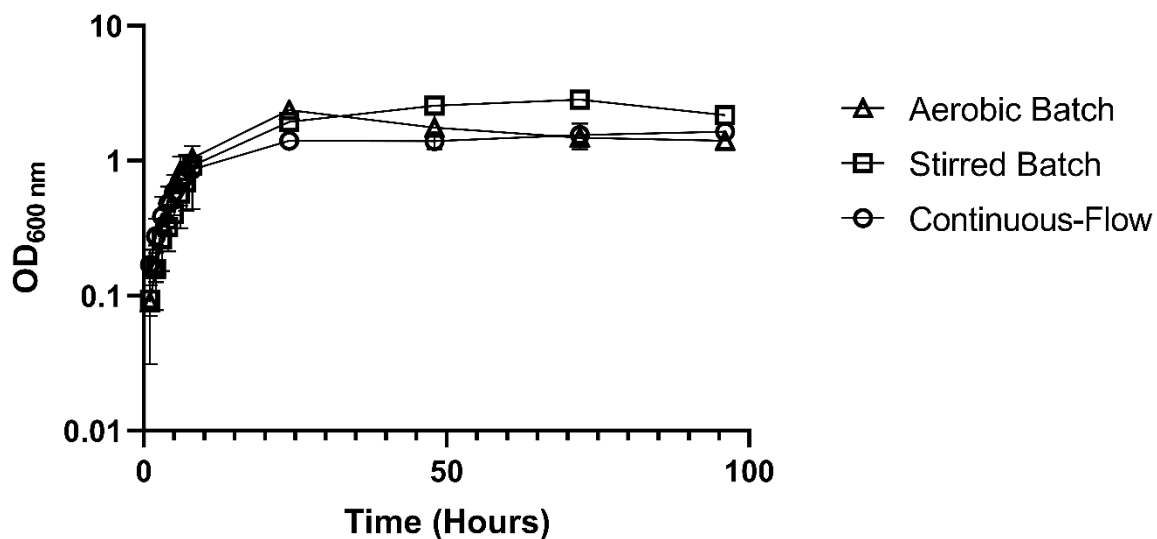


Figure 3.4 Growth of PA-SA co-cultures in batch and continuous-flow conditions.

Growth (monitored as OD_{600 nm}) of *P. aeruginosa* PAO1 and *S. aureus* 25923 dual species co-cultures in ASM in aerobic batch (triangles), stirred batch (squares) and continuous-flow (circles) growth conditions. $Q = 170 \mu\text{L min}^{-1}$ in the continuous-flow culture vessel. Data represented as the mean \pm standard deviation from three independent experiments.

species PA-CA biofilms display an up-regulation in the secretion of virulence factors, such as phenazines, rhamnolipids and pyoverdine, when compared with single-species PA biofilms (Cugini et al., 2007, Gibson et al., 2009, Hogan and Kolter, 2002, Hogan et al., 2004). Enhanced phenazine production can cause CA to switch from aerobic respiration to fermentation (Morales et al., 2013), thereby up-regulating the production of ethanol which causes PA to adopt a mucoid phenotype (DeVault et al., 1990, Morales et al., 2013). Furthermore, direct signalling events have been described between the two species. The PA QS molecule OdDHL promotes CA to grow as a yeast (Holcombe et al., 2010, McAlester et al., 2008), whereas farnesol produced by CA inhibits the production of PQS by *P. aeruginosa* (Cugini et al., 2007, Cugini et al., 2010), thereby modulating the expression of virulence factors and other genes under the control of this QS regulatory network (Lin et al., 2018). As in *Section 3.3*, no study has yet described the successful long-term co-culture of PA with CA, and therefore, how interspecies interactions between these common CF-associated organisms impacts upon gene expression or the evolutionary trajectory of these species.

3.4.2 Batch culture

When PA and *C. albicans* SC5314 are co-cultured in ASM under batch culture conditions, PA outcompetes CA in the culture vessel (*Figure 3.5*). During the aerobic batch co-culture, PA rapidly removes CA from the culture flask and no viable CA cells can be recovered after $T = 72$ h. A significant log-fold decrease ($P < 0.005$) in PA CFU mL⁻¹ counts also occurs between $T = 24$ hrs and $T = 96$ hrs (*Figure 3.5.A*). Under stirred batch conditions PA also outcompetes CA, albeit at a slower rate than the aerobic batch co-culture (*Figure 3.5.B*). Viable CA cells can still be recovered from the culture vessel at the final sampling point, but a significant 2 log-fold decrease in CA CFU mL⁻¹ counts occurs between 24 and 96 hrs of incubation.

3.4.3 Continuous-flow culture

A successful long-term PA-CA co-culture could be readily maintained under continuous-flow conditions (*Figure 3.6*). To prevent washout of CA from the culture vessel over time the flowrate of the model was decreased to $Q = 145 \mu\text{L min}^{-1}$. The culture carrying capacity for CA ($\approx 10^5$ CFU mL⁻¹) is approximately 3 log-fold lower than that of PA ($\approx 10^8$ CFU mL⁻¹) in the vessel. This notwithstanding, both species reached steady-state population densities after $T = 24$ hrs and no significant difference in PA or CA viable cell counts occurred after this point ($P > 0.1$).

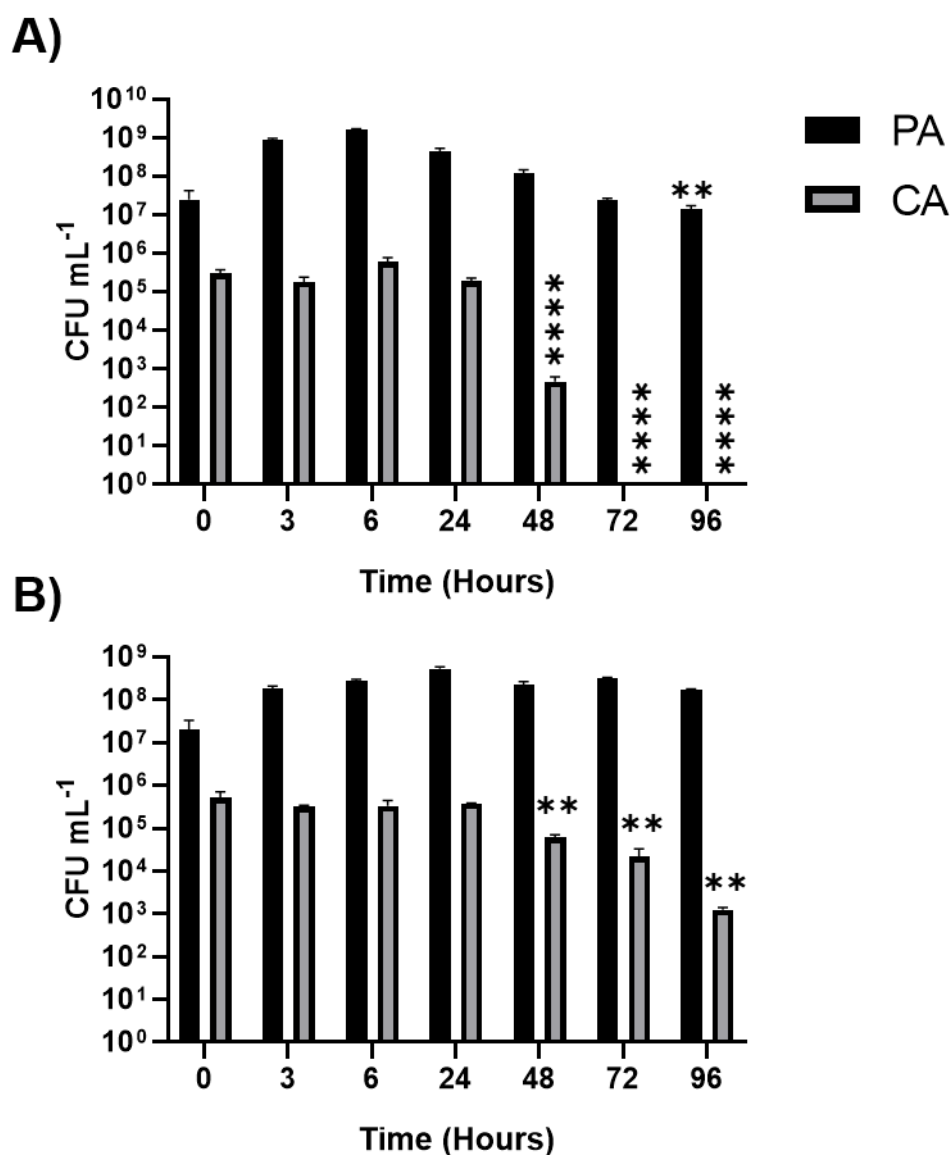


Figure 3.5 PA-CA co-culture during growth in batch culture conditions.

Viable cell counts (CFU mL⁻¹) of *P. aeruginosa* PAO1 (PA, black bars) and *C. albicans* SC5314 (CA, grey bars) during co-culture in ASM in **(A)** aerobic batch culture and **(B)** stirred batch culture conditions. Data represented as mean \pm standard deviation from three independent experiments. Asterisks represent significant (** $P < 0.005$, **** $P < 0.0001$) differences in CFU mL⁻¹ counts in comparison with the data from the 24 hrs time point.

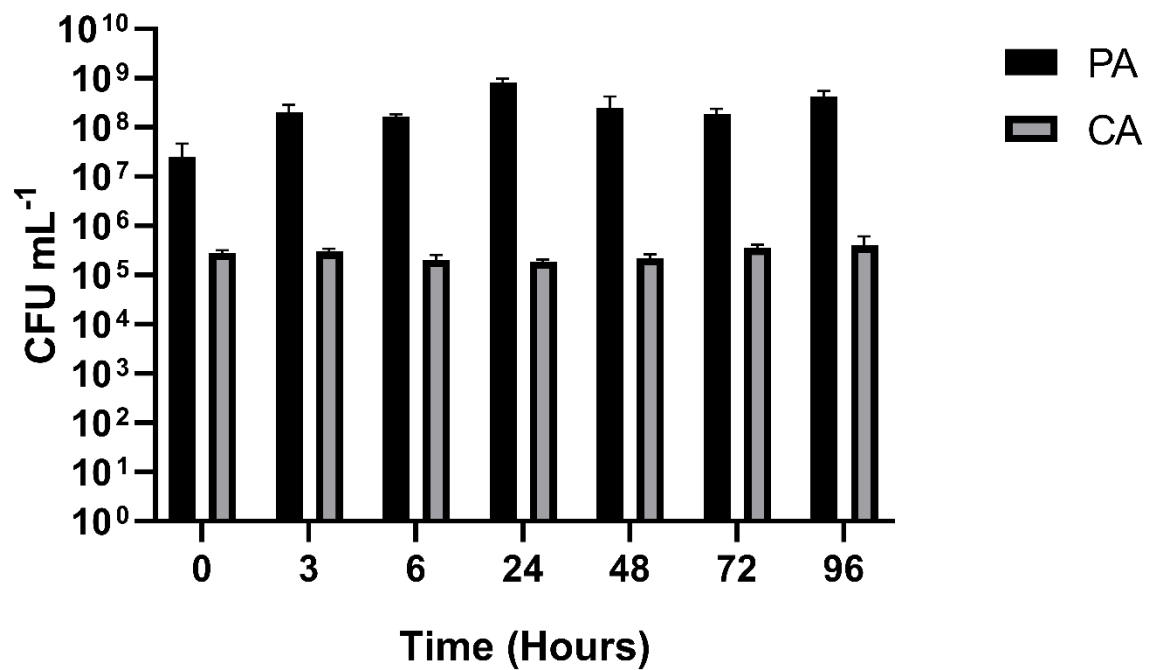


Figure 3.6 PA-SA co-culture during growth under continuous-flow conditions.

Viable cell counts (CFU mL⁻¹) of *P. aeruginosa* PAO1 (PA, black bars) and *C. albicans* SC5314 (CA, grey bars) during co-culture in ASM in the continuous-flow model. Flowrate (Q) = 145 μ L min⁻¹. Data represented as mean \pm standard deviation from three independent experiments.

3.4.4 OD_{600 nm} measurements

OD_{600 nm} of the PA-CA co-culture under aerobic batch culture conditions is significantly higher than the stirred batch and continuous-flow co-cultures after 8 hrs of incubation (*Figure 3.7*). At T = 24 hrs the cell density in the continuous-flow model is significantly lower than both the aerobic batch ($P < 0.001$) and stirred batch ($P < 0.05$) culture vessels. A steady-state carrying capacity (OD_{600 nm} \approx 1.0) is reached after 24 hrs of incubation in the continuous-flow vessel and optical density does not appreciably change for the remainder of the incubation period. The cell density of the aerobic batch co-culture peaks after 48 hrs of incubation (OD_{600 nm} = 4.9), followed by a significant 1.5 unit drop in OD_{600 nm} values every 24 hrs following this. The optical density of the stirred batch culture vessel increases exponentially after 24 hrs of incubation, reaching a final OD_{600 nm} of \approx 4.0 at T = 96 h, approaching values observed during the peak of aerobic batch culture growth.

3.5 Mixed species co-culture (SA-CA)

3.5.1 Comments

I next wanted to ensure a stable SA-CA co-culture could be maintained independent of the presence of PA in the continuous-flow model. As previously discussed, SA and CA are commonly isolated from CF sputum samples (Garczewska et al., 2016, Valenza et al., 2008), yet how these species interact within one another in the CF microenvironment is not known. CA and *Staphylococcus* species are commonly co-isolated from systemic bloodstream infections (Carolus et al., 2019, Kaufman et al., 2014) and SA aggregates on CA hyphae when co-cultured as polymicrobial biofilms (Peters et al., 2010, Tsui et al., 2016). The close physical association between these species suggests interspecies interactions may be prevalent between these microorganisms and a limited number of direct chemical interactions between SA and CA during co-culture have indeed been described. In addition to preventing yeast hyphal morphogenesis, thereby reducing SA-CA aggregation (Piispanen et al., 2011, Ramage et al., 2002), CA-produced farnesol can reduce the viability of SA cells through inducing an accumulation of intracellular reactive oxygen species (Vila et al., 2019). CA is also capable of inducing activation of the *agr* QS network of SA *via* an unelucidated mechanism, thereby directly modulating the expression of virulence factors and other QS-regulated genes during polymicrobial co-culture (Todd et al., 2019). Such interactions are, again, not all unidirectional, as lactate produced by SA during fermentation can prevent yeast hyphal morphogenesis (Liang et al., 2016).

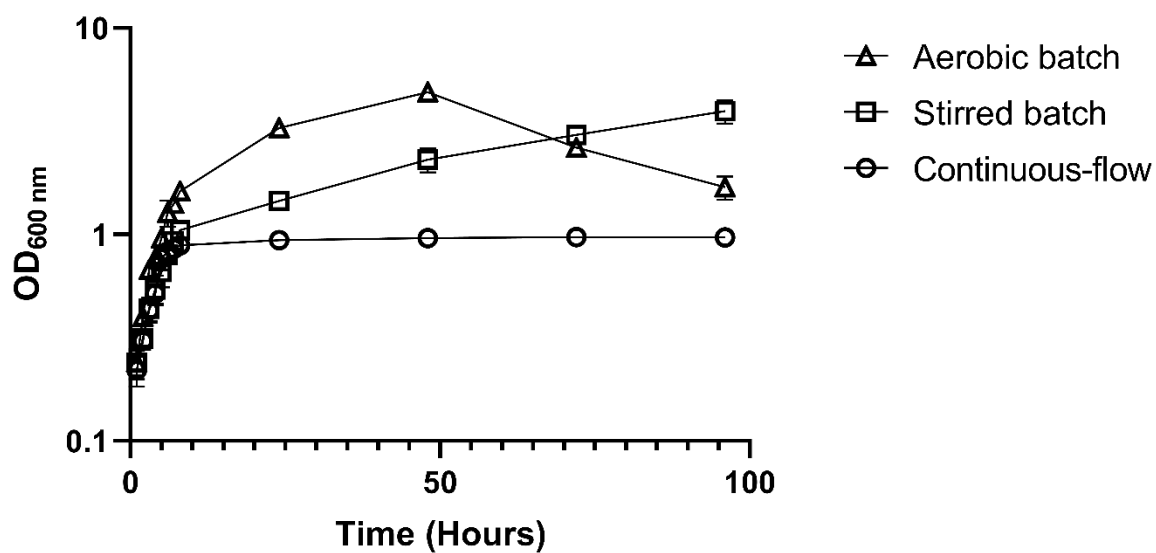


Figure 3.7 Growth of PA-CA co-cultures in batch and continuous-flow conditions.

Growth (monitored as OD_{600 nm}) of *P. aeruginosa* PAO1 and *C. albicans* SC5314 dual species co-cultures in ASM in aerobic batch (triangles), stirred batch (squares) and continuous-flow (circles) growth conditions. $Q = 145 \mu\text{L min}^{-1}$ in the continuous-flow culture vessel. Data represented as the mean \pm standard deviation from three independent experiments.

3.5.2 Batch culture

When SA and CA are co-cultured under batch conditions CA outcompetes SA present in the culture vessel (*Figure 3.8*), despite the fact CA comprises only 0.1% of the total microbial titres present within the aerobic and stirred batch co-cultures at $T = 24$ h. During co-culture under aerobic batch conditions a 3 log-fold decrease in SA cells occurs at each sampling point following 24 hrs of incubation and no viable SA cells could be recovered from the flask at $T = 96$ hrs (*Figure 3.8.A*). A significant 2 log-fold decrease ($P < 0.01$) in CA CFU mL⁻¹ counts also occurs between $T = 24$ and $T = 96$ hrs. Under stirred batch conditions viable SA cells could still be recovered from the culture vessel after 96 hrs of incubation, but a 5 log-fold decrease in SA CFU mL⁻¹ counts occurred between 24 and 96 hrs of incubation (*Figure 3.8.B*).

3.5.3 Continuous-flow culture

Under continuous-flow culture conditions ($Q = 145 \mu\text{L min}^{-1}$) a stable SA-CA co-culture could be readily maintained (*Figure 3.9*). As in *Section 3.4.4*, titres of both species reached a steady state by $T = 24$ hrs and the carrying capacity for CA within the culture is three orders of magnitude lower than that of SA within the culture vessel. The ratio of SA:CA remained unchanged and no significant difference ($P > 0.1$) in the titres of either species within the vessel occurred after 24 hrs of incubation.

3.5.4 OD_{600 nm} Measurements

OD_{600 nm} measurements of the SA-CA co-culture in the aerobic shake flask were significantly higher than the continuous-flow ($P < 0.0001$) and stirred batch ($P < 0.05$) culture vessels after 8 hrs of incubation (*Figure 3.10*). At $T = 24$ h, culture density in the continuous-flow model reached a steady-state carrying capacity ($\text{OD}_{600 \text{ nm}} \approx 1.35$) significantly lower than both the aerobic and stirred batch co-cultures ($P < 0.0001$).

No significant changes in OD_{600 nm} measurements were observed in the continuous-flow vessel after 24 hrs incubation ($P > 0.999$). Culture density of the SA-CA culture under aerobic batch conditions was significantly higher than the stirred batch culture from $T = 8$ to 72 hrs ($P < 0.001$). After $T = 48$ hrs the population within the aerobic batch culture appears to enter the stationary phase of growth and OD_{600 nm} measurements began to decrease after 72 hrs of incubation. Co-culture density within the stirred batch culture vessel steadily increased for the entire length of incubation, reaching a final optical density similar to that within the aerobic batch vessel at $T = 96$ hrs ($\text{OD}_{600 \text{ nm}} \approx 3.5$).

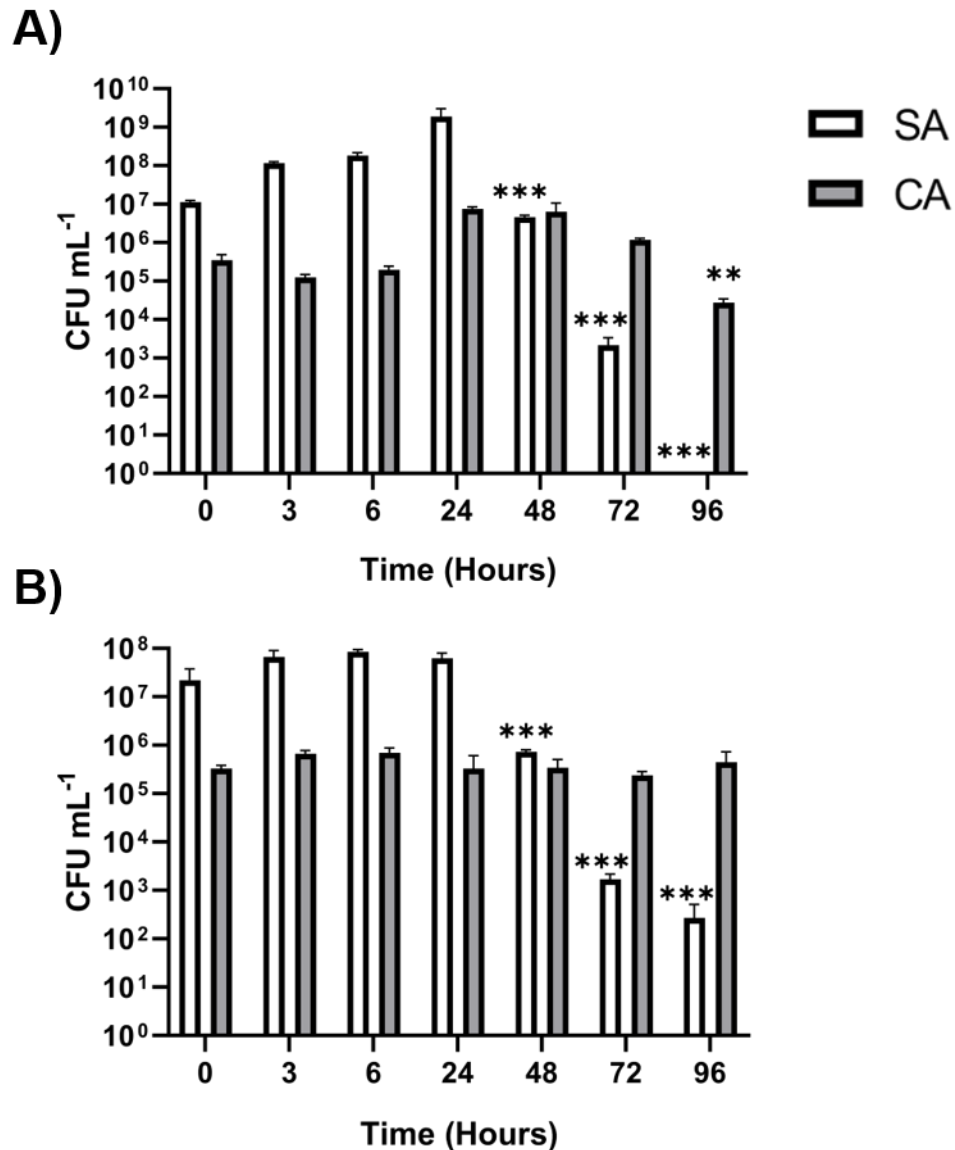


Figure 3.8 SA-CA co-culture grown in batch culture conditions.

Viable cell counts (CFU mL⁻¹) of *S. aureus* 25923 (SA, white bars) and *C. albicans* SC5314 (CA, grey bars) during co-culture in ASM in **(A)** aerobic batch culture and **(B)** stirred batch culture conditions. Data represented as mean \pm standard deviation from three independent experiments. Asterisks represent significant (** $P < 0.005$, *** $P < 0.001$) differences in CFU mL⁻¹ counts in comparison with the data from the 24 hrs time point.

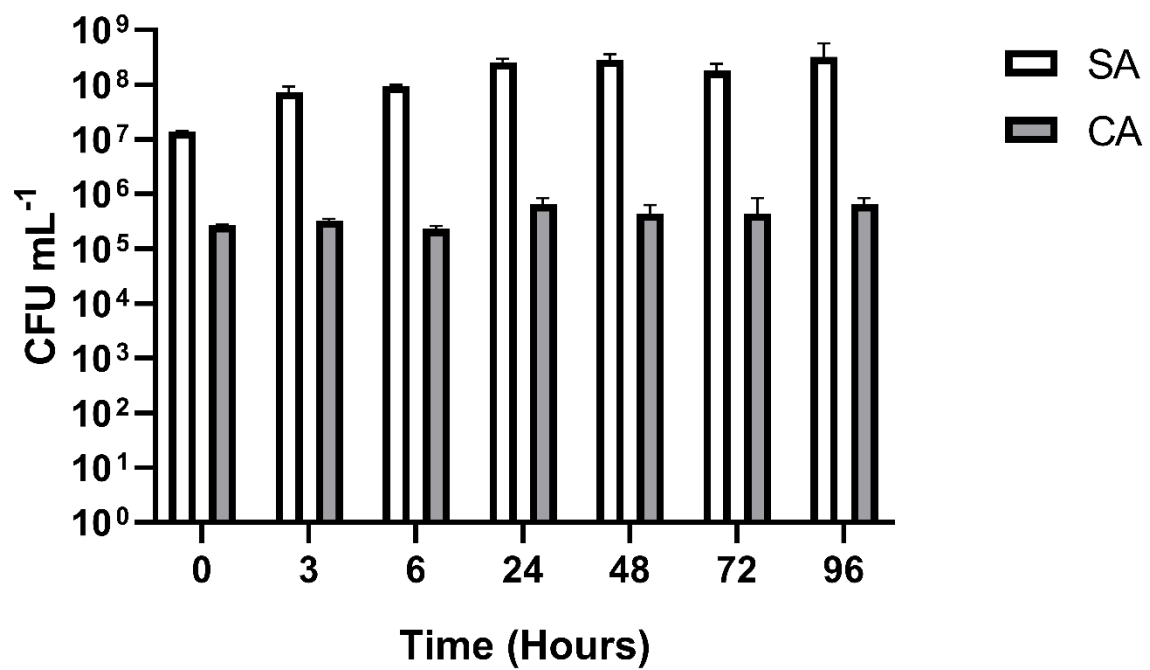


Figure 3.9 SA-CA co-culture grown under continuous-flow conditions.

Viable cell counts (CFU mL⁻¹) of *S. aureus* 25923 (SA, white bars) and *C. albicans* SC5314 (CA, grey bars) during co-culture in ASM in the continuous-flow model. Flowrate (Q) = 145 μ L min⁻¹. Data represented as mean \pm standard deviation from three independent experiments.

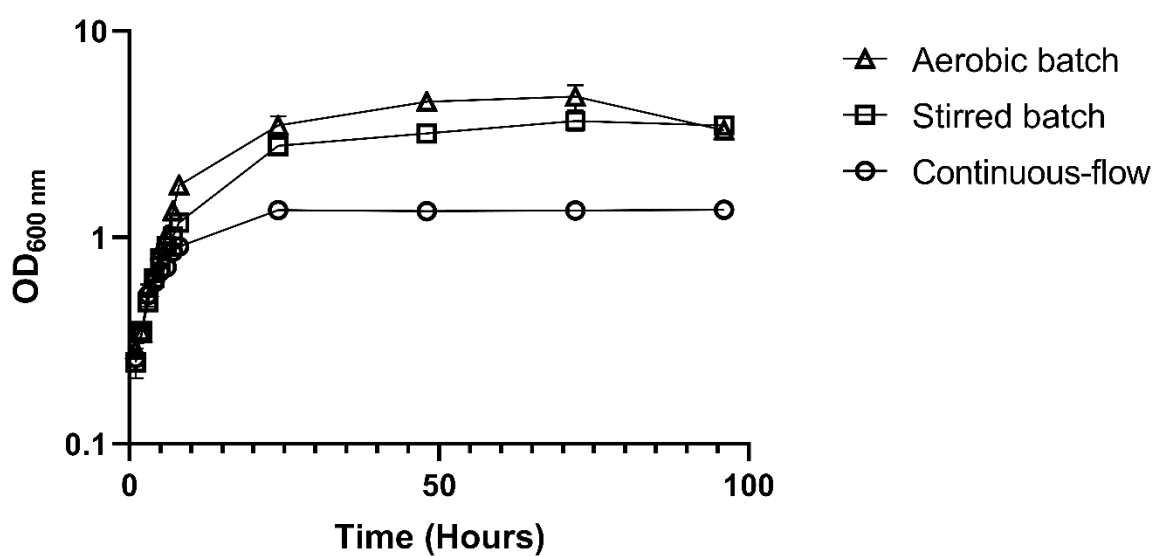


Figure 3.10 Growth of SA-CA co-cultures in batch and continuous-flow conditions.

Growth (monitored as OD_{600 nm}) of *S. aureus* 25923 and *C. albicans* SC5314 dual species co-cultures in ASM in aerobic batch (triangles), stirred batch (squares) and continuous-flow (circles) growth conditions. $Q = 145 \mu\text{L min}^{-1}$ in the continuous-flow culture vessel. Data represented as the mean \pm standard deviation from three independent experiments.

3.6 Triple species co-culture

3.6.1 Comments

The continuous-flow model can readily maintain dual species co-cultures of PA-SA, PA-CA and SA-CA that would ordinarily outcompete one another under batch culture conditions. I next wanted to determine if all three species could be maintained as a stable, steady-state polymicrobial community within the continuous-flow culture vessel. To the best of my knowledge, this is the first study to experimentally co-culture all three of these microorganisms associated with CF airway infections.

3.6.2 Batch culture

During triple species batch culture growth, both SA and CA were outcompeted by PA (*Figure 3.11*). Under aerobic batch culture conditions, a significant decline ($P < 0.001$) in SA CFUs recovered at each sampling point following $T = 24$ hrs was observed and no viable CA cells could be recovered from the flask at $T = 72$ hrs (*Figure 3.11.A*). No significant difference ($P > 0.1$) in PA CFU mL⁻¹ measurements occurred after $T = 24$ hrs. It should be noted that unlike the PA-SA dual species co-culture under aerobic batch conditions (*Section 3.3.2*), SA cells could still be recovered from the culture vessel at $T = 96$ hrs. When co-cultured under stirred batch conditions PA titres remained high ($\approx 10^9$ CFU mL⁻¹) and did not appreciably change ($P > 0.1$) after 24 hrs of incubation (*Figure 3.11.B*). In contrast, a significant decline ($P < 0.01$) in SA CFUs recovered from the flask occurred at each sampling point after $T = 24$ hrs. The slower removal of SA under stirred batch conditions, compared with aerobic batch conditions, was accompanied by a decreased rate in the decline of CA titres in the vessel after 24 hrs of incubation also.

3.6.3 Continuous-flow culture

A stable triple species co-culture of PA, SA and CA could be maintained in the continuous-flow culture vessel using $Q = 145 \mu\text{L min}^{-1}$ (*Figure 3.12*). After 24 hrs of incubation, all species reached a steady-state carrying capacity in the culture vessel and no significant difference ($P > 0.1$) in CFU mL⁻¹ counts for any species in the co-culture occurred following this point. Titres of PA and SA remained at $\approx 10^8$ CFU mL⁻¹ and CA titres ($\approx 10^5$ CFU mL⁻¹) were maintained at just 0.05% of the total population cell density present in the culture vessel.

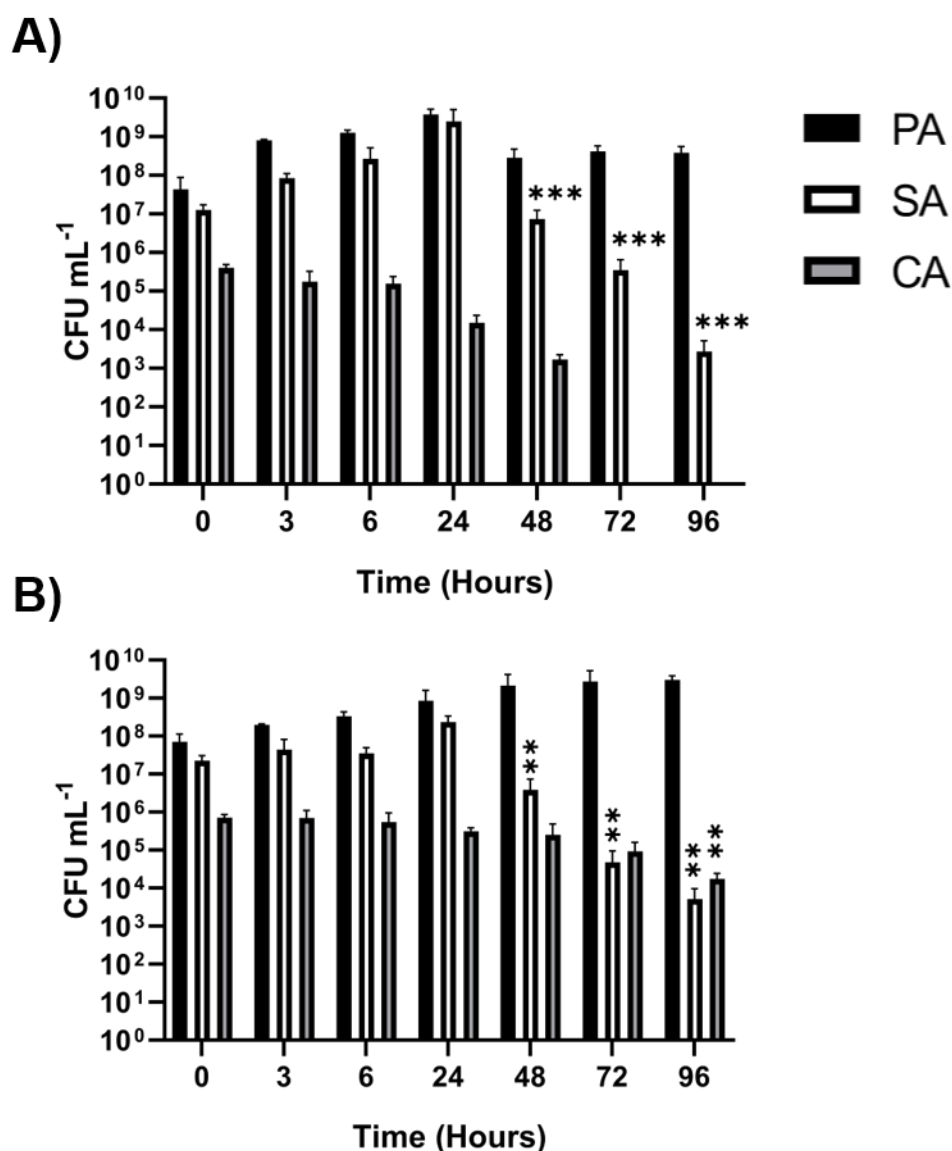


Figure 3.11 Triple species co-culture grown in batch culture conditions.

Viable cell counts (CFU mL⁻¹) of *P. aeruginosa* PAO1 (PA, black bars), *S. aureus* 25923 (SA, white bars) and *C. albicans* SC5314 (CA, grey bars) during co-culture in ASM in **(A)** aerobic batch culture and **(B)** stirred batch culture conditions. Data represented as mean \pm standard deviation from three independent experiments. Asterisks represent significant (** $P < 0.005$, *** $P < 0.001$) differences in CFU mL⁻¹ counts in comparison with the data from the 24 hrs time point.

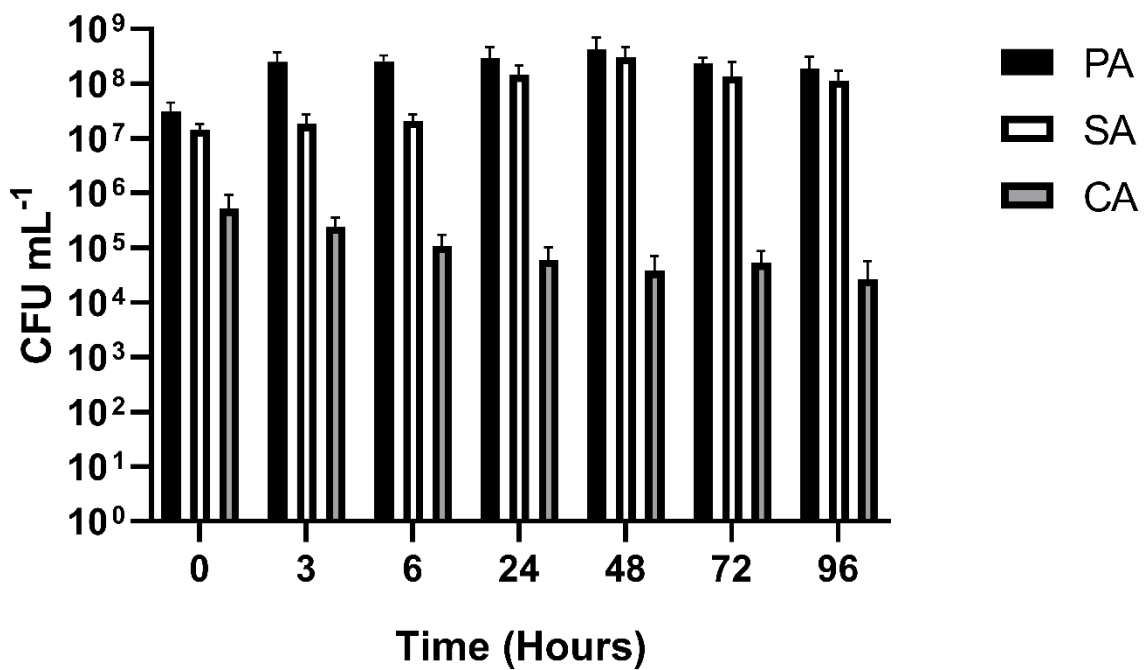


Figure 3.12 Triple species co-culture under continuous-flow conditions.

Viable cell counts (CFU mL⁻¹) of *P. aeruginosa* PAO1 (PA, black bars) *S. aureus* 25923 (SA, white bars) and *C. albicans* SC5314 (CA, grey bars) during co-culture in ASM in the continuous-flow model. Flowrate (Q) = 145 μ L min⁻¹. Data represented as mean \pm standard deviation from three independent experiments.

3.6.4 OD_{600 nm} Measurements

When comparing OD_{600 nm} measurements of the triple species co-cultures under the different culture conditions, the density of the aerobic batch co-culture is significantly higher ($P < 0.05$) than the continuous-flow and stirred batch cultures after $T = 4$ hrs (Figure 3.13). Culture density of the aerobic batch population then plateaued after 24 hrs of incubation ($OD_{600\text{ nm}} \approx 3.5$) and a significant decrease ($P < 0.0001$) in OD_{600 nm} values occurred at $T = 72$ hrs. Contrastingly, density of the continuous-flow and stirred batch co-cultures increases steadily for the first 48 hrs of incubation and no significant change ($P > 0.05$) in the culture density of either population occurred at the points following this. Culture density of the continuous-flow co-culture was significantly lower than both the aerobic batch ($P < 0.0001$) and stirred batch ($P < 0.001$) co-cultures after 24 hrs of incubation. OD_{600 nm} values of the continuous-flow co-culture remained approximately two units lower than the stirred batch culture for the entirety of the incubation period.

3.7 Conclusions

Using the simple continuous-flow model it is possible to maintain long-term *in vitro* co-cultures of three distinct microbial species (PA, SA and CA) associated with CF airway infections. Ordinarily these species would outcompete one another when co-cultured under batch culture conditions. These results indicate the continual supply of fresh media and removal of waste products is crucial for permitting the maintenance of polymicrobial co-cultures. The finding that CA is able to outcompete SA when co-cultured under batch conditions, despite comprising just 0.1% of the total microbial population after 24 hrs incubation, affirms the notion that a numerically minor members of a microbiota can impinge the growth of other species present within a polymicrobial population. Furthermore, the decreased rate of SA removal from the triple species co-culture when compared with the PA-SA dual species co-culture under the same conditions suggests CA, present at just 0.05% of the population, can protect SA from PA to some degree. This could be through a modulation of virulence factor production *via* interspecies interactions, such as the production of farnesol, but this would require further investigation. Taken together, these findings confirm the importance of viewing CF as polymicrobial infection and not simply studying the major pathogens in isolation.

A slower rate of species out-competition was observed in the stirred batch culture vessels when compared with the aerobic batch co-cultures of the same species. This may be due to the increased growth rate of species co-cultured under the aerobic batch conditions, evidenced by increased OD_{600 nm} measurements during the first 8 hrs of growth. Populations will grow to higher cell densities faster and quickly deplete the limited supply of nutrients,

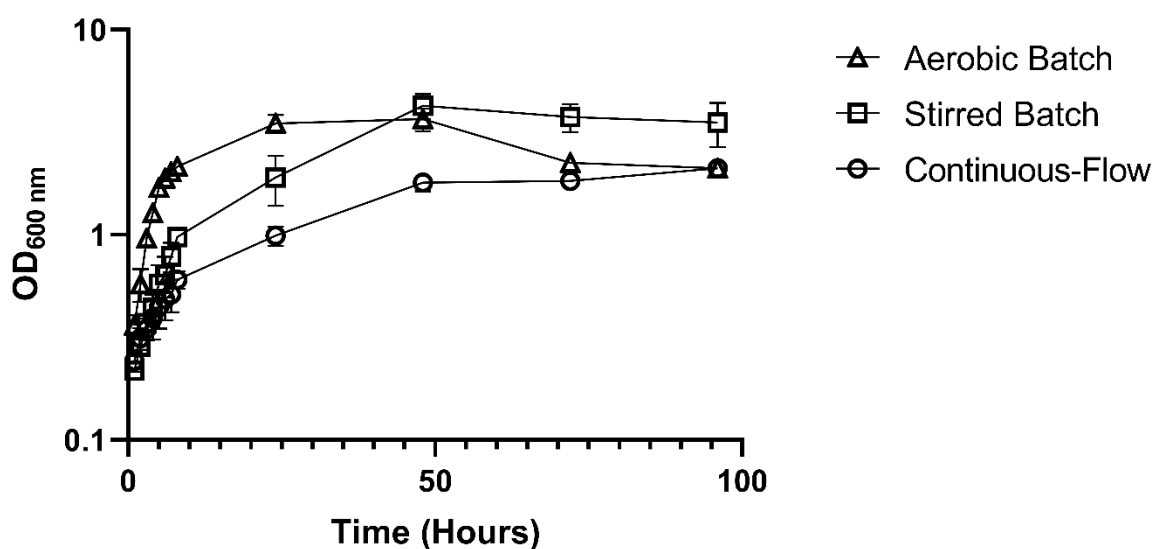


Figure 3.13 Growth of triple species co-culture in batch and continuous-flow conditions.

Growth (monitored as OD_{600 nm}) of *P. aeruginosa* PAO1, *S. aureus* 25923 and *C. albicans* SC5314 triple species co-cultures in ASM under aerobic batch (triangles), stirred batch (squares) and continuous-flow (circles) growth conditions. $Q = 145 \mu\text{L min}^{-1}$ in the continuous-flow culture vessel. Data represented as the mean \pm standard deviation from three independent experiments.

leading to an increase in interspecies competition and a faster removal of species from a co-culture. Additionally, less vigorous aeration of the stirred batch culture vessel may limit oxygen availability amongst the culture. Hypoxic conditions have been identified to prolong the lag-phase of microbial growth (Sabra et al., 2002). Furthermore, the action of PqsH, the enzyme responsible for catalysing the final step of PQS synthesis, is reliant on oxygen availability (Schertzer et al., 2010). Therefore, a decrease in the expression of PQS-controlled virulence factors and other gene may occur under these conditions. No information is available on how oxygen limitation affects the expression of CA virulence factors, but studies on other fungi (*A. fumigatus* and *Saccharomyces pombe*) suggest a down-regulation of virulence factor expression also occurs (Grahl et al., 2012).

OD_{600 nm} measurements were utilised to compare the total culture density of microbial populations. For every species co-culture combination, the density of the continuous-flow culture was kept below that of the batch cultures. For all dual species co-cultures, no significant changes in OD_{600 nm} values occurred after 24 hrs of incubation. Indicating the entire population is maintained at steady-state and does not enter the death phase of growth. Within the triple species continuous-flow vessel the culture density did increase after 24 hrs of incubation, this is due to Q being reduced to prevent the washout of CA from the co-culture. As PA and SA have a constant growth rate in ASM, the total culture density gradually increases over the entire period of incubation.

The results presented in this chapter provide the groundwork for the development of an *in vitro* culture model to permit the co-culture of an entire polymicrobial community associated with CF airway infections. They also provide proof-of-principle for an experimentally tractable model for studying long-term microbial co-cultures in conditions resembling the CF microenvironment.

4. Characterisation of Cultures

4.1 Introductory comments

As demonstrated in *Section 3*, polymicrobial communities of key pathogens associated with CF airway infections can be maintained for extended periods of time in the continuous-flow model. The work presented in this chapter aimed to characterise the metabolic state and mutability of microbial populations cultured in the model. Alongside investigating how the presence of co-cultivated species affects the accumulation of quorum sensing (QS) molecules and virulence-associated factors in the different conditions of growth to better understand why competition between species is decreased in the continuous-flow culture vessel. This work, where indicated, has been published in *Frontiers in Microbiology*.

4.2 Metabolic state of continuous-flow culture

To determine the metabolic state and growth phase of populations maintained in my continuous-flow model, the relative expression of exponential phase and stationary phase-specific genes was compared between mono-species PA populations cultured in stirred batch and continuous-flow conditions. As described in *Section 2.6*, four genes up-regulated during exponential growth and four genes up-regulated during the stationary phase of growth were targeted for quantitative real-time PCR (RT-PCR) analysis. These genes were selected from a published transcriptomic dataset gathered by former Welch Lab member Dr Helga Mikkelsen, studying PAO1 growth in AGSY growth medium (Mikkelsen et al., 2007). By targeting eight genes encoding different products differentially expressed between the exponential and stationary phases of growth, discrepancies in the expression of genes due to differences in growth media should be mitigated, making more obvious any general trends regarding the metabolic state of the culture. All RT-PCR results were normalised by quantifying the expression of the constitutively expressed 16S rRNA gene (Clarridge, 2004, Kolbert and Persing, 1999, Woese, 1987) and results analysed using the comparative $\Delta\Delta C_t$ method (Giulietti et al., 2001).

The relative expression of all target genes in a mon-species culture of PAO1 under continuous-flow conditions ($Q = 170 \mu\text{L min}^{-1}$) compared with stirred batch culture conditions ($Q = 0 \mu\text{L min}^{-1}$) over 96 hrs of incubation are shown in *Figure 4.1*. Interestingly, at $T = 6$ hrs (mid-log phase of PAO1 growth in ASM) all genes were expressed at higher levels in the continuous-flow culture relative to the batch culture. However, the differences in relative expression levels between the two cultures at 6 hrs of incubation are significantly smaller than at subsequent timepoints, suggesting that there is little difference in the expression of the

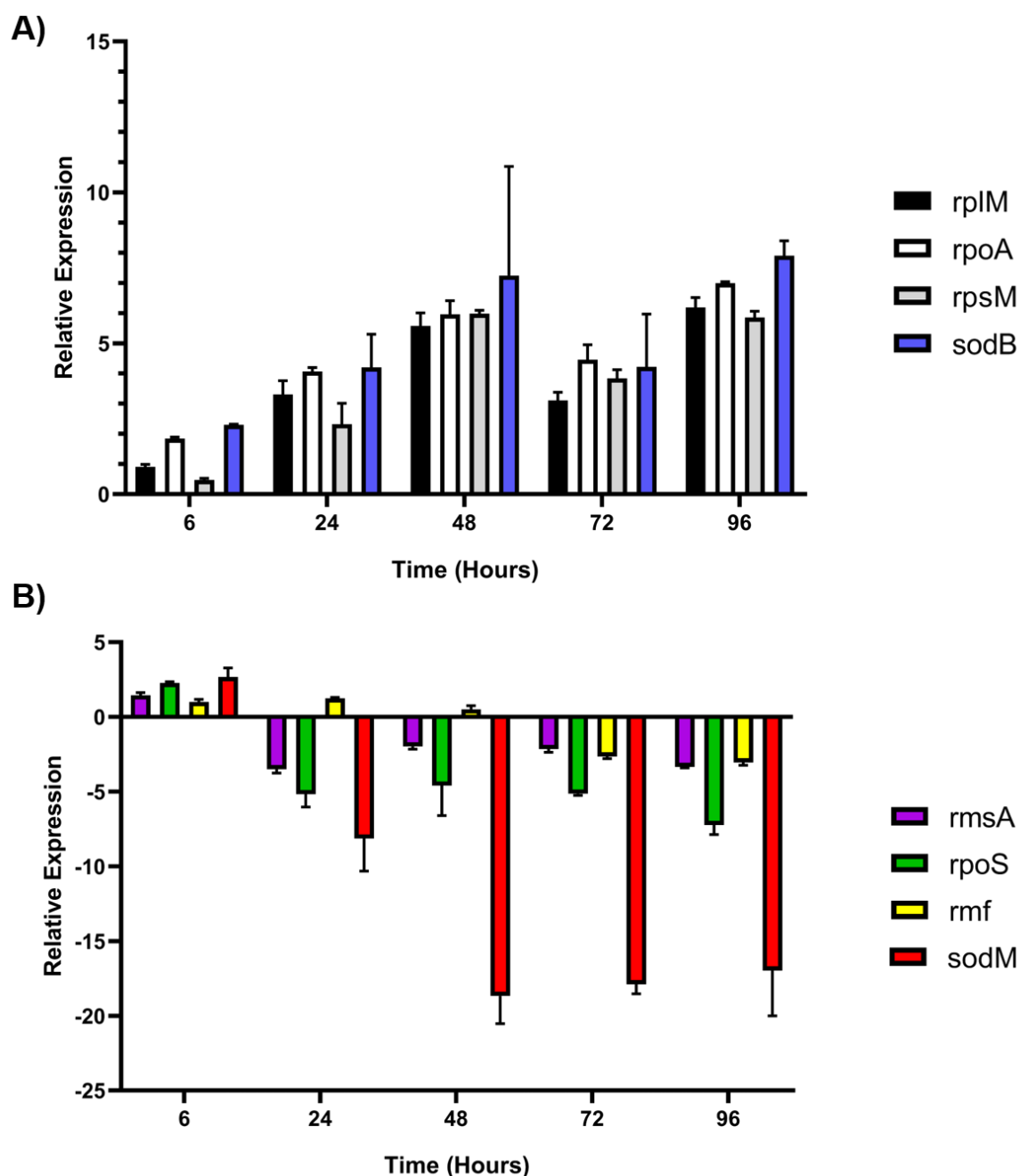


Figure 4.1 Relative expression of exponential and stationary phase specific genes by PA grown in batch and continuous-flow conditions.

The fold change in the expression of the listed genes between *P. aeruginosa* PAO1 mono-species cultures under continuous-flow ($Q = 170 \mu\text{L min}^{-1}$) and stirred batch ($Q = 0 \mu\text{L min}^{-1}$) conditions. **(A)** Genes associated with exponential growth phase; **(B)** genes associated with stationary phase of growth. Cycle threshold (C_t) values obtained by quantitative real-time PCR were normalised against expression of the 16S rRNA housekeeping gene and analysed using the comparative $\Delta\Delta C_t$ method. Data represented as the mean \pm standard deviation of three independent experiments.

target genes between the two culture conditions during this stage of growth. A significant increase ($P < 0.05$) in the relative expression of all genes associated with the exponential phase of growth occurs by $T = 24$ hrs (*Figure 4.1.A*). No significant change ($P > 0.05$) in the relative expression of *rpIM* (encoding an early assembly protein of the 50S ribosomal subunit) or *rpoA* (encoding DNA-directed RNA polymerase α -chain) occurs after 24 hrs of incubation. A significant increase ($P < 0.05$) in the relative expression of *rpsM* (encoding the 30S ribosomal subunit protein, S13) and *sodB* (encoding a superoxide dismutase) occurs between $T = 24$ hrs and $T = 96$ hrs. At the final point of sampling all exponential phase associated genes are expressed >5.5 units higher in the continuous-flow culture relative to the stirred batch culture.

Genes associated with the stationary phase of growth are displayed in *Figure 4.1.B*. All genes, except for *rmf*, had negative relative expression values by $T = 24$ hrs, indicating their decreased expression in the continuous-flow culture compared with the batch culture. The relative expression of *rmf* (encoding a ribosomal modulation factor that converts the 70S subunit to its inactive dimeric 100S form during the stationary phase) steadily decreases over time, becoming a negative value by $T = 72$ hrs. No significant difference in the relative expression of *rmsA* (encoding a putative carbon storage regulator) or *rpoS* (encoding an alternative sigma factor associated with the stationary phase stress response) occurred after 24 hrs of incubation. A significant decrease ($P < 0.0001$) in the relative expression of *sodM* (encoding a superoxide dismutase) occurred between $T = 24$ and $T = 48$ hrs, and relative expression values for this gene remained below -16.9 for the remainder of the incubation period. By the final point of sampling, all stationary phase associated genes were relatively expressed at fewer than -3.0 relative units under continuous-flow conditions compared with stirred batch conditions.

In summary, all exponential phase associated genes were positively up-regulated and all stationary phase associated genes negatively expressed under continuous-flow conditions relative to stirred batch conditions. Taken together, these results provide strong evidence to indicate that microbial populations maintained at a steady-state carrying capacity in the culture vessel remain metabolically active and do not enter the stationary phase of growth over the course of incubation.

4.3 Estimation of mutation rates

4.3.1 Comments

As discussed in *Section 1*, a possible use of the continuous-flow culture model would be to investigate how the presence of co-cultivated species affects the evolutionary trajectory of a

polymicrobial community. I therefore wanted to ensure that the co-culturing species and maintenance of populations in a steady-state carrying capacity for extended periods of time had no adverse effects on the mutability of members of the consortium. To investigate this, I determined the mutation rate (μ) of PA and SA when cultured independently or as a dual-species co-culture under continuous-flow and batch culture conditions using the methods described by Foster (2006), *Section 2.7*. Changes in μ overtime in the continuous-flow vessel were determined by measuring mutant accumulation (Kubitschek and Gustafson, 1964, Novick and Szilard, 1950) shortly after a steady-state population was attained ($T = 24$ hrs) and at the end of the experiment ($T = 96$ hrs). A modified version of the Luria-Delbrück fluctuation assay (Luria and Delbrück, 1943) and Jones median estimator (Jones et al., 1994) were used to determine μ for batch culture populations at $T = 24$ hrs, as described in *Section 2.7.3*. The emergence of spontaneous ciprofloxacin resistant (cip^r) isolates and rifampicin resistant (rif^r) isolates was used as a proxy to experimentally infer the rate of spontaneous mutation within a population. Part of the work in this section is published in *Frontiers in Microbiology* (O'Brien and Welch, 2019a).

To ensure that mutations in the genes responsible for conferring resistance to either ciprofloxacin or rifampicin did not provide a selective advantage or disadvantage for the growth of species under the culture conditions, potentially skewing any observations, the emergence of either cip^r or rif^r isolates in independent experiments was measured. It should be noted that due to differences in experimental design and methods for estimating mutation rates in a continuously dividing population (continuous-flow) or a population that enters the stationary phase of growth (batch culture), values for μ cannot be directly compared between assays.

4.3.2 Continuous-flow mutation rates

The mean number of rif^r -conferring and cip^r -conferring mutations per cell division are displayed in *Figure 4.2*. There was no significant difference ($P > 0.1$) in the values for μ calculated between samples when using either the emergence of rif^r -isolates (*Figure 4.2.A*) or cip^r -isolates (*Figure 4.2.B*) as proxy to estimate rates of spontaneous mutation. Values calculated for μ were between 8.97×10^{-9} and 2.55×10^{-8} mutations per cell division for all samples and timepoints. These values are comparable with previously reported PA and SA mutation rates (Dettman et al., 2016, Schaaff et al., 2002). Importantly, there was no significant change ($P > 0.1$) in μ between the cultures sampled at $T = 24$ hrs or $T = 96$ hrs and no significant difference ($P > 0.1$) in mutations per cell division of PA or SA when cultured axenically or as a co-culture. Taken together these results demonstrate that mutation rates remain stable and do not alter

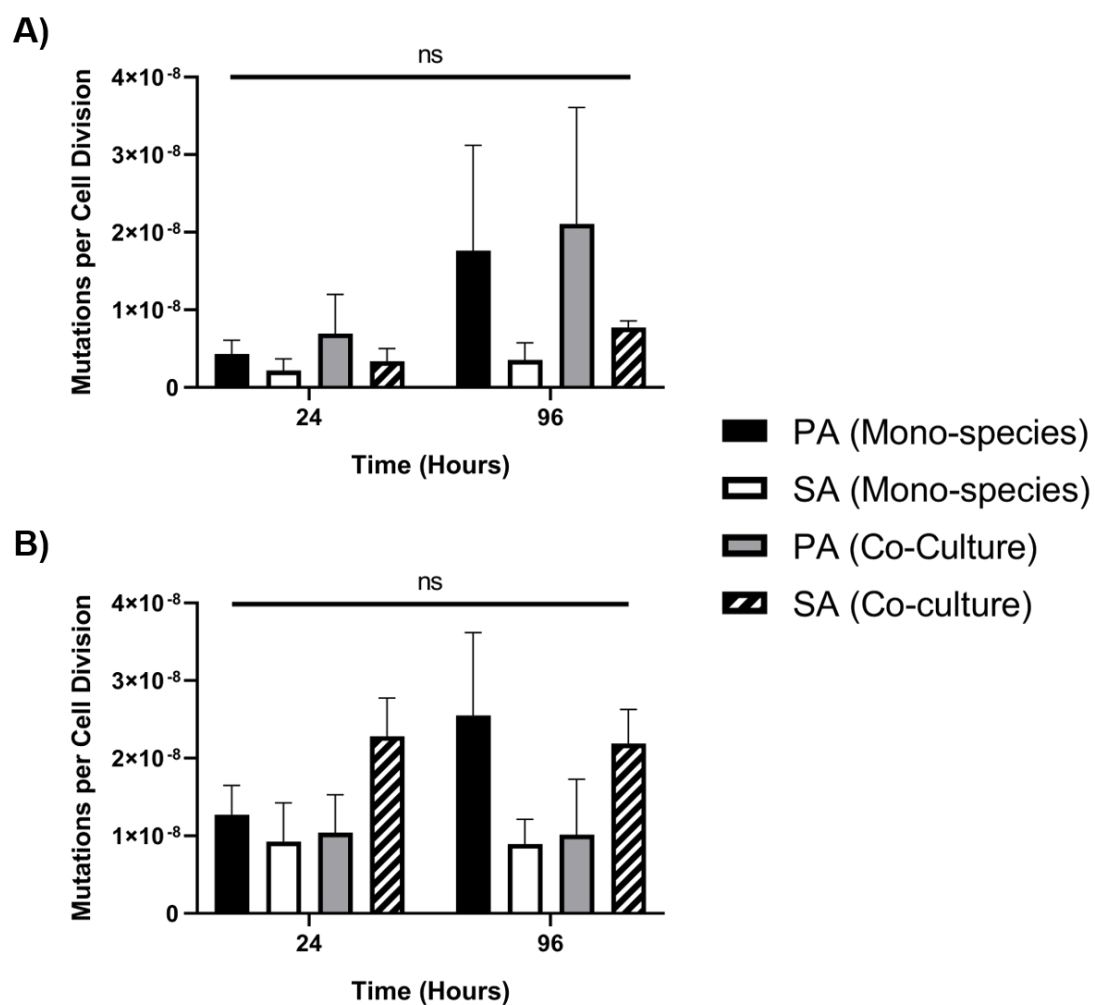


Figure 4.2 Estimation of mutation rates in the continuous-flow culture vessel.

Assumed mutation rates of *P. aeruginosa* PAO1 and *S. aureus* 25923 during single-species and dual species co-culture in the continuous-flow model after 24 and 96 hrs of incubation. Mutation rates were calculated as **(A)** the number of rif^r-conferring mutations per cell division, or **(B)** the number of cip^r-conferring mutations per cell division, using the methods described by (Foster, 2006). Data represented as the mean \pm standard deviation from three independent experiments. $P > 0.05$ is considered no significant difference (ns).

over time under continuous-flow conditions and that the maintenance of steady-state co-cultures of PA and SA in the model has no adverse effects on the mutability of either species.

4.3.3 Batch culture mutation rates

Mutation rates for PA and SA mono-species and dual species cultures incubated for 24 hrs under batch conditions are shown in *Figure 4.3*. As methods to estimate μ within a batch culture rely on the population not entering the death phase of growth, the $T = 96$ hrs point of sampling is not possible for this assay. As in *Section 4.3.3*, there was no significant difference ($P > 0.2$) in values for μ calculated using the emergence of *rif^r*-isolates (*Figure 3.3.A*) or *cip^r*-isolates (*Figure 4.3.B*) as a proxy to estimate the rate of spontaneous mutation amongst the populations cultured under batch conditions. There was a significant ($P < 0.05$) log-fold decrease in the mean number of *rif^r*-conferring mutations per cell division between PA cultured axenically and as a co-culture with SA. Similarly, a significant ($P < 0.01$) decrease in the mean number of *cip^r*-conferring mutations per cell division also occurred between PA cultured alone or as a batch co-culture with SA. No spontaneous *rif^r* or *cip^r* SA isolates could be recovered from the dual species co-culture, despite viable SA cells being recovered at $\approx 10^4 - 10^5$ CFU mL⁻¹ from the culture vessel at this point of sampling. As such, no value for μ can be calculated for SA when co-cultured with PA under batch conditions.

4.3.4 Conclusions

No significant difference in the assumed rate of mutation of any culture was observed when measuring the emergence of spontaneous *rif^r* or *cip^r* isolates in a population. This indicates that the acquisition of mutations conferring resistance to rifampicin or ciprofloxacin does not affect the fitness and growth of species in ASM under these culture conditions, and that values for μ are reliable. Furthermore, the mutation rates of species cultured under continuous-flow conditions remained unchanged irrespective of the length of incubation or presence of other species in the culture. This finding provides strong evidence to demonstrate that the maintenance of microbial populations at a steady-state in the continuous-flow culture vessel does not adversely affect the mutability of members of the population. This, in turn, reinforces the notion that the model is suitable for studying how the presence of co-habiting species may impact upon the evolutionary trajectory of a polymicrobial consortium.

By contrast the mutation rates of axenic and dual species populations were not stable under batch culture conditions, as evidenced by the significant decrease in μ observed when PA and SA are co-cultured together. This result contradicts the findings of Frapwell *et al.* (2018), who

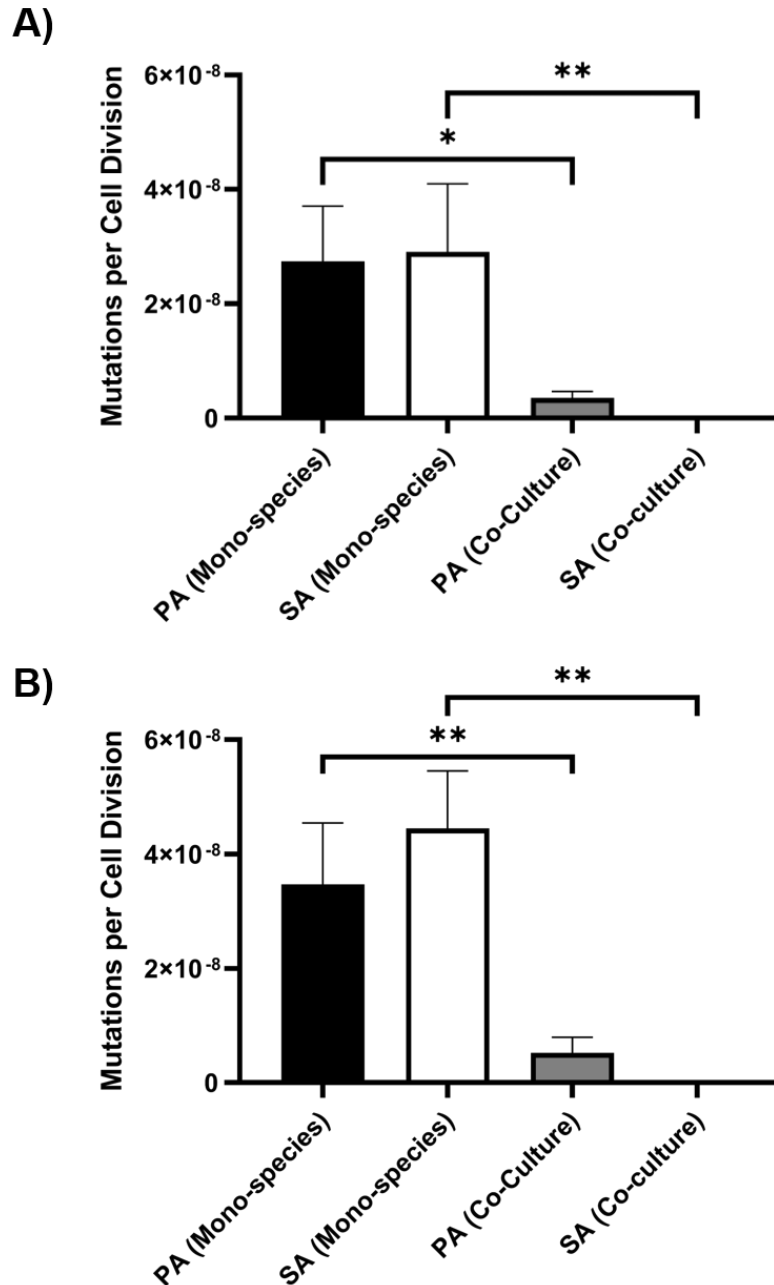


Figure 4.3 Estimation of mutation rates during batch culture.

Assumed mutation rates of *P. aeruginosa* PAO1 and *S. aureus* 25923 during single-species and dual species co-culture in batch culture conditions after 24 hrs of incubation. Mutation rates were calculated as **(A)** the number of rif^r-conferring mutations per cell division, or **(B)** the number of cip^r-conferring mutations per cell division, using the methods described by (Foster, 2006). Data represented as the mean \pm standard deviation from three independent experiments. Asterisks represent significant (* $P < 0.05$, ** $P < 0.01$) difference in mutations per cell division.

suggest that the genomic mutation rate of PA and SA is elevated during co-culture as a biofilm. Differences in the planktonic and biofilm microbial lifestyles may explain the inverse trend observed in this study, especially given that a 100-fold increase in μ has been previously reported between axenic planktonic and biofilm cultures of PA (Conibear et al., 2009) and that mutations are thought to accumulate more readily in biofilm populations (Banas et al., 2007). However, it is important to consider that stress and population density have also been found to affect the mutability of microbial species (Aanen and Debets, 2019, Frenoy and Bonhoeffer, 2018, Krašovec et al., 2014, Krašovec et al., 2017). Therefore, the increased competition for space and limited resources under batch culture conditions is likely to impose enhanced selection pressures on all members of a population. As previously mentioned, the acquisition of spontaneous mutations conferring resistance to rifampicin or ciprofloxacin are not likely to impact upon the fitness or growth of species in ASM. As such, mutations beneficial for the survival or improved competition between co-cultured species are likely to be selected for under batch culture conditions, possibly explaining the decrease in rif^r and cip^r isolates observed in the batch culture fluctuation tests. For these reasons, the co-culture of species using traditional batch culture approaches are pivotal in identifying genes essential for competition and survival in an acute infection setting. However, these culture methods say little about how a polymicrobial community evolves naturally over time, whereas the continuous-flow model provides a means to test this process in a seemingly unbiased and robust manner.

4.4 Pyocyanin quantification

4.4.1 Comments

As discussed in *Section 1.4*, PA produces a wide array of secreted extracellular factors such as phenazines, associated with virulence and competition between microbial species in the CF microenvironment. The most abundantly secreted phenazine by PA is pyocyanin, a blue-green redox-active pigment. The exact physiological role(s) of pyocyanin remain unclear but the compound has potent-antimicrobial activity and in its reduced form pyocyanin can react with molecular oxygen to form toxic reactive oxygen species (Baron and Rowe, 1981, Lau et al., 2004, Muller, 2002, Noto et al., 2017). As described in *Section 2.8*, the concentration of pyocyanin in the supernatant of a microbial population can be easily assayed *via* chloroform extraction of the pigment and photometric methods (Knight et al., 1979). Thus, quantification of pyocyanin was used as a simple proxy to assess the general virulence factor production by PA within mono-species and mixed species populations grown under the different culture

conditions described in *Section 2.3*. The work presented in this section is published in *Frontiers in Microbiology* (O'Brien and Welch, 2019a).

4.4.2 Concentration of pyocyanin

The concentration of pyocyanin present in the culture supernatant of mono-species and mixed species populations containing PA under continuous-flow and batch culture conditions after 96 hrs of incubation is shown in *Figure 4.4*. Axenic SA and CA cultures and the SA-CA co-culture produce no pyocyanin (data not shown). The endpoint concentration of pyocyanin was significantly lower ($P < 0.0001$) in the supernatant of all microbial species combinations grown under continuous-flow conditions compared with the aerobic and stirred batch cultures. There was no significant difference ($P > 0.3$) in the accumulation of pyocyanin between the different co-culture combinations under continuous-flow conditions, and the concentration of pyocyanin was less than $1.5 \mu\text{g mL}^{-1}$ for all continuous-flow culture supernatants. Under batch culture conditions the presence of SA caused a significant increase ($P < 0.0001$) in the accumulation of pyocyanin in the PA-SA dual species co-culture compared with the mono-species PA culture. Conversely, the presence of CA caused a significant decrease ($P < 0.0001$) in the accumulation of pyocyanin in the PA-CA co-culture under batch culture conditions compared with the mono-species PA culture. The concentration of pyocyanin present in the triple species batch cultures supernatants is significantly lower ($P < 0.0001$) than both the mono-species PA and PA-SA co-culture, yet is significantly higher ($P < 0.0001$) than the PA-CA co-culture.

4.4.3 Conclusions

Pyocyanin accumulation was measured as a proxy to assess the concentration of extracellularly secreted virulence factors present in the supernatants of microbial populations grown under the different culture conditions. The dramatic decrease in the endpoint concentration of pyocyanin observed within the continuous-flow vessel compared with the batch culture populations therefore suggests a likely decrease in the production of other virulence factors and competition between PA and other species in a co-culture under these conditions. This finding, in part, explains why populations of species that would ordinarily outcompete one another during co-culture can be maintained at a steady-state, with respect to microbial titres (*Section 3*), for extended periods of time in the continuous-flow model.

The presence of SA and CA within a co-culture under batch conditions did significantly alter the production of pyocyanin by PA. Just as Korganokar *et al.* (2013) reported that *N*-acetylglucosamine shed from the walls of Gram-positive species can up-regulate the

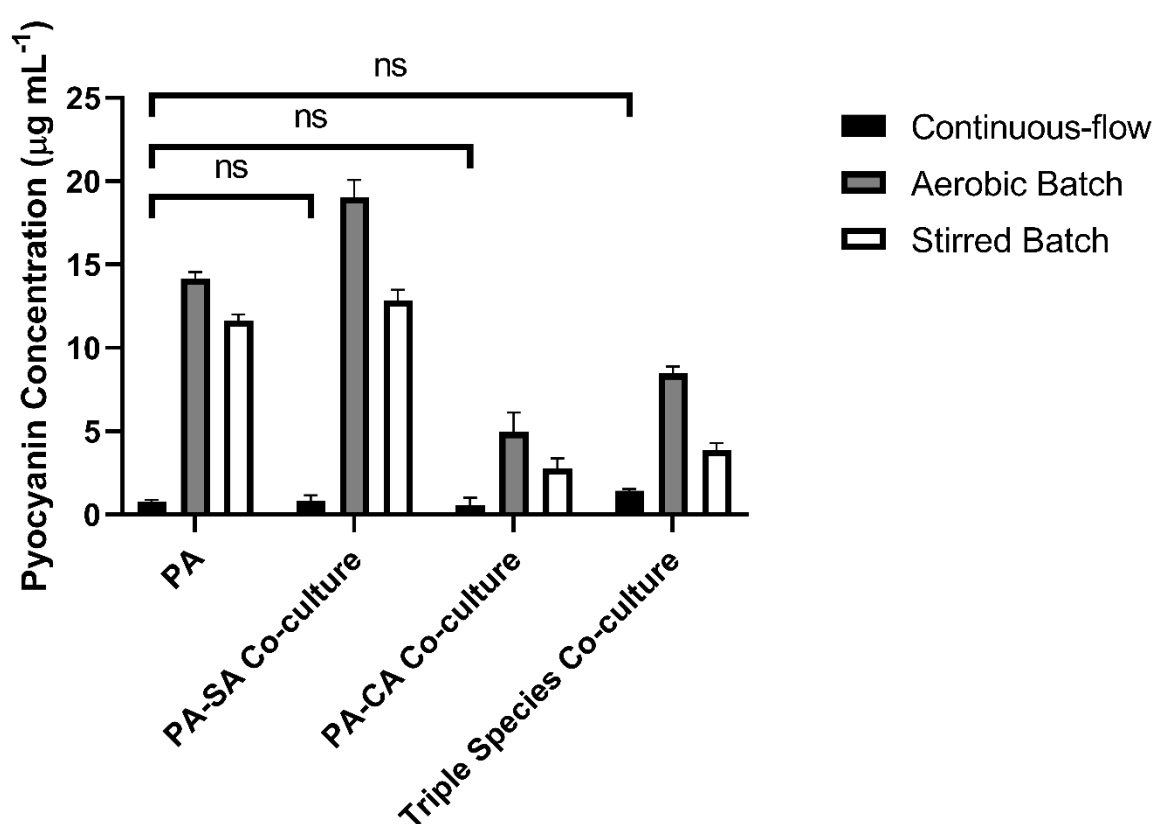


Figure 4.4 Quantification of pyocyanin concentration under different culture conditions.

The concentration ($\mu\text{g mL}^{-1}$) of pyocyanin in the supernatants of single-species and mixed species co-cultures of *P. aeruginosa* PAO1 (PA), *S. aureus* 25923 (SA) or *C. albicans* SC5314 (CA) after 96 hrs of incubation under: continuous-flow (black bars); aerobic batch (grey bars) and; stirred batch (white bars) culture conditions. Data represented as the mean \pm standard deviation of three independent experiments, $P > 0.05$ is considered no significant difference (ns).

production and secretion of PA extracellular virulence factors, SA caused a significant up-regulation in the accumulation of pyocyanin in the PA-SA co-culture. Furthermore, the presence of CA caused a significant decrease in the accumulation of pyocyanin during batch culture growth with PA, despite CA comprising less than 0.1% of the total microbial population of the PA-CA co-culture after 24 hrs of incubation (*Figure 3.4.2*). This is perhaps unsurprising, given that CA produced farnesol (up-regulated during times of stress) can inhibit QS in PA (*Section 1.3.5*) ultimately modulating the expression of genes under the control of this regulatory network, such as pyocyanin (Trejo-Hernández et al., 2014). The complex interplay of interspecies interactions amongst all members present within a polymicrobial consortium can be exemplified in the triple species co-culture. Here the concentration of pyocyanin lies between the values observed for the dual species co-cultures, suggesting that both SA and CA are simultaneously exerting an effect on PA gene expression under these culture conditions. Taken together, these findings strongly affirm the importance of viewing CF airway-associated infections as polymicrobial and to consider the impact which the presence of less abundant or avirulent species may have on the gene expression and virulence factor production by the dominant species and key pathogens.

4.5 Siderophore quantification

4.5.1 Comments

Iron is an important cofactor for many enzymes that catalyse redox reactions, making access to iron an essential requirement for all biological organisms needing to carry out fundamental cellular processes such as replication and respiration (Andrews et al., 2003, Kraemer et al., 2014). Bioavailability of iron is generally low in hosts, but it should be noted that iron levels within CF sputum are raised compared with healthy samples and that increased iron availability in the airways has been correlated with an increased ability of PA to establish persistent infections (Reid et al., 2007). Competition for iron acquisition between species is fierce and many microorganisms secrete iron scavenging molecules, termed siderophores, that bind iron for uptake *via* specific cell surface receptors (Guerinot, 1994, Miethke and Marahiel, 2007). PA is capable of synthesising two siderophores: pyoverdine and pyochelin (Cornelis and Matthijs, 2007), and SA produces a further two siderophores: staphyloferrin A and staphyloferrin B (Laakso et al., 2016). Siderophore production by PA and SA is essential for the full virulence of either species in *in vivo* models (Dale et al., 2004, Takase et al., 2000a, Takase et al., 2000b), where iron bioavailability is limited. Unlike other fungal species the CA genome does not harbour genes for the synthesis of siderophores (Haas, 2003), whereas *A. fumigatus* encodes for two siderophores (Hissen et al., 2004). However, CA does encode the

iron-chelate siderophore transporter complex Sti1/Arn1 enabling CA to uptake siderophores produced by other species (Ardon et al., 2001).

Given the importance of iron acquisition for supporting microbial growth and the wealth of unique siderophore molecules produced by a large number of distinct species, the role of siderophores in mediating interspecies interactions among a polymicrobial population is only now beginning to be realised (Almeida et al., 2009, Bisht et al., 2020, Cornelis and Dingemans, 2013, Harrison et al., 2008, Kramer et al., 2020, Lopez-Medina et al., 2015). Furthermore, the requirement of siderophores to establish full virulence within *in vivo* hosts makes these molecules a good proxy to study generalised virulence factor production amongst a population (Martin et al., 2011). The production of siderophores by cultures grown in ASM was measured using the chrome Azurol S (CAS) assay (Payne, 1994), as described in *Section 2.9*, to elucidate the role of interspecies competition with regards to the acquisition of iron between species cultured in a physiologically relevant CF growth medium under the different culture conditions.

4.5.2 Concentration of siderophores

The concentration of siderophores present in the culture supernatants of single-species and mixed species co-cultures under continuous-flow and batch culture conditions are shown in *Figure 4.5* and *Figure 4.6*, respectively. Single-species cultures of CA produced no siderophores under any culture condition (data not shown). For all species combinations under continuous-flow conditions siderophores were present at a concentration of $<1 \mu\text{M}$, significantly lower ($P < 0.0001$) than the concentration of siderophores present in all batch culture populations. There was no significant change ($P > 0.2$) in the concentration of siderophores present in the continuous-flow cultures over time.

Under aerobic batch culture conditions there was no significant difference ($P > 0.1$) in the concentration of siderophores between any of the species combinations at $T = 24$ hrs (*Figure 4.6.A*). There was a significant ($P < 0.0001$) 4-fold increase in the concentration of siderophores present in the PA mono-species culture between $T = 24$ and 48 hrs and no significant change ($P > 0.8$) in siderophore concentration after 48 hrs of incubation. Furthermore, siderophores were present at significantly higher concentration ($P < 0.001$) in the PA mono-species culture compared with all other species combinations after 48 hrs of incubation. There was a significant ($P < 0.05$) increase in siderophore concentration in the SA mono-species aerobic batch culture between $T = 24$ and 96 hrs of incubation. For the PA-SA dual species co-culture there was a significant ($P < 0.05$) 5-fold increase in siderophore concentration between $T = 24$ and 48 hrs, followed by a significant ($P < 0.05$) decrease in

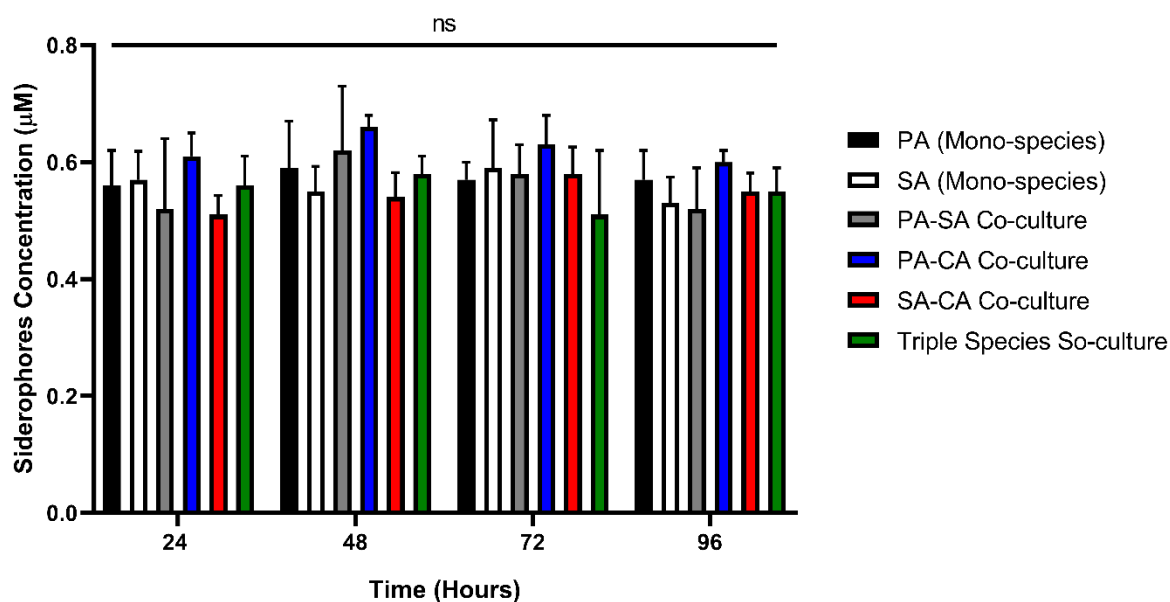
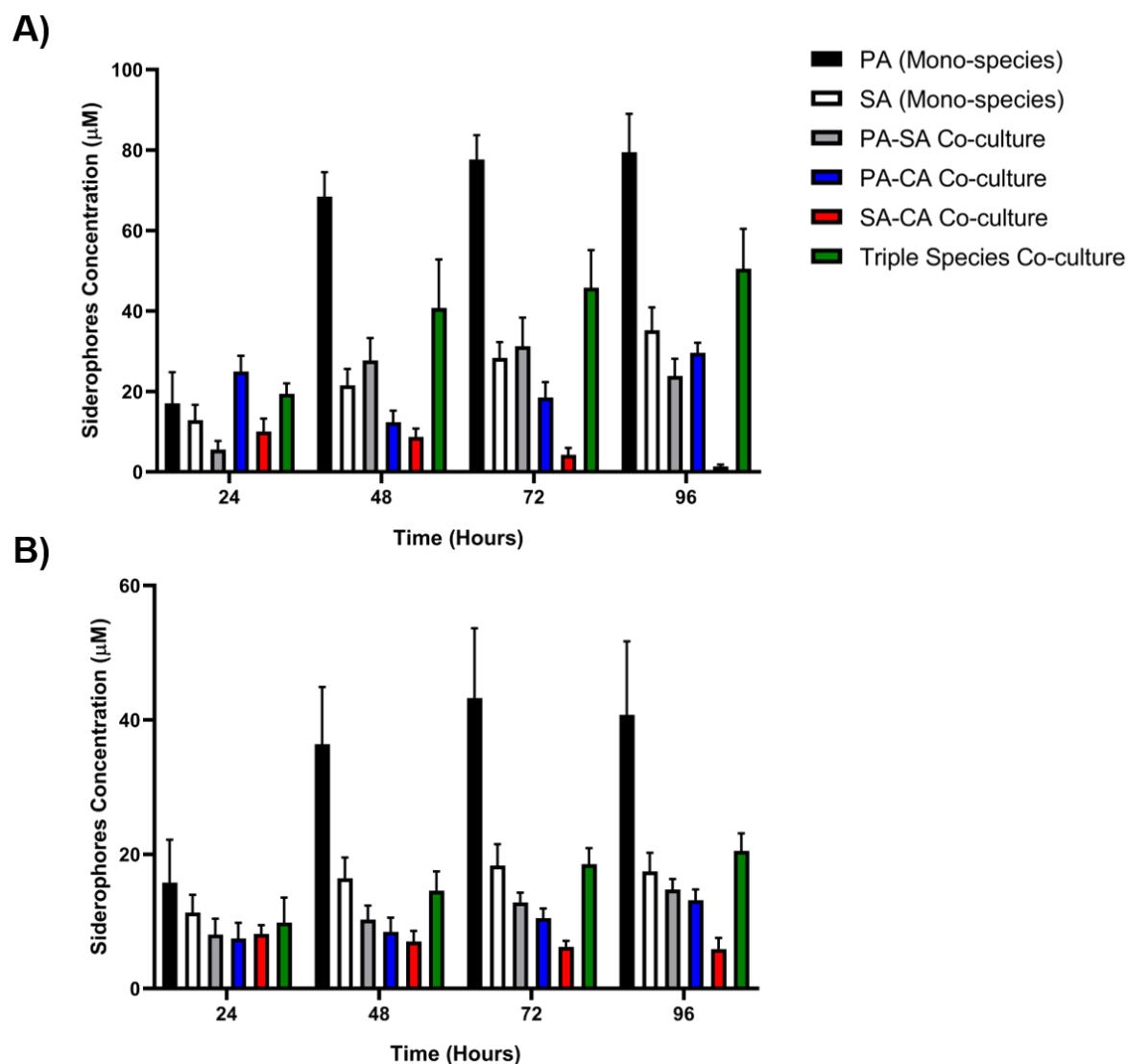


Figure 4.5 Quantification of siderophores under continuous-flow conditions.

Concentration (μM) of siderophores in the culture supernatants of single-species and mixed species populations of *P. aeruginosa* PAO1 (PA), *S. aureus* 25923 (SA) and *C. albicans* SC5314 (CA) cultured under continuous-flow conditions. Data represented as the mean \pm standard deviation of three independent experiments, $P > 0.05$ is considered no significant difference (ns).



siderophore concentration between T = 72 and 96 hrs. The inverse trend was observed for the PA-CA dual species co-culture. A significant ($P < 0.01$) 2-fold decrease in the concentration of siderophores occurred between T = 24 and 48 hrs, followed by a significant ($P < 0.001$) 1.5-fold increase in concentration between T = 72 and 96 hrs. The concentration of siderophores present in the supernatant of the SA-CA dual species co-culture significantly decreased ($P < 0.01$) from $\approx 10 \mu\text{M}$ at T = 24 hrs to just $1.35 \mu\text{M}$ at T = 96 hrs. A significant ($P < 0.001$) 2.6-fold increase occurred for the concentration of siderophores present in the triple species co-culture supernatant between T = 24 and 96 hrs. At the final point of sampling there was no significant difference ($P > 0.05$) in the concentration of siderophores present between the SA mono-species and PA-SA or PA-CA co-cultures, yet siderophores were present at significantly higher ($P < 0.001$) concentrations in the triple-species co-culture and significantly lower ($P < 0.001$) concentrations in the SA-CA co-culture.

As in the aerobic batch cultures, there was no significant difference ($P > 0.05$) in the concentration of siderophores between any species combination under stirred batch conditions at T = 24 hrs (*Figure 4.6.B*). There was a significant ($P < 0.01$) 2.3-fold increase in siderophores concentration in the PA mono-species culture between T = 24 and 48 hrs, followed by no significant change ($P > 0.9$) in values for the remainder of incubation. The concentration of siderophores in the PA mono-species culture was, again, significantly higher ($P < 0.001$) than all other species combinations at T = 48 hrs and the following timepoints. Under stirred batch conditions there was no significant difference in siderophore concentrations over time for any of the other species culture combinations following T = 24 hrs. There was a slight, but not statistically significant, increase in siderophores concentration in the triple species co-culture over the course of incubation and a non-significant, but gradual, decrease in concentration in the SA-CA culture. At the end point of sampling, the concentration of siderophores in the triple species culture was significantly higher ($P < 0.01$) than the SA-CA dual species culture. No significant difference was observed between siderophore concentrations of the SA mono-species, PA-SA or PA-CA dual species co-cultures at T = 96 hrs.

4.5.3 Conclusions

When using the continuous-flow culture vessel, the concentration of siderophores present in all culture supernatants was well below the concentrations observed during growth in batch culture conditions. Unlike the batch culture populations, siderophore concentrations did not change over time or with the presence of different species combinations in the polymicrobial consortium. I therefore hypothesise that under continuous-flow conditions, with a constant

supply of fresh nutrients such as iron (not unlike the situation in the CF airways) there is a decrease in competition for abundant resources among species. As such the production of siderophores, and by extension other virulence factors such as pyocyanin (*Section 4.4*), are reduced. Thus, a stable and steady-state polymicrobial population of PA, SA and CA is maintained for extended periods of time within the model.

There was a large alteration in the concentration of siderophores present in the supernatants of the different species combinations cultured under aerobic batch conditions, particularly after 24 hrs of incubation. Previous studies have established that siderophores are produced at the highest concentration between 24 and 48 hrs of growth (Ferreira et al., 2019), perhaps explaining why at the initial point of sampling there was no significant difference in siderophore concentrations between the differing populations.

Most notably, the presence of SA or CA caused a substantial decrease in the total concentration of siderophores present in the supernatant of co-culture populations when compared with the PA mono-species culture. The decrease in siderophore concentration in the PA-SA co-culture may be attributed to the ability of PA to lyse SA and utilise the resulting lysate as a source of free iron, as described by Mashburn *et al.* (2005), thereby decreasing the need of PA to produce siderophores for iron acquisition under these conditions. Alternatively, SA may down-regulate the production of siderophores *via* an, as yet, unelucidated mechanism. This finding directly contradicts the suggestion by Harrison *et al.* (2008) that co-culturing PA with SA causes an up-regulation in the production of siderophores. However, it should be noted that an iron chelating agent was present in the culture media used for this study. This is likely to not only decrease the bioavailability of iron, but also to chelate iron freed during SA lysis to cause an increased selection pressure for enhanced iron scavenging amongst the population.

As discussed in *Section 3.4*, several antagonistic interactions have been described between PA and CA, including the farnesol-mediated inhibition of QS networks within PA (Cugini et al., 2007, Fourie et al., 2016) and the subsequent suppression of pyochelin and pyoverdine biosynthesis (Lopez-Medina et al., 2015). The finding that the presence of CA caused a more pronounced decrease in siderophore concentration compared with the PA-SA co-culture may be attributable to the inability of CA to produce siderophores of its own, unlike SA. It is key to note that the complete removal of CA from the PA-CA co-culture under aerobic batch conditions by 72 hrs of incubation (*Figure 3.5.A*) was accompanied by an increase in siderophore production by the culture at this point. This demonstrates a clear role for interspecies interactions between the two microorganisms in modulating the production of siderophores by a co-culture. The loss of such interactions upon the removal of CA leads to

the production of siderophores at higher concentrations by the now axenic 'PA-only' population. Similarly, CA also caused a decrease in siderophore concentration in the SA-CA co-culture compared with the mono-species SA culture. This diminution may simply be attributed to the out-competition and complete removal of SA from the population by 72 hrs incubation (*Figure 3.8.A*). However, it is important not to disregard the impact that interspecies interactions may have upon this decrease in siderophore production, especially when considering that, when co-cultured with non-siderophore producing strains of *Enterococcus faecalis*, SA is known to down-regulate siderophore production in a *Caenorhabditis elegans* infection model (Ford et al., 2016).

In summary, the results presented in this section demonstrate that the concentrations of siderophores in the continuous-flow culture vessel are maintained at consistently low levels, irrespective of the length of incubation or combination of species present. By contrast, the presence of co-cultured CA, comprising just 0.05% of the total microbiota under iron limited batch culture conditions, caused a significant modulation in siderophore concentrations, highlighting the essential need to consider the presence of less abundant species when studying polymicrobial infections.

4.6 QS molecules quantification

4.6.1 Comments

As described in *Section 1.3.5*, quorum sensing (QS) regulatory networks coordinate multiple cellular processes, including the production of secondary metabolites and the expression of some extracellularly secreted and virulence associated compounds (Rutherford and Bassler, 2012). Recently the role of interspecies QS recognition among polymicrobial populations is becoming apparent (Abisado et al., 2018, Armbruster et al., 2010, Lewenza et al., 2002, Popat et al., 2012, Qazi et al., 2006). As previously discussed, the removal and out-competition of SA by PA during co-culture is thought to be dependent on the *lasR* QS system (Mashburn et al., 2005). Similarly, the QS-like signalling network identified in CA utilises farnesol as a signalling molecule (Nickerson et al., 2006). Farnesol is linked to interspecies communication events and is even known to modulate the action of PQS signalling in PA (Cugini et al., 2007, Cugini et al., 2010). Furthermore, cross-recognition of AHL signalling molecules has been identified among different microbial species, for instance PA is able to recognise AHL molecules produced by *B. cenocepacia*, another CF airway-associated pathogen (Lewenza et al., 2002). Such interspecies QS-regulated events have been described to be either cooperative or competitive in nature, yet their full extent upon modulating true polymicrobial communities is largely unknown.

The role of QS events is highly-dependent on environmental factors and the conditions of culture. In 2003, three independent transcriptomic studies were performed on PA in three different laboratories under three different culture conditions (Hentzer et al., 2003, Schuster et al., 2003, Wagner et al., 2003). Although these studies identified large numbers of QS-regulated genes, there was substantial divergence between expression profiles and only a small amount of overlap between the observed results. To determine how the presence of co-habiting microbial species may impinge on QS in PA cultured under continuous-flow and batch culture conditions, the concentration of: 2-heptyl-3-hydroxy-4-quinolone (PQS), *N*-(3-oxododecanoyl)-L-homoserine lactone (OdDHL) and *N*-butanoyl-L-homoserine lactone (BHL) present in the culture supernatants of axenic and mixed species cultures were measured using the biosensor strains and methods described in *Section 2.10*. The work presented in this section is published in *Frontiers in Microbiology* (O'Brien and Welch, 2019a).

4.6.2 Concentration of QS molecules

The concentration of all three PA QS molecules present in the supernatants of single and mixed species populations containing PA under the different culture conditions is shown in *Figure 4.7*. The concentration of all QS molecules in the continuous-flow model cultures was significantly lower ($P < 0.0001$) than their concentration in the aerobic and stirred batch cultures. Under continuous-flow conditions there were no significant changes ($P > 0.1$) in the concentration of PQS (*Figure 4.7.A*) or OdDHL (*Figure 4.7.B*) for any of the culture combinations between $T = 24$ and 96 hrs. There was, however, a significant ($P < 0.05$) 0.4 μM increase in the concentration of BHL (*Figure 4.7.C*) present in the PA-CA co-culture in the continuous-flow model over the incubation period. No other appreciable differences in the concentration of BHL present in the supernatants of co-cultures maintained at a steady-state in the continuous-flow model were observed.

There was no significant difference ($P > 0.9$) in the concentration of PQS present in the supernatants of the PA mono-species or PA-SA co-cultures under batch culture conditions. There was a non-significant ($P > 0.05$) $\approx 0.6 \mu\text{M}$ decrease in [PQS] present in the PA-CA co-culture compared with the PA mono-species or PA-SA co-culture under aerobic batch conditions for both $T = 24$ and 96 hrs. However, under stirred batch conditions the concentration of PQS present in the PA-CA co-culture was significantly higher ($P < 0.001$) than the PA mono-species or PA-SA co-cultures at both points of sampling. At $T = 24$ hrs the concentration of PQS in the triple species co-culture was significantly higher ($P < 0.05$) than it was in the PA mono-species or PA-SA co-culture under aerobic batch conditions. A significant ($P < 0.001$) 3-fold decrease in the concentration of PQS present in the triple species aerobic

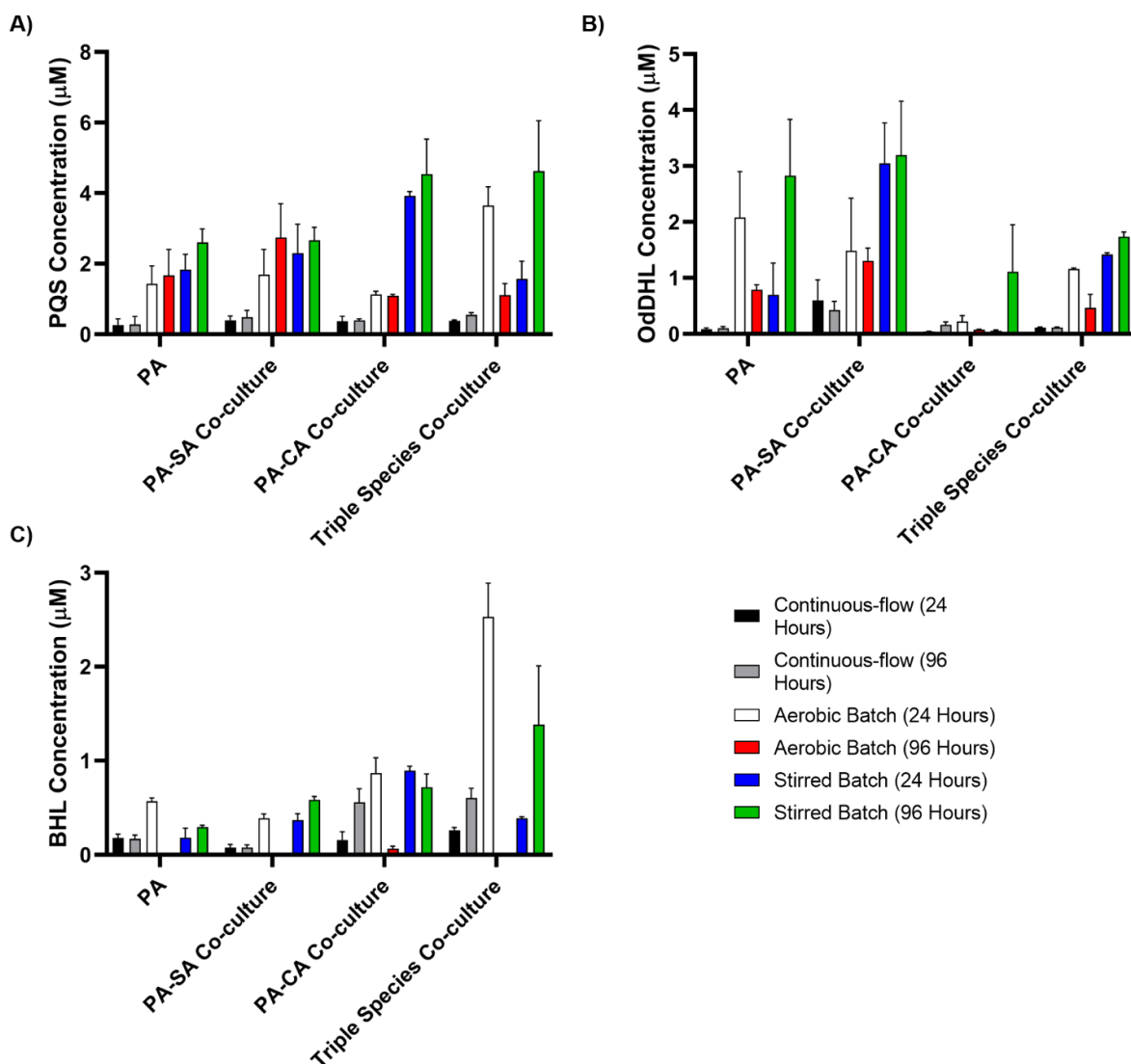


Figure 4.7 Quantification of quorum sensing molecule accumulation.

Concentration (μM) of the indicated quorum sensing molecules in the supernatants of single-species and mixed species populations of *P. aeruginosa* PAO1 (PA), *S. aureus* 25923 (SA) and *C. albicans* SC5314 (CA) cultured in the different culture conditions after 24 and 96 hrs of incubation (as indicated). **(A)** Pseudomonas quinolone signal (PQS); **(B)** *N*-(3-oxododecanoyl)-L-homoserine lactone (OdDHL); **(C)** *N*-butanoyl-L-homoserine lactone (BHL). Data represented as mean \pm standard deviation of three independent experiments.

batch culture occurred between $T = 24$ and 96 hrs, making the concentration of PQS present in the triple species co-culture significantly lower ($P < 0.05$) than the PA mono-species or PA-SA co-culture at the endpoint of incubation. The inverse trend was observed under batch culture conditions, as the concentration of PQS present within the triple species co-culture was significantly lower ($P < 0.05$) than the PA mono-species or PA-SA co-culture at $T = 24$ hrs. There was a significant ($P < 0.0001$) 3.3-fold increase in the concentration of PQS between 24 and 96 hrs of incubation in the triple species aerobic batch co-culture.

There was no significant difference in the concentration of OdDHL present in the PA mono-species culture between $T = 24$ and 96 hrs under aerobic batch conditions, or between the PA-SA co-cultures under both aerobic and stirred batch conditions. A significant increase ($P < 0.0001$) in the concentration of OdDHL present in the PA mono-species stirred batch culture occurred between the points of sampling. The concentration of OdDHL present in the PA-SA stirred co-culture was significantly higher ($P < 0.0001$) than the PA mono-species culture at after 24 hrs of incubation, but there was no significant difference between the two culture combinations at $T = 96$ hrs. OdDHL was also present at significantly higher ($P < 0.05$) levels in the PA-SA stirred batch culture compared with the same co-culture under aerobic conditions at both timepoints. The concentration of OdDHL present in the PA-CA co-culture under both aerobic and stirred batch conditions was significantly lower ($P < 0.05$) than the PA mono-species or PA-SA co-cultures at all timepoints. Furthermore, for all PA-CA batch co-cultures, except $T = 96$ hrs stirred co-culture, OdDHL was present at less than $0.25 \mu\text{M}$ and not statistically different than the concentration of OdDHL measured in the continuous-flow co-cultures. No significant difference in OdDHL concentrations were observed between the PA mono-species or PA-SA co-culture and triple species co-cultures under grown aerobic conditions or at $T = 24$ hrs under stirred batch conditions. After 96 hrs of incubation the concentration of OdDHL present in the triple species stirred batch co-culture was significantly lower ($P < 0.001$) than concentrations within the PA mono-species or PA-SA co-culture.

No BHL could be detected in the supernatants of any species combinations cultured under aerobic batch conditions at $T = 96$ hrs, except for the PA-CA co-culture where BHL was present at less than $0.1 \mu\text{M}$. The concentration of BHL present in the triple species aerobic batch culture was more than 3-fold higher ($P < 0.0001$) than the concentration of BHL observed for all other aerobic batch species combinations at $T = 24$ hrs. No significant difference in the concentration of BHL was observed between the PA mono-species and PA-SA co-culture at any time point under stirred batch conditions. BHL was present at a significantly higher ($P < 0.001$) concentration in the supernatant of the PA-CA co-culture compared with the PA mono-species and PA-SA co-culture at $T = 96$ and 24 hrs respectively. By the final point of sampling, the concentration of BHL present in the triple species aerobic

batch co-culture was significantly higher ($P < 0.001$) than all other species combinations grown under the same conditions.

4.6.3 Conclusions

Taken together these findings demonstrate that QS molecules accumulate to a much lower concentration in the continuous-flow model compared with batch culture populations. The simplest explanation for this finding is the continual dilution of QS signals with fresh media occurs in the continuous-flow vessel and causes a washout of QS molecules. However, it is crucial to note that previous work within the Welch laboratory has identified that QS molecules more than double their concentration over 2 hrs (Davenport et al., 2015). Using the faster flowrate of $Q = 170 \mu\text{L min}^{-1}$, it would take > 6 hrs to dilute the culture vessel by 50%, and all the while the culture continues to grow and produce more QS molecules. Assuming similar kinetics of QS production in ASM, these molecules should accumulate faster than they are diluted within the vessel. This finding therefore suggests that QS plays a less important role in populations maintained under continuous-flow conditions as opposed to batch culture conditions.

Unlike populations maintained in the continuous-flow vessel, the presence of co-cultivated species had a large and varied impact upon the production of QS molecules by PA under batch culture conditions. For example, the presence of SA during batch culture stimulated an up-regulation in OdDHL production. It has been demonstrated that OdDHL, but not the shorter chain BHL, can specifically bind to the SA membrane and cause a down-regulation in exotoxin and agr (the SA QS signalling molecule) production (Qazi et al., 2006). This finding suggests that PA QS molecules play a role in competition and the modulating the behaviour of other species *via* direct interaction with other species and not simply through the genes under the control of the QS network. The presence of CA caused a depression in the production of OdDHL, yet stimulated the production of PQS, and to a lesser extent BHL. It is interesting to note that alongside the aforementioned ability of CA produced farnesol to modulate the action of PQS signalling, the addition of exogenous PQS to an axenic CA culture stimulates growth (Curutiu et al., 2016). This highlights a complex network of direct and indirect cooperative and competitive interspecies interactions among polymicrobial populations and shows that the presence of a numerically minor species can have large effects on the behaviour of a polymicrobial consortium.

The lack of detectable BHL present in the supernatants of all aerobic batch cultures at $T = 96$ hrs and the decrease of OdDHL also observed at this time point is an interesting phenomenon, but one that can be answered through the alkaline pH of spent batch culture media (*Figure*

4.8). Hydrolysis of lactone rings is known to occur under alkaline conditions (Gómez-Bombarelli et al., 2013), causing a breakdown and decrease in the concentration of AHLs (BHL and OdDHL) but not the non-AHL PQS signalling molecule.

4.7 pH

The pH of axenic and mixed species cultures was examined after 96 hrs of incubation under the different culture conditions to see if values differed from the starting point of prewarmed ASM (\approx pH 6.7). The work presented in this section is published in *Frontiers in Microbiology* (O'Brien and Welch, 2019a).

The endpoint pH of all cultures maintained in the continuous-flow model were significantly lower ($P < 0.0001$) than the pH of species combinations grown under aerobic and stirred batch conditions (*Figure 4.8*). Furthermore, there was no significant difference ($P > 0.05$) between the pH measurements of any combination of species cultured under continuous-flow conditions, and the average pH of all continuous-flow populations (pH \approx 6.5) was comparable to that of sterile ASM. The endpoint pH of batch cultures containing PA and the SA-CA co-culture was significantly higher than sterile ASM, with an approximate 2-unit or 0.6-unit increase in pH observed in the aerobic and stirred batch cultures, respectively. A similar increase in pH occurred for the SA axenic culture grown under aerobic batch conditions, yet there was no significant difference in pH between the stirred batch and continuous-flow cultures. The endpoint pH of the mono-species CA cultured under aerobic batch conditions was significantly lower ($P < 0.01$) than the average pH of the continuous-flow populations and there was no significant difference ($P > 0.4$) in the pH of the stirred batch and continuous-flow cultures.

Unlike specific interspecies interactions, such as the sensing of extracellular secretions or the recognition of cell surface motifs, changes in the pH of a culture environment will be felt by all members of a population. Although little research has thus far been undertaken to examine to what extent changes in pH may play a role in mediating interspecies interactions or the competition/survival of species within a polymicrobial population, work on cyanobacteria co-cultures has established that changes in pH can facilitate out-competition between species (Yang et al., 2018). Environmental pH has also been linked to the expression of virulence factors by PA, SA and CA (De Bernardis et al., 1998, Harjai et al., 2005, Jenul and Horswill, 2018) and furthermore changes in pH have been implicated in competition between *H. influenzae* and *S. pneumoniae* within *in vitro* models (Tikhomirova and Kidd, 2013) and a 2-unit drop in the pH of sputum samples has been identified to occur prior to the onset of APEs in CF patients (Quinn et al., 2015). Interestingly, a study by Sankaralingam *et al.* (2014)

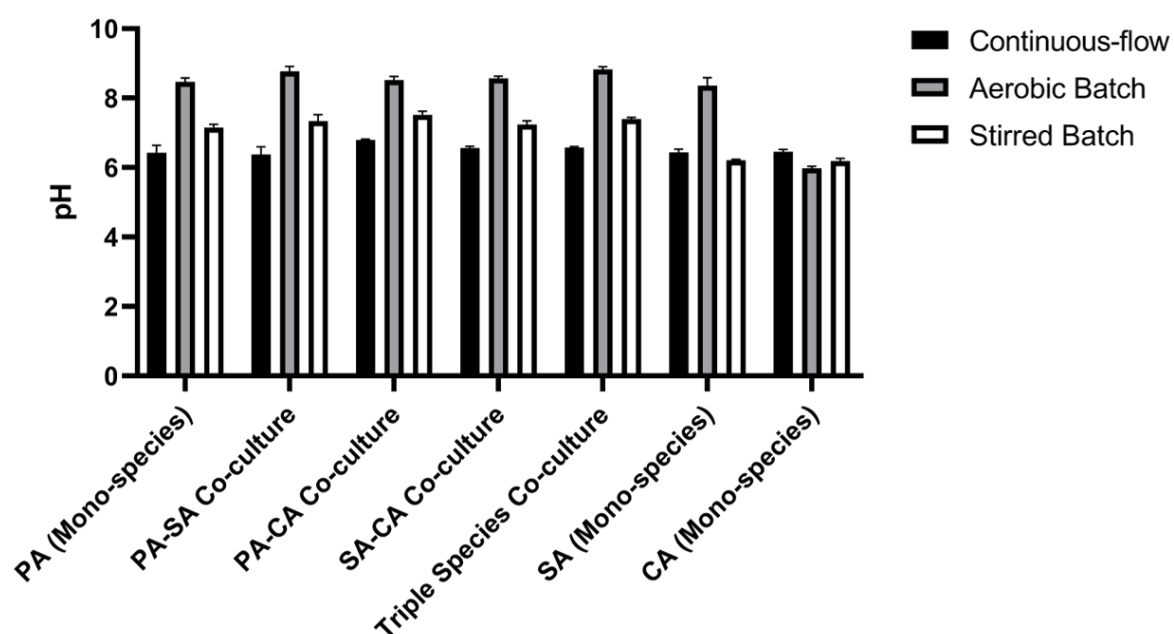


Figure 4.8 pH of microbial cultures.

Endpoint pH measurements of single-species and co-cultures of *P. aeruginosa* PAO1 (PA), *S. aureus* 25923 (SA) and *C. albicans* SC5341 (CA) after 96 hrs of incubation under: continuous-flow (black bars); aerobic batch (grey bars); and stirred batch (white bars) culture conditions. Data represented as mean \pm standard deviation of three independent experiments.

examining the effect of pH on phosphate-solubilising bacteria established that PA cultures grew to the highest density at pH 8 (Sankaralingam et al., 2014). Additional studies have also showed that PA up-regulates the production of some extracellular virulence factors, such as alginate and proteinase, at pH 8 also (Harjai et al., 2005). Contrastingly, an alkaline environment has been found to decrease *agr* expression *via* the repression of RNAlII transcription in SA, thereby decreasing the expression of genes important for virulence and competition under the control of the Gram-positive QS network (Regassa and Betley, 1992). Similarly, changes in pH are known to control yeast-hyphal morphogenesis in CA, and alkaline culture conditions are known to cause fungal stress by impairing nutrient uptake and repression of extracellular virulence factor production (Ardon et al., 2001, Vylkova et al., 2011).

The elevated pH of populations grown under batch culture conditions, where PA outcompetes SA and CA (*Section 3*), combined with previous reports suggesting that PA is able to thrive under alkaline conditions (yet SA and CA struggle to grow), suggests that modulations in the pH of an environment may play a crucial role in the removal of some species from a polymicrobial community. However, it cannot yet be concluded if species such as PA actively modulate their environment to favour or inhibit the growth of other members present within a polymicrobial community. What is apparent from the results presented in this section is that under continuous-flow conditions the pH of populations maintained in a steady-state was near neutral and remained close to the pH of sterile ASM. This demonstrates that a degree of environmental homeostasis is afforded by the culture model and that this may play a role in permitting the long-term maintenance of polymicrobial communities.

4.8 Conclusions

The results presented within this chapter demonstrate that extracellular secretions associated with virulence and interspecies competition, such as siderophores and pyocyanin, alongside QS signalling molecules, accumulate to a much lower concentration under continuous-flow culture conditions compared with batch culture conditions. Importantly, the measured concentration of extracellular products does not appreciably change over time or with the presence of different species combinations within a community. This indicates that the co-culture maintained in the continuous-flow model is stable with respect to interspecies competition and also with respect to species titres. Studies using PA and SA co-isolated from the same lobe of the CF lungs or co-evolved under *in vitro* conditions have demonstrated that the improved co-existence of these species is also accompanied by a suppression in virulence factor production (Baldan et al., 2014, Lorè et al., 2012). This suggests that repression of virulence factor production is linked to a decrease in competition between species and that, to

an extent, my *in vitro* model is promoting similar microbial behaviours to those thought to occur in the CF airways. However, the *in situ* behaviour of polymicrobial communities associated with this environmental niche are poorly understood, so no further comment can be made on this.

It is interesting to note that under continuous-flow conditions the accumulation of siderophores in the culture vessel is significantly decreased compared with the concentrations attained under batch culture conditions. This is despite access to iron remaining an essential requirement for the proliferation and survival of the same combination of microbial species present under both conditions. This is unsurprising given that pyoverdine synthesis is, in part, under the control of the *las/R* QS system (Stintzi et al., 1998) and that OdDHL accumulated to a much lower concentration in the continuous-flow cultures too. However, this observation clearly demonstrates that interspecies competition for resources is decreased using the novel *in vitro* culture system described in this work. It could be hypothesised that through the provision of a plentiful supply of nutrients, not unlike the overabundance of nutrient rich sputum available in the CF airway microenvironment due to the hyperproduction of airway secretions (Kreda et al., 2012), there is a suppression of interspecies virulence factor production typically used to compete for access to limited resources. Allowing mixed species communities that would ordinarily outcompete one another under nutrient-limited batch culture conditions to be successfully maintained using the continuous-flow model.

The presence of co-cultivating species, even if present at less than 0.05% of the total population (Section 3.5), caused significant and varied modulations in the accumulation of all the measured extracellular compounds under batch culture conditions. These findings are consistent with existing reports on the competition between species and a dysregulation of virulence factor production under nutrient-limited conditions. This affirms the need to consider how the presence of less abundant species, and not simply the principal pathogens, impinges upon the network of interspecies interactions present among a polymicrobial consortium.

Another key conclusion to be drawn from the data presented in this chapter is that the mutability of species cultured within the continuous-flow system is not adversely affected by the culture conditions, and mutation rates are stable irrespective of time or the presence of co-cultivated species. Furthermore, cells in the continuous-flow model appear to be maintained in a metabolically active and continually-dividing state for the entirety of the incubation period. Taken together these results indicate that the model provides an experimentally tractable system suitable for studying how the presence of additional species impacts upon the metabolic activity and evolutionary trajectory of mixed species populations cultured under nutritionally similar conditions to the CF microenvironment. The results

presented in this chapter provide a proof-of-principle to the robustness and versatility of the culture model. Any number of biochemical and phenotypic assays could be performed in real-time on any combination of microbial species maintained as a co-culture in the continuous-flow model. Thus allowing numerous biological questions pertaining to interspecies interactions and polymicrobial communities to be readily addressed.

5. Perturbation of steady-state microbial communities

5.1 Introduction of PA to SA-CA co-culture

5.1.1 Introductory Comments

As previously described (*Section 1.2*), the establishment of chronic PA infections is correlated with a worsened patient prognosis (Cox et al., 2010, Zhao et al., 2012). The airways of infant and adolescent patients remain largely free from PA colonisation (Conrad et al., 2013, Rogers et al., 2005, Tunney et al., 2008). Yet, by ages 18-20, 60-80% of persons with CF test positive for infection with PA (2015, Folkesson et al., 2012, Stressmann et al., 2011). Previous failings in the long-term co-cultivation of species associated with the CF microenvironment have prevented investigations into how PA interacts with a pre-existing microbial community. The continuous-flow model described in this work provides a physiologically relevant and robust method for the study of how the introduction of new species perturbs pre-existing, steady-state microbial populations. As a proof-of-principal for this concept, I initially studied how the introduction of PA, at different inoculum densities, perturbs the microbial titres of pre-established SA-CA co-cultures grown under continuous-flow conditions.

5.1.2 OD_{600 nm} Measurements

Average OD_{600 nm} measurements of pre-established steady-state SA-CA co-cultures following the introduction of PA at different inoculation densities are shown in *Figure 5.1*. There was no significant difference ($P > 0.9$) in the optical density of the SA-CA co-cultures before the introduction of PA ($T = 0$ hrs) and there was no statistically significant change ($P > 0.5$) in the optical density of any co-culture between $T = 1$ h and 8 hrs. Over this incubation period the average density of cultures inoculated with PA at an OD_{600 nm} 0.25 or 0.5 were significantly higher ($P < 0.01$) than the other cultures.

After 24 hrs incubation, there was no significant difference ($P > 0.8$) in the density of co-cultures inoculated with OD_{600 nm} 0.05 or 0.1 PA and there was no statistically significant change ($P > 0.9$) in the density of these cultures between $T = 24$ and 120 hrs. The cell density of the culture inoculated with OD_{600 nm} 0.5 PA was significantly higher ($P < 0.0001$) than all other co-cultures at $T = 24$ hrs and density of the culture inoculated with 0.25 PA was significantly higher ($P < 0.0001$) than the remaining co-cultures at this point of sampling. A significant ($P < 0.0001$) 0.55-unit decrease in the density of the co-culture inoculated with OD_{600 nm} 0.25 PA occurred between 24 and 72 hrs of incubation. There was no significant change ($P > 0.9$) in the average density of 0.25 inoculum co-culture after 72 hrs incubation

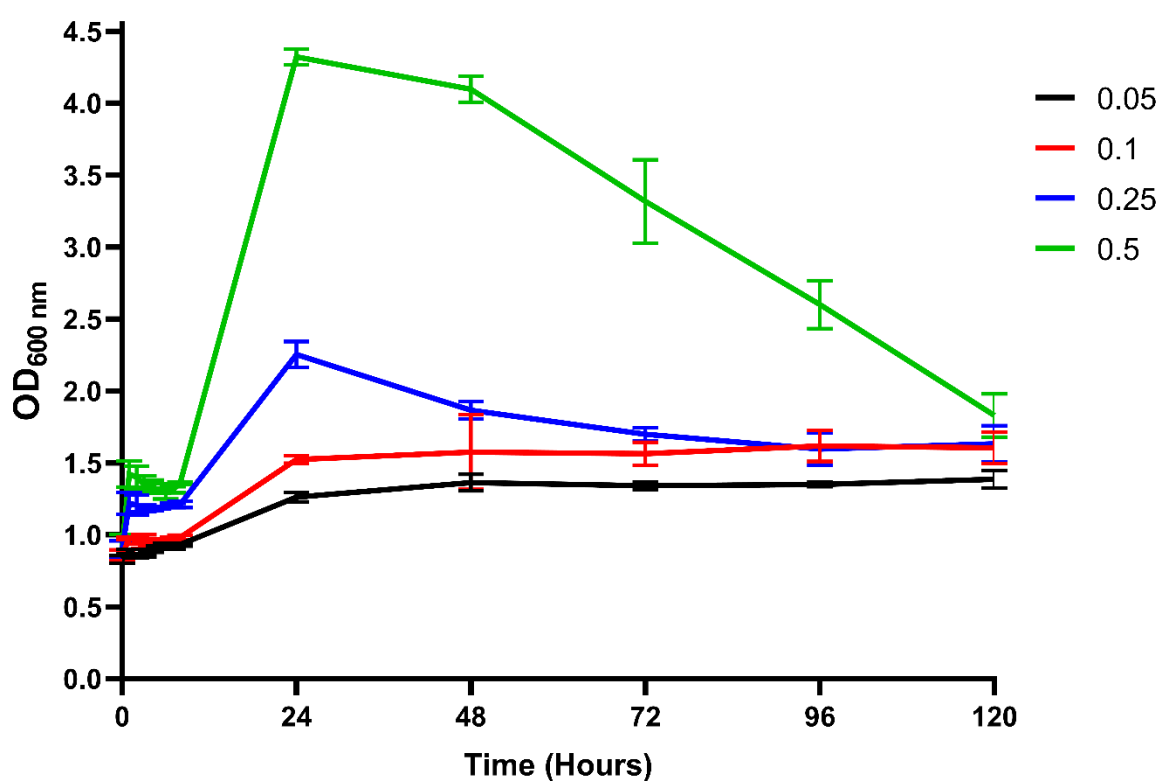


Figure 5.1 Population density following the addition of PA to a steady-state SA-CA co-culture.

Dual-species co-cultures of *S. aureus* 25923 and *C. albicans* SC5314 were grown for 24 hrs in ASM under continuous-flow conditions (as shown in *Section 3.5*). *P. aeruginosa* PAO1 was then inoculated into the culture vessel, at different densities, at T = 0 hrs and OD_{600 nm} measured for 120 h. Normalised overnight cultures of PA were introduced to the steady state co-cultures at the following densities: OD_{600 nm} 0.05 (black), 0.1 (red), 0.25 (blue) and 0.5 (green). Data represented as the mean \pm standard deviation from three independent experiments.

and there was no statistically significant difference ($P > 0.9$) between the density of co-cultures inoculated with OD_{600 nm} 0.1 or 0.25 PA between T = 72 and 120 hrs. A significant ($P < 0.0001$) ≈ 2.5 -unit decrease in the density of the culture inoculated with OD_{600 nm} 0.5 PA occurred between T = 24 and 120 hrs. There was no significant difference ($P > 0.5$) in average endpoint OD_{600 nm} measurements of the cultures inoculated with OD_{600 nm} 0.1, 0.25 and 0.5 PA) at the endpoint of sampling (OD_{600 nm} = 1.61, 1.63 and 1.83, respectively).

5.1.3 Viable cell counts

Viable cell counts of individual species present in pre-established SA-CA co-cultures following the introduction of PA at different inoculation densities are shown in *Figures 5.2 and 5.3*. There was no appreciable difference ($P > 0.9$) in viable SA or CA cell counts of any steady-state co-culture before the introduction of PA and the viable cell counts presented in *Section 3.5.4*. Furthermore, there was no significant change ($P > 0.9$) in SA or CA viable cell counts over the incubation period for co-cultures inoculated with OD_{600 nm} 0.05 or 0.1 PA (*Figure 5.2.A and 5.2.B*, respectively). Inoculation with OD_{600 nm} 0.05 or 0.1 PA resulted in the introduction of $\approx 8 \times 10^6$ or $\approx 3 \times 10^7$ PA CFU mL⁻¹ (respectively) into the steady-state co-culture. A 0.5-log fold increase in viable PA cell counts occurred between 0 and 24 hrs incubation for the co-culture inoculated with OD_{600 nm} 0.05 PA, although this change was not statistically significant ($P > 0.8$). By contrast, a significant ($P < 0.01$) log-fold increase in PA CFU mL⁻¹ occurred between T = 0 and 24 hrs in the culture vessel inoculated with OD_{600 nm} 0.1 PA. There was no significant change ($P > 0.9$) in PA titres in either co-culture after 24 hrs incubation.

Inoculation of PA into the culture vessel at an optical density of 0.25 resulted in the introduction of $\approx 4 \times 10^8$ CFU mL⁻¹ into the steady-state co-culture and there were significantly more ($P < 0.0001$) viable PA cells than SA or CA cells at this initial time point (*Figure 5.3.A*). A significant ($P < 0.0001$) 2.8×10^8 decrease in PA CFU mL⁻¹ occurred between T = 0 and 6 hrs, but was followed by a significant ($P < 0.0001$) log-fold increase in viable PA cells between T = 6 and 24 hrs, with $\approx 3 \times 10^9$ PA CFU mL⁻¹ present within the culture vessel at T = 24 hrs. A significant ($P < 0.0001$) log-fold decrease in viable PA cells present within the co-culture then occurred between 24 and 48 hrs incubation and there was no significant change ($P > 0.05$) in viable PA cell counts following T = 48 hrs. A respective 0.5-log and 1-log decrease in viable SA and CA cell counts occurred between 8 and 24 hrs incubation, yet this change was not statistically significant ($P > 0.9$). There was no appreciable difference in viable SA cell counts within the co-culture between T = 8 hrs and any time point following 48 hrs incubation and viable CA cell counts steadily increased from 10^4 back to 10^5 CFU mL⁻¹ between T = 24 and 96 hrs.

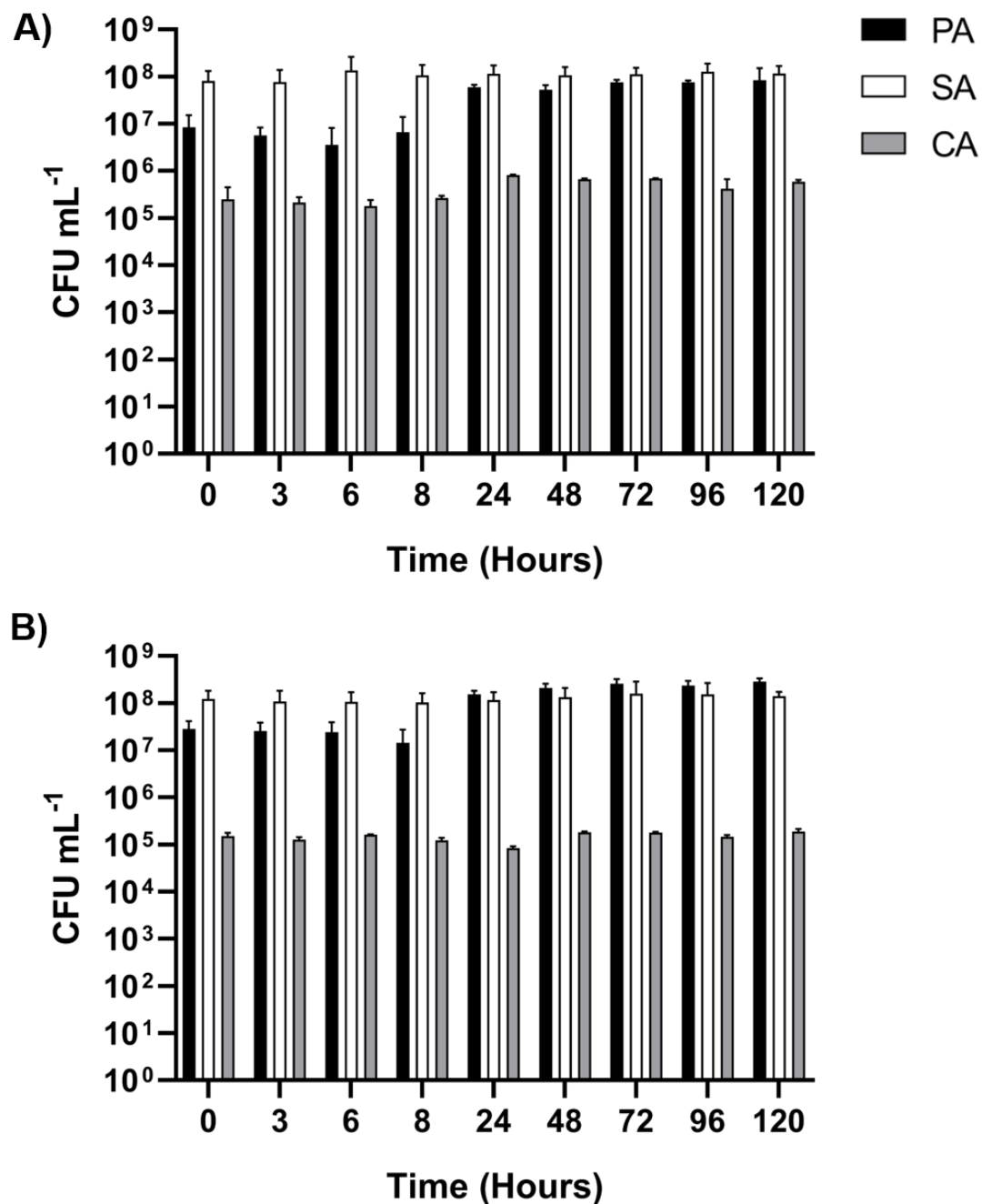


Figure 5.2 Viable cell counts of individual species following the addition of PA to a steady-state SA-CA co-culture.

Dual-species co-cultures of *S. aureus* 25923 and *C. albicans* SC5314 were grown under continuous-flow conditions for 24 hrs (as in Section 3.5). At $T = 0$ *P. aeruginosa* PAO1 was inoculated into the culture vessel at $OD_{600\text{ nm}}$ 0.05 (**A**) or 0.1 (**B**). Data represented as mean viable cell counts of PA (black), SA (white) and CA (grey) \pm standard deviation following inoculation of PA from three independent experiments.

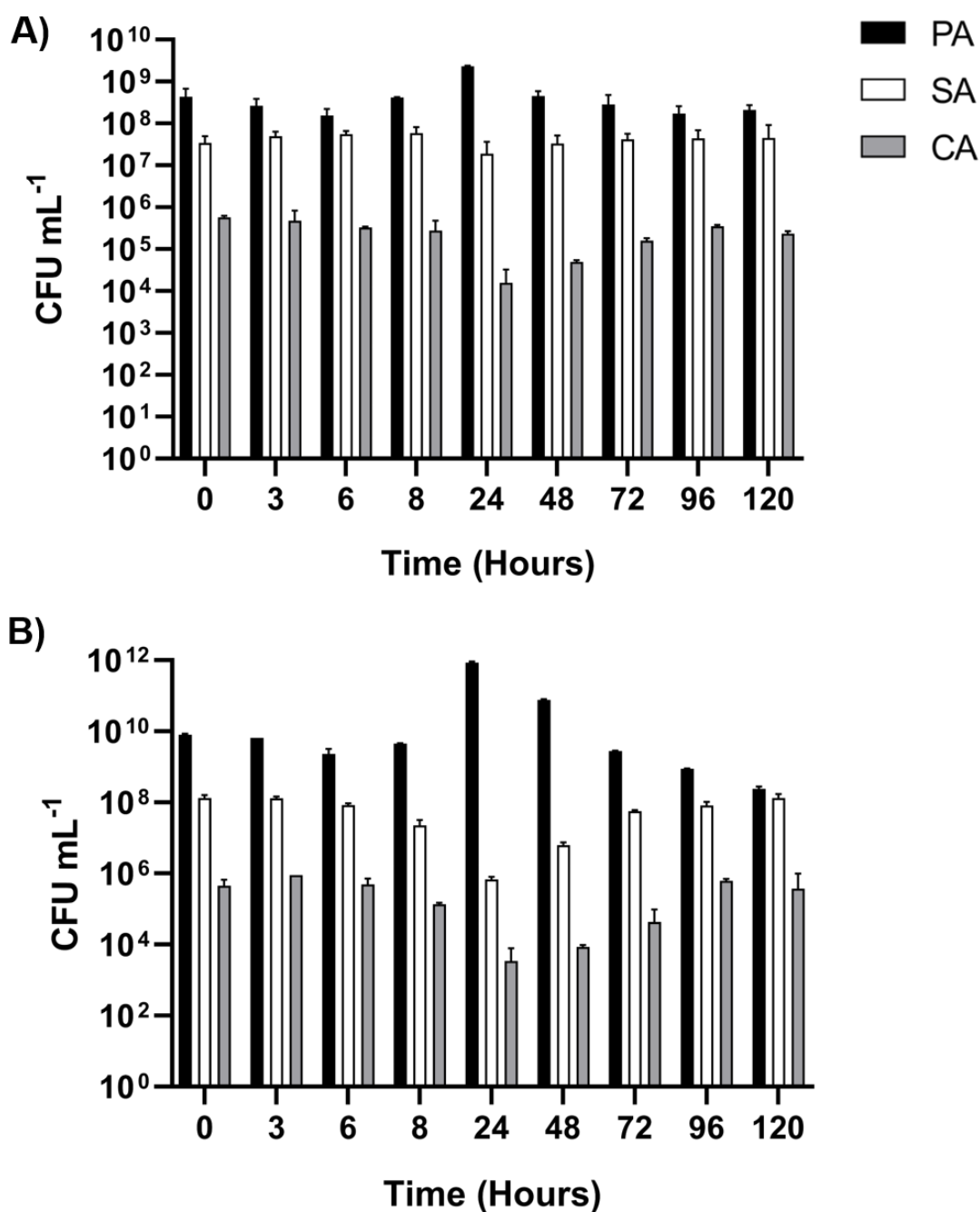


Figure 5.3 Viable cell counts of individual species following the addition of PA to a steady-state SA-CA co-culture.

Dual-species co-cultures of *S. aureus* 25923 and *C. albicans* SC5314 were grown under continuous-flow conditions for 24 hrs (as in Section 3.5). At T = 0 (above) *P. aeruginosa* PAO1 was inoculated into the culture vessel at OD_{600 nm} 0.25 (**A**) or 0.5 (**B**). Data represented as mean viable cell counts of PA (black), SA (white) and CA (grey) ± standard deviation following inoculation of PA from three independent experiments.

Inoculation of PA into the culture vessel at OD_{600 nm} 0.5 resulted in $\approx 8 \times 10^9$ PA CFU mL⁻¹ being introduced into the steady-state co-culture (*Figure 5.3.B*). There was no significant change ($P > 0.5$) in viable PA cell counts between T = 0 and 8 hrs. A significant ($P < 0.0001$) 2-log fold increase in PA viable cell counts occurred between T = 8 and 24 hrs, with $\approx 8.6 \times 10^{11}$ PA CFU mL⁻¹ being present in the co-culture at the 24 hrs timepoint. Following this, there was a significant ($P < 0.0001$) log-fold decrease in viable PA cell counts at every point of sampling between T = 24 and 96 hrs, and there was no statistically significant change ($P > 0.9$) in PA viable cell counts between 96 hrs and the final point of sampling. A significant ($P < 0.0001$) 2-log fold decrease in viable SA and CA cell counts present in the co-culture occurred between T = 0 and 24 hrs. Following this decline, an approximate log-fold increase in viable CA and SA cells occurred every 24 hrs until the final point of sampling. There was no appreciable difference in average viable SA or CA cell counts ($\approx 1.3 \times 10^8$ and $\approx 4.5 \times 10^5$ CFU mL⁻¹, respectively) present in the co-culture between T = 0 or 120 hrs and there was no significant difference ($P > 0.9$) in endpoint PA or SA viable cell counts. It is important to note that there was no significant difference in endpoint PA CFU mL⁻¹ counts between the co-cultures inoculated with PA at an optical density of 0.1, 0.25 or 0.5.

5.1.3 Conclusions

The introduction of PA, at any of the above inoculation densities, into pre-established microbial co-cultures maintained under continuous-flow conditions resulted in the same steady-state endpoint community, with respect to culture density and viable cell counts, maintained in the culture vessel. The reduction of viable PA cells observed between 24 and 120 hrs of incubation in the co-culture inoculated with the highest PA density (OD_{600 nm} 0.5), indicates that the endpoint microbial density measured in the co-cultures is the maximum steady-state carrying capacity supported by the *in vitro* model. The only significant perturbation of steady-state SA or CA viable cell counts occurred when introducing PA at the highest density into the culture vessel. Given that titres of viable SA and CA cells quickly recover to the level observed prior to the inoculation of PA, and that QS molecules and extracellular virulence factors do not accumulate in the culture vessel under continuous-flow conditions (*Section 4.*), this initial decrease in SA and CA cell counts may simply be attributed to a temporary displacement of cells from the culture vessel and not species out-competition. From the results presented in this sub-section, further investigation may be warranted into what changes occur in the gene expression and microbial physiology of species maintained in the co-culture between 0 and 24 hrs incubation in order to discern how PA modulates changes in microbial behaviour and what factor(s) are responsible for the initial diminution in the titres of co-cultivated species.

5.2 Antimicrobial treatment of single-species and mixed-species populations

5.2.1 Introductory comments

In the clinical setting, microbial infections are treated with antimicrobial compounds in an attempt to diminish the burden of a principal pathogenic species. For instance, the onset of APEs in persons with CF is met with aggressive antimicrobial treatment designed to reduce the titre of viable PA cells harboured within the airways. Antimicrobials are often designed with the treatment of a specific pathogen in mind and so are commonly developed and validated *in vitro* using axenic microbial cultures, yet little is known about how mixed microbial populations respond to antimicrobial intervention. As previously discussed in *Section 1* and demonstrated in *Section 4*, microbial species exhibit different behaviours and physiologies when grown as polymicrobial communities opposed to axenic cultures. Given the diversity of the microbiota associated with CF airway infections, it is likely that pathogens *in situ* respond in an unpredictable manner to the addition of antimicrobials and this may, in part, contribute towards refractory responses to treatment (Vandeplasseche et al., 2019).

Understanding how polymicrobial populations respond to antimicrobial perturbation is essential if we are to develop improved treatments to manage chronic airway infections. As previously detailed in *Section 3*, competition among species during traditional co-culture approaches hinder such studies, as mixed microbial co-cultures cannot be stably maintained *in vitro*. Previous studies have therefore relied on comparing the action of antimicrobials against single-species and mixed-species biofilms (Al-Bakri et al., 2005, Burmølle et al., 2006, Chen et al., 2019, Elias and Banin, 2012, Kara et al., 2006, Leriche et al., 2003, Whiteley et al., 2001). Although these studies are useful for studying a chronic infection scenario, microbial species behave very differently when grown as sessile or planktonic communities (Davey and O'Toole, 2000). As described in guidelines published by the European Committee on Antimicrobial Susceptibility Testing (EUCAST), standardised minimum inhibitory concentration (MIC) tests should be performed on liquid cultures (Clinical and Laboratory Standards Institute, 2019). It is therefore difficult to compare the results from the antimicrobial treatment of biofilms between experiments and with clinical breakpoint data. Furthermore, limited studies into the effects of antimicrobials on mixed bacterial populations grown as liquid cultures have identified altered responses to antimicrobials compared with axenic cultures (Galera-Laporta and Garcia-Ojalvo, 2020) affirming the need for further investigation into this phenomenon. As highlighted in *Section 1.5*, microbial physiology during biofilm growth more closely resembles the physiology of species during the stationary phase, where microbes are thought to be slow growing and more tolerant against antimicrobial action (Kamble and Pardesi, 2020). Conversely, steady-state microbial populations grown in the continuous-flow model are consistently maintained in the exponential growth phase (*Section 4.2*). Hence, the

continuous-flow model provides an unparalleled opportunity to robustly study how actively growing polymicrobial populations of key CF airway-associated pathogens respond to common clinically used antimicrobial compounds under physiologically relevant conditions, a feat that is simply not possible using existing *in vitro* models.

The results presented in this section describe the perturbation of pre-established steady-state mono-species and polymicrobial planktonic cultures of PA, SA and CA with three clinically-relevant species-specific antimicrobials: colistin, fusidic acid and fluconazole. It is important to note that antimicrobial compounds were added to the culture vessel after 24 hrs incubation and cultures were incubated under batch culture conditions for one hour before restoring liquid flow (as described in *Section 2.11.3*). As fresh ASM enters the culture vessel it gradually dilutes the antimicrobial, loosely mimicking the metabolism and excretion of antimicrobials when provided to a patient *in situ*.

Colistin (also known as polymyxin E) is a last-resort treatment for multi-drug resistant Gram-negative species, such as PA. Colistin is a bactericidal polycationic peptide that contains hydrophilic and lipophilic moieties. Cationic charges in the polypeptide portion of colistin are thought to electrostatically bind to the negatively charged lipopolysaccharide (LPS) in the outer membrane of PA. Colistin then displaces the membrane-stabilising divalent cations (Mg^{2+} and Ca^{2+}) in the outer membrane leading to disruption of the membrane integrity and subsequent lysis of Gram-negative bacteria in aqueous environments (Bialvaei and Samadi Kafil, 2015). Fusidic acid is a bacteriostatic steroidal compound effective against Gram-positive species and is primarily used as an antistaphylococcal antibiotic. Fusidic acid inhibits protein translation by binding to elongation factor G, preventing conformational changes in the enzyme and resulting in inhibition of peptide translocation and ribosome disassembly (Fernandes, 2016). Fluconazole is a broad-spectrum fungistatic or fungicidal compound, clinically used to treat numerous fungal infections, including candidiasis and cryptococcosis. This antifungal agent is a fluorine-substituted, bis-triazole that binds to fungal cytochrome P-450 and prevents the conversion of lanosterol to ergosterol, an essential component of the fungal cell wall (Pasko et al., 1990).

5.2.2 MIC of antimicrobials in ASM

Firstly, the MIC of the antimicrobial compounds against the different microbial species in ASM was determined (*Table 5.1*). The MIC of colistin against PA was $4\ \mu\text{g mL}^{-1}$, the MIC of fusidic

Species	Minimum Inhibitory Concentration ($\mu\text{g mL}^{-1}$)		
	Colistin	Fusidic Acid	Fluconazole
<i>P. aeruginosa</i> PAO1	4	>256	>256
<i>S. aureus</i> 25923	>256	0.0156	>256
<i>C. albicans</i> SC5314	>256	>256	1

Table 5.1 Minimum inhibitory concentration of antimicrobial compounds.

Minimum inhibitory concentration (MIC, $\mu\text{g mL}^{-1}$) of colistin, fusidic acid and fluconazole against *P. aeruginosa* PAO1, *S. aureus* 25923 and *C. albicans* SC5314 grown in ASM. MICs were determined using the EUCAST broth microdilution method and MIC considered as the lowest concentration able to inhibit visible microbial growth after 16 hrs incubation. MIC values were confirmed over three independent experiments using different batches of fresh ASM.

acid against SA was 15.6 ng mL^{-1} and the MIC of fluconazole against CA was $1 \text{ } \mu\text{g mL}^{-1}$. As expected from previous reports, the compounds were specifically active against the aforementioned species only and did not inhibit the growth of the other species at a concentration of $256 \text{ } \mu\text{g mL}^{-1}$. The MICs experimentally determined in ASM demonstrated in this sub-section are comparable with the published clinical breakpoint values collected using cation-adjusted Müller-Hinton II broth (EUCAST, 2020a, EUCAST, 2020b).

5.2.3 Treatment with colistin

5.2.3.1 Viable Cell Counts

Viable cell counts of pre-established PA mono-species and polymicrobial populations grown in ASM under continuous-flow conditions following the addition of 1 x MIC ($4 \text{ } \mu\text{g mL}^{-1}$), 2 x MIC ($8 \text{ } \mu\text{g mL}^{-1}$) or 5 x MIC ($20 \text{ } \mu\text{g mL}^{-1}$) colistin are shown in *Figure 5.4*, *5.5* and *5.6*, respectively. There was no appreciable difference in CFU mL^{-1} counts between any mono-species or polymicrobial culture before the addition of colistin. There was no statistically significant difference ($P > 0.9$) in viable cell counts between $T = 0$ and 24 hrs in the mono-species PA culture treated with 1 x MIC colistin (*Figure 5.4.A*). A significant ($P < 0.0001$) 2-log fold increase in PA CFU mL^{-1} counts was observed between $T = 0$ and 48 hrs. Similarly, there was no significant change ($P > 0.9$) in PA titres for the polymicrobial population treated with 1 x MIC colistin for the first 24 hrs of incubation and a significant ($P < 0.0001$) log-fold increase in viable PA cells occurred between $T = 0$ and 48 hrs (*Figure 5.4.B*). There was no significant change ($P > 0.9$) in SA or CA titres over the course of the incubation period.

A significant ($P < 0.001$) 4-log fold decrease in PA titres occurred in the mono-species culture vessel treated with 2 x MIC colistin between $T = 0$ and 3 hrs (*Figure 5.5.A*). Following this a, respective, log-fold and 2-log fold increase in PA CFU mL^{-1} counts occurred in the culture by 5 and 8 hrs incubation, although viable cell counts at these points remained significantly lower ($P < 0.01$) than the initial point of sampling. There was a significant ($P < 0.001$) log-fold increase in PA CFU mL^{-1} counts between $T = 0$ and 24 hrs and no significant change ($P > 0.9$) in viable cell counts occurred between 24 and 48 hrs incubation. A significant ($P < 0.01$) 2-log fold decrease in PA titres occurred between $T = 0$ and 3 hrs within the polymicrobial culture treated with 2 x MIC colistin. There was a 2-log fold increase in PA titres between $T = 3$ and 8 hrs and there was no statistically significant difference ($P > 0.9$) in PA titres between 0 and 8 hrs incubation. A significant ($P < 0.001$) log-fold increase in viable PA cell counts was observed between $T = 0$ and 24 or 48 hrs incubation. No significant change ($P > .0.9$) in viable SA or CA titres was observed across any point of sampling.

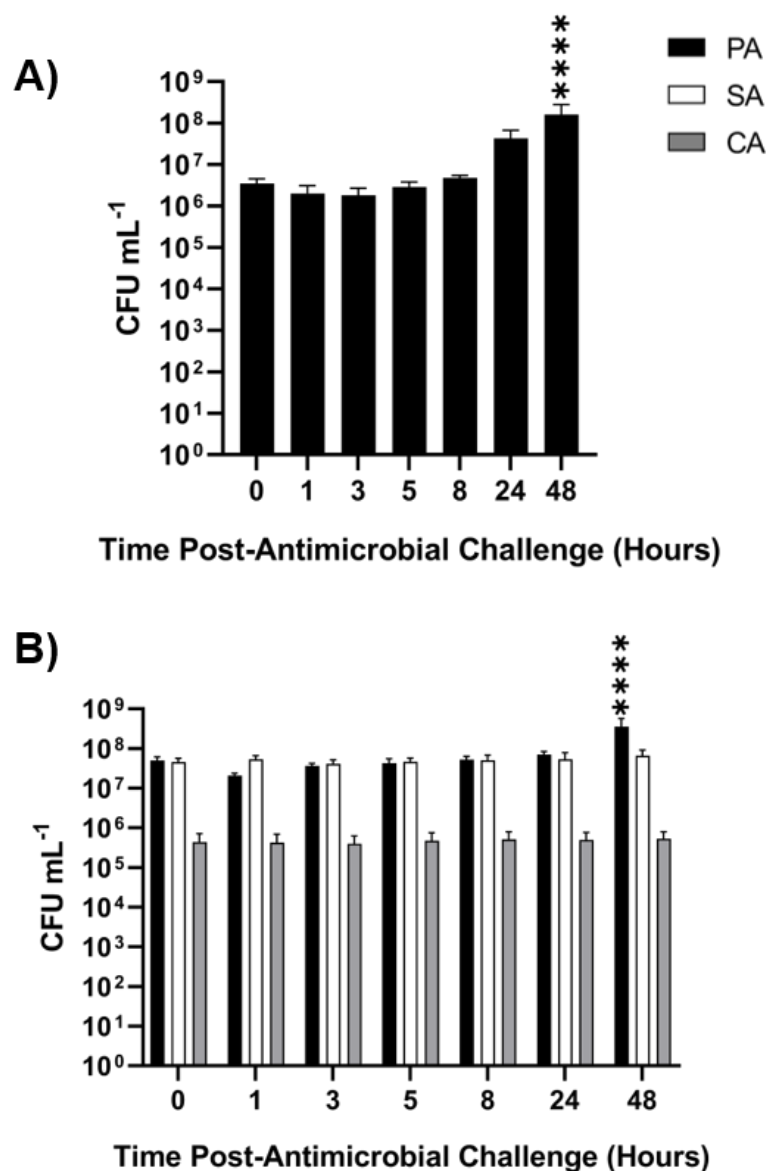


Figure 5.4 Addition of 1 x MIC colistin to steady-state microbial cultures.

Mono-species *P. aeruginosa* PAO1 and mixed-species cultures of *P. aeruginosa* PAO1 (black bars), *S. aureus* 25923 (white bars) and *C. albicans* SC5314 (grey bars) were grown to a steady-state in ASM under continuous-flow conditions. Bars represent viable cell counts (CFU mL⁻¹ in steady-state (24 hrs) **(A)** mono-species PA and **(B)** mixed-species populations following the addition of 4 µg mL⁻¹ colistin to the culture vessel at T = 0 hrs. Data represented as the mean ± standard deviation from three independent experiments. Asterisks represent significant (**** *P* < 0.0001) differences in PA CFU mL⁻¹ counts in comparison to counts at the 0 hrs timepoint.

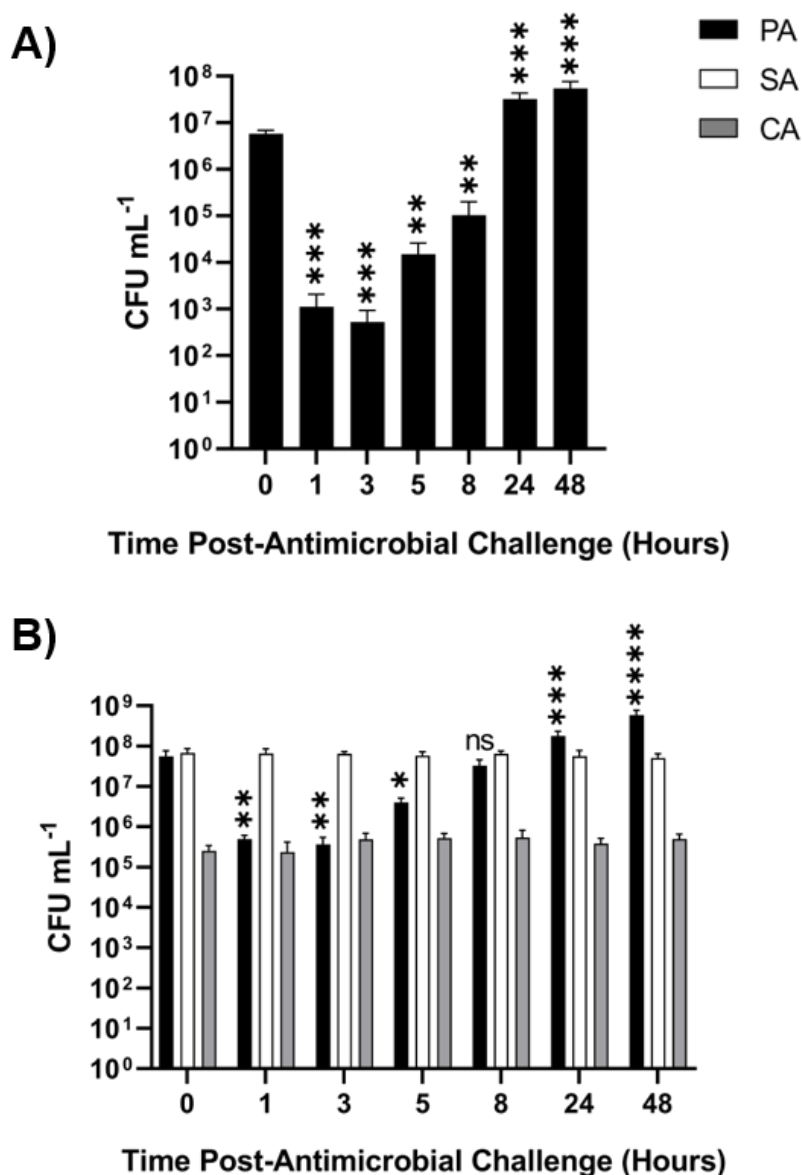


Figure 5.5 Addition of 2 x MIC colistin to steady-state microbial cultures.

Mono-species *P. aeruginosa* PAO1 and mixed-species cultures of *P. aeruginosa* PAO1 (black bars), *S. aureus* 25923 (white bars) and *C. albicans* SC5314 (grey bars) were grown to a steady-state in ASM under continuous-flow conditions. Bars represent viable cell counts (CFU mL⁻¹) in steady-state (24 hrs) **(A)** mono-species PA and **(B)** mixed-species populations following the addition of 8 µg mL⁻¹ colistin to the culture vessel at T = 0 hrs. Data represented as the mean ± standard deviation from three independent experiments. Asterisks represent significant (* *P* < 0.05, ** *P* < 0.01, *** *P* < 0.001, **** *P* < 0.0001) differences in PA CFU mL⁻¹ counts in comparison to counts at the 0 hrs timepoint. *P* > 0.05 is considered no significant difference (ns).

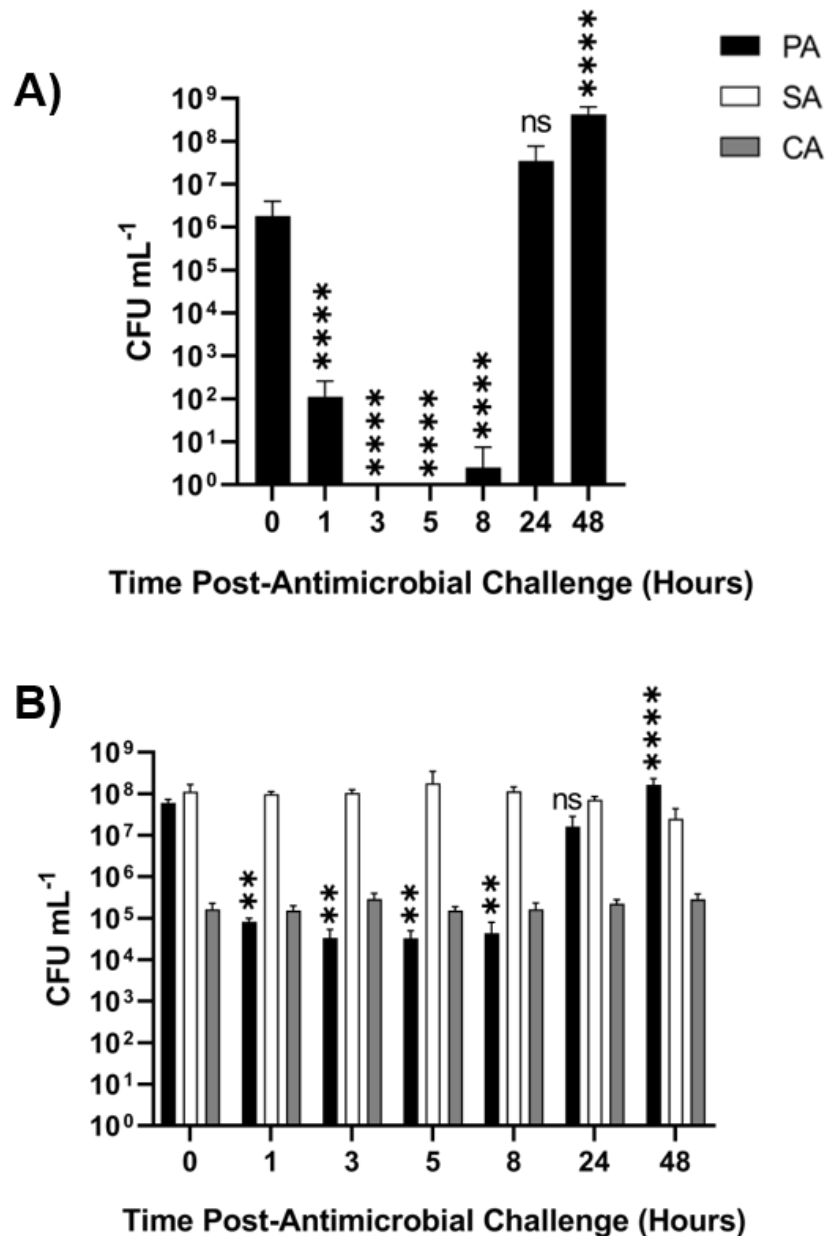


Figure 5.6 Addition of 5 x MIC colistin to steady-state microbial cultures.

Mono-species *P. aeruginosa* PAO1 and mixed-species cultures of *P. aeruginosa* PAO1 (black bars), *S. aureus* 25923 (white bars) and *C. albicans* SC5314 (grey bars) were grown to a steady-state in ASM under continuous-flow conditions. Bars represent viable cell counts (CFU mL⁻¹) in steady-state (24 hrs) **(A)** mono-species PA and **(B)** mixed-species populations following the addition of 20 µg mL⁻¹ colistin to the culture vessel at T = 0 hrs. Data represented as the mean ± standard deviation from three independent experiments. Asterisks represent significant (** *P* < 0.01, **** *P* < 0.0001) differences in PA CFU mL⁻¹ counts in comparison to counts at the 0 hrs timepoint. *P* > 0.05 is considered no significant difference (ns).

A significant ($P < 0.0001$) 4-log fold decrease in PA titres occurred between $T = 0$ and 1 hrs in the mono-species culture perturbed with 5 x MIC colistin (*Figure 5.6.A*). No viable PA cells were recovered from the culture vessel at 3 or 5 hrs incubation and fewer than 3 PA CFU mL⁻¹ were recovered from the culture vessels at 8 hrs of incubation. Following this, there was a significant 7-log fold increase in PA titres and there was no significant difference ($P > 0.9$) in CFU mL⁻¹ counts between $T = 0$ and 24 hrs. A further log-fold increase in PA cell counts occurred between the 24 and 48 hrs timepoints and final viable cell counts were significantly higher ($P < 0.0001$) than the initial point of sampling. A significant ($P < 0.01$) 2-log fold decrease in PA titres occurred between $T = 0$ and 1 hrs in the steady-state polymicrobial population treated with 5 x MIC colistin (*Figure 5.6.B*). There was no significant change ($P > 0.9$) in PA CFU mL⁻¹ counts between 1 and 8 hrs incubation. A 2-log fold increase in PA titres occurred between $T = 8$ and 24 hrs and there was no significant difference in PA CFU mL⁻¹ counts between 0 and 24 hrs incubation. A further log-fold increase in PA titres occurred between 24 and 48 hrs incubation and there was significantly more ($P < 0.0001$) PA CFU mL⁻¹ at the endpoint of sampling compared with the initial timepoint. No significant change ($P > 0.9$) in viable SA or CA titres was observed across any point of sampling.

5.2.3.2 OD_{600 nm} measurements

Average OD_{600 nm} measurements of single-species and polymicrobial populations treated with 1 x, 2 x or 5 x MIC colistin are displayed in *Figure 5.7*. The cell density of the polymicrobial populations were significantly higher ($P < 0.0001$) than that of the mono-species cultures and there was no appreciable difference in the starting OD_{600 nm} measurements of the pre-established cultures treated with different concentrations of colistin before the addition of the antimicrobial. There was no significant difference ($P > 0.9$) in OD_{600 nm} measurements between $T = 0$ and 8 hrs for both cultures treated with 1 x MIC colistin. There was a significant ($P < 0.05$) 0.2-unit increase in the density of the polymicrobial population treated with 1 x MIC colistin between 8 and 24 hrs incubation and a further significant ($P < 0.05$) 0.2-unit increase in average OD_{600 nm} measurements between $T = 24$ and 48 hrs. A significant ($P < 0.0001$) 0.4-unit increase in the density of the mono-species PA culture treated with 1 x MIC colistin occurred between $T = 8$ and 24 hrs and there was no significant difference ($P > 0.7$) in the cell density of the culture following this point.

Again, there was no significant difference ($P > 0.8$) in the density of both steady-state cultures treated with 2 x MIC colistin between $T = 0$ and 8 h. A significant ($P < 0.0001$) 0.6-unit increase in the density of the mono-species PA culture occurred between $T = 0$ and 24 hrs and there was no significant change in OD_{600 nm} measurements of the mono-species culture

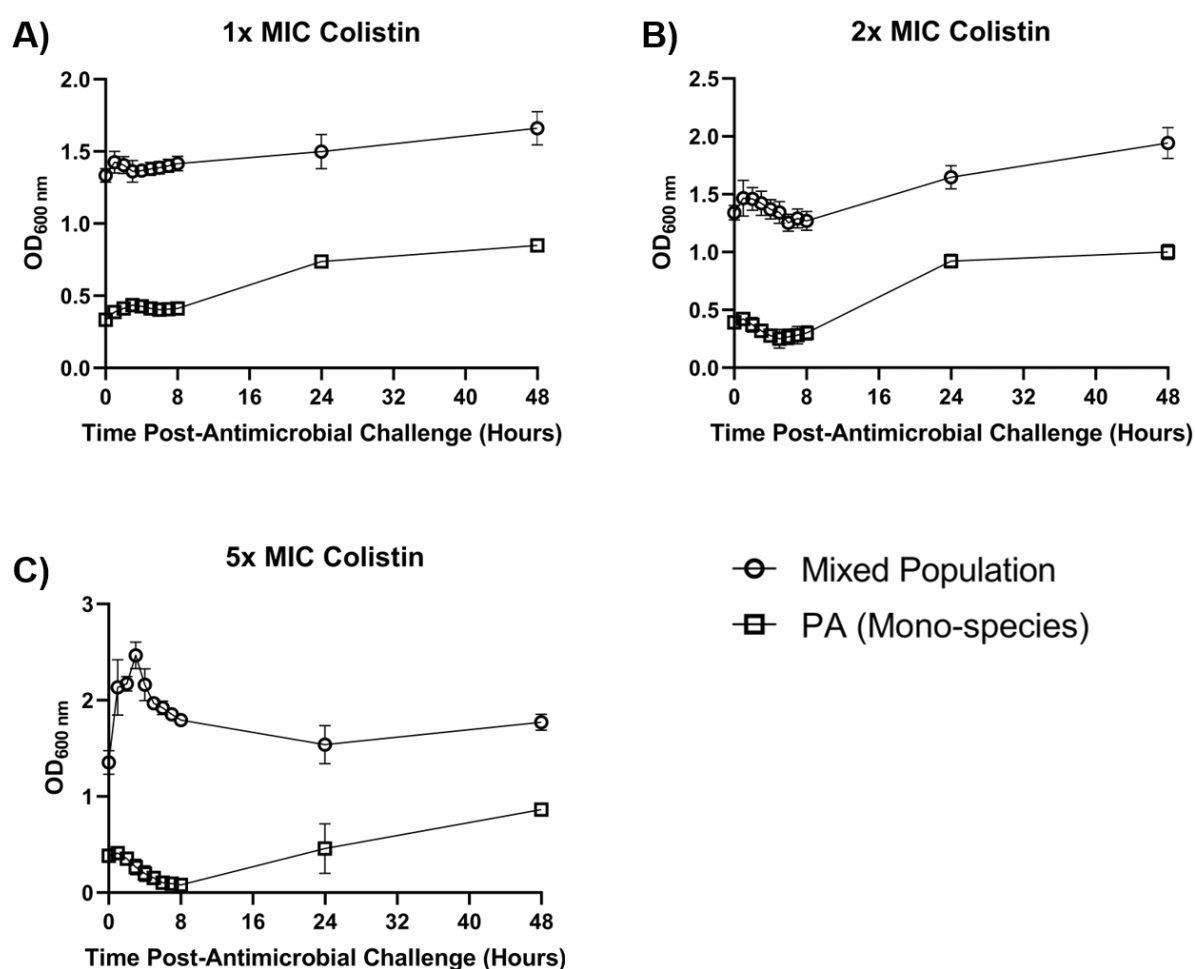


Figure 5.7 Optical density of steady-state cultures following the addition of colistin.

Mono-species *P. aeruginosa* PAO1 (squares) and mixed-species cultures of *P. aeruginosa* PAO1, *S. aureus* 25923 and *C. albicans* SC5314 (circles) were grown to a steady-state in ASM under continuous-flow conditions. Total culture density (OD_{600 nm}) was then measured following the addition of **(A)** 4; **(B)** 8 and **(C)** 20 $\mu\text{g mL}^{-1}$ colistin to the culture vessel. Data represented as the mean \pm standard deviation from three independent experiments.

between 24 and 48 hrs incubation. A significant ($P < 0.01$) 0.3-unit increase in optical density measurements occurred between $T = 0$ and 24 hrs within the polymicrobial population and a further significant ($P < 0.01$) 0.3-unit increase in cell density occurred between 24 and 48 hrs incubation.

A 0.3-unit decrease in average $OD_{600\text{ nm}}$ measurements occurred between $T = 0$ ($OD_{600\text{ nm}}$ 0.38) and 8 hrs ($OD_{600\text{ nm}}$ 0.08) in the PA mono-species culture treated with 5 x MIC colistin, although this change was not statistically significant ($P > 0.05$). An ≈ 0.4 -unit increase in average cell density measurements then occurred between 8 and 24 hrs incubation and there was no significant difference ($P > 0.9$) in $OD_{600\text{ nm}}$ values at $T = 0$ or 24 hrs. A further ≈ 0.4 -unit increase in $OD_{600\text{ nm}}$ measurements occurred between 24 and 48 hrs incubation and the average endpoint optical density measurements of the mono-species culture ($OD_{600\text{ nm}}$ 0.88) were significantly higher ($P < 0.01$) than the initial point of sampling. There was a significant ($P < 0.0001$) 0.8-unit increase in the average optical density of the polymicrobial population treated with 5 x MIC colistin between $T = 0$ hrs ($OD_{600\text{ nm}}$ 1.35) and 1 h ($OD_{600\text{ nm}}$ 2.13). Optical density continued to increase until $T = 3$ hrs ($OD_{600\text{ nm}}$ 2.47) and there was a significant ($P < 0.0001$) 0.7-unit decline in the density of the culture between 3 and 8 hrs incubation. There was no significant difference ($P > 0.9$) in average $OD_{600\text{ nm}}$ measurements of the polymicrobial culture between $T = 0$ and 24 hrs, however optical density measurements of the co-culture at the endpoint of sampling ($OD_{600\text{ nm}}$ 1.77) were significantly higher ($P < 0.05$) than the density of the culture before the addition of colistin.

5.2.4 Treatment with fusidic acid

5.2.4.1 Viable Cell Counts

Viable cell counts of pre-established SA mono-species and polymicrobial populations grown in ASM under continuous-flow conditions following the addition of 1 x MIC (15.6 ng mL⁻¹), 2 x MIC (31.2 ng mL⁻¹) or 5 x MIC (78 ng mL⁻¹) fusidic acid are shown in *Figure 5.8*, *5.9* and *5.10*, respectively. There was no appreciable difference in CFU mL⁻¹ counts between any mono-species or polymicrobial culture before the addition of fusidic acid. There was no statistically significant ($P > 0.05$) change in SA titres present in the mono-species culture treated with 1 x MIC fusidic acid between $T = 0$ and any subsequent point of sampling (*Figure 5.8.A*). A 0.4-log fold decrease in viable cell counts did occur between 0 and 5 hrs incubation and SA CFU mL⁻¹ counts at this point were significant lower ($P < 0.01$) than endpoint CFU counts. There was no significant difference ($P > 0.6$) in viable cell counts of any species within the polymicrobial culture treated with 1 x MIC fusidic acid across the entire period of incubation (*Figure 5.8.B*).

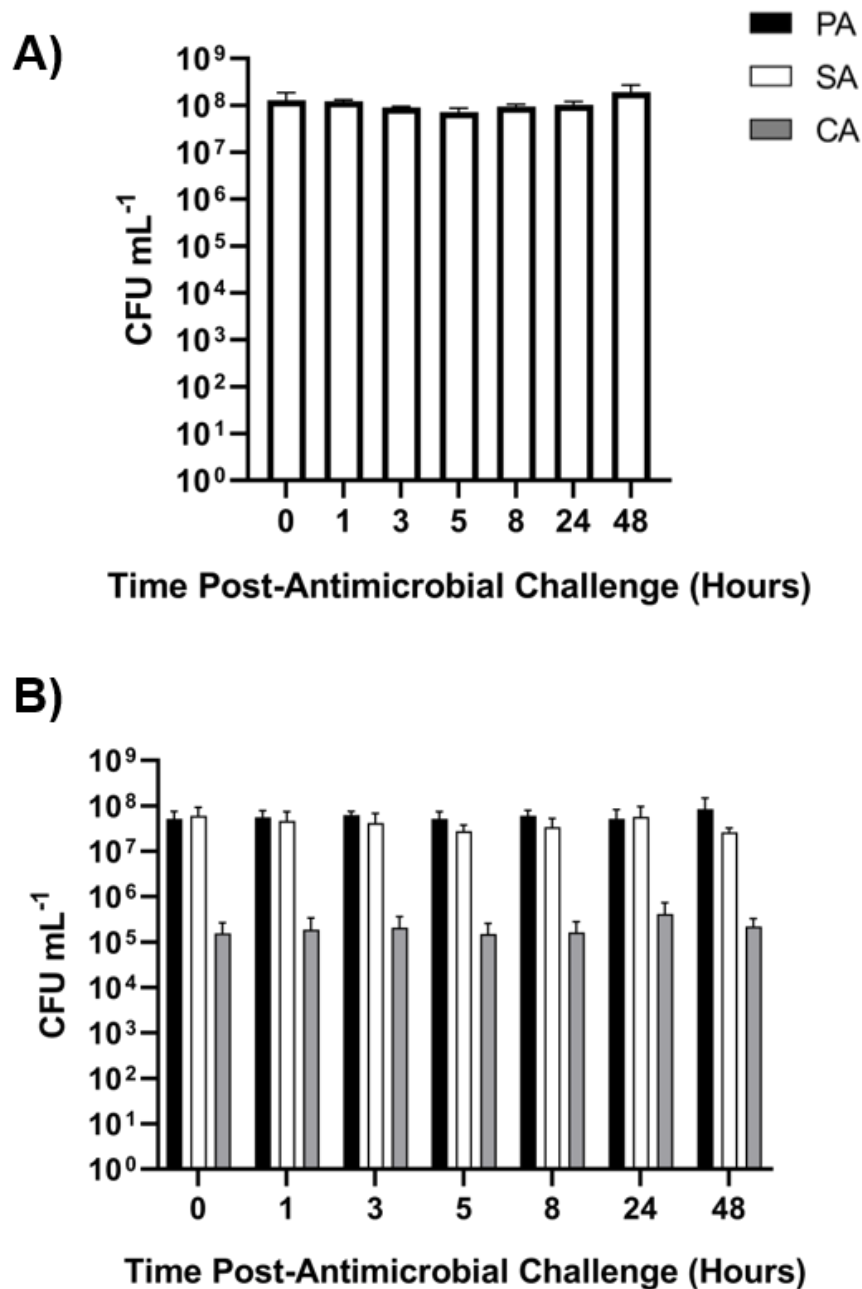


Figure 5.8 Addition of 1 x MIC fusidic acid to steady-state microbial cultures.

Mono-species *S. aureus* 25923 and mixed-species cultures of *P. aeruginosa* PAO1 (black bars), *S. aureus* 25923 (white bars) and *C. albicans* SC5314 (grey bars) were grown to a steady-state in ASM under continuous-flow conditions. Bars represent viable cell counts (CFU mL⁻¹) in steady-state (24 hrs) **(A)** mono-species SA and **(B)** mixed-species populations following the addition of 15.6 ng mL⁻¹ fusidic acid to the culture vessel at T = 0 hrs. Data represented as the mean ± standard deviation from three independent experiments.

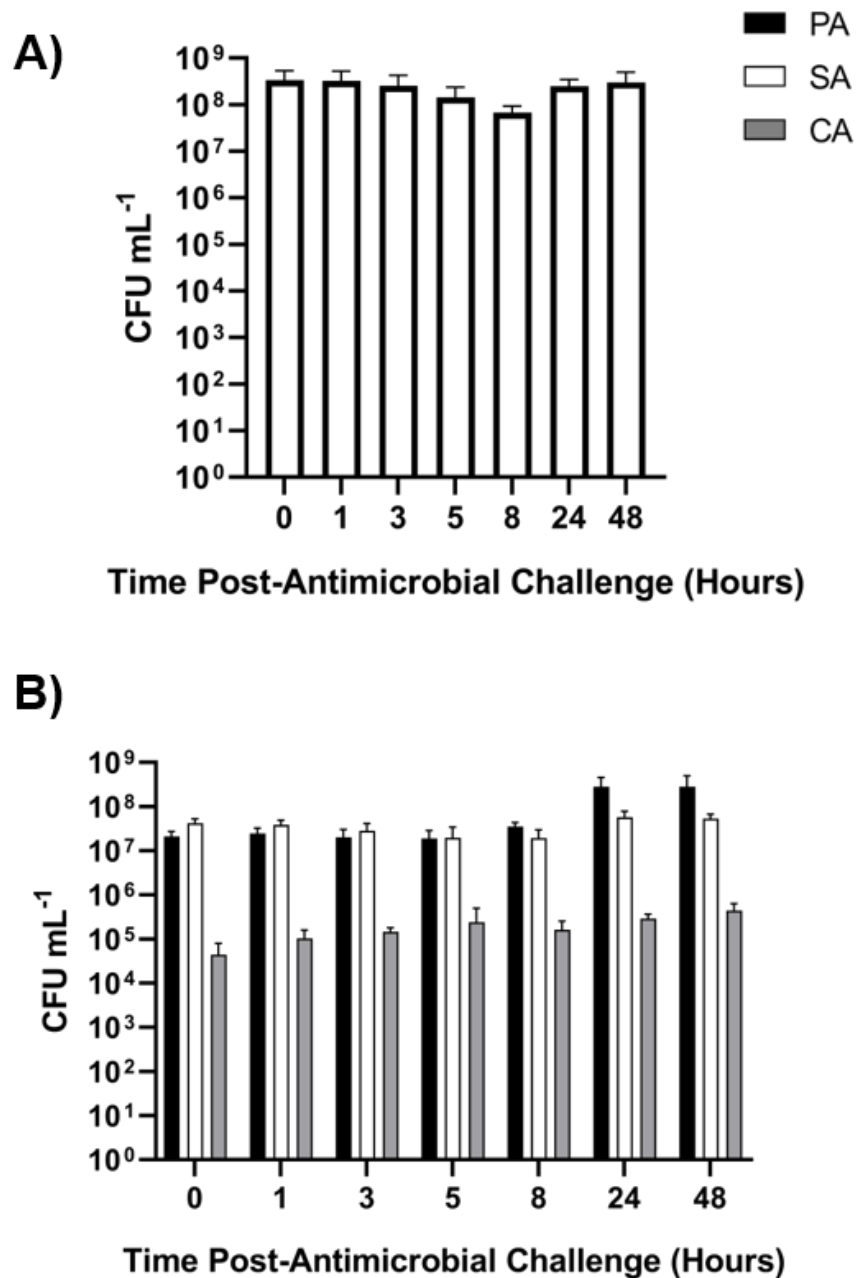


Figure 5.9 Addition of 2 x MIC fusidic acid to steady-state microbial cultures.

Mono-species *S. aureus* 25923 and mixed-species cultures of *P. aeruginosa* PAO1 (black bars), *S. aureus* 25923 (white bars) and *C. albicans* SC5314 (grey bars) were grown to a steady-state in ASM under continuous-flow conditions. Bars represent viable cell counts (CFU mL⁻¹) in steady-state (24 hrs) **(A)** mono-species SA and **(B)** mixed-species populations following the addition of 31.2 ng mL⁻¹ fusidic acid to the culture vessel at T = 0 hrs. Data represented as the mean ± standard deviation from three independent experiments.

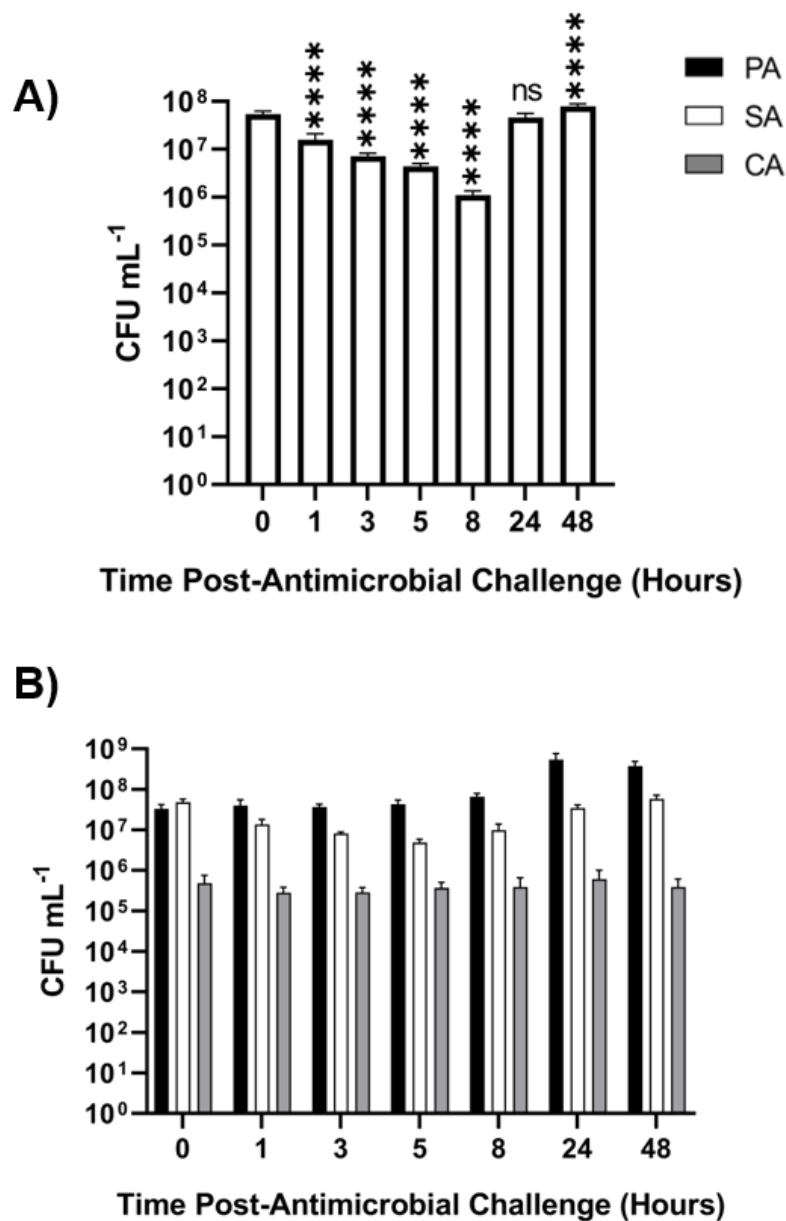


Figure 5.10 Addition of 5 x MIC fusidic acid to steady-state microbial cultures.

Mono-species *S. aureus* 25923 and mixed-species cultures of *P. aeruginosa* PAO1 (black bars), *S. aureus* 25923 (white bars) and *C. albicans* SC5314 (grey bars) were grown to a steady-state in ASM under continuous-flow conditions. Bars represent viable cell counts (CFU mL⁻¹) in steady-state (24 hrs) **(A)** mono-species SA and **(B)** mixed-species populations following the addition of 78 ng mL⁻¹ fusidic acid to the culture vessel at T = 0 hrs. Data represented as the mean \pm standard deviation from three independent experiments. Asterisks represent significant (**** $P < 0.0001$) differences in SA CFU mL⁻¹ counts in comparison to counts at the 0 hrs timepoint. $P > 0.05$ is considered no significant difference (ns).

Similarly, no statistically significant ($P > 0.05$) change in SA titres could be observed across any timepoint for the mono-species SA culture treated with 2 x MIC fusidic acid (*Figure 5.9.A*). As in *Figure 5.9.A*, there was a non-significant 0.8-log fold decrease in SA CFU mL⁻¹ between T = 0 and 8 hrs. There was no significant change in SA or CA titres for the entire period of incubation within the polymicrobial population treated with 2 x MIC fusidic acid (*Figure 5.9.B*). Interestingly, a significant ($P < 0.001$) log-fold increase in PA CFU mL⁻¹ counts occurred between T = 0 and 24 hrs and there was no appreciable change ($P > 0.9$) in viable PA cell counts following the 24 hrs point of sampling.

A significant ($P < 0.0001$) 1.4-log fold decrease in SA CFU mL⁻¹ counts occurred between T = 0 and 8 hrs within the mono-species SA culture treated with 5 x MIC fusidic acid (*Figure 5.10.A*). SA titres in the culture vessel then increased between 8 and 24 hrs incubation and there was no significant difference ($P > 0.2$) in SA CFU mL⁻¹ counts between T = 0 and 24 hrs. Yet, there was a significant ($P < 0.0001$) 0.5-log fold increase in SA titres between T = 0 and 48 hrs. There was no statistically significant ($P > 0.8$) change in SA or CA titres across any time point for the polymicrobial culture perturbed with 5 x MIC fusidic acid (*Figure 5.10.B*). Yet an approximate log-fold decrease in average SA CFU mL⁻¹ counts was observed between T = 0 and 5 hrs. A significant ($P < 0.0001$) log-fold increase in PA titres occurred within the polymicrobial co-culture between T = 0 and 24 hrs and there was no significant change ($P > 0.9$) in PA CFU mL⁻¹ counts following this point of sampling.

5.2.4.2 OD_{600 nm} measurements

Average OD_{600 nm} measurements of single-species and polymicrobial populations treated with 1 x, 2 x or 5 x MIC fusidic acid are displayed in *Figure 5.11*. There was no significant change ($P > 0.8$) in OD_{600 nm} measurements of either of the steady-state cultures treated with 1 x MIC fusidic acid or the polymicrobial culture treated with 2 x MIC fusidic acid across all timepoints. A significant ($P < 0.01$) 0.1-unit decrease in average OD_{600 nm} measurements occurred between T = 0 and 8 hrs for the SA mono-species population treated with 2 x MIC fusidic acid. This was followed by an 0.1-unit increase in optical density measurements between T = 8 and 24 hrs and a further 0.1-unit increase in OD_{600 nm} values between 24 and 48 hrs incubation. The endpoint cell density of the 2 x MIC treated mono-species SA culture was significantly higher ($P > 0.05$) than the density of the culture at the initial point of sampling. There was a significant ($P < 0.01$) 0.2-unit drop in OD_{600 nm} measurements for the SA mono-species steady-state culture treated with 5 x MIC fusidic acid between T = 0 and 8 hrs. Density of the cell culture then increased by 0.2-units between 8 and 24 hrs incubation and there was no

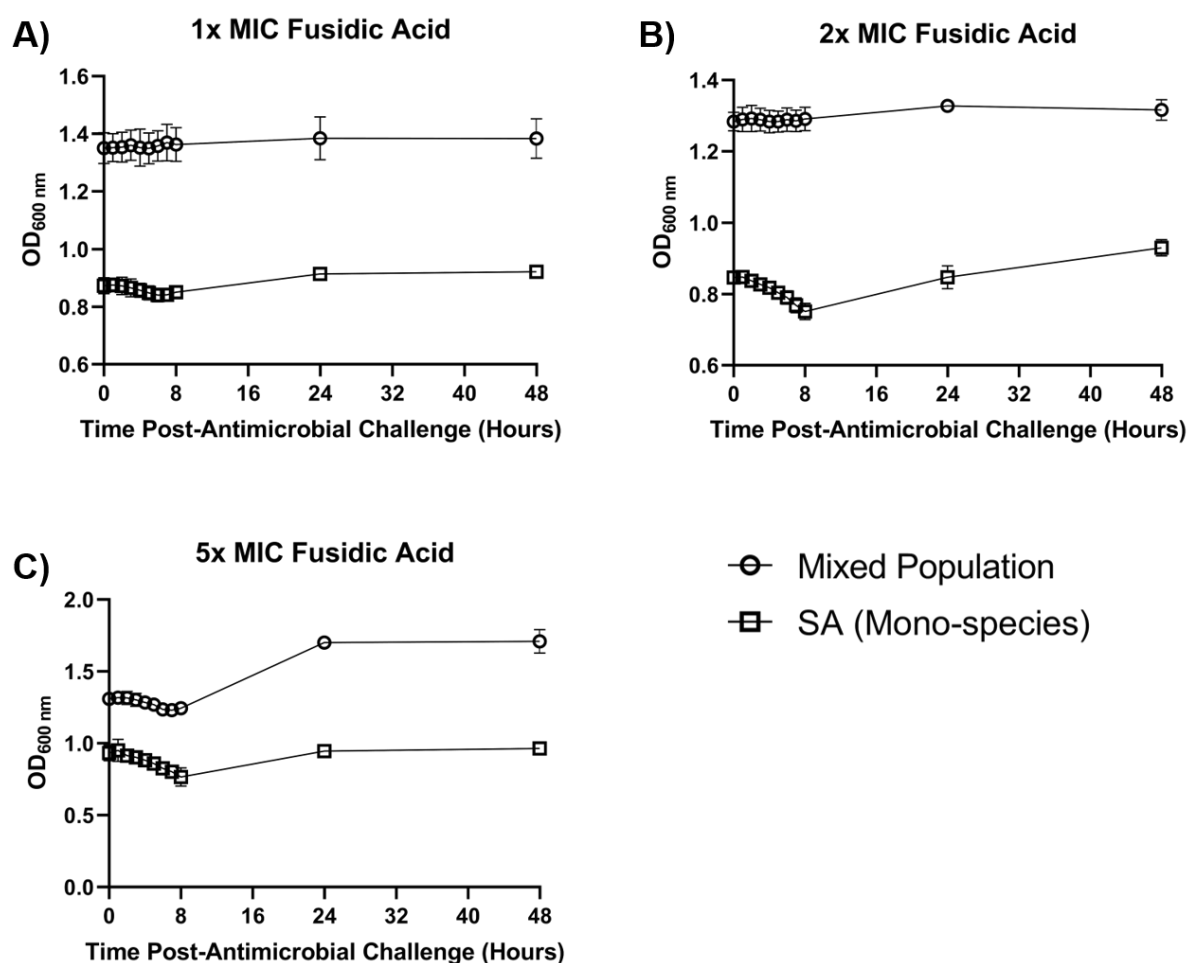


Figure 5.11 Optical density of steady-state cultures following the addition of fusidic acid.

Mono-species *S. aureus* 25923 (squares) and mixed-species cultures of *P. aeruginosa* PAO1, *S. aureus* 25923 and *C. albicans* SC5314 (circles) were grown to a steady-state in ASM under continuous-flow conditions. Total culture density (OD_{600 nm}) was then measured following the addition of **(A)** 15.6; **(B)** 31.2 and **(C)** 78 ng mL⁻¹ fusidic acid to the culture vessel. Data represented as the mean ± standard deviation from three independent experiments.

significant difference in OD_{600 nm} measurements of the culture at T = 0, 24 or 48 hrs. There was no significant difference ($P > 0.9$) in the optical density of the polymicrobial culture treated with 5 x MIC fusidic acid between T = 0 and 8 hrs. A significant ($P < 0.0001$) 0.45-unit increase in average OD_{600 nm} values then occurred between T = 8 and 24 hrs and there was no appreciable change ($P > 0.9$) in the density of the co-culture between 24 and 48 hrs incubation.

5.2.5 Treatment with fluconazole

5.2.5.1 Viable Cell Counts

Viable cell counts of pre-established CA mono-species and polymicrobial populations grown in ASM under continuous-flow conditions following the addition of 1 x MIC (1 µg mL⁻¹), 2 x MIC (2 µg mL⁻¹) or 5 x MIC (5 µg mL⁻¹) fluconazole are shown in *Figure 5.12*, *5.13* and *5.14*, respectively. No appreciable difference in CFU mL⁻¹ counts could be observed between any mono-species or polymicrobial culture before the addition of fluconazole. There was no significant difference ($P > 0.7$) in CA titres within the mono-species culture treated with 1 x MIC fluconazole between T = 0 hrs and any subsequent timepoint (*Figure 5.12.A*). Similarly, there was no statistically significant change ($P > 0.9$) in CA, PA or SA titres between T = 0 and any other point of sampling within the polymicrobial culture treated with 1 x MIC fluconazole (*Figure 5.12.B*).

A significant ($P < 0.01$) log-fold decrease in CA titres occurred between T = 0 and 8 hrs in the CA mono-species population treated with 2 x MIC fluconazole (*Figure 5.13.A*). A 0.5-log fold increase in CA CFU mL⁻¹ counts then occurred between 8 and 24 hrs of incubation, but viable cell counts remained significantly lower ($P < 0.05$) than the initial point of sampling. At the endpoint of incubation, there was no significant difference ($P > 0.1$) in CA titres compared with T = 0 hrs. There was no statistically significant change ($P > 0.2$) in CA, PA or SA titres across all sample points for the polymicrobial population treated with 2 x MIC fluconazole (*Figure 5.13.B*). However, a 0.5-log fold decrease in CA titres can be observed between 0 and 8 hrs incubation.

A significant ($P < 0.0001$) ≈ 2-log fold decrease in CA titres occurred between 0 and 8 hrs within the mono-species CA culture treated with 5 x MIC fluconazole (*Figure 5.14.A*). An approximate 0.6-log fold increase in CA CFU mL⁻¹ counts then occurred between T = 8 and 24 hrs and this was followed by a further 0.6-log fold increase in CA titres present in the culture vessel between 24 and 48 hrs incubation. Despite this increase in CA cells, endpoint CA CFU mL⁻¹ counts remaining significantly lower ($P < 0.05$) than the initial point of sampling. As with perturbation with 2 x MIC fluconazole. There was no statistically significant change ($P > 0.2$) in CA or SA CFU mL⁻¹ counts across all points of sampling for the polymicrobial culture

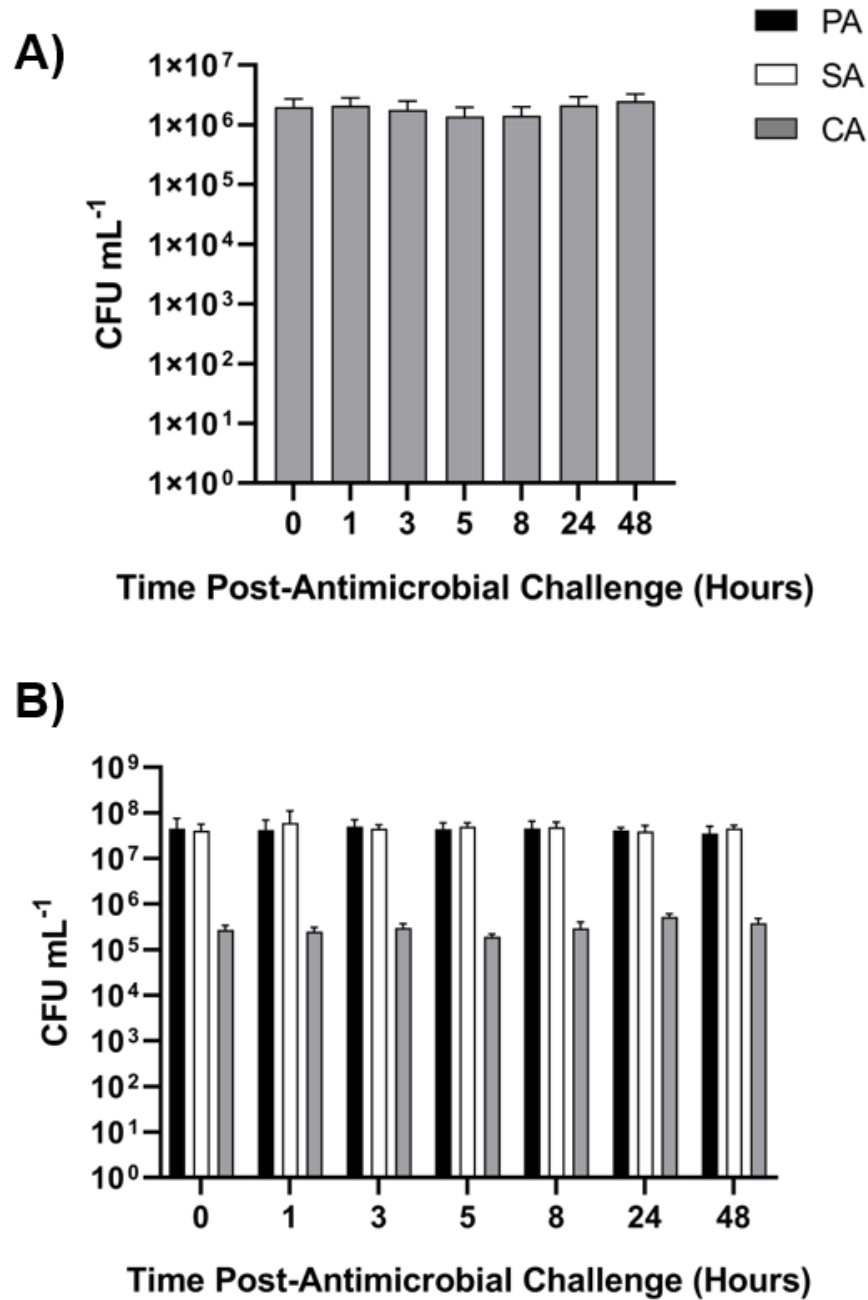


Figure 5.12 Addition of 1 x MIC fluconazole to steady-state microbial cultures.

Mono-species *C. albicans* SC5314 and mixed-species cultures of *P. aeruginosa* PAO1 (black bars), *S. aureus* 25923 (white bars) and *C. albicans* SC5314 (grey bars) were grown to a steady-state in ASM under continuous-flow conditions. Bars represent viable cell counts (CFU mL⁻¹) in steady-state (24 hrs) **(A)** mono-species PA and **(B)** mixed-species populations following the addition of 1 µg mL⁻¹ fluconazole to the culture vessel at T = 0 hrs. Data represented as the mean ± standard deviation from three independent experiments.

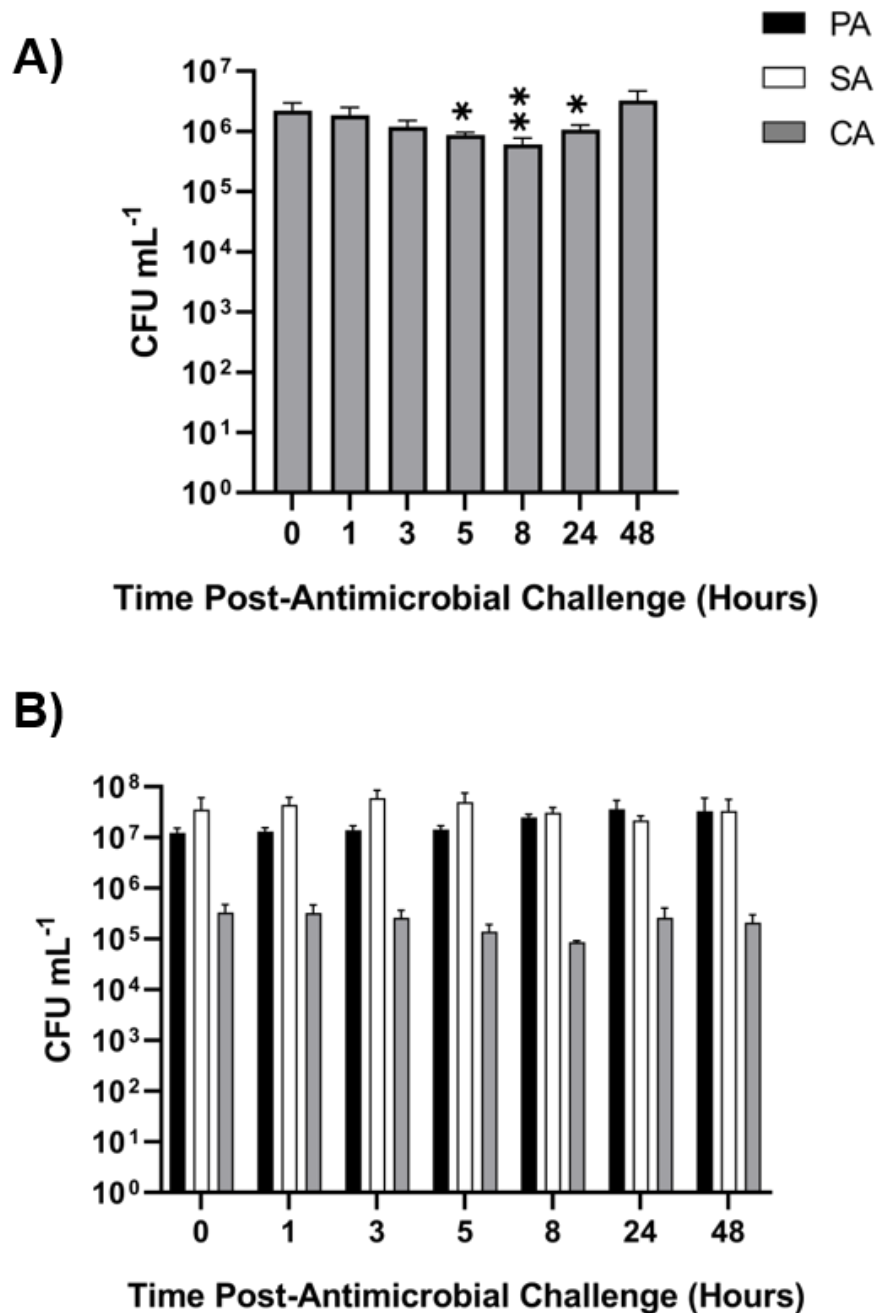


Figure 5.13 Addition of 2 x MIC fluconazole to steady-state microbial cultures.

Mono-species *C. albicans* SC5314 and mixed-species cultures of *P. aeruginosa* PAO1 (black bars), *S. aureus* 25923 (white bars) and *C. albicans* SC5314 (grey bars) were grown to a steady-state in ASM under continuous-flow conditions. Bars represent viable cell counts (CFU mL⁻¹) in steady-state (24 hrs) **(A)** mono-species PA and **(B)** mixed-species populations following the addition of 2 µg mL⁻¹ fluconazole to the culture vessel at T = 0 hrs. Data represented as the mean ± standard deviation from three independent experiments. Asterisks represent significant (* *P* < 0.05, ** *P* < 0.01) differences in CA CFU mL⁻¹ counts in comparison to counts at the 0 hrs timepoint.

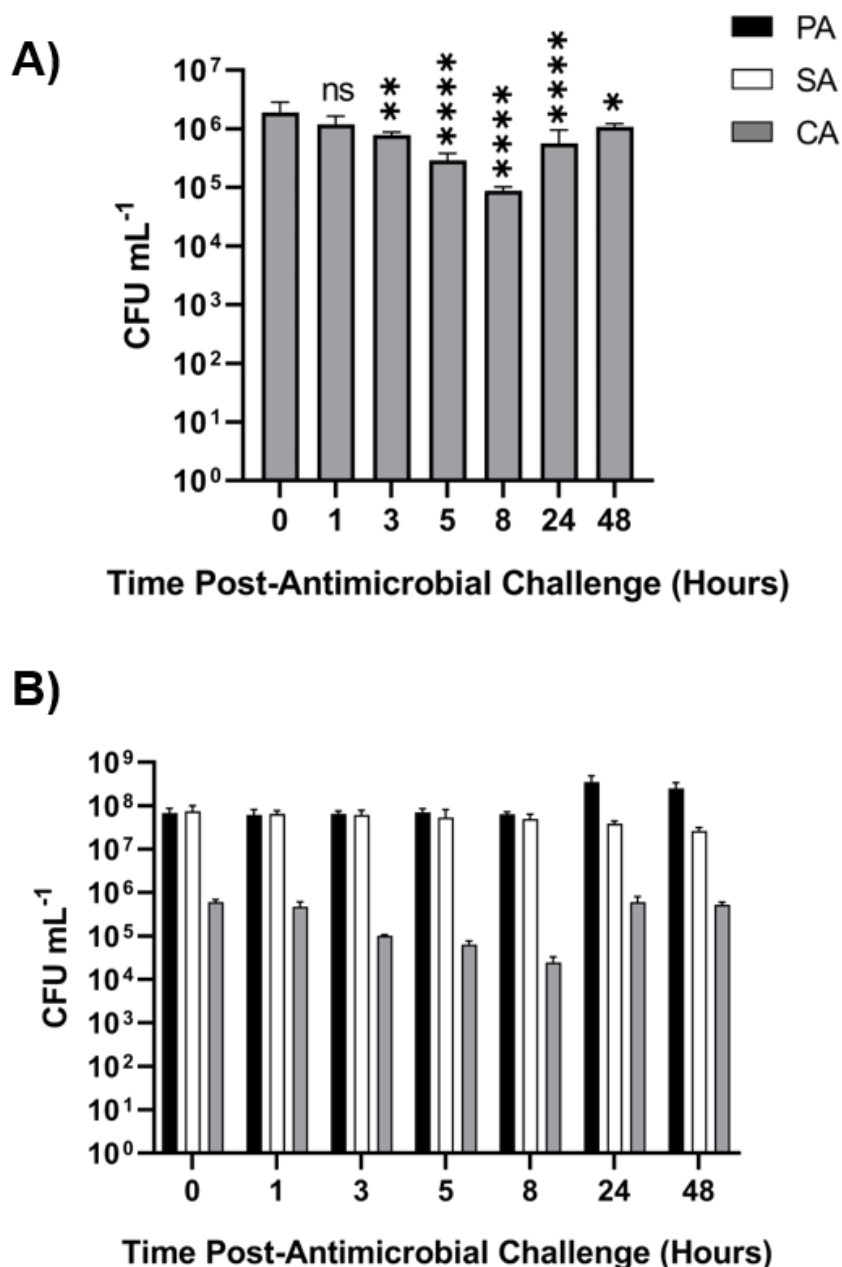


Figure 5.14 Addition of 5 x MIC fluconazole to steady-state microbial cultures.

Mono-species *C. albicans* SC5314 and mixed-species cultures of *P. aeruginosa* PAO1 (black bars), *S. aureus* 25923 (white bars) and *C. albicans* SC5314 (grey bars) were grown to a steady-state in ASM under continuous-flow conditions. Bars represent viable cell counts (CFU mL⁻¹) in steady-state (24 hrs) **(A)** mono-species PA and **(B)** mixed-species populations following the addition of 5 µg mL⁻¹ fluconazole to the culture vessel at T = 0 hrs. Data represented as the mean ± standard deviation from three independent experiments. Asterisks represent significant (* *P* < 0.05, ** *P* < 0.01, **** *P* < 0.0001) differences in CA CFU mL⁻¹ counts in comparison to counts at the 0 hrs timepoint. *P* > 0.05 is considered no significant difference (ns).

treated with 5 x MIC fluconazole (*Figure 5.14.B*). However, a non-significant \approx log-fold decrease in CA titres was observed between 0 and 8 hrs incubation. By contrast, a significant ($P < 0.001$) log-fold increase in PA CFU mL⁻¹ counts occurred between 0 and 24 hrs incubation and there was no significant change ($P > 0.9$) in PA titres following this.

5.2.5.2 OD_{600 nm} measurements

Average OD_{600 nm} measurements of single-species and polymicrobial populations treated with 1 x, 2 x or 5 x MIC fluconazole are shown in *Figure 5.15*. Across all time points there was no statistically significant change ($P > 0.4$) in OD_{600 nm} measurements of the mono-species or polymicrobial steady-state cultures treated with 1 x MIC or 2 x MIC fluconazole. There was a significant ($P < 0.05$) 0.3-unit increase in OD_{600 nm} measurements between 0 and 2 hrs incubation (OD_{600 nm} 1.78 and 2.08, respectively) for the mono-species CA culture treated with 5 x MIC fluconazole. This was followed by a significant ($P < 0.0001$) 0.5-unit decrease in the cell density between T = 2 and 8 hrs (OD_{600 nm} 1.54), yet there was no statistically significant difference ($P > 0.1$) the density of the culture between T = 0 and 8 hrs. A steady, but non-significant ($P > 0.9$) increase in OD_{600 nm} values then occurred between 8, 24 and 48 hrs of incubation. Endpoint average cell density of the mono-species population treated with 5 x MIC fluconazole was not statistically different ($P > 0.5$) from the density at the initial point of sampling. A significant ($P < 0.0001$) 0.4-unit increase in optical density of the polymicrobial population treated with 5 x MIC fluconazole occurred between T = 0 and 24 hrs (OD_{600 nm} 1.42 and 1.84, respectively). There was no appreciable change ($P < 0.9$) in optical density measurements of the polymicrobial co-culture between 24 and 48 hrs incubation.

5.2.6 Conclusions

Several key conclusions pertaining to the understanding of the antimicrobial perturbation of steady-state polymicrobial populations can be drawn from the results presented in this subsection. Firstly, the treatment of polymicrobial populations with species-specific antimicrobials had less impact on the target microorganism compared with treatment of mono-species populations with the same antimicrobial agent. This demonstrates a diminution in the efficacy of both microbicidal and microbiostatic compounds when treating mixed species populations. Secondly, colistin caused the fastest onset and most pronounced decrease in viable cell counts, in both mono-species and polymicrobial cultures, compared with the bacteriostatic/fungistatic compounds. This difference might be explained by the rapid lysis of PA cells by colistin *via* disruption of the outer membrane. By contrast fusidic acid and

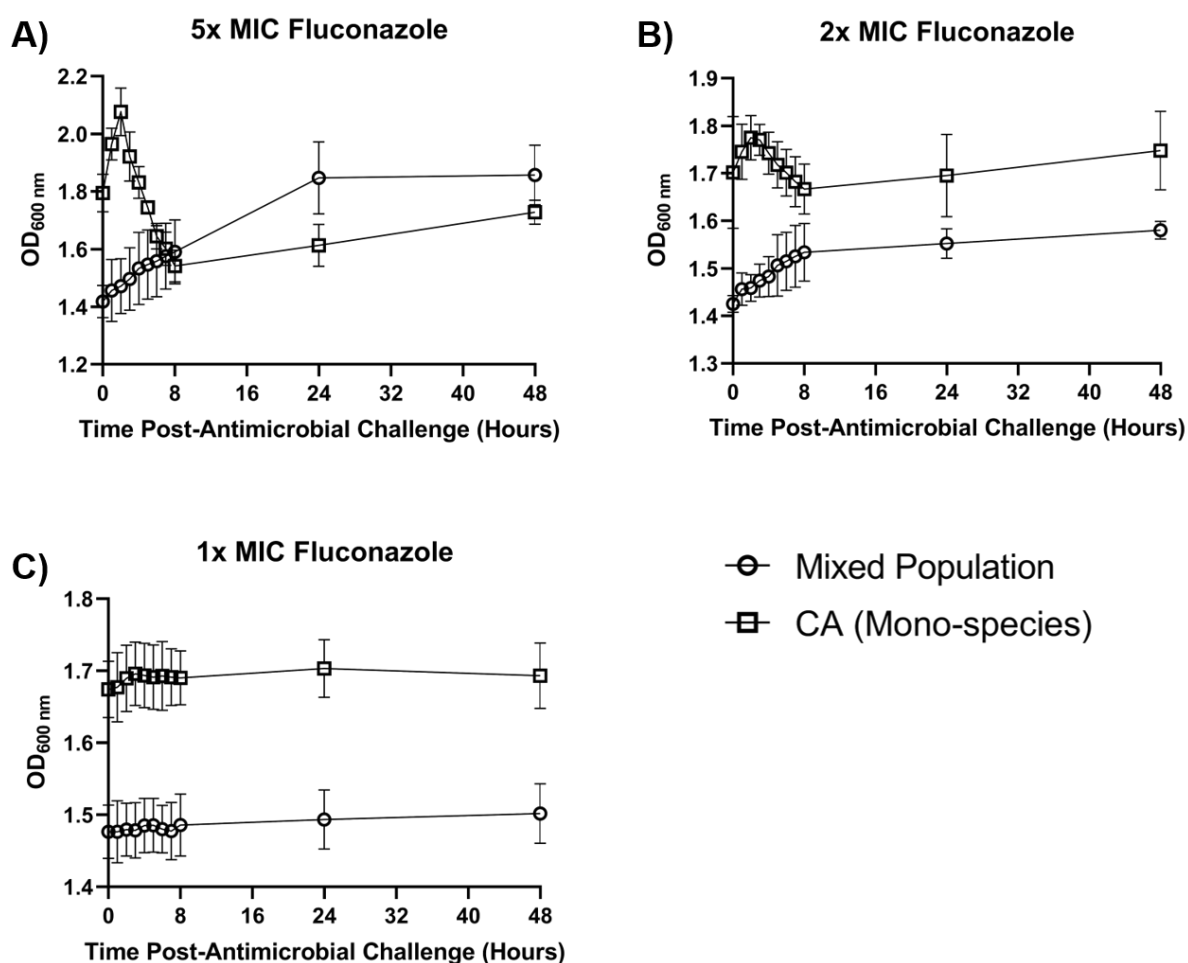


Figure 5.15 Optical density of steady-state cultures following the addition of fusidic acid.

Mono-species *C. albicans* SC5314 (squares) and mixed-species cultures of *P. aeruginosa* PAO1, *S. aureus* 25923 and *C. albicans* SC5314 (circles) were grown to a steady-state in ASM under continuous-flow conditions. Total culture density (OD_{600 nm}) was then measured following the addition of **(A)** 1; **(B)** 2 and **(C)** 5 $\mu\text{g mL}^{-1}$ fluconazole to the culture vessel. Data represented as the mean \pm standard deviation from three independent experiments.

fluconazole arrest the growth of actively dividing SA and CA cells present in a pre-established culture but do not cause cell lysis. Non-replicating populations of SA and CA are then gradually displaced from the culture vessel due to the continuous-flow of fresh medium. Incidentally, the addition of ASM to the culture vessel dilutes the antimicrobials present and permits the growth of species to recommence at later timepoints once sub-MIC concentrations of the antimicrobial are reached. These preliminary results suggest that the treatment of pre-established chronic microbial infections with bactericidal compounds likely result in more effective clearance of the target pathogen. However, further investigation into whether this observation is true for different antimicrobial compound classes is required. It is also important to note that the *in vitro* model cannot account for the action of an immune system when clearing microbial infections *in situ*.

The treatment of steady-state polymicrobial populations with 5 x MIC fusidic acid or fluconazole caused a slight inhibition in the growth of the target species. However, this decrease in SA and CA titres in the culture vessel was accompanied by a significant increase in PA CFU mL⁻¹ counts in both populations. This demonstrates the ability of PA to capitalize on exogenous perturbation of a polymicrobial community and increase its population in response to a diminution in the cell counts of a co-habiting species. This observation is in support of the climax-attack model (CAM) of the CF airway-associated microbial ecology proposed by Conrad *et al.* (2013). The CAM hypothesises that PA is a member of both the stable and disturbed polymicrobial consortium and becomes the dominant pathogen associated with the CF microenvironment by being the most adept at surviving immune clearance or clinical intervention. Following the removal of other species during exogenous perturbation PA expands into the newly liberated environmental niche previously inhabited by other microbial species. Treatment of either steady-state population with colistin or the treatment of mono-species SA population with 5 x MIC fusidic acid resulted in a significant increase in CFU mL⁻¹ counts between the initial and endpoint of sampling. This finding highlights that the failed eradication of a microbial population with antimicrobial compounds may select for mutant variants that can rapidly expand to occupy recently-vacated niches previously occupied by co-habiting strains/species. Taken in combination, these findings affirm the importance of fully understanding how antimicrobial compounds perturb complete polymicrobial communities to limit the emergence of pathogenic species whilst treating the polymicrobial communities associated with CF airway infections.

5.3 Antimicrobial resistance vs tolerance

5.3.1 Resistance profiles of isolates

It could not be determined whether the modulated decrease in the titres of a target pathogen from a polymicrobial co-culture following the addition of an antimicrobial resulted from an increased selection of mutants with inheritable resistance mechanisms within the population or if this phenomenon was simply a protective or tolerance effect resulting from the presence of other species during co-culture. To investigate this, 48 isolates were randomly collected throughout the incubation of both the mono-species and polymicrobial populations treated with the different concentration of antimicrobials (as described in *Section 2.11.4*). The resistance profiles of these isolates were compared against the susceptibility of the parental strain reported in *Section 5.2.2*.

There was no difference in the MIC of fusidic acid required to inhibit growth of the parental SA strain and any SA isolate collected from either the mono-species or polymicrobial cultures treated with any concentration fusidic acid (data not shown). This demonstrates that the decreased removal of viable SA cells from a polymicrobial population following treatment with this antimicrobial arises from a protective mechanism owing to the presence of other species during co-culture, not an inherited mechanism of resistance.

The percentage of PA or CA isolates able to grow in the presence of increasing concentrations of colistin or fluconazole are shown in *Figure 5.16* and *Figure 5.17*, respectively. The resistance profiles of the individual isolates against different antimicrobial concentrations are shown in *Table 5.2* and *Table 5.3*, respectively. Unlike the SA isolates, 89.6% and 83.3% of the PA strains isolated from the polymicrobial or mono-species cultures, respectively, could grow in the concentration of colistin required to inhibit the growth of the parental strain ($4 \mu\text{g mL}^{-1}$). Similarly, 83.3% and 75% of the CA isolates collected from the polymicrobial or mono-species cultures, respectively, could grow in the concentration of fluconazole required to inhibit the parental strain ($1 \mu\text{g mL}^{-1}$). No CA isolates could grow in the presence of $10 \mu\text{g mL}^{-1}$ fluconazole, yet 31.2% of isolates collected from the polymicrobial culture and 18.8% of the isolates from the single-species culture could grow in $5 \mu\text{g mL}^{-1}$ fluconazole. Likewise, 29.2% and 16.7% of the PA isolates collected from the polymicrobial or mono-species cultures were able to grow in $40 \mu\text{g mL}^{-1}$ colistin. Furthermore, 14.6% of the polymicrobial culture and 8.3% of the axenic culture PA isolates could grow in ASM supplemented with 1 mg mL^{-1} colistin and so are considered fully resistant to this antimicrobial compound. Interestingly, 70.8% of the CA isolates and all of the PA isolates able to grow in the presence of the highest concentration of the antimicrobials were recovered from the culture vessels treated with 2 x MIC colistin or fluconazole. Just 5% of the isolates able to grow in $5 \mu\text{g mL}^{-1}$ fluconazole or $40 \mu\text{g mL}^{-1}$ colistin

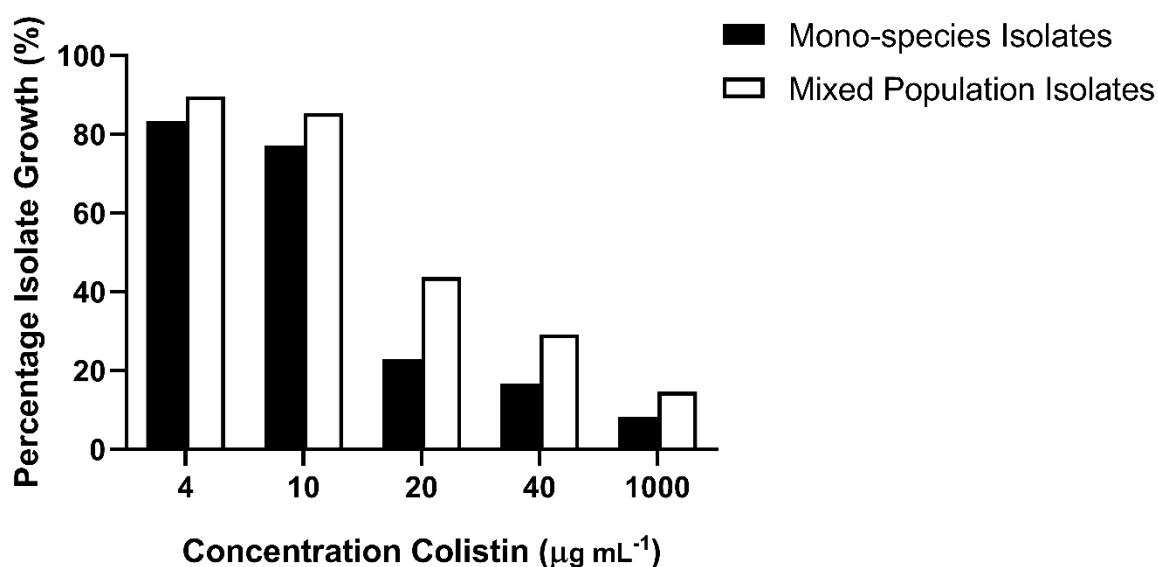


Figure 5.16 Growth of *P. aeruginosa* isolates in ASM with colistin.

Percentage (%) of *P. aeruginosa* PAO1 isolates able to grow in ASM containing the indicated concentration of colistin ($\mu\text{g mL}^{-1}$). Isolates (48 from each condition) were randomly collected from single-species (black bars) and mixed-species (white bars) steady-state continuous-flow populations challenged with colistin (as described in *Section 2.11.4*). Ability of isolates to grow in different colistin concentrations was determined in microtiter plates incubated at 37°C for 16 hrs with 100 rpm shaking and results were confirmed over three independent experiments using fresh batches of ASM.

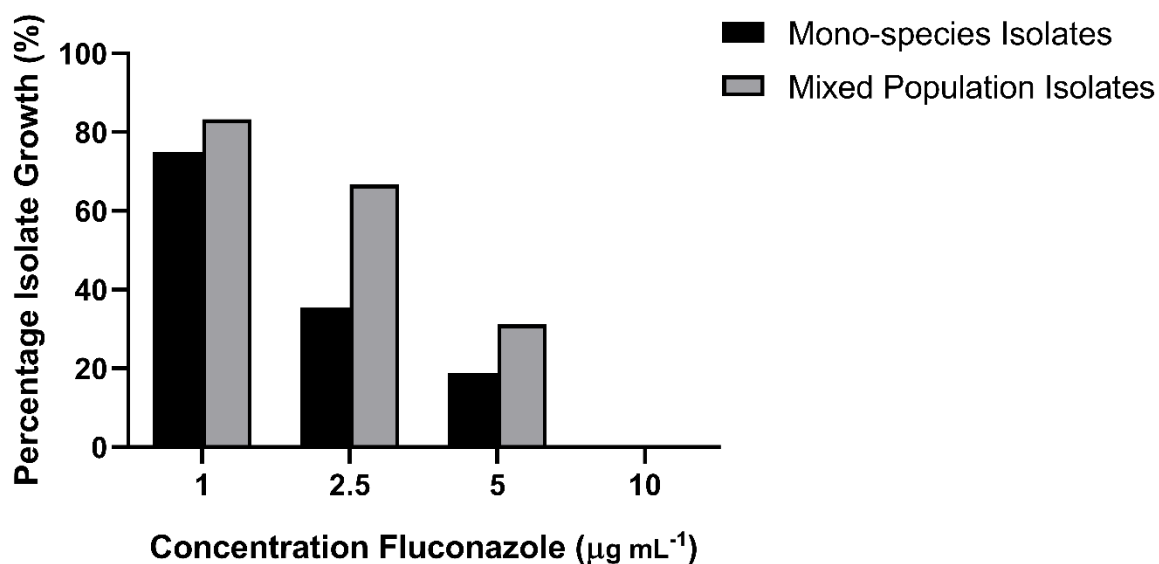


Figure 5.17 Growth of *C. albicans* isolates in ASM with fluconazole.

Percentage (%) of *C. albicans* SC5314 isolates able to grow in ASM containing the indicated concentration of fluconazole ($\mu\text{g mL}^{-1}$). Isolates (48 from each condition) were randomly collected from single-species (black bars) and mixed-species (white bars) steady-state continuous-flow populations challenged with fluconazole (as described in *Section 2.11.4*). Ability of isolates to grow in different colistin concentrations was determined in microtiter plates incubated at 37°C for 24 hrs with 100 rpm shaking and results were confirmed over three independent experiments using fresh batches of ASM.

Time (Hours)	MIC ($\mu\text{g mL}^{-1}$) of colistin against isolates collected from mono-species culture challenged with:											
	1 x MIC colistin				2 x MIC colistin				5 x MIC colistin			
1	4	10	20	20	25	45	>1000	>1000	20	25	45	45
8	4	10	20	20	20	45	>1000	>1000	20	25	20	20
24	4	4	4	20	20	20	20	20	20	20	20	20
48	4	4	4	10	20	20	20	20	20	20	20	20
	MIC ($\mu\text{g mL}^{-1}$) of colistin against isolates collected from polymicrobial co-culture challenged with:											
	1 x MIC colistin				2 x MIC colistin				5 x MIC colistin			
1	4	4	4	10	45	45	>1000	>1000	20	20	25	45
8	20	20	20	20	45	>1000	>1000	>1000	25	25	45	45
24	4	20	20	20	25	45	>1000	>1000	20	20	25	25
48	4	10	20	20	20	20	20	20	20	20	20	20

Table 5.2 Resistance profiles of PA isolates collected from steady-state cultures challenged with different concentrations of colistin.

Isolates of *P. aeruginosa* were randomly collected from mono-species *P. aeruginosa* PAO1 (top rows) or polymicrobial *P. aeruginosa* PAO1, *S. aureus* 25923 and *C. albicans* SC3514 polymicrobial (bottom rows) steady-state cultures challenged with 1 x minimum inhibitory concentration (MIC, left columns), 2 x MIC (middle columns) or 5 x MIC (right columns) colistin (4, 8, 20 $\mu\text{g mL}^{-1}$, respectively) after 1, 8, 24 or 48 hrs incubation. Strains with an MIC of 4, 20, 25 and 45 $\mu\text{g mL}^{-1}$ colistin are, respectively, denoted by the green, light blue, dark blue, yellow and orange cells. Resistant isolates able to grow in the presence of 1000 $\mu\text{g mL}^{-1}$ colistin are denoted by the red cells.

Time (Hours)	MIC ($\mu\text{g mL}^{-1}$) of fluconazole against isolates collected from mono-species culture challenged with:											
	1 x MIC fluconazole				2 x MIC fluconazole				5 x MIC fluconazole			
3	1	1	1	1	2.5	2.5	2.5	10	2.5	2.5	2.5	2.5
8	1	5	2.5	2.5	5	10	10	10	5	5	10	10
24	1	1	2.5	2.5	5	5	10	10	2.5	5	5	10
48	1	1	1	1	2.5	2.5	2.5	2.5	1	2.5	2.5	2.5
	MIC ($\mu\text{g mL}^{-1}$) of fluconazole against isolates collected from polymicrobial co-culture challenged with:											
	1 x MIC fluconazole				2 x MIC fluconazole				5 x MIC fluconazole			
3	2.5	2.5	2.5	2.5	5	10	10	10	5	5	5	10
8	2.5	5	5	10	5	10	10	10	5	5	10	10
24	1	2.5	5	5	5	5	10	10	2.5	5	5	10
48	1	1	1	1	2.5	5	10	10	1	1	1	2.5

Table 5.3 Resistance profiles of CA isolates collected from steady-state cultures challenged with different concentrations of fluconazole.

Isolates of *C. albicans* were randomly collected from mono-species *C. albicans* SC3541 (top rows) or polymicrobial *P. aeruginosa* PAO1, *S. aureus* 25923 and *C. albicans* SC3514 polymicrobial (bottom rows) steady-state cultures challenged with 1 x minimum inhibitory concentration (MIC, left columns), 2 x MIC (middle columns) or 5 x MIC (right columns) fluconazole (1, 2, 5 $\mu\text{g mL}^{-1}$, respectively) after 3, 8, 24 or 48 hrs incubation. Strains with an MIC of 1, 2.5, 5 or 10 $\mu\text{g mL}^{-1}$ fluconazole are, respectively, denoted by the green, yellow, orange and red cells.

were collected from the culture vessel at T = 48 hrs. By contrast 17.1%, 45.7% and 31.4% of the isolates able to survive the higher antimicrobial challenges were collected at T = 1 or 3, 8 and 24 hrs, respectively.

5.3.2 Whole genome sequencing of resistant isolates

To identify the genomic single nucleotide polymorphisms (SNPs) responsible for conferring a heritable resistance to the action of 1 mg mL⁻¹ colistin in ASM (*Section 5.3.1*) whole genome sequencing (WGS) was carried out on 8 PA isolates collected from the continuous-flow culture vessel challenged with 2 x MIC colistin (8 µg mL⁻¹, *Section 5.2.2*). Two resistant isolates independently collected from the mono-species PA culture after 1 h (isolates A and B) or 8 hrs (isolates E and F) exposure to colistin were sequenced alongside the progenitor *P. aeruginosa* PAO1 strain used to inoculate the culture vessel in all experiments. Two resistant isolates independently collected from the polymicrobial co-culture after 1 h (isolates C and D) or 8 hrs (isolates G and H) exposure to colistin were also sequenced. A summary of the SNPs differentiating the genome of the colistin-resistant isolates and the parental strain are shown in *Table 5.4*.

All sequenced isolates contain the insertion of a single cytosine in the intragenic region of *dppA1* (PA4496), which encodes a dipeptide ABC transporter substrate-binding protein. Although important for the uptake and utilisation of di- and tri-peptides by PA (Pletzer et al., 2014), this insertion occurs in the non-coding region of *dppA1* and so is predicted to have no effect on the functionality or expression of the gene product.

All isolates, except D and H, contain mutations in one of three genes (*pilM*, *pilW* or *pilF*) associated with the biogenesis of the type IV fimbrial protein (also called type IV pilin). More than 40 genes are involved in the regulation and synthesis of type IV pilin; I refer the reader to (Mattick, 2002) for an overview of these. Isolates A, B and C contain a GCGCATAGGA insertion at position 531 in *pilM* (PA5044), resulting in a frameshift mutation at amino acid 177 onwards. Isolates F and G contain the deletion of a guanosine at position 361 in *pilW* (PA4552), resulting in a frameshift mutation at amino acid 187. Finally, isolate E contains a single nucleotide polymorphism (SNP) guanosine to adenine substitution at position 581 in *pilF* (PA3805), resulting in an alanine to valine substitution at amino acid position 194.

Isolates A, D, E, F and H contain non-synonymous mutations within *wzy* (PA3154) encoding for the B-band O-antigen polymerase. This enzyme catalyses the polymerisation of a repeating O-antigen oligosaccharide in the periplasmic space and is essential for lipopolysaccharide (LPS, also called endotoxin) biogenesis. After polymerisation, O-anti

Isolate	Culture Type	Time (h)	Locus	Gene	Product	Type	Effect	NT Position	AA Position
A	Mono	1	PA3154	<i>wzy</i>	B-band O-antigen polymerase	SNP	missense	1238/ 1317	413/ 438
			PA5044	<i>pilM</i>	Type 4 fimbrial biogenesis protein	ins	frameshift	531/ 1065	177/ 357
			PA4496	<i>dppA1</i>	ABC transporter	ins	intragenic		
B	Mono	1	PA3159	<i>wbpA</i>	UDP- <i>N</i> -acetyl- <i>D</i> -glucosamine 6-dehydrogenase	SNP	missense	150/1311	50/436
			PA5044	<i>pilM</i>	Type 4 fimbrial biogenesis protein	ins	frameshift	531/ 1065	177/ 357
			PA4496	<i>dppA1</i>	ABC transporter	ins	intragenic		
C	Poly	1	PA3155	<i>wbpE</i>	UDP-2-acetamido-2-deoxy-3-oxo- <i>D</i> -glucuronate aminotransferase	SNP	missense	701/1080	234/359
			PA5044	<i>pilM</i>	Type 4 fimbrial biogenesis protein	ins	frameshift	531/ 1065	177/ 357
			PA4496	<i>dppA1</i>	ABC transporter	ins	intragenic		
			PA5001	<i>ssg</i>	Hypothetical protein	SNP	missense	569/957	190/318
D	Poly	1	PA3154	<i>wzy</i>	B-band O-antigen polymerase	ins	frameshift	129/1317	43/438
			PA4496	<i>dppA1</i>	ABC transporter	ins	intragenic		
E	Mono	8	PA3154	<i>wzy</i>	B-band O-antigen polymerase	ins	frameshift	129/131	43/438
			PA3805	<i>pilF</i>	Type 4 fimbrial biogenesis protein	SNP	missense	581/759	194/252
			PA4496	<i>dppA1</i>	ABC transporter	ins	intragenic		
F	Mono	8	PA3154	<i>wzy</i>	B-band O-antigen polymerase	SNP	missense	1238/ 1317	413/ 438
			PA4552	<i>pilW</i>	Type 4 fimbrial biogenesis protein	del	frameshift	561/825	187/274
			PA4496	<i>dppA1</i>	ABC transporter	ins	intragenic		
G	Poly	8	PA4552	<i>pilW</i>	Type 4 fimbrial biogenesis protein	del	frameshift	561/825	187/274
			PA4496	<i>dppA1</i>	ABC transporter	ins	intragenic		
H	Poly	8	PA3154	<i>wzy</i>	B-band O-antigen polymerase	ins	frameshift	266/1317	89/438
			PA4496	<i>dppA1</i>	ABC transporter	ins	intragenic		

Table 5.4 Non-synonymous genetic mutations between parental strain and colistin resistant isolates.

Summary of non-synonymous mutations identified between the genomes of PA isolates resistant to the action of 1 mg mL⁻¹ colistin and the genome of the progenitor strain (PAO1) during variant calling analysis. All isolates sequenced were collected from a steady-state continuous-flow culture after 1 or 8 hrs exposure to 8 µg mL⁻¹ colistin. Culture type identifies if the isolate was obtained from a mono-species (Mono) or polymicrobial (Poly) culture. Mutation type is abbreviated to ins (insertion), del (deletion) or SNP (single nucleotide polymorphism). Final columns, respectively, denote the nucleotide (NT) or amino acid (AA) position of the mutation within the total length of the gene or product.

ligase (encoded by *waaL*) attaches a lipid-A core “tail” to the polymerised O-antigen chain to anchor the LPS in the outer membrane of PA (Burrows et al., 1996, King et al., 2009). Isolates D, E and hrs contain a thymidine insertion at position 129 within *wzy*, resulting in a frameshift mutation from amino acid 43. Isolate A contains a cytosine to thymidine SNP at position 1238, resulting in a glycine to aspartic acid substitution at amino acid 413 and isolate F contains a guanine to thymidine transversion at position 266 resulting in a premature stop codon at amino acid position 89 in the B-band O-antigen polymerase enzyme.

Isolates B and C contain SNPs in genes belonging to the *wbp* cluster responsible for the biosynthesis of the repeating O-antigen oligosaccharide molecule. Isolate B contains a cytosine to adenosine transversion at position 150 in *wbpA* (PA3159), which encodes a UDP-*N*-acetyl-*D*-glucosamine 6-dehydrogenase (responsible for the dehydrogenation of UDP-*D*-GlcNAc to yield UDP-*D*-GlcNAcA (King et al., 2009)), resulting in a lysine to asparagine substitution at amino acid position 50. Isolate C contains a thymidine to cytosine SNP at position 701 within *wbpE* (PA3155), which encodes a UDP-2-acetamido-2-dideoxy-*D*-ribo-hex-3-uluronic acid transaminase (responsible for the transamination of UDP-3-keto-*D*-GlcNAcA to UDP-*D*-GlcNAc3NA (King et al., 2009)), resulting in a glycine to arginine substitution at amino acid position 234.

Isolate C also contains a SNP thymidine to cytosine substitution at position 569 within *ssg* (PA5001) resulting in a tyrosine to cysteine missense transition at amino acid position 190. Although *ssg* encodes for a hypothetical protein in PA, BLAST alignment of this gene reveals an orthologous gene encoding a putative glycotransferase involved in the biosynthesis of LPS in *Pseudomonas alkylphenolia* (Veeranagouda et al., 2011).

5.4 Conclusions

Examination of the MICs of SA isolates collected from the steady-state axenic and polymicrobial cultures challenged with different concentrations of fusidic acid revealed that there was no difference in the antimicrobial susceptibility of the parental strain or any recovered isolate. This demonstrates that the reduced removal of viable SA cells from a steady-state polymicrobial co-culture compared with an axenic SA population is not an inherited mechanism of resistance, but is likely to be the result of a protective phenotypic effect owing to the presence of PA and/or CA in the co-culture. By contrast, a higher percentage of PA or CA isolates collected from the polymicrobial co-cultures treated with colistin or fluconazole displayed an increased MIC against the action of the antimicrobials in isolation compared with isolates collected from perturbed mono-species steady-state populations. This finding is significant as it suggests that PA or CA grown as part of a polymicrobial community

increases the emergence of isolates that are inherently resistant to the action(s) of the two clinically relevant antimicrobial compounds studied as part of this work.

WGS of PA isolates resistant to the action of 1 mg mL⁻¹ colistin revealed that there was no difference in the non-synonymous mutations identified in the isolates collected from the mono-species or polymicrobial co-culture populations. This demonstrates that growth as part of a polymicrobial population does not cause the emergence of novel mechanisms of colistin resistance, but that growth as part of a polymicrobial consortium simply increases the prevalence of which these resistance mechanisms arise under continuous-flow conditions. As no WGS was performed on the CA isolates with increased resistance profiles, no further comments can be made on whether this hypothesis is also true for this microorganism.

Analysis of the non-synonymous mutations likely to be responsible for conferring the complete resistance of PA isolates against the action of colistin identified that all candidate genes predicted to impinge upon the production of a functional gene product are involved in the biogenesis of LPS or pilin (*Table 5.4*). It may even be hypothesised that *ssg*, encoding for a hypothetical protein in PA, is also involved in LPS biosynthesis given its sequence similarity to a putative glycotransferase involved in LPS production in *P. alkylphenolia* (as mentioned in *Section 5.2* (Veeranagouda et al., 2011)). Earlier reports have previously implicated the loss of functional LPS biosynthesis in Gram-negative bacteria as a mechanism implicated in possible resistance against the action of colistin (Han et al., 2018, Kadurugamuwa et al., 1993, King et al., 2009). This is perhaps unsurprising, as loss of LPS from the cell envelope prevents colistin from forming electrostatic interactions with, and disrupting the integrity, of the outer membrane of bacteria. Previous WGS studies have demonstrated that a decrease in the expression of genes in the *wbp* cluster are associated with increased colistin-resistance in clinical PA isolates (Gutu et al., 2015). However, the aforementioned study only demonstrated that mutations within *cprA* were responsible for the down-regulation of *wbp* genes and not SNPs within the gene cluster itself. Furthermore, no study has yet demonstrated that SNPs in *wzy* are responsible for conferring colistin-resistance in PA.

SNPs in genes involved in the biosynthesis of the type IV fimbrial protein were also found in most of the sequenced PA isolates in this study. Interestingly, mutations in the pilin biogenesis genes have been identified in two separate WGS studies of clinical PA isolates resistant to the action of colistin (Lee et al., 2014, Lee et al., 2016). However, no direct evidence has yet correlated the loss/mutation of pilin synthesis with conferring colistin resistance or their role in the emergence of antimicrobial resistance. Given that isolate G can grow in the presence of 1 mg mL⁻¹ colistin and only contains a non-synonymous mutation within *pilW*, this study provides strong evidence to suggest that the loss of type IV pilin synthesis pathways can also give rise

to colistin-resistant PA strains. The results presented across *Section 5.3* identify novel SNPs within 7 genes involved in the synthesis of LPS or pilin (*wzy*, *wbpA*, *wbpE*, *ssg*, *pilF*, *pilM* and *pilW*) that are likely to result in resistance to colistin and present a new avenue to pursue the targeted inhibition of the emergence of colistin resistance *in situ*.

Through examining the MIC of the PA and CA isolates collected over the various time points (*Table 5.2* and *5.3*), it is apparent that isolates gathered from both the mono-species and polymicrobial co-cultures at the initial points of sampling (1/3 or 8 hrs post-antimicrobial exposure) have higher MICs compared with the isolates collected from the later time points (24 or 48 hrs post-antimicrobial exposure). This phenomenon demonstrates a gradual loss of inherited resistance mechanisms from the culture vessel over time once the selection pressure is removed *via* the continuous displacement of the antimicrobial compounds with fresh ASM. This may indicate a fitness cost associated with the loss of LPS or pilin biosynthetic pathways under continuous-flow conditions. However, it should be noted that these genes are generally considered to be important *in vivo* virulence factors important for mediating bacterium-host interactions (Bucior et al., 2012, Persat et al., 2015) and evidence in the literature suggests they are not important for *in vitro* growth (Ramphal et al., 1991). Instead, it is possible that the overall diminution of microbial titres following an antimicrobial challenge allows for faster growing isolates, lacking colistin/fluconazole resistance mechanisms, to emerge in a perturbed microbial population within the continuous-flow culture vessel in the absence of a selection pressure (as is proposed by the CAM model, discussed in *Section 5.2.5* (Conrad et al., 2013)). Thus, these faster growing, but more susceptible isolates, reduce the prevalence of the resistant isolates maintained in the culture vessel. This hypothesis is supported by the significant increase in viable cell counts observed within the culture vessel after 48 hrs antimicrobial exposure, despite Q remaining constant. The increased cell density of the culture maintained in the continuous-flow vessel at the later points of sampling thereby demonstrates an elevated growth rate of species above the rate of dilution previously suitable for maintaining a stable, steady-state microbial population *in vitro*.

The majority of PA or CA isolates displaying the highest colistin or fluconazole MIC in ASM were recovered from the axenic and polymicrobial populations treated with 2 x MIC of the antimicrobials discerned in *Table 5.1*. In combination with the viable cell counts presented across *Section 5.2*, this finding suggests that challenging the continuous-flow culture vessel with 1 x MIC of an antimicrobial (quickly becoming a sub-inhibitory concentration of the compound due to the flow of fresh ASM) does little to perturb a steady-state microbial community and does not exert a significant pressure to select for antimicrobial resistant mutants. Conversely, treating a population with a supra-concentration of an antimicrobial (5 x MIC) limits the emergence of highly-resistant microbial strains within a population under

continuous-flow conditions. These findings therefore indicate that there might be significant clinical benefit to treating infections with a high concentration of antimicrobials to limit the emergence of resistant isolates *in situ*.

6. Polymicrobial biofilms

6.1 Introductory comments

As described in *Section 1.5*, biofilm formation is often cited as the major reason chronic microbial infections are not effectively cleared by the immune system or display refractory responses to therapeutic intervention. In fact, the establishment of chronic PA biofilms during CF infection is the best described example of biofilm formation in medicine (Høiby et al., 2017). With the importance of understanding how interspecies interactions modulate changes in microbial behaviour now apparent, attention is moving towards understanding the formation and behaviour of polymicrobial biofilms using a range of models and experimental approaches (Haney et al., 2018). However, only a handful of published studies have utilised physiologically relevant CF growth medium (*i.e.* ASM or synthetic cystic fibrosis sputum) for the growth and characterisation of microbial biofilms. The work of Sriramulu *et al.* (2005) successfully demonstrated that PA cultured in ASM forms microcolonies resembling *in situ* CF airway growth (Sriramulu et al., 2005) and Diaz Iglesias *et al.* (2019) have recently characterised the growth of SA biofilms in ASM (Diaz Iglesias et al., 2019). The main focus of previous studies utilising ASM to study biofilms has focused on understanding the evolutionary diversification of PA biofilms (Davies et al., 2017) or assessing the effects of novel therapeutics on single-species PA biofilms (Grassi et al., 2019, Kosztolowicz et al., 2020, Maisetta et al., 2017). A literature search reveals a single paper describing the co-culture of PA and SA biofilms using ASM (Haley et al., 2012).

The work presented in this chapter aims to characterise the temporal formation of axenic and polymicrobial biofilms grown in ASM under nutrient limited (batch culture, see *Section 2.12.1*) and nutrient rich (continuous-flow, see *Section 2.12.2*) conditions. I also sought to develop a novel method of biofilm cultivation compatible with my existing continuous-flow model (*Section 2.11.3*). A comparison of mono-species and polymicrobial biofilm growth on two different solid substrata, agar cubes or sections of *ex vivo* porcine lung tissue (EVPL), is also presented in this chapter. Experiments using EVPL were conducted by myself under the guidance and supervision of Dr Freya Harrison at the University of Warwick.

To address the limitations of commonly-used biofilm assays a complimentary and combinatorial approach to assess biofilm growth over time was utilised. Crystal violet (CV) staining of microbial populations attached to microtiter plate wells, popularised in the 1990's (Mack et al., 1994, O'Toole et al., 1999), was used as a rapid and cost-effective method of quantifying the total adherent biomass of the biofilms. Indiscriminate staining of not just microbial cells, but any material adhering to the surface of a plate (e.g. EPS matrix components) is the major limitation of the CV staining assay, making it impossible to quantify

the exact number of adherent microbes in a biofilm (Merritt et al., 2005). Therefore, a colorimetric tetrazolium assay utilising conversion of XTT to an orange formazan product by actively respiring cells (see *Section 2.12*) was used as a proxy to determine the viability of biofilms (Corte et al., 2019). Although XTT staining is useful for assessing overall biofilm metabolic activity it cannot differentiate between the species present in a polymicrobial culture. Hence, as in *Section 3.*, the laborious enumeration of individual species *via* plating onto selective agar plates was used to determine changes in the ecological composition of polymicrobial biofilms over time.

6.2 Batch culture polymicrobial biofilms

6.2.1 Crystal violet staining assays

Normalised absorbance values ($Abs_{595\text{ nm}}$) measured for single-species and polymicrobial biofilms grown in ASM under batch culture conditions and stained using CV (as described in *Section 2.12.1*) are shown in *Figure 6.1*. There was no significant difference ($P < 0.01$) in the total biomass of the PA and CA single-species cultures for the first 6 hrs of incubation. After 12 hrs of incubation the biomass of the CA mono-species biofilm was 3-fold greater than that of the PA mono-species biofilm. By $T = 24$ hrs the biomass of the CA mono-species biofilm was the largest of all the species combinations tested and there was no significant change ($P > 0.9$) in $Abs_{595\text{ nm}}$ values between 24 and 48 hrs of incubation. Biomass of the PA mono-species biofilm increased 4-fold between $T = 12$ hrs to $T = 24$ hrs followed by a subsequent 4-fold decrease in $Abs_{595\text{ nm}}$ values at $T = 48$ hrs. There was no significant difference ($P > 0.9$) in $Abs_{595\text{ nm}}$ values of the PA mono-species biofilm between $T = 12$ hrs and $T = 48$ hrs. For the 24 hrs of incubation the total biomass of the SA mono-species biofilm was significantly lower ($P < 0.0001$) than the biomass of the other mono-species biofilms. This was followed by a significant ($P < 0.0001$) 4-fold increase in total biomass of the SA mono-species biofilm between 24 and 48 hrs of incubation. There was no significant difference ($P > 0.99$) in $Abs_{595\text{ nm}}$ values between the CA and SA mono-species cultures at $T = 48$ hrs.

For all co-culture species combinations containing PA, the biofilm biomass increased steadily for the first 12 hrs of incubation. After 12 hrs of incubation the triple-species biofilm had the greatest total biomass of all the culture combinations. For the PA-SA and triple-species co-cultures there was a significant ($P < 0.001$) 3.5-fold decrease in total biofilm mass between $T = 12$ and 24 hrs, followed by a further 2-fold decrease at $T = 48$ hrs. A similar, yet less pronounced, trend was also observed for the PA-CA co-culture. There was no significant difference ($P > 0.9$) in $Abs_{595\text{ nm}}$ values between the PA-only, PA-SA, PA-CA and triple-species cultures at $T = 48$ hrs. Interestingly, the SA-CA co-culture steadily increased in biomass

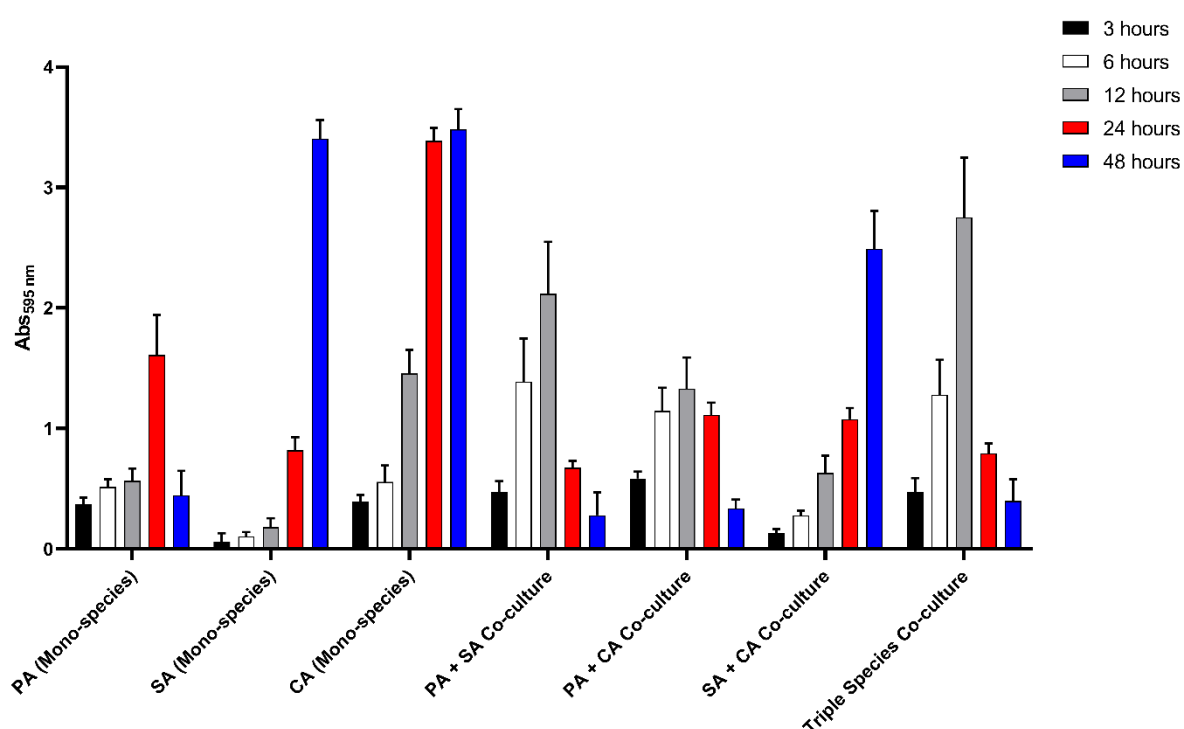


Figure 6.1 Crystal violet-stained batch culture biofilms.

Normalised Abs_{595 nm} values of solubilised biofilm biomass stained with crystal violet. Single-species and co-culture populations of *P. aeruginosa* PAO1 (PA), *S. aureus* 25923 (SA) and *C. albicans* SC5314 (CA) were incubated for 3, 6, 12, 24 and 48 hours (black, white, grey, blue and red bars respectively) in ASM in microtiter plates under batch culture conditions (as described in Section 2.11.1). Data represented as the mean \pm standard deviation of three independent experiments.

throughout the entire period of incubation, yet at T = 48 hrs, Abs_{595 nm} values for the SA-CA co-culture were 1.4-fold lower than either the SA or CA single-species cultures.

6.2.2 XTT staining assays

Normalised absorbance values (Abs_{450 nm}) measured for XTT assays of single-species and polymicrobial biofilms grown in ASM under batch culture conditions are shown in *Figure 6.2*. For the first 12 hrs of incubation the metabolic activity of the CA mono-species biofilm was significantly higher than all other species combinations, a significant ($P < 0.0001$) 1.7-fold decrease in Abs_{450 nm} then occurred by T = 24 hrs. There was no significant difference ($P > 0.1$) in the metabolic activity of the PA and SA mono-species biofilms for the first 12 hrs of incubation. Between T = 12 and 24 hrs, there was a significant ($P < 0.0001$) 6.4-fold increase in the metabolic activity of the SA mono-species biofilm and no significant difference ($P > 0.9$) in Abs_{450 nm} values of the SA biofilm following this point. The SA mono-species biofilm was the most metabolically active of all batch culture combinations after 24 hrs of incubation. There was no statistically significant difference ($P > 0.1$) in the metabolic activity of the PA mono-species biofilm following 12 hrs of incubation.

For all polymicrobial biofilms, the metabolic activity of the biofilm increased by approximately 3-fold between 3 and 12 hrs of incubation, although this increase was not statistically significant. A significant ($P < 0.05$) >2-fold decrease in Abs_{450 nm} values then occurred for the polymicrobial biofilms containing PA between 12 and 24 hrs of incubation. This was followed by an increase in the metabolic activity of PA-containing mixed species biofilms between T = 24 and 48 hrs, although this trend was only statistically significant ($P < 0.0001$) in the PA-SA co-culture. The metabolic activity of the SA-CA biofilm steadily increased for the first 24 hrs of incubation and was followed by a significant ($P < 0.0001$) 2.3-fold decrease in Abs_{450 nm} measurements at T = 48 hrs. There was no significant difference ($P > 0.2$) in the metabolic activity of the CA mono-species, PA-SA and SA-CA biofilms at 48 hrs of incubation.

6.2.3 CFU mL⁻¹ counts

Viable cell counts for mono-species and polymicrobial biofilms grown under batch culture conditions are displayed in *Figure 6.3.A* and pairwise CFU mL⁻¹ counts from the planktonic fraction of the same cultures are displayed in *Figure 6.3.B*. There was a steady increase in the viable cell counts of all single species biofilms for the first 24 hrs of incubation. A log-fold

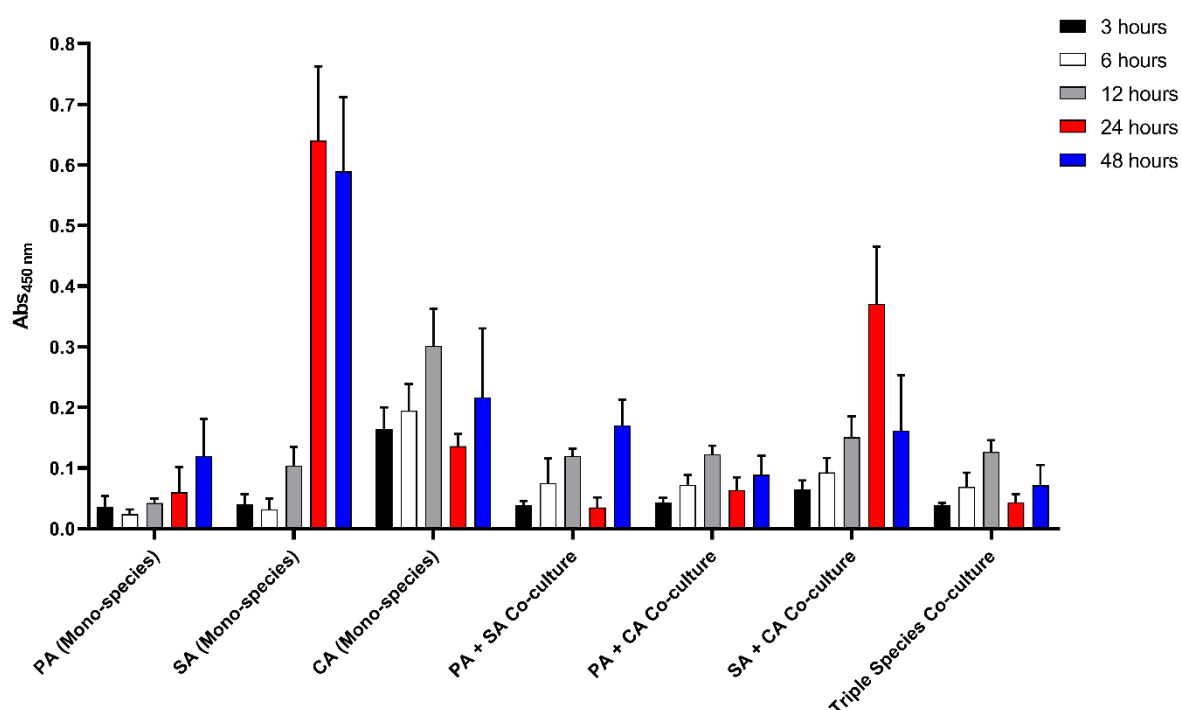


Figure 6.2 XTT-stained batch culture biofilms.

Normalised Abs_{450 nm} values of biofilms incubated with XTT to quantify the metabolic activity of the adhered cells. Single-species and co-culture populations of *P. aeruginosa* PAO1 (PA), *S. aureus* 25923 (SA) and *C. albicans* SC5314 (CA) were incubated for 3, 6, 12, 24 and 48 hours (black, white, grey, blue and red bars respectively) in ASM in microtiter plates under batch culture conditions (as described in Section 2.11.1). Data represented as the mean \pm standard deviation of three independent experiments.

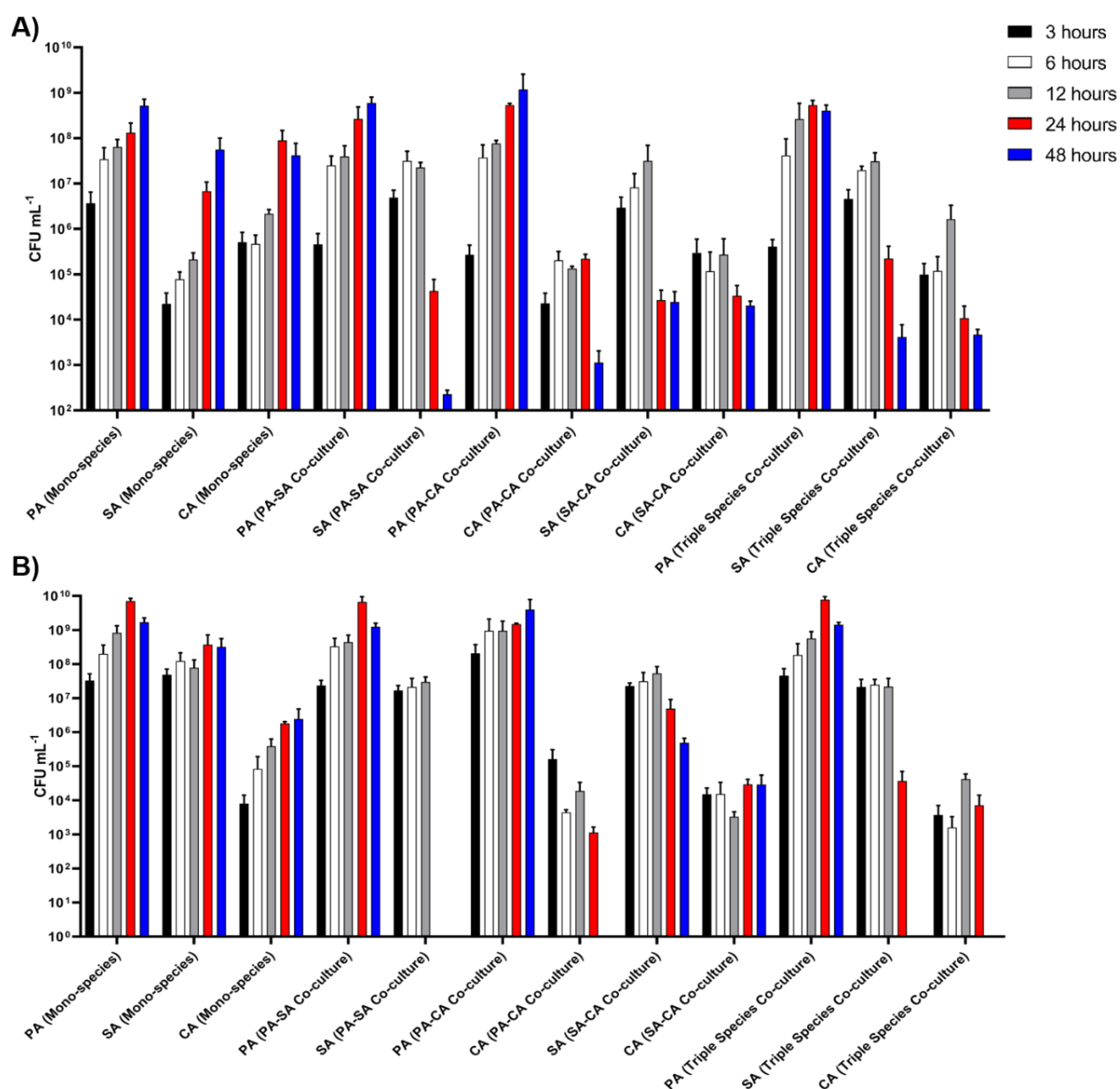


Figure 6.3 CFU mL⁻¹ counts of batch culture biofilms.

Viable *P. aeruginosa* PAO1 (PA), *S. aureus* 25923 (SA) and *C. albicans* SC5314 (CA) cell counts (CFU mL⁻¹) in the **(A)** biofilm and **(B)** planktonic fraction of single-species and polymicrobial cultures incubated for 3, 6, 12, 24 and 48 hours (black, white, grey, red and blue bars respectively) in microtiter plates under batch culture conditions, as described in *Section 2.11.1*. Data represented as mean \pm standard deviation from three independent experiments.

reduction in CFU mL⁻¹ counts in the PA mono-species biofilm occurred at T = 48 hrs, conversely there was a log-fold increase in viable SA cell counts in the single-species biofilm at this point. The SA mono-species biofilm had the fewest cell titres of the single-species cultures for the first 24 hrs of incubation, yet by T = 48 hrs there was no significant difference ($P > 0.9$) in viable cell counts between the SA and CA mono-species biofilms. There was no significant difference ($P > 0.9$) in viable cell counts of the PA mono-species biofilm sampled at T = 12 or 48 hrs.

PA cell titres in all mixed species biofilms increased for the first 24 hrs of incubation, reaching $>5 \times 10^8$ CFU mL⁻¹ by this point in all instances. There was no statistically significant change in PA titres for any mixed species biofilm between T = 24 and 48 hrs. The number of viable SA cells in the PA-SA biofilm was a log-fold higher than the number of viable cells present in the SA mono-species biofilm for the first 12 hrs of incubation. A significant ($P < 0.0001$) 4-log fold reduction in SA CFU mL⁻¹ counts occurred between 12 and 24 hrs of incubation and a further 2-log fold reduction in viable cell counts occurred at T = 48 hrs. At the final point of sampling there were fewer than 300 SA CFU mL⁻¹ present in the PA-SA co-culture biofilm. There was a greater than 1-log fold reduction in CA titres present in the PA-CA biofilm compared with the CA mono-species culture across all points of sampling. At T = 6 hrs there was $\approx 2 \times 10^5$ CA CFU mL⁻¹ present in the PA-CA biofilm and there was no statistically significant change until a 2-log fold reduction in CA titres at T = 48 hrs.

Compared with the SA mono-species biofilm there was a 2-log fold increase in SA CFU mL⁻¹ present in the SA-CA biofilm for the first 12 hrs of incubation. This was followed by a 3-log fold reduction in viable SA counts after 24 hrs of incubation and no change in CFU mL⁻¹ counts occurred thereafter. No significant difference ($P > 0.9$) existed in CA CFU mL⁻¹ present in the SA-CA biofilm and the mono-species culture for the first 12 hrs of incubation. However, at T = 24 and 48 hrs there was a 3-log fold reduction in CA CFU mL⁻¹ counts compared with the single-species CA biofilm at these points. Titres of all three species increased for the first 12 hrs of incubation in the triple species biofilm. There was no significant difference ($P > 0.9$) in PA or CA titres present in the biofilm compared with their respective single-species cultures. However, there was a 2-log fold increase in SA CFU mL⁻¹ counts between 3 and 12 hrs of incubation. A 2-log fold reduction in viable SA and CA titres then occurred in the triple species biofilm between T = 12 and 24 hrs. Followed by a further log-fold reduction in CFU mL⁻¹ counts for both species at T = 48 hrs.

As expected, there was a steady increase in viable cell counts in the planktonic fraction of all three mono-species cultures over incubation period (*Figure 6.3.B*). A similar loss of species from the planktonic fraction of the microbial co-cultures was observed as reported for the

polymicrobial batch cultures in *Section 3*. Briefly, no viable SA cells could be recovered from the PA-SA and triple-species co-cultures after 24 and 48 hrs respectively. Similarly, no viable CA cells were recovered from the PA-CA or triple species co-cultures at T = 48 hrs and a reduction in viable SA titres occurred in planktonic fraction of the SA-CA co-culture following 12 hrs of incubation.

6.2.4 Key Findings

Under batch culture conditions, SA forms the least dense biofilm with respect to total biomass and lowest viable cell counts during the initial 12 hrs of incubation, whereas PA forms the biofilm with the most viable cells and CA the greatest total biomass and metabolic activity. Despite the small biomass of the SA mono-species biofilm, it is as metabolically active as the PA mono-species biofilm for the first 12 hrs of growth. The presence of PA or CA increases the initial attachment of SA cells to the biofilm, as evidenced by an increase in SA titres. Conversely, the presence of PA or SA reduced the initial number of viable CA cells found in the mixed population biofilms.

A significant reduction in the biomass of the PA mono-species biofilm occurred after 48 hrs of growth. This observation may be attributed to dispersal of the mature biofilm in response to the depletion of available nutrients under batch culture conditions (Maunder and Welch, 2017, Sauer et al., 2004). It is interesting to note that a reduction in biomass also occurs for all polymicrobial biofilms containing PA and that the total biomass of the PA-SA, PA-CA and triple-species biofilms is comparable to that of the mono-species biofilm at the endpoint of sampling. This reduction in biomass occurs after only 24 hrs of incubation and coincides with a reduction in viable SA and CA titres but no appreciable change in PA titres in the biofilm. This finding is in support of existing reports that microbial species, in this instance PA, produce extracellular factors that degrade the extracellular matrix of competing species to displace and remove these from a biofilm community (Kaplan, 2010).

Also of note is that the removal of species from the biofilm fraction of the co-cultures was significantly lower compared with the loss of species from the planktonic portion of the co-culture. This observation suggests that the expression of extracellular factors responsible for the out-competition of co-cultivated species is decreased during the biofilm mode of growth in ASM. In support of this hypothesis, studies into *Streptococcus suis* and *Actinobacillus pleuropneumoniae* have demonstrated a decreased expression of virulence associated genes during biofilm growth (Li et al., 2008, Wang et al., 2011). Alternatively, the diffusion coefficient in biofilms is severely diminished compared to aqueous solutions due to the presence of polymeric substances, extracellular DNA and abiotic particles that comprise the EPS in which

microbial cells are embedded during biofilm growth (Sankaran et al., 2019, Stewart, 2003). This matrix is thought to act as a molecular sieve and may simply retard the diffusion of extracellular factors responsible for the out-competition of co-cultivated species through the biofilm. This decreased diffusion of extracellular factors may therefore improve the longevity of species rapidly removed from the planktonic portion of the co-culture. However, as described in *Section 3.6*, the rate of SA and CA removal from the triple-species biofilm population was decreased when compared with the rate of removal from the dual-species biofilms. This indicates that modulation of microbial behaviours in response to the presence of a co-cultivated species is also evident during the biofilm mode of growth.

6.3 Continuous-flow polymicrobial biofilms

6.3.1 Crystal violet staining assays

Normalised absorbance values ($Abs_{595\text{ nm}}$) measured for single-species and polymicrobial biofilms grown in ASM under continuous-flow conditions using the Kadouri drip-plate model (as described in *Section 2.12.2*) are displayed in *Figure 6.4*. A significant increase ($P < 0.01$) in the total biomass of all mono-species biofilms occurred between 6 and 48 hrs of incubation. Total biomass of the CA mono-species biofilm was significantly higher ($P < 0.0001$) than the other single-species biofilms across all points of sampling and the SA mono-species biofilm had the lowest total biomass of the single-species cultures. There was no significant difference ($P > 0.1$) in the total biomass of any polymicrobial biofilm at $T = 6$ hrs and a significant ($P < 0.0001$) greater than 4-fold increase in total biomass of all polymicrobial biofilms occurred between $T = 6$ and 24 hrs. $Abs_{595\text{ nm}}$ values for the PA-SA biofilm then increased by a further 3-units between $T = 24$ and 48 hrs. Contrastingly, a significant ($P < 0.05$) 4-unit decrease in $Abs_{595\text{ nm}}$ values of the PA-CA biofilm and a significant ($P < 0.0001$) 50% reduction in the total biomass of the triple-species biofilm occurred between $T = 24$ and 48 hrs. There was no significant difference ($P > 0.2$) in the total biomass of the SA-CA biofilm between 24 and 48 hrs of incubation.

6.3.2 XTT staining assays

Normalised absorbance values ($Abs_{450\text{ nm}}$) measured for XTT assays of single-species and polymicrobial biofilms grown in ASM under continuous-flow conditions using the Kadouri drip-plate model (as described in *Section 2.12.2*) are displayed in *Figure 6.5*. The metabolic activity of all biofilms significantly increased ($P < 0.001$) at each point of sampling for the first 24 hrs

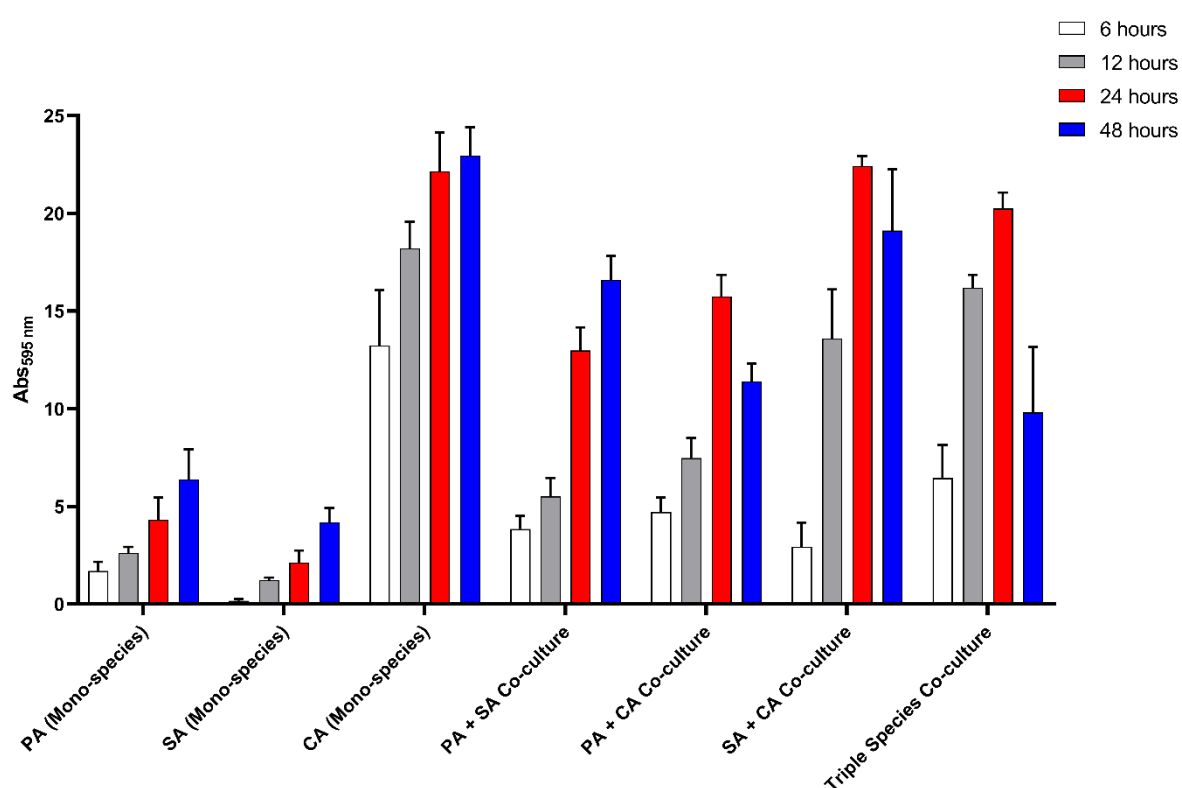


Figure 6.4 Crystal violet-stained continuous-flow microtiter plate biofilms.

Normalised Abs_{595 nm} values of solubilised biofilm biomass stained with crystal violet. Single-species and co-culture populations of *P. aeruginosa* PAO1 (PA), *S. aureus* 25923 (SA) and *C. albicans* SC5314 (CA) were incubated in ASM in the continuous-flow microtiter plate (Kadouri drip-fed) model described in Section 2.11.2. The flowrate was 55 $\mu\text{L min}^{-1}$. Cultures were incubated for 6, 12, 24 and 48 hrs (white, grey, blue and red bars respectively). Data represented as the mean \pm standard deviation of three independent experiments.

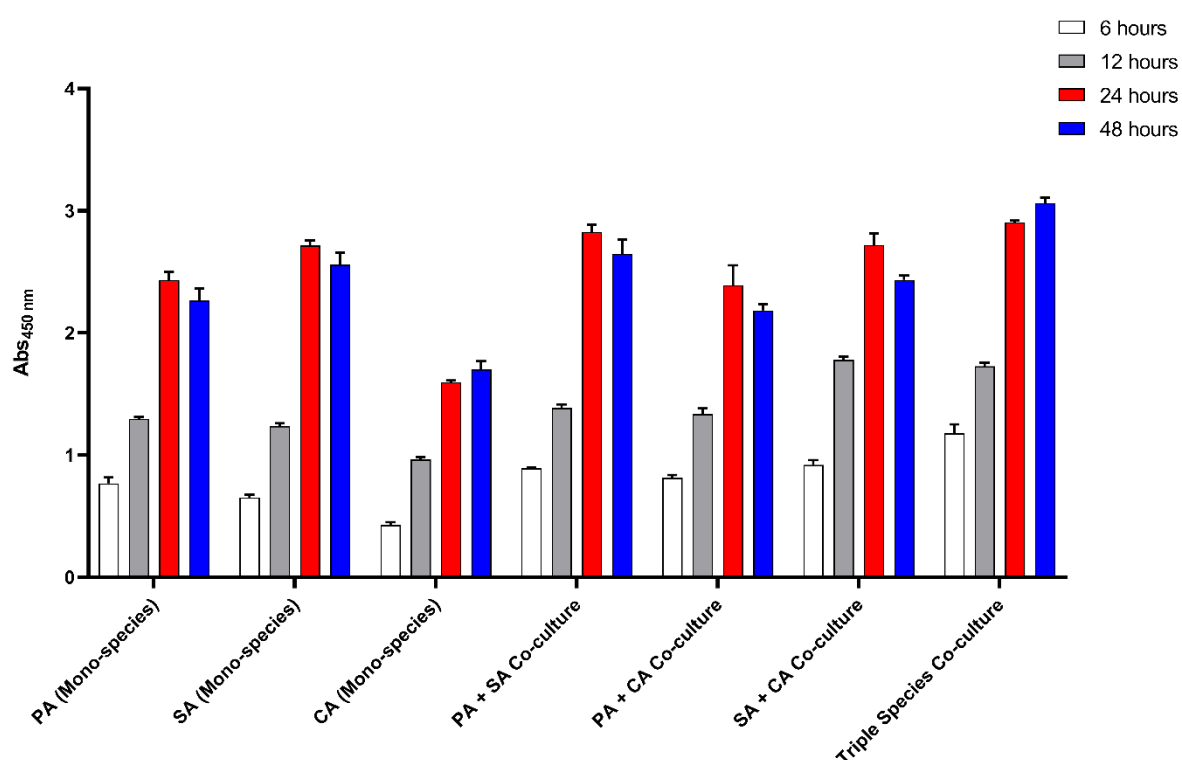


Figure 6.5 XTT-stained continuous-flow microtiter plate biofilms.

Normalised Abs_{450 nm} values of biofilms incubated with XTT to quantify the metabolic activity of adhered cells. Single-species and co-culture populations of *P. aeruginosa* PAO1 (PA), *S. aureus* 25923 (SA) and *C. albicans* SC5314 (CA) were incubated in ASM in the continuous-flow microtiter plate (Kadouri drip-fed) model described in *Section 2.11.2*. The flowrate was 55 $\mu\text{L min}^{-1}$. Cultures were incubated for 6, 12, 24 and 48 hrs (white, grey, blue and red bars respectively). Data represented as the mean \pm standard deviation of three independent experiments.

of incubation. The metabolic activity of the CA mono-species biofilm was significantly lower ($P < 0.0001$) than all other species combinations across all points of sampling. At $T = 24$ hrs, the total metabolic activity of the triple species biofilm was significantly higher than the PA mono-species and PA-CA co-culture ($P < 0.0001$), CA mono-species ($P < 0.01$) and SA-CA co-culture ($P < 0.05$) biofilms. There was no significant difference ($P > 0.05$) in $Abs_{450\text{ nm}}$ measurements between the triple-species and PA-SA co-culture biofilms at 24 hrs of incubation. There was no significant difference ($P < 0.01$) in the metabolic activity of the PA-SA, SA-CA and CA-only biofilms at $T = 24$ hrs and $Abs_{450\text{ nm}}$ values of the PA mono-species biofilm was significantly lower ($P < 0.0001$) than these co-cultures at this point of sampling.

There was a significant decrease ($P < 0.05$) in the metabolic activity of the PA-only, PA-SA, PA-CA and SA-CA biofilms between $T = 24$ and 48 hrs and there was no significant difference ($P > 0.1$) in $Abs_{450\text{ nm}}$ values of the SA or CA mono-species and triple-species biofilms between these points. At the final point of sampling, the metabolic activity of the triple-species biofilm was significantly higher ($P < 0.0001$) than all other species combinations. There was no significant difference ($P > 0.4$) in $Abs_{450\text{ nm}}$ values measured for the CA-only and PA-SA, or the mono-species PA and SA-CA biofilms at 48 hrs of incubation. Metabolic activity of the CA and PA-SA biofilms was significantly higher ($P < 0.01$) than the PA and SA-CA biofilms and $Abs_{450\text{ nm}}$ values measured for the PA-CA biofilm were significantly lower ($P < 0.001$) than those measured for all co-culture combinations at $T = 48$ hrs.

6.3.3 CFU mL⁻¹ counts

Viable cell counts for mono-species and polymicrobial biofilms grown under continuous-flow conditions using the Kadouri drip-plate model (as described in *Section 2.12.2*) are displayed in *Figure 6.6.A* and pairwise CFU mL⁻¹ counts from the planktonic fraction of the same culture are displayed in *Figure 6.6.B*. There was a 2-log and 5-log fold increase, respectively, in viable cell counts of PA and SA in the mono-species biofilms between $T = 6$ and 48 hrs. A log-fold increase in CFU mL⁻¹ counts occurred in the CA mono-species biofilm between $T = 6$ and 12 hrs and there was no significant difference ($P > 0.9$) in cell titres after this timepoint. The SA mono-species biofilm had significantly fewer ($P < 0.0001$) viable cells over the initial 12 hrs of incubation compared to all other species combinations, yet there was no significant difference ($P > 0.9$) in PA or SA titres present in the mono-species biofilms at the final point of sampling. There was a >1-log fold decrease in viable PA cell counts in all polymicrobial biofilms for the initial 12 hrs of incubation compared with the mono-species PA biofilm. By contrast, a >2-log fold increase in SA titres was observed in the polymicrobial biofilms at $T = 6$ and 12 hrs compared with the mono-species biofilm. There was little difference in the number of viable

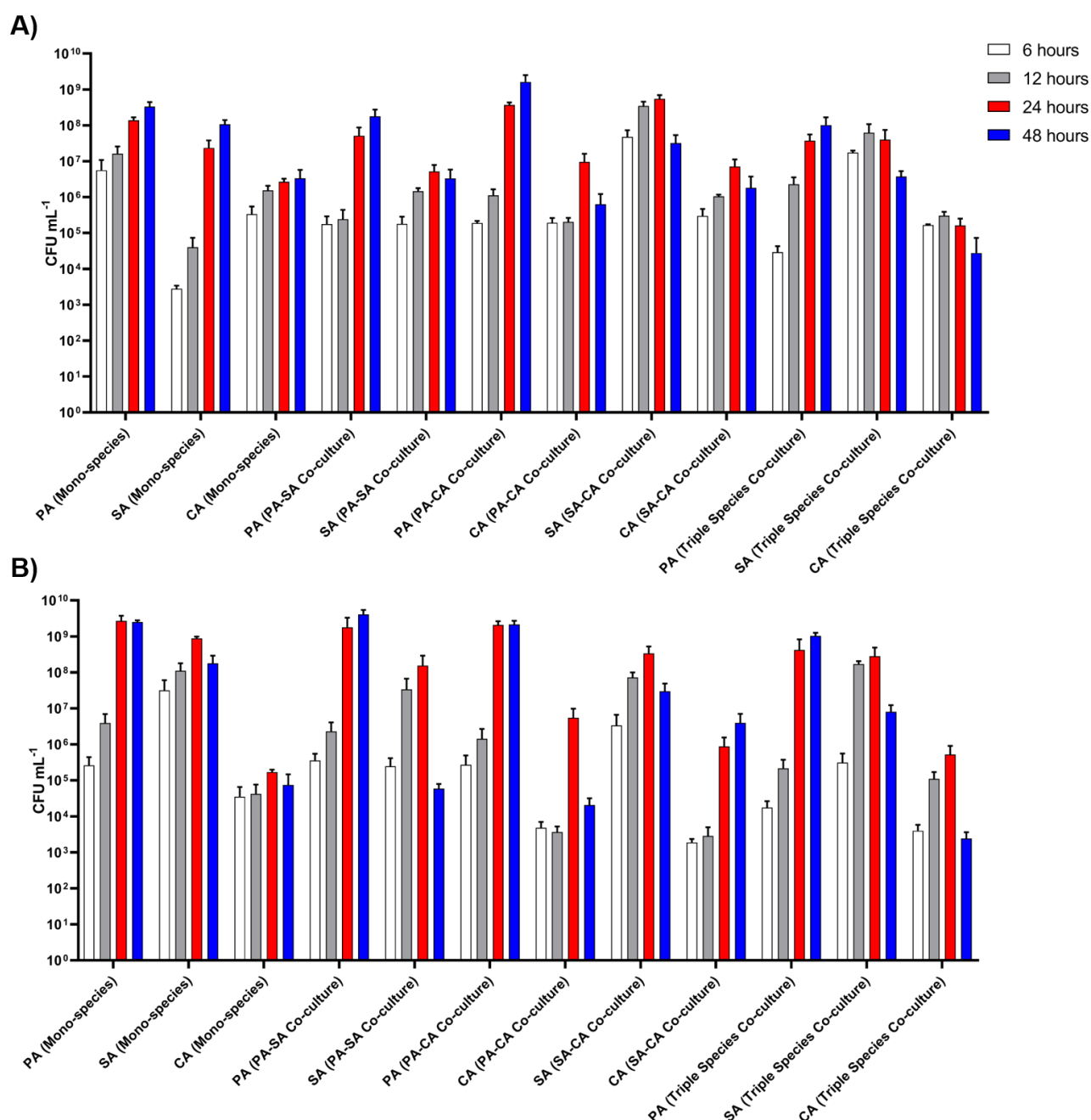


Figure 6.6 CFU mL⁻¹ counts of continuous-flow microtiter plate.

Viable *P. aeruginosa* PAO1 (PA), *S. aureus* 25923 (SA) and *C. albicans* SC5314 (CA) cell counts (CFU mL⁻¹) in the **(A)** biofilm and **(B)** planktonic fraction of single-species and polymicrobial cultures incubated in ASM in the continuous-flow microtiter plate (Kadouri drip-fed) model described in Section 2.11.2. The flowrate was 55 $\mu\text{L min}^{-1}$. Cultures were incubated for 6, 12, 24 and 48 hrs (white, grey, blue and red bars respectively). Data represented as the mean \pm standard deviation of three independent experiments.

CA cells present in the mono-species or polymicrobial biofilms across the first 12 hrs of incubation. In all polymicrobial biofilms there was a significant increase ($P < 0.01$) in PA CFU mL⁻¹ counts between the initial and final points of sampling. By T = 48 hrs, there were significantly more ($P < 0.01$) viable PA cells present in all polymicrobial biofilms compared with CFU mL⁻¹ counts of the other species present in their respective biofilm co-cultures. In the PA-SA biofilm, a log-fold increase in SA CFU mL⁻¹ counts occurred between T = 6 and 24 hrs but there was no significant change ($P > 0.9$) in microbial titres following this. After 24 hrs of incubation there were $>10^7$ SA CFU mL⁻¹ in the SA-CA and triple-species biofilms, >2 -log fold more than the PA-SA co-culture and >4 -log fold more than the mono-species biofilm at this point. In the SA-CA and triple-species biofilms, a significant ($P < 0.01$) log-fold reduction in viable SA titres occurred between T = 24 and 48 hrs.

At the final point of sampling there were approximately 10 and 100 more SA CFU mL⁻¹ in the mono-species biofilm compared, respectively, with the SA-CA and triple-species co-cultures. There was no statistically significant difference ($P > 0.9$) in CA titres of the mono-species and any polymicrobial biofilm for the first 12 hrs of incubation. An approximate 2-log increase in CA CFU mL⁻¹ occurred in the PA-CA biofilm between T = 12 and 24 hrs. This was subsequently followed by a log-fold decrease in CA titres at 48 hrs incubation. A similar, but less pronounced, trend can be observed for viable CA counts in the SA-CA biofilm. There was no statistically significant difference in CA titres between T = 12 and 48 hrs in both the PA-CA and SA-CA polymicrobial biofilms. There was little difference in CA CFU mL⁻¹ counts of the triple-species co-culture for the first 24 hrs of incubation, with cell counts never exceeding 4×10^5 CFU mL⁻¹. A log-fold reduction in CA cell titres occurred between T = 24 and 48 hrs in the triple-species biofilm, however this change was not statically significant ($P > 0.9$).

Similar to the continuous-flow results described in *Section 3.*, planktonic CFU mL⁻¹ counts of all species in mono-species and co-culture combinations increased for the first 24 hrs of growth. However, and unlike the results described in *Section 3.*, there was a significant decrease in SA titres in the planktonic fraction of all polymicrobial cultures between T = 24 and 48 hrs. Additionally, there was a significant decrease in CA CFU mL⁻¹ counts in the PA-CA and triple-species planktonic fractions between 24 hrs and the final point of sampling. As in *Section 3.*, there was no significant difference ($P > 0.1$) in the cell counts of the planktonic fraction of any other species combination between 24 and 48 hrs of growth.

6.3.4 Key Findings

A continual increase in the total biomass, metabolic activity and viable cell counts of all species and culture combinations occurred for the first 24 hrs of incubation using the continuous-flow

Kadouri drip-plate culture method. As in *Section 6.2*, CA formed the largest total biomass yet was the least metabolically active of the mono-species biofilms across all points of sampling. Conversely, the SA mono-species biofilm was the most metabolically active despite having fewer viable cells than the PA mono-species biofilm. Unlike the results described in *Section 6.2.4*, biomass and CFU mL⁻¹ of the PA-only biofilm did not decrease between 24 and 48 hrs of incubation, suggesting that with an increased supply of nutrients available to the sessile community there is a suppression of biofilm dispersal (Sauer et al., 2004). As with the batch culture biofilms (*Section 6.2.3*), the presence of PA or CA increased the initial number of viable SA cells present in the polymicrobial biofilms compared with the mono-species culture. Furthermore, the presence of PA or SA decreased CA titres present in the polymicrobial biofilms across all points of sampling. Crucially, there was no out-competition of SA from the PA-SA biofilm co-culture under continuous-flow conditions, as evidenced by no significant change in SA CFU mL⁻¹ counts occurring after 24 hrs of incubation. There was a reduction, albeit at a much lower rate than that observed in *Figure 6.3.A*, in SA cell titres present in the SA-CA and triple-species biofilms between T = 24 and 48 hrs of incubation. This reduction in SA CFU mL⁻¹ was accompanied by a decrease in the total metabolic activity of the biofilms. Similarly, the removal of viable CA cells from polymicrobial biofilms was only significant in the PA-CA co-culture at the final point of sampling and was accompanied by a decrease in the total biomass of the biofilm.

6.4 Biofilms grown in the continuous-flow model

Viable cell counts for mono-species and polymicrobial biofilms adhered to agar cubes or sections of *ex vivo* porcine lung tissue (EVPL) in the continuous-flow culture vessel (as described in *Section 2.12.3*) are shown in *Figure 6.7* and *Figure 6.8*, respectively. There was no significant difference in viable cell counts of the planktonic fraction of any species combination compared with the continuous-flow results described in *Section 3* (data not shown). No PA, SA or CA cells could be isolated from uninfected EVPL sections after any period of incubation (data not shown).

6.4.1 Agar associated biofilms

A significant ($P < 0.05$) log-fold increase in PA titres occurred in the mono-species biofilm between T = 24 and 96 hrs. There was also a significant ($P < 0.0001$) 2-log fold increase in SA titres in the mono-species biofilm over the incubation period. There was no statistically significant ($P > 0.5$) difference in CA titres in the mono-species biofilm or any species in the polymicrobial biofilm between 24 and 96 hrs of incubation. There was no significant difference

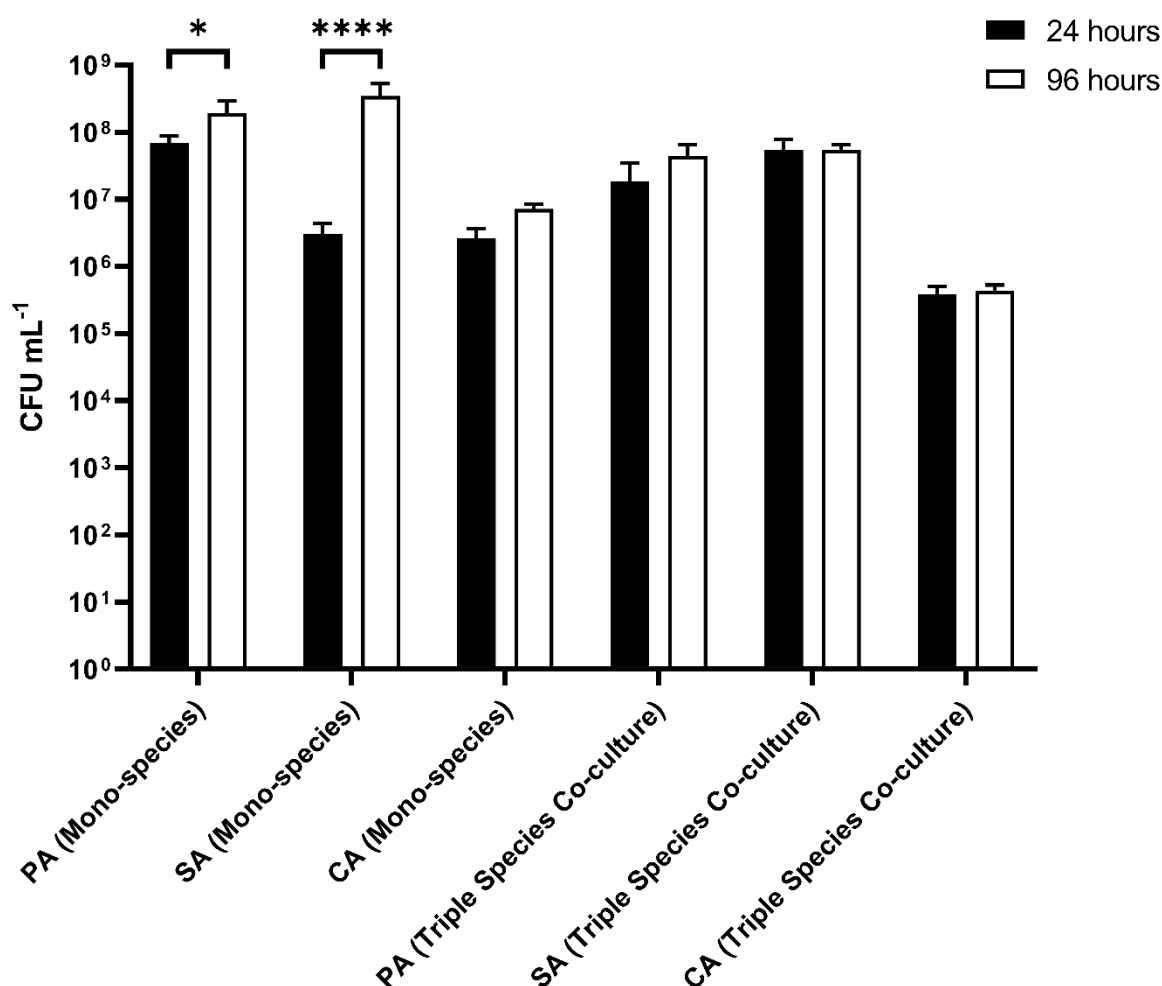


Figure 6.7 CFU mL⁻¹ counts of biofilms adhered to agar chunks.

Viable *P. aeruginosa* PAO1 (PA), *S. aureus* 25923 (SA) and *C. albicans* SC5314 (CA) cell counts (CFU mL⁻¹) adhered to 2.5% agar chunks after incubation for 24 (black bars) or 96 hrs (white bars) in the continuous-flow culture model as described in Section 2.11.3.

Asterisks represent significant (* $P < 0.05$, **** $P < 0.0001$) differences in CFU mL⁻¹ counts between the 24 and 96 hrs timepoints of individual species in their respective culture. Data represented as the mean \pm standard deviation of three independent experiments.

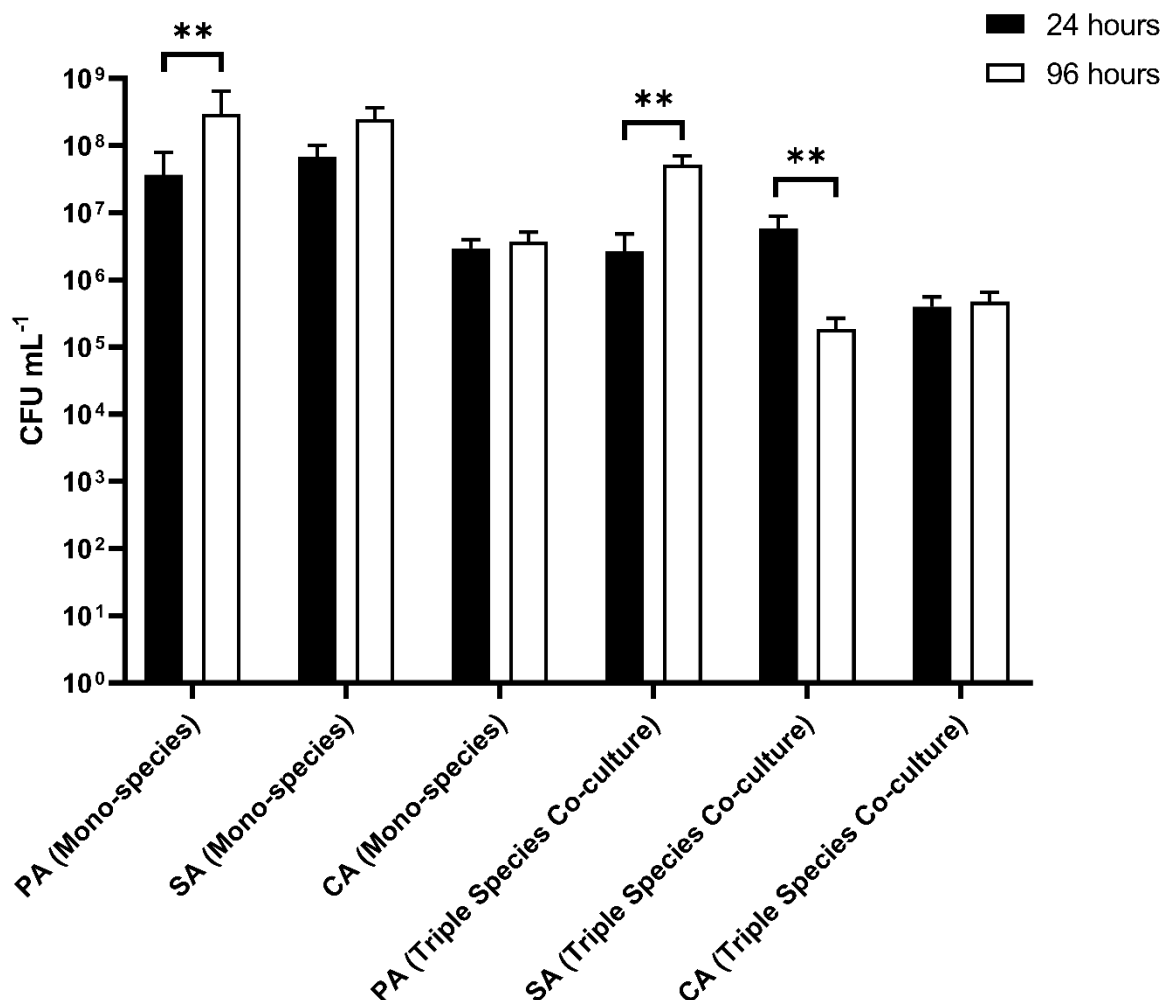


Figure 6.8 CFU mL⁻¹ counts of biofilms adhered to porcine bronchiole tissue.

Viable *P. aeruginosa* PAO1 (PA), *S. aureus* 25923 (SA) and *C. albicans* SC5314 (CA) cell counts (CFU mL⁻¹) adhered to sections of *ex vivo* porcine lung tissue after incubation for 24 (black bars) or 96 hrs (white bars) in the continuous-flow culture model as described in Section 2.11.3. Asterisks represent significant (** $P < 0.01$) differences in CFU mL⁻¹ counts between the 24 and 96 hrs timepoints of individual species in their respective culture. Data represented as the mean \pm standard deviation of three independent experiments.

($P > 0.8$) in PA or SA CFU mL⁻¹ counts in the polymicrobial biofilm at either point of sampling and cell counts of both species were 3-log fold ($P < 0.0001$) higher than CA CFU mL⁻¹ counts in the polymicrobial biofilm at T = 24 and 96 hrs. There were 1-log fold fewer CA CFU mL⁻¹ in the polymicrobial biofilm compared to the mono-species biofilm at both points of sampling.

After 24 hrs of incubation, there no significant difference ($P > 0.9$) between SA or CA CFU mL⁻¹ counts in the mono-species biofilms and there were significantly more ($P < 0.001$) PA CFU mL⁻¹ in the mono-species PA biofilm at this point. There was no significant difference ($P > 0.9$) in PA CFU mL⁻¹ counts in the mono-species biofilm and PA or SA titres in the polymicrobial biofilm at the first point of sampling. At T = 96 hrs, there was no significant difference ($P > 0.9$) in PA or SA CFU mL⁻¹ counts in the mono-species biofilm and the CA mono-species biofilm had significantly fewer ($P < 0.0001$) viable cells at this point. PA and SA titres present in the polymicrobial biofilm were 1-log fold fewer than their respective mono-species biofilms after 96 hrs of incubation. Furthermore, there were 2-log fold fewer CA CFU mL⁻¹ than PA or SA CFU mL⁻¹ in the polymicrobial biofilm at the final point of sampling.

6.4.2 EVPL associated biofilms

A significant ($P < 0.01$) log-fold increase in viable cell counts in the PA mono-species biofilm occurred between T = 24 and 96 hrs. There was no statistically significant ($P > 0.1$) change in SA or CA CFU mL⁻¹ counts in their respective mono-species biofilms between the two points of sampling. Likewise, there was no change in CA titres in the polymicrobial biofilm between T = 24 and 96 hrs. There was a significant ($P < 0.01$) log-fold increase in PA CFU mL⁻¹ in the polymicrobial biofilm between 24 and 96 hrs of incubation. Conversely, there was a log-fold decrease ($P < 0.01$) in SA CFU mL⁻¹ in the mixed-species biofilm between the first and final time points. There was no significant difference ($P > 0.9$) in cell titres of the PA or SA mono-species biofilms between either point of sampling and there was less than 1-log fold fewer CA CFU mL⁻¹ in the CA mono-species biofilm. Across both timepoints there was 1-log fold fewer CA titres in the mono-species biofilm compared to the polymicrobial co-culture.

At T = 24 hrs, there was no significant difference ($P > 0.9$) in PA or SA CFU mL⁻¹ counts in the polymicrobial biofilm, but the titres of each species were 1-log fold lower than their respective mono-species biofilms at this point. SA titres in the polymicrobial biofilm at the final point of sampling were 3-log fold lower than PA or SA mono-species cell titres and 1-log fold lower than CA mono-species cell counts. There was no significant difference ($P > 0.9$) in SA or CA viable cell counts in the polymicrobial biofilm at T = 96 hrs, yet there were significantly more PA CFU mL⁻¹ in the mixed species biofilm.

6.4.3 Comparison between agar and EVPL biofilms

When comparing the formation of biofilms on agar chunks with EVPL sections, there was no significant difference ($P > 0.8$) in viable PA or CA titres in the mono-species or polymicrobial biofilms at either $T = 24$ or 96 hrs. The only appreciable difference in CFU mL⁻¹ counts when using different solid substrata was observed for SA titres. There was a log-fold increase in viable SA cells adhered to EVPL sections in the mono-species culture at the first point of sampling. Yet there is a 2-log fold reduction in SA titres present in the EVPL polymicrobial biofilm compared with the agar-associated polymicrobial biofilm at $T = 96$ hrs.

6.5 Conclusions

The results presented in this chapter indicate that PA-mediated biofilm dispersal and competition among species in a polymicrobial biofilm are suppressed during growth under continuous-flow conditions. This was demonstrated by the continual increase in total biomass and steady total metabolic rates of all species combinations over time during co-cultivation using the Kadouri drip-plate culture method (*Section 6.3*). This, in combination with the results presented in *Section 3*., highlight the importance of providing fresh nutrients and removing excess cells and waste products to ensure the stable *in vitro* co-culture of CF associated species in both the planktonic and sessile modes of growth. It is key to note that antagonistic interactions are still observed under continuous-flow conditions in the microtiter plate. A significant, albeit decreased, removal of CA and SA does occur in their respective continuous-flow PA-CA or SA-CA biofilms. Furthermore, the presence of co-cultivated species decreased CA CFU mL⁻¹ present in the polymicrobial biofilms compared with CA mono-species biofilms. These observations suggest interspecies competition is not simply linked to nutrient limitation. As physical space (surface area) is finite in microtiter plate wells and CA forms the largest total biomass of any mono-species biofilm, competition for this limited commodity could be hypothesised to enhance interspecies competition (Poletto et al., 2015). Alternatively, separate contact-dependent cues (Gates et al., 2018) or the recognition of extracellular products (Jayathilake et al., 2017) may trigger the up-regulation virulence factors in polymicrobial biofilms.

In the polymicrobial biofilms there is also clear evidence of synergistic interactions between species. During the initial 12 hrs of biofilm formation, SA forms the smallest, yet most metabolically active, mono-species biofilm adhered to the bottom of the microtiter plates. Attachment of SA is significantly improved under both batch and continuous-flow culture conditions in the presence of co-cultivated species. This suggests that SA cells are able to readily embed themselves in the EPS matrix (Nocelli et al., 2016) produced in abundance by

both PA (Wei and Ma, 2013) and CA (Da et al., 2019) during their biofilm mode of growth. Given that SA is known to be an early coloniser of the CF airways (Bogaert et al., 2004, Rosenfeld et al., 2012), this finding may be significant as the initial successful attachment of this species in the CF microenvironment may also be improved by the presence of other early coloniser species (Conrad et al., 2013, Rogers et al., 2005, Tunney et al., 2008). Further investigation into these synergistic interactions could lead to the identification of novel therapeutic targets for improved management of early airway CF airway infections and the prevention of chronic SA colonisation in infants.

Interestingly, the formation of mono-species SA biofilms on solid substratum in the *in vitro* continuous-flow model after 24 hrs incubation is significantly improved on EVPL sections compared with the initial attachment of SA biofilms using agar as a solid substratum. This enhanced ability to form biofilms on bronchiole tissue sections sharing a high degree of similarity to human airway tissue (Judge et al., 2014) may help explain why SA is an effective early coloniser of the CF airways. The growth of biofilms on EVPL sections stimulated a decrease of viable SA CFU mL⁻¹ counts in polymicrobial biofilms after 96 hrs incubation; a decrease that was not observed using agar chunks as a substratum. Although dual-species biofilm co-cultures were not studied due to time constraints and a limitation of available EVPL sections in the Harrison Lab, this initial finding suggests that microbial interaction with host tissue may up-regulate the localised production of virulence factors and enhanced interspecies competition (Döring et al., 2011, Malhotra et al., 2019). This hypothesis is further supported by studies using a PA-SA co-culture incubated in the presence of a mono-layer of human bronchiole epithelial cells homozygous for the phe508del mutation. These researchers reported that an up-regulation of microbial competition, dependent on the action of siderophores and 2-heptyl-4-hydroxyquinolone *N*-oxide, drives SA towards a fermentative metabolic profile (Filkins et al., 2015). Furthermore, it can be hypothesised that recognition of both airway epithelial cells and SA is required to drive the observed changes in PA behaviour under continuous-flow conditions as increased competition is not observed when using an abiotic substratum, such as agar chunks. The implications of this finding are twofold: firstly, the EVPL biofilm model could be an effective approach for studying how late-stage CF pathogens displace species overtime in a physiologically relevant polymicrobial model of CF airway infection. Secondly, agar is more suitable substratum for promoting long-term and stable, steady-state growth of polymicrobial biofilms in my continuous flow model and so was used in subsequent experiments aimed at culturing entire sputum-derived polymicrobial populations in the *in vitro* model (Section 7).

7. Growth of Patient-Derived Polymicrobial Populations

7.1 Introductory Comments

As demonstrated in *Section 3*, co-cultures of domesticated microbial species can be stably maintained in the continuous-flow model. I sought to further refine culture conditions of the culture vessel to permit the recapitulation of entire polymicrobial communities contained in CF sputum samples *in vitro*. Unfortunately, due to the complexity of this task and the global outbreak of SARS-CoV-2 this goal was not fully realised. However, the preliminary work presented in this chapter provides a framework to guide future optimisation efforts.

7.2 Growth of CF-sputum Samples in ASM

Clinical strains isolated from patients are found to have extended lag phases compared to their commonly studied and well characterised domesticated reference strain counterparts (Theophel et al., 2014). The lag phase is the most poorly understood of the microbial growth phases and as such has no universally defined physiological or biochemical criteria (Madigan and Martinko, 2000). It is however assumed that this phase promotes microbial fitness by allowing species to undergo adaptations necessary for nutrient acquisition and the exploitation of new environmental conditions (Bertrand, 2019, Madigan and Martinko, 2000, Rolfe et al., 2012). It is also interesting to note that an extended lag phase may offer a survival advantage against antimicrobial stress (Bertrand, 2019, Li et al., 2016), possibly explaining why species with extended lag phases can be isolated from chronic clinical infection scenarios.

To prevent the initial washout of microbial species and ensure the successful growth of polymicrobial populations found within expectorated CF sputum samples, I first determined the growth rate of the microbial species contained within CF sputum samples in ASM under batch culture conditions. OD_{600 nm} measurements afforded a rapid and cost-effective technique for estimating the total microbial density of microbial populations of an unknown composition. To take automated OD_{600 nm} measurements, the model was fitted with an in-line spectrophotometer, as described in *Section 2.3.1*. To create a “closed-loop” system with no net displacement of culture media (*i.e.* $Q = 0 \text{ } \mu\text{L min}^{-1}$) the spectrophotometer outlet was fed into the inlet HPLC port on the culture vessel and $Q = 200 \text{ } \mu\text{L min}^{-1}$ was applied to cycle culture media through the spectrophotometer. Homogenised expectorated sputum sampled (*Section 2.13.1*) independently collected from three different persons with CF were inoculated into separate culture vessels and OD_{600 nm} measured every 30 min.

Culture density of CF sputum-associated microbial populations grown in ASM followed a typical microbial growth curve (*Figure 7.1*). Sputum derived populations exhibited a long initial

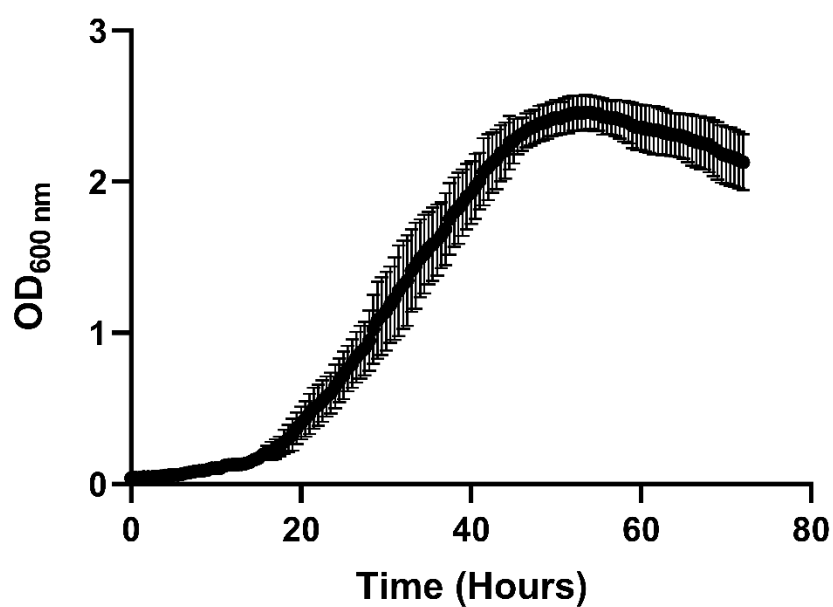


Figure 7.1 Growth of microbial populations from CF sputum in ASM.

Optical density (OD_{600 nm}) measurements following the growth of pooled homogenised expectorated sputum samples from three separate persons with CF in ASM under batch culture conditions in the continuous-flow culture vessel. Data represented as the mean ± standard deviation from three independent experiments.

lag phase, with average culture turbidity not exceeding $OD_{600\text{ nm}}$ 0.2 for the first 16 hrs of incubation. Populations were in the exponential growth phase between $T = 17$ and 45 hrs, with an average doubling time of ≈ 5 hrs. Changes in $OD_{600\text{ nm}}$ measurements plateaued as the culture reached the presumed stationary phase of growth. Average peak culture density ($OD_{600\text{ nm}}$ 2.54) was reached at $T = 54$ hrs. Microbial populations then entered the presumed death phase, as evidenced by an approximate 0.5-unit drop in average $OD_{600\text{ nm}}$ values occurring between 54 and 72 hrs.

To account for the long lag phase and prevent species washout from the model, in subsequent experiments, culture vessels inoculated with CF sputum were incubated using $Q = 0\text{ }\mu\text{L min}^{-1}$ for 24 hrs to ensure that microbial populations enter the mid-logarithmic growth phase before applying an appropriate flowrate of fresh ASM (determination of Q is described in *Section 7.3*).

7.3 Flowrate Optimisation

7.3.1 Comments

Clinical and environmental isolates often have longer doubling times compared with domesticated laboratory strains (Gibson et al., 2018). This slow growth is often cited as a survival strategy to support growth in nutrient limited conditions and to withstand starvation (Biselli et al., 2020, Chesbro et al., 1990, Eguchi et al., 1996, Postgate and Hunter, 1962). Furthermore, slow growth rates are considered a mechanism to tolerate immune clearance (Kaldalu and Tenson, 2019) and resist antimicrobial action during growth as planktonic or biofilm communities (Ciofu and Tolker-Nielsen, 2019, Katayama et al., 2017, Pontes and Groisman, 2019, Yamaguchi et al., 2019). It may therefore be unsurprising that slow growing organisms are often isolated from the polymicrobial communities associated with chronic CF airway infections (Burns and Rolain, 2014). The maintenance of slow growing homogenous mono-species cultures in continuous-flow conditions is well characterised (Allen and Waclaw, 2019, Biselli et al., 2020, Chesbro et al., 1990, Smith and Waltman, 1995). It is known that the rate of media displacement (retention time, R_t) is essential for maintaining stable steady-state microbial populations in continuous-flow culture vessels. If Q is too high, species growth will not match the rate of displacement and cultures will be “washed-out” from the system. If Q is too low, the culture will grow to a high cell density and enter the stationary phase of growth and species out-competition is more likely occur among members of a polymicrobial consortium.

The slow growth of CF sputum-derived microbial populations is evident from the results presented in *Section 7.1*, and the importance of using a suitable value for Q was identified while optimising the continuous-flow model to maintain the growth of CA as part of a

polymicrobial consortium (*Section 3*). I therefore performed a screen of different flow rates to identify the culture conditions most suitable for permitting a diverse polymicrobial population to be maintained. Aliquots of a homogenised CF sputum sample were inoculated into the continuous-flow vessel, as described in *Section 2.14.2*, and variable Q applied. $OD_{600\text{ nm}}$ was used to measure the total density of the sputum-derived microbial population over time. Illumina MiSeq-based sequencing of the hypervariable region of the bacterial 16S rRNA gene encoding for the 30S ribosomal subunit was also used to identify changes in bacterial ecology between the initial inoculum and populations maintained in the culture vessel after incubation for 120 hrs.

To fully explore changes in microbial composition in the sequencing libraries, a combination of phylogenetic metric tests was employed. Faith's phylogenetic diversity, defined as "the sum of branch lengths of a phylogenetic tree connecting all species in the target assembly" (Faith, 1992), was used as a phylogenetic generalization of species richness and to provide an overview of species presence/absence in samples. The Bray-Curtis dissimilarity test was used to quantify species dissimilarity among ecological populations by measuring the abundance of different operational taxonomic units (OTUs) in sequencing library samples (Bray, 1957). UniFrac analysis of variants build upon this dissimilarity metric by incorporating assumed phylogenetic differences between compositions when computing taxonomic distance (Lozupone and Knight, 2005). Whereas unweighted UniFrac measurements simply account for the presence/absence of species providing a qualitative measure of dissimilarity amongst samples, the weighted UniFrac analysis accounts for the relative abundance and relatedness of OTUs in samples, providing a quantitative measure of dissimilarity.

7.3.2 $OD_{600\text{ nm}}$

Average $OD_{600\text{ nm}}$ values of sputum-associated microbial populations grown under continuous-flow conditions in ASM are shown in *Figure 7.2*. There was no significant difference ($P > 0.9$) in the optical density of any sputum derived population for the first 24 hrs of incubation, *i.e.* before Q was applied to the system. Using $Q = 145\text{ }\mu\text{L min}^{-1}$ (the flow rate previously used to maintain triple-species populations of reference strains in the model) there was a steady decline in total microbial density over time, with an approximate 0.3-unit reduction in $OD_{600\text{ nm}}$ values occurring between $T = 24$ and 120 hrs. For all other flowrates a stable steady-state carrying capacity, with respect to culture turbidity, was achieved by ≈ 48 hrs. As could be expected from previous studies characterising microbial growth in chemostats (Smith and Waltman, 1995), total microbial carrying capacity in the continuous-flow model is intrinsically

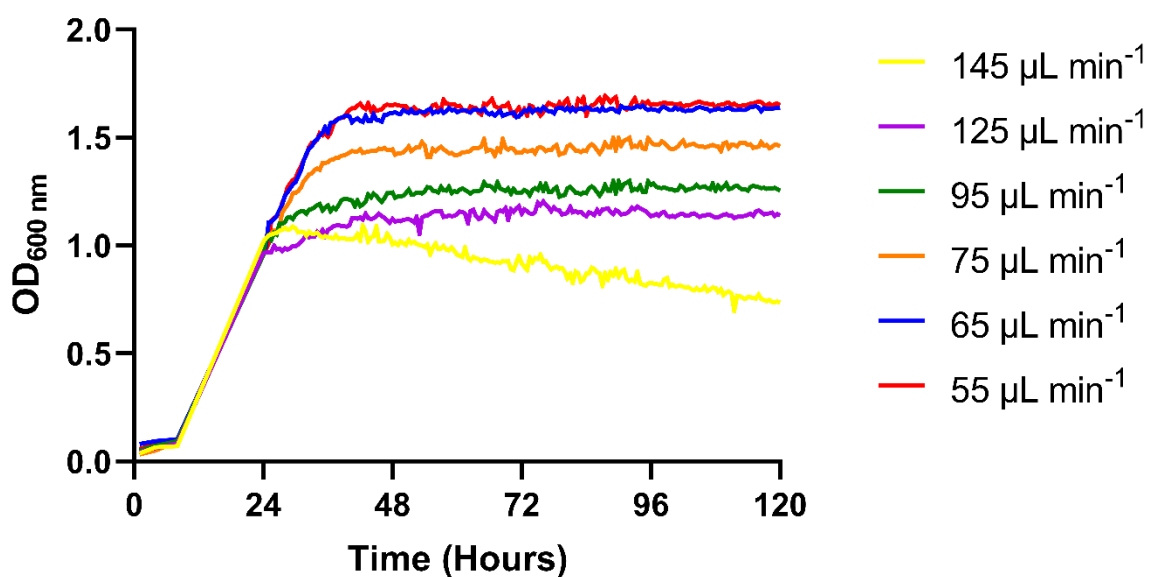


Figure 7.2 Growth of CF sputum-derived microbial populations in the continuous-flow model using different flow rates.

Optical density ($\text{OD}_{600 \text{ nm}}$) measurements following total microbial density of polymicrobial populations derived from homogenised expectorated sputum samples collected from the same person with CF in ASM under continuous-flow conditions (*Section 2.14*). $Q = 145$ (yellow); 125 (purple); 95 (green); 75 (orange); 65 (blue) and $55 \mu\text{L min}^{-1}$ (red). Data represented as the mean from two independent experiments.

linked with Q . A lower flowrate resulted in higher $OD_{600\text{ nm}}$ measurements in the culture vessel. After 48 hrs incubation an average $OD_{600\text{ nm}}$ of 1.15, 1.25 and 1.45 was reached using $Q = 125, 95$ and $75\text{ }\mu\text{L min}^{-1}$, respectively. There was no significant difference ($P > 0.9$) in the average steady-state carrying capacity in the culture vessel ($OD_{600\text{ nm}}$ 1.6) using $Q = 65$ or $55\text{ }\mu\text{L min}^{-1}$.

7.3.3 Bacterial Ecology

7.3.3.1 Relative abundance taxa plots

Relative abundance taxa bar plots of the initial inoculum and planktonic/biofilm samples after 120 hrs incubation using variable flowrates are shown in *Figure 7.3*. Although some heterogeneity could be observed for the relative abundance of OTUs present in the initial CF sputum aliquots, five OTUs were present in detectable abundances across all samples. Bacteria within the inoculum were present in the following average relative abundances: *P. aeruginosa* (PA) $67.52 \pm 24.4\%$; *Enterobacteriaceae* $27.29 \pm 25.64\%$; Lactobacillales (unassigned family) $2.49 \pm 1.66\%$; Bacilli (unassigned order) $0.81 \pm 0.7\%$ and *Anaereosinus glycerini* (member of the *Veillonellaceae* family (Strömpl et al., 1999)) $0.78 \pm 0.51\%$. It should also be noted that the inoculum sample introduced into the $Q = 55\text{ }\mu\text{L min}^{-1}$ culture vessel also contained an OTU corresponding to a Gammaproteobacteria of unassigned taxonomical order at a relative abundance of 6.5%.

Endpoint bacterial populations using $Q = 145\text{ }\mu\text{L min}^{-1}$ were dominated by PA, with the planktonic and biofilm samples containing PA at a relative abundance of 99.7% and 99.9%, respectively. Only *Enterobacteriaceae* could be detected at a relative abundance of just 0.23% in the endpoint planktonic sample using the highest flowrate. Using $Q = 125$ and $95\text{ }\mu\text{L min}^{-1}$ caused a decrease in the relative abundance of PA in the endpoint planktonic samples. For $Q = 125\text{ }\mu\text{L min}^{-1}$ PA was present at 18.74% (43% reduction in relative abundance), whereas Lactobacillales comprised 79.11% (76.46% increase in relative abundance) and *Enterobacteriaceae* 2.08% relative abundance at $T = 120$ hrs. Using $Q = 95\text{ }\mu\text{L min}^{-1}$ PA comprised 29.95% of the planktonic sample (28.7% reduction in relative abundance) and Lactobacillales and *Enterobacteriaceae* were present at a relative abundance of 63.33% and 6.64%, respectively. The endpoint biofilm sample using $Q = 125\text{ }\mu\text{L min}^{-1}$ consisted entirely of PA (99.9% relative abundance) and the biofilm sample utilising $Q = 95\text{ }\mu\text{L min}^{-1}$ comprised of PA (96.48%), Lactobacillales (3.17%) and Bacilli (0.165%).

Using $Q = 75$ and $65\text{ }\mu\text{L min}^{-1}$ there was a respective 25.11% and 16.9% increase in the relative abundance of PA between the inoculum and endpoint sputum samples. For $Q = 75\text{ }\mu\text{L min}^{-1}$ PA was present at a relative abundance of 98.84% and Lactobacillales and Bacilli

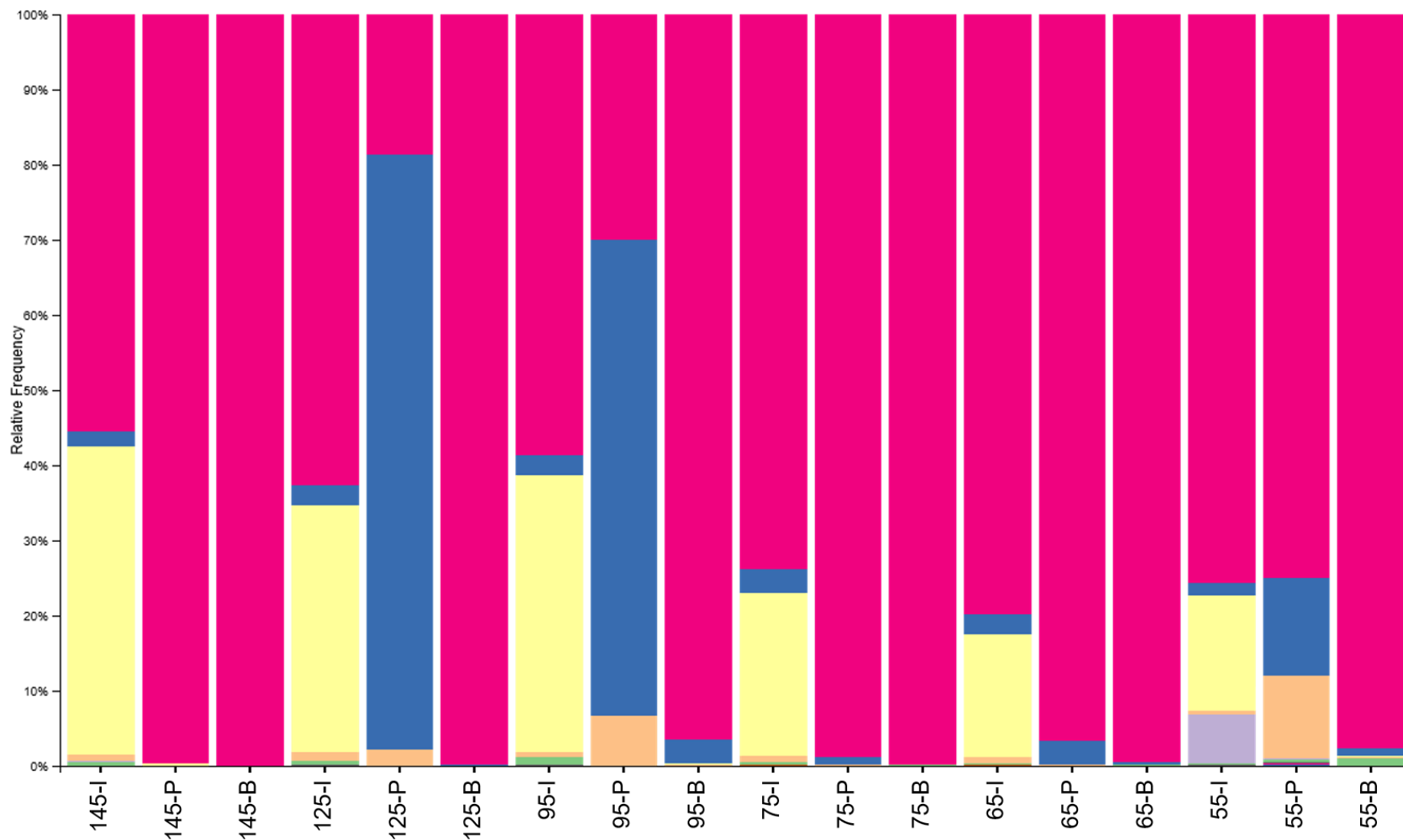
















Figure 7.3 Relative bacterial species abundance in flowrate optimisation sequencing libraries.

Relative abundance of bacterial species in the initial CF sputum inoculum and in the corresponding endpoint planktonic or biofilm samples following 120 hrs incubation. Each bar represents a different sample. Labels below samples denote flowrate ($\mu\text{L min}^{-1}$, Q) -inoculum (I); -planktonic (P) or -biofilm (B). For example, 125-P \equiv Q = 125 $\mu\text{L min}^{-1}$ planktonic. *Legend 7.1* is the corresponding legend for this taxa plot.

 (P): Proteobacteria, (C): Gammaproteobacteria, (O): Pseudomonadales, (F): Pseudomonadaceae, (G): Pseudomonas, (S): aeruginosa
 (P): Firmicutes, (C): Bacilli, (O): Lactobacillales
 (P): Proteobacteria, (C): Gammaproteobacteria, (O): Enterobacteriales, (F): Enterobacteriaceae
 (P): Firmicutes, (C): Bacilli
 (P): Proteobacteria, (C): Gammaproteobacteria
 (P): Proteobacteria, (C): Gammaproteobacteria, (O): Pseudomonadales, (F): Pseudomonadaceae
 (P): Unassigned
 (P): Proteobacteria
 (P): Firmicutes, (C): Bacilli, (O): Bacillales, (F): Bacillaceae
 (P): Firmicutes, (C): Bacilli, (O): Bacillales
 (P): Proteobacteria, (C): Betaproteobacteria, (O): Neisseriales, (F): Neisseriaceae
 (P): Firmicutes
 (P): Proteobacteria, (C): Betaproteobacteria, (O): Neisseriales, (F): Neisseriaceae, (G): Neisseria
 (P): Firmicutes, (C): Clostridia, (O): Clostridiales, (F): Veillonellaceae, (G): Anaerostipes (S): glycerini

Legend 7.1 Relative bacterial species abundance in flowrate optimisation sequencing libraries.

Legend corresponding to *Figure 7.3*. Denoting: phylum (P); classification (C); order (O); family (F); genus (G) and species (S) at the highest level which could be unambiguously assigned to aligned quality filtered sequence reads.

were present at 1.06% and 0.05%, respectively in the planktonic sample at T = 120 hrs. Using $Q = 65 \mu\text{L min}^{-1}$ PA, Lactobacillales and Bacilli were present at a relative abundance of 96.7%, 3.12% and 0.14%, respectively in the endpoint planktonic sample. Again, PA dominated the biofilm fraction of these cultures, being present at a relative abundance of 99.85% and 99.5% in the $Q = 75$ and $65 \mu\text{L min}^{-1}$ endpoint biofilm samples, respectively. Importantly, *A. glycerini* an obligate anaerobe could also be detected at a relative abundance of 0.21% in the polymicrobial biofilm sample incubated using $Q = 65 \mu\text{L min}^{-1}$.

Using the lowest flowrate possible with the digital peristaltic pump ($Q = 55 \mu\text{L min}^{-1}$) resulted in the smallest change (0.52%) in PA relative abundance between the initial inoculum (75.6% relative abundance) and endpoint planktonic (75.08% relative abundance) sample. The $Q = 55 \mu\text{L min}^{-1}$ planktonic sample contained the most diverse species abundance of any endpoint sample, also containing: *Enterobacteriaceae* (relative abundance 0.1%), Lactobacillales (12.91%), Bacilli (11.03%), *A. glycerini* (0.37%) and unassigned Pseudomonadaceae and Bacillaceae (0.37% and 0.15% relative abundance, respectively). There was a respective 12.75% and 10.6% increase in the relative abundance of Lactobacillales and Bacilli present in the initial and planktonic samples over the course of incubation. Conversely, there was a 15.3% decrease in the relative abundance of *Enterobacteriaceae* present in the culture vessel between T = 0 and 120 hrs. All five distinct OTUs identified in the initial sputum inoculums could also be detected in the $Q = 55 \mu\text{L min}^{-1}$ endpoint biofilm sample. Like the other biofilm samples, PA was present in the highest relative abundance (97.6%) and *Enterobacteriaceae*, Lactobacillales, Bacilli and *A. glycerini* were present at a relative abundance of 0.12%, 0.1%, 0.12% and 0.89% respectively. Demonstrating a 0.52% increase in the relative abundance of anaerobic *A. glycerini* between $Q = 55$ and $65 \mu\text{L min}^{-1}$ biofilm samples when using the slower flowrate.

7.3.3.2 Faith's Phylogenetic Diversity

Box plots representing Faith's phylogenetic diversity of bacterial communities present in the combined initial inoculums and in the combined planktonic and biofilm endpoint samples for the different flowrates are shown in *Figure 7.4*. The phylogenetic biodiversity of the inoculum samples was significantly higher ($P < 0.05$) than all endpoint samples, demonstrating a reduction in the overall phylogenetic diversity present in the culture vessels over 120 hrs of incubation. Despite it being clear that the phylogenetic diversity of endpoint samples using $Q = 55 \mu\text{L min}^{-1}$ is greater than endpoint samples using higher flowrates, this difference is not statistically significant ($P > 0.05$) when using Faith's measure of biodiversity.

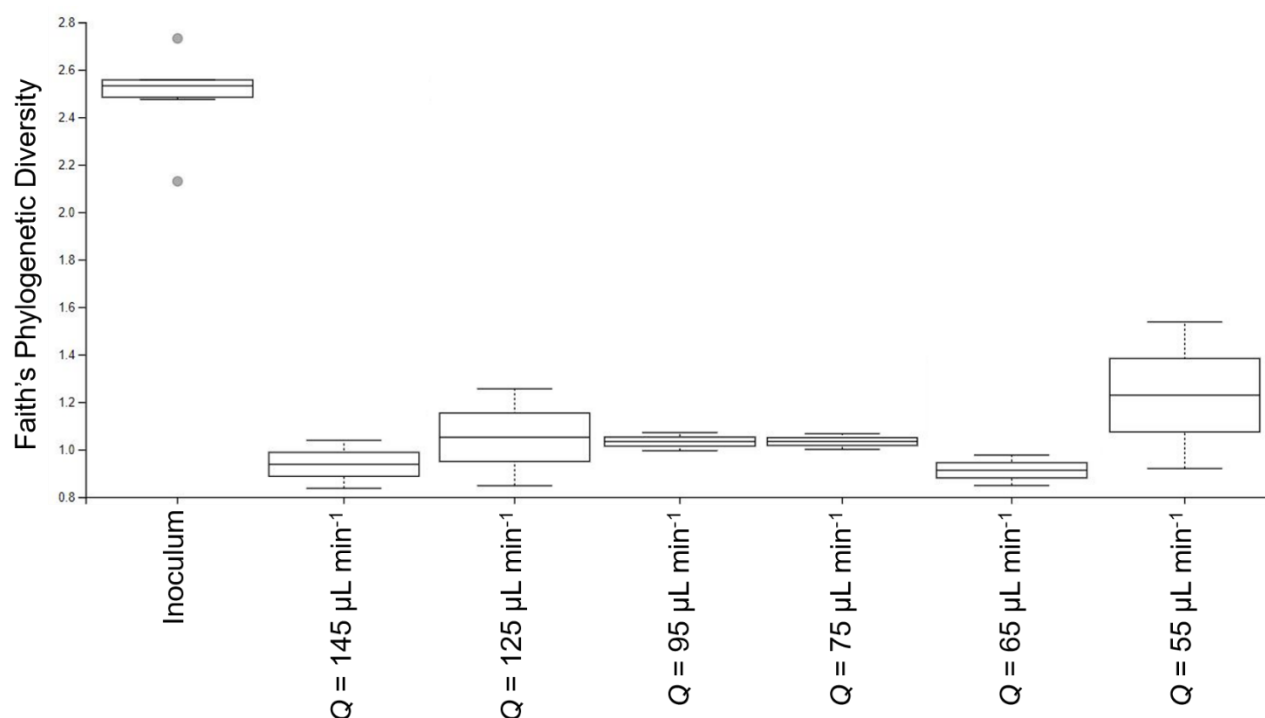


Figure 7.4 Faith's phylogenetic diversity of flowrate optimisation samples.

Boxplots representing Faith's phylogenetic diversity of bacterial communities in the initial CF sputum inoculum and combined endpoint planktonic and biofilm samples after 120 hrs incubation in ASM under continuous-flow conditions using different flowrates (Q). $n = 6$ for inoculum and $n = 2$ for endpoint samples.

7.3.3.2 Bray-Curtis Dissimilarity Test

Principal coordinate analysis (PCoA) plots based upon Bray-Curtis dissimilarity test of bacterial communities present in the initial inoculum, endpoint planktonic and endpoint point biofilm samples for the different flowrates are shown in *Figure 7.5*. The PCoA plot resulted in a 3-dimensional solution in which PC1 accounted for 53.64% of the variation and PC2 and PC3 accounted for 27.71% and 20.35%, respectively. The inoculum samples clustered together in one region, with little variance observed in PC1 or PC2. Planktonic samples of the three fastest flowrates (145, 125 and 95 $\mu\text{L min}^{-1}$) did not cluster with each other or the other endpoint samples and were the most dissimilar compared with the inoculum samples. All other endpoint samples, except $Q = 55 \mu\text{L min}^{-1}$ planktonic sample, formed a tight cluster with little variance compared to the inoculum samples along PC1 and PC2. When compared to the cluster of endpoint samples, the $Q = 55 \mu\text{L min}^{-1}$ planktonic sample was closer to the inoculum samples along PC3, approximately equidistant from the inoculum samples along PC2 and further from the inoculum samples along PC1.

7.3.3.3 UniFrac Analysis

PCoA analysis plots based upon unweighted and weighted variants of UniFrac distance for the bacterial communities present in the initial inoculum, endpoint planktonic and endpoint biofilm samples for the different flowrates are shown in *Figure 7.6* and *Figure 7.7*, respectively. The unweighted PCoA plot resulted in a 3-dimensional solution in which PC1 accounted for 60.15% of the variation and PC2 and PC3 accounted for 9.51% and 7.91%, respectively. The inoculum samples clustered together in a region separated from all endpoint samples along PC1. There was no obvious clustering of endpoint planktonic and biofilm samples. However, $Q = 75$ and $65 \mu\text{L min}^{-1}$ planktonic and $Q = 145, 95, 65$ and $55 \mu\text{L min}^{-1}$ biofilm samples did cluster with respect to PC2, this loose cluster showed little variance from the initial inoculum samples along PC2. $Q = 145, 65$ and $55 \mu\text{L min}^{-1}$ biofilm samples were least dissimilar from the inoculum cluster along PC3. With respect to PC1, $Q = 55 \mu\text{L min}^{-1}$ planktonic sample was closest to the cluster of inoculum samples. As in *Figure 7.5*, $Q = 145, 125$ and $95 \mu\text{L min}^{-1}$ planktonic samples were the most dissimilar to the inoculum samples with respect to all axes.

The weighted PCoA plot resulted in a 3-dimensional solution in which PC1 accounted for 96.05% of the variance and PC2 and PC3 accounted for 3.48% and 0.31% respectively. All samples, except $Q = 125, 95$ and $55 \mu\text{L min}^{-1}$ planktonic samples, clustered tightly with little variance with respect to PC1. This cluster can be further split into two distinct clusters along PC2, comprising of the initial inoculum (top) and endpoint (bottom) samples. For the

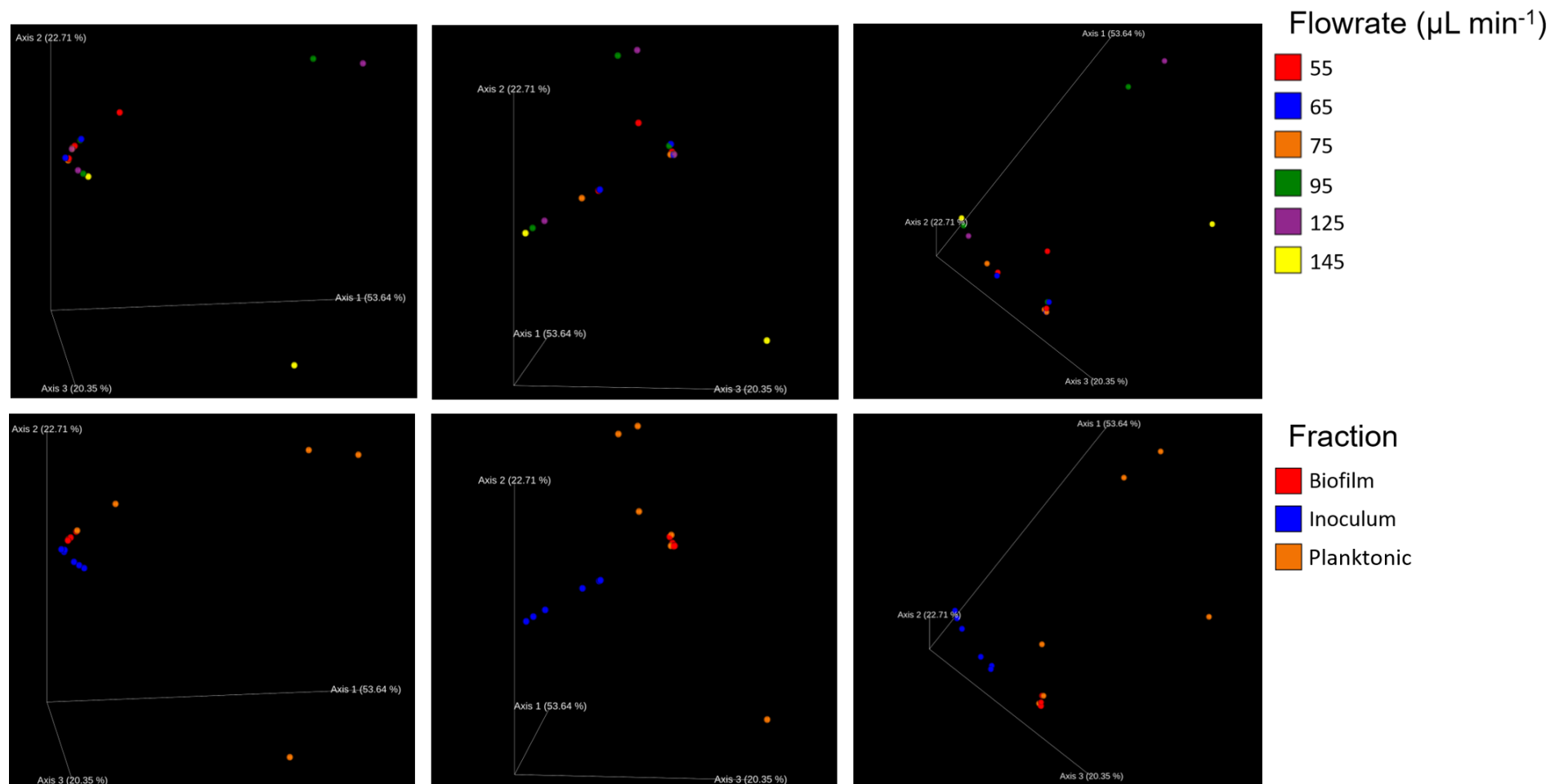


Figure 7.5 Bray-Curtis dissimilarity test of flowrate optimisation samples

Principal coordinate analysis (PCoA) based on Bray-Curtis dissimilarity test of initial inoculum, endpoint planktonic and endpoint biofilm samples. Endpoint samples were incubated in ASM under continuous flow conditions for 120 hrs using different flowrates (Q). Top panels denote the different flowrates: $Q = 145$ (yellow); 125 (purple); 95 (green); 75 (orange); 65 (blue) and $55 \mu\text{L min}^{-1}$ (red). Bottom panels denote the different sample types (fraction): initial inoculum (blue); endpoint planktonic (orange) and endpoint biofilm (blue).

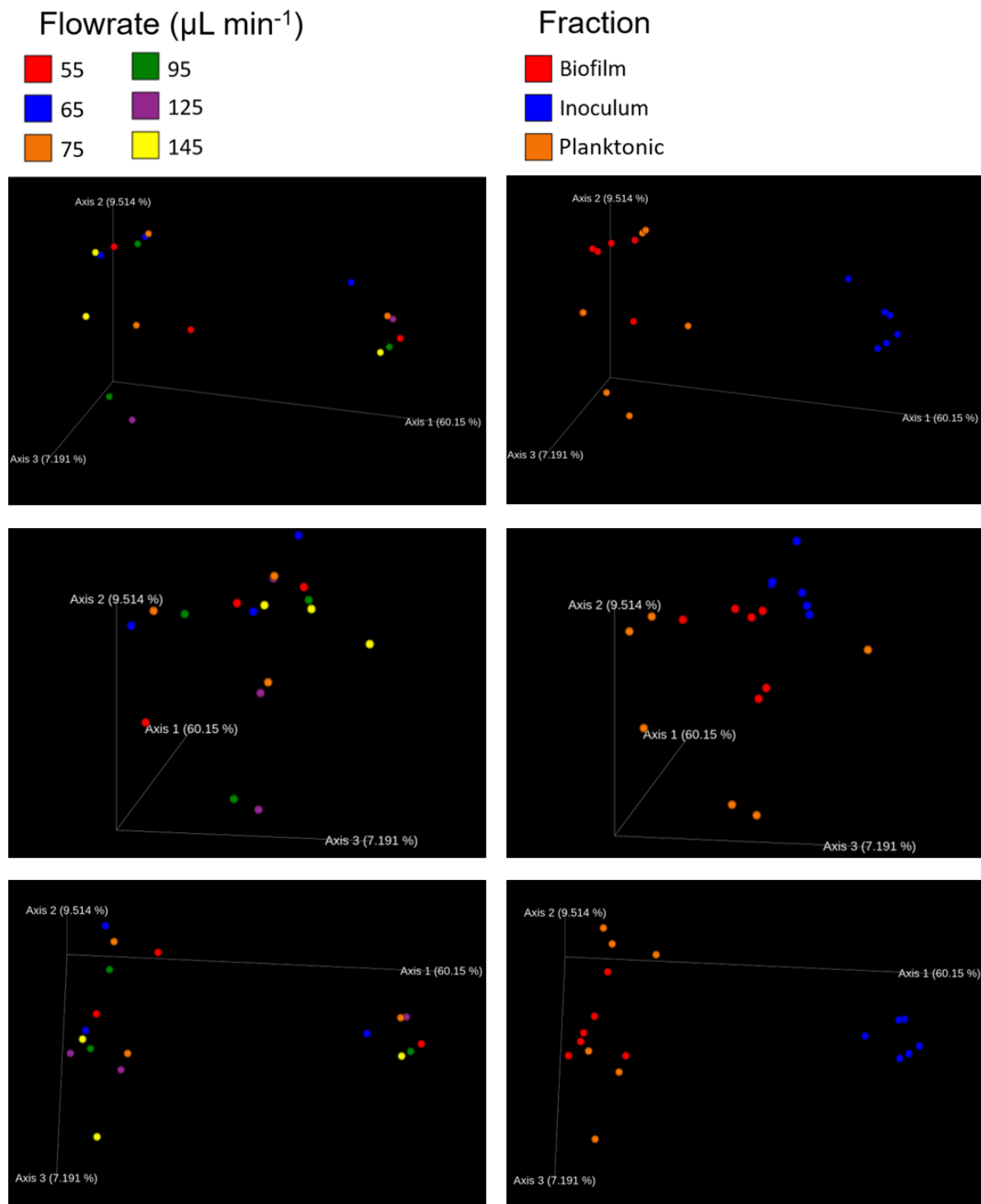


Figure 7.6 Unweighted UniFrac of flowrate optimisation samples

Principal coordinate analysis (PCoA) based on unweighted variants of UniFrac for inoculum, endpoint planktonic and endpoint biofilm bacterial samples. Endpoint samples were incubated in ASM under continuous flow conditions for 120 hrs using different flowrates (Q). Left panels denote the different flowrates: $Q = 145$ (yellow); 125 (purple); 95 (green); 75 (orange); 65 (blue) and $55 \mu\text{L min}^{-1}$ (red). Right panels denote the different sample types (fraction): initial inoculum (blue); endpoint planktonic (orange) and endpoint biofilm (blue).

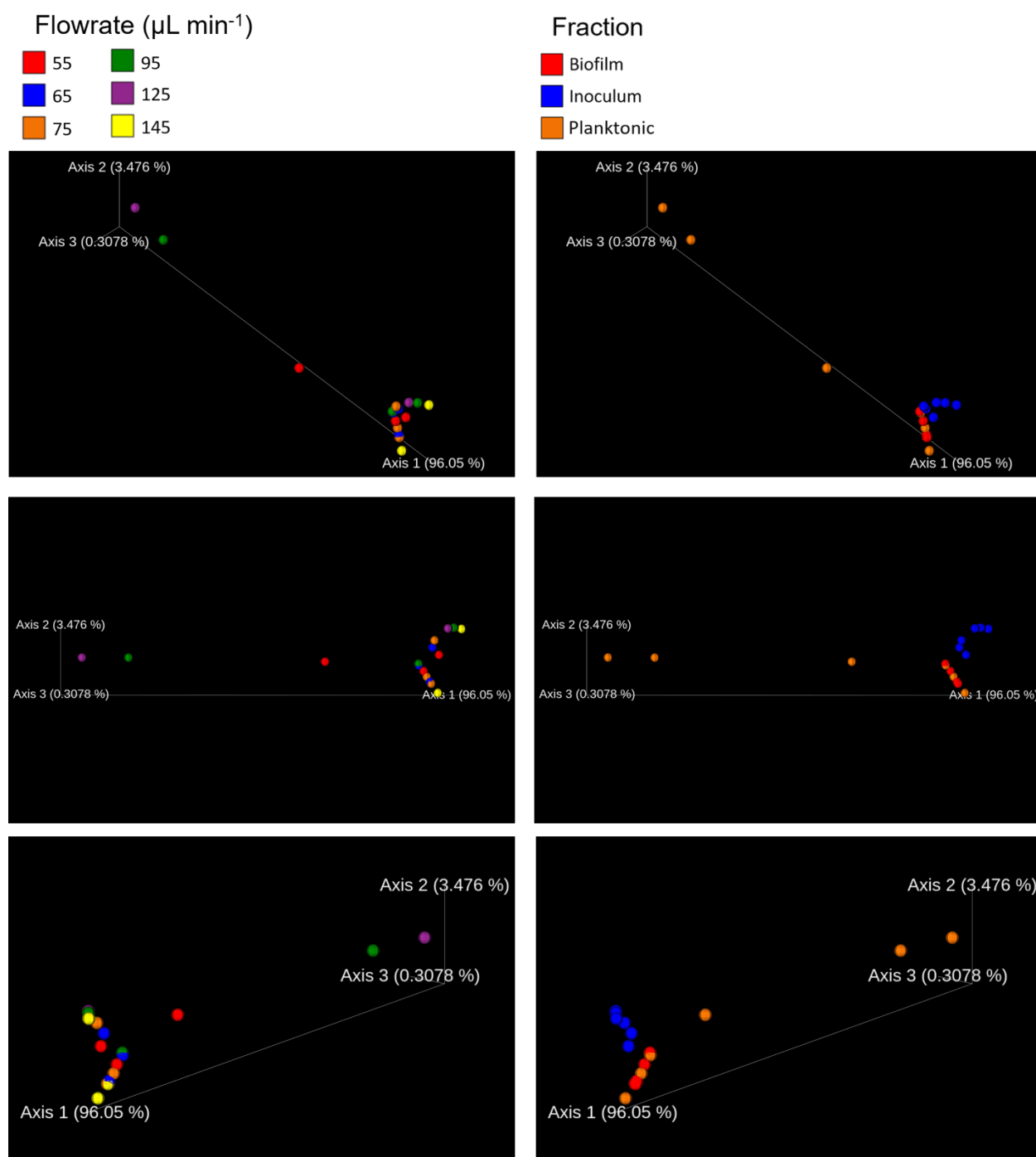


Figure 7.7 Weighted UniFrac of flowrate optimisation samples

Principal coordinate analysis (PCoA) based on weighted UniFrac analysis of inoculum, endpoint planktonic and endpoint biofilm bacterial samples. Endpoint samples were incubated in ASM under continuous flow conditions for 120 hrs using different flowrates (Q). Left panels denote the different flowrates: $Q = 145$ (yellow); 125 (purple); 95 (green); 75 (orange); 65 (blue) and 55 $\mu\text{L min}^{-1}$ (red). Right panels denote the different sample types (fraction): initial inoculum (blue); endpoint planktonic (orange) and endpoint biofilm (blue).

endpoint sample cluster, the $Q = 65$ and $55 \mu\text{L min}^{-1}$ biofilm samples were least dissimilar to their respective inoculum samples and the $Q = 65 \mu\text{L min}^{-1}$ planktonic sample was the closest planktonic sample to its respective inoculum sample. The endpoint samples that did not cluster showed little variance from the other samples along PC2 and PC3 and of these samples, $Q = 125$ and $55 \mu\text{L min}^{-1}$ showed the most and least variance to the initial inoculums along PC1, respectively.

7.3.4 Conclusions

In combination, the results presented in this sub-section highlight several key conclusions. Firstly, using $Q = 145 \mu\text{L min}^{-1}$ resulted in a washout of sputum-derived microbial species from the culture vessel, as evidenced by the decline in culture density over time. All other flowrates permitted stable microbial carrying capacities, of various average optical densities, to be maintained over the period of incubation. The faster flowrates, 125 and $95 \mu\text{L min}^{-1}$, resulted in an increase in the relative abundance of Lactobacillales in the planktonic fraction of the culture. Whereas $Q = 75$ and $65 \mu\text{L min}^{-1}$ resulted in PA being the dominant bacterial species in the planktonic fraction at the endpoint of incubation.

Importantly $Q = 55 \mu\text{L min}^{-1}$ permitted the most diverse bacterial populations to be maintained in the planktonic and biofilm fractions of the co-culture. This notion is supported by Faith's phylogenetic diversity analysis (*Figure 7.4*) and that all five OTUs present in the initial inoculum are present in the endpoint biofilm and planktonic populations (*Figure 7.3*). Furthermore, these samples are the least dissimilar from the initial culture inoculums with respect to PC1 in the PCoA analysis based upon the Bray-Curtis dissimilarity test (*Figure 7.5*) and unweighted UniFrac analysis of variance (*Figure 7.6*). Taken together, these results demonstrate that $Q = 55 \mu\text{L min}^{-1}$ is the most suitable flowrate for the maintenance of diverse sputum-derived polymicrobial cultures. Hence this flowrate was used for the culture of sputum samples in all subsequent experiments. However, it is clear from the data that there is still a change in species diversity over time using this flowrate. For example, the $Q = 55 \mu\text{L min}^{-1}$ planktonic sample shows significant variance from the initial inoculum samples along PC1 in the weighted UniFrac PCoA (*Figure 7.7*). Although this variance is attributed to an increase in the relative abundance Lactobacillales in the sample, it demonstrates that optimisation of Q alone is not sufficient for the exact recapitulation of microbial communities at the abundancies found in CF sputum using the continuous-flow model.

The results presented in this sub-section also identify distinct differences in the bacterial ecology of the planktonic and biofilm populations grown from the same polymicrobial inoculum. For example, it is key to note that the biofilms of the two slowest flowrates permitted the growth

of *A. glycerini*, an obligate anaerobe. Biofilms are often found to have hypoxic and anoxic regions crucial for permitting the survival of anaerobic species (Karampatzakis et al., 2017, Wu et al., 2018). Similarly, the CF microenvironment is found to have steep oxygen gradients and hypoxic regions (Worlitzsch et al., 2002) suitable for harbouring the growth of anaerobic species. Some key anaerobic species such as *Veillonella*, *Prevotella* and *Rothia* are persistent members of chronic CF airway infections (Carmody et al., 2018, Rogers et al., 2004, Tunney et al., 2008, Zemanick et al., 2010). Previous studies have demonstrated that these anaerobic fermenters, such as *A. glycerini*, may trigger proinflammatory immune responses (Ghorbani et al., 2015, Mirković et al., 2015) and contribute towards the pathogenicity of conventional CF pathogens (Flynn et al., 2016). However, the role of anaerobes in CF airway infections is still hotly debated (Caverly and LiPuma, 2018). It is therefore important that anaerobes can be maintained in the *in vitro* model to discern their potential role in the modulation of microbial physiology *via* interspecies interactions in future experiments. As well as highlighting the need to consider the endpoint composition of both the planktonic and biofilm populations when further optimising continuous-flow culture conditions.

7.4 Supplementation of ASM

7.4.1 Comments

Optimisation of *Q* alone was not sufficient for maintaining the full diversity of microorganisms found in CF sputum *in vitro* (Section 7.3). It is well known that fastidious and auxotrophic species often require supplementation with exogenous growth factors to promote their growth *ex situ*. I therefore performed a search of the literature to identify exogenous supplements previously found improve the laboratory growth of microbial species and then screened the following modified ASM compositions to identify factors which enhanced the diversity of sputum derived polymicrobial communities maintained in the continuous-flow model:

(1) ASM + 40 μM FeSO_4 (ASM- FeSO_4). As described previously (Section 1.) iron acquisition is essential for biological growth and a scarcity of this resource has been found to increase microbial pathogenesis and competition amongst species (Mashburn et al., 2005). ASM containing an excess of free iron (10-times the amount in standard ASM) may reduce interspecies competition and provide sufficient free iron to support the *in vitro* growth of some fastidious microorganisms.

(2) ASM + 50 mg L^{-1} desferrioxamine (ASM-desferrioxamine). Microbial “cheaters” are often isolated from chronic polymicrobial infections. These species do not produce metabolically expensive public goods, such as siderophores, but exploit the global production of such molecules from other members of a microbial consortium (Kramer et al., 2020, Kümmerli,

2015, Vacca, 2017). The cross-recognition and uptake of xenosiderophores by bacterial and fungal species is well documented and the addition of exogenous siderophores has been shown to improve the growth of some microbial species (Guan et al., 2001, Meyer, 1992, Miethke et al., 2013, Visca et al., 2013). I therefore supplemented ASM with desferrioxamine (a commercially available bacterial siderophore) at a concentration previously shown to improve bacterial growth to investigate if this would support the growth of fastidious species that do not encode their own iron scavenging molecules.

(3) ASM + micronutrients (ASM-micronutrients). Trace elements act as cofactors for some essential enzymatic reactions (Nimbalkar et al., 2018). Although different microorganisms require different combinations of essential micronutrients (also known as trace elements) the usual elements required for bacterial growth are Mn, Co, Zn, Cu and Mo (Costa et al., 2020, Demirel and Scherer, 2011, Glass and Orphan, 2012). ASM was therefore supplemented with the micronutrient stock described by LaBauve and Wargo (2012), containing the standard essential micronutrients.

(4) ASM + vitamins (ASM-vitamins). Some bacteria and fungi also require vitamins to support their growth. In particular, water-soluble vitamins have been shown to improve microbial growth (Omotani et al., 2017). ASM was therefore supplemented with stock solutions of the key water-soluble vitamins described in *Table 2.9*.

(5) ASM + 1 mM KNO₃ (ASM-KNO₃). As described in *Section 7.3.4*, it is essential the model can support the growth of anaerobic species. Increased levels of nitrate have previously improved the *in vitro* growth of anaerobic species and supported anoxic growth by denitrification of PA at growth rates reported in CF sputum (Line et al., 2014). Hence, ASM-KNO₃ was supplemented with 3.5-times more KNO₃ than standard ASM to determine if this could promote the growth of sputum-derived microbes under continuous-flow conditions.

(6) ASM + 5 mM methionine and cysteine (ASM-Met/Cys). Anaerobic fermentation of amino acids is a conserved feature of microbial fermentation under anoxic conditions and may be crucial for the survival of anaerobes in microaerobic environments (Loddeke et al., 2017, Palego, 2015). The breakdown of sulfur-containing amino acids may generate localised anoxic regions, particularly in biofilms, as released can react with dissolved oxygen in the media (Aklujkar et al., 2014, Alcántara et al., 2004). I therefore supplemented ASM with an excess of Met and Cys to see if an increased concentration of sulfur-containing amino acids would improve the growth of anaerobic fermenters present in CF sputum.

(7) ASM + 5% heat-inactivated fetal bovine calf serum (FBS, ASM-FBS). FBS is a common cell-culture supplement rich in eukaryotic growth factors that can also improve the growth of microorganisms. FBS is an essential supplement for the *in vitro* growth of *Helicobacter pylori*

(Bessa et al., 2012, Testerman et al., 2001) and further improves the growth of several other bacterial species (Giengkam et al., 2015, Gifford et al., 2002, Hanson, 1987, Leonhard et al., 2018). Heat-inactivated FBS was used as a supplement to minimise the inhibitory effects of heat-labile immune factors found in FBS on growth of the microbial consortium.

(8) ASM + 100 μ M sodium pyrophosphate (ASM- $\text{Na}_2\text{H}_2\text{P}_2\text{O}_7$). Increased phosphorus bioavailability is viewed as the most important factor for permitting the expansion of aquatic microbial populations. Furthermore, access to inorganic phosphorus is essential for maintaining diverse microbial populations and niche species in activated sludge (Miettinen et al., 1997, Zheng et al., 2019). Hence, I supplemented ASM with sodium pyrophosphate to increase the concentration of inorganic phosphorus in the growth media and determine the effects of this supplement on the growth of sputum derived polymicrobial communities.

(9) ASM + 1 mg L^{-1} *N*-acetylmuramic acid (ASM-NAM). Exogenous NAM, obtained from the walls of dead bacterial cells in a polymicrobial consortium *in situ* (Borisova et al., 2016), has been identified as an essential factor for the *in vitro* growth of some oral and airway-associated pathogens (Hottmann et al., 2018, Mayer et al., 2019). Provision of this essential bacterial cell wall component may therefore stimulate the growth of such auxotrophic species early during incubation, where no NAM is available to be recycled from dead cells and prevent the early washout of such species from the culture vessel.

Aliquots of homogenised CF sputum samples were inoculated into the continuous-flow culture vessel containing different ASM compositions, as described in *Section 2.14.2*. $Q = 55 \mu\text{L min}^{-1}$. As in *Section 7.3*, $\text{OD}_{600 \text{ nm}}$ was used to assess the total density of co-cultures and Illumina MiSeq-based 16S rRNA amplicon sequencing was used to identify changes in bacterial ecology over 120 hrs incubation.

7.4.2 Micronutrient Supplementation

7.4.2.1 $\text{OD}_{600 \text{ nm}}$

Average $\text{OD}_{600 \text{ nm}}$ values of sputum-associated microbial populations grown under continuous-flow conditions in different ASM compositions are shown in *Figure 7.8*. All sputum-derived microbial populations, except the population grown in ASM-Met/Cys, reached a total steady-state microbial carrying capacity by $T = 48$ hrs. There was no significant difference ($P > 0.9$) in the average $\text{OD}_{600 \text{ nm}}$ measurements of sputum samples cultured in standard ASM compared with average culture densities observed using the same flowrate in *Section 7.3.2*. There was no significant difference ($P > 0.1$) between average steady-state carrying capacities

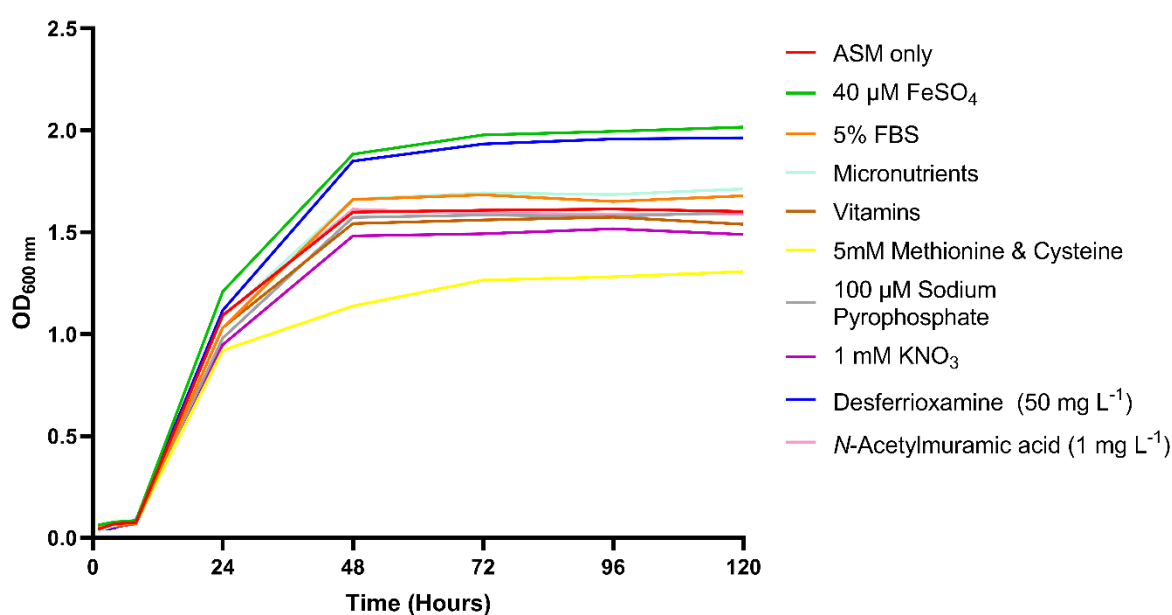


Figure 7.8 Growth of CF sputum derived microbial populations in different ASM compositions.

Optical density (OD_{600 nm}) measurements following total microbial density of microbial populations derived from homogenised expectorated sputum samples collected from the same person with CF under continuous-flow conditions. $Q = 55 \mu\text{L min}^{-1}$. Culture media was ASM with the following supplements: + no supplement (red); + 40 μM FeSO₄ (green); + 5% FBS (orange); + micronutrients (cyan); + vitamins (brown); + 5mM methionine and cysteine (yellow); + 100 μM sodium pyrophosphate (grey); + 1 mM KNO₃ (purple); + 50 mg L⁻¹ desferrioxamine (purple); + 1 mg L⁻¹ N-acetylmuramic acid (pink). Data represented as the mean from two independent experiments.

of populations cultured in: ASM-only ($OD_{600\text{ nm}} \approx 1.6$); ASM-FBS (1.67); ASM-micronutrients (1.68); ASM-vitamins (1.55); ASM- $Na_2H_2P_2O_7$ (1.58); ASM- KNO_3 (1.5) or ASM-NAM (1.59). Carrying capacities of sputum-derived microbial populations cultured in ASM supplemented with increased $FeSO_4$ or desferrioxamine were significantly higher ($P < 0.05$) than the density of the other cultures, average $OD_{600\text{ nm}}$ 1.97 and 1.93 respectively. Sputum-derived populations cultured in ASM-Met/Cys did not reach a stable steady-state carrying capacity until $T = 72$ hrs and the average steady-state culture density ($OD_{600\text{ nm}}$ 1.3) was significantly lower ($P < 0.05$) than that of the ASM-only culture.

7.4.3 Bacterial Ecology

7.4.3.1 Taxa Plots

Relative abundance taxa bar plots of the initial inoculum and planktonic/biofilm samples after 120 hrs incubation in different compositions of ASM are shown in *Figure 7.9*. Although there was considerable heterogeneity in the relative abundance of the initial bacterial inoculum present in the sputum aliquots, three distinct OTUs were present at $>1\%$ relative abundance across all samples. These three dominant bacteria were present in the following average relative abundancies: *P. aeruginosa* $67.63 \pm 19.38\%$, Lactobacillales (unassigned family) $19.56 \pm 16.13\%$ and Bacilli (unassigned order) $7.8 \pm 4.54\%$. Inoculum samples introduced into ASM supplemented with desferrioxamine, NAM, sodium pyrophosphate and increased methionine/cysteine also contained a prominent OTU corresponding to Bacteroidetes (unassigned classification) at a relative abundance of $15.38 \pm 9.34\%$. Furthermore, the samples inoculated into ASM-desferrioxamine or ASM- Met/Cys included Micrococcaceae (unassigned genus) at a relative abundance of 2.82% and 1.09%, respectively. The sample inoculated into ASM- KNO_3 contained Lactobacillales and *Enterobacteriaceae* at a relative abundance of 2% and 41.02%, respectively. Across all samples, the remaining inoculum comprised of the other bacteria listed in *Legend 7.2* in varied proportions at $<0.2\%$ total relative abundance.

A 4.22% decrease in the relative abundance of PA occurred between the initial inoculum (relative abundance = 70.93%) and the endpoint planktonic sample (66.71%) cultured in ASM-only. By contrast, Lactobacillales increased in relative abundance from 21.32 to 31.72% and Bacilli decreased in relative abundance from 7.15 to 1.49% over the course of incubation. A Gammaproteobacteria (unassigned order) was also present in the ASM-only planktonic endpoint sample at a relative abundance of 0.03% but all other inoculum species were lost over the course of incubation. As in *Section 7.3*, PA was the dominant species in the ASM-

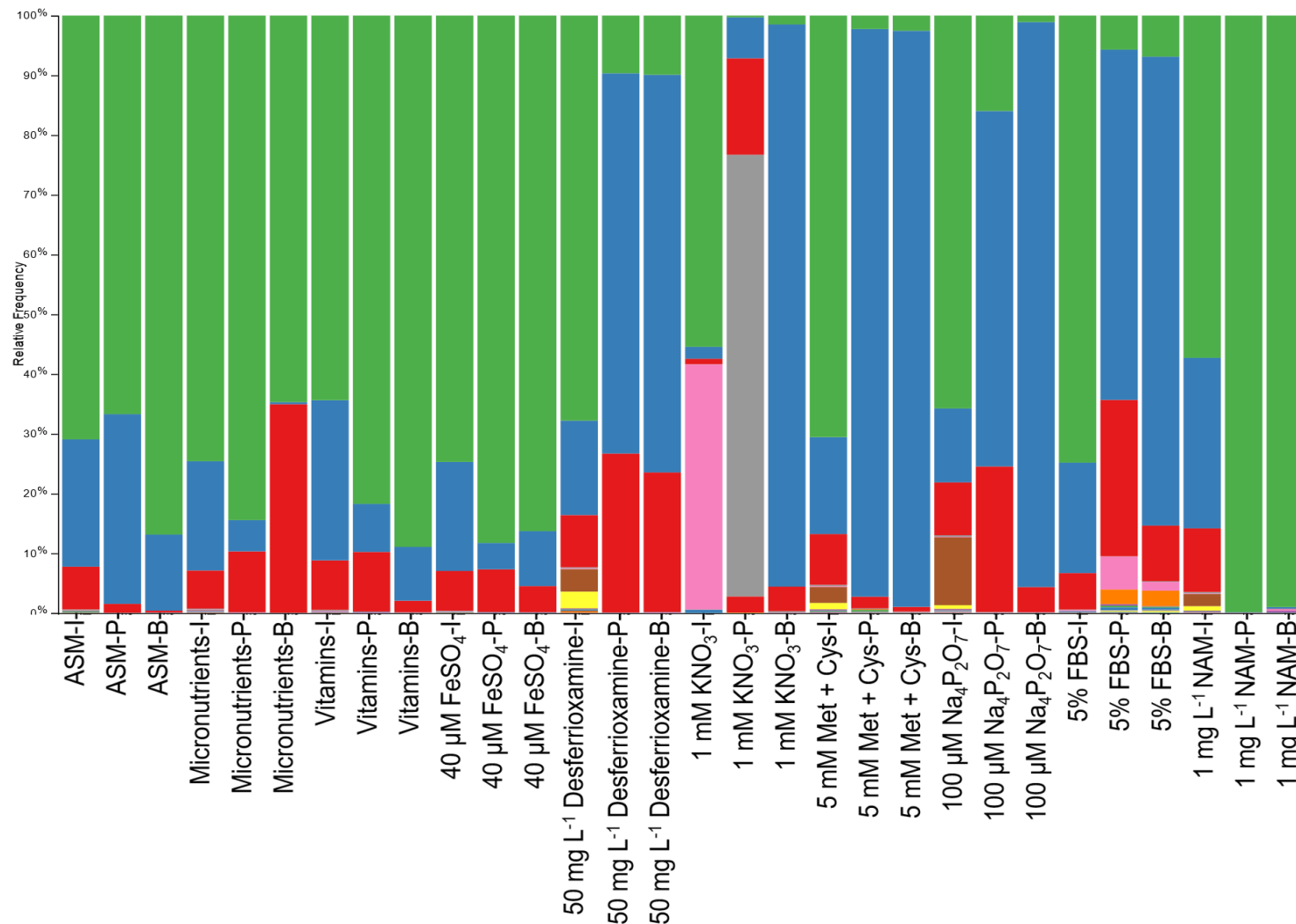


Figure 7.9 Relative bacterial species abundance in different ASM composition sequencing libraries.

Relative abundance of bacterial species in the initial CF sputum inoculum and in the corresponding endpoint planktonic or biofilm samples following 120 hrs incubation under continuous-flow conditions in different compositions of ASM. $Q = 55 \mu\text{L min}^{-1}$. Each bar represents a different sample. Labels below samples denote the ASM supplement: -inoculum (I); -planktonic (P) or -biofilm (B). For example, $\text{Na}_4\text{P}_2\text{O}_7\text{-P} \equiv \text{ASM} + 100 \mu\text{M}$ sodium pyrophosphate-planktonic. *Legend 7.2* is the corresponding legend for this taxa plot.

	(P): Proteobacteria, (C): Gammaproteobacteria, (O): Pseudomonadales, (F): Pseudomonadaceae, (G): Pseudomonas, (S): aeruginosa
	(P): Firmicutes, (C): Bacilli, (O): Lactobacillales
	(P): Firmicutes, (C): Bacilli
	(P): Firmicutes
	(P): Proteobacteria, (C): Gammaproteobacteria, (O): Enterobacteriales, (F): Enterobacteriaceae
	(P): Bacteroidetes
	(P): Actinobacteria, (C): Actinobacteria, (O): Actinomycetales, (F): Micrococcaceae
	(P): Firmicutes, (C): Bacilli, (O): Bacillales, (F): Bacillaceae
	(P): Proteobacteria, (C): Gammaproteobacteria
	(P): Unassigned
	(P): Proteobacteria, (C): Gammaproteobacteria, (O): Pseudomonadales, (F): Pseudomonadaceae
	(P): Firmicutes, (C): Clostridia, (O): Clostridiales
	(P): Firmicutes, (C): Bacilli, (O): Bacillales
	(P): Proteobacteria
	(P): Actinobacteria, (C): Actinobacteria, (O): Actinomycetales, (F): Micrococcaceae, (G): Rothia
	(P): Firmicutes, (C): Bacilli, (O): Bacillales, (F): Listeriaceae, (G): Listeria, (S) weihenstephanensis
	(P): Actinobacteria, (C): Actinobacteria, (O): Actinomycetales
	(P): Firmicutes, (C): Bacilli, (O): Lactobacillales, (F): Streptococcaceae, (G): Streptococcus, (S): agalactiae
	(P): Proteobacteria, (C): Betaproteobacteria, (O): Neisseriales, (F): Neisseriaceae
	(P): Firmicutes, (C): Bacilli, (O): Bacillales, (F): Staphylococcaceae, (G): Micrococcus, (S): brunensis
	(P): Proteobacteria, (C): Betaproteobacteria, (O): Neisseriales, (F): Neisseriaceae, (G): Neisseria
	(P): Firmicutes, (C): Clostridia, (O): Clostridiales, (F): Lachnospiraceae, (G): Lachnoanaerobaculum
	(P): Proteobacteria, (C): Gammaproteobacteria, (O): Pseudomonadales
	(P): Firmicutes, (C): Bacilli, (O): Lactobacillales, (F): Aerococcaceae, (G): Abiotrophia, (S): defectiva
	(P): Firmicutes, (C): Clostridia, (O): Clostridiales, (F): Veillonellaceae
	(P): Bacteroidetes, (C): Bacteroidia, (O): Bacteroidales
	(P): Firmicutes, (C): Clostridia, (O): Clostridiales, (F): Lachnospiraceae
	(P): Firmicutes, (C): Bacilli, (O): Bacillales, (F): Listeriaceae, (G): Listeria
	(P): Actinobacteria, (C): Actinobacteria, (O): Bifidobacteriales, (F): Bifidobacteriaceae, (G): Alloscardovia
	(P): Proteobacteria, (C): Betaproteobacteria, (O): Burkholderiales

Legend 7.2 Relative bacterial species abundance in different ASM composition sequencing libraries.

Legend corresponding to *Figure 7.9*. Denoting: phylum (P); classification (C); order (O); family (F); genus (G) and species (S) at the highest level which could be unambiguously assigned to aligned quality filtered sequence reads.

only endpoint biofilm sample (relative abundance 86.86%) and Lactobacillales, Bacilli and Pseudomonadaceae (unassigned genus) were present at a relative abundance of 12.7, 0.32 and 0.01%, respectively. Similar changes in bacterial ecology were observed over time for the sputum samples cultured in ASM supplemented with micronutrients and vitamins. Compared with the initial inoculums, there was a respective 9.86 and 7.14% increase in the relative abundance of PA in endpoint ASM-micronutrients (84.7%) and ASM-vitamins (81.73%) planktonic samples. An approximate 13% decrease in the relative abundance of Lactobacillales occurred between the initial inoculum and endpoint ASM-micronutrients or ASM-vitamins planktonic samples, with this OTU, respectively, present in these samples at 5.23 and 8.04%. Bacilli, Pseudomonadaceae and Proteobacteria (unassigned classification) were, respectively, present at 10.21/10.02%, 0.03/0.09% and 0.06/0.08% relative abundance in the ASM-micronutrients or ASM-vitamins samples. The composition of the ASM-vitamins biofilm sample closely resembled that of ASM-only, with PA; Lactobacillales; Bacilli and Pseudomonadaceae present at a relative abundance of 88.93, 8.99, 1.96 and 0.02%, respectively. However, the composition of the ASM-micronutrients biofilm sample was markedly different, with Bacilli present at a relative abundance of 34.92% and PA, Lactobacillales and Gammaproteobacteria at 64.7, 0.034 and 0.01%, respectively.

For the planktonic sample cultured in ASM-FeSO₄ there was an ≈13% increase/decrease, respectively, in the endpoint relative abundance of PA (88.26%) and Lactobacillales (4.41%). The relative abundance of Bacilli decreased by just 0.58% over 120 hrs incubation and Pseudomonadaceae was present in the endpoint planktonic sample at a relative abundance of 0.08%. The composition of the endpoint biofilm sample was similar to the planktonic fraction, with PA, Lactobacillales, Bacilli and Pseudomonadaceae present at a relative abundance of 86.29, 9.2, 4.4 and 0.07%, respectively. Interestingly, the endpoint planktonic sample cultured in ASM-desferrioxamine was dominated by Lactobacillales (relative abundance 63.64%). Bacilli, PA and Proteobacteria were present at a relative abundance of 26.44, 9.66 and 0.03%, respectively. The composition of the endpoint biofilm sample for this supplement closely resembled that of the planktonic sample with PA, Lactobacillales, Bacilli and Proteobacteria present at a relative abundance of 9.91, 66.55, 23.41 and 0.07%, respectively.

The endpoint planktonic and biofilm samples cultured in ASM-Na₂H₂P₂O₇ were both dominated by Lactobacillales at a relative abundance of 59.48 and 94.55%, respectively. There was an ≈50% decrease and ≈15% increase, respectively, in the endpoint relative abundances of PA (15.98%) and Bacilli (24.36%) in the planktonic fraction, compared with the initial inoculum. Unlike the ASM-desferrioxamine endpoint samples, *Enterobacteriaceae*, Pseudomonadaceae, Proteobacteria and Bacillales (unassigned family) were present in the

ASM- $\text{Na}_2\text{H}_2\text{P}_2\text{O}_7$ endpoint planktonic fraction at a relative abundance of 0.09, 0.01, 0.04 and 0.04%, respectively. Alongside the Lactobacillales, the endpoint ASM- $\text{Na}_2\text{H}_2\text{P}_2\text{O}_7$ biofilm fraction contained PA at a relative abundance of just 1.09%, with *Enterobacteriaceae* (0.02%), Pseudomonadaceae (0.05%) and Bacillales (0.3%). Similarly, endpoint planktonic and biofilm samples cultured in ASM-Met/Cys contained Lactobacillales at a relative abundance of 94.99 and 96.41%, respectively. PA relative abundance decreased by 68.3% over the incubation period and this species comprised just 2.26% of the ASM-Met/Cys planktonic fraction at T = 120 hrs. Bacilli, Firmicutes (unassigned order), Bacillaceae and an OTU corresponding to an unclassified bacterium were present in the endpoint ASM-Met/Cys planktonic sample at a relative abundance of 0.15, 0.11, 0.27 and 0.23%, respectively. The endpoint biofilm sample for this supplement also contained PA, Bacilli and an unassigned bacterium at a relative abundance of 2.55, 0.8 and 0.05%, respectively.

A 55.14% decrease in the relative abundance of PA occurred over the course of incubation in ASM- KNO_3 . Unlike the other endpoint planktonic samples, Firmicutes (unassigned classification) comprised 73.94% of the ASM- KNO_3 planktonic OTUs, with PA, Lactobacillales, Bacilli, Clostridiales (unassigned family) and Veillonellaceae (unassigned family) present at a relative abundance of 0.3, 6.86, 16.13, 2.7 and 0.05%, respectively. Interestingly, the ASM- KNO_3 biofilm sample was dissimilar to the planktonic sample and comprised the following species abundances: PA (1.49%), Lactobacillales (94.09%), Bacilli (4.1%) *Enterobacteriaceae* (0.06%) and Gammaproteobacteria (0.003%). In endpoint planktonic and biofilm samples of ASM supplemented with NAM, PA was the dominant species, present at a respective relative abundance of 99.85 and 98.99%. Lactobacillales and *Enterobacteriaceae* comprised the remaining 0.09 and 0.02% of the planktonic sample and Lactobacillales, *Enterobacteriaceae*, Gammaproteobacteria and Pseudomonadaceae were present at 0.3, 0.27, 0.31 and 0.2% relative abundance in the biofilm sample, respectively.

Endpoint planktonic and biofilm samples of CF sputum cultured in ASM-FBS contained the most diverse bacterial populations. The ASM-FBS endpoint planktonic sample contained: PA (5.7%, 69.12% decrease in abundance), Lactobacillales (58.63%, 40.15% increase in abundance), Bacilli (26.18%, 20.08% increase in abundance), *Enterobacteriaceae* (5.5%), Bacillaceae (unassigned genus, 2.46%), Gammaproteobacteria (0.24%), Pseudomonadaceae (0.45%), Bacillales (0.12%), *Listeria weihenstephanensis* (0.17%), *Macrococcus brunensis* (0.12%), Pseudomonadales (0.04%), Firmicutes (0.03%) and an unassigned OTU (0.29%). The endpoint ASM-FBS biofilm sample resembled the planktonic community and consisted of: PA (6.88%), Lactobacillales (78.48%), Bacilli (9.3%), *Enterobacteriaceae* (1.47%), Bacillaceae (2.61%), Gammaproteobacteria (0.08%),

Pseudomonadaceae (0.31%), Bacillales (0.24%), *L. weihenstephanensis* (0.23%), *M. brunensis* (0.1%), Firmicutes (0.11%) and an unassigned OTU (0.18%).

7.4.3.2 Faith's Phylogenetic Diversity

Box plots representing Faith's phylogenetic diversity of bacterial communities present in the combined initial inoculum samples and in the combined endpoint planktonic and biofilm samples cultured in different ASM compositions are shown in *Figure 7.10*. The phylogenetic biodiversity of the inoculum samples was significantly higher ($P < 0.05$) than all endpoint samples, demonstrating a loss of species diversity in the different ASM compositions over the incubation period. The phylogenetic diversity of the combined endpoint ASM-FBS sample was significantly higher ($P < 0.05$) than that of all other endpoint samples cultured using different ASM compositions. There was no statistically significant difference ($P > 0.1$) in the overall species diversity of the other endpoint bacterial populations using Faith's measure of biodiversity.

7.4.3.3 Bray-Curtis Dissimilarity Test

Principal coordinate analysis (PCoA) plots based upon Bray-Curtis dissimilarity test of bacterial communities present in the initial inoculum, endpoint planktonic fraction and endpoint point biofilm samples cultured in different ASM compositions are shown in *Figure 7.11*. The PCoA plot resulted in a 3-dimensional solution in which PC1 accounted for 68.7% of the variation and PC2 and PC3 accounted for 12.17% and 7.82%, respectively. All samples, except for the ASM-KNO₃ planktonic sample, clustered into three distinct groups. Firstly, the initial inoculum clustered in one region with little variance along any axis. Secondly, endpoint planktonic and biofilm samples cultured in ASM-only or ASM supplemented with micronutrients, vitamins or 40 µM FeSO₄ clustered with little variance along PC1 and PC3. This cluster was the most similar to the cluster of initial inoculum samples with respect to all axis. The third cluster consisted of the endpoint planktonic and biofilm samples cultured in ASM supplemented with desferrioxamine, FBS, NAM, 5 mM Met/Cys, sodium pyrophosphate and the ASM-KNO₃ biofilm sample. The third cluster differed significantly from the initial inoculum along PC1 but showed comparatively little variance to this cluster with respect to PC2 and PC3.

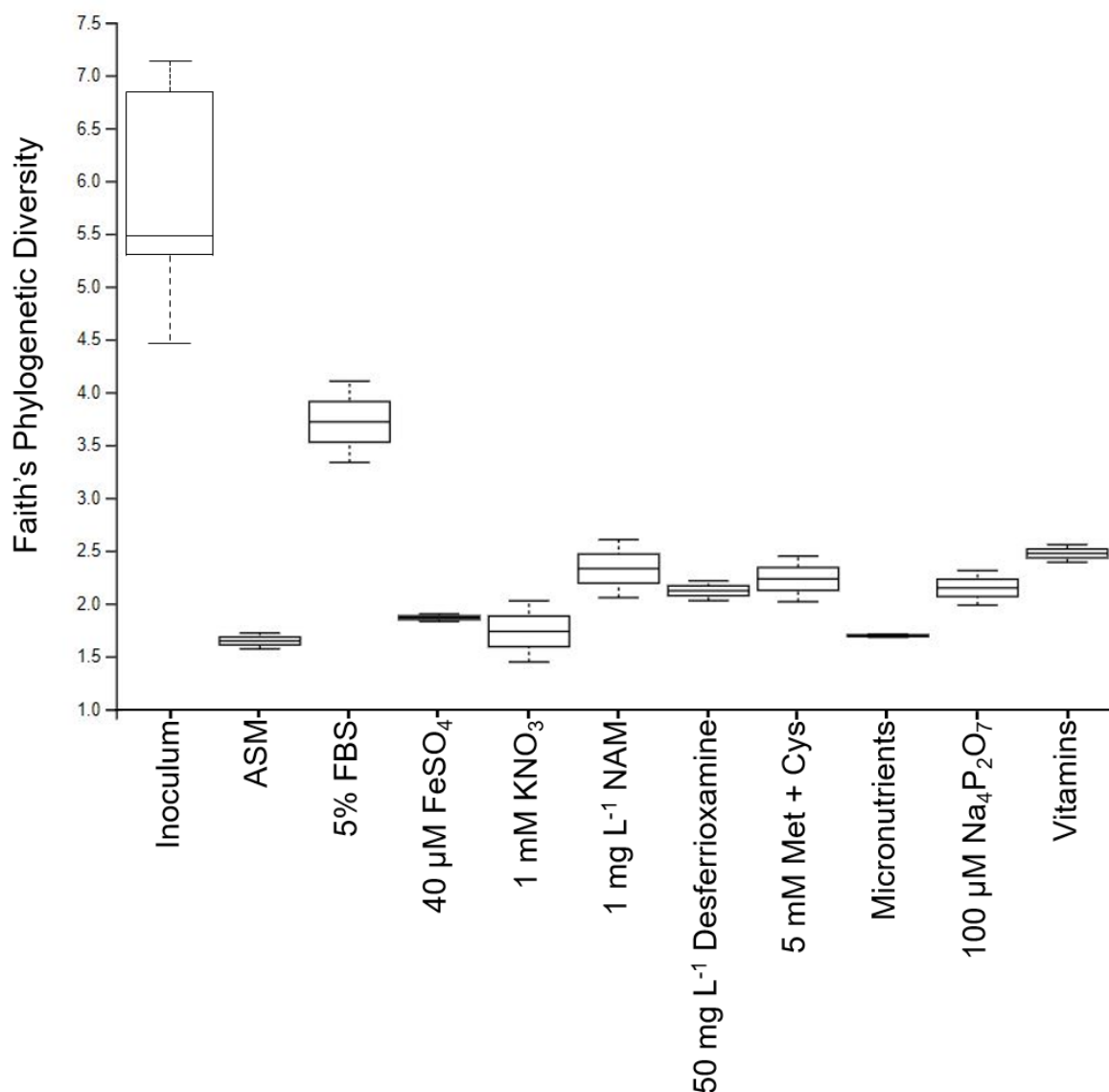
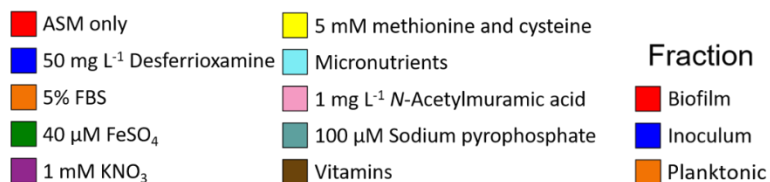


Figure 7.10 Faith's phylogenetic diversity of supplemented ASM samples.

Boxplots representing Faith's phylogenetic diversity of bacterial communities in the initial CF sputum inoculum and combined endpoint planktonic and biofilm samples. Endpoint samples were incubated in different compositions of ASM under continuous-flow conditions for 120 hrs. $Q = 55 \mu\text{L min}^{-1}$. Sample labels denote the ASM supplement. $n = 10$ for inoculum and $n = 2$ for endpoint samples.

Supplement



Fraction

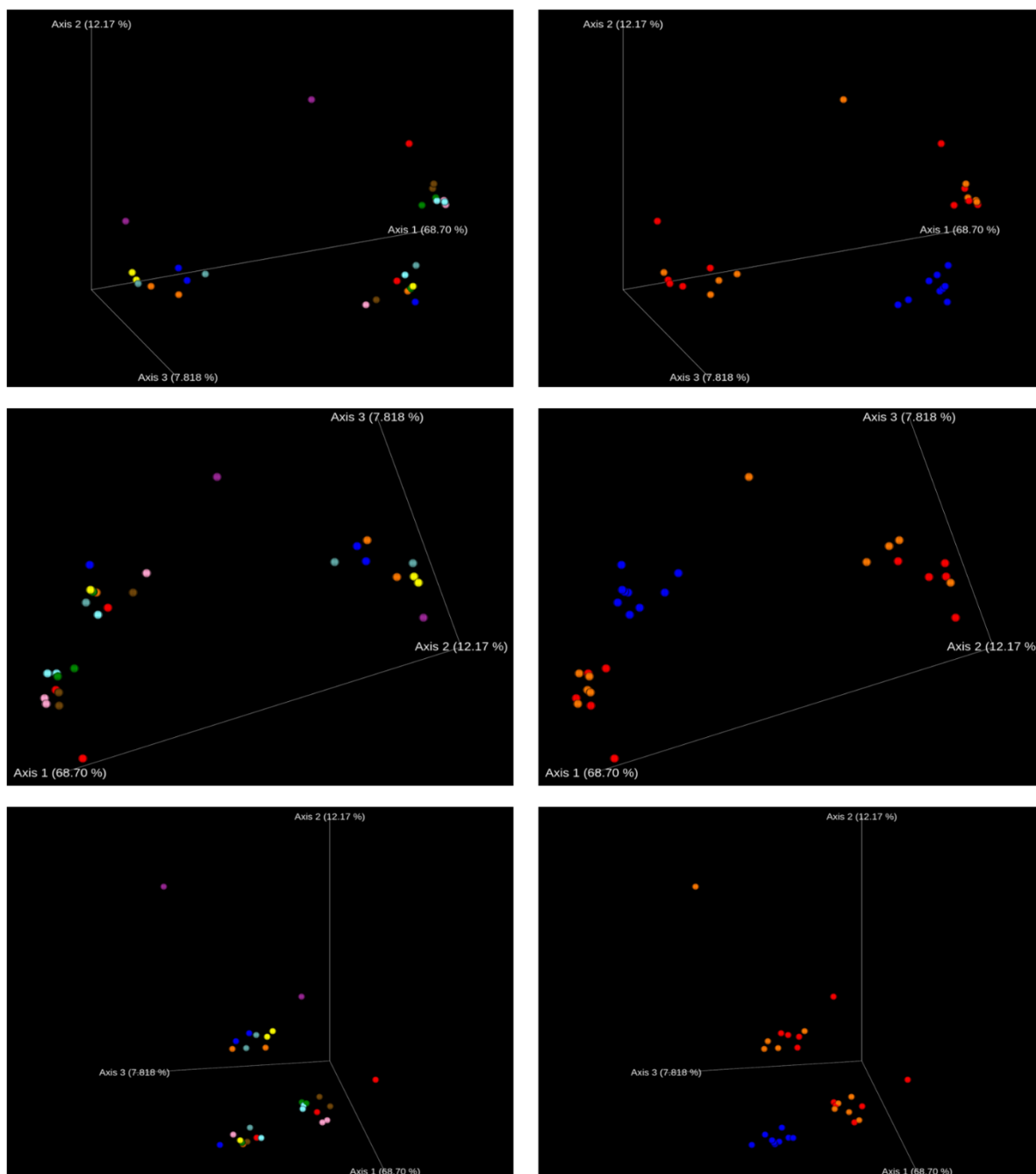


Figure 7.11 Bray-Curtis dissimilarity test of supplemented ASM samples.

Principal coordinate analysis (PCoA) based on Bray-Curtis dissimilarity test of initial inoculum, endpoint planktonic and endpoint biofilm samples. Endpoint samples were incubated in different ASM compositions under continuous flow conditions for 120 hrs. $Q = 55 \mu\text{L min}^{-1}$. Left panels denote the different supplements: + no supplement (red); + 40 μM FeSO₄ (green); + 5% FBS (orange); + micronutrients (cyan); + vitamins (brown); + 5mM methionine and cysteine (yellow); + 100 μM sodium pyrophosphate (grey); + 1 mM KNO₃ (purple); + 50 mg L⁻¹ desferrioxamine (purple); + 1 mg L⁻¹ *N*-acetylmuramic acid (pink). Right panels denote the different sample types (fraction): initial inoculum (blue); endpoint planktonic (orange) and endpoint biofilm (blue).

7.4.3.4 UniFrac Analysis

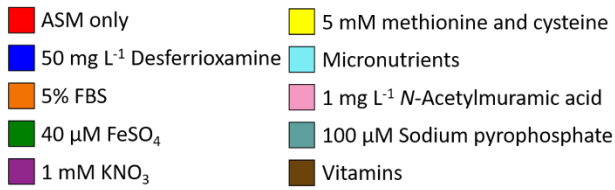
PCoA analysis plots based upon unweighted and weighted variants of UniFrac distance for the bacterial communities present in the initial inoculum, endpoint planktonic fraction and endpoint biofilm samples cultured in different ASM compositions are shown in *Figure 7.12* and *Figure 7.13*, respectively. The unweighted PCoA plot resulted in a 3-dimensional solution in which PC1 accounted for 46.59 % of the variation and PC2 and PC3 accounted for 11.72% and 9.05%, respectively. Samples corresponding to the initial inoculum clustered into two separate regions, dissimilar only with respect to PC3. The endpoint samples formed a loose cluster distributed across PC2. The ASM-FBS biofilm sample was the most dissimilar to the other endpoint samples and was closest to the inoculum samples with respect to PC1. Interestingly, the ASM-FBS planktonic sample was the highest endpoint sample with respect to PC2 and the second closest to the inoculum samples along PC1. The endpoint planktonic and biofilm samples for ASM-only, ASM-micronutrients and ASM-FeSO₄ clustered tightly at the polar end of axis 2 in comparison to the ASM-FBS samples.

The weighted PCoA plot resulted in a 3-dimensional solution in which PC1 accounted for 94.96% of the variance and PC2 and PC3 accounted for 2.81% and 1.6%, respectively. The endpoint ASM-KNO₃ planktonic sample did not cluster with any other sample and the remaining samples clustered into four regions. Cluster 1 comprised of a cluster of all initial inoculum samples. The ASM-vitamins and ASM-NAM inoculum samples displayed some variance within cluster 1 with respect to PC1 and PC2. Importantly, the endpoint ASM-only planktonic and ASM-micronutrients biofilm samples clustered in group 1 and were highly similar to the ASM-vitamins inoculum sample. Secondly, cluster 2 contained the endpoint ASM-only biofilm, ASM-micronutrients planktonic and the ASM-vitamins, ASM-NAM, ASM-FeSO₄ planktonic and biofilm samples. Cluster 2 was distributed along PC1 and showed some variance to cluster 1 with respect to PC2. The remaining samples were dissimilar from clusters 1 and 2 with respect to PC1 and could be divided into two clusters. Cluster 3 contained the endpoint ASM-sodium pyrophosphate planktonic and ASM-FBS/ASM-desferrioxamine planktonic and biofilm samples. Cluster 3 was similar to cluster 1 with respect to both PC2 and PC3. The remaining samples formed a tight cluster that showed little variance to cluster 2 with respect to PC2 and PC3.

7.4.4 Conclusions

Several conclusions can be drawn from the data presented in this sub-section. Firstly, increased iron bioavailability, *via* supplementing ASM with excess FeSO₄ or with an exogenous siderophore, significantly increased the total microbial carrying capacity in the

Supplement



Fraction

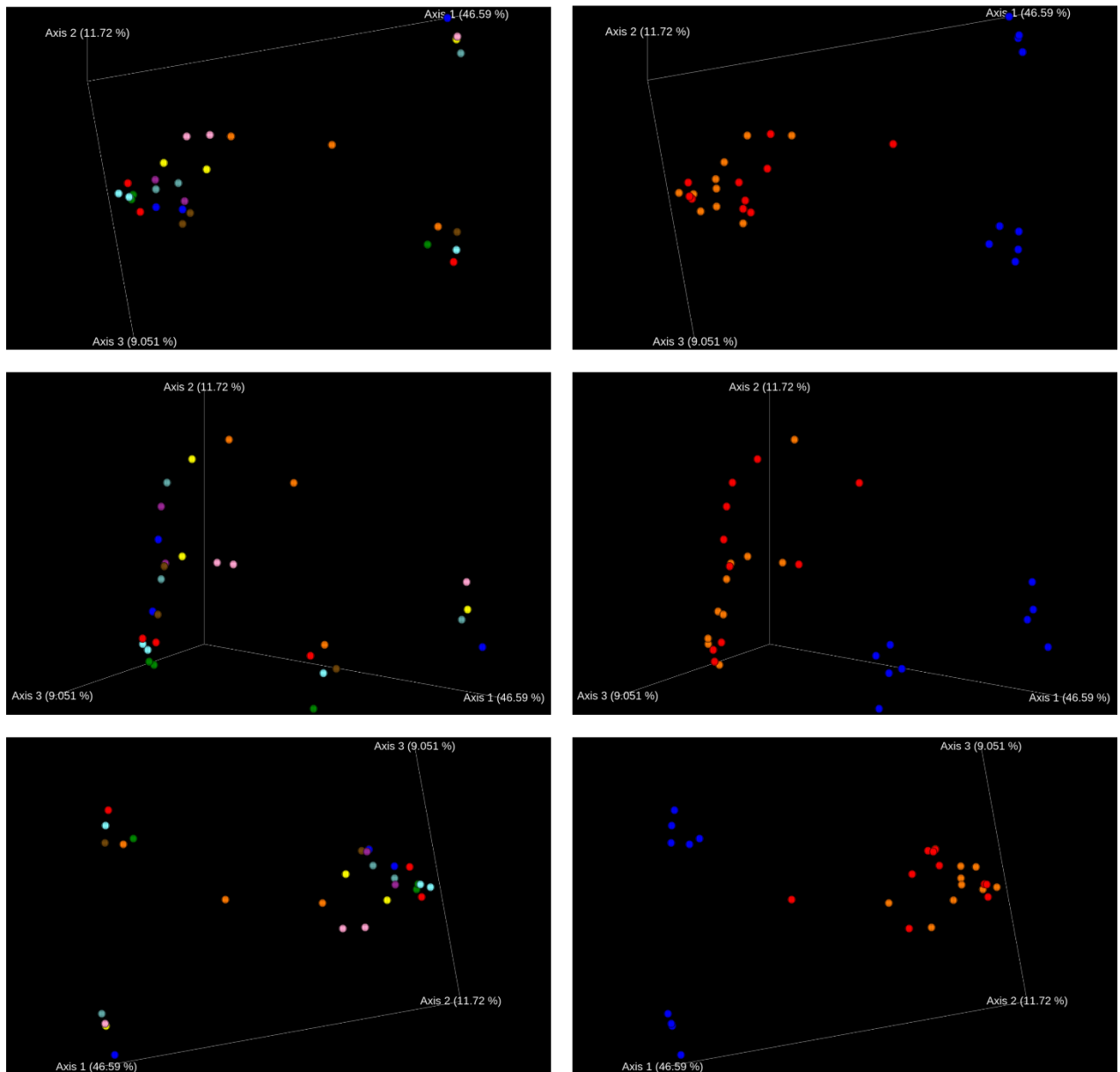


Figure 7.12 Unweighted UniFrac of supplemented ASM samples.

Principal coordinate analysis (PCoA) based on unweighted variants of UniFrac of initial inoculum, endpoint planktonic and endpoint biofilm samples. Endpoint samples were incubated in different ASM compositions under continuous flow conditions for 120 hrs. $Q = 55 \mu\text{L min}^{-1}$. Left panels denote the different supplements: + no supplement (red); + 40 μM FeSO₄ (green); + 5% FBS (orange); + micronutrients (cyan); + vitamins (brown); + 5mM methionine and cysteine (yellow); + 100 μM sodium pyrophosphate (grey); + 1 mM KNO₃ (purple); + 50 mg L⁻¹ desferrioxamine (purple); + 1 mg L⁻¹ *N*-acetylmuramic acid (pink). Right panels denote the different sample types (fraction): initial inoculum (blue); endpoint planktonic (orange) and endpoint biofilm (blue).

Supplement

- ASM only
- 50 mg L⁻¹ Desferrioxamine
- 5% FBS
- 40 μM FeSO₄
- 1 mM KNO₃
- 5 mM methionine and cysteine
- Micronutrients
- 1 mg L⁻¹ N-Acetylmuramic acid
- 100 μM Sodium pyrophosphate
- Vitamins

Fraction

- Biofilm
- Inoculum
- Planktonic

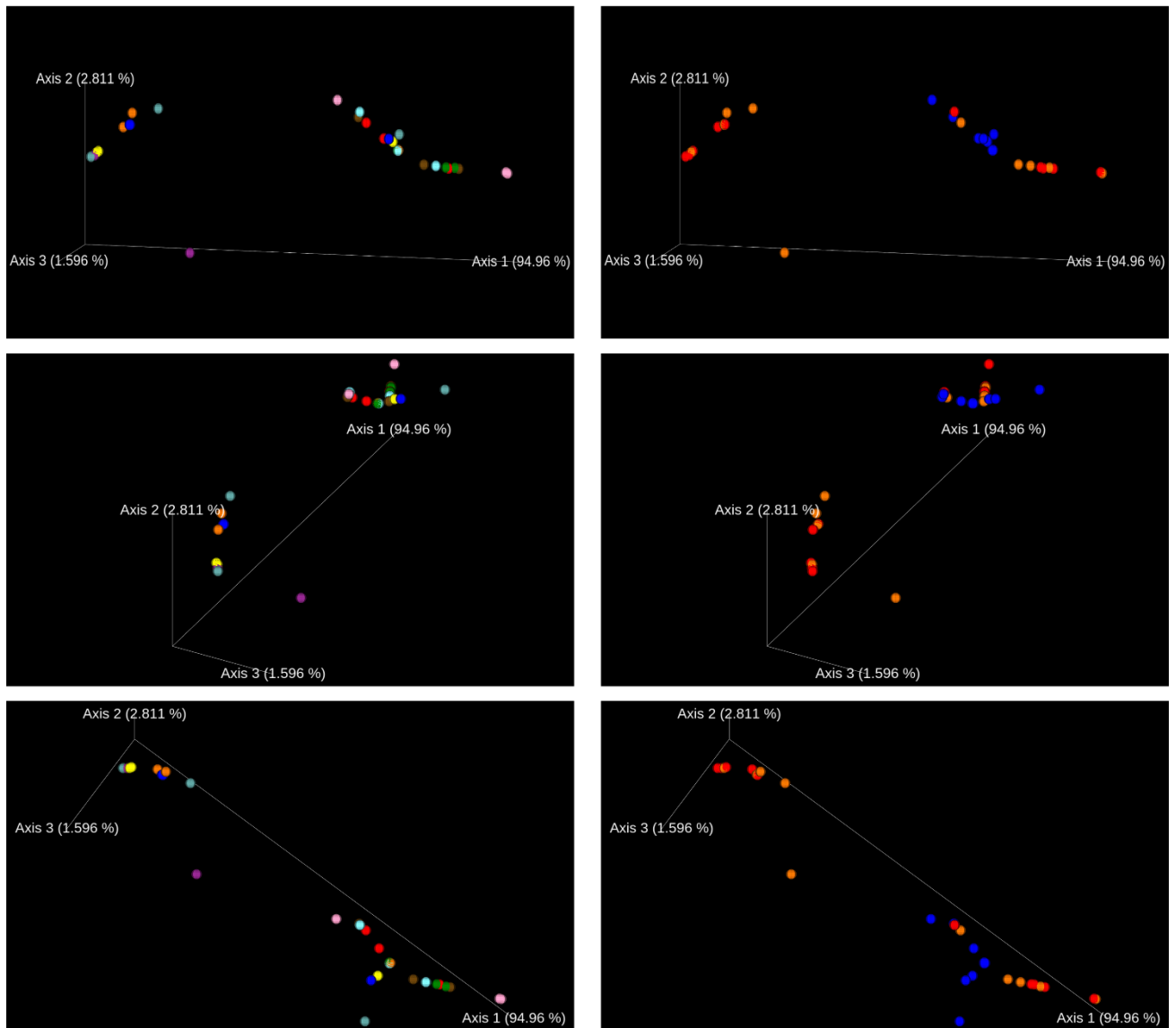


Figure 7.13 Weighted UniFrac of supplemented ASM samples.

Principal coordinate analysis (PCoA) based on weighted variants of UniFrac of initial inoculum, endpoint planktonic and endpoint biofilm samples. Endpoint samples were incubated in ASM supplemented with different ASM compositions under continuous-flow conditions for 120 hrs. $Q = 55 \mu\text{L min}^{-1}$. Left panels denote the different supplements: + no supplement (red); + 40 μM FeSO₄ (green); + 5% FBS (orange); + micronutrients (cyan); + vitamins (brown); + 5mM methionine and cysteine (yellow); + 100 μM sodium pyrophosphate (grey); + 1 mM KNO₃ (purple); + 50 mg L⁻¹ desferrioxamine (purple); + 1 mg L⁻¹ N-acetylmuramic acid (pink). Right panels denote the different sample types (fraction): initial inoculum (blue); endpoint planktonic (orange) and endpoint biofilm (blue)

culture vessel (*Figure 7.8*). Simply increasing the concentration of free iron did not improve the growth of less abundant species present in the inoculum but permitted PA to grow to a higher endpoint titre. This finding may be unsurprising given that PA can produce two siderophores with the ability to sequester iron from other species in the culture (*Section 4.5*). Addition of desferrioxamine to ASM enabled Lactobacillales to grow to a higher endpoint titre and outcompete PA in the culture vessel, suggesting Lactobacillales, but no other species, can recognise and take up this siderophore, perhaps also making it less available to the other species present.

As evidenced by Faith's measure of phylogenetic diversity, there was an overall decrease in bacterial biodiversity over time (*Figure 7.10*). In general, anaerobic species were lost from most ASM compositions. However, supplementing the media with 1 mM KNO₃ permitted the long-term maintenance of Firmicutes, Veillonellaceae and Clostridiales. Although anaerobes dominated the ASM-KNO₃ culture, aerobes were also present at low relative abundance in the community at the endpoint of sampling. This finding suggests that, with further optimisation, it should be possible to maintain an entire polymicrobial community of aerobic and anaerobic species for extended periods of time in the continuous-flow model.

It is interesting to note that an increase in species diversity is observed across samples in which PA is not the dominant bacterium. This supports previous findings that PA encodes for an arsenal of extracellular virulence factors able to outcompete other species during co-culture (*Section 1.4.4*) and highlights a link between the presence of PA and a decline in diversity amongst the airway-associated microbiota. Furthermore, some evidence suggests that a decrease in diversity among the CF-airway associated polymicrobial community is linked with a decline in pulmonary function (Zhao et al., 2012, Paganin et al., 2015). This indicates that there may be some therapeutic potential in promoting the growth of less abundant species in the CF microenvironment.

Supplementing ASM with FBS maintained the most diverse microbial community and caused a significant increase in the relative abundance of species comprising <0.2% of the initial inoculum. FBS is an undefined culture supplement, hence the exact factor responsible for the increased diversity of these endpoint samples cannot be discerned. Firstly, the cocktail of different chemicals in FBS may prove to include essential growth factors for some fastidious microbial species. Secondly, albumin (comprising ≈50% of the FBS protein content (Issaq et al., 2007)) has recently been found to inhibit QS networks in PA and modulate interspecies interactions among polymicrobial communities (Smith et al., 2017).

A further screen of the following ASM compositions was performed to: (i) discern which component of FBS was responsible for enhancing the biodiversity of polymicrobial populations

cultured *in vitro*, and (ii) to screen refined ASM compositions to find a culture medium suitable for the steady-state maintenance of sputum-derived polymicrobial communities at a similar relative abundancies to inoculum communities.

(1 – 3) 1%, 5% and 10% FBS, respectively (ASM-1%FBS, ASM-5%FBS, ASM-10%FBS). To explore the effects of different FBS concentrations on polymicrobial community growth.

(4) 2.5% bovine serum albumin (ASM-BSA). Albumin comprises ≈50% of the proteins in FBS, hence this concentration is comparable to that present when adding 5% FBS. This supplement was used to discern if QS inhibition alone was responsible for promoting the growth of diverse sputum-derived polymicrobial communities *in vitro*.

(5) 5% charcoal-stripped FBS (ASM-charcoal-FBS). Dextran treated charcoal selectively removes hormones and lipids from FBS. This supplement was used to determine if these molecules contributed towards increased the increased biodiversity of communities during *in vitro* cultivation.

(6 – 8) <5, 5-30 and >30 kDa fractions of 5% FBS, respectively (ASM-<5kDa-FBS, ASM-5-30kDa-FBS and ASM->30kDa-FBS). FBS (5%) was fractionated by passing the supplement through 5 and 30 kDa “molecular weight cut-off” membranes to determine which portion of FBS contributed towards increasing overall species diversity in the model.

(9) 0.1 g L⁻¹ hemin (ASM-hemin). Hemin is required some anaerobic species for the reduction of nitrate during fermentation (Jacobs et al., 1964), therefore exogenous supplementation of this cofactor may promote the growth of such anaerobic fermenters in ASM. Hemin may also provide an additional source of iron to promote microbial growth.

(10) 0.1 g L⁻¹ hemoglobin (ASM-hemoglobin). As above (9), ASM was supplemented with hemoglobin to examine how the presence of this heme-group containing protein altered the growth and ecology of *in vitro* polymicrobial populations.

(11) Micronutrients + vitamins + 40 μM FeSO₄ (ASM-micronutrients-vitamins-FeSO₄). Combination of the three supplements that yielded the least dissimilar endpoint planktonic or biofilm sample compositions compared to the initial inoculum samples according to weighted UniFrac analysis of variance (*Figure 7.13*).

(12) Micronutrients + vitamins + 40 μM FeSO₄ + 5% FBS (ASM-micronutrients-vitamins-FeSO₄-FBS). Combination of the above (11) supplements and the supplement yielding the most diverse endpoint microbiota.

7.5 Further ASM Supplementation

7.5.1 OD_{600 nm}

Average OD_{600 nm} values of sputum-associated microbial populations grown under continuous-flow conditions are shown in *Figure 7.14*. All sputum-derived microbial populations reached a steady-state carrying capacity, with respect to culture density, by T = 48 hrs. Cultures grown in ASM supplemented with micronutrients-vitamins-FeSO₄ (40 µM), hemoglobin or micronutrients-vitamins-FeSO₄ (40 µM)-FBS reached significantly higher ($P < 0.05$) steady state carrying capacities (OD_{600 nm} ≈ 2.0, 1.88 and 1.82, respectively) than other ASM compositions (OD_{600 nm} ≈ 1.6), except ASM supplemented with hemin. Differences in the average steady-state culture density of ASM-hemin (OD_{600 nm} ≈ 1.7) were not statistically significant compared with other ASM compositions.

7.5.2 Bacterial Ecology

7.5.2.1 Taxa plots

Relative abundance taxa bar plots of initial inoculum and planktonic/biofilm samples after 120 hrs incubation in additional ASM compositions are shown in *Figure 7.15*. Inoculum samples contained distinct key OTUs at the following average relative abundancies: *P. aeruginosa* 45.91 ± 21.97%, Lactobacillales (unassigned family) 25.14 ± 14.89%, Bacilli (unassigned order) 12.45 ± 5.67%, Bacteroidetes (unassigned classification) 10.91 ± 11.62%, Micrococcaceae (unassigned genus) 1.25 ± 2.66%, Firmicutes (unassigned classification) 0.8 ± 0.9%, Enterobacteriaceae (unassigned genus) 0.83 ± 1.29%, *Rothia* (unassigned species) 0.62 ± 2.65% and Gammaproteobacteria (unassigned order) 0.37 ± 0.91%. Across all samples, the remaining inoculum comprised of the other bacteria listed in *Legend 7.3* in varied proportions at <0.1% relative abundance.

Samples cultured in standard ASM contained bacterial OTUs in the endpoint planktonic/biofilm fractions, respectively, at the following relative abundancies: Lactobacillales 23.51/74.96%, Bacilli 63.92/21.09%, Bacillaceae (unassigned genus) 11.93/1.38%, Firmicutes 0.1/0.04% and Lactobacillaceae (unassigned genus) 0.09/0.39%. Unlike *Section 7.3.3* and *7.4.3*, PA was lost from the endpoint of all culture samples except ASM-micronutrients-vitamins-FeSO₄, where this species comprised just 0.88% relative abundance of the planktonic sample. This finding was unexpected and is discussed further in *Section 7.5.3*. Despite the loss of detectable PA from all culture vessels, some interesting trends can still be inferred from the bacterial ecology of the endpoint samples supplemented with different compounds.

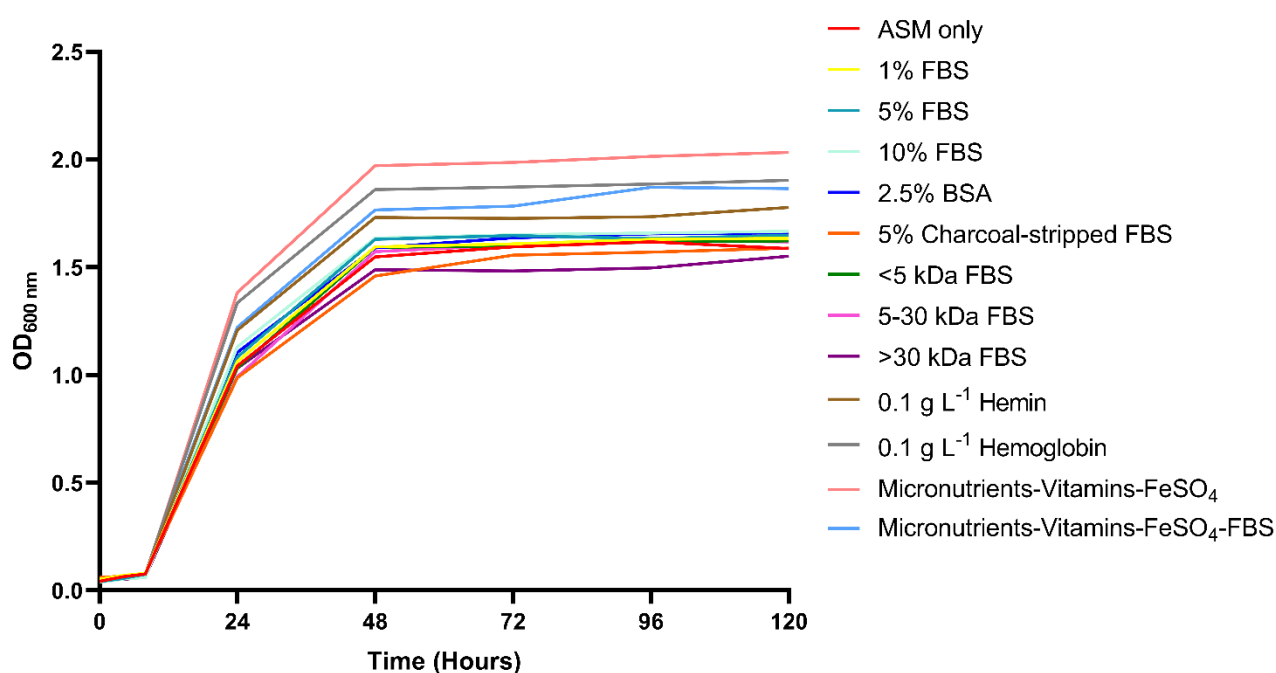


Figure 7.14 Growth of CF sputum-derived microbial populations in further supplemented ASM.

Optical density ($OD_{600\text{ nm}}$) measurements following total density of microbial populations derived from homogenised expectorated sputum samples collected from the same person with CF under continuous-flow conditions. $Q = 55\text{ }\mu\text{L min}^{-1}$. Culture medium was ASM supplemented with the following: no supplement (red); + 1% FBS (yellow); + 5% FBS (teal); 10% FBS (cyan); + 2.5% BSA (blue); + 5% charcoal-stripped FBS (orange); + <5 kDa FBS fraction (green); + 5-30 kDa FBS fraction (pink); + >30 kDa FBS fraction (purple); 0.1 g L^{-1} hemin (brown); + 0.1 g L^{-1} hemoglobin (grey); + micronutrients, vitamins, $40\text{ }\mu\text{M FeSO}_4$, 5% FBS (light blue) +; + micronutrients, vitamins, $40\text{ }\mu\text{M FeSO}_4$ (salmon pink). Data represented as the mean from two independent experiments.

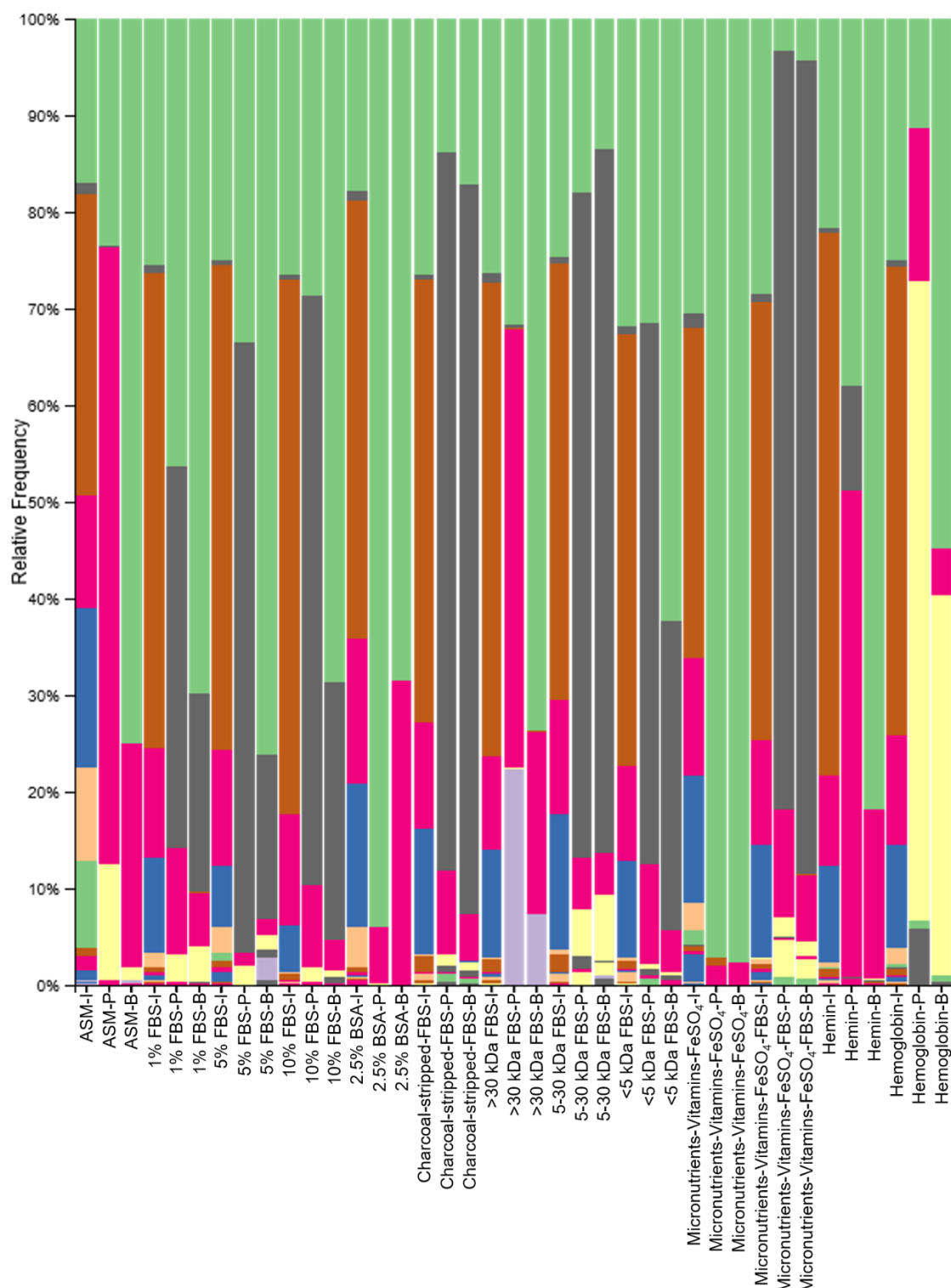



























Figure 7.15 Relative bacterial species abundance in further ASM supplemented sequencing libraries.

Relative abundance of bacterial species in the initial CF sputum inoculum and in the corresponding endpoint planktonic or biofilm samples following 120 hrs incubation under continuous-flow conditions in different compositions of ASM. $Q = 55 \mu\text{L min}^{-1}$. Each bar represents a different sample. Labels below samples denote the ASM supplement: -inoculum (I); -planktonic (P) or -biofilm (B). For example, 2.5%BSA-P \equiv ASM+ 2.5% bovine serum albumin-planktonic. *Legend 7.3* is the corresponding legend for this taxa plot.

 (P): Firmicutes, (C): Bacilli, (O): Lactobacillales
 (P): Firmicutes
 (P): Proteobacteria, (C): Gammaproteobacteria, (O): Pseudomonadales, (F): Pseudomonadaceae, (G): Pseudomonas, (S): aeruginosa
 (P): Firmicutes, (C): Bacilli
 (P): Bacteroidetes
 (P): Firmicutes, (C): Bacilli, (O): Bacillales, (F): Bacillaceae
 (P): Actinobacteria, (C): Actinobacteria, (O): Actinomycetales, (F): Micrococcaceae
 (P): Firmicutes, (C): Bacilli, (O): Lactobacillales, (F): Lactobacillaceae
 (P): Actinobacteria, (C): Actinobacteria, (O): Actinomycetales
 (P): Firmicutes, (C): Bacilli, (O): Bacillales
 (P): Proteobacteria, (C): Gammaproteobacteria, (O): Enterobacteriales, (F): Enterobacteriaceae
 (P): Unassigned
 (P): Actinobacteria, (C): Actinobacteria, (O): Actinomycetales, (F): Micrococcaceae, (G): Rothia
 (P): Firmicutes, (C): Clostridia, (O): Clostridiales
 (P): Proteobacteria, (C): Gammaproteobacteria
 (P): Firmicutes, (C): Clostridia, (O): Clostridiales, (F): Lachnospiraceae, (G): Lachnoanaerobaculum, (S): orale
 (P): Firmicutes, (C): Clostridia, (O): Clostridiales, (F): Veillonellaceae
 (P): Firmicutes, (C): Clostridia, (O): Clostridiales, (F): Veillonellaceae, (G): Anaerostipes, (S): glycerini
 (P): Firmicutes, (C): Bacilli, (O): Lactobacillales, (F): Streptococcaceae, (G): Streptococcus, (S): agalactiae
 (P): Proteobacteria, (C): Gammaproteobacteria, (O): Pseudomonadales, (F): Pseudomonadaceae
 (P): Bacteroidetes, (C): Flavobacteriia, (O): Flavobacteriales, (F): Flavobacteriaceae
 (P): Proteobacteria
 (P): Actinobacteria, (C): Actinobacteria, (O): Bifidobacteriales, (F): Bifidobacteriaceae, (G): Alloscardovia
 (P): Actinobacteria, (C): Actinobacteria
 (P): Fusobacteria, (C): Fusobacteriia, (O): Fusobacteriales, (F): Leptotrichiaceae

Legend 7.3 Relative bacterial species abundance in further ASM supplemented sequencing libraries

Legend corresponding to *Figure 7.15*. Denoting: phylum (P); classification (C); order (O); family (F); genus (G) and species (S) at the highest level which could be unambiguously assigned to aligned quality filtered sequence reads.

Alongside PA, endpoint planktonic/biofilm samples cultured in ASM-micronutrients-vitamins-FeSO₄ also contained Lactobacillales and Bacilli at a relative abundance of 97.19/97.68% and 1.96/2.25%, respectively. Similarly, endpoint ASM-BSA samples only contained Lactobacillales and Bacilli in the planktonic/biofilm fractions at a relative abundance of 93.96/68.4% and 5.9/31.54%, respectively. Whereas endpoint planktonic/biofilm samples of ASM-micronutrients-vitamins-FeSO₄-FBS contained OTUs at the following relative abundancies, respectively: Firmicutes (78.35/84.25%), Lactobacillales (3.41/5.33%), Bacilli (11.18/6.86%), Bacillaceae (2.07/1.52%), Veillonellaceae (0.8/0.64%) and Clostridiales (3.82/2.05%). Endpoint samples cultured in ASM supplemented with 1% or 10% FBS shared very similar bacterial ecology. In the ASM-1%FBS samples, Lactobacillales, Firmicutes, Bacilli, Bacillaceae and Bacillales comprised: 46.4/69.88%; 39.46/20.54%; 10.89/5.57%; 2.82/3.73% and 0/0.082% of the planktonic/biofilm samples, respectively. Importantly, Veillonellaceae (unassigned genus) was present at a relative abundance of 0.08% in the ASM-10%FBS planktonic sample. The relative abundance of other OTUs present in planktonic/biofilm samples of ASM-10%FBS were as follows: Lactobacillales (28.73/68.65%), Firmicutes (60.98/26.76%), Bacilli (8.43/3.03%), Bacillaceae (1.47/0.1%) and Bacillales (0.1/0.66%).

As in Section 7.4, supplementing ASM with 5% FBS resulted in a more diverse endpoint microbiota. Firmicutes was the dominant OTU in the endpoint planktonic sample (63.07% relative abundance) alongside Lactobacillales (33.57%), Bacilli (1.42%), Bacillaceae (1.58%), Clostridiales (0.22%), Veillonellaceae (0.2%) and Lactobacillaceae (0.01%). For the ASM-5%FBS biofilm sample Lactobacillales was present at a relative abundance of 76.09%, followed by Firmicutes (17.07%), *Lachnoanaerobaculum orale* (2.33%), Bacilli (1.73%), Bacillaceae (1.49%), Bacillales (0.74%) and *Anaerosinus glycerini* (0.49%). Supplementing ASM with 5% charcoal-stripped FBS or the 5-30 kDa fraction of 5% FBS resulted in similar endpoint bacterial compositions to ASM-5%FBS. Endpoint planktonic/biofilm samples of ASM-charcoal-FBS contained OTUs at the following relative abundancies, respectively: Firmicutes (74.31/75.59%), Lactobacillales (13.89/17.11%), Bacilli (8.71/4.88%), Bacillaceae (1.08/0.99%), Veillonellaceae (0.77/0.48%), Bacillales (0.62/0.64%) and *Anaerosinus glycerini* (0.2/0.4%). Endpoint planktonic/biofilm samples of ASM-5-30kDa-FBS contained OTUs at the following relative abundancies, respectively: Firmicutes (68.91/72.88%), Lactobacillales (17.93/13.43%), Bacilli (5.23/4.32%), Bacillaceae (4.87/6.83%), Bacillales (1.32/0.15%), Clostridiales (1.19/1.31%), *Lachnoanaerobaculum orale* (0.02/0.36%) and *Anaerosinus glycerini* (0/0.65%).

Supplementing ASM with the >30 kDa or <5kDa fractions of 5% FBS resulted in similar bacterial ecologies after 120 hrs incubation. Bacilli and Lactobacillales were the most

abundant OTUs in the planktonic and biofilm ASM->30kDa-FBS samples, respectively, and the most abundant OTU in the ASM-<5kDa-FBS sample corresponded to Firmicutes of an unassigned order. OTUs were present in the ASM->30kDa-FBS planktonic/biofilm endpoint samples at the following relative abundancies: Lactobacillales (31.7/73.7%), Bacilli (45.48/18.9%), Lactobacillaceae (22.35/7.24%), Firmicutes (0.35/0.04%), Bacteroidetes (0/0.01%) and Gammaproteobacteria (0/0.04%). Endpoint ASM-<5kDa-FBS planktonic/biofilm samples were comprised of OTUs at the following relative abundancies: Lactobacillales (31.55/62.31%), Firmicutes (56/32%), Bacilli (10.24/4.36%), Bacillaceae (0.44/0.25%), Bacillales (0.75/0.61%) and Veillonellaceae (0.59/0%).

Endpoint samples cultured in ASM supplemented with hemin or hemoglobin shared bacterial ecologies closely resembling those of the >30 kDa or <5 kDa FBS supplement samples. ASM-hemin endpoint planktonic/biofilm samples contained OTUs at the following, respective, relative abundancies: Lactobacillales (38.07/81.79%), Bacilli (50.26/17.43%), Firmicutes (10.8/0.07%), Bacillaceae (0.06/0.14%), Bacillales (0/0.26%) and Enterobacteriaceae (0/0.15%). Endpoint ASM-hemoglobin planktonic/biofilm samples comprised of: Lactobacillales (11.37/54.78%), Bacilli (15.71/7.8%), Firmicutes (0/0.11%), Bacillaceae (66.2/39.34%), Bacillales (5.83/0.19%) and Actinomycetales (0.86/0.7%).

7.5.2.2 Faith's Phylogenetic Diversity

Box plots representing Faith's phylogenetic diversity of bacterial communities present in combined initial inoculum and in combined endpoint planktonic and biofilm samples cultured in additional ASM compositions are shown in *Figure 7.16*. The phylogenetic biodiversity of the combined inoculum samples was significantly higher ($P < 0.05$) than all endpoint samples, again demonstrating a loss in species diversity over time during *in vitro* cultivation. Compared with the ASM-only endpoint samples, supplementing the growth medium with FBS (any type, fraction or concentration), hemin or hemoglobin caused a slight increase in the phylogenetic biodiversity of endpoint samples, but this trend is not statistically significant ($P > 0.8$). Conversely, supplementing ASM with BSA (2.5%) caused a noticeable reduction in endpoint sample phylogenetic biodiversity, but again this change is not statistically significant ($P > 0.2$).

7.5.2.3 Principal Coordinate Analysis

Principal coordinate analysis (PCoA) plots based upon Bray-Curtis dissimilarity test or unweighted and weighted variants of UniFrac distance for bacterial communities present in the initial inoculum, endpoint planktonic fraction and endpoint biofilm samples cultured in additional ASM compositions are shown in *Figure 7.17*, *Figure 7.18* and *Figure 7.19*,

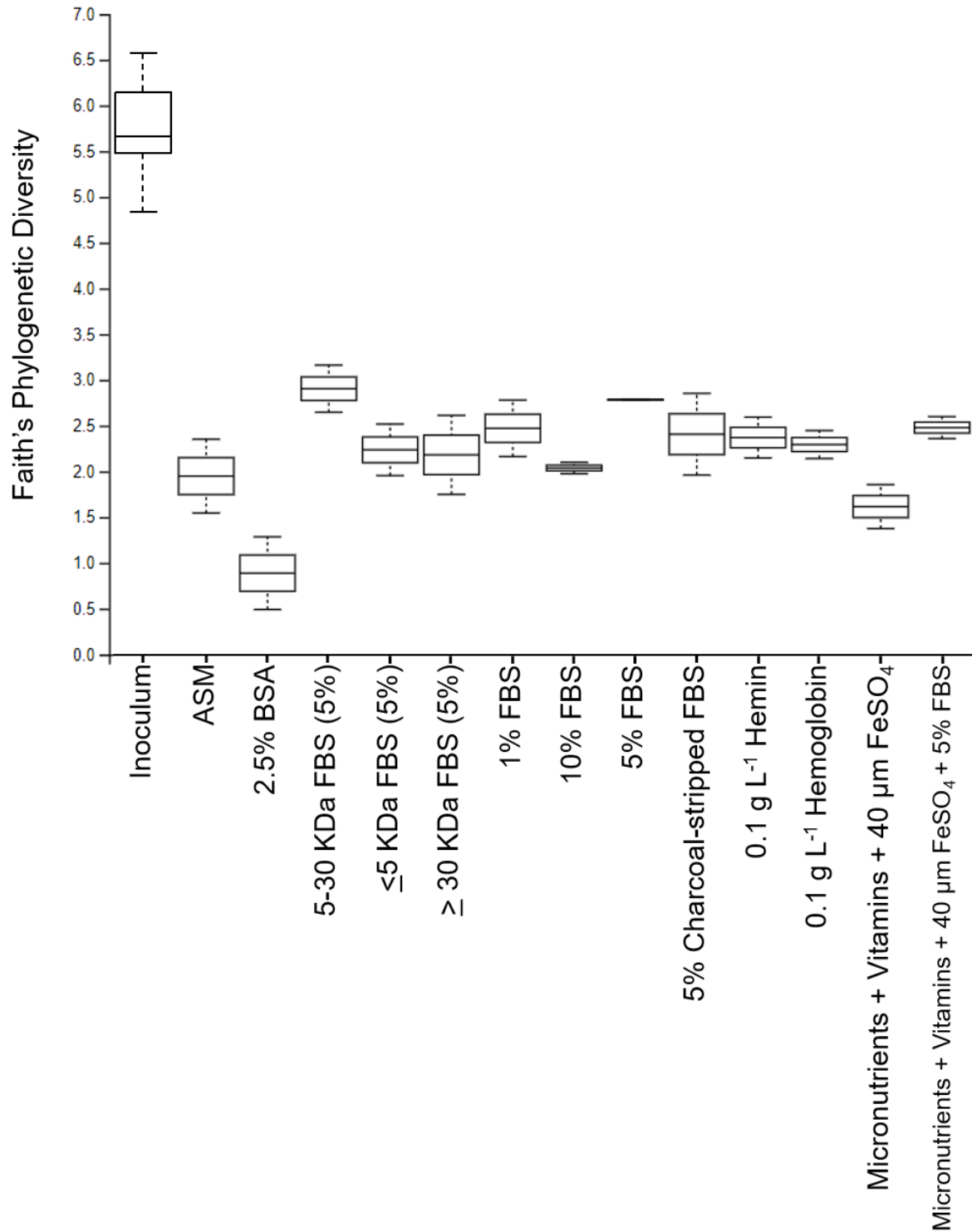


Figure 7.16 Faith's phylogenetic diversity of further supplemented ASM samples

Boxplots representing Faith's phylogenetic diversity of bacterial communities in the initial CF sputum inoculum and combined endpoint planktonic and biofilm samples. Endpoint samples were incubated in different compositions of ASM under continuous-flow conditions for 120 h. $Q = 55 \mu\text{L min}^{-1}$. Sample labels denote the ASM supplement. $n = 13$ for inoculum and $n = 2$ for endpoint samples.

respectively. For all PCoA plots the inoculum samples clustered tightly in one region separated from all endpoint samples with respect to PC1. This trend is to be expected given the loss of a key OTU corresponding to PA from most bacterial communities at the endpoint of sampling.

The PCoA plot based upon Bray-Curtis dissimilarity test resulted in a 3-dimensional solution in which PC1 accounted for 35.7% of the variation and PC2 and PC3 accounted for 23.98% and 11.75%, respectively. Endpoint planktonic and biofilm samples cultured in ASM-BSA, ASM-micronutrients-vitamins-FeSO₄ and biofilm samples cultured in ASM-only, ASM->30kDa-FBS and ASM-hemin clustered tightly at the bottom of axis 2 and the remaining samples were distributed along this axis. With respect to PC2, planktonic samples cultured in ASM-10%FBS, ASM-micronutrients-vitamins-FeSO₄-FBS and ASM->30kDa-FBS and both endpoint samples from the ASM-5-10kDa-FBS culture were closest to the inoculum samples. Yet the ASM-charcoal-FBS planktonic and biofilm samples and ASM-only, ASM-5%FBS and ASM->30kDa-FBS planktonic samples were closest to the inoculum with respect to PC1. A large cluster of endpoint planktonic and biofilm samples cultured in ASM supplemented with: 1, 5 and 10% FBS, the <5 and 5-30 kDa fractions of FBS (5%) and micronutrients-vitamins-FeSO₄-FBS(5%) showed little variance to the inoculum cluster with respect to PC3.

The unweighted PCoA plot resulted in a 3-dimensional solution in which PC1 accounted for 38.51% of the variation and PC2 and PC3 accounted for 10.92 % and 10.32%, respectively. There was little variance, with respect to PC1, amongst all endpoint samples and these samples were distributed across axis 3. Endpoint samples could be clustered into two groups with respect to PC2. Cluster 1, consisting of planktonic and biofilm samples cultured in standard ASM and ASM supplemented with BSA, hemoglobin and micronutrients-vitamins-FeSO₄, was most dissimilar to the inoculum cluster with respect to PC2. Cluster 2 consisted of the remaining endpoint samples and displayed little variance along PC2 compared with the inoculum samples. Planktonic samples cultured in ASM-1%FBS, ASM-10%FBS and ASM-<5kDa-FBS formed a tight sub-cluster at the bottom of axis 2 and were more dissimilar to the inoculum samples with respect to PC2.

The weighted PCoA plot resulted in a 3-dimensional solution in which PC1 accounted for 84.5% of the variance and PC2 and PC3 accounted for 7.82% and 4.06%, respectively. Endpoint samples were widely distributed across PC2 and could be split into two clusters separated along axis 1. Cluster 1 contained the samples with the most diverse endpoint species compositions and consisted of both endpoint samples cultured in ASM-charcoal-FBS, ASM-micronutrients-vitamins-FeSO₄-FBS and ASM-5-30kDa-FBS and planktonic samples cultured in ASM-5%FBS, ASM-10%FBS and ASM-5-10kDa-FBS. Cluster 2 contained the remaining endpoint samples and could be further broken into two sub-clusters. The first sub-

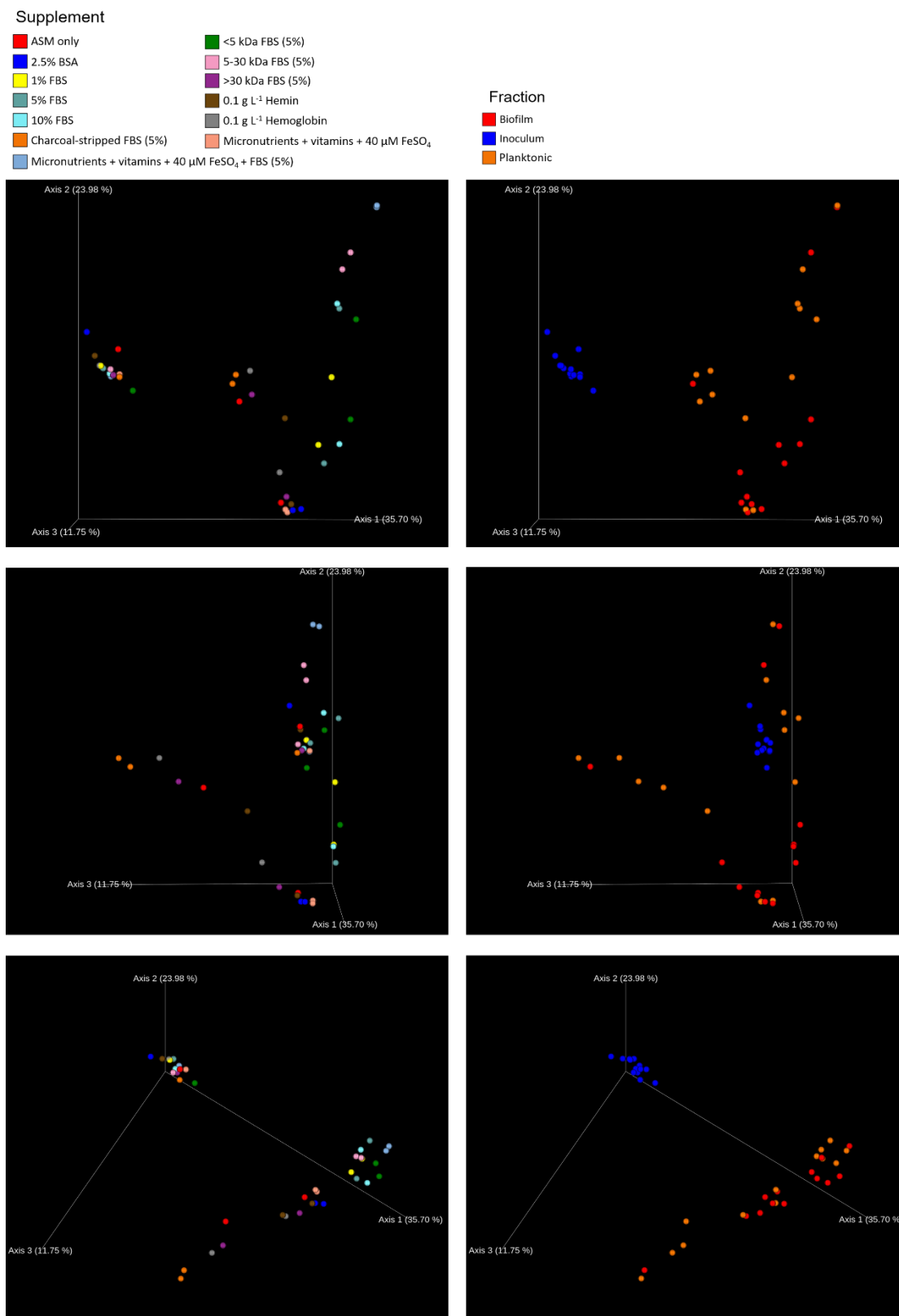
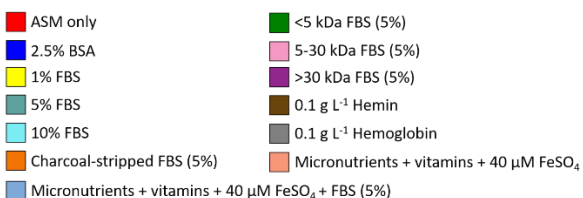


Figure 7.17 Bray-Curtis dissimilarity test of further supplemented ASM samples

Principal coordinate analysis (PCoA) based on Bray-Curtis dissimilarity test of initial inoculum, endpoint planktonic and endpoint biofilm samples. Endpoint samples were incubated in different ASM compositions under continuous flow conditions for 120 hrs. $Q = 55 \mu\text{L min}^{-1}$. Left panels denote the different supplements: no supplement (red); + 2.5% BSA (blue); + 1% FBS (yellow); + 5% FBS (teal); 10% FBS (cyan); + 5% charcoal-stripped FBS (orange); + micronutrients, vitamins, 40 μM FeSO_4 , 5% FBS (light blue); + <5 kDa FBS (green); + 5-30 kDa FBS (pink); + >30 kDa FBS (purple); + 0.1 g L^{-1} hemin (brown); + 0.1 g L^{-1} hemoglobin (grey); + micronutrients, vitamins, 40 μM FeSO_4 (salmon pink). Right panels denote the different sample types (fraction): initial inoculum (blue); endpoint planktonic (orange) and endpoint biofilm (blue).

Supplement



Fraction

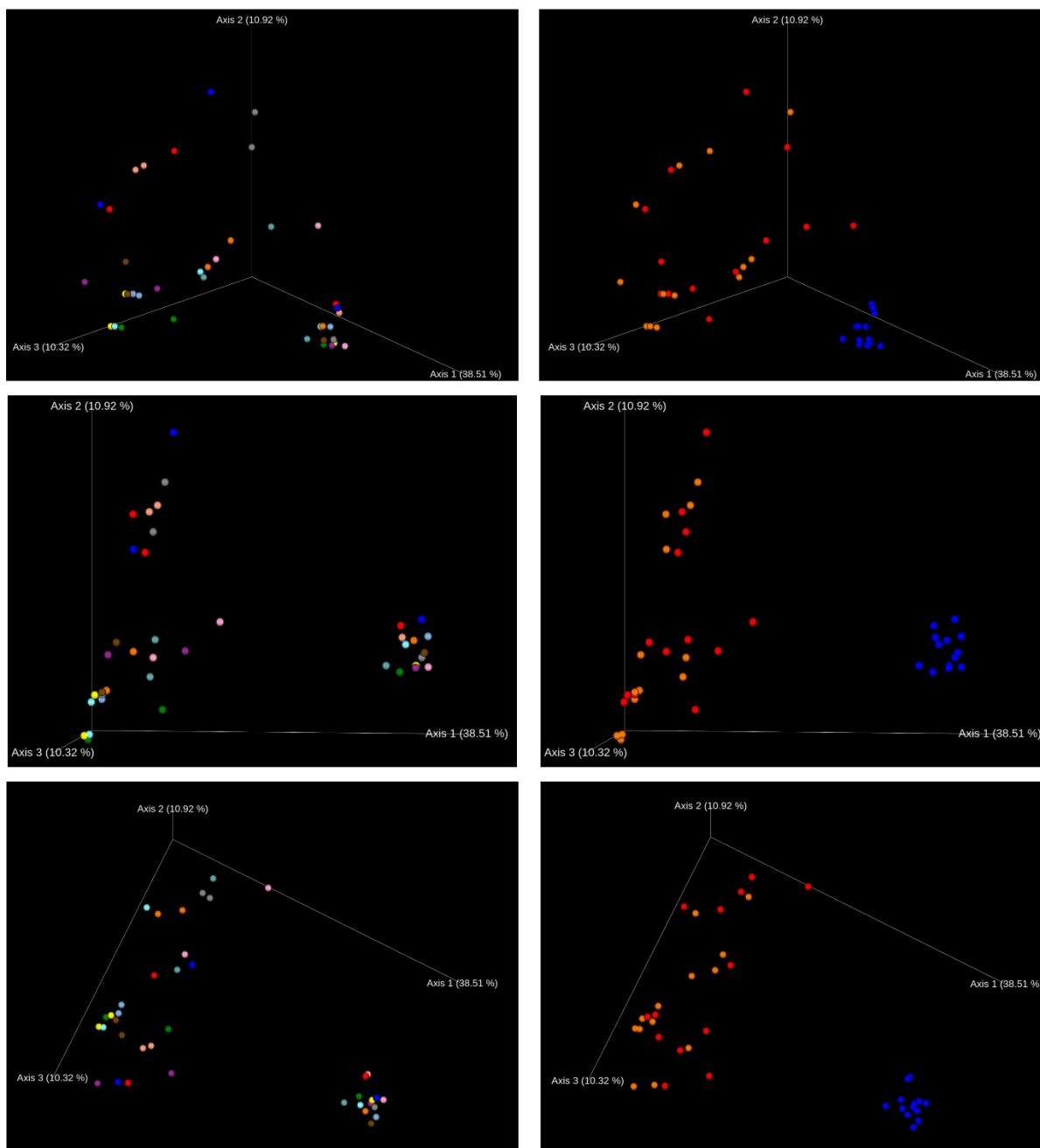
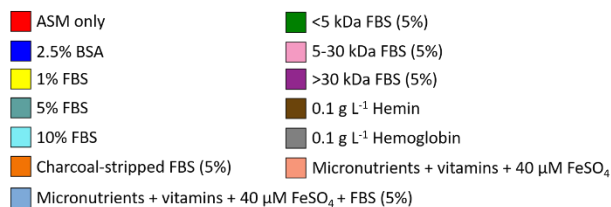


Figure 7.18 Unweighted UniFrac of further supplemented ASM samples

Principal coordinate analysis (PCoA) based on unweighted variants of UniFrac of initial inoculum, endpoint planktonic and endpoint biofilm samples. Endpoint samples were incubated in different ASM compositions under continuous flow conditions for 120 hrs. $Q = 55 \mu\text{L min}^{-1}$. Left panels denote the different supplements: no supplement (red); + 2.5% BSA (blue); + 1% FBS (yellow); + 5% FBS (teal); 10% FBS (cyan); + 5% charcoal-stripped FBS (orange); + micronutrients, vitamins, 40 μM FeSO₄, 5% FBS (light blue); + <5 kDa FBS (green); + 5-30 kDa FBS (pink); + >30 kDa FBS (purple); + 0.1 g L⁻¹ hemin (brown); + 0.1 g L⁻¹ hemoglobin (grey); + micronutrients, vitamins, 40 μM FeSO₄ (salmon pink). Right panels denote the different sample types (fraction): initial inoculum (blue); endpoint planktonic (orange) and endpoint biofilm (blue).

Supplement



Fraction

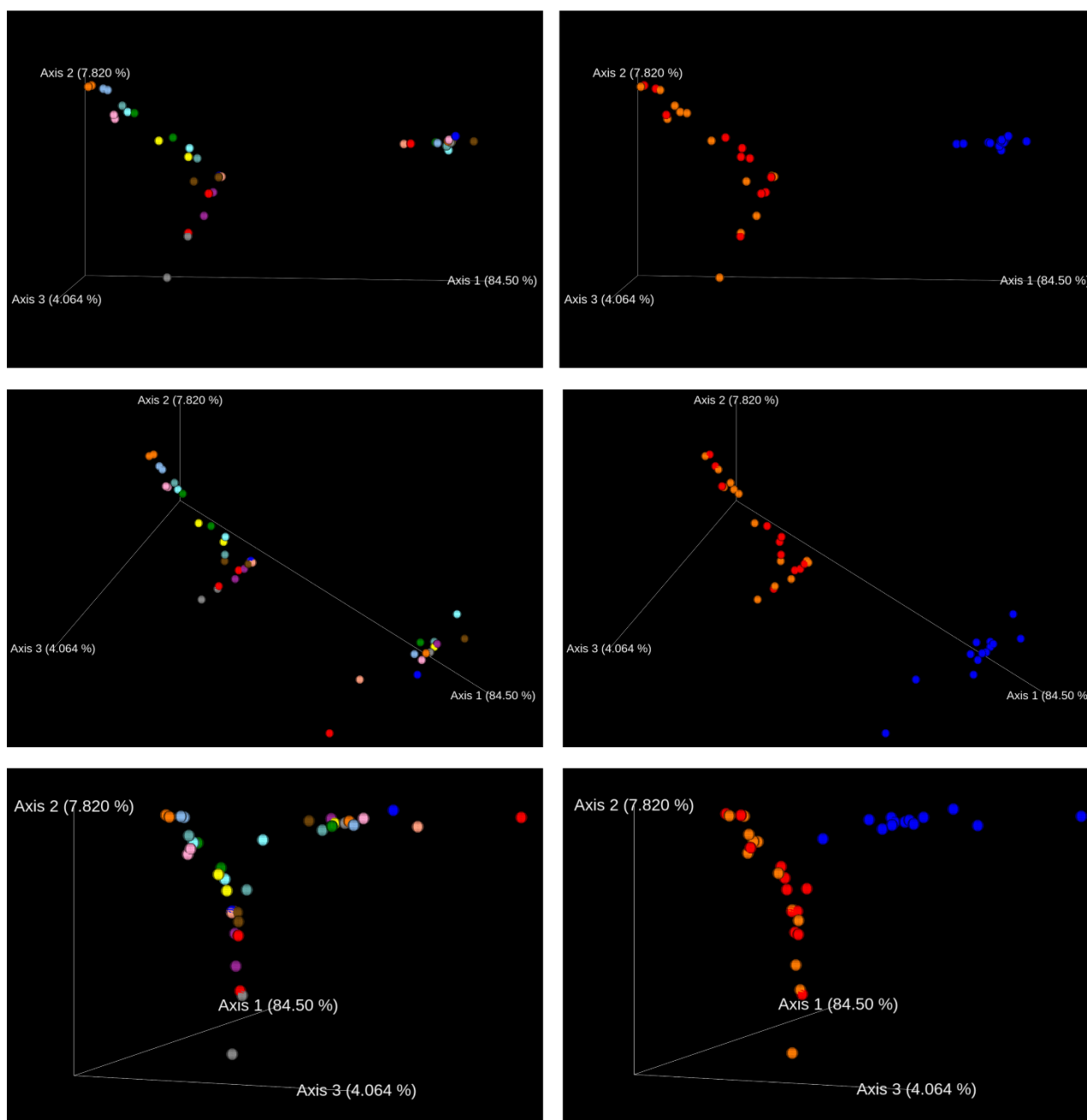


Figure 7.19 Weighted UniFrac of further supplemented ASM samples

Principal coordinate analysis (PCoA) based on weighted variants of UniFrac of initial inoculum, endpoint planktonic and endpoint biofilm samples. Endpoint samples were incubated in different ASM compositions under continuous flow conditions for 120 hrs. $Q = 55 \mu\text{L min}^{-1}$. Left panels denote the different supplements: no supplement (red); + 2.5% BSA (blue); + 1% FBS (yellow); + 5% FBS (teal); 10% FBS (cyan); + 5% charcoal-stripped FBS (orange); + micronutrients, vitamins, 40 μM FeSO₄, 5% FBS (light blue); + <5 kDa FBS (green); + 5-30 kDa FBS (pink); + >30 kDa FBS (purple); + 0.1 g L⁻¹ hemin (brown); + 0.1 g L⁻¹ hemoglobin (grey); + micronutrients, vitamins, 40 μM FeSO₄ (salmon pink). Right panels denote the different sample types (fraction): initial inoculum (blue); endpoint planktonic (orange) and endpoint biofilm (blue).

cluster showed little variance with respect to PC3 and consisted: of both samples cultured in ASM-1%FBS; biofilm samples cultured in ASM supplemented with 5% FBS, 10% FBS and <5 kDa FBS fraction and the ASM-hemin planktonic fraction. The remaining samples formed the second sub-cluster and were distributed along PC3 but were the least dissimilar from the inoculum samples with respect to PC1.

7.5.3 Comments

As shown in *Figure 7.15*, PA was lost from the endpoint samples of almost every culture, including standard ASM. This is despite all previous sections demonstrating the strong growth of this bacterium in ASM under continuous-flow conditions. The reasons for this may be two-fold. Firstly, sputum samples collected from a different person with CF were inoculated into the continuous-flow model. It is possible the strain(s) of PA in these sputum aliquots was slow growing and simply washed out from the culture vessel. Yet, given that PA was still present in the endpoint planktonic sample cultured in ASM supplemented with micronutrients-vitamins-FeSO₄ this explanation seems unlikely. Secondly, unlike previous experiments studying biofilm growth in the continuous-flow vessel, the phenomenon of microbial-mediated biocorrosion of the stainless-steel biofilm container was observed (*Figure 7.20*). Although the contribution of polymicrobial consortia towards the biocorrosion of metals has not been extensively studied outside of an industrial manufacturing setting, it should be noted that species of *Bacillus*, *Clostridium* and *Pseudomonas* (all of which were present in the inoculum sample) are thought to cause the biocorrosion of steel *via* metal oxidation (Kip and van Veen, 2015, Narenkumar et al., 2019). Furthermore, the ability of some fungi to reduce iron (Ottow and Von Klopotek, 1969) or produce organic acids (Liaud et al., 2014) significantly contributes towards biocorrosion (Wu et al., 2020). As only the bacterial 16S rRNA was sequenced, the presence of such fungal species in the cultures could not be discerned. Nevertheless, this finding highlights that stainless-steel is not a suitable material for studying biofilm growth in the model and a thermoplastic alternative, e.g. silicon, should be trialled in future experiments.

Some tentative conclusions can be drawn from the preliminary data presented in this subsection, but it is essential to note that all hypotheses should be validated in future experiments. As in *Section 7.4*, an enhanced availability of free iron increased the total steady-state carrying capacity of the culture vessel, despite a vastly different composition of bacteria existing in the model after 120 hrs incubation. Supplementing the medium with albumin alone caused a decrease in endpoint species diversity, indicating that the speculated inhibition of QS networks in PA alone is not sufficient for the maintenance of a diverse sputum-derived microbial consortium *in vitro*. Species diversity was enhanced the most when supplementing ASM with 5% FBS, suggesting that lower concentrations (1% FBS) do not contain sufficient essential

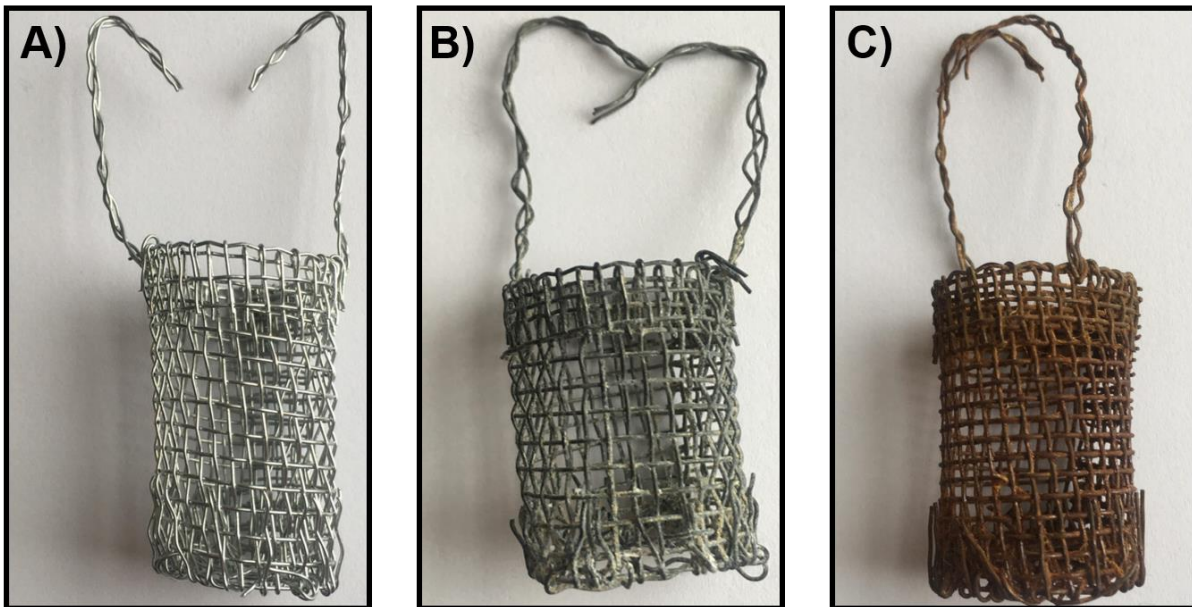


Figure 7.20 Microbial-mediated biocorrosion of biofilm containers.

Representative stainless-steel biofilm containers described in *Section 2.12.3* **(A)** Biofilm container before incubation in continuous-flow model. **(B)** Biofilm container after 120 hrs incubation in standard ASM inoculated with CF sputum samples described in *Section 7.4*. **(C)** Biofilm container after 120 hrs incubation in standard ASM inoculated with CF sputum samples described in *Section 7.5*. (B) and (C) were incubated under the same conditions for the same time period, yet (C) rusted significantly. As the microbial inoculum was the only difference between the two cultures it can be deduced that corrosion of container (C) is microbially induced.

growth factors to enhance the growth of fastidious species and that increased albumin concentration (in 10% FBS) inhibits microbial growth. Furthermore, supplementation of ASM with charcoal stripped FBS resulted in a similar endpoint microbiota as ASM-5%FBS, demonstrating that hormones or other lipids in FBS are likely not the factor contributing to increased endpoint species diversity. Similarly, the 5-30 kDa fraction of FBS (lacking albumin, molecular weight 66.5 kDa) resulted in a microbiota comparable to 5% FBS, indicating this fraction of the undefined culture supplement contained the growth factor(s) most likely to improve the growth of diverse CF associated polymicrobial communities *in vitro*.

7.6 Conclusions

The key conclusions that can be drawn from the results presented in this chapter will help guide future efforts in optimising continuous-flow culture conditions for the *in vitro* recapitulation of entire polymicrobial communities associated with CF airway infections. Firstly, an extended lag-phase associated with the growth of sputum-derived microbial populations in ASM was noted (*Section 7.2*). To prevent washout of the culture vessel, sputum samples should be incubated under batch culture conditions for 24 hrs before applying media flowrate to ensure populations are in the logarithmic phase of growth. Secondly, $Q = 55 \mu\text{L min}^{-1}$ was found to be the most suitable flowrate for maintaining sputum-derived microbial populations in a steady-state (*Section 7.3*). This flowrate permitted some species present at a low relative abundance in the initial inoculum, e.g. *A. glycerini* and Enterobacteriaceae, to be maintained in the culture vessel over the incubation period. Using $Q = 55 \mu\text{L min}^{-1}$ also resulted in the smallest change in the relative abundance of PA between the initial and endpoint planktonic fraction samples. However, across all samples there was a clear decrease in the phylogenetic diversity of sputum-derived bacterial populations grown *in vitro*, especially the loss of anaerobic species from the planktonic fraction. As indicated in *Section 7.4*, subtly optimising the concentration of nitrate in ASM may improve the maintenance of anaerobic bacteria in the model at a similar relative abundance to the starting inoculum.

A loss of PA from endpoint samples generally correlated with an increase in overall species diversity. Furthermore, supplementing ASM with FBS clearly increased the bacterial diversity of endpoint samples (*Section 7.4* and *7.5*). Preliminary experiments to decipher which component(s) of the FBS supplement were responsible for enhancing bacterial biodiversity during *in vitro* growth suggest that albumin-mediated modulation of interspecies interactions (Smith et al., 2017) is not the sole explanation for this observation. As suggested in *Section 7.5*, it is likely that an unidentified non-lipid component of FBS, 5-30 kDa in size enhances the growth of microbial species present at low abundancies in CF sputum, yet this hypothesis

remains to be validated. Overall, these preliminary findings highlight the value in pinpointing individual factors to promote the growth of fastidious microbial species, and in utilising these to subtly refine the composition of ASM. These approaches should prove a fruitful line of investigation in the search for conditions that faithfully recapitulate entire CF polymicrobial community(s) *in vitro*.

8. Discussion

8.1 Maintenance and characterisation of polymicrobial co-cultures

The results presented throughout this study clearly demonstrate that the polymicrobial populations of pathogenic species associated with CF airway infections – including species that would ordinarily outcompete each other using traditional culture methods - can be maintained as co-cultures for extended periods of time under continuous-flow conditions. Populations were held in a stable, steady-state with respect to microbial titres (*Figure 3.3, 3.6, 3.9 and 3.12*), genomic mutability (*Figure 4.2*) the accumulation of extracellular virulence factors (*Figure 4.4 and 4.5*) and QS molecules (*Figure 4.7*) in the culture vessel for the entirety of the incubation period. To my knowledge, this is the first study to describe the successful *in vitro* co-culture of key CF associated pathogens using ASM. The three reference strains chosen for this work (PA, SA and CA) were selected to represent the three different classes of microbes commonly associated with CF airway infections (Gram-negative bacteria, Gram-positive bacteria and fungi, respectively). Crucially, stable microbial titres of each distinct species could be readily maintained in the co-culture (*Section 3*), indicating that other combinations of microbial species from the CF microenvironment can also likely be maintained *in vitro* as part of a steady-state co-culture as long as the correct flow rate is established. This hypothesis is currently being tested by other members of the Welch laboratory, who are working towards the co-culture of additional species associated with CF using my continuous-flow model.

The importance of studying mixed microbial populations is reiterated by the findings presented in *Sections 3 and 4*. The presence of numerically minor species (such as CA, which comprised just 0.05% by numbers in the polymicrobial consortium (*Figure 3.12*)), can cause significant and varied modulations in the accumulation of extracellular signalling molecules or virulence factors (*Section 4*). Furthermore, the presence of these less-abundant species can modulate the microbial titres of a polymicrobial consortium maintained under batch culture conditions (*Section 3*). Given the diversity of the microbiota thought to be associated with the CF airways throughout a patient's life (Carmody et al., 2015, Zhao et al., 2012) and the ubiquitous presence of less abundant, or “rare”, species (comprising <0.1% of the total relative abundance) in CF sputum samples (*Section 7*), this work demonstrates the essential need to consider the impact of low-abundance species on the modulation of microbial behaviour. They also open up the possibility of experimentally examining how inter-species interactions may contribute towards an increase/decrease in microbial pathogenicity.

The stability of individual microbial titres in co-cultures maintained under continuous-flow conditions (*Section 3*) may be attributed to the diminished accumulation of extracellular

virulence factors, e.g. siderophores and pyocyanin previously identified to be essential for infection in *in vivo* models (van Delden, 2004) in the culture vessel (*Section 4*). Although only two virulence factors were studied in this work, the diminished accumulation of QS molecules under continuous-flow conditions suggests that the expression of other extracellular factors under the control of these signalling networks is also likely to be repressed. Precisely why these factors do not accumulate in the model system is not yet known. As discussed in *Section 4.6*, previous studies suggest that QS molecules should accumulate faster than the rate of dilution in the continuous-flow culture vessel (Davenport et al., 2015). Two likely explanations may account for the observed decrease in extracellular factors in the culture vessel. First, the continuous displacement of spent media with fresh ASM ensures an abundant supply of fresh nutrients. This culture method was chosen to loosely represent the overproduction of sputum in persons with CF, where PA and SA are known to co-habit over the course of a patient's life (Hogan et al., 2016, Limoli et al., 2016, Wakeman et al., 2016, Zolin et al., 2019). As there is a reduced need to compete for available nutrients it is possible that the production of "expensive" extracellular goods utilised in competition between species is simply not required. Second, as demonstrated in *Section 4.2*, steady-state microbial populations are maintained in an actively growing state for the entirety of the incubation. As secondary metabolites are often produced during the stationary growth phase, it is possible that the biosynthesis or secretion of these factors is repressed in the actively-growing state. It should be noted that these two hypotheses are intrinsically linked. Increasing the retention time (R_t) within the culture vessel, *via* decreasing Q , would cause a population to transition into the stationary phase of growth once the carrying capacity in the culture vessel is reached. At the same time, increased R_t would decrease nutrient availability in the culture, likely leading to increased interspecies competition for limited resources. Hence, no further comment on these assumptions can yet be made.

It is interesting to note that an accumulation of PA mutants lacking functional QS networks and strains with repressed virulence factor expression are often isolated from chronic infection scenarios, suggesting a diminished importance for these metabolic pathways *in situ* (Kostylev et al., 2019, LaFayette et al., 2015, Waters and Goldberg, 2019). Furthermore, PA isolates from late-stage airway infections do not outcompete co-cultivated species as quickly as commonly-used reference strains or isolates obtained from acute infection scenarios. For example, in certain mucoid strains able to exist in a co-culture with SA, there is a marked down-regulation of rhamnolipids, siderophores and HQNO (Briaud et al., 2019, Hotterbeekx et al., 2017, Price et al., 2020). These reports, taken in combination with the results provided in this study provide strong evidence to suggest the use of a continuous-flow model for the study of microbial behaviours associated with the chronic stages of infection. Additionally,

increasing R_i of the culture vessel should also allow the more aggressive acute infection scenario to be studied (as competition for limited nutrients would increase).

As demonstrated in *Section 4.2*, RT-PCR can be successfully and reproducibly performed on microbial populations maintained under continuous-flow conditions. It is important to note that the relative expression of any gene can be quantified using RT-PCR, ensuring that the model system provides a robust tool to monitor changes in the expression of key genes during growth in co-culture. For example, quantifying the expression of the pyocyanin or siderophore biosynthetic genes (*phz* (Mavrodi et al., 2001) or *pch/pvd* (Bonneau et al., 2020), respectively) could indicate if the low accumulation of associated extracellular factors is due to displacement from the vessel or due to a decrease in gene expression. An untargeted transcriptomic approach, such as using RNA-seq (Owens et al., 2019), to compare the expression profiles of axenic and polymicrobial steady-state populations would be a powerful approach to discern subtle and unexpected changes in the genetic profiles of species over time. Although expensive, this approach could identify key genes important for the successful establishment/maintenance of pathogenic species in a polymicrobial consortium and may also identify potentially novel therapeutic targets.

Environmental homeostasis is afforded during growth in the continuous-flow culture model (*Section 4.7*), yet previous reports have implicated changes in environmental conditions, such as a decrease in pH, in triggering the onset of APEs (Quinn et al., 2014, Quinn et al., 2015). Other studies have further established that changes in available eDNA and mucin concentrations in a growth medium can modulate microbial behaviour and promote biofilm formation (Sriramulu et al., 2005). As ASM is a chemically-defined culture medium, my *in vitro* model provides an unparalleled opportunity to decipher how changes in environmental conditions or chemical factors, *via* changing pH or the nutritional composition of ASM, alters the behaviour of polymicrobial populations. Exogenous molecules could also be added to the culture vessel to discern how they impinge upon interspecies interactions among the community. For example, purified signalling molecules specific for either Gram-positive or Gram-negative QS networks, could be introduced into the culture vessel to determine how the activation of these regulatory networks affects steady-state microbial co-cultures. As a tractable experimental culture model, any number of subtle interspecies interactions could be studied in real-time and at a depth that is simply not possible using *in vivo* models of infection.

The genomic mutability of co-cultivated microbial species maintained under continuous-flow conditions is extremely stable (*Figure 4.2*). The model therefore provides a unique research tool for studying the co-evolution of mixed microbial species associated with CF infections under nutritionally relevant conditions over an indefinite period of incubation. Through

comparing the genome sequences of parental strains and their progeny, common conserved evolutionary changes likely to be beneficial for survival in the CF environment may be identified. Hypermutator strains lacking the DNA mismatch repair genes (e.g. *mutS* in PA (Oliver et al., 2002) and SA (Prunier and Leclercq, 2005) or *MSH2* and *PMS1* in CA (Legrand et al., 2007)) could also be introduced into stable microbial co-cultures to accelerate the rate of evolution of species in a seemingly unbiased manner. This approach should however be used with caution, as the emergence of fast-growing mutant strains could lead to the imbalance of microbial titres and further perturbations in the steady-state community. Tn-Seq analysis (van Opijnen et al., 2009) of PA or other key CF pathogens maintained in a co-culture could also be used to define the genes essential for survival as part of a polymicrobial community. These genes may prove to be attractive targets for the development of novel therapeutic treatments to prevent the effective *in situ* establishment of chronic airway infections.

8.2 External perturbation of steady-state microbial populations

The results presented in *Section 5* provide a proof-of-principal for the use of my novel culture vessel for studying the robust and tractable perturbation of steady-state microbial communities *in vitro*. These findings demonstrate that my model can be successfully used to study the response of stable planktonic co-cultures treated with antimicrobial compounds and the introduction of new species or strain variants. Furthermore, the model could be utilised for the development of effective combinational therapy approaches designed to limit the emergence of antimicrobial resistant isolates in a polymicrobial consortium, and prevent the establishment of chronic airway infections with keystone respiratory pathogens. Due to time constraints, only a small sub-set of microbial co-cultures and their response to antimicrobial compounds were examined in this study. However, hypothetically, it should be possible to study how any combination of microbial species or an entire patient-derived polymicrobial population responds to exogenous perturbation.

No matter the cell density of the PA inoculum introduced to a pre-established steady-state SA-CA co-culture, the same composition of microbial species, with respect to viable cell numbers, was achieved by the end point of incubation (*Figures 5.2 and 5.3*). Given that competition among species appears to be mitigated under continuous-flow conditions (*Sections 3 and 4*), this finding indicates that a maximum carrying capacity is achieved during growth in the culture vessel. When cell titres reach this maximum carrying capacity, cell numbers converge towards the same steady-state over time. Through altering the R_t in the model, it is possible to modulate the total microbial carrying capacity, as demonstrated in *Figure 7.2*. Upon

introduction of very high PA titres to a steady-state co-culture (*Figure 5.3.B*) there was a temporary diminution in SA and CA CFU mL⁻¹ during the subsequent 24 hrs of incubation. This temporary decrease in SA and CA titres may arise due to a severe limitation of nutrients caused by the introduction of a high density of PA cells to the culture vessel. Following this, and as PA cells are displaced with fresh ASM, the SA and CA titres recover to the steady-state titres achieved prior to the exogenous introduction of PA to the microbial community. As suggested in *Section 8.1*, transcriptomic analysis of a steady-state PA-negative microbial community following perturbation with a large PA challenge could identify genes up-regulated during the initial stages of co-culture with other species. Furthermore, Tn-Seq analysis could reveal genes crucial for PA to establish an effective infection in a polymicrobial community. The corresponding gene products may prove attractive targets for the development of prophylactic therapeutics to prevent the establishment of chronic PA infections in the CF airways.

The decreased efficacy of antimicrobial compounds against their target microorganism when grown as part of a polymicrobial community is evident from the results presented in *Section 5* (*Figures 5.4 – 5.14*). This observation highlights an essential need to consider the role of additional species at a site of infection and how they might modulate the response of a principal pathogen to therapeutic intervention. From the antimicrobials tested in this study it is also clear that bacteriostatic compounds are less efficacious at treating pre-established microbial cultures under continuous-flow conditions compared with bactericidal compounds. This finding affirms the notion that the use of bactericidal antimicrobials against chronic CF infections is preferable in the clinical setting (Pankey and Sabath, 2004). It should be noted that the role of a host's immune system in clearing microbial infections is not accounted for in this or any other *in vitro* model. However, and mitigating, impaired immune clearance of infections in the CF airway is well reported in the literature (Cohen and Prince, 2012, Bonfield and Chmiel, 2017, Bruscia and Bonfield, 2016, Ratner and Mueller, 2012).

The decreased loss of viable SA cells from a polymicrobial consortium treated with fusidic acid, compared to an axenic SA culture, is not an inherited mechanism of resistance but arises due to the presence of PA and/or CA in the co-culture (discussed in *Section 5.3*). Given that antimicrobials are less efficacious against microbial biofilms (Fux et al., 2005, Høiby et al., 2010a, Parsek, 2003, Sharma et al., 2019, Stewart, 2002) and that SA is found to form significantly denser biofilms in the presence of PA and CA (*Figures 6.3, 6.6, 6.7 and 6.8 and Section 8.3*), this phenomenon is likely to arise as a result of enhanced biofilm formation during co-culture. This finding supports the importance of ongoing research efforts to disrupt/inhibit biofilm formation during the treatment of chronic infections (Verderosa et al., 2019). Future research efforts can easily adopt my model to robustly discern the key species responsible for

modulating antimicrobial action during co-culture and test the efficacy of novel treatment regimens.

More PA and CA isolates displaying enhanced antimicrobial resistance profiles were collected from the steady-state polymicrobial cultures perturbed with either colistin or fluconazole than were collected from the perturbed axenic cultures (*Figures 5.16 and 5.17*). This finding demonstrates an increased emergence of inherited mechanisms of resistance, alongside increased antimicrobial tolerance (discussed above) during microbial co-culture. WGS analysis of PA isolates resistant to the action of 1 mg mL⁻¹ colistin revealed no difference in the genes containing SNPs identified between isolates recovered from the axenic or polymicrobial cultures. These findings demonstrate that the growth of PA as part of a polymicrobial community does not necessarily drive the emergence of novel inherited mechanisms of antimicrobial resistance. Instead growth as part of a polymicrobial consortium increases the emergence of PA isolates containing SNPs in genes conferring resistance to colistin within a mixed microbial population. Interestingly, all of the non-synonymous colistin resistance-conferring SNPs in PA were found in genes encoding cell surface-associated virulence factors such as LPS and type IV pilin (*Table 5.4*). Most of these have not previously been directly linked to conferring resistance against colistin. This finding suggests that the down-regulation of these cell surface moieties may benefit PA growth as part of a polymicrobial consortium. Perhaps by preventing the effective recognition of PA by other members of a community which may trigger an up-regulation of interspecies competition events. Although the affected genes are known to be important for mediating host-bacterium interactions (Lam et al., 2011), these genes are not essential for the growth of PA *in vitro*, and pilin-deficient PA strains are proven to effectively interact with purified mucin *in vitro* (Ramphal et al., 1991). Importantly, mutations in LPS and pilin biosynthetic genes are often identified in clinical PA isolates recovered from late-stage CF airway infections (Smith et al., 2006). Existing studies have also demonstrated that late-stage PA isolates can be co-cultivated with other bacterial species for longer periods of time under batch culture conditions due to a reduction in virulence factor production (Baldan et al., 2014). This provides some evidence to support the hypothesis that a down-regulation of genes encoding cell surface associated virulence factors permits improved co-culture of PA with other species. Mutants defective in such genes would therefore be expected to be selected for in co-cultures. Although WGS analysis of CA isolates displaying increased fluconazole resistance was not performed as part of this study, future investigation into this could confirm if there is also an alteration in fungal cell surface moieties during growth as a polymicrobial community.

The stability of microbial mutation rates in co-cultures maintained in the model for extended periods of time (*Figure 4.2*) and the emergence of key genomic mutations commonly identified

in situ in CF airway infection scenarios provides strong evidence to support the utility of the continuous-flow model for studying the evolutionary trajectory of key CF associated pathogens when grown as a part of a polymicrobial community.

In the cultures treated with supra-MIC concentrations (5 x MIC) of colistin or fusidic acid there was a significant increase in viable PA cell counts between the steady-state community prior to antimicrobial exposure (T = 0 hrs) and the final point of sampling (T = 48 hrs) (*Figures 5.6 and 5.10*). This demonstrates ability of PA to expand into a vacant environmental niche following the perturbation of a microbial community. Furthermore, this finding supports the CAM model of changes within a polymicrobial community following clinical intervention or immune clearance proposed by Conrad *et al.* (2013). In brief, this hypothesis suggests that keystone pathogens of late-stage CF airway infections can resist clearance from the airway and acquire adaptations that enable them to occupy a newly-liberated environmental niche. This often complicates future treatment regimens and leads to a worsening patient prognosis. Given that targeting SA with a large fusidic acid challenge caused a significant increase in PA titres and a reduction in SA titres, this observation affirms the importance of understanding how an entire polymicrobial population responds to antimicrobial treatment, and not simply the principal pathogen being targeted. One key use of the model system in the future is to examine how complex and patient-derived polymicrobial consortia respond to global perturbation, *i.e.* antimicrobial action, in order to develop effective combination therapies to limit the emergence of key pathogens.

8.3 Formation of polymicrobial biofilms in ASM

A combined approach of different experimental assays was employed to study the temporal formation of biofilms in ASM. This revealed complementary information regarding the dynamics of biofilm formation that would otherwise be missed when studying biofilms with a single technique. For example, CA initially formed biofilms with the largest total biomass (*Figure 6.1 and 6.4*) but these biofilms were the least metabolically active (*Figure 6.2 and 6.5*). By contrast, SA formed the least dense but most metabolically active biofilms in ASM. Given that a number of conventional antimicrobials are more active against vigorously-growing microbial populations (Agrawal *et al.*, 2019, Anderl *et al.*, 2003, Keren *et al.*, 2004, Matsuo *et al.*, 2011, Pletnev *et al.*, 2015) and that the EPS encasing cells in biofilms is known to hamper the penetration of various antimicrobial compounds (Hall and Mah, 2017, Harjai *et al.*, 2005, Høiby *et al.*, 2010a), this finding indicates that *in situ* biofilms comprising of SA may be more susceptible to antimicrobial treatment compared with biofilms containing CA. By extension it may be reasonable to predict that biofilms containing both PA and CA (showing low metabolic

activity and high biomass production) would be more tolerant to antimicrobial action compared with biofilms of the other species combinations studied as part of this work. Indeed, it has recently been demonstrated that the CA biofilm matrix can protect SA against vancomycin, a “last-resort” glycopeptide antimicrobial, during polymicrobial co-culture (Kong et al., 2016). Furthermore, PA-derived exogenous alginate can also protect SA from killing during growth as a polymicrobial biofilm (Price et al., 2020, Schurr, 2020). Although the perturbation of polymicrobial biofilms with antimicrobials was not studied here, the results presented in *Sections 5 and 6* demonstrate that my model system provides a tractable tool for investigating this in detail. No matter the research question being addressed, the results presented in *Section 6* highlight the importance of using multiple experimental techniques when studying biofilm formation, especially in a polymicrobial scenario where it may be impossible to discern which species are responsible for the production of extracellular products such as EPS.

Consistent with previous studies, the out-competition and removal of microbial species during co-culture was diminished in the biofilm mode of growth compared with growth as a planktonic culture (*Figure 6.3 and 6.6*). As discussed in *Section 6.5*, diffusion coefficients of small molecules are lower in a biofilm matrix (Sankaran et al., 2019) thereby limiting the rate of release of extracellular products from or within the biofilm (Janissen et al., 2015, Jayathilake et al., 2017). This is likely to result in a heterogenous distribution of extracellular factors, such as those associated with virulence. By extension the diffusion of fresh nutrients into the biofilm will also be limited and may explain why increased interspecies competition and a reduction in SA and CA titres occurs in some of the polymicrobial biofilms cultured using the Kadouri drip-plate continuous-flow method (*Figure 6.6*). It is also important to note that the flow rate was lower during experiments using the continuous-flow microtiter plate format ($Q = 55 \mu\text{L min}^{-1}$ as opposed to $>145 \mu\text{L min}^{-1}$ during growth in the 100 mL culture vessel). The lower flow rate was necessary to prevent rapid washout of cells from the smaller well volume present in the drip-plates. However, as described previously (*Section 8.1*) this, in turn, is likely to increase competition amongst microbial species. This notion is supported by the observation that polymicrobial biofilms grown on agar in the continuous-flow system (with a higher Q) do not demonstrate any microbial out-competition over the 96 hrs incubation period (*Figure 6.7*). Alongside this, biofilms containing PA did not demonstrate signs of biofilm dispersal during growth using the Kadouri drip-plate method (*Figure 6.4 and 6.6*). In combination, these findings provide further support for my hypothesis that microbial competition is suppressed under growth conditions with an ample supply of nutrients, not unlike the nutrient-rich CF microenvironment (Palmer et al., 2005, Palmer et al., 2007, Son et al., 2007). Ultimately these findings also demonstrate the suitability of the continuous-flow model for the long-term study of sessile polymicrobial communities *in vitro*.

In addition to some microbial competition occurring in the polymicrobial biofilms during the late stages of incubation (after 24 hrs incubation), antagonistic and synergistic interspecies interactions are also present during the initial stages of mixed species biofilm formation under both continuous-flow and batch culture conditions. As discussed in *Section 6.5*, the presence of PA or CA in a co-culture increased the attachment of viable SA cells in the biofilm during the first 12 hrs of incubation (*Figure 6.3* and *6.6*). Conversely, the presence of PA or SA in the co-culture decreased the attachment of viable CA cells in the biofilm. Earlier publications have established the importance of an EPS matrix for the formation of sessile microbial communities (Limoli et al., 2015). Direct evidence also demonstrates that EPS components, such as alginate produced by PA, may encapsulate other species in polymicrobial biofilms to provide an anchor point for the improved attachment of species to a surface (Flemming and Wingender, 2010). Furthermore, polymeric substances can protect co-cultured species from antimicrobial action or clearance *via* the immune system (Paulsson and Riesbeck, 2018). As identified through CV staining (*Figure 6.1* and *6.4*) SA produces the smallest biomass of the three reference strains studied throughout this work. When co-cultured with species producing a large amount of biomass, *i.e.* PA or CA, SA appears to be more efficient in attaching to the biofilm during the initial stages of biofilm formation. Indeed existing reports have shown that *Staphylococcus* spp. interact synergistically with fungal species, such as CA, during the initial stages of biofilm formation (Adam et al., 2002, Costerton et al., 1999, Shirliff et al., 2009) and SA has been demonstrated to show strong adherence to the CA hyphal adhesin protein, Als3p, during biofilm growth (Peters et al., 2012b). In contrast, PA can prevent the CA yeast-hyphal morphogenesis associated with the maturation of fungal biofilms. Such antagonistic interactions between species can explain the decrease in viable CA cells in polymicrobial biofilms compared with mono-species biofilms observed in the current work (*Figure 6.3, 6.6, 6.7* and *6.8*).

The ability of the solid substratum to modulate microbial behaviour is also evident from the results presented in *Section 6*. Despite being identified as an early coloniser of the CF microenvironment and strong biofilm producer *in situ* (Kiedrowski et al., 2018), SA formed the least dense biofilms on abiotic surfaces such as plastic (*Figure 6.1, 6.3, 6.4* and *6.6*) and agar chunks (*Figure 6.7*) during growth in ASM. When cultured on bronchiole tissue sections (*Figure 6.8*) SA established a significantly denser mono-species biofilms compared with growth on agar chunks. The increased attachment of SA to EVPL tissue sections indicates that proteins and/or lipids on the surface of the bacterium are involved in the recognition and/or adhesion of SA to epithelial cells in the CF microenvironment (Josse et al., 2017), but are not as effective at promoting biofilm formation *in vitro* on abiotic surfaces. Although α -toxin produced by SA is essential for the intracellular invasion of human epithelial cells (da Silva et

al., 2004), no specific cell-surface receptor has yet been identified as essential for the direct interaction of SA with CF airway epithelial cells. Tn-seq analysis of SA (Valentino et al., 2014) cultured on EVPL sections in ASM under continuous-flow conditions would prove useful in identifying genes important for the initial establishment of SA biofilms *in situ*, and also genes essential for the long-term maintenance of biofilms on epithelial cells. The associated gene products may prove to be attractive drug targets to prevent the establishment of chronic biofilms in the CF microenvironment.

When comparing the endpoint viable cell counts of the polymicrobial biofilms grown on agar chunks (*Figure 6.7*) and EVPL sections (*Figure 6.8*), increased interspecies competition among the biofilms grown upon bronchiole tissue sections is clearly evidenced by a reduction in SA titres. This diminution in viable cell counts was not observed on agar chunks. This finding reinforces the ability of PA and/or CA to recognise bronchiole tissue and modulate their behaviour towards a more aggressive state. Due to time constraints, I was unable to examine the growth of dual-species biofilms on EVPL sections as part of this collaborative study (carried out during a visit to the University of Warwick). However, evidence in the literature demonstrates that PA up-regulates the production of extracellular virulence factors, e.g. HQNO and siderophores, when grown on a monolayer of airway epithelial cells (Filkins et al., 2015) and that CA undergoes yeast-to-hyphae morphogenesis to invade tissues when grown upon epithelial cells (Maza et al., 2017, Richardson et al., 2018). Combined with a decrease in SA titres when co-cultured in batch with either PA or CA (*Figure 3.2* and *3.8*), it seems likely that both PA and CA contribute towards the lower titres of viable SA cells in EVPL-associated biofilms, although this hypothesis remains to be proven. As aforementioned (*Section 6.5*), an increase in virulence during culture upon EVPL sections can be exploited in future work studying an acute or more aggressive infection scenario. Importantly, histopathological studies of EVPL sections cultured with a steady-state microbial population can also be undertaken to discern how tissue damage or cell invasion is altered during growth as a polymicrobial community. To investigate this further, Dr. Marwa Hassan (University of Warwick) is performing histopathological studies on the EVPL sections collected throughout this study as part of the ongoing collaboration. In contrast abiotic surfaces, such as agar chunks, do not seemingly cause an increase in interspecies competition and so are more likely suited for the maintenance of stable polymicrobial biofilms for extended periods of time in the *in vitro* model (*Section 7*).

Although not the primary focus of this study, the continuous-flow model provides a defined and reproducible tool for the study of interspecies interactions and competition in polymicrobial biofilms on various substrata. Overall, it is evident that biofilms behave differently under batch and continuous-flow conditions and there is a difference in the ecological composition of

patient derived communities between the planktonic and biofilm mode of growth (*Figures 7.3 – 7.19*). Through understanding and exploiting such interspecies interactions it may be possible to promote the growth of avirulent species, thereby preventing keystone pathogens from establishing chronic airway infections. Alternatively, such avirulent species may drive the behaviours of pathogens towards a less virulent profile. It should be reiterated that the stainless-steel biofilm containers I designed and built throughout this work were suitable for co-culturing reference strains but are not suitable for the *in vitro* cultivation of populations of unknown compositions, which may contain strains or species able to oxidise and corrode the container (*Figure 7.20*). The use of a thermostable plastic, e.g. silicone or polypropylene, alternative material should be explored in future experiments co-culturing polymicrobial populations derived from CF sputum samples.

8.4 *In vitro* cultivation of patient-derived polymicrobial communities

With the stable co-culture of domesticated microbial species for extended periods of time possible under continuous-flow conditions, I wanted to explore if the recapitulation of an entire polymicrobial population derived from the CF airways could be achieved using my *in vitro* model. No published work has yet described the successful co-culture of an entire patient-specific microbial community, such as those contained in CF sputum samples, using *in vitro* or *in vivo* models (O'Brien and Welch, 2019b). Success in realising this aim would provide a simple and novel research tool to enable the robust and tractable study of true polymicrobial consortia in the lab. Furthermore, studying the growth of entire patient-specific microbial communities *in vitro* helps to bridge the “bench-to-bedside research gap” (van der Laan and Boenink, 2015) and would no doubt reveal the key interspecies interactions likely to be occurring *in situ* that may prove to be attractive drug targets. Although this goal was not fully realised in this study, the results presented across *Section 7* provide a useful framework for guiding future optimisation efforts to enable the recapitulation of the entire microbiota associated with the CF airways *in vitro*. This work is currently being continued by a PhD student, Éva Benyei, in the Welch lab.

The extended lag phase and slow growth rate of microbial species derived from CF sputum samples, compared with the well-studied laboratory reference strains used in the work presented in *Sections 3 – 6*, is clearly evident in *Figure 7.1*. As previously discussed in *Section 7.2* and *7.3*, the longer lag phase and slower doubling time of some microbial species can be associated with enhanced resistance and/or tolerance to antimicrobial action and immune clearance (Bertrand, 2019, Burns and Rolain, 2014, Ciofu and Tolker-Nielsen, 2019, Kaldalu and Tenson, 2019, Li et al., 2016, Pontes and Groisman, 2019, Yamaguchi et al., 2019). Given

the aggressive antimicrobial treatment of CF airway associated infections at the onset of APEs throughout a patient's life, it may perhaps be unsurprising that sputum samples collected from adult persons with CF (as in this study) contain slow-growing microbial strains more likely to survive such clinical intervention. This finding is consistent with previous studies conducted in the Welch laboratory into the reduced growth rate of clinical PA isolates collected from the CF airway environment and from surgical wound infections (personal communications). Importantly, these observations suggested that was essential to pre-incubate sputum-derived polymicrobial communities inoculated into the culture vessel under batch culture conditions ($0 \mu\text{L min}^{-1}$) for ≈ 24 hrs until the population had entered the exponential phase of growth. This prevented the rapid washout of microbial cells during the initial stages of incubation, where not all of the inoculated cells were actively dividing. Furthermore, $Q = 55 \mu\text{L min}^{-1}$ was identified as the optimal flow rate to compensate for the slow growth rate of species associated with CF sputum samples. This flow rate also yielded the smallest change in the relative abundance of PA between the initial and endpoint sequencing samples in a screen of different flow rates (Figure 7.3). This lower flow rate also proved to be suitable for maintaining the most diverse microbiota in both the planktonic and biofilm communities for extended periods of incubation (Figures 7.3 – 7.7). Alongside $Q = 65 \mu\text{L min}^{-1}$, the slowest flow rate also enabled the highest total microbial carrying capacity, with respect to optical density, to be maintained *in vitro* (Figure 7.2). It is interesting to note that, as in a traditional chemostat or microbial fermenter, altering Q increases or decreases the total microbial carrying capacity of the culture vessel. This may prove useful in the study of different disease states and interspecies interactions occurring between populations of different cell densities in future studies of sputum-derived microbial populations.

As demonstrated in Sections 3 and 4, species of low relative abundance in a polymicrobial population, such as CA, which comprised less than 0.05% of the total microbiota in the triple-species co-cultures (Figure 3.11 and 3.12), can significantly modulate the microbial ecology and secretion of extracellular products by other members of the consortium. An assortment of low-abundance species comprising less than 0.1% of the total polymicrobial community, such as *A. glycerini*, *M. brunensis*, *S. agalactiae* and *Rothia/Prevotella* spp., were ubiquitously present in all of the cultured sputum samples (Figure 7.3, 7.9 and 7.15). Although the “classical” and more abundant bacterial species, such as PA and *Streptococcus* spp., can be easily maintained in my *in vitro* model, most low-abundance species were lost from the culture vessel at the endpoint of sampling under almost every culture condition. Given that little is known about the behaviour of such low-abundance species and that they may play an essential role in modulating the physiology and behaviour of “classical” CF airway associated pathogens *in situ*, it is crucial that the loss of these species during *in vitro* growth is mitigated.

As discussed in detail in *Section 7.4*, I attempted to subtly alter the nutritional composition of ASM to identify factors essential for promoting the growth of less abundant species present in the sputum samples. With little-to-no research published on the axenic growth of the low abundance species identified in the sputum inoculum or the growth of entire polymicrobial populations *ex situ* in general, the empirical selection of suitable ASM supplements was challenging. I therefore chose to focus on media supplements previously identified to improve the *in vitro* growth of fastidious microorganisms in the literature (see *Section 7.4* for details on these supplements). From the results presented across *Section 7.4* and *7.5*, most nutritional supplements tested did not improve the growth of less-abundant microbial species. However, it was clear that some supplements did modulate microbial ecology and cause global changes in the growth of the population. For instance, increased iron bioavailability or an increase in the concentration of sulfur-containing amino acids in the ASM caused a significant increase or decrease, respectively, in the total microbial carrying capacity of the system (*Figure 7.8*).

As described in *Sections 1.1, 1.2, 1.3* and *7.4*, obstruction of the CF airways with thick mucus plugs ensures the formation of steep oxygen gradients and hypoxic regions in the microenvironment (Worlitzsch et al., 2002). The heterogenous distribution of oxic and anoxic zones permits a mixture of aerobic and anaerobic microorganisms to be persistent members of such microenvironments (Carmody et al., 2018, Rogers et al., 2004, Tunney et al., 2008, Zemanick et al., 2010). Furthermore, such anaerobic species have been implicated in triggering the onset of severe inflammatory immune responses or worsening the pathogenicity of conventional CF pathogens (Flynn et al., 2016, Ghorbani et al., 2015, Mirković et al., 2015). Experimental limitations have prevented the successful co-culture of anaerobic and aerobic species associated with the CF microenvironment, hindering the study of such behaviours and causing the role of anaerobic species in driving changes in microbial physiology to still be contested in the literature (Caverly and LiPuma, 2018). Importantly, supplementing ASM with an excess of potassium nitrate did enable robust growth of anaerobic species in the *in vitro* model, largely at the expense of the growth of aerobic species (*Figure 7.9*). However, this observation, that a patient-derived population of anaerobic and aerobic bacteria can be maintained as a co-culture for 6 days using the continuous-flow model, indicates that by further optimising the concentration of nitrate in ASM it should eventually be possible to stably co-culture a balanced population in the same culture vessel.

The supplementation of ASM with FBS had the most dramatic and promising effect on promoting the growth of less abundant microbial species (*Figure 7.3*) and increasing the endpoint biodiversity of planktonic and sessile bacterial communities cultured *in vitro* (*Figure 7.4*). However, it is important to note that a loss of numerous low-abundance bacterial species present in the sputum inoculum still occurred and that altering the nutritional composition of

ASM must be treated with caution. Global transcriptomic studies comparing the growth of PA in ASM and airway secretions obtained from CF patients have revealed near identical gene expression profiles (Fung et al., 2010, Turner et al., 2015, Palmer et al., 2005). Hence, altering the chemical composition of the medium may result in a departure of microbial behaviour and physiology from what may be occurring *in situ*. However, this change in the physiological similarity of ASM to airway secretions may be a necessary trade-off to permit the *in vitro* co-culture of entire patient-derived polymicrobial populations. In *Section 7.5* I aimed to screen different fractions of FBS to try and decipher the specific component(s) of the supplement responsible for enhancing the growth of less abundant and fastidious bacteria. As supplementing ASM with a single additive or a small number of key chemically-defined additives is the best route towards reproducibility and measuring subtle interspecies interactions within confidence.

As detailed in *Section 7.5*, it may be hypothesised that a non-lipophilic component of FBS, 5-30 kDa in size, is responsible for enhancing the endpoint bacterial diversity of polymicrobial populations cultured under continuous-flow conditions (*Figure 7.14*). However, as already discussed the biocorrosion of the stainless-steel biofilm containers (*Figure 7.20*) and the loss of PA from all co-cultures (*Figure 7.15*) means that no further comment on this hypothesis can be made at this time. However, further systematic screening of this supplement fraction at different concentrations would corroborate and/or identify the key supplement(s) for enhancing the growth of less abundant bacteria. My initial hypothesis that albumin-mediated inhibition of PA QS networks (Smith et al., 2017) might lead to a decrease in virulence factor production, thereby enabling the growth of the rarer sputum-associated bacteria appears to be incorrect. This is because the species diversity in endpoint samples obtained from the culture vessel supplemented with BSA alone were lower than they were in unadulterated ASM (*Figure 7.14*). Although a complex and onerous undertaking, future systematic refinement of ASM supplements will be necessary to maintain a true polymicrobial microbiota *in vitro*, given that optimisation of Q alone is not sufficient for this goal to be realised.

A correlation between the loss of PA and an increase in overall bacterial species diversity in endpoint polymicrobial populations co-cultured *in vitro* can be observed across the results presented in *Section 7*. This is consistent with existing reports that a worsening of CF patient prognosis and pulmonary lung function is linked to both the establishment of chronic infection with PA and a decrease in species diversity within the airways (Zhao et al., 2012). Once PA establishes an infection in the CF airways it is near-impossible to eradicate with aggressive clinical and antimicrobial interventions (Fodor et al., 2012, Pressler et al., 2011). This observation may therefore suggest some therapeutic potential in encouraging the controlled growth of avirulent species in the CF microenvironment to beneficially provide a degree of

colonisation resistance (Kim et al., 2017) against the establishment of chronic infection with virulent pathogenic species *in situ*. Once fully refined, the *in vitro* continuous-flow model may provide an experimentally tractable tool to investigate this hypothesis in future research projects.

It is important to note that, due to the high costs associated with the preparation and sequencing of libraries for MiSeq analysis, only the bacterial ecology of sputum samples cultured *in vitro*, via sequencing of the V3/4 hypervariable region of the 16S rRNA gene, was assessed throughout this work and is a major limitation of the present study. Hence, changes in the ecology of the fungal population (potentially) present in the sputum samples over time in response to changes in bacterial ecology could not be discerned. However, MiSeq analysis of the ITS region of the 18S rRNA gene from fungal species and comparison of the output with the ITS2 gene database (Schultz et al., 2006) would be simple to perform. Combined with 16S analysis this would powerfully describe entire community wide changes in microbial ecology over time in the model.

8.5 Benefits and limitations of the continuous-flow model

As an *in vitro* model, the continuous-flow culture vessel has several advantages and limitations compared with existing models used in the study of infections associated with the CF airways. First, like all *in vitro* models it is inexpensive to set up and run, with the largest expense being the initial cost of a peristaltic pump and culture vessel components. Furthermore, the model is purposefully simple in design to enable users with little-to-no experience to set up and operate. In combination these factors make the model very accessible and help promote uptake among other research groups regardless of expertise or experience. Samples could even be removed from a steady-state microbial population, freeze dried and sent to other research groups using the model for reconstitution and further analysis. This would enable effective peer-to-peer collaboration, an assurance of experimental reproducibility and the mitigation of user/lab bias when studying complex polymicrobial consortia. Second, the simplicity and modular nature of the model ensures it is easy to multiplex the number of culture vessels studied in tandem and to include additional in-line analytical instruments, such as the in-line spectrophotometer described in *Section 2.3.1* or novel components such as real-time O₂ and pH probes. The only limiting factor for increasing the model's throughput is the labour-intensive production and filtration of fresh ASM.

As an *in vitro* alternative to animal models, there are no ethical concerns when using the continuous-flow system and my model is fully compliant with the “3Rs” (the replacement, refinement and reduction of the use of animals in research). Although the exact figures are

hard to extract, it is estimated that in the UK alone over 90,000 mice die per annum as a direct result of research into respiratory infections (personal communication with the NC3Rs). Widespread uptake of my model would therefore directly reduce the burdening cost of animal life when studying CF airway infections or polymicrobial community interactions. Perhaps more importantly, the conditions in the culture vessels are defined and there need be no inherent genetic variation among the host organism inocula. The lack of variation between culture vessels ensures that the model is extremely robust, as evidenced by the remarkably stable cell titres and small error bars observed between independent experiments presented across this study.

Given that ASM is a biochemically defined growth medium, subtle interspecies interactions and changes in environmental homeostasis or microbe behaviour can be measured with confidence and not attributed to changes in a host organism's biology as the result of infection. This also enables the facile experimental perturbation of culture conditions, *i.e.* through altering the composition of ASM, environmental conditions such as temperature or the exogenous perturbation of a steady-state culture with antimicrobials or new species/strain variants, as demonstrated in *Section 5*. An *in vitro* model also enables the time-resolved and sequential sampling of the same steady-state culture. This enables the longitudinal study of a polymicrobial consortium for an indefinite amount of time, something not possible with *in situ* sampling or when sacrificing *in vivo* models at various time points. These factors ensure that the continuous-flow model will prove to be a valuable research tool for the study of chronic CF airway infection scenarios.

The continuous-flow model is also subject to a number of perceived disadvantages. Although ASM is biochemically representative of CF airway secretions, and PA gene expression in this medium displays virtually no transcriptomic differences compared with growth in CF sputum (Fung et al., 2010, Turner et al., 2015), the *in vitro* model lacks the spatial organisation of the CF airway microenvironment *in situ*. Existing studies have shown that microbial growth *ex situ* on porcine lung tissue, which shares a remarkable degree of spatial homology with the human airways (Meurens et al., 2012, Rogers et al., 2008), displays similar behavioural growth characteristics to those observed *in situ* (Harrison et al., 2014, Harrison and Diggle, 2016). The introduction of removable sections of solid substrata, *i.e.* *ex vivo* porcine lung tissue sections (*Section 6.4*), to the culture vessel also results in significant changes in the dynamics of biofilm formation (discussed in *Section 8.3*). This shows that, where required, an element of *ex situ* spatial organisation can be easily introduced to my *in vitro* model. However, caution should be taken when introducing undefined elements (such as animal tissue) to the chemically-defined culture medium to ensure uniformity across experiments.

The absence of host cells/tissues and the role of an immune system in modulating microbial behaviour is another key limitation of the *in vitro* model. These factors limit the use of my model in the study of host-microbe interactions and how a polymicrobial consortium responds to, or causes, changes in environmental conditions, *i.e.* during acute pulmonary exacerbations. This being said, it is important to note that few *in vivo* models accurately capture the human CF airway environment, and no such model has yet been successful in recapitulating an entire CF polymicrobial community within the laboratory (O'Brien and Welch, 2019b). The simplicity and well-defined nature of the continuous-flow model is beneficial for the study of purely microbe-microbe interspecies interactions under defined environmental conditions. Furthermore, it allows for the direct comparison of results between experiments without the added complication of host-microbe interactions and changes driven by the actions of an immune system; something difficult to reproducibly achieve when utilising animal models. Hypothetically it may be possible to introduce a CF relevant human cell line, such as immortalised phe508del CFTR tracheal epithelial cells (Kunzelmann et al., 1993), to the culture vessel using bioengineering methods such as hollow fibre cell culture (Storm et al., 2016). Although complicated to achieve, this may enable the stable co-cultivation of a polymicrobial community with clinically relevant host tissues to discern key host-microbe interactions that would greatly benefit the development and validation of effective CF therapeutics. This notwithstanding, the original aims of this study were to develop a model to permit the stable long-term co-culture of microbial communities to enable the future investigation of interspecies interactions and changes in community architecture overtime. Consequently, the possibilities of stable host-bacterium culture methods were not explored.

An important experimental consideration and potential limitation when using the continuous-flow culture model in the study of novel and uncharacterised polymicrobial populations is the need to optimise Q between experiments utilising different microorganisms. The optimisation of Q is a balancing act of simultaneously preventing species washout while preventing population overgrowth and entry into the stationary phase due to nutrient limitation. The importance of optimising Q was made apparent throughout this work, both when culturing CA as part of a triple-species co-culture (*Section 3*) and when cultivating the polymicrobial communities derived from CF sputum samples (*Section 7*). As demonstrated in *Section 7.3*, Q can be optimised for the study of entire polymicrobial populations, although some refinement will be essential for the *in vitro* study of faster or slower growing microorganisms.

9. Final Conclusions

The role of interspecies interactions in modulating changes in the metabolism, behaviour and gene expression of microbial species is now clearly apparent in the field of medical microbiology. There is an increasingly important need to consider the presence of co-cultivated and low-abundance species when studying clinical infection scenarios, something particularly relevant in the context of CF airway infections. Chronic obstruction of the airways predisposes such patients to lifelong (and often terminal) infections with dense and diverse polymicrobial ecosystems. Despite intensive research efforts, once established, these airway infections are near impossible to eradicate with existing treatment options; treatment options that are often validated against axenic microbial populations. A detailed understanding of how an entire microbial community behaves and responds to therapeutic intervention would enable the development of more efficacious treatments to treat and limit the establishment of chronic airway infections to improve the longevity and welfare of persons with CF.

Effective research into the behaviours of mixed microbial populations has been hindered by the out-competition and removal of species when grown as a co-culture using traditional batch techniques. I redress this issue in the current study by describing the development, optimisation and characterisation of a novel, continuous-flow model that permits long-term maintenance of a diverse group of microbial species including *P. aeruginosa* (Gram-negative bacterium), *S. aureus* (Gram-positive bacterium) and *C. albicans* (dimorphic fungi), all of which are commonly associated with CF airway infections. To the best of my knowledge, this is the first *in vitro*, *in vivo* or *ex vivo* model that permits the stable co-culture of these pathogens with respect to cell titres, metabolic state, mutation rates and virulence factor production. I also demonstrate that low-abundance species, representing less than 0.05% (by cell numbers) in a population, can significantly modulate microbial behaviour and the formation of polymicrobial biofilms. Furthermore, I demonstrate an increased refractory response of pre-established polymicrobial communities to treatment with clinically-relevant antimicrobial compounds and identify novel SNPs in the *P. aeruginosa* genome that confer a complete resistance to the action of colistin.

Although I was not able to recapitulate an entire, stable polymicrobial consortium derived from the airways of a persons with CF, this work provides the groundwork for future research efforts in doing so. Success in achieving this aim would enable the facile and detailed experimental study of polymicrobial interactions in a reproducible setup. Such a system would also help to bridge the bench-to-bedside gap when studying chronic obstructive pulmonary disorders and enable the development of improved airway management treatments. The purposefully simple, modular and robust nature of my model should hopefully promote widespread uptake

of the system by other research groups. In summary, any number of fundamental biological questions pertaining to the understanding of interspecies interactions, and to the growth of entire microbial communities in the context of CF could be investigated using my continuous-flow model.

10. References

- Cystic Fibrosis Foundation (www.cff.org).
- Cystic Fibrosis Mutation Database (www.genet.sickkids.on.20ca/cftr/).
2015. Cystic Fibrosis Foundation Patient Registry Annual Data Report 2015. Bethesda.
- AANEN, D. K. & DEBETS, A. J. M. 2019. Mutation-rate plasticity and the germline of unicellular organisms. *Proc Biol Sci*, 286, 20190128.
- ABISADO, R. G., BENOMAR, S., KLAUS, J. R., DANDEKAR, A. A. & CHANDLER, J. R. 2018. Bacterial Quorum Sensing and Microbial Community Interactions. *mBio*, 9.
- ADAM, B., BAILLIE, G. S. & DOUGLAS, L. J. 2002. Mixed species biofilms of *Candida albicans* and *Staphylococcus epidermidis*. *J Med Microbiol*, 51, 344-349.
- AGRAWAL, A., RANGARAJAN, N. & WEISSHAAR, J. C. 2019. Resistance of early stationary phase *E. coli* to membrane permeabilization by the antimicrobial peptide Cecropin A. *Biochim Biophys Acta Biomembr*, 1861, 182990.
- AHMED, B., COX, M. J., CUTHBERTSON, L., JAMES, P., COOKSON, W. O. C., DAVIES, J. C., MOFFATT, M. F. & BUSH, A. 2019. Longitudinal development of the airway microbiota in infants with cystic fibrosis. *Sci Rep*, 9, 5143.
- AHMED, B., COX, M. J., CUTHBERTSON, L., JAMES, P. L., COOKSON, W. O. C., DAVIES, J. C., MOFFATT, M. F. & BUSH, A. 2018. Comparison of the upper and lower airway microbiota in children with chronic lung diseases. *PLoS One*, 13, e0201156.
- AKLUJKAR, M., RISSO, C., SMITH, J., BEAULIEU, D., DUBAY, R., GILTEAUX, L., DIBURRO, K. & HOLMES, D. 2014. Anaerobic degradation of aromatic amino acids by the hyperthermophilic archaeon *Ferroglobus placidus*. *Microbiology (Reading)*, 160, 2694-2709.
- AL-BAKRI, A. G., GILBERT, P. & ALLISON, D. G. 2005. Influence of gentamicin and tobramycin on binary biofilm formation by co-cultures of *Burkholderia cepacia* and *Pseudomonas aeruginosa*. *J Basic Microbiol*, 45, 392-6.
- ALCÁNTARA, S., VELASCO, A. & REVAH, S. 2004. Sulfur formation by steady-state continuous cultures of a sulfoxidizing consortium and *Thiobacillus thioparus* ATCC 23645. *Environ Technol*, 25, 1151-7.
- ALLEN, R. J. & WACLAW, B. 2019. Bacterial growth: a statistical physicist's guide. *Rep Prog Phys*, 82, 016601.
- ALMEIDA, R. S., WILSON, D. & HUBE, B. 2009. *Candida albicans* iron acquisition within the host. *FEMS Yeast Res*, 9, 1000-12.
- AMIR, A., MCDONALD, D., NAVAS-MOLINA, J. A., KOPYLOVA, E., MORTON, J. T., ZECH XU, Z., KIGHTLEY, E. P., THOMPSON, L. R., HYDE, E. R., GONZALEZ, A. & KNIGHT, R. 2017. Deblur Rapidly Resolves Single-Nucleotide Community Sequence Patterns. *mSystems*, 2.
- ANDERL, J. N., ZÄHLER, J., ROE, F. & STEWART, P. S. 2003. Role of nutrient limitation and stationary-phase existence in *Klebsiella pneumoniae* biofilm resistance to ampicillin and ciprofloxacin. *Antimicrob Agents Chemother*, 47, 1251-6.
- ANDREWS, S. C., ROBINSON, A. K. & RODRÍGUEZ-QUIÑONES, F. 2003. Bacterial iron homeostasis. *FEMS Microbiol Rev*, 27, 215-37.
- ANTONIC, V., STOJADINOVIC, A., ZHANG, B., IZADJOO, M. J. & ALAVI, M. 2013. *Pseudomonas aeruginosa* induces pigment production and enhances virulence in a white phenotypic variant of *Staphylococcus aureus*. *Infect Drug Resist*, 6, 175-86.
- ARDON, O., BUSSEY, H., PHILPOTT, C., WARD, D. M., DAVIS-KAPLAN, S., VERRONEAU, S., JIANG, B. & KAPLAN, J. 2001. Identification of a *Candida albicans* ferrichrome transporter and its characterization by expression in *Saccharomyces cerevisiae*. *J Biol Chem*, 276, 43049-55.
- ARMBRUSTER, C. E., HONG, W., PANG, B., WEIMER, K. E., JUNEAU, R. A., TURNER, J. & SWORDS, W. E. 2010. Indirect pathogenicity of *Haemophilus influenzae* and *Moraxella catarrhalis* in polymicrobial otitis media occurs via interspecies quorum signaling. *mBio*, 1.

- ARMBRUSTER, C. R., WOLTER, D. J., MISHRA, M., HAYDEN, H. S., RADEY, M. C., MERRIHEW, G., MACCOSS, M. J., BURNS, J., WOZNIAK, D. J., PARSEK, M. R. & HOFFMAN, L. R. 2016. Staphylococcus aureus Protein A Mediates Interspecies Interactions at the Cell Surface of Pseudomonas aeruginosa. *mBio*, 7.
- ARMITAGE, P. 1952. The Statistical Theory of Bacterial Populations Subject to Mutation. Journal of the Royal Statistical Society. Series B (Methodological).
- ASOKAN, G. V., RAMADHAN, T., AHMED, E. & SANAD, H. 2019. WHO Global Priority Pathogens List: A Bibliometric Analysis of Medline-PubMed for Knowledge Mobilization to Infection Prevention and Control Practices in Bahrain. *Oman Med J*, 34, 184-193.
- ASTERIS, G. & SARKAR, S. 1996. Bayesian procedures for the estimation of mutation rates from fluctuation experiments. *Genetics*, 142, 313-26.
- BALDAN, R., CIGANA, C., TESTA, F., BIANCONI, I., DE SIMONE, M., PELLIN, D., DI SERIO, C., BRAGONZI, A. & CIRILLO, D. M. 2014. Adaptation of Pseudomonas aeruginosa in Cystic Fibrosis airways influences virulence of Staphylococcus aureus in vitro and murine models of co-infection. *PLoS One*, 9, e89614.
- BANAS, J. A., MILLER, J. D., FUSCHINO, M. E., HAZLETT, K. R., TOYOFUKU, W., PORTER, K. A., REUTZEL, S. B., FLORCZYK, M. A., MCDONOUGH, K. A. & MICHALEK, S. M. 2007. Evidence that accumulation of mutants in a biofilm reflects natural selection rather than stress-induced adaptive mutation. *Appl Environ Microbiol*, 73, 357-61.
- BARNABIE, P. M. & WHITELEY, M. 2015. Iron-Mediated Control of Pseudomonas aeruginosa-Staphylococcus aureus Interactions in the Cystic Fibrosis Lung. *J Bacteriol*, 197, 2250-1.
- BARON, S. S. & ROWE, J. J. 1981. Antibiotic action of pyocyanin. *Antimicrob Agents Chemother*, 20, 814-20.
- BEAUME, M., KÖHLER, T., FONTANA, T., TOGNON, M., RENZONI, A. & VAN DELDEN, C. 2015. Metabolic pathways of Pseudomonas aeruginosa involved in competition with respiratory bacterial pathogens. *Front Microbiol*, 6, 321.
- BELL, S. C., MALL, M. A., GUTIERREZ, H., MACEK, M., MADGE, S., DAVIES, J. C., BURGEL, P. R., TULLIS, E., CASTAÑOS, C., CASTELLANI, C., BYRNES, C. A., CATHCART, F., CHOTIRMALL, S. H., COSGRIFF, R., EICHLER, I., FAJAC, I., GOSS, C. H., DREVINEK, P., FARRELL, P. M., GRAVELLE, A. M., HAVERMANS, T., MAYER-HAMBLETT, N., KASHIRSKAYA, N., KEREM, E., MATHEW, J. L., MCKONE, E. F., NAEHRLICH, L., NASR, S. Z., OATES, G. R., O'NEILL, C., PYPOPS, U., RARAIGH, K. S., ROWE, S. M., SOUTHERN, K. W., SIVAM, S., STEPHENSON, A. L., ZAMPOLI, M. & RATJEN, F. 2020. The future of cystic fibrosis care: a global perspective. *Lancet Respir Med*, 8, 65-124.
- BEN HAJ KHALIFA, A., MOISSENET, D., VU THIEN, H. & KHEDHER, M. 2011. [Virulence factors in Pseudomonas aeruginosa: mechanisms and modes of regulation]. *Ann Biol Clin (Paris)*, 69, 393-403.
- BERNHARD, W., HOFFMANN, S., DOMBROWSKY, H., RAU, G. A., KAMLAGE, A., KAPPLER, M., HAITSMA, J. J., FREIHORST, J., VON DER HARDT, H. & POETS, C. F. 2001. Phosphatidylcholine molecular species in lung surfactant: composition in relation to respiratory rate and lung development. *Am J Respir Cell Mol Biol*, 25, 725-31.
- BERTRAND, R. L. 2019. Lag Phase Is a Dynamic, Organized, Adaptive, and Evolvable Period That Prepares Bacteria for Cell Division. *J Bacteriol*, 201.
- BESSA, L. J., CORREIA, D. M., CELLINI, L., AZEVEDO, N. F. & ROCHA, I. 2012. Optimization of culture conditions to improve Helicobacter pylori growth in Ham's F-12 medium by response surface methodology. *Int J Immunopathol Pharmacol*, 25, 901-9.
- BIALVAEI, A. Z. & SAMADI KAFIL, H. 2015. Colistin, mechanisms and prevalence of resistance. *Curr Med Res Opin*, 31, 707-21.
- BISELLI, E., SCHINK, S. J. & GERLAND, U. 2020. Slower growth of Escherichia coli leads to longer survival in carbon starvation due to a decrease in the maintenance rate. *Mol Syst Biol*, 16, e9478.

- BISHT, K., BAISHYA, J. & WAKEMAN, C. A. 2020. *Pseudomonas aeruginosa* polymicrobial interactions during lung infection. *Curr Opin Microbiol*, 53, 1-8.
- BITTAR, F. & ROLAIN, J. M. 2010. Detection and accurate identification of new or emerging bacteria in cystic fibrosis patients. *Clin Microbiol Infect*, 16, 809-20.
- BJARNSHOLT, T. & GIVSKOV, M. 2007. The role of quorum sensing in the pathogenicity of the cunning aggressor *Pseudomonas aeruginosa*. *Anal Bioanal Chem*, 387, 409-14.
- BJARNSHOLT, T., JENSEN, P., FIANDACA, M. J., PEDERSEN, J., HANSEN, C. R., ANDERSEN, C. B., PRESSLER, T., GIVSKOV, M. & HØIBY, N. 2009. *Pseudomonas aeruginosa* biofilms in the respiratory tract of cystic fibrosis patients. *Pediatr Pulmonol*, 44, 547-58.
- BJORNSON, H. S., COLLEY, R., BOWER, R. H., DUTY, V. P., SCHWARTZ-FULTON, J. T. & FISCHER, J. E. 1982. Association between microorganism growth at the catheter insertion site and colonization of the catheter in patients receiving total parenteral nutrition. *Surgery*, 92, 720-7.
- BLATTNER, F. R., PLUNKETT, G., BLOCH, C. A., PERNA, N. T., BURLAND, V., RILEY, M., COLLADO-VIDES, J., GLASNER, J. D., RODE, C. K., MAYHEW, G. F., GREGOR, J., DAVIS, N. W., KIRKPATRICK, H. A., GOEDEN, M. A., ROSE, D. J., MAU, B. & SHAO, Y. 1997. The complete genome sequence of *Escherichia coli* K-12. *Science*, 277, 1453-62.
- BLEVES, S., VIARRE, V., SALACHA, R., MICHEL, G. P., FILLOUX, A. & VOULHOUX, R. 2010. Protein secretion systems in *Pseudomonas aeruginosa*: A wealth of pathogenic weapons. *Int J Med Microbiol*, 300, 534-43.
- BOBADILLA, J. L., MACEK, M., FINE, J. P. & FARRELL, P. M. 2002. Cystic fibrosis: a worldwide analysis of CFTR mutations--correlation with incidence data and application to screening. *Hum Mutat*, 19, 575-606.
- BOGAERT, D., VAN BELKUM, A., SLUIJTER, M., LUIJENDIJK, A., DE GROOT, R., RÜMKE, H. C., VERBRUGH, H. A. & HERMANS, P. W. 2004. Colonisation by *Streptococcus pneumoniae* and *Staphylococcus aureus* in healthy children. *Lancet*, 363, 1871-2.
- BOLYEN, E., RIDEOUT, J. R., DILLON, M. R., BOKULICH, N. A., ABNET, C. C., AL-GHALITH, G. A., ALEXANDER, H., ALM, E. J., ARUMUGAM, M., ASNICAR, F., BAI, Y., BISANZ, J. E., BITTINGER, K., BREJNROD, A., BRISLAWN, C. J., BROWN, C. T., CALLAHAN, B. J., CARABALLO-RODRÍGUEZ, A. M., CHASE, J., COPE, E. K., DA SILVA, R., DIENER, C., DORRESTEIN, P. C., DOUGLAS, G. M., DURALL, D. M., DUVALLET, C., EDWARDSON, C. F., ERNST, M., ESTAKI, M., FOUQUIER, J., GAUGLITZ, J. M., GIBBONS, S. M., GIBSON, D. L., GONZALEZ, A., GORLICK, K., GUO, J., HILLMANN, B., HOLMES, S., HOLSTE, H., HUTTENHOWER, C., HUTTLEY, G. A., JANSSEN, S., JARMUSCH, A. K., JIANG, L., KAEHLER, B. D., KANG, K. B., KEEFE, C. R., KEIM, P., KELLEY, S. T., KNIGHTS, D., KOESTER, I., KOSCIOLEK, T., KREPS, J., LANGILLE, M. G. I., LEE, J., LEY, R., LIU, Y. X., LOFTFIELD, E., LOZUPONE, C., MAHER, M., MAROTZ, C., MARTIN, B. D., MCDONALD, D., MCIVER, L. J., MELNIK, A. V., METCALF, J. L., MORGAN, S. C., MORTON, J. T., NAIMEY, A. T., NAVAS-MOLINA, J. A., NOTHIAS, L. F., ORCHANIAN, S. B., PEARSON, T., PEOPLES, S. L., PETRAS, D., PREUSS, M. L., PRUESSE, E., RASMUSSEN, L. B., RIVERS, A., ROBESON, M. S., ROSENTHAL, P., SEGATA, N., SHAFFER, M., SHIFFER, A., SINHA, R., SONG, S. J., SPEAR, J. R., SWAFFORD, A. D., THOMPSON, L. R., TORRES, P. J., TRINH, P., TRIPATHI, A., TURNBAUGH, P. J., UL-HASAN, S., VAN DER HOOFT, J. J. J., VARGAS, F., VÁZQUEZ-BAEZA, Y., VOGTMANN, E., VON HIPPEL, M., WALTERS, W., et al. 2019. Reproducible, interactive, scalable and extensible microbiome data science using QIIME 2. *Nat Biotechnol*, 37, 852-857.
- BONFIELD, T. & CHMIEL, J. F. 2017. Impaired innate immune cells in cystic fibrosis: Is it really a surprise? *J Cyst Fibros*, 16, 433-435.
- BONNEAU, A., ROCHE, B. & SCHALK, I. J. 2020. Iron acquisition in *Pseudomonas aeruginosa* by the siderophore pyoverdine: an intricate interacting network including periplasmic and membrane proteins. *Sci Rep*, 10, 120.
- BORISOVA, M., GAUPP, R., DUCKWORTH, A., SCHNEIDER, A., DALÜGGE, D., MÜHLECK, M., DEUBEL, D., UNSLEBER, S., YU, W., MUTH, G., BISCHOFF, M., GÖTZ, F. & MAYER, C. 2016.

- Peptidoglycan Recycling in Gram-Positive Bacteria Is Crucial for Survival in Stationary Phase. *mBio*, 7.
- BOUCHER, J. C., YU, H., MUDD, M. H. & DERETIC, V. 1997. Mucoid *Pseudomonas aeruginosa* in cystic fibrosis: characterization of muc mutations in clinical isolates and analysis of clearance in a mouse model of respiratory infection. *Infect Immun*, 65, 3838-46.
- BOUCHER, R. C. 2002. An overview of the pathogenesis of cystic fibrosis lung disease. *Advanced Drug Delivery Reviews*, 54, 1359 - 1371.
- BOUTIN, S., GRAEBER, S. Y., WEITNAUER, M., PANITZ, J., STAHL, M., CLAUSZNITZER, D., KADERALI, L., EINARSSON, G., TUNNEY, M. M., ELBORN, J. S., MALL, M. A. & DALPKE, A. H. 2015. Comparison of microbiomes from different niches of upper and lower airways in children and adolescents with cystic fibrosis. *PLoS One*, 10, e0116029.
- BOYD, A. & CHAKRABARTY, A. M. 1995. *Pseudomonas aeruginosa* biofilms: role of the alginate exopolysaccharide. *J Ind Microbiol*, 15, 162-8.
- BOYLE, M. P. & DE BOECK, K. 2013. A new era in the treatment of cystic fibrosis: correction of the underlying CFTR defect. *Lancet Respir Med*, 1, 158-63.
- BRAGONZI, A., FARULLA, I., PARONI, M., TWOMEY, K. B., PIRONE, L., LORÈ, N. I., BIANCONI, I., DALMASTRI, C., RYAN, R. P. & BEVIVINO, A. 2012. Modelling co-infection of the cystic fibrosis lung by *Pseudomonas aeruginosa* and *Burkholderia cenocepacia* reveals influences on biofilm formation and host response. *PLoS One*, 7, e52330.
- BRAY, J. R. A. C. J. T. 1957. An Ordination of the Upland Forest Communities of Southern Wisconsin. *Ecological Monographs*, 27, 325-349.
- BRIAUD, P., CAMUS, L., BASTIEN, S., DOLÉANS-JORDHEIM, A., VANDENESCH, F. & MOREAU, K. 2019. Coexistence with *Pseudomonas aeruginosa* alters *Staphylococcus aureus* transcriptome, antibiotic resistance and internalization into epithelial cells. *Sci Rep*, 9, 16564.
- BRUSCIA, E. M. & BONFIELD, T. L. 2016. Cystic Fibrosis Lung Immunity: The Role of the Macrophage. *J Innate Immun*, 8, 550-563.
- BUCIOR, I., PIELAGE, J. F. & ENGEL, J. N. 2012. *Pseudomonas aeruginosa* pili and flagella mediate distinct binding and signaling events at the apical and basolateral surface of airway epithelium. *PLoS Pathog*, 8, e1002616.
- BURMØLLE, M., WEBB, J. S., RAO, D., HANSEN, L. H., SØRENSEN, S. J. & KJELLEBERG, S. 2006. Enhanced biofilm formation and increased resistance to antimicrobial agents and bacterial invasion are caused by synergistic interactions in multispecies biofilms. *Appl Environ Microbiol*, 72, 3916-23.
- BURNS, J. L. & ROLAIN, J. M. 2014. Culture-based diagnostic microbiology in cystic fibrosis: can we simplify the complexity? *J Cyst Fibros*, 13, 1-9.
- BURROWS, L. L., CHARTER, D. F. & LAM, J. S. 1996. Molecular characterization of the *Pseudomonas aeruginosa* serotype O5 (PAO1) B-band lipopolysaccharide gene cluster. *Molecular Biology*, 22, 481 - 495.
- C.J., F., R.P., H., O., S., B.T., M., C.M., D., R.N., A., A.R., H., P., S., Y., H., A.R.M., C. & S., W. J. 2018. Increased rates of genomic mutation in a biofilm co-culture model of *Pseudomonas aeruginosa* and *Staphylococcus aureus*. *BioRx*.
- CARDOZO, V. F., OLIVEIRA, A. G., NISHIO, E. K., PERUGINI, M. R., ANDRADE, C. G., SILVEIRA, W. D., DURÁN, N., ANDRADE, G., KOBAYASHI, R. K. & NAKAZATO, G. 2013. Antibacterial activity of extracellular compounds produced by a *Pseudomonas* strain against methicillin-resistant *Staphylococcus aureus* (MRSA) strains. *Ann Clin Microbiol Antimicrob*, 12, 12.
- CARLSSON, M., SJÖHOLM, A. G., ERIKSSON, L., THIEL, S., JENSENIUS, J. C., SEGELMARK, M. & TRUEDSSON, L. 2005. Deficiency of the mannan-binding lectin pathway of complement and poor outcome in cystic fibrosis: bacterial colonization may be decisive for a relationship. *Clin Exp Immunol*, 139, 306-13.

- CARMODY, L. A., CAVERLY, L. J., FOSTER, B. K., ROGERS, M. A. M., KALIKIN, L. M., SIMON, R. H., VANDEVANTER, D. R. & LIPUMA, J. J. 2018. Fluctuations in airway bacterial communities associated with clinical states and disease stages in cystic fibrosis. *PLoS One*, 13, e0194060.
- CARMODY, L. A., ZHAO, J., KALIKIN, L. M., LEBAR, W., SIMON, R. H., VENKATARAMAN, A., SCHMIDT, T. M., ABDO, Z., SCHLOSS, P. D. & LIPUMA, J. J. 2015. The daily dynamics of cystic fibrosis airway microbiota during clinical stability and at exacerbation. *Microbiome*, 3, 12.
- CARMODY, L. A., ZHAO, J., SCHLOSS, P. D., PETROSINO, J. F., MURRAY, S., YOUNG, V. B., LI, J. Z. & LIPUMA, J. J. 2013. Changes in cystic fibrosis airway microbiota at pulmonary exacerbation. *Ann Am Thorac Soc*, 10, 179-87.
- CAROLUS, H., VAN DYCK, K. & VAN DIJCK, P. 2019. *Candida albicans* and *Staphylococcus* species: A Threatening Twosome. *Front Microbiol*, 10, 2162.
- CAVERLY, L. J. & LIPUMA, J. J. 2018. Good cop, bad cop: anaerobes in cystic fibrosis airways. *Eur Respir J*, 52.
- CHAMBERS, L. A., ROLLINS, B. M. & TARRAN, R. 2007. Liquid movement across the surface epithelium of large airways. *Respir Physiol Neurobiol*, 159, 256-70.
- CHARLSON, E. S., BITTINGER, K., HAAS, A. R., FITZGERALD, A. S., FRANK, I., YADAV, A., BUSHMAN, F. D. & COLLMAN, R. G. 2011. Topographical continuity of bacterial populations in the healthy human respiratory tract. *Am J Respir Crit Care Med*, 184, 957-63.
- CHATTORAJ, S. S., MURTHY, R., GANESAN, S., GOLDBERG, J. B., ZHAO, Y., HERSHENSON, M. B. & SAJJAN, U. S. 2010. *Pseudomonas aeruginosa* alginate promotes *Burkholderia cenocepacia* persistence in cystic fibrosis transmembrane conductance regulator knockout mice. *Infect Immun*, 78, 984-93.
- CHEN, P., WANG, J. J., HONG, B., TAN, L., YAN, J., ZHANG, Z., LIU, H., PAN, Y. & ZHAO, Y. 2019. Characterization of Mixed-Species Biofilm Formed by *Vibrio parahaemolyticus* and *Listeria monocytogenes*. *Front Microbiol*, 10, 2543.
- CHESBRO, W., ARBIGE, M. & EIFERT, R. 1990. When nutrient limitation places bacteria in the domains of slow growth: metabolic, morphologic and cell cycle behaviour *FEMS Microbiology Letters*, 74, 103 - 119.
- CHEW, S. C., KUNDUKAD, B., SEVIOUR, T., VAN DER MAAREL, J. R., YANG, L., RICE, S. A., DOYLE, P. & KJELLEBERG, S. 2014. Dynamic remodeling of microbial biofilms by functionally distinct exopolysaccharides. *mBio*, 5, e01536-14.
- CHMIEL, J. F. & DAVIS, P. B. 2003. State of the art: why do the lungs of patients with cystic fibrosis become infected and why can't they clear the infection? *Respir Res*, 4, 8.
- CHOTIRMALL, S. H., O'DONOGHUE, E., BENNETT, K., GUNARATNAM, C., O'NEILL, S. J. & MCELVANEY, N. G. 2010. Sputum *Candida albicans* presages FEV₁ decline and hospital-treated exacerbations in cystic fibrosis. *Chest*, 138, 1186-95.
- CIANCIOOTTO, N. P. 2005. Type II secretion: a protein secretion system for all seasons. *Trends Microbiol*, 13, 581-8.
- CIGANA, C., BIANCONI, I., BALDAN, R., DE SIMONE, M., RIVA, C., SIPIONE, B., ROSSI, G., CIRILLO, D. M. & BRAGONZI, A. 2018. *Staphylococcus aureus* Impacts *Pseudomonas aeruginosa* Chronic Respiratory Disease in Murine Models. *J Infect Dis*, 217, 933-942.
- CIOFU, O., HANSEN, C. R. & HØIBY, N. 2013. Respiratory bacterial infections in cystic fibrosis. *Curr Opin Pulm Med*, 19, 251-8.
- CIOFU, O. & TOLKER-NIELSEN, T. 2019. Tolerance and Resistance of *Pseudomonas aeruginosa* Biofilms to Antimicrobial Agents- How *P. aeruginosa* Can Escape Antibiotics. *Front Microbiol*, 10, 913.
- CLARK, D. 1981. Regulation of fatty acid degradation in *Escherichia coli*: analysis by operon fusion. *J Bacteriol*, 148, 521-6.
- CLARRIDGE, J. E. 2004. Impact of 16S rRNA gene sequence analysis for identification of bacteria on clinical microbiology and infectious diseases. *Clin Microbiol Rev*, 17, 840-62.

- COHEN, T. S. & PRINCE, A. 2012. Cystic fibrosis: a mucosal immunodeficiency syndrome. *Nat Med*, 18, 509-19.
- CONIBEAR, T. C., COLLINS, S. L. & WEBB, J. S. 2009. Role of mutation in *Pseudomonas aeruginosa* biofilm development. *PLoS One*, 4, e6289.
- CONRAD, D., HAYNES, M., SALAMON, P., RAINEY, P. B., YOULE, M. & ROHWER, F. 2013. Cystic fibrosis therapy: a community ecology perspective. *Am J Respir Cell Mol Biol*, 48, 150-6.
- CORNELIS, P. & DINGEMANS, J. 2013. *Pseudomonas aeruginosa* adapts its iron uptake strategies in function of the type of infections. *Front Cell Infect Microbiol*, 3, 75.
- CORNELIS, P. & MATTHIJS, S. 2007. *Pseudomonas Siderophores and their Biological Significance*, In: Varma A., Chincholkar S.B. (eds) *Microbial Siderophores*. Soil Biology, vol 12. Springer, Berlin, Heidelberg.
- CORTE, L., CASAGRANDE PIERANTONI, D., TASCINI, C., ROSCINI, L. & CARDINALI, G. 2019. Biofilm Specific Activity: A Measure to Quantify Microbial Biofilm. *Microorganisms*, 7.
- COSTA, O. Y. A., OGUEJIOFOR, C., ZÜHLKE, D., BARRETO, C. C., WÜNSCHE, C., RIEDEL, K. & KURAMAE, E. E. 2020. Impact of Different Trace Elements on the Growth and Proteome of Two Strains of *Granulicella*, Class "Acidobacteriia". *Front Microbiol*, 11, 1227.
- COSTERTON, J. W., GEESEY, G. G. & CHENG, K. J. 1978. How bacteria stick. *Sci Am*, 238, 86-95.
- COSTERTON, J. W., STEWART, P. S. & GREENBERG, E. P. 1999. Bacterial biofilms: a common cause of persistent infections. *Science*, 284, 1318-22.
- COX, M. J., ALLGAIER, M., TAYLOR, B., BAEK, M. S., HUANG, Y. J., DALY, R. A., KARAOZ, U., ANDERSEN, G. L., BROWN, R., FUJIMURA, K. E., WU, B., TRAN, D., KOFF, J., KLEINHENZ, M. E., NIELSON, D., BRODIE, E. L. & LYNCH, S. V. 2010. Airway microbiota and pathogen abundance in age-stratified cystic fibrosis patients. *PLoS One*, 5, e11044.
- CRUSZ, S. A., POPAT, R., RYBTKE, M. T., CÁMARA, M., GIVSKOV, M., TOLKER-NIELSEN, T., DIGGLE, S. P. & WILLIAMS, P. 2012. Bursting the bubble on bacterial biofilms: a flow cell methodology. *Biofouling*, 28, 835-42.
- CUGINI, C., CALFEE, M. W., FARROW, J. M., MORALES, D. K., PESCI, E. C. & HOGAN, D. A. 2007. Farnesol, a common sesquiterpene, inhibits PQS production in *Pseudomonas aeruginosa*. *Mol Microbiol*, 65, 896-906.
- CUGINI, C., MORALES, D. K. & HOGAN, D. A. 2010. *Candida albicans*-produced farnesol stimulates *Pseudomonas* quinolone signal production in LasR-defective *Pseudomonas aeruginosa* strains. *Microbiology*, 156, 3096-107.
- CURUTIU, C. H., OLBAN, A. M., DITU, L. M., BUGNAR, O., STEFAN, A., IORDACHE, F., BLEOTU, C., LAZAR, V. & CHIFIRIUC, M. C. 2016. Influence of cell-to-cell interactions and QS molecules on *Candida albicans* and *Pseudomonas aeruginosa* growth and adherence features. *26th European Congress of Clinical Microbiology and Infectious Diseases*. Amsterdam, Netherlands.
- CUTHBERTSON, L., ROGERS, G. B., WALKER, A. W., OLIVER, A., HAFIZ, T., HOFFMAN, L. R., CARROLL, M. P., PARKHILL, J., BRUCE, K. D. & VAN DER GAST, C. J. 2014. Time between collection and storage significantly influences bacterial sequence composition in sputum samples from cystic fibrosis respiratory infections. *J Clin Microbiol*, 52, 3011-6.
- CUTTING, G. R. 2010. Modifier genes in Mendelian disorders: the example of cystic fibrosis. *Ann N Y Acad Sci*, 1214, 57-69.
- DA SILVA, M. C., ZAHM, J. M., GRAS, D., BAJOLET, O., ABELY, M., HINNERSKY, J., MILLIOT, M., DE ASSIS, M. C., HOLOGNE, C., BONNET, N., MERTEN, M., PLOTKOWSKI, M. C. & PUCHELLE, E. 2004. Dynamic interaction between airway epithelial cells and *Staphylococcus aureus*. *Am J Physiol Lung Cell Mol Physiol*, 287, L543-51.
- DA, W., SHAO, J., LI, Q., SHI, G., WANG, T., WU, D. & WANG, C. 2019. Extraction of Extracellular Matrix in Static and Dynamic *Candida* Biofilms Using Cation Exchange Resin and Untargeted Analysis of Matrix Metabolites by Ultra-High-Performance Liquid Chromatography-Tandem Quadrupole Time-of-Flight Mass Spectrometry (ULPC-Q-TOF-MS). *Front Microbiol*, 10, 752.

- DALE, S. E., DOHERTY-KIRBY, A., LAJOIE, G. & HEINRICHS, D. E. 2004. Role of siderophore biosynthesis in virulence of *Staphylococcus aureus*: identification and characterization of genes involved in production of a siderophore. *Infect Immun*, 72, 29-37.
- DALTON, T., DOWD, S. E., WOLCOTT, R. D., SUN, Y., WATTERS, C., GRISWOLD, J. A. & RUMBAUGH, K. P. 2011. An in vivo polymicrobial biofilm wound infection model to study interspecies interactions. *PLoS One*, 6, e27317.
- DAVENPORT, P. W., GRIFFIN, J. L. & WELCH, M. 2015. Quorum Sensing Is Accompanied by Global Metabolic Changes in the Opportunistic Human Pathogen *Pseudomonas aeruginosa*. *J Bacteriol*, 197, 2072-82.
- DAVEY, M. E. & O'TOOLE, G. A. 2000. Microbial biofilms: from ecology to molecular genetics. *Microbiol Mol Biol Rev*, 64, 847-67.
- DAVIES, E. V., JAMES, C. E., BROCKHURST, M. A. & WINSTANLEY, C. 2017. Evolutionary diversification of *Pseudomonas aeruginosa* in an artificial sputum model. *BMC Microbiol*, 17, 3.
- DAVIES, E. V., JAMES, C. E., WILLIAMS, D., O'BRIEN, S., FOTHERGILL, J. L., HALDENBY, S., PATERSON, S., WINSTANLEY, C. & BROCKHURST, M. A. 2016. Temperate phages both mediate and drive adaptive evolution in pathogen biofilms. *Proc Natl Acad Sci U S A*, 113, 8266-71.
- DE BERNARDIS, F., MÜHLSCHLEGEL, F. A., CASSONE, A. & FONZI, W. A. 1998. The pH of the host niche controls gene expression in and virulence of *Candida albicans*. *Infect Immun*, 66, 3317-25.
- DE KIEVIT, T. R. 2009. Quorum sensing in *Pseudomonas aeruginosa* biofilms. *Environ Microbiol*, 11, 279-88.
- DELEON, S., CLINTON, A., FOWLER, H., EVERETT, J., HORSWILL, A. R. & RUMBAUGH, K. P. 2014. Synergistic interactions of *Pseudomonas aeruginosa* and *Staphylococcus aureus* in an in vitro wound model. *Infect Immun*, 82, 4718-28.
- DEMIREL, B. & SCHERER, P. 2011. Trace element requirements of agricultural biogas digesters during biological conversion of renewable biomass to methane. *Biomass and Bioenergy*, 35, 992 - 998.
- DERETIC, V., GOVAN, J. R., KONYECSNI, W. M. & MARTIN, D. W. 1990. Mucoicid *Pseudomonas aeruginosa* in cystic fibrosis: mutations in the muc loci affect transcription of the *algR* and *algD* genes in response to environmental stimuli. *Mol Microbiol*, 4, 189-96.
- DETTMAN, J. R., SZTEPANACZ, J. L. & KASSEN, R. 2016. The properties of spontaneous mutations in the opportunistic pathogen *Pseudomonas aeruginosa*. *BMC Genomics*, 17, 27.
- DEVAULT, J. D., KIMBARA, K. & CHAKRABARTY, A. M. 1990. Pulmonary dehydration and infection in cystic fibrosis: evidence that ethanol activates alginate gene expression and induction of mucoidy in *Pseudomonas aeruginosa*. *Mol Microbiol*, 4, 737-45.
- DIAZ IGLESIAS, Y., WILMS, T., VANBEVER, R. & VAN BAMBEKE, F. 2019. Activity of Antibiotics against *Staphylococcus aureus* in an. *Antimicrob Agents Chemother*, 63.
- DIGGLE, S. P., CORNELIS, P., WILLIAMS, P. & CÁMARA, M. 2006. 4-quinolone signalling in *Pseudomonas aeruginosa*: old molecules, new perspectives. *Int J Med Microbiol*, 296, 83-91.
- DIGGLE, S. P., GRIFFIN, A. S., CAMPBELL, G. S. & WEST, S. A. 2007. Cooperation and conflict in quorum-sensing bacterial populations. *Nature*, 450, 411-4.
- DIGGLE, S. P., WINZER, K., CHHABRA, S. R., WORRALL, K. E., CÁMARA, M. & WILLIAMS, P. 2003. The *Pseudomonas aeruginosa* quinolone signal molecule overcomes the cell density-dependency of the quorum sensing hierarchy, regulates *rhl*-dependent genes at the onset of stationary phase and can be produced in the absence of LasR. *Mol Microbiol*, 50, 29-43.
- DONLAN, R. M. 2002. Biofilms: microbial life on surfaces. *Emerg Infect Dis*, 8, 881-90.
- DRAKE, J. W. 1970. *The Molecular Basis of Mutation*, Holden-Day, Inc.; San Francisco, CA.
- DUARTE, A., COTTER, S. C., DE GASPERIN, O., HOUSLAY, T. M., BONCORAGLIO, G., WELCH, M. & KILNER, R. M. 2017. No evidence of a cleaning mutualism between burying beetles and their phoretic mites. *Sci Rep*, 7, 13838.

- DÖRING, G., HOIBY, N. & GROUP, C. S. 2004. Early intervention and prevention of lung disease in cystic fibrosis: a European consensus. *J Cyst Fibros*, 3, 67-91.
- DÖRING, G., PARAMESWARAN, I. G. & MURPHY, T. F. 2011. Differential adaptation of microbial pathogens to airways of patients with cystic fibrosis and chronic obstructive pulmonary disease. *FEMS Microbiol Rev*, 35, 124-46.
- EGUCHI, M., NISHIKAWA, T., MACDONALD, K., CAVICCHIOLI, R., GOTTSCHAL, J. C. & KJELLEBERG, S. 1996. Responses to Stress and Nutrient Availability by the Marine Ultramicrobacterium *Sphingomonas* sp. Strain RB2256. *Appl Environ Microbiol*, 62, 1287-94.
- ELBORN, J. S. 2016. Cystic fibrosis. *Lancet*, 388, 2519-2531.
- ELIAS, S. & BANIN, E. 2012. Multi-species biofilms: living with friendly neighbors. *FEMS Microbiol Rev*, 36, 990-1004.
- EMERSON, J., ROSENFELD, M., MCNAMARA, S., RAMSEY, B. & GIBSON, R. L. 2002. *Pseudomonas aeruginosa* and other predictors of mortality and morbidity in young children with cystic fibrosis. *Pediatr Pulmonol*, 34, 91-100.
- ENGEL, J. & BALACHANDRAN, P. 2009. Role of *Pseudomonas aeruginosa* type III effectors in disease. *Curr Opin Microbiol*, 12, 61-6.
- ESPINOSA-URGEL, M. 2003. Resident parking only: rhamnolipids maintain fluid channels in biofilms. *J Bacteriol*, 185, 699-700.
- EUCAST 2020a. Breakpoint tables for interpretation of MICs and zone diameters. Version 10.0, 2020. www.eucast.org.
- EUCAST 2020b. Breakpoint tables for interpretation of MICs for antifungal agents. Version 10.0. www.eucast.org.
- FAITH, D. P. 1992. Conservation evaluation and phylogenetic diversity. *Biological Conservation*, 61, 1 - 10.
- FERNANDES, P. 2016. Fusidic Acid: A Bacterial Elongation Factor Inhibitor for the Oral Treatment of Acute and Chronic Staphylococcal Infections. *Cold Spring Harb Perspect Med*, 6, a025437.
- FERREIRA, C. M. H., VILAS-BOAS, Â., SOUSA, C. A., SOARES, H. M. V. M. & SOARES, E. V. 2019. Comparison of five bacterial strains producing siderophores with ability to chelate iron under alkaline conditions. *AMB Express*, 9, 78.
- FIELD, T. R., SIBLEY, C. D., PARKINS, M. D., RABIN, H. R. & SURETTE, M. G. 2010. The genus *Prevotella* in cystic fibrosis airways. *Anaerobe*, 16, 337-44.
- FILKINS, L. M., GRABER, J. A., OLSON, D. G., DOLBEN, E. L., LYND, L. R., BHUJU, S. & O'TOOLE, G. A. 2015. Coculture of *Staphylococcus aureus* with *Pseudomonas aeruginosa* Drives *S. aureus* towards Fermentative Metabolism and Reduced Viability in a Cystic Fibrosis Model. *J Bacteriol*, 197, 2252-64.
- FLEMMING, H. C. & WINGENDER, J. 2010. The biofilm matrix. *Nat Rev Microbiol*, 8, 623-33.
- FLETCHER, M. P., DIGGLE, S. P., CÁMARA, M. & WILLIAMS, P. 2007. Biosensor-based assays for PQS, HHQ and related 2-alkyl-4-quinolone quorum sensing signal molecules. *Nat Protoc*, 2, 1254-62.
- FLYNN, J. M., NICCUM, D., DUNITZ, J. M. & HUNTER, R. C. 2016. Evidence and Role for Bacterial Mucin Degradation in Cystic Fibrosis Airway Disease. *PLoS Pathog*, 12, e1005846.
- FODOR, A. A., KLEM, E. R., GILPIN, D. F., ELBORN, J. S., BOUCHER, R. C., TUNNEY, M. M. & WOLFGANG, M. C. 2012. The adult cystic fibrosis airway microbiota is stable over time and infection type, and highly resilient to antibiotic treatment of exacerbations. *PLoS One*, 7, e45001.
- FOLKESSON, A., JELSBÄK, L., YANG, L., JOHANSEN, H. K., CIOFU, O., HØIBY, N. & MOLIN, S. 2012. Adaptation of *Pseudomonas aeruginosa* to the cystic fibrosis airway: an evolutionary perspective. *Nat Rev Microbiol*, 10, 841-51.
- FORD, S. A., KAO, D., WILLIAMS, D. & KING, K. C. 2016. Microbe-mediated host defence drives the evolution of reduced pathogen virulence. *Nat Commun*, 7, 13430.

- FOSTER, P. L. 2006. Methods for determining spontaneous mutation rates. *Methods Enzymol*, 409, 195-213.
- FOURIE, R., ELLS, R., SWART, C. W., SEBOLAI, O. M., ALBERTYN, J. & POHL, C. H. 2016. Candida albicans and Pseudomonas aeruginosa Interaction, with Focus on the Role of Eicosanoids. *Front Physiol*, 7, 64.
- FRANKLIN, M. J., NIVENS, D. E., WEADGE, J. T. & HOWELL, P. L. 2011. Biosynthesis of the Pseudomonas aeruginosa Extracellular Polysaccharides, Alginate, Pel, and Psl. *Front Microbiol*, 2, 167.
- FRASER-PITT, D. & O'NEIL, D. 2015. Cystic fibrosis - a multiorgan protein misfolding disease. *Future Sci OA*, 1, FSO57.
- FRAYMAN, K. B., ARMSTRONG, D. S., CARZINO, R., FERKOL, T. W., GRIMWOOD, K., STORCH, G. A., TEO, S. M., WYLIE, K. M. & RANGANATHAN, S. C. 2017a. The lower airway microbiota in early cystic fibrosis lung disease: a longitudinal analysis. *Thorax*, 72, 1104-1112.
- FRAYMAN, K. B., ARMSTRONG, D. S., GRIMWOOD, K. & RANGANATHAN, S. C. 2017b. The airway microbiota in early cystic fibrosis lung disease. *Pediatr Pulmonol*, 52, 1384-1404.
- FRENOY, A. & BONHOEFFER, S. 2018. Death and population dynamics affect mutation rate estimates and evolvability under stress in bacteria. *PLoS Biol*, 16, e2005056.
- FUGÈRE, A., LALONDE SÉGUIN, D., MITCHELL, G., DÉZIEL, E., DEKIMPE, V., CANTIN, A. M., FROST, E. & MALOUIN, F. 2014. Interspecific small molecule interactions between clinical isolates of Pseudomonas aeruginosa and Staphylococcus aureus from adult cystic fibrosis patients. *PLoS One*, 9, e86705.
- FUNG, C., NAUGHTON, S., TURNBULL, L., TINGPEJ, P., ROSE, B., ARTHUR, J., HU, H., HARMER, C., HARBOUR, C., HASSETT, D. J., WHITCHURCH, C. B. & MANOS, J. 2010. Gene expression of Pseudomonas aeruginosa in a mucin-containing synthetic growth medium mimicking cystic fibrosis lung sputum. 59, 1089-1100.
- FUX, C. A., COSTERTON, J. W., STEWART, P. S. & STOODLEY, P. 2005. Survival strategies of infectious biofilms. *Trends Microbiol*, 13, 34-40.
- GALERA-LAPORTA, L. & GARCIA-OJALVO, J. 2020. Antithetic population response to antibiotics in a polybacterial community. *Sci Adv*, 6, eaaz5108.
- GARCZEWSKA, B., JARZYŃKA, S., KUŚ, J., SKORUPA, W. & AUGUSTYNOWICZ-KOPEĆ, E. 2016. Fungal infection of cystic fibrosis patients - single center experience. *Pneumonol Alergol Pol*, 84, 151-9.
- GATES, D. E., VALLETTA, J. J., BONNEAUD, C. & RECKER, M. 2018. Quantitative host resistance drives the evolution of increased virulence in an emerging pathogen. *J Evol Biol*, 31, 1704-1714.
- GENTZSCH, M. & MALL, M. A. 2018. Ion Channel Modulators in Cystic Fibrosis. *Chest*, 154, 383-393.
- GERMERODT, S., BOHL, K., LÜCK, A., PANDE, S., SCHRÖTER, A., KALETA, C., SCHUSTER, S. & KOST, C. 2016. Pervasive Selection for Cooperative Cross-Feeding in Bacterial Communities. *PLoS Comput Biol*, 12, e1004986.
- GHIO, A. J., ROGGLI, V. L., SOUKUP, J. M., RICHARDS, J. H., RANDELL, S. H. & MUHLEBACH, M. S. 2013. Iron accumulates in the lavage and explanted lungs of cystic fibrosis patients. *J Cyst Fibros*, 12, 390-8.
- GHORBANI, P., SANTHAKUMAR, P., HU, Q., DJIADEU, P., WOLEVER, T. M., PALANIYAR, N. & GRASEMANN, H. 2015. Short-chain fatty acids affect cystic fibrosis airway inflammation and bacterial growth. *Eur Respir J*, 46, 1033-45.
- GIBSON, B., WILSON, D. J., FEIL, E. & EYRE-WALKER, A. 2018. The distribution of bacterial doubling times in the wild. *Proc Biol Sci*, 285.
- GIBSON, J., SOOD, A. & HOGAN, D. A. 2009. Pseudomonas aeruginosa-Candida albicans interactions: localization and fungal toxicity of a phenazine derivative. *Appl Environ Microbiol*, 75, 504-13.
- GIENGKAM, S., BLAKES, A., UTSAHAJIT, P., CHAEMCHUEN, S., ATWAL, S., BLACKSELL, S. D., PARIS, D. H., DAY, N. P. & SALJE, J. 2015. Improved Quantification, Propagation, Purification and

- Storage of the Obligate Intracellular Human Pathogen *Orientia tsutsugamushi*. *PLoS Negl Trop Dis*, 9, e0004009.
- GIFFORD, A. H., KLIPPENSTEIN, J. R. & MOORE, M. M. 2002. Serum stimulates growth of and proteinase secretion by *Aspergillus fumigatus*. *Infect Immun*, 70, 19-26.
- GILL, C., VAN DE WIJGERT, J. H., BLOW, F. & DARBY, A. C. 2016. Evaluation of Lysis Methods for the Extraction of Bacterial DNA for Analysis of the Vaginal Microbiota. *PLoS One*, 11, e0163148.
- GILLUM, A. M., TSAY, E. Y. & KIRSCH, D. R. 1984. Isolation of the *Candida albicans* gene for orotidine-5'-phosphate decarboxylase by complementation of *S. cerevisiae* *ura3* and *E. coli* *pyrF* mutations. *Mol Gen Genet*, 198, 179-82.
- GIULIETTI, A., OVERBERGH, L., VALCKX, D., DECALLONNE, B., BOUILLON, R. & MATHIEU, C. 2001. An overview of real-time quantitative PCR: applications to quantify cytokine gene expression. *Methods*, 25, 386-401.
- GJØDSBØL, K., CHRISTENSEN, J. J., KARLSMARK, T., JØRGENSEN, B., KLEIN, B. M. & KROGFELT, K. A. 2006. Multiple bacterial species reside in chronic wounds: a longitudinal study. *Int Wound J*, 3, 225-31.
- GLASS, J. B. & ORPHAN, V. J. 2012. Trace metal requirements for microbial enzymes involved in the production and consumption of methane and nitrous oxide. *Front Microbiol*, 3, 61.
- GOVAN, J. R. & NELSON, J. W. 1993. Microbiology of cystic fibrosis lung infections: themes and issues. *J R Soc Med*, 86 Suppl 20, 11-8.
- GRAHL, N., SHEPARDSON, K. M., CHUNG, D. & CRAMER, R. A. 2012. Hypoxia and fungal pathogenesis: to air or not to air? *Eukaryot Cell*, 11, 560-70.
- GRASEMANN, H., IOANNIDIS, I., TOMKIEWICZ, R. P., DE GROOT, H., RUBIN, B. K. & RATJEN, F. 1998. Nitric oxide metabolites in cystic fibrosis lung disease. *Arch Dis Child*, 78, 49-53.
- GRASSI, L., BATONI, G., OSTYN, L., RIGOLE, P., VAN DEN BOSSCHE, S., RINALDI, A. C., MAISETTA, G., ESIN, S., COENYE, T. & CRABBÉ, A. 2019. The Antimicrobial Peptide lin-SB056-1 and Its Dendrimeric Derivative Prevent. *Front Microbiol*, 10, 198.
- GREEN, E. R. & MECSAS, J. 2016. Bacterial Secretion Systems: An Overview. *Microbiol Spectr*, 4.
- GREENBERG, D. P. & STUTMAN, H. R. 1991. Cystic fibrosis. Infection and immunity to *Staphylococcus aureus* and *Haemophilus influenzae*. *Clin Rev Allergy*, 9, 75-86.
- GUAN, L. L., KANO, K. & KAMINO, K. 2001. Effect of exogenous siderophores on iron uptake activity of marine bacteria under iron-limited conditions. *Appl Environ Microbiol*, 67, 1710-7.
- GUERINOT, M. L. 1994. Microbial iron transport. *Annu Rev Microbiol*, 48, 743-72.
- GUTU, A. D., RODGERS, N. S., PARK, J. & MOSKOWITZ, S. M. 2015. *Pseudomonas aeruginosa* high-level resistance to polymyxins and other antimicrobial peptides requires *cprA*, a gene that is disrupted in the PAO1 strain. *Antimicrob Agents Chemother*, 59, 5377-87.
- GÓMEZ-BOMBARELLI, R., CALLE, E. & CASADO, J. 2013. Mechanisms of lactone hydrolysis in neutral and alkaline conditions. *J Org Chem*, 78, 6868-79.
- HAAS, H. 2003. Molecular genetics of fungal siderophore biosynthesis and uptake: the role of siderophores in iron uptake and storage. *Appl Microbiol Biotechnol*, 62, 316-30.
- HALEY, C. L., COLMER-HAMOOD, J. A. & HAMOOD, A. N. 2012. Characterization of biofilm-like structures formed by *Pseudomonas aeruginosa* in a synthetic mucus medium. *BMC Microbiol*, 12, 181.
- HALL, C. W. & MAH, T. F. 2017. Molecular mechanisms of biofilm-based antibiotic resistance and tolerance in pathogenic bacteria. *FEMS Microbiol Rev*, 41, 276-301.
- HAN, M. L., ZHU, Y., CREEK, D. J., LIN, Y. W., ANDERSON, D., SHEN, H. H., TSUJI, B., GUTU, A. D., MOSKOWITZ, S. M., VELKOV, T. & LI, J. 2018. Alterations of Metabolic and Lipid Profiles in Polymyxin-Resistant *Pseudomonas aeruginosa*. *Antimicrob Agents Chemother*, 62.
- HANCOCK, R. E. & BRINKMAN, F. S. 2002. Function of *pseudomonas* porins in uptake and efflux. *Annu Rev Microbiol*, 56, 17-38.

- HANEY, E. F., TRIMBLE, M. J., CHENG, J. T., VALLÉ, Q. & HANCOCK, R. E. W. 2018. Critical Assessment of Methods to Quantify Biofilm Growth and Evaluate Antibiofilm Activity of Host Defence Peptides. *Biomolecules*, 8.
- HANSON, B. 1987. Factors influencing Rickettsia tsutsugamushi infection of cultured cells. *Am J Trop Med Hyg*, 36, 621-30.
- HARJAI, K., KHANDWAHA, R. K., MITTAL, R., YADAV, V., GUPTA, V. & SHARMA, S. 2005. Effect of pH on production of virulence factors by biofilm cells of Pseudomonas aeruginosa. *Folia Microbiol (Praha)*, 50, 99-102.
- HARRISON, F. & DIGGLE, S. P. 2016. An ex vivo lung model to study bronchioles infected with Pseudomonas aeruginosa biofilms. *Microbiology*, 162, 1755-1760.
- HARRISON, F., MURULI, A., HIGGINS, S. & DIGGLE, S. P. 2014. Development of an ex vivo porcine lung model for studying growth, virulence, and signaling of Pseudomonas aeruginosa. *Infect Immun*, 82, 3312-23.
- HARRISON, F., PAUL, J., MASSEY, R. C. & BUCKLING, A. 2008. Interspecific competition and siderophore-mediated cooperation in Pseudomonas aeruginosa. *ISME J*, 2, 49-55.
- HAUSER, A. R., JAIN, M., BAR-MEIR, M. & MCCOLLEY, S. A. 2011. Clinical significance of microbial infection and adaptation in cystic fibrosis. *Clin Microbiol Rev*, 24, 29-70.
- HENRICI, A. T. 1933. Studies of Freshwater Bacteria: I. A Direct Microscopic Technique. *J Bacteriol*, 25, 277-87.
- HENTZER, M., EBERL, L. & GIVSKOV, M. 2005. Transcriptome analysis of Pseudomonas aeruginosa biofilm development: anaerobic respiration and iron limitation. *Biofilms*, 2, 37-61.
- HENTZER, M., TEITZEL, G. M., BALZER, G. J., HEYDORN, A., MOLIN, S., GIVSKOV, M. & PARSEK, M. R. 2001. Alginate overproduction affects Pseudomonas aeruginosa biofilm structure and function. *J Bacteriol*, 183, 5395-401.
- HENTZER, M., WU, H., ANDERSEN, J. B., RIEDEL, K., RASMUSSEN, T. B., BAGGE, N., KUMAR, N., SCHEMBRI, M. A., SONG, Z., KRISTOFFERSEN, P., MANEFIELD, M., COSTERTON, J. W., MOLIN, S., EBERL, L., STEINBERG, P., KJELLEBERG, S., HØIBY, N. & GIVSKOV, M. 2003. Attenuation of Pseudomonas aeruginosa virulence by quorum sensing inhibitors. *EMBO J*, 22, 3803-15.
- HERSHBERGER, C. D., YE, R. W., PARSEK, M. R., XIE, Z. D. & CHAKRABARTY, A. M. 1995. The algT (algU) gene of Pseudomonas aeruginosa, a key regulator involved in alginate biosynthesis, encodes an alternative sigma factor (sigma E). *Proc Natl Acad Sci U S A*, 92, 7941-5.
- HIBBING, M. E., FUQUA, C., PARSEK, M. R. & PETERSON, S. B. 2010. Bacterial competition: surviving and thriving in the microbial jungle. *Nat Rev Microbiol*, 8, 15-25.
- HISSEN, A. H., CHOW, J. M., PINTO, L. J. & MOORE, M. M. 2004. Survival of Aspergillus fumigatus in serum involves removal of iron from transferrin: the role of siderophores. *Infect Immun*, 72, 1402-8.
- HOFFMAN, L. R., DÉZIEL, E., D'ARGENIO, D. A., LÉPINE, F., EMERSON, J., MCNAMARA, S., GIBSON, R. L., RAMSEY, B. W. & MILLER, S. I. 2006. Selection for Staphylococcus aureus small-colony variants due to growth in the presence of Pseudomonas aeruginosa. *Proc Natl Acad Sci U S A*, 103, 19890-5.
- HOGAN, D. A. & KOLTER, R. 2002. Pseudomonas-Candida interactions: an ecological role for virulence factors. *Science*, 296, 2229-32.
- HOGAN, D. A., VIK, A. & KOLTER, R. 2004. A Pseudomonas aeruginosa quorum-sensing molecule influences Candida albicans morphology. *Mol Microbiol*, 54, 1212-23.
- HOGAN, D. A., WILLGER, S. D., DOLBEN, E. L., HAMPTON, T. H., STANTON, B. A., MORRISON, H. G., SOGIN, M. L., CZUM, J. & ASHARE, A. 2016. Analysis of Lung Microbiota in Bronchoalveolar Lavage, Protected Brush and Sputum Samples from Subjects with Mild-To-Moderate Cystic Fibrosis Lung Disease. *PLoS One*, 11, e0149998.
- HOLCOMBE, L. J., MCALESTER, G., MUNRO, C. A., ENJALBERT, B., BROWN, A. J. P., GOW, N. A. R., DING, C., BUTLER, G., O'GARA, F. & MORRISSEY, J. P. 2010. Pseudomonas aeruginosa

- secreted factors impair biofilm development in *Candida albicans*. *Microbiology*, 156, 1476-1486.
- HOLLOWAY, B. W. 1955. Genetic recombination in *Pseudomonas aeruginosa*. *J Gen Microbiol*, 13, 572-81.
- HOTTERBEEKX, A., KUMAR-SINGH, S., GOOSSENS, H. & MALHOTRA-KUMAR, S. 2017. *In vivo* and *In vitro* Interactions between *Pseudomonas aeruginosa* and *Staphylococcus* spp. *Front Cell Infect Microbiol*, 7, 106.
- HOTTMANN, I., MAYER, V. M. T., TOMEK, M. B., FRIEDRICH, V., CALVERT, M. B., TITZ, A., SCHÄFFER, C. & MAYER, C. 2018. *N*-Acetylmuramic Acid (MurNAc) Auxotrophy of the Oral Pathogen *Tannerella forsythia*: Characterization of a MurNAc Kinase and Analysis of Its Role in Cell Wall Metabolism. *Front Microbiol*, 9, 19.
- HWANG, T. C. & KIRK, K. L. 2013. The CFTR ion channel: gating, regulation, and anion permeation. *Cold Spring Harb Perspect Med*, 3, a009498.
- HØIBY, N., BJARNSHOLT, T., GIVSKOV, M., MOLIN, S. & CIOFU, O. 2010a. Antibiotic resistance of bacterial biofilms. *Int J Antimicrob Agents*, 35, 322-32.
- HØIBY, N., BJARNSHOLT, T., MOSER, C., JENSEN, P., KOLPEN, M., QVIST, T., AANAES, K., PRESSLER, T., SKOV, M. & CIOFU, O. 2017. Diagnosis of biofilm infections in cystic fibrosis patients. *APMIS*, 125, 339-343.
- HØIBY, N., CIOFU, O. & BJARNSHOLT, T. 2010b. *Pseudomonas aeruginosa* biofilms in cystic fibrosis. *Future Microbiol*, 5, 1663-74.
- HØIBY, N., DÖRING, G. & SCHIØTZ, P. O. 1987. Pathogenic mechanisms of chronic *Pseudomonas aeruginosa* infections in cystic fibrosis patients. *Antibiot Chemother (1971)*, 39, 60-76.
- IBBERSON, C. B., STACY, A., FLEMING, D., DEES, J. L., RUMBAUGH, K., GILMORE, M. S. & WHITELEY, M. 2017. Co-infecting microorganisms dramatically alter pathogen gene essentiality during polymicrobial infection. *Nat Microbiol*, 2, 17079.
- IBBERSON, C. B. & WHITELEY, M. 2020. The social life of microbes in chronic infection. *Curr Opin Microbiol*, 53, 44-50.
- ILLUMINA 2013. 16S Metagenomic Sequencing Library Preparation. emea.support.illumina.com.
- INSTITUTE, C. A. L. S. 2019. *Performance Standards for Antimicrobial Susceptibility Testing*, Wayne, PA.
- ISSAQ, H. J., XIAO, Z. & VEENSTRA, T. D. 2007. Serum and plasma proteomics. *Chem Rev*, 107, 3601-20.
- JACOBS, N. J., HEADY, R. E., JACOBS, J. M., CHAN, K. & DEIBEL, R. H. 1964. Effect of Hemin and Oxygen Tension of Growth and Nitrate Reduction by Bacteria. *J Bacteriol*, 87, 1406-11.
- JANISSEN, R., MURILLO, D. M., NIZA, B., SAHOO, P. K., NOBREGA, M. M., CESAR, C. L., TEMPERINI, M. L., CARVALHO, H. F., DE SOUZA, A. A. & COTTA, M. A. 2015. Spatiotemporal distribution of different extracellular polymeric substances and filamentation mediate *Xylella fastidiosa* adhesion and biofilm formation. *Sci Rep*, 5, 9856.
- JARRY, T. M. & CHEUNG, A. L. 2006. *Staphylococcus aureus* escapes more efficiently from the phagosome of a cystic fibrosis bronchial epithelial cell line than from its normal counterpart. *Infect Immun*, 74, 2568-77.
- JAYATHILAKE, P. G., JANA, S., RUSHTON, S., SWAILES, D., BRIDGENS, B., CURTIS, T. & CHEN, J. 2017. Extracellular Polymeric Substance Production and Aggregated Bacteria Colonization Influence the Competition of Microbes in Biofilms. *Front Microbiol*, 8, 1865.
- JENSEN, P., BJARNSHOLT, T., PHIPPS, R., RASMUSSEN, T. B., CALUM, H., CHRISTOFFERSEN, L., MOSER, C., WILLIAMS, P., PRESSLER, T., GIVSKOV, M. & HØIBY, N. 2007. Rapid necrotic killing of polymorphonuclear leukocytes is caused by quorum-sensing-controlled production of rhamnolipid by *Pseudomonas aeruginosa*. *Microbiology*, 153, 1329-1338.
- JENUL, C. & HORSWILL, A. R. 2018. Regulation of. *Microbiol Spectr*, 6.

- JONES, K. L., HEGAB, A. H., HILLMAN, B. C., SIMPSON, K. L., JINKINS, P. A., GRISHAM, M. B., OWENS, M. W., SATO, E. & ROBBINS, R. A. 2000. Elevation of nitrotyrosine and nitrate concentrations in cystic fibrosis sputum. *Pediatr Pulmonol*, 30, 79-85.
- JONES, M. E., THOMAS, S. M. & CLARKE, K. 1999. The application of a linear algebra to the analysis of mutation rates. *J Theor Biol*, 199, 11-23.
- JONES, M. E., THOMAS, S. M. & ROGERS, A. 1994. Luria-Delbrück fluctuation experiments: design and analysis. *Genetics*, 136, 1209-16.
- JORTH, P., EHSAN, Z., REZAYAT, A., CALDWELL, E., POPE, C., BREWINGTON, J. J., GOSS, C. H., BENSCOTER, D., CLANCY, J. P. & SINGH, P. K. 2019. Direct Lung Sampling Indicates That Established Pathogens Dominate Early Infections in Children with Cystic Fibrosis. *Cell Rep*, 27, 1190-1204.e3.
- JOSSE, J., LAURENT, F. & DIOT, A. 2017. Staphylococcal Adhesion and Host Cell Invasion: Fibronectin-Binding and Other Mechanisms. *Front Microbiol*, 8, 2433.
- JUDGE, E. P., HUGHES, J. M., EGAN, J. J., MAGUIRE, M., MOLLOY, E. L. & O'DEA, S. 2014. Anatomy and bronchoscopy of the porcine lung. A model for translational respiratory medicine. *Am J Respir Cell Mol Biol*, 51, 334-43.
- JUNGE, S., GÖRLICH, D., DEN REIJER, M., WIEDEMANN, B., TÜMMLER, B., ELLEMUNTER, H., DÜBBERS, A., KÜSTER, P., BALLMANN, M., KOERNER-RETTBERG, C., GROßE-ONNEBRINK, J., HEUER, E., SEXTRO, W., MAINZ, J. G., HAMMERMANN, J., RIETHMÜLLER, J., GRAEPLER-MAINKA, U., STAAB, D., WOLLSCHLÄGER, B., SZCZEPANSKI, R., SCHUSTER, A., TEGTMEYER, F. K., SUTHARSAN, S., WALD, A., NOFER, J. R., VAN WAMEL, W., BECKER, K., PETERS, G. & KAHL, B. C. 2016. Factors Associated with Worse Lung Function in Cystic Fibrosis Patients with Persistent *Staphylococcus aureus*. *PLoS One*, 11, e0166220.
- KADURUGAMUWA, J. L., LAM, J. S. & BEVERIDGE, T. J. 1993. Interaction of gentamicin with the A band and B band lipopolysaccharides of *Pseudomonas aeruginosa* and its possible lethal effect. *Antimicrob Agents Chemother*, 37, 715-21.
- KALDALU, N. & TENSON, T. 2019. Slow growth causes bacterial persistence. *Sci Signal*, 12.
- KAMBLE, E. & PARDESI, K. 2020. Antibiotic Tolerance in Biofilm and Stationary-Phase Planktonic Cells of *Staphylococcus aureus*. *Microb Drug Resist*.
- KAPLAN, J. B. 2010. Biofilm dispersal: mechanisms, clinical implications, and potential therapeutic uses. *J Dent Res*, 89, 205-18.
- KARA, D., LUPPENS, S. B. & CATE, J. M. 2006. Differences between single- and dual-species biofilms of *Streptococcus mutans* and *Veillonella parvula* in growth, acidogenicity and susceptibility to chlorhexidine. *Eur J Oral Sci*, 114, 58-63.
- KARAMPATZAKIS, A., SANKARAN, J., KANDASWAMY, K., RICE, A., CHOEN, Y. & WOHLAND, T. 2017. Measurement of oxygen concentrations in bacterial biofilms using transient state monitoring by single plane illumination microscopy
- Biomed Phys Eng Express*, 3, 035020.
- KATAYAMA, Y., AZECHI, T., MIYAZAKI, M., TAKATA, T., SEKINE, M., MATSUI, H., HANAKI, H., YAHARA, K., SASANO, H., ASAKURA, K., TAKAKU, T., OCHIAI, T., KOMATSU, N. & CHAMBERS, H. F. 2017. Prevalence of Slow-Growth Vancomycin Nonsusceptibility in Methicillin-Resistant *Staphylococcus aureus*. *Antimicrob Agents Chemother*, 61.
- KAUFMAN, D. A., BROWN, A. T., EISENHUTH, K. K., YUE, J., GROSSMAN, L. B. & HAZEN, K. C. 2014. More serious infectious morbidity and mortality associated with simultaneous candidemia and coagulase-negative staphylococcal bacteremia in neonates and in vitro adherence studies between *Candida albicans* and *Staphylococcus epidermidis*. *Early Hum Dev*, 90 Suppl 1, S66-70.
- KEREM, B., ROMMENS, J. M., BUCHANAN, J. A., MARKIEWICZ, D., COX, T. K., CHAKRAVARTI, A., BUCHWALD, M. & TSUI, L. C. 1989. Identification of the cystic fibrosis gene: genetic analysis. *Science*, 245, 1073-80.

- KEREN, I., KALDALU, N., SPOERING, A., WANG, Y. & LEWIS, K. 2004. Persister cells and tolerance to antimicrobials. *FEMS Microbiology Letters*, 230, 13 - 18.
- KIEDROWSKI, M. R., GASTON, J. R., KOCAK, B. R., COBURN, S. L., LEE, S., PILEWSKI, J. M., MYERBURG, M. M. & BOMBERGER, J. M. 2018. Biofilm Growth on Cystic Fibrosis Airway Epithelial Cells Is Enhanced during Respiratory Syncytial Virus Coinfection. *mSphere*, 3.
- KIM, S., COVINGTON, A. & PAMER, E. G. 2017. The intestinal microbiota: Antibiotics, colonization resistance, and enteric pathogens. *Immunol Rev*, 279, 90-105.
- KING, J. D., KOCÍNCOVÁ, D., WESTMAN, E. L. & LAM, J. S. 2009. Review: Lipopolysaccharide biosynthesis in *Pseudomonas aeruginosa*. *Innate Immun*, 15, 261-312.
- KIP, N. & VAN VEEN, J. A. 2015. The dual role of microbes in corrosion. *ISME J*, 9, 542-51.
- KIRCHNER, S., FOTHERGILL, J. L., WRIGHT, E. A., JAMES, C. E., MOWAT, E. & WINSTANLEY, C. 2012. Use of artificial sputum medium to test antibiotic efficacy against *Pseudomonas aeruginosa* in conditions more relevant to the cystic fibrosis lung. *J Vis Exp*, e3857.
- KIRKETERP-MØLLER, K., JENSEN, P., FAZLI, M., MADSEN, K. G., PEDERSEN, J., MOSER, C., TOLKER-NIELSEN, T., HØIBY, N., GIVSKOV, M. & BJARNSHOLT, T. 2008. Distribution, organization, and ecology of bacteria in chronic wounds. *J Clin Microbiol*, 46, 2717-22.
- KLEPAC-CERAJ, V., LEMON, K. P., MARTIN, T. R., ALLGAIER, M., KEMBEL, S. W., KNAPP, A. A., LORY, S., BRODIE, E. L., LYNCH, S. V., BOHANNAN, B. J., GREEN, J. L., MAURER, B. A. & KOLTER, R. 2010. Relationship between cystic fibrosis respiratory tract bacterial communities and age, genotype, antibiotics and *Pseudomonas aeruginosa*. *Environ Microbiol*, 12, 1293-303.
- KNIGHT, M., HARTMAN, P. E., HARTMAN, Z. & YOUNG, V. M. 1979. A new method of preparation of pyocyanin and demonstration of an unusual bacterial sensitivity. *Anal Biochem*, 95, 19-23.
- KNOWLES, M. R. & BOUCHER, R. C. 2002. Mucus clearance as a primary innate defense mechanism for mammalian airways. *J Clin Invest*, 109, 571-7.
- KOLBERT, C. P. & PERSING, D. H. 1999. Ribosomal DNA sequencing as a tool for identification of bacterial pathogens. *Curr Opin Microbiol*, 2, 299-305.
- KONG, E. F., TSUI, C., KUCHARÍKOVÁ, S., ANDES, D., VAN DIJCK, P. & JABRA-RIZK, M. A. 2016. Commensal Protection of *Staphylococcus aureus* against Antimicrobials by *Candida albicans* Biofilm Matrix. *mBio*, 7.
- KORGAONKAR, A., TRIVEDI, U., RUMBAUGH, K. P. & WHITELEY, M. 2013. Community surveillance enhances *Pseudomonas aeruginosa* virulence during polymicrobial infection. *Proc Natl Acad Sci U S A*, 110, 1059-64.
- KORGAONKAR, A. K. & WHITELEY, M. 2011. *Pseudomonas aeruginosa* enhances production of an antimicrobial in response to N-acetylglucosamine and peptidoglycan. *J Bacteriol*, 193, 909-17.
- KOSTYLEV, M., KIM, D. Y., SMALLEY, N. E., SALUKHE, I., GREENBERG, E. P. & DANDEKAR, A. A. 2019. Evolution of the *Pseudomonas aeruginosa* quorum-sensing hierarchy. *Proc Natl Acad Sci U S A*, 116, 7027-7032.
- KOSZTOŁOWICZ, T., METZLER, R., WĄSIK, S. & ARABSKI, M. 2020. Model of ciprofloxacin subdiffusion in *Pseudomonas aeruginosa* biofilm formed in artificial sputum medium. *bioRxiv*, 2020.02.26.966507.
- KRAEMER, S. M., DUCKWORTH, O. W., HARRINGTON, J. M. & SCHENKEVELD, W. D. C. 2014. Metallophores and Trace Metal Biogeochemistry. *Aquatic Geochemistry*, 21, 159 - 195.
- KRAMER, J., ÖZKAYA, Ö. & KÜMMERLI, R. 2020. Bacterial siderophores in community and host interactions. *Nat Rev Microbiol*, 18, 152-163.
- KRAŠOVEC, R., BELAVKIN, R. V., ASTON, J. A., CHANNON, A., ASTON, E., RASH, B. M., KADIRVEL, M., FORBES, S. & KNIGHT, C. G. 2014. Mutation rate plasticity in rifampicin resistance depends on *Escherichia coli* cell-cell interactions. *Nat Commun*, 5, 3742.
- KRAŠOVEC, R., RICHARDS, H., GIFFORD, D. R., HATCHER, C., FAULKNER, K. J., BELAVKIN, R. V., CHANNON, A., ASTON, E., MCBAIN, A. J. & KNIGHT, C. G. 2017. Spontaneous mutation rate is

- a plastic trait associated with population density across domains of life. *PLoS Biol*, 15, e2002731.
- KREDA, S. M., DAVIS, C. W. & ROSE, M. C. 2012. CFTR, mucins, and mucus obstruction in cystic fibrosis. *Cold Spring Harb Perspect Med*, 2, a009589.
- KUBITSCHKE, H. E. & GUSTAFSON, L. A. 1964. Mutation in Continuous Cultures III: Mutational Responses in *Escherichia coli*. *J Bacteriol*, 88, 1595-7.
- KULASEKARA, B. R. & LORY, S. 2004. The Genome of *Pseudomonas aeruginosa*. In: RAMOS JL. (EDS) *PSEUDOMONAS*. SPRINGER, B., MA (ed.).
- KUNG, V. L., OZER, E. A. & HAUSER, A. R. 2010. The accessory genome of *Pseudomonas aeruginosa*. *Microbiol Mol Biol Rev*, 74, 621-41.
- KUNZELMANN, K., SCHWIEBERT, E. M., ZEITLIN, P. L., KUO, W. L., STANTON, B. A. & GRUENERT, D. C. 1993. An immortalized cystic fibrosis tracheal epithelial cell line homozygous for the delta F508 CFTR mutation. *Am J Respir Cell Mol Biol*, 8, 522-9.
- KÜMMERLI, R. 2015. Cheat invasion causes bacterial trait loss in lung infections. *Proc Natl Acad Sci U S A*, 112, 10577-8.
- LAAKSO, H. A., MAROLDA, C. L., PINTER, T. B., STILLMAN, M. J. & HEINRICHS, D. E. 2016. A Heme-responsive Regulator Controls Synthesis of Staphyloferrin B in *Staphylococcus aureus*. *J Biol Chem*, 291, 29-40.
- LABAUVE, A. E. & WARGO, M. J. 2012. Growth and laboratory maintenance of *Pseudomonas aeruginosa*. *Curr Protoc Microbiol*, Chapter 6, Unit 6E.1.
- LAFAYETTE, S. L., HOULE, D., BEAUDOIN, T., WOJEWODKA, G., RADZIOCH, D., HOFFMAN, L. R., BURNS, J. L., DANDEKAR, A. A., SMALLEY, N. E., CHANDLER, J. R., ZLOSNIK, J. E., SPEERT, D. P., BERNIER, J., MATOUK, E., BROCHIERO, E., ROUSSEAU, S. & NGUYEN, D. 2015. Cystic fibrosis-adapted *Pseudomonas aeruginosa* quorum sensing *lasR* mutants cause hyperinflammatory responses. *Sci Adv*, 1.
- LAM, J. S., TAYLOR, V. L., ISLAM, S. T., HAO, Y. & KOCÍNCOVÁ, D. 2011. Genetic and Functional Diversity of *Pseudomonas aeruginosa* Lipopolysaccharide. *Front Microbiol*, 2, 118.
- LAMMERTYN, E. J., VANDERMEULEN, E., BELLON, H., EVERAERTS, S., VERLEDEN, S. E., VAN DEN EYNDE, K., BRACKE, K. R., BRUSSELLE, G. G., GOEMINNE, P. C., VERBEKEN, E. K., VANAUDENAERDE, B. M. & DUPONT, L. J. 2017. End-stage cystic fibrosis lung disease is characterised by a diverse inflammatory pattern: an immunohistochemical analysis. *Respir Res*, 18, 10.
- LAU, G. W., HASSETT, D. J., RAN, H. & KONG, F. 2004. The role of pyocyanin in *Pseudomonas aeruginosa* infection. *Trends Mol Med*, 10, 599-606.
- LE, K. Y. & OTTO, M. 2015. Quorum-sensing regulation in staphylococci-an overview. *Front Microbiol*, 6, 1174.
- LEA, D. E. & COULSON, C. A. 1949. The distribution of the numbers of mutants in bacterial populations. *J Genet*, 49, 264-85.
- LEE, J. & ZHANG, L. 2015. The hierarchy quorum sensing network in *Pseudomonas aeruginosa*. *Protein Cell*, 6, 26-41.
- LEE, J. Y., NA, I. Y., PARK, Y. K. & KO, K. S. 2014. Genomic variations between colistin-susceptible and -resistant *Pseudomonas aeruginosa* clinical isolates and their effects on colistin resistance. *J Antimicrob Chemother*, 69, 1248-56.
- LEE, J. Y., PARK, Y. K., CHUNG, E. S., NA, I. Y. & KO, K. S. 2016. Evolved resistance to colistin and its loss due to genetic reversion in *Pseudomonas aeruginosa*. *Sci Rep*, 6, 25543.
- LEEKHA, S., TERRELL, C. L. & EDSON, R. S. 2011. General principles of antimicrobial therapy. *Mayo Clin Proc*, 86, 156-67.
- LEGRAND, M., CHAN, C. L., JAUERT, P. A. & KIRKPATRICK, D. T. 2007. Role of DNA mismatch repair and double-strand break repair in genome stability and antifungal drug resistance in *Candida albicans*. *Eukaryot Cell*, 6, 2194-205.

- LEID, J. G., WILLSON, C. J., SHIRTLIFF, M. E., HASSETT, D. J., PARSEK, M. R. & JEFFERS, A. K. 2005. The exopolysaccharide alginate protects *Pseudomonas aeruginosa* biofilm bacteria from IFN- γ -mediated macrophage killing. *J Immunol*, 175, 7512-8.
- LEONHARD, M., ZATORSKA, B., MOSER, D., TAN, Y. & SCHNEIDER-STICKLER, B. 2018. Evaluation of combined growth media for in vitro cultivation of oropharyngeal biofilms on prosthetic silicone. *J Mater Sci Mater Med*, 29, 45.
- LERICHE, V., BRIANDET, R. & CARPENTIER, B. 2003. Ecology of mixed biofilms subjected daily to a chlorinated alkaline solution: spatial distribution of bacterial species suggests a protective effect of one species to another. *Environ Microbiol*, 5, 64-71.
- LEWENZA, S., VISSER, M. B. & SOKOL, P. A. 2002. Interspecies communication between *Burkholderia cepacia* and *Pseudomonas aeruginosa*. *Can J Microbiol*, 48, 707-16.
- LI, B., QIU, Y., SHI, H. & YIN, H. 2016. The importance of lag time extension in determining bacterial resistance to antibiotics. *Analyst*, 141, 3059-67.
- LI, H., LI, X., WANG, Z., FU, Y., AI, Q., DONG, Y. & YU, J. 2015. Autoinducer-2 regulates *Pseudomonas aeruginosa* PAO1 biofilm formation and virulence production in a dose-dependent manner. *BMC Microbiol*, 15, 192.
- LI, H., LUO, Y. F., WILLIAMS, B. J., BLACKWELL, T. S. & XIE, C. M. 2012. Structure and function of OprD protein in *Pseudomonas aeruginosa*: from antibiotic resistance to novel therapies. *Int J Med Microbiol*, 302, 63-8.
- LI, L., ZHOU, R., LI, T., KANG, M., WAN, Y., XU, Z. & CHEN, H. 2008. Enhanced biofilm formation and reduced virulence of *Actinobacillus pleuropneumoniae* luxS mutant. *Microb Pathog*, 45, 192-200.
- LI, X. Z. & NIKAIDO, H. 2009. Efflux-mediated drug resistance in bacteria: an update. *Drugs*, 69, 1555-623.
- LIANG, W., GUAN, G., DAI, Y., CAO, C., TAO, L., DU, H., NOBILE, C. J., ZHONG, J. & HUANG, G. 2016. Lactic acid bacteria differentially regulate filamentation in two heritable cell types of the human fungal pathogen *Candida albicans*. *Mol Microbiol*, 102, 506-519.
- LIAUD, N., GINIES, C., NAVARRO, D., FABRE, N., CRAPART, S., GIMBERT, I., LEVASSEUR, A., RAOUCHE, S. & SIGOILLOT, J.-C. 2014. Exploring fungal biodiversity: organic acid production by 66 strains of filamentous fungi. *Fungal Biology and Biotechnology*, 1, 1.
- LIMOLI, D. H., JONES, C. J. & WOZNIAK, D. J. 2015. Bacterial Extracellular Polysaccharides in Biofilm Formation and Function. *Microbiol Spectr*, 3.
- LIMOLI, D. H., YANG, J., KHANSAHEB, M. K., HELFMAN, B., PENG, L., STECENKO, A. A. & GOLDBERG, J. B. 2016. *Staphylococcus aureus* and *Pseudomonas aeruginosa* co-infection is associated with cystic fibrosis-related diabetes and poor clinical outcomes. *Eur J Clin Microbiol Infect Dis*, 35, 947-53.
- LIN, J., CHENG, J., WANG, Y. & SHEN, X. 2018. The *Pseudomonas* Quinolone Signal (PQS): Not Just for Quorum Sensing Anymore. *Front Cell Infect Microbiol*, 8, 230.
- LINE, L., ALHEDE, M., KOLPEN, M., KÜHL, M., CIOFU, O., BJARNSHOLT, T., MOSER, C., TOYOFUKU, M., NOMURA, N., HØIBY, N. & JENSEN, P. 2014. Physiological levels of nitrate support anoxic growth by denitrification of *Pseudomonas aeruginosa* at growth rates reported in cystic fibrosis lungs and sputum. *Front Microbiol*, 5, 554.
- LIPUMA, J. J. 2010. The changing microbial epidemiology in cystic fibrosis. *Clin Microbiol Rev*, 23, 299-323.
- LIZEWSKI, S. E., SCHURR, J. R., JACKSON, D. W., FRISK, A., CARTERSON, A. J. & SCHURR, M. J. 2004. Identification of AlgR-regulated genes in *Pseudomonas aeruginosa* by use of microarray analysis. *J Bacteriol*, 186, 5672-84.
- LODDEKE, M., SCHNEIDER, B., OGURI, T., MEHTA, I., XUAN, Z. & REITZER, L. 2017. Anaerobic Cysteine Degradation and Potential Metabolic Coordination in *Salmonella enterica* and *Escherichia coli*. *J Bacteriol*, 199.

- LOPES, S. P., AZEVEDO, N. F. & PEREIRA, M. O. 2017. Developing a model for cystic fibrosis sociomicrobiology based on antibiotic and environmental stress. *Int J Med Microbiol*, 307, 460-470.
- LOPES, S. P., CERI, H., AZEVEDO, N. F. & PEREIRA, M. O. 2012. Antibiotic resistance of mixed biofilms in cystic fibrosis: impact of emerging microorganisms on treatment of infection. *Int J Antimicrob Agents*, 40, 260-3.
- LOPEZ-MEDINA, E., FAN, D., COUGHLIN, L. A., HO, E. X., LAMONT, I. L., REIMMANN, C., HOOPER, L. V. & KOH, A. Y. 2015. Candida albicans Inhibits Pseudomonas aeruginosa Virulence through Suppression of Pyochelin and Pyoverdine Biosynthesis. *PLoS Pathog*, 11, e1005129.
- LORÈ, N. I., CIGANA, C., DE FINO, I., RIVA, C., JUHAS, M., SCHWAGER, S., EBERL, L. & BRAGONZI, A. 2012. Cystic fibrosis-niche adaptation of Pseudomonas aeruginosa reduces virulence in multiple infection hosts. *PLoS One*, 7, e35648.
- LOZUPONE, C. & KNIGHT, R. 2005. UniFrac: a new phylogenetic method for comparing microbial communities. *Appl Environ Microbiol*, 71, 8228-35.
- LUBAMBA, B., DHOOGHE, B., NOEL, S. & LEAL, T. 2012. Cystic fibrosis: insight into CFTR pathophysiology and pharmacotherapy. *Clin Biochem*, 45, 1132-44.
- LURIA, S. E. & DELBRÜCK, M. 1943. Mutations of Bacteria from Virus Sensitivity to Virus Resistance. *Genetics*, 28, 491-511.
- LYCZAK, J. B., CANNON, C. L. & PIER, G. B. 2002. Lung infections associated with cystic fibrosis. *Clin Microbiol Rev*, 15, 194-222.
- MACK, D., NEDELMANN, M., KROKOTSCH, A., SCHWARZKOPF, A., HEESEMANN, J. & LAUFS, R. 1994. Characterization of transposon mutants of biofilm-producing Staphylococcus epidermidis impaired in the accumulative phase of biofilm production: genetic identification of a hexosamine-containing polysaccharide intercellular adhesin. *Infect Immun*, 62, 3244-53.
- MADIGAN, M. T. & MARTINKO, J. M. 2000. *Brock biology of microorganisms*, Prentice-Hall, Upper Saddle River, NJ.
- MAGALHÃES, A. P., LOPES, S. P. & PEREIRA, M. O. 2016. Insights into Cystic Fibrosis Polymicrobial Consortia: The Role of Species Interactions in Biofilm Development, Phenotype, and Response to In-Use Antibiotics. *Front Microbiol*, 7, 2146.
- MAHBOUBI, M. A., CARMODY, L. A., FOSTER, B. K., KALIKIN, L. M., VANDEVANTER, D. R. & LIPUMA, J. J. 2016. Culture-Based and Culture-Independent Bacteriologic Analysis of Cystic Fibrosis Respiratory Specimens. *J Clin Microbiol*, 54, 613-9.
- MAISETTA, G., GRASSI, L., ESIN, S., SERRA, I., SCORCIAPINO, M. A., RINALDI, A. C. & BATONI, G. 2017. The Semi-Synthetic Peptide Lin-SB056-1 in Combination with EDTA Exerts Strong Antimicrobial and Antibiofilm Activity against Pseudomonas aeruginosa in Conditions Mimicking Cystic Fibrosis Sputum. *Int J Mol Sci*, 18.
- MAKOVCOVA, J., BABAK, V., KULICH, P., MASEK, J., SLANY, M. & CINCAROVA, L. 2017. Dynamics of mono- and dual-species biofilm formation and interactions between Staphylococcus aureus and Gram-negative bacteria. *Microb Biotechnol*, 10, 819-832.
- MALHOTRA, S., HAYES, D. & WOZNIAK, D. J. 2019. Cystic Fibrosis and Pseudomonas aeruginosa: the Host-Microbe Interface. *Clin Microbiol Rev*, 32.
- MALL, M., GRUBB, B. R., HARKEMA, J. R., O'NEAL, W. K. & BOUCHER, R. C. 2004. Increased airway epithelial Na⁺ absorption produces cystic fibrosis-like lung disease in mice. *Nat Med*, 10, 487-93.
- MARKUSSEN, T., MARVIG, R. L., GÓMEZ-LOZANO, M., AANÆS, K., BURLEIGH, A. E., HØIBY, N., JOHANSEN, H. K., MOLIN, S. & JELSKAK, L. 2014. Environmental heterogeneity drives within-host diversification and evolution of Pseudomonas aeruginosa. *mBio*, 5, e01592-14.
- MARTIN, L. W., REID, D. W., SHARPLES, K. J. & LAMONT, I. L. 2011. Pseudomonas siderophores in the sputum of patients with cystic fibrosis. *Biometals*, 24, 1059-67.

- MASELLI, J. H., SONTAG, M. K., NORRIS, J. M., MACKENZIE, T., WAGENER, J. S. & ACCURSO, F. J. 2003. Risk factors for initial acquisition of *Pseudomonas aeruginosa* in children with cystic fibrosis identified by newborn screening. *Pediatr Pulmonol*, 35, 257-62.
- MASHBURN, L. M., JETT, A. M., AKINS, D. R. & WHITELEY, M. 2005. *Staphylococcus aureus* serves as an iron source for *Pseudomonas aeruginosa* during in vivo coculture. *J Bacteriol*, 187, 554-66.
- MASTROPAOLO, M. D., EVANS, N. P., BYRNES, M. K., STEVENS, A. M., ROBERTSON, J. L. & MELVILLE, S. B. 2005. Synergy in polymicrobial infections in a mouse model of type 2 diabetes. *Infect Immun*, 73, 6055-63.
- MATSUO, M., OOGAI, Y., KATO, F., SUGAI, M. & KOMATSUZAWA, H. 2011. Growth-phase dependence of susceptibility to antimicrobial peptides in *Staphylococcus aureus*. *Microbiology (Reading)*, 157, 1786-1797.
- MATTICK, J. S. 2002. Type IV pili and twitching motility. *Annu Rev Microbiol*, 56, 289-314.
- MAUNDERS, E. & WELCH, M. 2017. Matrix exopolysaccharides; the sticky side of biofilm formation. *FEMS Microbiol Lett*, 364.
- MAVRODI, D. V., BONSALL, R. F., DELANEY, S. M., SOULE, M. J., PHILLIPS, G. & THOMASHOW, L. S. 2001. Functional analysis of genes for biosynthesis of pyocyanin and phenazine-1-carboxamide from *Pseudomonas aeruginosa* PAO1. *J Bacteriol*, 183, 6454-65.
- MAYER, V. M. T., HOTTMANN, I., FIGL, R., ALTMANN, F., MAYER, C. & SCHÄFFER, C. 2019. Peptidoglycan-type analysis of the N-acetylmuramic acid auxotrophic oral pathogen *Tannerella forsythia* and reclassification of the peptidoglycan-type of *Porphyromonas gingivalis*. *BMC Microbiol*, 19, 200.
- MAZA, P. K., BONFIM-MELO, A., PADOVAN, A. C. B., MORTARA, R. A., ORIKAZA, C. M., RAMOS, L. M. D., MOURA, T. R., SORIANI, F. M., ALMEIDA, R. S., SUZUKI, E. & BAHIA, D. 2017. : The Ability to Invade Epithelial Cells and Survive under Oxidative Stress Is Unlinked to Hyphal Length. *Front Microbiol*, 8, 1235.
- MCALESTER, G., O'GARA, F. & MORRISSEY, J. P. 2008. Signal-mediated interactions between *Pseudomonas aeruginosa* and *Candida albicans*. *J Med Microbiol*, 57, 563-9.
- MCCLEAN, M., STANLEY, T., GOLDSMITH, C. E., MILLAR, B. C., MCCLURG, B., ELBORN, J. S., LOWERY, C. J., DOOLEY, J. S., RENDALL, J. C. & MOORE, J. E. 2010. Determination of optimum incubation time for release of bacteria from sputum of patients with cystic fibrosis using dithiothreitol (sputasol). *Br J Biomed Sci*, 67, 89-91.
- MERRITT, J. H., KADOURI, D. E. & O'TOOLE, G. A. 2005. Growing and analyzing static biofilms. *Curr Protoc Microbiol*, Chapter 1, Unit 1B.1.
- MEURENS, F., SUMMERFIELD, A., NAUWYNCK, H., SAIF, L. & GERDTS, V. 2012. The pig: a model for human infectious diseases. *Trends Microbiol*, 20, 50-7.
- MEYER, J. M. 1992. Exogenous siderophore-mediated iron uptake in *Pseudomonas aeruginosa*: possible involvement of porin OprF in iron translocation. *J Gen Microbiol*, 138, 951-8.
- MICHALSKA, M. & WOLF, P. 2015. *Pseudomonas* Exotoxin A: optimized by evolution for effective killing. *Front Microbiol*, 6, 963.
- MIETHKE, M., KRAUSHAAR, T. & MARAHIEL, M. A. 2013. Uptake of xenosiderophores in *Bacillus subtilis* occurs with high affinity and enhances the folding stabilities of substrate binding proteins. *FEBS Lett*, 587, 206-13.
- MIETHKE, M. & MARAHIEL, M. A. 2007. Siderophore-based iron acquisition and pathogen control. *Microbiol Mol Biol Rev*, 71, 413-51.
- MIETTINEN, I. T., VARTIAINEN, T. & MARTIKAINEN, P. J. 1997. Phosphorus and bacterial growth in drinking water. *Appl Environ Microbiol*, 63, 3242-5.
- MIKKELSEN, H., DUCK, Z., LILLEY, K. S. & WELCH, M. 2007. Interrelationships between colonies, biofilms, and planktonic cells of *Pseudomonas aeruginosa*. *J Bacteriol*, 189, 2411-6.
- MIRKOVIĆ, B., MURRAY, M. A., LAVELLE, G. M., MOLLOY, K., AZIM, A. A., GUNARATNAM, C., HEALY, F., SLATTERY, D., MCNALLY, P., HATCH, J., WOLFGANG, M., TUNNEY, M. M., MUHLEBACH, M.

- S., DEVERY, R., GREENE, C. M. & MCELVANEY, N. G. 2015. The Role of Short-Chain Fatty Acids, Produced by Anaerobic Bacteria, in the Cystic Fibrosis Airway. *Am J Respir Crit Care Med*, 192, 1314-24.
- MITCHELL, G., SÉGUIN, D. L., ASSELIN, A. E., DÉZIEL, E., CANTIN, A. M., FROST, E. H., MICHAUD, S. & MALOUIN, F. 2010. Staphylococcus aureus sigma B-dependent emergence of small-colony variants and biofilm production following exposure to Pseudomonas aeruginosa 4-hydroxy-2-heptylquinoline-N-oxide. *BMC Microbiol*, 10, 33.
- MORALES, D. K., GRAHL, N., OKEGBE, C., DIETRICH, L. E., JACOBS, N. J. & HOGAN, D. A. 2013. Control of Candida albicans metabolism and biofilm formation by Pseudomonas aeruginosa phenazines. *mBio*, 4, e00526-12.
- MOREAU-MARQUIS, S., STANTON, B. A. & O'TOOLE, G. A. 2008. Pseudomonas aeruginosa biofilm formation in the cystic fibrosis airway. *Pulm Pharmacol Ther*, 21, 595-9.
- MOWAT, E., PATERSON, S., FOTHERGILL, J. L., WRIGHT, E. A., LEDSON, M. J., WALSHAW, M. J., BROCKHURST, M. A. & WINSTANLEY, C. 2011. Pseudomonas aeruginosa population diversity and turnover in cystic fibrosis chronic infections. *Am J Respir Crit Care Med*, 183, 1674-9.
- MULLER, M. 2002. Pyocyanin induces oxidative stress in human endothelial cells and modulates the glutathione redox cycle. *Free Radic Biol Med*, 33, 1527-33.
- NARENKUMAR, J., ALSALHI, M. S., ARUL PRAKASH, A., ABILAJI, S., DEVANESAN, S., RAJASEKAR, A. & ALFURAYDI, A. A. 2019. Impact and Role of Bacterial Communities on Biocorrosion of Metals Used in the Processing Industry. *ACS Omega*, 4, 21353-21360.
- NGUYEN, A. T., JONES, J. W., RUGE, M. A., KANE, M. A. & OGLESBY-SHERROUSE, A. G. 2015. Iron Depletion Enhances Production of Antimicrobials by Pseudomonas aeruginosa. *J Bacteriol*, 197, 2265-75.
- NGUYEN, A. T. & OGLESBY-SHERROUSE, A. G. 2016. Interactions between Pseudomonas aeruginosa and Staphylococcus aureus during co-cultivations and polymicrobial infections. *Appl Microbiol Biotechnol*, 100, 6141-8.
- NICKERSON, K. W., ATKIN, A. L. & HORNBLY, J. M. 2006. Quorum sensing in dimorphic fungi: farnesol and beyond. *Appl Environ Microbiol*, 72, 3805-13.
- NIKAIDO, H. 2003. Molecular basis of bacterial outer membrane permeability revisited. *Microbiol Mol Biol Rev*, 67, 593-656.
- NIMBALKAR, P. R., KHEDKAR, M. A., PARULEKAR, R. S., CHANDGUDE, V. K., SONAWANE, K. D., CHAVAN, P. V. & BANKAR, S. B. 2018. Role of Trace Elements as Cofactor: An Efficient Strategy toward Enhanced Biobutanol Production. *ACS Sustain Chem Eng*, 6, 9304-9313.
- NOCELLI, N., BOGINO, P. C., BANCHIO, E. & GIORDANO, W. 2016. Roles of Extracellular Polysaccharides and Biofilm Formation in Heavy Metal Resistance of Rhizobia. *Materials (Basel)*, 9.
- NOTO, M. J., BURNS, W. J., BEAVERS, W. N. & SKAAR, E. P. 2017. Mechanisms of Pyocyanin Toxicity and Genetic Determinants of Resistance in Staphylococcus aureus. *J Bacteriol*, 199.
- NOVICK, A. & SZILARD, L. 1950. Description of the chemostat. *Science*, 112, 715-6.
- O'BRIEN, S. & FOTHERGILL, J. L. 2017. The role of multispecies social interactions in shaping Pseudomonas aeruginosa pathogenicity in the cystic fibrosis lung. *FEMS Microbiol Lett*, 364.
- O'BRIEN, T. J. & WELCH, M. 2019a. A Continuous-Flow Model for *in vitro* Cultivation of Mixed Microbial Populations Associated with Cystic Fibrosis Airway Infections. *Front Microbiol*, 10, 2713.
- O'BRIEN, T. J. & WELCH, M. 2019b. Recapitulation of polymicrobial communities associated with cystic fibrosis airway infections: a perspective. *Future Microbiol*, 14, 1437-1450.
- O'TOOLE, G. A., PRATT, L. A., WATNICK, P. I., NEWMAN, D. K., WEAVER, V. B. & KOLTER, R. 1999. Genetic approaches to study of biofilms. *Methods Enzymol*, 310, 91-109.
- OLIVER, A., BAQUERO, F. & BLÁZQUEZ, J. 2002. The mismatch repair system (mutS, mutL and uvrD genes) in Pseudomonas aeruginosa: molecular characterization of naturally occurring mutants. *Mol Microbiol*, 43, 1641-50.

- OMOTANI, S., TANI, K., NAGAI, K., HATSUDA, Y., MUKAI, J. & MYOTOKU, M. 2017. Water Soluble Vitamins Enhance the Growth of Microorganisms in Peripheral Parenteral Nutrition Solutions. *Int J Med Sci*, 14, 1213-1219.
- OTTOW, J. C. & VON KLOPOTEK, A. 1969. Enzymatic reduction of iron oxide by fungi. *Appl Microbiol*, 18, 41-3.
- OWENS, N. D. L., DE DOMENICO, E. & GILCHRIST, M. J. 2019. An RNA-Seq Protocol for Differential Expression Analysis. *Cold Spring Harb Protoc*, 2019.
- PAGANIN, P., FISCARELLI, E. V., TUCCIO, V., CHIANCIANESI, M., BACCI, G., MORELLI, P., DOLCE, D., DALMASTRI, C., DE ALESSANDRI, A., LUCIDI, V., TACCETTI, G., MENGONI, A. & BEVIVINO, A. 2015. Changes in cystic fibrosis airway microbial community associated with a severe decline in lung function. *PLoS One*, 10, e0124348.
- PALEGO, L. A. B. L. A. G. G. 2015. Sulfur Metabolism and Sulfur-Containing Amino Acids: I-Molecular Effectors.
- PALLERONI, N. A. M. E. 2004. Taxonomy of Pseudomonads: Experimental Approaches. 3-44.
- PALMER, K. L., AYE, L. M. & WHITELEY, M. 2007. Nutritional cues control *Pseudomonas aeruginosa* multicellular behavior in cystic fibrosis sputum. *J Bacteriol*, 189, 8079-87.
- PALMER, K. L., MASHBURN, L. M., SINGH, P. K. & WHITELEY, M. 2005. Cystic fibrosis sputum supports growth and cues key aspects of *Pseudomonas aeruginosa* physiology. *J Bacteriol*, 187, 5267-77.
- PAN, X., YANG, Y. & ZHANG, J. R. 2014. Molecular basis of host specificity in human pathogenic bacteria. *Emerg Microbes Infect*, 3, e23.
- PANG, Z., RAUDONIS, R., GLICK, B. R., LIN, T. J. & CHENG, Z. 2019. Antibiotic resistance in *Pseudomonas aeruginosa*: mechanisms and alternative therapeutic strategies. *Biotechnol Adv*, 37, 177-192.
- PANKEY, G. A. & SABATH, L. D. 2004. Clinical relevance of bacteriostatic versus bactericidal mechanisms of action in the treatment of Gram-positive bacterial infections. *Clin Infect Dis*, 38, 864-70.
- PAPENFORT, K. & BASSLER, B. L. 2016. Quorum sensing signal-response systems in Gram-negative bacteria. *Nat Rev Microbiol*, 14, 576-88.
- PARSEK, M. R. A. S. P. K. 2003. Bacterial Biofilms: An Emerging Link to Disease Pathogenesis. *Annual Review of Microbiology*, 57, 677-701.
- PASKO, M. T., PISCITELLI, S. C. & VAN SLOOTEN, A. D. 1990. Fluconazole: a new triazole antifungal agent. *DICP*, 24, 860-7.
- PAULSSON, M. & RIESBECK, K. 2018. How bacteria hack the matrix and dodge the bullets of immunity. *Eur Respir Rev*, 27.
- PAYNE, S. M. 1994. Detection, isolation, and characterization of siderophores. *Methods Enzymol*, 235, 329-44.
- PERSAT, A., INCLAN, Y. F., ENGEL, J. N., STONE, H. A. & GITAI, Z. 2015. Type IV pili mechanoechemically regulate virulence factors in *Pseudomonas aeruginosa*. *Proc Natl Acad Sci U S A*, 112, 7563-8.
- PETERS, B. M., JABRA-RIZK, M. A., O'MAY, G. A., COSTERTON, J. W. & SHIRTLIFF, M. E. 2012a. Polymicrobial interactions: impact on pathogenesis and human disease. *Clin Microbiol Rev*, 25, 193-213.
- PETERS, B. M., JABRA-RIZK, M. A., SCHEPER, M. A., LEID, J. G., COSTERTON, J. W. & SHIRTLIFF, M. E. 2010. Microbial interactions and differential protein expression in *Staphylococcus aureus* - *Candida albicans* dual-species biofilms. *FEMS Immunol Med Microbiol*, 59, 493-503.
- PETERS, B. M., OVCHINNIKOVA, E. S., KROM, B. P., SCHLECHT, L. M., ZHOU, H., HOYER, L. L., BUSSCHER, H. J., VAN DER MEI, H. C., JABRA-RIZK, M. A. & SHIRTLIFF, M. E. 2012b. *Staphylococcus aureus* adherence to *Candida albicans* hyphae is mediated by the hyphal adhesin Als3p. *Microbiology (Reading)*, 158, 2975-2986.

- PEZZULO, A. A., TANG, X. X., HOEGGER, M. J., ABOU ALAIWA, M. H., RAMACHANDRAN, S., MONINGER, T. O., KARP, P. H., WOHLFORD-LENANE, C. L., HAAGSMAN, H. P., VAN EIJK, M., BÁNFI, B., HORSWILL, A. R., STOLTZ, D. A., MCCRAY, P. B., WELSH, M. J. & ZABNER, J. 2012. Reduced airway surface pH impairs bacterial killing in the porcine cystic fibrosis lung. *Nature*, 487, 109-13.
- PIHET, M., CARRERE, J., CIMON, B., CHABASSE, D., DELHAES, L., SYMOENS, F. & BOUCHARA, J. P. 2009. Occurrence and relevance of filamentous fungi in respiratory secretions of patients with cystic fibrosis--a review. *Med Mycol*, 47, 387-97.
- PIISPANEN, A. E., BONNEFOI, O., CARDEN, S., DEVEAU, A., BASSILANA, M. & HOGAN, D. A. 2011. Roles of Ras1 membrane localization during *Candida albicans* hyphal growth and farnesol response. *Eukaryot Cell*, 10, 1473-84.
- PLETNEV, P., OSTERMAN, I., SERGIEV, P., BOGDANOV, A. & DONTSOVA, O. 2015. Survival guide: *Escherichia coli* in the stationary phase. *Acta Naturae*, 7, 22-33.
- PLETZER, D., LAFON, C., BRAUN, Y., KÖHLER, T., PAGE, M. G., MOUREZ, M. & WEINGART, H. 2014. High-throughput screening of dipeptide utilization mediated by the ABC transporter DppBCDF and its substrate-binding proteins DppA1-A5 in *Pseudomonas aeruginosa*. *PLoS One*, 9, e111311.
- POLETO, C., MELONI, S., VAN METRE, A., COLIZZA, V., MORENO, Y. & VESPIGNANI, A. 2015. Characterising two-pathogen competition in spatially structured environments. *Sci Rep*, 5, 7895.
- PONTES, M. H. & GROISMAN, E. A. 2019. Slow growth determines nonheritable antibiotic resistance in. *Sci Signal*, 12.
- POOLE, K. 2011. *Pseudomonas aeruginosa*: resistance to the max. *Front Microbiol*, 2, 65.
- POPAT, R., CRUSZ, S. A., MESSINA, M., WILLIAMS, P., WEST, S. A. & DIGGLE, S. P. 2012. Quorum-sensing and cheating in bacterial biofilms. *Proc Biol Sci*, 279, 4765-71.
- POSTGATE, J. R. & HUNTER, J. R. 1962. The survival of starved bacteria. *J Gen Microbiol*, 29, 233-63.
- PRESSLER, T., BOHMOVA, C., CONWAY, S., DUMCIUS, S., HJELTE, L., HØIBY, N., KOLLBERG, H., TÜMMLER, B. & VAVROVA, V. 2011. Chronic *Pseudomonas aeruginosa* infection definition: EuroCareCF Working Group report. *J Cyst Fibros*, 10 Suppl 2, S75-8.
- PREVAES, S. M., DE STEENHUIJSEN PITERS, W. A., DE WINTER-DE GROOT, K. M., JANSSENS, H. M., TRAMPER-STRANDERS, G. A., CHU, M. L., TIDDENS, H. A., VAN WESTREENEN, M., VAN DER ENT, C. K., SANDERS, E. A. & BOGAERT, D. 2017. Concordance between upper and lower airway microbiota in infants with cystic fibrosis. *Eur Respir J*, 49.
- PRICE, C. E., BROWN, D. G., LIMOLI, D. H., PHELAN, V. V. & O'TOOLE, G. A. 2020. Exogenous Alginate Protects *Staphylococcus aureus* from Killing by *Pseudomonas aeruginosa*. *J Bacteriol*, 202.
- PROESMANS, M., BALINSKA-MISKIEWICZ, W., DUPONT, L., BOSSUYT, X., VERHAEGEN, J., HØIBY, N. & DE BOECK, K. 2006. Evaluating the "Leeds criteria" for *Pseudomonas aeruginosa* infection in a cystic fibrosis centre. *Eur Respir J*, 27, 937-43.
- PRUNIER, A. L. & LECLERCQ, R. 2005. Role of *mutS* and *mutL* genes in hypermutability and recombination in *Staphylococcus aureus*. *J Bacteriol*, 187, 3455-64.
- PULCRANO, G., IULA, D. V., RAIA, V., ROSSANO, F. & CATANIA, M. R. 2012. Different mutations in *mucA* gene of *Pseudomonas aeruginosa* mucoid strains in cystic fibrosis patients and their effect on *algU* gene expression. *New Microbiol*, 35, 295-305.
- QAZI, S., MIDDLETON, B., MUHARRAM, S. H., COCKAYNE, A., HILL, P., O'SHEA, P., CHHABRA, S. R., CÁMARA, M. & WILLIAMS, P. 2006. N-acylhomoserine lactones antagonize virulence gene expression and quorum sensing in *Staphylococcus aureus*. *Infect Immun*, 74, 910-9.
- QUINN, R. A., LIM, Y. W., MAUGHAN, H., CONRAD, D., ROHWER, F. & WHITESON, K. L. 2014. Biogeochemical forces shape the composition and physiology of polymicrobial communities in the cystic fibrosis lung. *MBio*, 5, e00956-13.
- QUINN, R. A., WHITESON, K., LIM, Y. W., SALAMON, P., BAILEY, B., MIENARDI, S., SANCHEZ, S. E., BLAKE, D., CONRAD, D. & ROHWER, F. 2015. A Winogradsky-based culture system shows an

- association between microbial fermentation and cystic fibrosis exacerbation. *ISME J*, 9, 1052.
- QUINTON, P. M. 1983. Chloride impermeability in cystic fibrosis. *Nature*, 301, 421-2.
- RAJAN, S. & SAIMAN, L. 2002. Pulmonary infections in patients with cystic fibrosis. *Semin Respir Infect*, 17, 47-56.
- RAMAGE, G., SAVILLE, S. P., WICKES, B. L. & LÓPEZ-RIBOT, J. L. 2002. Inhibition of *Candida albicans* biofilm formation by farnesol, a quorum-sensing molecule. *Appl Environ Microbiol*, 68, 5459-63.
- RAMPHAL, R., KOO, L., ISHIMOTO, K. S., TOTTEN, P. A., LARA, J. C. & LORY, S. 1991. Adhesion of *Pseudomonas aeruginosa* pilin-deficient mutants to mucin. *Infect Immun*, 59, 1307-11.
- RATJEN, F., BELL, S. C., ROWE, S. M., GOSS, C. H., QUITTNER, A. L. & BUSH, A. 2015. Cystic fibrosis. *Nat Rev Dis Primers*, 1, 15010.
- RATJEN, F., HUG, C., MARIGOWDA, G., TIAN, S., HUANG, X., STANOJEVIC, S., MILLA, C. E., ROBINSON, P. D., WALTZ, D., DAVIES, J. C. & GROUP, V.-I. 2017. Efficacy and safety of lumacaftor and ivacaftor in patients aged 6-11 years with cystic fibrosis homozygous for F508del-CFTR: a randomised, placebo-controlled phase 3 trial. *Lancet Respir Med*, 5, 557-567.
- RATNER, D. & MUELLER, C. 2012. Immune responses in cystic fibrosis: are they intrinsically defective? *Am J Respir Cell Mol Biol*, 46, 715-22.
- REGASSA, L. B. & BETLEY, M. J. 1992. Alkaline pH decreases expression of the accessory gene regulator (*agr*) in *Staphylococcus aureus*. *J Bacteriol*, 174, 5095-100.
- REID, D. W., CARROLL, V., O'MAY, C., CHAMPION, A. & KIROV, S. M. 2007. Increased airway iron as a potential factor in the persistence of *Pseudomonas aeruginosa* infection in cystic fibrosis. *Eur Respir J*, 30, 286-92.
- RENWICK, J., MCNALLY, P., JOHN, B., DESANTIS, T., LINNANE, B., MURPHY, P. & CF, S. 2014. The microbial community of the cystic fibrosis airway is disrupted in early life. *PLoS One*, 9, e109798.
- RENWICK, M. J., SIMPKIN, V. & MOSSIALOS, E. 2016. Targeting innovation in antibiotic drug discovery and development: The need for a One Health – One Europe – One World Framework.
- RICHARDSON, J. P., HO, J. & NAGLIK, J. R. 2018. *Candida*-Epithelial Interactions. *J Fungi (Basel)*, 4.
- RIORDAN, J. R., ROMMENS, J. M., KEREM, B., ALON, N., ROZMAHEL, R., GRZELCZAK, Z., ZIELENSKI, J., LOK, S., PLAUSIC, N. & CHOU, J. L. 1989. Identification of the cystic fibrosis gene: cloning and characterization of complementary DNA. *Science*, 245, 1066-73.
- ROGERS, C. S., ABRAHAM, W. M., BROGDEN, K. A., ENGELHARDT, J. F., FISHER, J. T., MCCRAY, P. B., MCLENNAN, G., MEYERHOLZ, D. K., NAMATI, E., OSTEDGAARD, L. S., PRATHER, R. S., SABATER, J. R., STOLTZ, D. A., ZABNER, J. & WELSH, M. J. 2008. The porcine lung as a potential model for cystic fibrosis. *Am J Physiol Lung Cell Mol Physiol*, 295, L240-63.
- ROGERS, G. B., CARROLL, M. P. & BRUCE, K. D. 2009. Studying bacterial infections through culture-independent approaches. *J Med Microbiol*, 58, 1401-18.
- ROGERS, G. B., CARROLL, M. P., SERISIER, D. J., HOCKEY, P. M., JONES, G. & BRUCE, K. D. 2004. characterization of bacterial community diversity in cystic fibrosis lung infections by use of 16s ribosomal DNA terminal restriction fragment length polymorphism profiling. *J Clin Microbiol*, 42, 5176-83.
- ROGERS, G. B., CARROLL, M. P., SERISIER, D. J., HOCKEY, P. M., KEHAGIA, V., JONES, G. R. & BRUCE, K. D. 2005. Bacterial activity in cystic fibrosis lung infections. *Respir Res*, 6, 49.
- ROGERS, G. B., HOFFMAN, L. R., WHITELEY, M., DANIELS, T. W., CARROLL, M. P. & BRUCE, K. D. 2010a. Revealing the dynamics of polymicrobial infections: implications for antibiotic therapy. *Trends Microbiol*, 18, 357-64.
- ROGERS, G. B., STRESSMANN, F. A., WALKER, A. W., CARROLL, M. P. & BRUCE, K. D. 2010b. Lung infections in cystic fibrosis: deriving clinical insight from microbial complexity. *Expert Rev Mol Diagn*, 10, 187-96.

- ROGNES, T., FLOURI, T., NICHOLS, B., QUINCE, C. & MAHÉ, F. 2016. VSEARCH: a versatile open source tool for metagenomics. *PeerJ*, 4, e2584.
- ROLFE, M. D., RICE, C. J., LUCCHINI, S., PIN, C., THOMPSON, A., CAMERON, A. D., ALSTON, M., STRINGER, M. F., BETTS, R. P., BARANYI, J., PECK, M. W. & HINTON, J. C. 2012. Lag phase is a distinct growth phase that prepares bacteria for exponential growth and involves transient metal accumulation. *J Bacteriol*, 194, 686-701.
- ROMMENS, J. M., IANNUZZI, M. C., KEREM, B., DRUMM, M. L., MELMER, G., DEAN, M., ROZMAHEL, R., COLE, J. L., KENNEDY, D. & HIDAKA, N. 1989. Identification of the cystic fibrosis gene: chromosome walking and jumping. *Science*, 245, 1059-65.
- ROSCHE, W. A. & FOSTER, P. L. 2000. Determining mutation rates in bacterial populations. *Methods*, 20, 4-17.
- ROSENFELD, M., BERNARDO-OCAMPO, C., EMERSON, J., GENATOSSIO, A., BURNS, J. & GIBSON, R. 2012. Prevalence of cystic fibrosis pathogens in the oropharynx of healthy children and implications for cystic fibrosis care. *J Cyst Fibros*, 11, 456-7.
- ROSLEV, P. & KING, G. M. 1993. Application of a tetrazolium salt with a water-soluble formazan as an indicator of viability in respiring bacteria. *Appl Environ Microbiol*, 59, 2891-6.
- RUTHERFORD, S. T. & BASSLER, B. L. 2012. Bacterial quorum sensing: its role in virulence and possibilities for its control. *Cold Spring Harb Perspect Med*, 2.
- RÖMLING, U., FIEDLER, B., BOSSHAMMER, J., GROTHUES, D., GREIPEL, J., VON DER HARDT, H. & TÜMMLER, B. 1994. Epidemiology of chronic *Pseudomonas aeruginosa* infections in cystic fibrosis. *J Infect Dis*, 170, 1616-21.
- SABRA, W., KIM, E. J. & ZENG, A. P. 2002. Physiological responses of *Pseudomonas aeruginosa* PAO1 to oxidative stress in controlled microaerobic and aerobic cultures. *Microbiology*, 148, 3195-3202.
- SAJJAN, U., THANASSOULIS, G., CHERAPANOV, V., LU, A., SJOLIN, C., STEER, B., WU, Y. J., ROTSTEIN, O. D., KENT, G., MCKERLIE, C., FORSTNER, J. & DOWNEY, G. P. 2001. Enhanced susceptibility to pulmonary infection with *Burkholderia cepacia* in *Cftr*(-/-) mice. *Infect Immun*, 69, 5138-50.
- SALTER, S. J., COX, M. J., TUREK, E. M., CALUS, S. T., COOKSON, W. O., MOFFATT, M. F., TURNER, P., PARKHILL, J., LOMAN, N. J. & WALKER, A. W. 2014. Reagent and laboratory contamination can critically impact sequence-based microbiome analyses. *BMC Biol*, 12, 87.
- SAMBROOK, J. & RUSSELL, D. W. 2006. Preparation and Transformation of Competent *E. coli* Using Calcium Chloride. *CSH Protoc*, 2006.
- SANDS, K., WILLIAMS, D. W., WILSON, M., LEWIS, M. & WISE, M. P. 2013. The dynamics of polymicrobial biofilms. *Am J Respir Crit Care Med*, 188, 1266.
- SANKARALINGAM, S., ESWARAN, S., BALAKAN, B., SUNDARAM, V. & SHANKAR, T. 2014. Screening and Growth Characterization of Phosphate Solubilizing Bacterium *Pseudomonas aeruginosa*. *Advances in Environmental Biology*, 8, 673-680.
- SANKARAN, J., TAN, N. J. H. J., BUT, K. P., COHEN, Y., RICE, S. A. & WOHLAND, T. 2019. Single microcolony diffusion analysis in *Pseudomonas aeruginosa* biofilms. *NPJ Biofilms Microbiomes*, 5, 35.
- SAUER, K. 2003. The genomics and proteomics of biofilm formation. *Genome Biol*, 4, 219.
- SAUER, K., CULLEN, M. C., RICKARD, A. H., ZEEF, L. A., DAVIES, D. G. & GILBERT, P. 2004. Characterization of nutrient-induced dispersion in *Pseudomonas aeruginosa* PAO1 biofilm. *J Bacteriol*, 186, 7312-26.
- SCHAAFF, F., REIPERT, A. & BIERBAUM, G. 2002. An elevated mutation frequency favors development of vancomycin resistance in *Staphylococcus aureus*. *Antimicrob Agents Chemother*, 46, 3540-8.
- SCHERTZER, J. W., BROWN, S. A. & WHITELEY, M. 2010. Oxygen levels rapidly modulate *Pseudomonas aeruginosa* social behaviours via substrate limitation of PqsH. *Mol Microbiol*, 77, 1527-38.

- SCHICK, A. & KASSEN, R. 2018. Rapid diversification of *Pseudomonas aeruginosa* in cystic fibrosis lung-like conditions. *Proc Natl Acad Sci U S A*, 115, 10714-10719.
- SCHULTZ, J., MÜLLER, T., ACHTZIGER, M., SEIBEL, P. N., DANDEKAR, T. & WOLF, M. 2006. The internal transcribed spacer 2 database--a web server for (not only) low level phylogenetic analyses. *Nucleic Acids Res*, 34, W704-7.
- SCHURR, M. J. 2020. *Pseudomonas aeruginosa* Alginate Benefits *Staphylococcus aureus*? *J Bacteriol*, 202.
- SCHUSTER, M. & GREENBERG, E. P. 2006. A network of networks: quorum-sensing gene regulation in *Pseudomonas aeruginosa*. *Int J Med Microbiol*, 296, 73-81.
- SCHUSTER, M., LOSTROH, C. P., OGI, T. & GREENBERG, E. P. 2003. Identification, timing, and signal specificity of *Pseudomonas aeruginosa* quorum-controlled genes: a transcriptome analysis. *J Bacteriol*, 185, 2066-79.
- SHAH, I. M., LAABERKI, M. H., POPHAM, D. L. & DWORKIN, J. 2008. A eukaryotic-like Ser/Thr kinase signals bacteria to exit dormancy in response to peptidoglycan fragments. *Cell*, 135, 486-96.
- SHARMA, D., MISBA, L. & KHAN, A. U. 2019. Antibiotics versus biofilm: an emerging battleground in microbial communities. *Antimicrob Resist Infect Control*, 8, 76.
- SHIRTLIFF, M. E., PETERS, B. M. & JABRA-RIZK, M. A. 2009. Cross-kingdom interactions: *Candida albicans* and bacteria. *FEMS Microbiol Lett*, 299, 1-8.
- SIBLEY, C. D., PARKINS, M. D., RABIN, H. R., DUAN, K., NORGAARD, J. C. & SURETTE, M. G. 2008. A polymicrobial perspective of pulmonary infections exposes an enigmatic pathogen in cystic fibrosis patients. *Proc Natl Acad Sci U S A*, 105, 15070-5.
- SIBLEY, C. D., RABIN, H. & SURETTE, M. G. 2006. Cystic fibrosis: a polymicrobial infectious disease. *Future Microbiol*, 1, 53-61.
- SINGH, P. K., SCHAEFER, A. L., PARSEK, M. R., MONINGER, T. O., WELSH, M. J. & GREENBERG, E. P. 2000. Quorum-sensing signals indicate that cystic fibrosis lungs are infected with bacterial biofilms. *Nature*, 407, 762-4.
- SMITH, A. C., RICE, A., SUTTON, B., GABRILSKA, R., WESSEL, A. K., WHITELEY, M. & RUMBAUGH, K. P. 2017. Albumin Inhibits *Pseudomonas aeruginosa* Quorum Sensing and Alters Polymicrobial Interactions. *Infect Immun*, 85.
- SMITH, E. E., BUCKLEY, D. G., WU, Z., SAENPHIMMACHAK, C., HOFFMAN, L. R., D'ARGENIO, D. A., MILLER, S. I., RAMSEY, B. W., SPEERT, D. P., MOSKOWITZ, S. M., BURNS, J. L., KAUL, R. & OLSON, M. V. 2006. Genetic adaptation by *Pseudomonas aeruginosa* to the airways of cystic fibrosis patients. *Proc Natl Acad Sci U S A*, 103, 8487-92.
- SMITH, H. L. & WALTMAN, P. 1995. *The Theory of the Chemostat: Dynamics of Microbial Competition*. Cambridge University Press.
- SOBERÓN-CHÁVEZ, G., LÉPINE, F. & DÉZIEL, E. 2005. Production of rhamnolipids by *Pseudomonas aeruginosa*. *Appl Microbiol Biotechnol*, 68, 718-25.
- SON, M. S., MATTHEWS, W. J., KANG, Y., NGUYEN, D. T. & HOANG, T. T. 2007. In vivo evidence of *Pseudomonas aeruginosa* nutrient acquisition and pathogenesis in the lungs of cystic fibrosis patients. *Infect Immun*, 75, 5313-24.
- SOUSA, A. M., MONTEIRO, R. & PEREIRA, M. O. 2018. Unveiling the early events of *Pseudomonas aeruginosa* adaptation in cystic fibrosis airway environment using a long-term in vitro maintenance. *Int J Med Microbiol*, 308, 1053-1064.
- SOUSA, A. M. & PEREIRA, M. O. 2014. *Pseudomonas aeruginosa* Diversification during Infection Development in Cystic Fibrosis Lungs-A Review. *Pathogens*, 3, 680-703.
- SPIERS, A. J., BUCKLING, A. & RAINEY, P. B. 2000. The causes of *Pseudomonas* diversity. *Microbiology*, 146 (Pt 10), 2345-2350.
- SRIRAMULU, D. D., LÜNSDORF, H., LAM, J. S. & RÖMLING, U. 2005. Microcolony formation: a novel biofilm model of *Pseudomonas aeruginosa* for the cystic fibrosis lung. *J Med Microbiol*, 54, 667-76.

- STANOJEVIC, S., MCDONALD, A., WATERS, V., MACDONALD, S., HORTON, E., TULLIS, E. & RATJEN, F. 2017. Effect of pulmonary exacerbations treated with oral antibiotics on clinical outcomes in cystic fibrosis. *Thorax*, 72, 327-332.
- STENBIT, A. E. & FLUME, P. A. 2011. Pulmonary exacerbations in cystic fibrosis. *Curr Opin Pulm Med*, 17, 442-7.
- STEWART, P. S. 2002. Mechanisms of antibiotic resistance in bacterial biofilms. *Int J Med Microbiol*, 292, 107-13.
- STEWART, P. S. 2003. Diffusion in biofilms. *J Bacteriol*, 185, 1485-91.
- STINTZI, A., EVANS, K., MEYER, J. M. & POOLE, K. 1998. Quorum-sensing and siderophore biosynthesis in *Pseudomonas aeruginosa*: lasR/lasI mutants exhibit reduced pyoverdine biosynthesis. *FEMS Microbiol Lett*, 166, 341-5.
- STOODLEY, P., SAUER, K., DAVIES, D. G. & COSTERTON, J. W. 2002. Biofilms as complex differentiated communities. *Annu Rev Microbiol*, 56, 187-209.
- STOREY, D. G., UJACK, E. E. & RABIN, H. R. 1992. Population transcript accumulation of *Pseudomonas aeruginosa* exotoxin A and elastase in sputa from patients with cystic fibrosis. *Infect Immun*, 60, 4687-94.
- STORM, M. P., SORRELL, I., SHIPLEY, R., REGAN, S., LUETCHFORD, K. A., SATHISH, J., WEBB, S. & ELLIS, M. J. 2016. Hollow Fiber Bioreactors for In Vivo-like Mammalian Tissue Culture. *J Vis Exp*.
- STOVER, C. K., PHAM, X. Q., ERWIN, A. L., MIZOGUCHI, S. D., WARRENER, P., HICKEY, M. J., BRINKMAN, F. S., HUFNAGLE, W. O., KOWALIK, D. J., LAGROU, M., GARBER, R. L., GOLTRY, L., TOLENTINO, E., WESTBROCK-WADMAN, S., YUAN, Y., BRODY, L. L., COULTER, S. N., FOLGER, K. R., KAS, A., LARBIG, K., LIM, R., SMITH, K., SPENCER, D., WONG, G. K., WU, Z., PAULSEN, I. T., REIZER, J., SAIER, M. H., HANCOCK, R. E., LORY, S. & OLSON, M. V. 2000. Complete genome sequence of *Pseudomonas aeruginosa* PAO1, an opportunistic pathogen. *Nature*, 406, 959-64.
- STRESSMANN, F. A., ROGERS, G. B., MARSH, P., LILLEY, A. K., DANIELS, T. W., CARROLL, M. P., HOFFMAN, L. R., JONES, G., ALLEN, C. E., PATEL, N., FORBES, B., TUCK, A. & BRUCE, K. D. 2011. Does bacterial density in cystic fibrosis sputum increase prior to pulmonary exacerbation? *J Cyst Fibros*, 10, 357-65.
- STRESSMANN, F. A., ROGERS, G. B., VAN DER GAST, C. J., MARSH, P., VERMEER, L. S., CARROLL, M. P., HOFFMAN, L., DANIELS, T. W., PATEL, N., FORBES, B. & BRUCE, K. D. 2012. Long-term cultivation-independent microbial diversity analysis demonstrates that bacterial communities infecting the adult cystic fibrosis lung show stability and resilience. *Thorax*, 67, 867-73.
- STRÖMPL, C., TINDALL, B. J., JARVIS, G. N., LÜNSDORF, H., MOORE, E. R. & HIPPE, H. 1999. A re-evaluation of the taxonomy of the genus *Anaerovibrio*, with the reclassification of *Anaerovibrio glycerini* as *Anaerosinus glycerini* gen. nov., comb. nov., and *Anaerovibrio burkinabensis* as *Anaeroarcus burkinensis* [corrig.] gen. nov., comb. nov. *Int J Syst Bacteriol*, 49 Pt 4, 1861-72.
- SUGAI, M., FUJIWARA, T., AKIYAMA, T., OHARA, M., KOMATSUZAWA, H., INOUE, S. & SUGINAKA, H. 1997. Purification and molecular characterization of glycylglycine endopeptidase produced by *Staphylococcus capitis* EPK1. *J Bacteriol*, 179, 1193-202.
- SUN, Z., KANG, Y., NORRIS, M. H., TROYER, R. M., SON, M. S., SCHWEIZER, H. P., DOW, S. W. & HOANG, T. T. 2014. Blocking phosphatidylcholine utilization in *Pseudomonas aeruginosa*, via mutagenesis of fatty acid, glycerol and choline degradation pathways, confirms the importance of this nutrient source in vivo. *PLoS One*, 9, e103778.
- SURI, R. 2005. The use of human deoxyribonuclease (rhDNase) in the management of cystic fibrosis. *BioDrugs*, 19, 135-44.
- SZWEDA, P., KOTŁOWSKI, R. & KUR, J. 2005. New effective sources of the *Staphylococcus simulans* lysostaphin. *J Biotechnol*, 117, 203-13.

- TAKASE, H., NITANAI, H., HOSHINO, K. & OTANI, T. 2000a. Impact of siderophore production on *Pseudomonas aeruginosa* infections in immunosuppressed mice. *Infect Immun*, 68, 1834-9.
- TAKASE, H., NITANAI, H., HOSHINO, K. & OTANI, T. 2000b. Requirement of the *Pseudomonas aeruginosa* tonB gene for high-affinity iron acquisition and infection. *Infect Immun*, 68, 4498-504.
- TART, A. H., WOLFGANG, M. C. & WOZNIAK, D. J. 2005. The alternative sigma factor AlgT represses *Pseudomonas aeruginosa* flagellum biosynthesis by inhibiting expression of fleQ. *J Bacteriol*, 187, 7955-62.
- TATE, S., MACGREGOR, G., DAVIS, M., INNES, J. A. & GREENING, A. P. 2002. Airways in cystic fibrosis are acidified: detection by exhaled breath condensate. *Thorax*, 57, 926-9.
- TESTERMAN, T. L., MCGEE, D. J. & MOBLEY, H. L. 2001. *Helicobacter pylori* growth and urease detection in the chemically defined medium Ham's F-12 nutrient mixture. *J Clin Microbiol*, 39, 3842-50.
- THEOPHEL, K., SCHACHT, V. J., SCHLÜTER, M., SCHNELL, S., STINGU, C. S., SCHAUMANN, R. & BUNGE, M. 2014. The importance of growth kinetic analysis in determining bacterial susceptibility against antibiotics and silver nanoparticles. *Front Microbiol*, 5, 544.
- THOMAS, P., SEKHAR, A. C., UPRETI, R., MUJAWAR, M. M. & PASHA, S. S. 2015. Optimization of single plate-serial dilution spotting (SP-SDS) with sample anchoring as an assured method for bacterial and yeast cfu enumeration and single colony isolation from diverse samples. *Biotechnol Rep (Amst)*, 8, 45-55.
- TIKHOMIROVA, A. & KIDD, S. P. 2013. *Haemophilus influenzae* and *Streptococcus pneumoniae*: living together in a biofilm. *Pathog Dis*, 69, 114-26.
- TODD, O. A., FIDEL, P. L., HARRO, J. M., HILLIARD, J. J., TKACZYK, C., SELLMAN, B. R., NOVERR, M. C. & PETERS, B. M. 2019. *Candida albicans* Augments *Staphylococcus aureus* Virulence by Engaging the Staphylococcal agr Quorum Sensing System. *mBio*, 10.
- TOLKER-NIELSEN, T. & MOLIN, S. 2004. The Biofilm Lifestyle of *Pseudomonads*. In: Ramos JL. (eds) *Pseudomonas*. Springer, Boston, MA.
- TREANGEN, T. J., MAYBANK, R. A., ENKE, S., FRISS, M. B., DIVIAK, L. F., KARAOLIS, D. K., KOREN, S., ONDOV, B., PHILLIPPY, A. M., BERGMAN, N. H. & ROSOVITZ, M. J. 2014. Complete Genome Sequence of the Quality Control Strain *Staphylococcus aureus* subsp. *aureus* ATCC 25923. *Genome Announc*, 2.
- TREJO-HERNÁNDEZ, A., ANDRADE-DOMÍNGUEZ, A., HERNÁNDEZ, M. & ENCARNACIÓN, S. 2014. Interspecies competition triggers virulence and mutability in *Candida albicans*-*Pseudomonas aeruginosa* mixed biofilms. *ISME J*, 8, 1974-88.
- TSUI, C., KONG, E. F. & JABRA-RIZK, M. A. 2016. Pathogenesis of *Candida albicans* biofilm. *Pathog Dis*, 74, ftw018.
- TUNNEY, M. M., FIELD, T. R., MORIARTY, T. F., PATRICK, S., DOERING, G., MUHLEBACH, M. S., WOLFGANG, M. C., BOUCHER, R., GILPIN, D. F., MCDOWELL, A. & ELBORN, J. S. 2008. Detection of anaerobic bacteria in high numbers in sputum from patients with cystic fibrosis. *Am J Respir Crit Care Med*, 177, 995-1001.
- TURNER, K. H., WESSEL, A. K., PALMER, G. C., MURRAY, J. L. & WHITELEY, M. 2015. Essential genome of *Pseudomonas aeruginosa* in cystic fibrosis sputum. *Proc Natl Acad Sci U S A*, 112, 4110-5.
- VACCA, I. 2017. Bacterial ecology: Cheaters take advantage. *Nat Rev Microbiol*, 15, 575.
- VALENTINO, M. D., FOULSTON, L., SADAKA, A., KOS, V. N., VILLET, R. A., SANTA MARIA, J., LAZINSKI, D. W., CAMILLI, A., WALKER, S., HOOPER, D. C. & GILMORE, M. S. 2014. Genes contributing to *Staphylococcus aureus* fitness in abscess- and infection-related ecologies. *mBio*, 5, e01729-14.
- VALENZA, G., TAPPE, D., TURNWALD, D., FROSCH, M., KÖNIG, C., HEBESTREIT, H. & ABELE-HORN, M. 2008. Prevalence and antimicrobial susceptibility of microorganisms isolated from sputa of patients with cystic fibrosis. *J Cyst Fibros*, 7, 123-7.

- VAN DELDEN, C. 2004. Virulence Factors in *Pseudomonas Aeruginosa*. In: Ramos JL. (eds) Virulence and Gene Regulation. Springer, Boston, MA.
- VAN DER LAAN, A. L. & BOENINK, M. 2015. Beyond bench and bedside: disentangling the concept of translational research. *Health Care Anal*, 23, 32-49.
- VAN OPIJNEN, T., BODI, K. L. & CAMILLI, A. 2009. Tn-seq: high-throughput parallel sequencing for fitness and genetic interaction studies in microorganisms. *Nat Methods*, 6, 767-72.
- VANDEPLASSCHE, E., TAVERNIER, S., COENYE, T. & CRABBÉ, A. 2019. Influence of the lung microbiome on antibiotic susceptibility of cystic fibrosis pathogens. *Eur Respir Rev*, 28.
- VEERANAGOUDA, Y., LEE, K., CHO, A. R., CHO, K., ANDERSON, E. M. & LAM, J. S. 2011. Ssg, a putative glycosyltransferase, functions in lipo- and exopolysaccharide biosynthesis and cell surface-related properties in *Pseudomonas alkylphenolia*. *FEMS Microbiol Lett*, 315, 38-45.
- VEGA, N. M., ALLISON, K. R., SAMUELS, A. N., KLEMPNER, M. S. & COLLINS, J. J. 2013. Salmonella typhimurium intercepts Escherichia coli signaling to enhance antibiotic tolerance. *Proc Natl Acad Sci U S A*, 110, 14420-5.
- VENDEVILLE, A., WINZER, K., HEURLIER, K., TANG, C. M. & HARDIE, K. R. 2005. Making 'sense' of metabolism: autoinducer-2, LuxS and pathogenic bacteria. *Nat Rev Microbiol*, 3, 383-96.
- VERDEROSA, A. D., TOTSIKA, M. & FAIRFULL-SMITH, K. E. 2019. Bacterial Biofilm Eradication Agents: A Current Review. *Front Chem*, 7, 824.
- VILA, T., KONG, E. F., IBRAHIM, A., PIEPENBRINK, K., SHETTY, A. C., MCCracken, C., BRUNO, V. & JABRA-RIZK, M. A. 2019. quorum-sensing molecule farnesol modulates staphyloxanthin production and activates the thiol-based oxidative-stress response in. *Virulence*, 10, 625-642.
- VISCA, P., BONCHI, C., MINANDRI, F., FRANGIPANI, E. & IMPERI, F. 2013. The dual personality of iron chelators: growth inhibitors or promoters? *Antimicrob Agents Chemother*, 57, 2432-3.
- VYLKOVA, S., CARMAN, A. J., DANHOF, H. A., COLLETTE, J. R., ZHOU, H. & LORENZ, M. C. 2011. The fungal pathogen *Candida albicans* autoinduces hyphal morphogenesis by raising extracellular pH. *mBio*, 2, e00055-11.
- WADA, A. 2001. An improved method for purifying bacterial genomic DNAs for direct sequencing by capillary automated sequencer. *Technical Tips Online*, 6, 12 - 14.
- WAGNER, V. E., BUSHNELL, D., PASSADOR, L., BROOKS, A. I. & IGLEWSKI, B. H. 2003. Microarray analysis of *Pseudomonas aeruginosa* quorum-sensing regulons: effects of growth phase and environment. *J Bacteriol*, 185, 2080-95.
- WAINWRIGHT, C. E., ELBORN, J. S. & RAMSEY, B. W. 2015. Lumacaftor-Ivacaftor in Patients with Cystic Fibrosis Homozygous for Phe508del CFTR. *N Engl J Med*, 373, 1783-4.
- WAKEMAN, C. A., MOORE, J. L., NOTO, M. J., ZHANG, Y., SINGLETON, M. D., PRENTICE, B. M., GILSTON, B. A., DOSTER, R. S., GADDY, J. A., CHAZIN, W. J., CAPRIOLI, R. M. & SKAAR, E. P. 2016. The innate immune protein calprotectin promotes *Pseudomonas aeruginosa* and *Staphylococcus aureus* interaction. *Nat Commun*, 7, 11951.
- WANG, Y., ZHANG, W., WU, Z. & LU, C. 2011. Reduced virulence is an important characteristic of biofilm infection of *Streptococcus suis*. *FEMS Microbiol Lett*, 316, 36-43.
- WANNER, U. & EGLI, T. 1990. Dynamics of microbial growth and cell composition in batch culture. *FEMS Microbiol Rev*, 6, 19-43.
- WARD, C. L., OMURA, S. & KOPITO, R. R. 1995. Degradation of CFTR by the ubiquitin-proteasome pathway. *Cell*, 83, 121-7.
- WATERS, C. M. & GOLDBERG, J. B. 2019. *Pseudomonas aeruginosa* in cystic fibrosis: A chronic cheater. *Proc Natl Acad Sci U S A*, 116, 6525-6527.
- WEI, Q. & MA, L. Z. 2013. Biofilm matrix and its regulation in *Pseudomonas aeruginosa*. *Int J Mol Sci*, 14, 20983-1005.
- WEIMER, K. E., ARMBRUSTER, C. E., JUNEAU, R. A., HONG, W., PANG, B. & SWORDS, W. E. 2010. Coinfection with *Haemophilus influenzae* promotes pneumococcal biofilm formation during

- experimental otitis media and impedes the progression of pneumococcal disease. *J Infect Dis*, 202, 1068-75.
- WEISBURG, W. G., BARNES, S. M., PELLETIER, D. A. & LANE, D. J. 1991. 16S ribosomal DNA amplification for phylogenetic study. *J Bacteriol*, 173, 697-703.
- WHITELEY, M., BANGERA, M. G., BUMGARNER, R. E., PARSEK, M. R., TEITZEL, G. M., LORY, S. & GREENBERG, E. P. 2001. Gene expression in *Pseudomonas aeruginosa* biofilms. *Nature*, 413, 860-4.
- WINSON, M. K., SWIFT, S., FISH, L., THROUP, J. P., JØRGENSEN, F., CHHABRA, S. R., BYCROFT, B. W., WILLIAMS, P. & STEWART, G. S. 1998. Construction and analysis of luxCDABE-based plasmid sensors for investigating N-acyl homoserine lactone-mediated quorum sensing. *FEMS Microbiol Lett*, 163, 185-92.
- WINSTANLEY, C., O'BRIEN, S. & BROCKHURST, M. A. 2016. *Pseudomonas aeruginosa* Evolutionary Adaptation and Diversification in Cystic Fibrosis Chronic Lung Infections. *Trends Microbiol*, 24, 327-337.
- WOESE, C. R. 1987. Bacterial evolution. *Microbiol Rev*, 51, 221-71.
- WOLCOTT, R., COSTERTON, J. W., RAOULT, D. & CUTLER, S. J. 2013. The polymicrobial nature of biofilm infection. *Clin Microbiol Infect*, 19, 107-12.
- WOOD, D. E. & SALZBERG, S. L. 2014. Kraken: ultrafast metagenomic sequence classification using exact alignments. *Genome Biol*, 15, R46.
- WOODS, P. W., HAYNES, Z. M., MINA, E. G. & MARQUES, C. N. H. 2018. Maintenance of *S. aureus* in co-culture with *P. aeruginosa* while growing as biofilms. *Front Microbiol*, 9, 3291.
- WORLITZSCH, D., TARRAN, R., ULRICH, M., SCHWAB, U., CEKICI, A., MEYER, K. C., BIRRER, P., BELLON, G., BERGER, J., WEISS, T., BOTZENHART, K., YANKASKAS, J. R., RANDELL, S., BOUCHER, R. C. & DÖRING, G. 2002. Effects of reduced mucus oxygen concentration in airway *Pseudomonas* infections of cystic fibrosis patients. *J Clin Invest*, 109, 317-25.
- WU, Y., KLAPPER, I. & STEWART, P. S. 2018. Hypoxia arising from concerted oxygen consumption by neutrophils and microorganisms in biofilms. *Pathog Dis*, 76.
- WU, Y., SHAO, X., JIAO, H., SONG, X., HE, K. & LI, Z. 2020. Tracking the fungus-assisted biocorrosion of lead metal by Raman imaging and scanning electron microscopy technique. *Journal of Raman Spectroscopy*, 51, 508-513.
- XU, X. L., LEE, R. T., FANG, H. M., WANG, Y. M., LI, R., ZOU, H., ZHU, Y. & WANG, Y. 2008. Bacterial peptidoglycan triggers *Candida albicans* hyphal growth by directly activating the adenylyl cyclase Cyr1p. *Cell Host Microbe*, 4, 28-39.
- YAMAGUCHI, T., ANDO, R., MATSUMOTO, T., ISHII, Y. & TATEDA, K. 2019. Association between cell growth and vancomycin resistance in clinical community-associated methicillin-resistant. *Infect Drug Resist*, 12, 2379-2390.
- YANG, J., TANG, H., ZHANG, X., ZHU, X., HUANG, Y. & YANG, Z. 2018. High temperature and pH favor *Microcystis aeruginosa* to outcompete *Scenedesmus obliquus*. *Environ Sci Pollut Res Int*, 25, 4794-4802.
- ZANNONI, D. 1989. The respiratory chains of pathogenic pseudomonads. *Biochimica et Biophysica Acta (BBA) - Bioenergetics*, 975, 299 - 316.
- ZEMANICK, E. T., WAGNER, B. D., SAGEL, S. D., STEVENS, M. J., ACCURSO, F. J. & HARRIS, J. K. 2010. Reliability of quantitative real-time PCR for bacterial detection in cystic fibrosis airway specimens. *PLoS One*, 5, e15101.
- ZHAO, J., SCHLOSS, P. D., KALIKIN, L. M., CARMODY, L. A., FOSTER, B. K., PETROSINO, J. F., CAVALCOLI, J. D., VANDEVANTER, D. R., MURRAY, S., LI, J. Z., YOUNG, V. B. & LIPUMA, J. J. 2012. Decade-long bacterial community dynamics in cystic fibrosis airways. *Proc Natl Acad Sci U S A*, 109, 5809-14.
- ZHENG, L., REN, M., XIE, E., DING, A., LIU, Y., DENG, S. & ZHANG, D. 2019. Roles of Phosphorus Sources in Microbial Community Assembly for the Removal of Organic Matters and Ammonia in Activated Sludge. *Front Microbiol*, 10, 1023.

- ZIV, N., BRANDT, N. J. & GRESHAM, D. 2013. The use of chemostats in microbial systems biology. *J Vis Exp*.
- ZOBELL, C. E. 1943. The Effect of Solid Surfaces upon Bacterial Activity. *J Bacteriol*, 46, 39-56.
- ZOLIN, A., ORENTI, A., VAN RENS, J., FOX, A., KRASNYK, M., JUNG, A., MEI-ZAHAV, M., COSGRIFF, R., STORMS, V. & NAEHRLICH, L. 2019. ECFS Patient Registry Annual Data Report 2017.
- ZUGHAIER, S. M. & CORNELIS, P. 2018. Editorial: Role of Iron in Bacterial Pathogenesis. *Front Cell Infect Microbiol*, 8, 344.
- ZUMFT, W. G. 2004. Denitrification by Pseudomonads: control and assembly processes. In Ramos, J. L. (ed.), *Pseudomonas*. Springer, Boston, MA.

11. Appendices

Appendix 2.1	Preparation of artificial sputum medium (ASM).....	7
Appendix 2.2	Production and purification of recombinant lysostaphin.....	7
Appendix 2.3	Pipeline and commands for processing sequencing data using QIIME.....	9
Appendix 3.1	Growth of species in ASM.....	13
Appendix 3.2	Dual species (PA-SA) continuous-flow optical density measurement.....	17
Appendix 3.3	Triple species continuous-flow optical density measurements.....	22

Appendix 2.1 Preparation of artificial sputum medium (ASM)

The following protocol was used to prepare 1 L of ASM, this modified recipe is a combination of previously published protocols for the production of SCFM2 (Palmer *et al.* (2007) and Turner *et al.* (2015) and ASM (Kirchner *et al.* (2012)).

1. Add 5 g of mucin from porcine stomach, type-II (Sigma-Aldrich) to 250 mL of sterile 1 x PBS (Oxoid) (final concentration = 1.25 g L^{-1}) and leave to dissolve with stirring overnight at 4°C .
2. Add 4 g of fish sperm DNA (Sigma-Aldrich) to 250 mL of sterile double distilled H_2O (dd H_2O) (final concentration = 1 g L^{-1}) and leave to dissolve overnight in a shaking water bath at 35°C , 180 rpm.
3. In a clean beaker, add 250 mL of d H_2O and make up the SCFM2 buffered base and amino acid mix using the recipe below (*Table S1*).

Amino acid stocks							
Chemical	[Stock]	stock volume	fw	Mass to add	Stock to add to beaker	Final Conc	Notes
	(M)	(mL)	(g/mol)	(g)	(mL)	(mM)	-
NaH_2PO_4	0.2	25	137.99	0.690	8.125	1.3	-
Na_2HPO_4	0.2	25	141.96	0.710	6.252	1.25	-
KNO_3	1	25	101.103	2.528	0.348	0.348	-
K_2SO_4	0.25	25	174.259	1.089	1.084	0.271	-
<i>Add solids below directly to beaker</i>							
NH_4Cl			53.491	0.124		2.2808	-
KCl			74.5513	1.116		14.943	-
NaCl			58.44	3.032		51.848	-
MOPS			209.2633	2.092		10	-
Amino Acids							
Ser	0.1	50	105.09	0.525	14.46	1.446	-
Glu.HCl	0.1	50	183.59	0.918	15.492	1.549	-
Pro	0.1	50	115.13	0.576	16.612	1.661	-
Gly	0.1	50	75.07	0.375	12.032	1.203	-
Ala	0.1	50	89.09	0.445	17.8	1.78	-
Val	0.1	50	117.15	0.586	11.172	1.117	-
Met	0.1	50	149.21	0.746	6.332	0.633	-
Ile	0.1	50	131.17	0.656	11.212	1.121	-
Leu	0.1	50	131.17	0.656	16.092	1.609	-
Orn.HCl	0.1	50	168.62	0.843	6.76	0.676	-
Lys.HCl	0.1	50	182.6	0.913	21.28	2.128	-
Arg.HCl	0.1	50	210.7	1.054	3.06	0.306	-

Trp	0.1	50	204.23	1.021	0.132	0.013	Prep in 0.2 M NaOH
Asp	0.1	50	133.1	0.666	8.272	0.827	Prep in 0.5 M NaOH
*Tyr	0.1	50	181.19	0.906	8.02	0.802	Prep in 1.0 M NaOH
*Thr	0.1	50	119.12	0.596	10.72	1.072	-
*Cys.HCl	0.1	50	157.6	0.788	1.6	0.16	-
*Phe	0.1	50	165.19	0.826	5.3	0.53	-
*His.HCl.H ₂ O	0.1	50	209.6	1.048	5.192	0.519	-

Table S1. Instructions for the preparation of stock solutions required to make the buffered base and amino acid mixture. The amount of each solution required to make 1 L of ASM is shown alongside the concentration (mM) of each constituent component within the culture media. Note that all amino acid stock solutions can be kept in the dark at 4°C for 1 month, stock solutions annotated with “*” must be made fresh on the day of preparation.

- Combine the dissolved mucin and DNA solutions and pellet undissolved particles by centrifugation at 4000 × g for 30 min (4°C).
- Without disturbing the pellet, carefully remove the supernatant and combine with the buffered base amino acid mix.
- Adjust the pH of the media to 6.8.
- Add the final components of ASM as shown in Table S2.

Chemical	[Stock]	Stock volume	fw	Mass to add	Stock to add to 1L mL BB	[Final]	Notes
	(M)	(mL)	(g/mol)	(g)	(mL)	(mM)	
Dextrose (D-glucose)	1	25	180.16	4.504	1.2	3	
L-lactic acid	1	25	90.08	2.252	9.3	9.3	pH stock to 7 with NaOH
CaCl ₂ ·2H ₂ O	1	25	147.014	3.67535	1.754	1.754	
MgCl ₂ ·6H ₂ O	1	25	203.31	5.08275	0.606	0.606	
FeSO ₄ ·7H ₂ O	0.0036	50	278.05	0.05	1	0.0036	Make fresh on day of preparation
N-acetylglucosamine	0.25	25	221.21	1.383	1.2	0.3	
Egg yolk emulsion					5		Premade stock from Sigma

Table S2. Instructions for the preparation of stock solutions of the final reagents required to make ASM. The amount of each stock solution required to make 1 L ASM is shown alongside the final concentration (mM) of each constituent component within the culture media. Note that the FeSO₄ stock must be prepared fresh on the day of preparation.

8. Adjust the final volume to 1 L with dH₂O.
9. Filter sterilise media using a 0.22 µm Millipore stericup (Sigma-Aldrich) attached to a vacuum pump. Note that this process can be slow and may take up to two days.
10. Store filtered ASM in the dark at 4°C for up to one month.

Appendix 2.2 Production and purification of recombinant lysostaphin

Addition of mutanolysin, lysostaphin and lysozyme for the efficient lysis of Gram-positive and Gram-negative species and improved total genomic DNA (gDNA) extraction from complex polymicrobial communities prior to high-throughput sequencing has been described previously (Gill et al., 2016, Wada, 2001). . The following protocol details the production and purification of recombinant lysostaphin used in this study.

S.2.2.1 Generation of DE3 (pET23Lys)

Following the manufacturer's instructions, plasmid pET23Lys was purified from a routine overnight culture of DH5 α (pET23Lys) using a GeneJET Plasmid Miniprep Kit (ThermoFisher). pET23Lys was then transformed into chemically competent Rosetta DE3 cells (Novagen) using the standard heat shock protocol described by (Sambrook and Russell, 2006). Correct transformants were selected for by plating recovered cells onto LB-A plates supplemented with 50 $\mu\text{g mL}^{-1}$ carbenicillin (plasmid selection) and 25 $\mu\text{g mL}^{-1}$ chloramphenicol (Rosetta DE3 selection), incubated overnight at 37°C.

S.2.2.2 Lysostaphin overexpression

Induction medium was prepared by evenly dividing 800 ml 2xYT broth supplemented with appropriate selection (carbenicillin and chloramphenicol) and 0.1 M Isopropyl β -D-thiogalactopyranoside (IPTG, Bioline) to induce protein expression between two 2 L baffled flasks. An overnight starter culture of DE3(pET23Lys) was sub-cultured (1 mL) into both flasks containing induction medium and incubated at 25°C for 72 hrs with shaking (200 rpm). Cells were harvested by centrifugation (5000 $\times g$, 20 min, 4°C) and the supernatant discarded. Cell pellets were then resuspended in 30 mL lysis buffer and stored at -80°C.

S.2.2.3 Protein purification

Frozen cell pellets were thawed at room temperature before 20 mg of lysozyme from chicken egg white (Sigma) and 5 μL of DNase I (ThermoFisher) was added to each pellet. Cells were pooled and sonicated on ice using a 3 mm probe, with 60-70% amplitude for 14 cycles of 20 secs on and 40 secs off. The resulting lysate was centrifuged (18,000 $\times g$, 45 min, 4°C) to sediment cell debris and the supernatant collected and filter sterilised (0.22 μm pore size). Using the manufacturers pre-set 'Affinity AC' protocol on an ÄKTA start protein purification system (GE Life Sciences), His-tagged lysostaphin was purified on a HisTrap FF 5 ml Ni-resin column (GE Life Sciences), using ice cold equilibration and elution buffer in lines A and B of

the ÄKTA respectively. Fractions containing the eluted protein were pooled in a 3,000 Da MWCO dialysis membrane (FisherScientific) and dialysed overnight in 2 L of dialysis buffer at 4°C.

S.2.2.4 Assessing lysostaphin purity

The concentration of dialysed lysostaphin was quantified using Quick Start Bradford Protein Assay kit (BioRad), following the manufactures instructions and using a bovine serum albumin (BSA) standard curve. Recombinant lysostaphin was stored in working aliquots at -80°C.

1D-SDS PAGE (one-dimensional sodium dodecyl sulfate polyacrylamide gel electrophoresis) was used to assess the purity of lysostaphin. Dialysed protein was mixed with SDS sample buffer at a 1:1 ratio and boiled at 95°C for 10 min, then left to cool at room temperature. Samples were loaded into the wells of a polyacrylamide gel (containing 5% stacking and 8% resolving gel, size: 100 mm x 100 mm x 1 mm) alongside a Precision Plus Protein Unstained Protein Standard ladder (BioRad). Polyacrylamide gels were resolved in SDS running buffer at 200 V for 1 hrs in a Mini-PROTEAN Tetra Vertical Electrophoresis Cell (BioRad). Once resolved, gels were visualised by incubation for 1 hrs in Coomassie staining solution followed by 24 hrs incubation in destaining solution. Stained gels were imaged using a ChemiDoc Imaging System (BioRad). A single clear band corresponding to the approximate molecular weight of lysostaphin (26.9 kDa) can be seen on the 1D-SDS PAGE gel, demonstrating successful purification of recombinant lysostaphin (*Figure S.2.1*).

S.2.2.4 Assessing lysostaphin activity

Lysostaphin is a glycyglycine endopeptidase capable of cleaving crosslinking pentaglycine bridges found in the cell wall peptidoglycan of certain Gram-positive bacteria (such as SA), causing the lysis of quiescent and actively growing cells (Sugai et al., 1997). To test the functionality of purified protein, the kinetics of SA lysis by lysostaphin was assessed by following the reduction in turbidity of a bacterial suspension. Cells from overnight cultures were harvested by centrifugation (4000 x g, 10 min, room temp) and resuspended in fresh LB at OD_{600 nm} 0.5. Normalised cultures were added to wells of a clear, flat-bottomed 96-well plate and lysostaphin added to final concentration of 10 µg mL⁻¹. The same volume of fresh dialysis buffer was used as a negative control. Plates were incubated at 37°C with 100 rpm shaking in a FLUOstar Omega plate reader and OD₆₀₀ measured every 5 min. Purified lysostaphin caused a rapid reduction in turbidity of the bacterial suspension, whereas no difference in turbidity was detected for the buffer only control, demonstrating the protein is functional (*Figure S.2.2*, below).

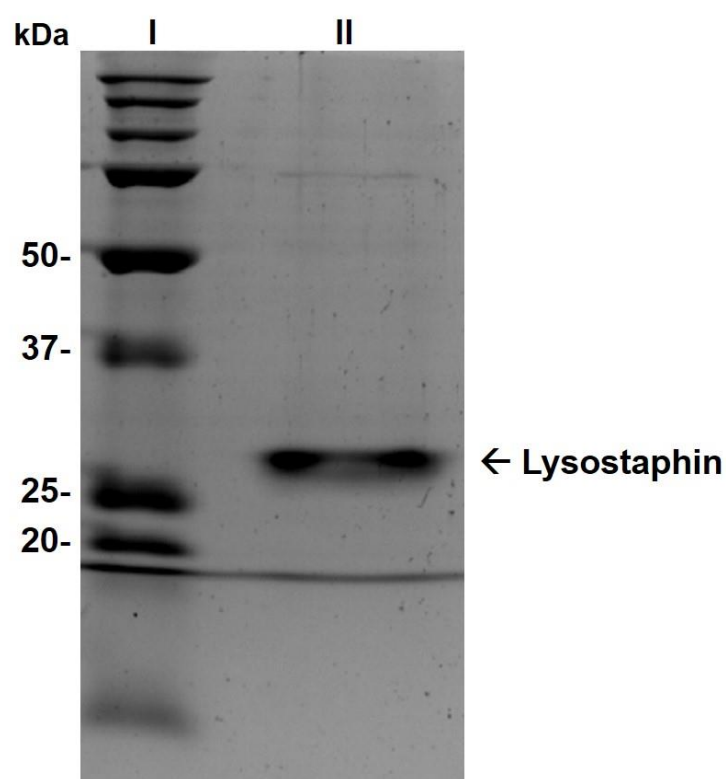


Figure S.2.1 Purification of lysostaphin.

1D-SDS PAGE gel of purified recombinant lysostaphin. Lane I: Precision Plus Protein Unstained Protein Standard molecular weight marker (BioRad), molecular weight is indicated in kDa. Lane II: purified lysostaphin. A single band approximately 27 kDa in size is clearly visible in lane II which corresponds to the molecular weight of lysostaphin (26.9 kDa).

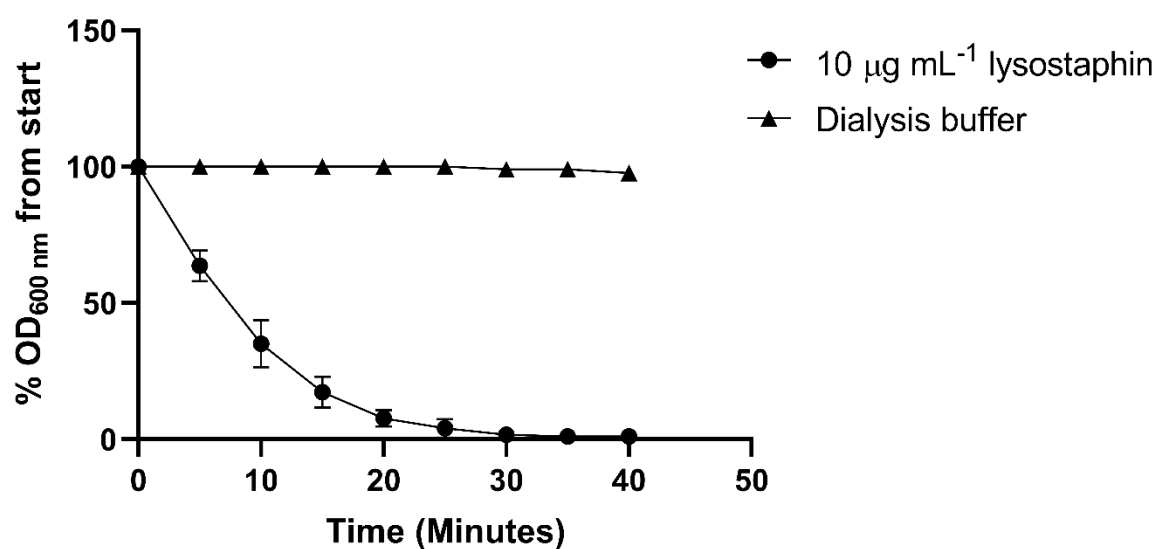


Figure S.2.2 Quality check of recombinant lysostaphin activity.

Lysis of *S. aureus* 25923 cell suspension by lysostaphin. Normalised bacterial cultures, OD_{600 nm} 0.5, incubated with 10 µg mL⁻¹ lysostaphin (circles) or dialysis buffer only (triangles). Turbidity of bacterial solution was measured at OD_{600 nm} every 5 min. Lysostaphin causes a rapid reduction in turbidity of the cell suspension, indicating the purified protein is functional. Data represented as mean ± standard deviation from three separate experiments.

Appendix 2.3 Pipeline and commands for processing sequencing data using QIIME2

Sequence reads from high-throughput paired end sequencing using an Illumina MiSeq instrument were returned from the DNA Sequencing Facility as separate paired-end demultiplexed fastq. files in the CASAVA 1.8 format. The following protocol details the pipeline and commands used to generate relative abundance taxa bar plots and compute core diversity metrics from the resulting data using the opensource bioinformatics software QIIME2 (software version QIIME 2 2020.6.0) within a VirtualBox 64-bit Ubuntu operating system (Oracle VM virtualbox).

1. Metadata files for the sequencing data were generated on Google Sheets and validated for use in QIIME2 with the Keemai plugin (keemei.qiime2.org/)
2. Files were compiled into a compressed .zip folder named `casva-18-paired-end.zip`. The compressed folder and sample metadata file were imported into QIIME 2

3. Compressed folder containing sequence data was unzipped:

```
unzip -q casava-18-paired-end-demultiplexed.zip
```

4. Sequence data was imported as a QIIME2 artifact in the `qza.` file format:

```
qiime tools import \  
--type 'SampleData[PairedEndSequencesWithQuality]' \  
--input-path casava-18-paired-end-demultiplexed \  
--input-format CasavaOneEightSingleLanePerSampleDirFmt \  
--output-path demux-paired-end.qza
```

5. Paired-end reads were joined using the `q2-vsearch` plugin (Rognes et al., 2016) (Rognes et al., 2016):

```
qiime vsearch join-pairs \  
--i-demultiplexed-seqs demux-paired-end.qza \  
--o-joined-sequences demux-joined.qza
```

6. A summary of the `demux-joined.qza` artifact was generated. The resulting interactive `qzv.` File was used to explore the quality of sequence reads in the artifact

and determine a suitable max length of sequence reads (as described in the QIIME2 tutorial: docs.qiime2.org/2018.2/tutorials/read-joining/):

```
qiime demux summarize \  
  --i-data demux-joined.qza \  
  --o-visualization demux-joined.qzv
```

7. Quality control was applied to sequences in the `demux-joined.qza` artifact:

```
qiime quality-filter q-score-joined \  
  --i-demux demux-joined.qza \  
  --o-filtered-sequences filtered-demux-joined.qza \  
  --o-filter-stats filtered-demux-joined-stats.qza
```

8. Sequences were denoised using Deblur (Amir et al., 2017). With `--p-trim-length` `x` passed as the sequence length previously selected in step 5:

```
qiime deblur denoise-16S \  
  --i-demultiplexed-seqs filtered-demux-joined.qza \  
  --p-trim-length x \  
  --p-sample-stats \  
  --o-representative-sequences rep-seqs.qza \  
  --o-table filtered-table.qza \  
  --o-stats filtered-deblur-stats.qza
```

9. Rooted and unrooted phylogenetic trees relating features in the sequencing samples were then generated:

```
qiime phylogeny align-to-tree-mafft-fasttree \  
  --i-sequences rep-seqs.qza \  
  --o-alignment aligned-rep-seqs.qza \  
  --o-masked-alignment masked-aligned-rep-seqs.qza \  
  --o-tree unrooted-tree.qza \  
  --o-rooted-tree rooted-tree.qza
```

10. A summary table of the number of features in samples of the `filtered-table.qza` artifact was generated. Passing the mapping file `--m-sample-metadata-file` as the imported sample metadata file (`sample-metadata.tsv`) generated in step 1:

```
qiime feature-table summarize \  
  --i-table filtered-table.qza \  
  --o-visualization filtered-table.qzv \  
  --m-sample-metadata-file sample-metadata.tsv
```

11. Core alpha and beta diversity metrics (see below ^[1]) were calculated using the `qiime diversity` plugin. With `--p-sampling-depth x` passed as the number of features present in the smallest sample identified from the `filtered-table.qzv` file*:

```
qiime diversity core-metrics-phylogenetic \
--i-phylogeny rooted-tree.qza \
--i-table filtered-table.qza \
--p-sampling-depth x \
--m-metadata-file sample-metadata.tsv \
--output-dir core-metrics
```

**Alpha rarefaction plots computed using the `qiime diversity alpha-rarefaction` visualiser were used to determine if the richness of samples was fully observed in the above core diversity metrics and sampling depth in the above computation refined accordingly.*

12. Significant associations between the microbial composition of samples in the context of the sample metadata (contained in the `sample-metadata.tsv` file) were explored within the Faith's phylogenetic (alpha) diversity metric (computed in step 11) using Kruskal-Wallis one-way analysis of variance:

```
qiime diversity alpha-group-significance \
--i-alpha-diversity core-metrics/faith_pd_vector.qza \
--m-metadata-file sample-metadata.tsv \
--o-visualization core-metrics /faith-pd-group-significance.qzv
```

13. Taxonomy was assigned to sequences in the `FeatureData[sequences]` QIIME2 artifact (generated in step 8) using the pre-trained Naïve Bayes classifier and the `qiime feature-classifier` plugin*:

```
qiime feature-classifier classify-sklearn \
--i-classifier gg-13-8-99-515-806-nb-classifier.qza \
--i-reads rep-seqs.qza \
--o-classification taxonomy.qza
```

**This classifier (passed as `gg-13-8-99-515-806-nb-classifier.qza` above) was trained on Greengenes 13_8 99% OTUs sample preparation and sequencing parameters, compatible with the sample library preparation and sequencing methods described in Section 2.14.4.*

14. Finally, bar plots demonstrating taxonomic composition of samples in the sequencing libraries were generated using the `taxonomy.qza` artifact from step 13:

```
qiime taxa barplot \
  --i-table filtered-table.qza \
  --i-taxonomy filtered-taxonomy.qza \
  --m-metadata-file sample-metadata.tsv \
  --o-visualization filtered-taxa-bar-plots.qzv
```

^[1]Core diversity metric outputs generated using this pipeline:

Alpha diversity metrics:

- Shannon's diversity index (a quantitative measure of community richness)
- Observed OTUs (a qualitative measure of community richness)
- Faith's Phylogenetic Diversity (a qualitative measure of community richness that incorporates phylogenetic relationships between the features)
- Evenness (or Pielou's Evenness; a measure of community evenness)

Beta diversity metrics:

- Jaccard distance (a qualitative measure of community dissimilarity)
- Bray-Curtis distance (a quantitative measure of community dissimilarity)
- unweighted UniFrac distance (a qualitative measure of community dissimilarity that incorporates phylogenetic relationships between the features)
- weighted UniFrac distance (a quantitative measure of community dissimilarity that incorporates phylogenetic relationships between the features)

Appendix 3.1 Growth of species in ASM

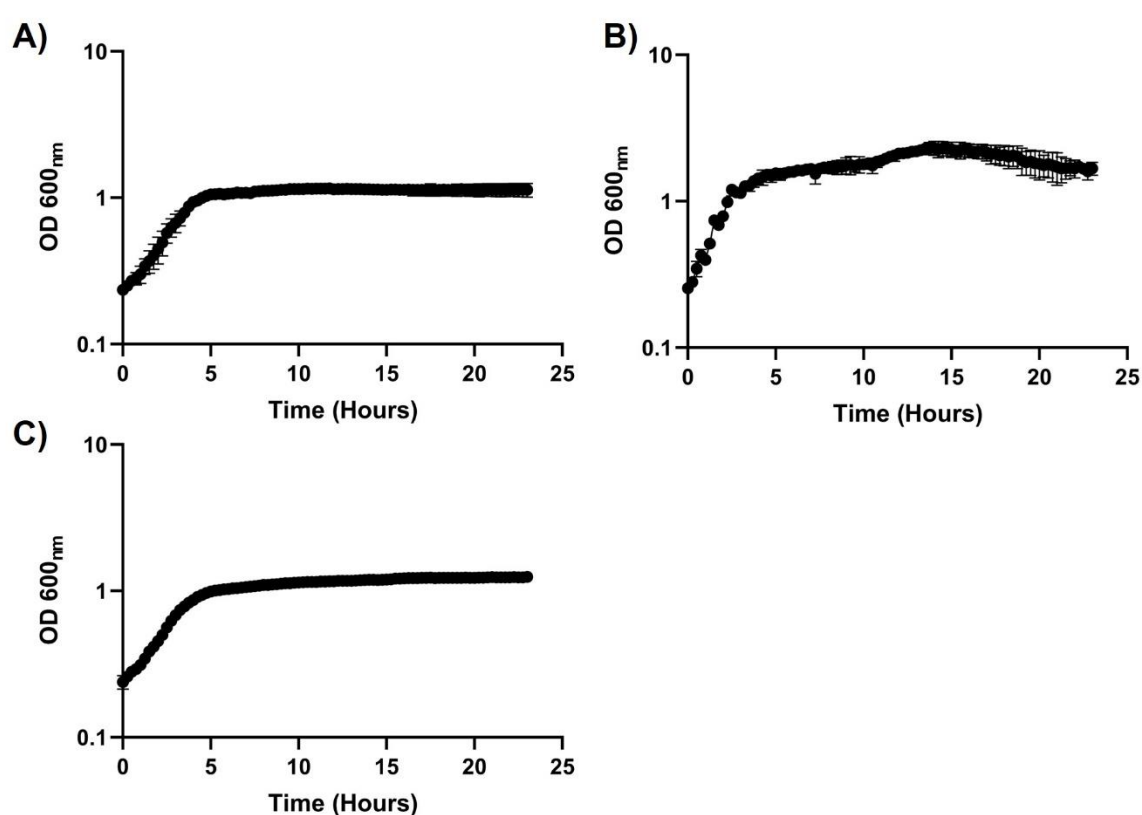


Figure S.3.1 Single species growth in ASM.

Growth of **(A)** *Pseudomonas aeruginosa* PAO1; **(B)** *Staphylococcus aureus* 25923; **(C)** *Candida albicans* SC5314 in ASM. All cultures were grown in flat-bottomed 96 well microtiter plates (Nunc) incubated at 37°C. Measurements were taken every 15 min using a FLUOstar Omega plate reader (BGM) with 180 rpm orbital shaking during idle time between reads. Optical density at 600 nm is plotted on a log₁₀ scale with data presented as the mean \pm standard deviation from at least 3 independent experiments.

Appendix 3.2 Dual species (PA-SA) continuous-flow optical density measurements

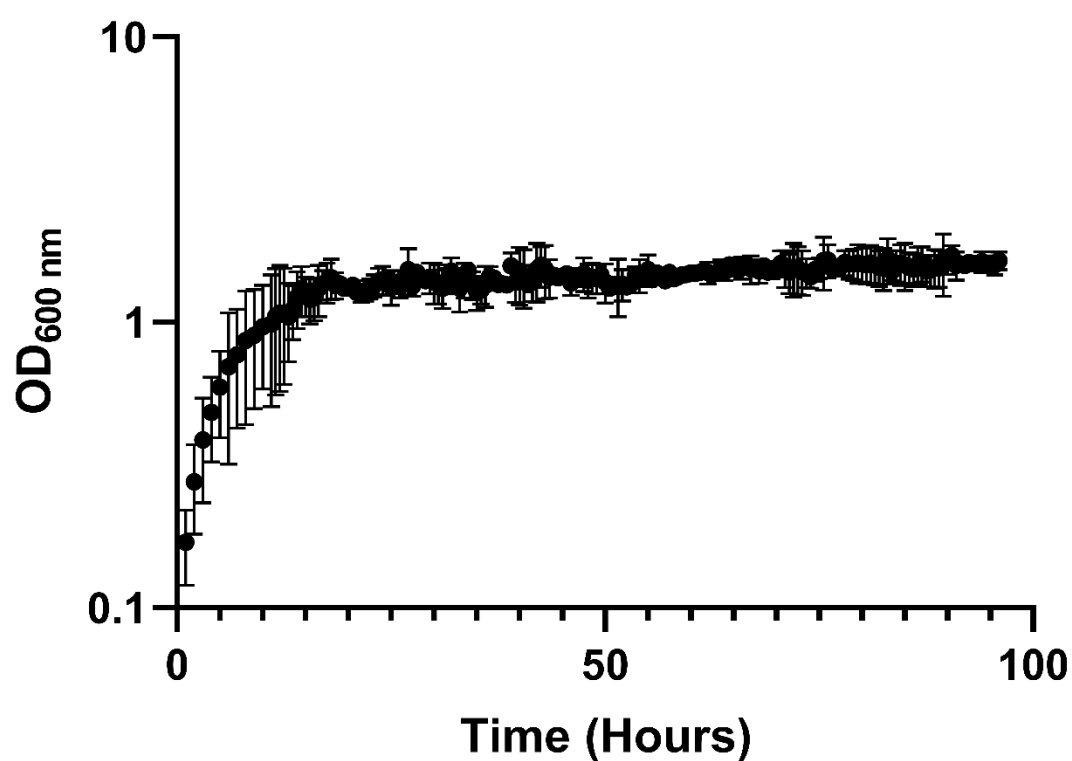


Figure S.3.2 Growth of dual species PA-SA co-culture under continuous-flow conditions.

Growth (monitored as OD_{600 nm}) of *P. aeruginosa* PAO1 – *S. aureus* 25923 co-culture in ASM in the continuous-flow culture vessel ($Q = 170 \mu\text{L min}^{-1}$). Automated OD_{600 nm} measurements were taken every 30 min using an in-line spectrometer fitted with a continuous-flow cuvette (as described in *Section 2.3.1*). Data represented as the mean \pm standard deviation from 3 independent experiments.

Appendix 3.3 Triple species continuous-flow optical density measurements

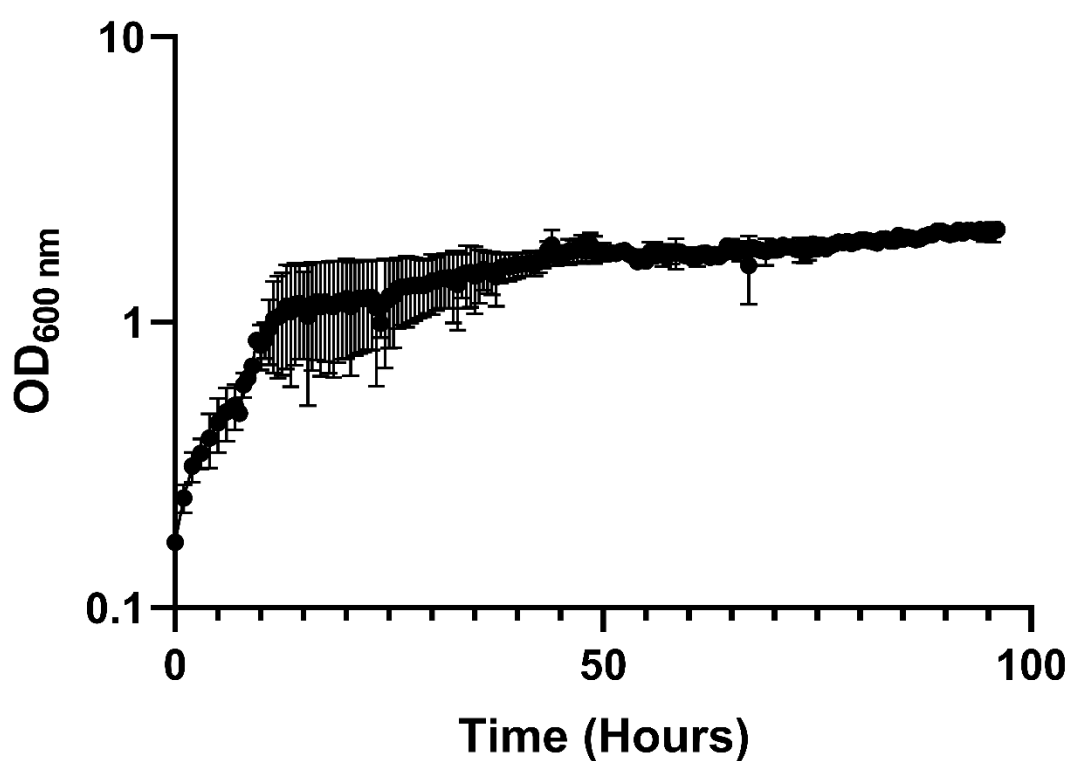


Figure S.3.3 Growth of triple-species (PA-SA-CA) co-culture under continuous-flow conditions.

Growth (monitored as OD_{600 nm}) of *P. aeruginosa* PAO1, *S. aureus* 25923 and *C. albicans* SC5314 co-culture in ASM in the continuous-flow culture vessel ($Q = 145 \mu\text{L min}^{-1}$). Automated OD_{600 nm} measurements were taken every 30 min using an in-line spectrometer fitted with a continuous-flow cuvette (as described in Section 2.3.1). Data represented as the mean \pm standard deviation from 3 independent experiments.

12. Publications

1. O'Brien, T.J. and Welch M. (2019) A continuous-flow model for *in vitro* cultivation of mixed microbial populations associated with cystic fibrosis airway infections. *Front Microbiol.* eCollection 10:2713.
2. O'Brien, T.J. and Welch M. (2019) Recapitulation of polymicrobial communities associated with cystic fibrosis airway infections: a perspective. *Future Microbiol.* 14 (16), 1437-1450.
3. Sifuna A.M., Reva O., O'Brien T.J., Figueroa W., Dina V., Shivoga W. and Welch M. (2021). Virulence and antimicrobial resistance genes are enriched in the plasmidome of clinical *Escherichia coli* isolates compared with wastewater isolates from Western Kenya. *J Infect., Gene. and Evol.* 91:104784.



A Continuous-Flow Model for *in vitro* Cultivation of Mixed Microbial Populations Associated With Cystic Fibrosis Airway Infections

Thomas James O'Brien and Martin Welch*

Department of Biochemistry, University of Cambridge, Cambridge, United Kingdom

OPEN ACCESS

Edited by:

Giovanna Batoni,
University of Pisa, Italy

Reviewed by:

Giordano Rampioni,
Roma Tre University, Italy
Emanuela Frangipani,
University of Urbino Carlo Bo, Italy

*Correspondence:

Martin Welch
mw240@cam.ac.uk

Specialty section:

This article was submitted to
Microbial Physiology and Metabolism,
a section of the journal
Frontiers in Microbiology

Received: 17 September 2019

Accepted: 08 November 2019

Published: 22 November 2019

Citation:

O'Brien TJ and Welch M (2019) A
Continuous-Flow Model for *in vitro*
Cultivation of Mixed Microbial
Populations Associated With Cystic
Fibrosis Airway Infections.
Front. Microbiol. 10:2713.
doi: 10.3389/fmicb.2019.02713

The airways of people with cystic fibrosis (CF) provide a nutrient-rich environment which favours colonisation by a variety of bacteria and fungi. Although the dominant pathogen associated with CF airway infections is *Pseudomonas aeruginosa*, it is becoming increasingly clear that inter-species interactions between *P. aeruginosa* and other colonists in the airways may have a large impact on microbial physiology and virulence. However, there are currently no suitable experimental models that permit long-term co-culture of *P. aeruginosa* with other CF-associated pathogens. Here, we redress this problem by describing a “3R’s-compliant” continuous-flow *in vitro* culture model which enables long-term co-culture of three representative CF-associated microbes: *P. aeruginosa*, *Staphylococcus aureus* and *Candida albicans*. Although these species rapidly out-compete one another when grown together or in pairs in batch culture, we show that in a continuously-fed setup, they can be maintained in a very stable, steady-state community. We use our system to show that even numerically (0.1%) minor species can have a major impact on intercellular signalling by *P. aeruginosa*. Importantly, we also show that co-culturing does not appear to influence species mutation rates, further reinforcing the notion that the system favours stability rather than divergence. The model is experimentally tractable and offers an inexpensive yet robust means of investigating inter-species interactions between CF pathogens.

Keywords: cystic fibrosis, continuous-flow, co-culture, *in vitro*, *Pseudomonas aeruginosa*, *Staphylococcus aureus*, *Candida albicans*

INTRODUCTION

Cystic fibrosis (CF) is the most common life-limiting genetic disorder within the Caucasian population (Cystic Fibrosis Foundation, 2019), with 1 in 40 people estimated to carry the common $\Delta F508$ mutation in the CF transmembrane conductance regulator (CFTR) gene (Bobadilla et al., 2002; Cystic Fibrosis Mutation Database, 2019). The most striking consequence of dysfunctional CFTR activity is the overproduction of nutrient-rich, mucilaginous sputum. This blocks the airways and generates a heterogeneous environment with steep oxygen gradients and a lowered pH (Boucher, 2002; Tate et al., 2002; Worlitzsch et al., 2002). This environmental niche is rich in nutrients such as mucin, amino acids, iron, and nitrate making the CF airway prone to colonisation by a variety of microbial species (Grasemann et al., 1998; Jones et al., 2000; Palmer et al., 2007; Ghio et al., 2013).

The resulting infections often persist for decades, leading to respiratory failure and eventually, premature death (Lyczak et al., 2002; Rajan and Saiman, 2002; Carmody et al., 2013, 2015; Elborn, 2016). Traditionally, these CF-associated infections have been linked with a relatively small number of easily-culturable pathogens, such as *Pseudomonas aeruginosa* or *Staphylococcus aureus*. However, the introduction of culture-independent molecular profiling approaches revealed that expectorated CF sputum samples often contain a much wider range of bacterial and fungal species (Sibley et al., 2006, 2008; Rogers et al., 2010a; Zhao et al., 2012; Carmody et al., 2013, 2015; Short et al., 2014; Boutin et al., 2015). This suggests that the CF airways may harbour a highly-diverse microbial community, although this notion has been challenged recently through the direct sampling of lavage fluid from the lungs of CF children. These new data suggest that to a large extent, the diversity of the previously reported CF-associated microbiome arises from contamination of the sample during passage through the oral cavity, and following sample processing (Jorth et al., 2019). Nevertheless, these newer studies still suggest that the CF airways harbour a core population of “non-conventional” pathogens, including *Prevotella*, *Veillonella* and *Staphylococcus* species, as well as “traditional CF pathogens” such as *P. aeruginosa* (PA).

The polymicrobial character of many CF-associated airway infections makes it crucial to consider what impact inter-species interactions have on the physiology and composition of the microbial consortium. Previous reports demonstrate that co-culturing bacterial species *in vitro* and *in vivo* causes significant alterations in gene essentiality (Ibberson et al., 2017). This can lead to changes in microbial lifestyle, impacting upon the expression of virulence factors (Rogers et al., 2009, 2010a,b; Hibbing et al., 2010; Leekha et al., 2011; Elias and Banin, 2012; Quinn et al., 2014; Limoli et al., 2016). For example, PA senses peptidoglycan shed from Gram-positive bacteria, and this stimulates the production of extracellular lytic virulence factors (Korgaonkar et al., 2013). Polymicrobial communities also display altered responses to therapeutic intervention. This may explain why many of the currently used clinical interventions designed to target PA show varying degrees of efficacy between patients (Lopes et al., 2012; Peters et al., 2012). As a consequence of these conceptual realisations, research focus is gradually moving away from studying individual species in isolation toward co-cultivating the major CF associated pathogens (Spasenovski et al., 2010; Bragonzi et al., 2012; Filkins et al., 2015; Magalhães et al., 2016; Lopes et al., 2017; Makovcova et al., 2017). However, these efforts are hampered by the paucity of adequate polymicrobial infection models. The development of a model which enables the stable and long-term recapitulation of CF polymicrobial communities is therefore highly-desirable.

Here we describe the development of a simple *in vitro* continuous-flow co-culture model which utilises artificial sputum medium (ASM). ASM is known to physiologically recapitulate the nutritional composition of CF airway secretions (Palmer et al., 2007; Kirchner et al., 2012; Turner et al., 2015). To the best of our knowledge, our co-culture model (Figure 1) is the first to permit the long-term, steady-state co-culture

of three distinct microbial species: PA, *Staphylococcus aureus* (SA), and *Candida albicans* (CA). Through viable cell counting and optical density measurements, we demonstrate that the abundance of each member of this microbial population remains unchanged over the course of 4 days and that a total carrying capacity can be reached and maintained within the culture vessel. By contrast, and in line with previous reports, when these species are co-cultured under batch conditions, PA rapidly outcompetes the other species (Machan et al., 1992; Duan et al., 2003; Hogan et al., 2004; Mashburn et al., 2005; McAlester et al., 2008; Cugini et al., 2010; Holcombe et al., 2010; Morales et al., 2010; Park et al., 2012; Korgaonkar et al., 2013; Baldan et al., 2014; Fugère et al., 2014; Rüger et al., 2014; Barnabie and Whiteley, 2015; Filkins et al., 2015; Nguyen et al., 2015; Zago et al., 2015; Nguyen and Oglesby-Sherrouse, 2016). Our *in vitro* model provides a defined and experimentally tractable system which can be used to dissect interspecies interactions and determine the long-term impact of co-cultivation on the physiology and gene expression profiles of CF-associated pathogens. Our *in vitro* model also provides a robust and cheaper alternative to existing *in vivo* infection models, making it compliant with the current trend toward the refinement, replacement and reduction (3Rs) of animal models in research.

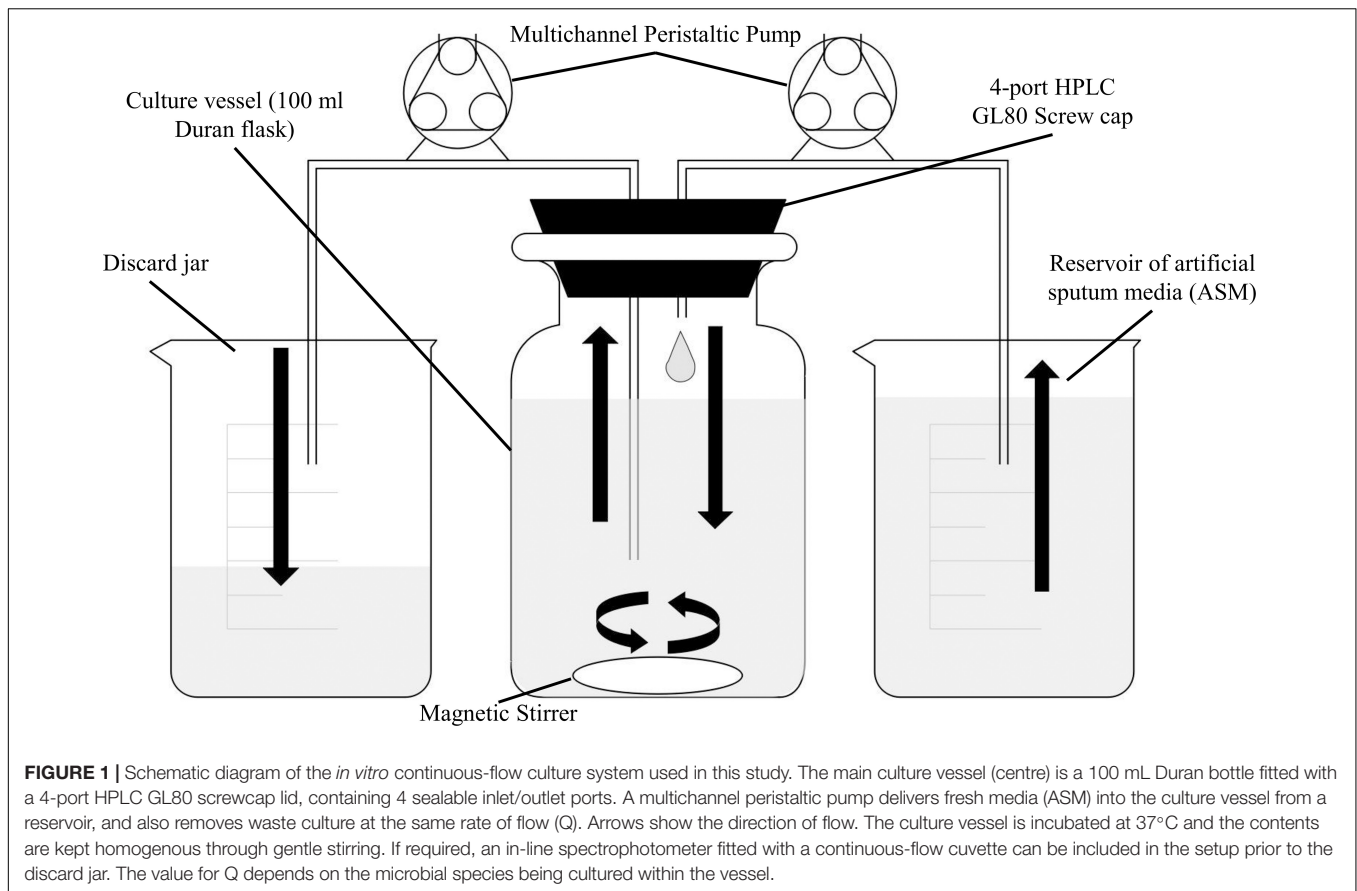
The species chosen for inoculation into our co-culture model represent three distinct classes of microorganisms; a Gram-negative species and dominant CF-associated pathogen (PA), a Gram-positive species, often associated with CF airway infections (SA) and a dimorphic fungus (CA), also commonly found in CF airway secretions (Conrad et al., 2013). As such, our continuous-flow model lays a solid groundwork for the development and optimisation of an *in vitro* co-culture model which can be directly inoculated with expectorated CF sputum. This will hopefully enable, in the longer-term, full recapitulation of the CF-associated polymicrobial community in defined laboratory conditions.

MATERIALS AND METHODS

Microbial Strains and Culture Conditions

The bacterial/fungal strains used in this study are shown in Table 1. All bacterial strains were routinely cultured in lysogeny broth (LB) (Formedium) with vigorous aeration at 37°C overnight. Where necessary, cultures were supplemented with 50 µg mL⁻¹ carbenicillin (to maintain pSB1057 in the *N*-(3-Oxododecanoyl)-L-homoserine lactone OdDHL biosensor strain) or 10 µg mL⁻¹ tetracycline (to maintain pSB536 in the *N*-butanoyl-L-homoserine lactone BHL biosensor strain).

Artificial sputum medium was used for every mono-, dual-, and triple-species cultivation. ASM was made using a modified version of the recipe published by Turner et al. (2015). Briefly, bovine maxillary mucin was replaced with 1.25 g L⁻¹ porcine stomach mucin type-II (Sigma-Aldrich) and salmon sperm DNA was replaced with 1 g L⁻¹ fish sperm DNA (Sigma-Aldrich) as described by Kirchner et al. (2012). A detailed protocol for preparing ASM can be found in the **Supplementary Information** (SI.1).



Continuous-Flow Culture Vessel and Culture Conditions

A schematic of the continuous-flow culture system is shown in **Figure 1**. The culture vessel consists of a 100 mL flask (Duran), fitted with an assembled 4-port HPLC GL80 screw cap (Duran). A 24-channel IPC ISM934C standard-speed digital peristaltic pump (Ismatec) was used to deliver sterile ASM at a defined flow rate (Q) through 1.5 mm bore sterilin silicon tubing (Fisher Scientific) to the culture vessel. A different channel on the same pump was used to remove waste culture into a discard jar at the same flow-rate. The culture vessel was maintained at 37°C and its contents were kept homogenous by stirring (100 rpm) using a magnetic stir bar. When necessary, the culture optical density was monitored at 600 nm ($OD_{600\text{ nm}}$) by passing the removed waste culture through an in-line 6715 UV series spectrophotometer (Jenway) fitted with a continuous-flow cuvette.

Overnight cultures were washed three times in sterile 1 × phosphate buffered saline (PBS, Oxoid) prior to inoculating the culture vessel. Pre-warmed ASM (100 mL) in the culture vessels was inoculated with the required combination of microbial species. Each species was introduced into the culture vessel to achieve a starting $OD_{600\text{ nm}}$ of 0.05. The vessel was incubated for 3 h prior to starting the flow of medium. For mono-species and co-culture experiments not containing CA, the flow rate (Q) was set at $170\ \mu\text{L min}^{-1}$. For co-culture experiments including CA, Q was decreased to $145\ \mu\text{L min}^{-1}$. For all

continuous-flow experiments, samples (1 mL volume) for cell enumeration were withdrawn using a syringe fitted with a sterile needle inserted through the rubber septa in the HPLC ports.

Aerobic and Stirred Batch Culture Conditions

For aerobic batch cultures, 250 mL Erlenmeyer flasks containing pre-warmed ASM (inoculated with the indicated strains to a starting $OD_{600\text{ nm}}$ of 0.05) were incubated at 37°C with vigorous shaking (180 rpm). Stirred batch cultures were set up as described for the continuous-flow experiments (see section “Continuous-Flow Culture Vessel and Culture Conditions”), except with $Q = 0\ \mu\text{L min}^{-1}$. For both types of batch culture, samples (1 mL volume) were taken from the culture vessel for $OD_{600\text{ nm}}$ analysis and viable cell counting.

Microbial CFU mL^{-1} Enumeration

Colony forming units (CFU) per mL of culture were determined using the single plate-serial dilution spotting (SP-SDS), as described previously (Thomas et al., 2015). Serial dilutions were made in sterile PBS and 20 μL of each dilution was spotted onto the appropriate selective agar. PA was isolated using pseudomonas agar base (Oxoid) supplemented with cetrимide ($200\ \mu\text{g mL}^{-1}$) and sodium nalidixate ($15\ \mu\text{g mL}^{-1}$). SA was isolated on mannitol salt agar (Oxoid). CA was isolated on BiGGY agar (Oxoid). During co-culture experiments involving CA, the agar plates used to isolate PA and SA were further

TABLE 1 | Microbial strains used in this study.

Strain	Description	References
PAO1	<i>Pseudomonas aeruginosa</i> , spontaneous chloramphenicol-resistant derivative. Used worldwide as a laboratory reference strain (isolated Melbourne, 1954).	Holloway, 1955
ATCC 25923	<i>Staphylococcus aureus</i> Rosenbach (ATCC® 25923D-5™), methicillin sensitive clinical isolate. Laboratory reference strain lacking recombinases and <i>mecA</i> (isolated Seattle, 1945).	Treangen et al., 2014
SC5314	<i>Candida albicans</i> , clinical isolate commonly used as a wild-type laboratory reference strain (isolated New York, 1980s).	Gillum et al., 1984
PAO1 $\Delta pqsA$ CTX- <i>lux::pqsA</i>	PQS biosensor strain. $\Delta pqsA$ mutant of PAO1 containing a <i>pqsA</i> promoter:: <i>luxCDABE</i> fusion integrated at a neutral site in the chromosome.	Fletcher et al., 2007
JM109 (pSB1057)	OdDHL biosensor strain. <i>Escherichia coli</i> JM109 containing pSB1057.	Winson et al., 1998
JM109 (pSB536)	BHL biosensor strain. <i>Escherichia coli</i> JM109 containing pSB536.	Winson et al., 1998

supplemented with 5 $\mu\text{g mL}^{-1}$ itraconazole to inhibit the growth of CA. All plates were incubated at 37°C. *Pseudomonas* agar base and mannitol salt plates were incubated overnight (16 h). BiGGY agar plates were incubated for 24 h. CFU mL^{-1} counts are averages taken from three technical repeats. There was no significant difference between total CFU mL^{-1} counts of pure microbial cultures plated onto either non-selective (LB-agar) or any of the selective agar (*data not shown*).

Quantification of Quorum Sensing Molecules

Aliquots (1.5 mL) of culture were collected after 24 and 96 h (as indicated) of incubation. The cells were pelleted by centrifugation (15,000 $\times g$, 5 min, 20°C) and the supernatant was filtered (0.22 μm pore size). Aliquots of the supernatant were snap frozen in liquid N_2 and stored at -20°C until use. OdDHL was detected using JM109 (pSB1057). BHL was detected using JM109 (pSB536). PQS was detected using PAO1 $\Delta pqsA$ CTX-*lux::pqsA*. Overnight starter cultures of the reporter strains were sub-cultured in LB supplemented with the appropriate antibiotics and grown to $\text{OD}_{600\text{nm}} = 1.0$. Following this, aliquots (60 μL volume) of the normalised cell culture were transferred to a sterile clear-bottomed black opaque 96-well plate (Greiner Bio-One) containing an equal volume of thawed culture supernatant. The plates were incubated at 30°C with shaking (100 rpm) for 3 h. Bioluminescence was recorded using a FLOUstar Omega plate reader (BMG). Standard curves to calibrate the biosensor outputs were constructed using known concentrations of synthetic quorum sensing molecules dissolved in ASM.

Quantification of Pyocyanin

Pyocyanin quantification was performed following chloroform extraction of the pigment (Knight et al., 1979). Aliquots (10 mL volume) of culture were collected after 96 h growth and the cells were pelleted (4000 $\times g$, 30 min, 4°C). The culture supernatants were filter sterilised (0.22 μm pore size). Chloroform (4.5 mL) was added to 7.5 mL of the cell-free culture supernatant and the suspension was vigorously vortexed for 30 s. The immiscible layers were separated by centrifugation (4000 $\times g$, 10 min, 4°C). An aliquot (3 mL volume) of the blue-green chloroform phase was removed and mixed with 1.5 mL 0.2M HCl. The immiscible layers were then separated by centrifugation and

1 mL of the rose-pink phase was transferred to a cuvette. The pyocyanin absorbance was measured at 520 nm using a BioSpectrometer Kinetic spectrophotometer (Eppendorf) and converted to concentration ($\mu\text{g mL}^{-1}$) by multiplying the $A_{520\text{ nm}}$ value by 26.6.

Estimation of Mutation Rates

Mutation rates in the chemostat were measured as described by Foster (2006). Initially, the rate constant (λ) associated with exponential growth of PA and SA co-cultured in ASM, was determined by enumeration of CFU mL^{-1} on selective agar plates. Next, the total cell count (N) within the culture vessel at steady-state growth was determined. The number of spontaneous rifampicin resistant PA or SA mutants, r , was measured after $t_1 = 0$ h, $t_2 = 24$ h and $t_3 = 96$ h of incubation. Total cell numbers in the chemostat did not change appreciably between 24 and 96 h. The value of r was determined by plating aliquots (100 μL volume) of culture onto either *pseudomonas* isolation agar supplemented with 60 $\mu\text{g mL}^{-1}$ rifampicin (for PA), or mannitol salt agar supplemented with 0.05 $\mu\text{g mL}^{-1}$ rifampicin (for SA). The mutation rate per cell per generation (m) was calculated according to Eq. 2 in Foster (2006);

$$\mu = \frac{1}{N\lambda} \frac{(r_2 - r_1)}{(t_2 - t_1)}$$

Statistical Analysis

Unless otherwise stated, all data represent the mean \pm SD of three independent biological experiments. Results were analysed by one-way or two-way ANOVA (as indicated), or Student's unpaired *t*-test using GraphPad Prism version 8.2.0, with $P < 0.05$ being considered statistically significant.

RESULTS

Mono-Species Continuous-Flow Culture (PAO1)

As a first step, we confirmed that PA, SA and CA could all grow in ASM. This was done by inoculating each species into flat-bottomed microtitre plates containing ASM. The plates were incubated at 37°C with vigorous shaking (180 rpm) in a FluoStar Omega plate reader, and the culture optical density (OD_{600})

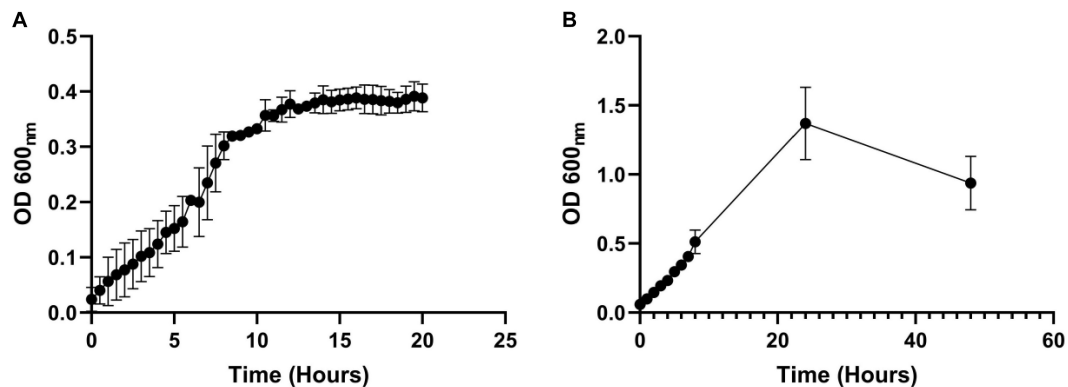


FIGURE 2 | Growth of *P. aeruginosa* in ASM in batch and continuous flow culture conditions. Growth (monitored as OD₆₀₀) of PA in ASM during **(A)** continuous-flow culture ($Q = 170 \mu\text{L min}^{-1}$); **(B)** batch culture ($Q = 0 \mu\text{L min}^{-1}$). Data represent the mean \pm standard deviation from three independent experiments.

was monitored every 15 min. PA, SA and CA grew rapidly in ASM, achieving a final OD₆₀₀ of > 1 after 24 h in all cases (**Supplementary Figure S1**).

Next, we measured whether a mono-species culture of PA could be maintained with stable steady-state titres in our continuous-flow setup. The laboratory reference strain, PAO1, was inoculated into the continuous-flow system using a flow-rate $Q = 170 \mu\text{L min}^{-1}$ and the OD₆₀₀ was measured every 30 min as described in Section “Continuous-Flow Culture Vessel and Culture Conditions.” The OD₆₀₀ increased almost linearly for the first 8 h and then reached a plateau (OD₆₀₀ ≈ 0.4) after 10 h of incubation (**Figure 2A**). By comparison, during growth in the same medium and experimental setup with $Q = 0 \mu\text{L min}^{-1}$ (i.e., in stirred batch mode), the PA culture reached a final OD₆₀₀ of > 1 (**Figure 2B**). We conclude that during continuous-flow operation, the setup allows the culture to achieve a steady-state carrying capacity with an OD₆₀₀ well-below the final OD₆₀₀ associated with entry into the stationary phase of growth in the same medium.

Dual-Species Co-culture (PA-SA)

Staphylococcus aureus is also associated with CF airway infection and is particularly prevalent in adolescent patients (Goss and Muhlebach, 2011; Conrad et al., 2013; Jorth et al., 2019). Despite PA and SA being frequently co-isolated from CF patients, numerous antagonistic interactions have been identified between these species, and PA readily outcompetes SA *in vitro* in mixed cultures (Machan et al., 1992; Duan et al., 2003; Mashburn et al., 2005; Park et al., 2012; Korgaonkar et al., 2013; Baldan et al., 2014; Fugère et al., 2014; Rüger et al., 2014; Filkins et al., 2015; Nguyen et al., 2015). We therefore wanted to determine if the two species could be stably maintained in our continuous-flow culture system. We found that a mixed species co-culture of PA and SA could be readily maintained to yield an apparently stable steady-state composition using $Q = 170 \mu\text{L min}^{-1}$. The CFU counts for each species are shown in **Figure 3A**, and the co-culture OD₆₀₀ measurements are shown in **Supplementary Figure S2**. A steady state composition of around 10^7 SA CFU mL⁻¹ and 10^8 PA CFU mL⁻¹ was established by 24 h of growth,

and there were no significant differences in the viable cell counts following this ($P > 0.05$) up to 96 h of growth. By contrast, during aerobic batch culture in flasks, PA rapidly outcompeted SA and no viable SA could be recovered at the 96 h sampling point (**Figure 3B**). PA also outcompeted SA during stirred batch co-culture conditions ($Q = 0 \mu\text{L min}^{-1}$) in the continuous-flow vessel (**Figure 3C**), albeit at a slower rate. Taken together, these data indicate that a continual supply of fresh media and removal of waste products is crucial for permitting a successful PA-SA co-culture *in vitro*.

Dual-Species Co-culture (PA-CA)

Fungi, such as *Candida* sp. and *Aspergillus* sp. are also associated with CF airway infections (Williams et al., 2016; Bouchara et al., 2018). We therefore examined whether *Candida albicans* (CA) could be maintained alongside PA in the continuous-flow setup. This is important because inter-kingdom interactions between PA and CA have been previously shown to affect virulence factor production by both species (Hogan et al., 2004; McAlester et al., 2008; Cugini et al., 2010; Holcombe et al., 2010). We found that a co-culture of PA and CA could be readily maintained in the continuous-flow setup (**Figure 4A**), although to prevent a wash-out of CA from the culture vessel over time we had to decrease the flow rate ($Q = 145 \mu\text{L min}^{-1}$). The culture carrying capacity for CA (ca. 10^5 CFU mL⁻¹) was lower than it was for PA (ca. 10^8 CFU mL⁻¹), but once a steady-state had been achieved (after 24 h incubation) no statistically significant differences in PA or CA viable cell counts were observed ($P > 0.05$). In contrast, CA titres rapidly declined during aerobic batch co-culture (**Figure 4B**). A similar, albeit slower decline in CA titres was observed during stirred batch growth (**Figure 4C**).

Dual-Species Co-culture (SA-CA)

We next wanted to confirm that a stable co-culture of SA and CA could be maintained independent of PA. Using $Q = 145 \mu\text{L min}^{-1}$, this was indeed the case (**Figure 5A**), and after 24 h growth, the ratio of SA:CA remained essentially unchanged. As in the PA-CA co-culture, at steady-state, the carrying capacity (ca. 10^5 CFU mL⁻¹) for CA was lower than

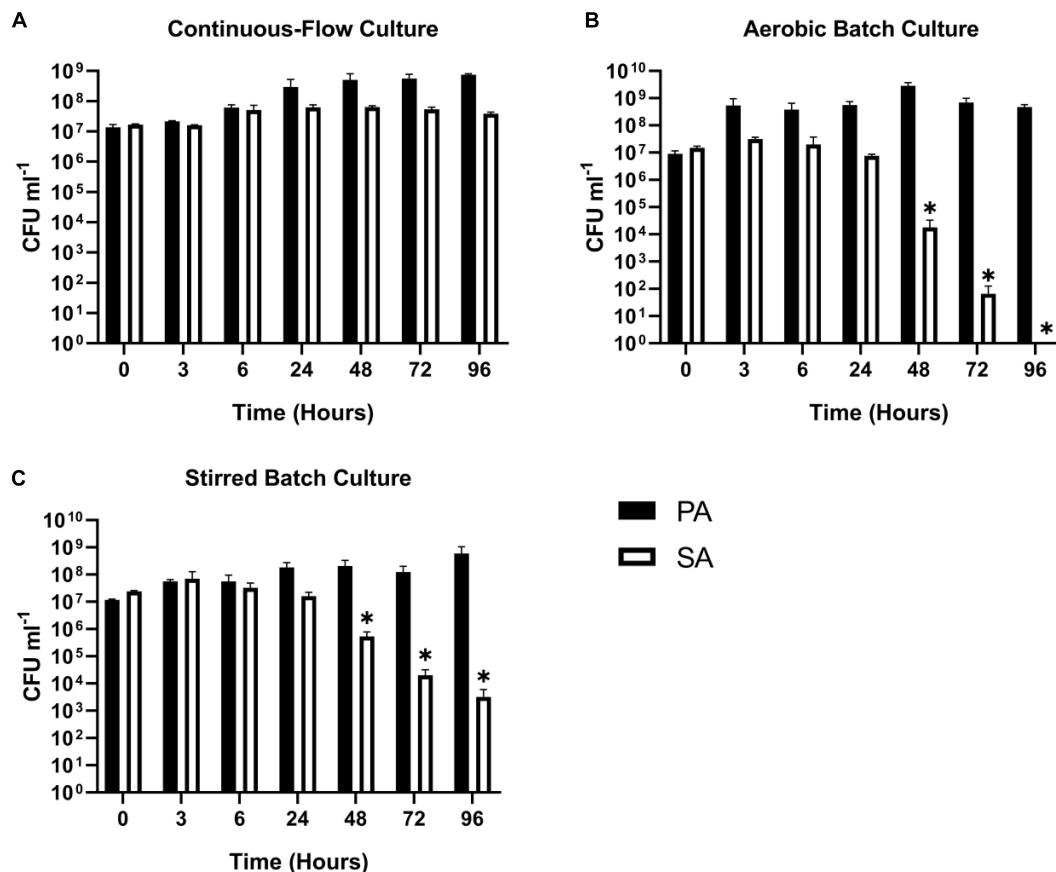


FIGURE 3 | Continuous-flow culture allows *P. aeruginosa* and *S. aureus* to be maintained in a stable steady-state. Viable cell counts [colony forming units (CFUs)] of *P. aeruginosa* PAO1 (PA, black bars) and *S. aureus* 25923 (SA, white bars) during co-culture in ASM using: **(A)** a continuous-flow setup; **(B)** aerobic batch culture; and **(C)** stirred batch culture. Data represent as mean \pm standard deviation from three independent experiments. Asterisks represent significant (* $P < 0.05$) differences in CFU mL⁻¹ counts in comparison with the data from the 24 h time point.

it was for SA (ca. 10^8 CFU mL⁻¹). Unexpectedly, we noted that following aerobic and stirred batch culture, the CA outcompeted the SA (**Figures 5B,C**). This confirms that in mixed cultures, a species comprising just 0.1% of the microbiota can potentially have a major impact on titres of the [initially] numerically-dominant organism.

Triple-Species Co-culture

With the continuous-flow culture system clearly capable of maintaining dual-species co-cultures of PA-SA, PA-CA and CA-SA, we next wanted to determine if all three species could be co-cultured to achieve a stable steady-state composition. We found that setting $Q = 145 \mu\text{L min}^{-1}$, a mixed population of all three microbial species could be maintained at a steady state for 96 h of incubation (**Figure 6A**; the corresponding in-line OD₆₀₀ data are shown in **Supplementary Figure S3**). Once the steady-state had been achieved (i.e., after 24 h of growth) there were no significant differences in the CFU mL⁻¹ counts for each species for the remaining duration of the co-culture ($P > 0.1$). The PA and SA titres remained at around 10^8 – 10^9 CFU mL⁻¹, and the CA titres remained at around 10^5 CFU mL⁻¹. By contrast,

when co-cultured in aerobic batch culture, both SA and CA were outcompeted by PA (**Figure 6B**). Indeed, there was a progressive decrease in the number of SA CFUs in each of the samples harvested after the 24 h time-point ($P < 0.0005$), and by 72 h, no viable CA CFU could be recovered. However, and unlike the PA-SA aerobic dual cultures (**Figure 3B**), SA could still be recovered at the 96 h sampling point, suggesting that the presence of CA affords a degree of protection, perhaps by decreasing the direct competition between PA and SA for shared resources. The stirred batch co-cultures yielded a somewhat different pattern (**Figure 6C**). Here, following the 24 h sampling point, PA titres remained high (ca. 10^9 – 10^{10} CFU mL⁻¹) and constant, but there was a significant and progressive decrease in SA titres ($P < 0.05$). Unlike the aerobic batch culture, this was accompanied by a much slower decline in CA titres.

Quantification of *P. aeruginosa* Quorum Sensing Molecules

Quorum sensing (QS) mediated signalling pathways are linked to the regulation of secondary metabolite and extracellular virulence factor production by PA. Some of these QS-regulated

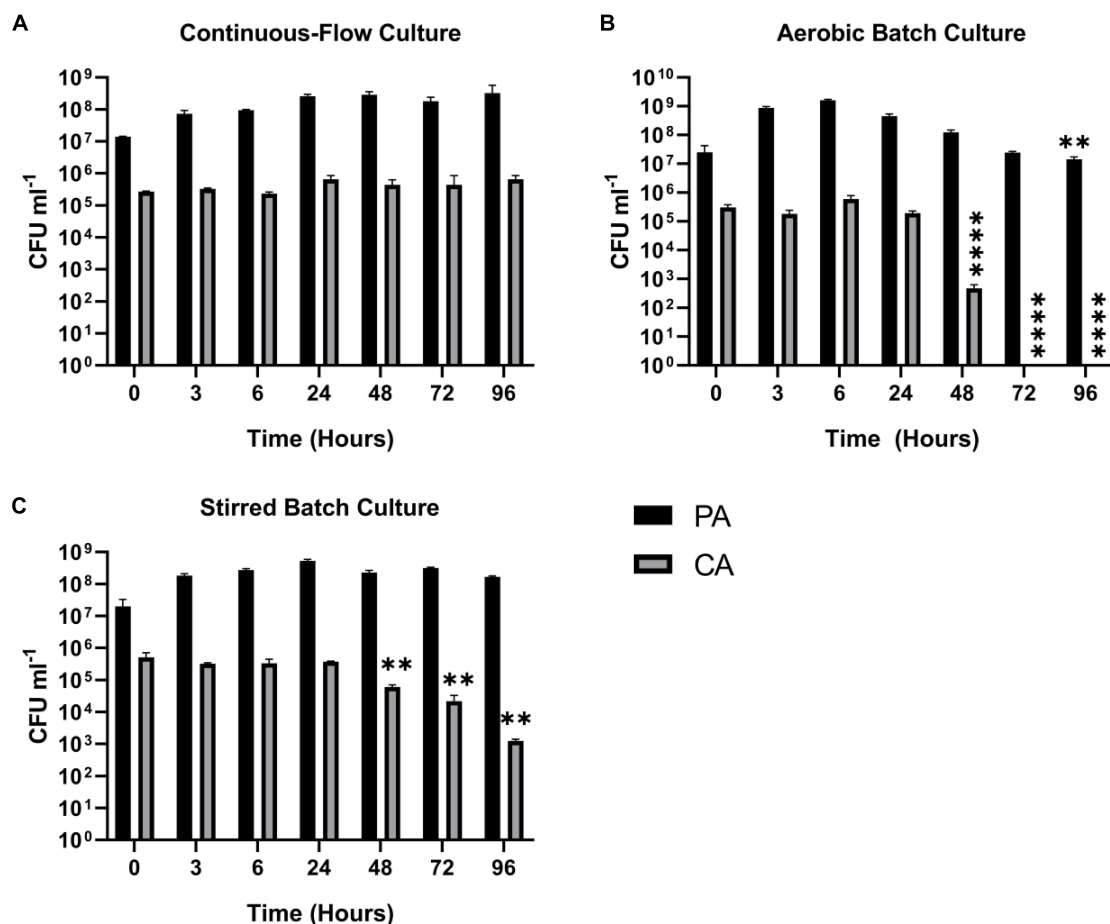


FIGURE 4 | Continuous-flow culture allows *P. aeruginosa* and *C. albicans* to be maintained in a stable steady-state. Viable cell counts (CFU) of *P. aeruginosa* PAO1 (PA, black bars) and *C. albicans* SC5314 (CA, grey bars) during co-culture in ASM using: **(A)** a continuous-flow setup; **(B)** aerobic batch culture; and **(C)** stirred batch culture. Data represent as mean \pm standard deviation from three independent experiments. Asterisks represent significant differences in CFU mL⁻¹ counts in comparison with the data from the 24 h time point (** $P < 0.005$, *** $P < 0.0001$).

factors have been implicated in mediating interactions with other microbial species (Gambello et al., 1993; Smith and Iglewski, 2003; Lau et al., 2004; Schuster and Greenberg, 2006; Dekimpe and Déziel, 2009; Antunes et al., 2010). To examine how other microbial species might impinge on QS in PA, we therefore determined the concentration of the *Pseudomonas* quinolone signal (PQS), *N*-(3-Oxododecanoyl)-L-homoserine lactone (OdDHL) and *N*-butanoyl-L-homoserine lactone (BHL) in the culture supernatant of single and mixed species co-cultures (Figures 7A–C, respectively).

The concentration of all three QS molecules was significantly ($P < 0.0001$) lower in the continuous-flow setup compared with the aerobic- and stirred-batch cultures. In the continuous-flow setup, there was no significant difference in the concentration of PQS between the 24 and 96 h sampling points, or of OdDHL between these sampling points ($P > 0.1$), although we did note an increase in BHL concentration in the PA-CA co-culture over this period ($P > 0.05$). In contrast, QS molecules accrued to much higher concentrations in the aerobic- and stirred-batch cultures. Moreover, the presence of co-cultivated species had a

large, but differential impact on QS molecule production by PA. For example, in batch culture, SA appeared to stimulate OdDHL production, whereas CA appeared to depress OdDHL levels and stimulate PQS (and to a lesser extent, also BHL) production. Taken together, our data indicate that QS molecules accumulate to a much lower concentration in the continuous-flow setup compared with batch cultures.

Quantification of Pyocyanin

Pyocyanin is a redox-active PA secondary metabolite, and is linked with virulence and competition between microbial species in the CF lung (Castric, 1975; Hoffman et al., 2006; Voggu et al., 2006; Biswas et al., 2009; Filkins et al., 2015; Noto et al., 2017). We measured pyocyanin levels in the different culture setups at the endpoint of each experiment (Figure 8). Pyocyanin concentrations were significantly lower for all microbial species combinations in the continuous-flow setup compared with the aerobic- or stirred-batch cultures ($P < 0.0001$). No significant differences were observed in pyocyanin accumulation between the different microbial co-culture combinations following growth

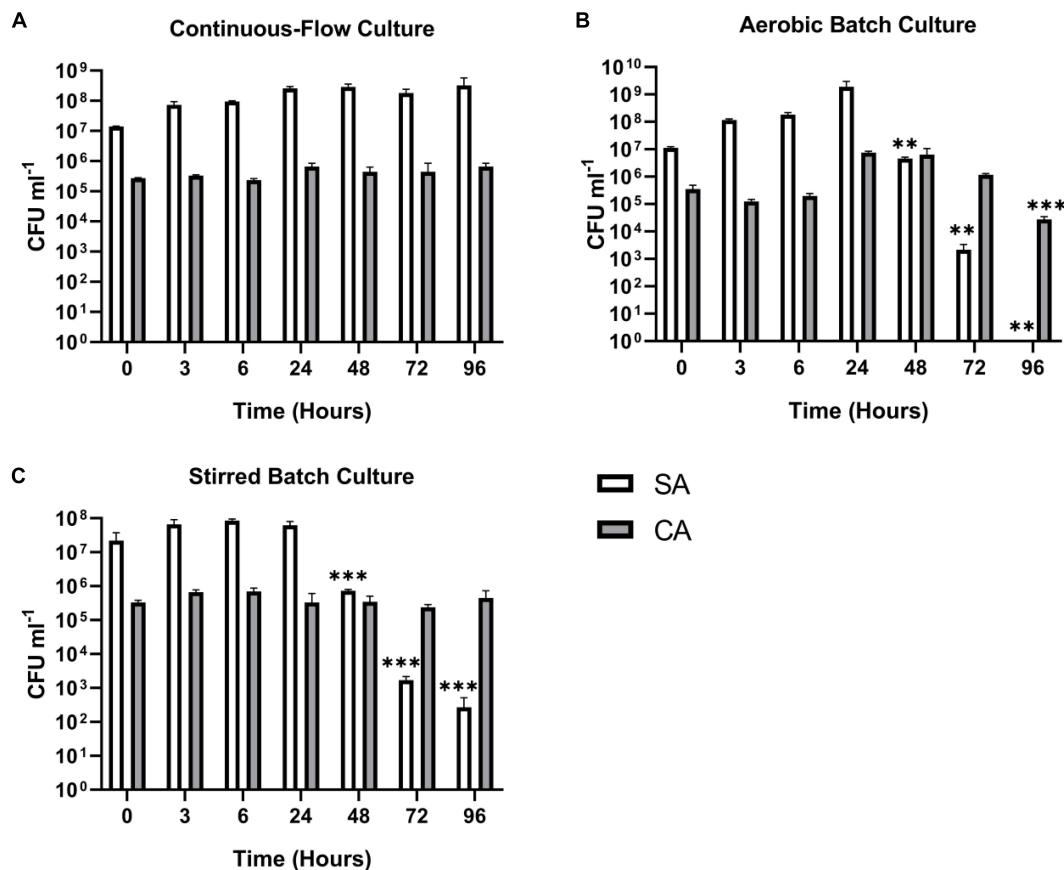


FIGURE 5 | Continuous-flow culture allows *S. aureus* and *C. albicans* to be maintained in a stable steady-state. Viable cell counts of *S. aureus* 25923 (SA, white bars) and *C. albicans* SC5314 (CA, grey bars) co-cultures in ASM in: **(A)** a continuous-flow setup; **(B)** aerobic batch culture; and **(C)** stirred batch culture. Data represented as mean \pm standard deviation of three independent experiments. CFU mL⁻¹ values are plotted on a log₁₀ scale and asterisks represent significant differences in CFU mL⁻¹ counts in comparison with the data from the 24 h time point (** $P < 0.005$, *** $P < 0.001$, **** $P < 0.0001$).

in the continuous-flow setup ($P > 0.3$). However, we did note that in the batch cultures, the presence of CA depressed pyocyanin accumulation.

Estimation of Mutation Rates in Co-cultures of *P. aeruginosa* and *S. aureus*

One possible use of the continuous-flow system described here would be to investigate how the presence of co-habiting species affects evolutionary trajectory(s). To gauge this, we measured the mutation rate of each species during co-culture. Mutation rates were measured as described by Foster (2006) and were assessed shortly after the steady-state had been attained (i.e., at the 24 h time-point) and at the end of the experiment (96 h time-point). The mean number of Rif^R-conferring mutations per cell division was comparable with previously-reported values [$\approx 10^{-8}$ – 10^{-9} mutations/cell/division (Schaaff et al., 2002; Dettman et al., 2016)] and was consistently low for both PA and SA, with no statistically significant differences between the 24 and 96 h sampling points ($P > 0.1$) (Figure 9). We conclude that PA and SA do not exhibit abnormal mutability in the continuous-flow

setup and that co-culture of these species has no apparent impact on their respective mutation rate.

Continuous-Flow Cultures Maintain a Constant pH

We also examined the endpoint pH of mixed-species cultures to see whether this differed from the starting pH of ASM (pH 6.7). We found that irrespective of the microbes and combinations of microbes being tested, the continuous flow cultures maintained a remarkably constant pH that was close to the starting pH. Stirred batch cultures maintained a pH of ca. 7, whereas aerobic batch cultures exhibited an endpoint pH > 8 (Supplementary Figure S4).

DISCUSSION

In this work, we have shown that a simple *in vitro* continuous-flow co-culture system enables long-term co-culture of three distinct microbial species (PA, SA and CA) associated with CF airway infections. When co-cultured in batch, these organisms ordinarily outcompete one another, leading to domination by

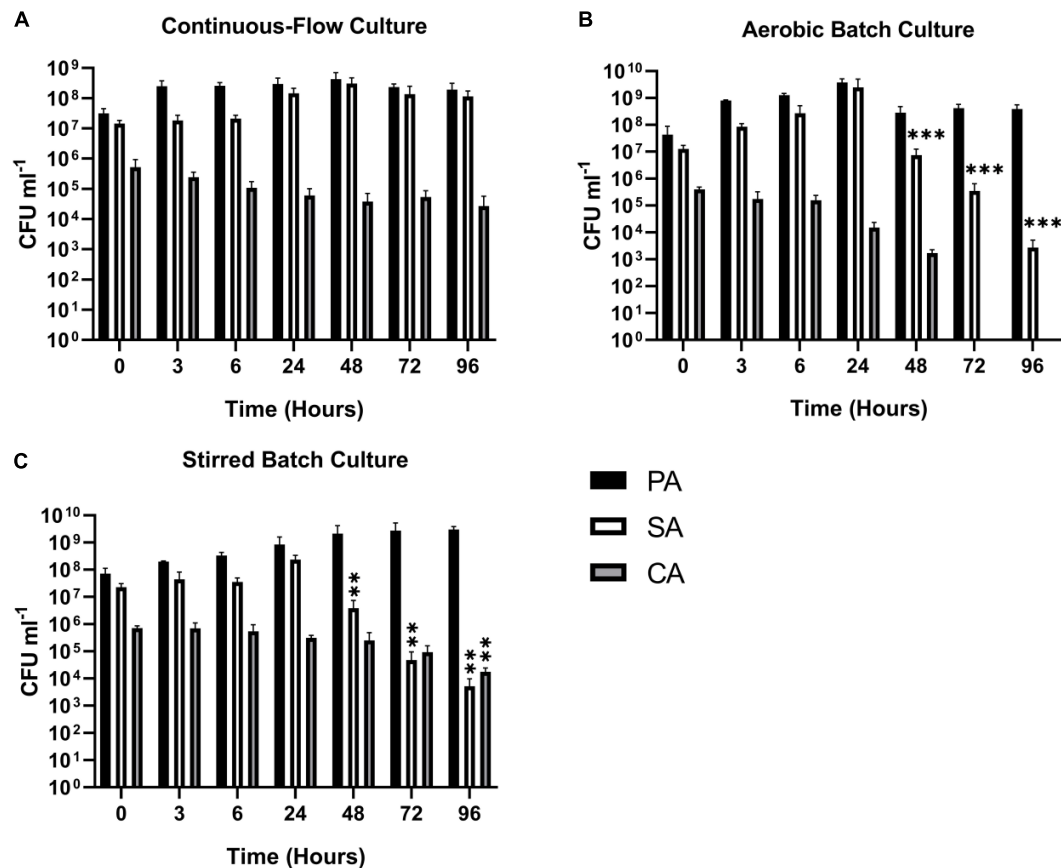


FIGURE 6 | Continuous-flow culture allows *P. aeruginosa*, *C. albicans*, and *S. aureus* to be maintained in a stable steady-state. Viable cell counts of *P. aeruginosa* PAO1 (PA, black bars) *S. aureus* 25923 (SA, white bars) and *C. albicans* SC5314 (CA, grey bars) co-cultures in ASM in: (A) a continuous-flow setup; (B) aerobic batch culture; and (C) stirred batch culture. Data represented as mean \pm standard deviation of three independent experiments. CFU mL⁻¹ values are plotted on a log₁₀ scale and asterisks represent significant differences in CFU mL⁻¹ counts in comparison with the data from the 24 h time point (** P < 0.05, *** P < 0.001).

a single species. However, in the setup described here, once a steady-state has been achieved (after around 24 h incubation) each inoculated species can be maintained at a constant titre, presumably reflecting the carrying capacity for each organism in the culture. Significantly, we show that even low-abundance species (represented by CA in our model) can be stably maintained, and that the presence of such species can have a major impact on the population trajectory of numerically more-abundant organisms such as SA, as well as inter-cellular signalling by PA.

The airways of people with CF have been shown to harbour a diverse polymicrobial community, comprising both bacteria and fungi (Sibley et al., 2006, 2008; Rogers et al., 2010a; Zhao et al., 2012; Carmody et al., 2013, 2015; Short et al., 2014; Boutin et al., 2015), and through the efforts of several teams, we now have a well-defined ASM for *in vitro* analyses. Indeed, PA grown in ASM has an almost identical gene expression profile compared with PA grown directly in sputum derived from CF patients (Turner et al., 2015). In spite of this, to date, there have been no reports describing the successful, long-term co-culture of CF-associated microbes in ASM. As we demonstrate in the current work,

simply adding mixed-species inocula into ASM is not a recipe for the long-term maintenance of a stable population. Perhaps the best measure of the lack of progress on this front is seen when considering PA and SA. These two species are common in CF infections, and decades of work have revealed a wealth of knowledge about their physiology and nutritional requirements in axenic culture. However, until now, there have been no studies describing the successful long-term co-cultivation of these two species *in vitro*. One possible reason for this is that in iron limited conditions, PA lyses SA and uses the resulting lysate as a source of iron (Mashburn et al., 2005). By providing a continual supply of fresh media (which presumably mimics the unrelenting and exuberant production of airway secretions in the CF lung) we speculate that this nutritional limitation may be overcome.

The *in vitro* system described here offers a number of advantages. First, it is inexpensive to set up, making it accessible as a model to most researchers. Second, it is compliant with the “3Rs” (the replacement, refinement and reduction of animal research). Third, it is robust, as attested by the remarkably constant titres of each species following attainment of the steady-state condition. Fourth, early indications are that it can faithfully

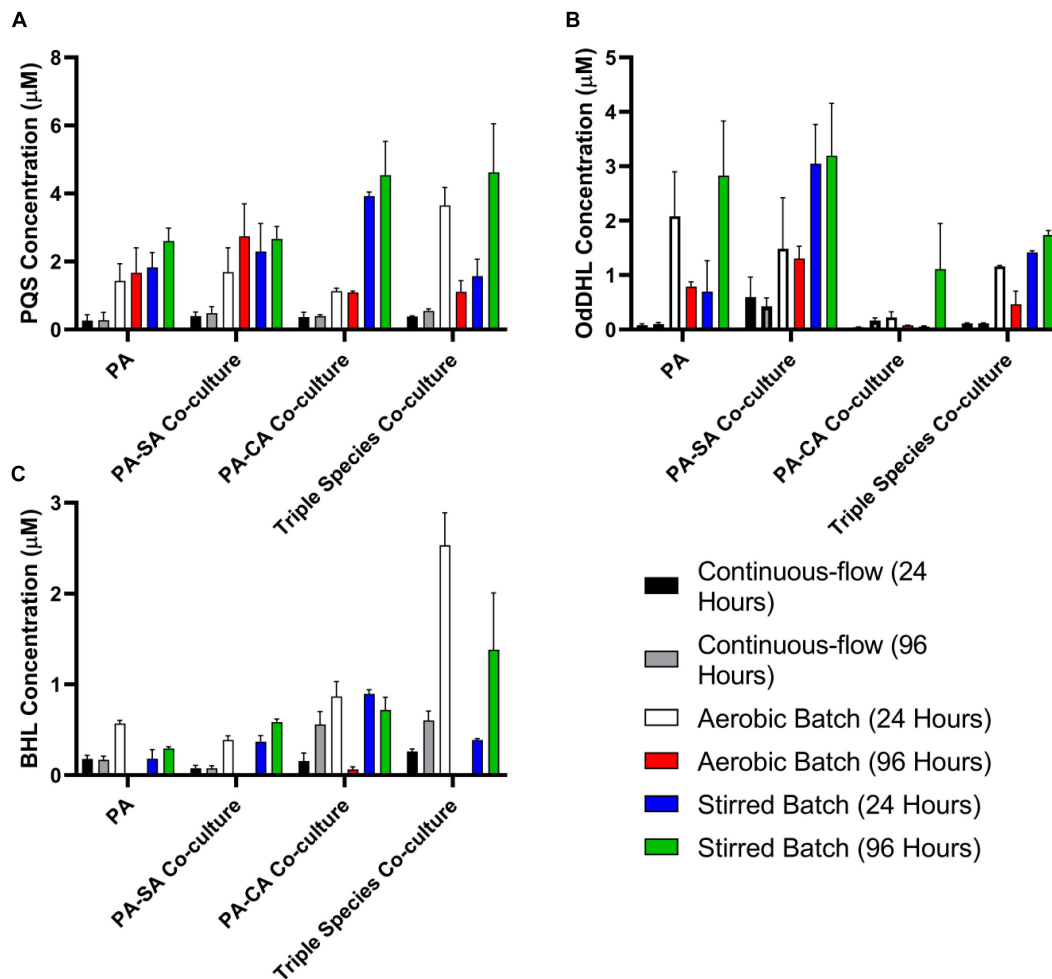
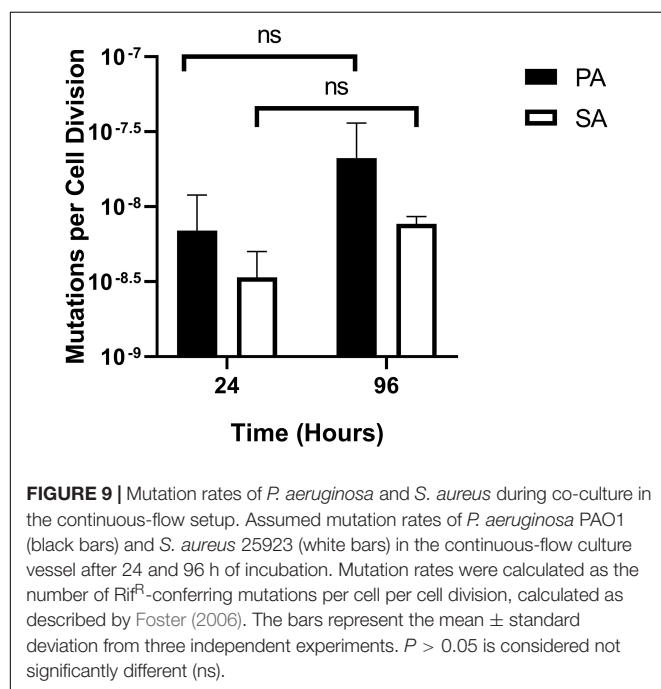
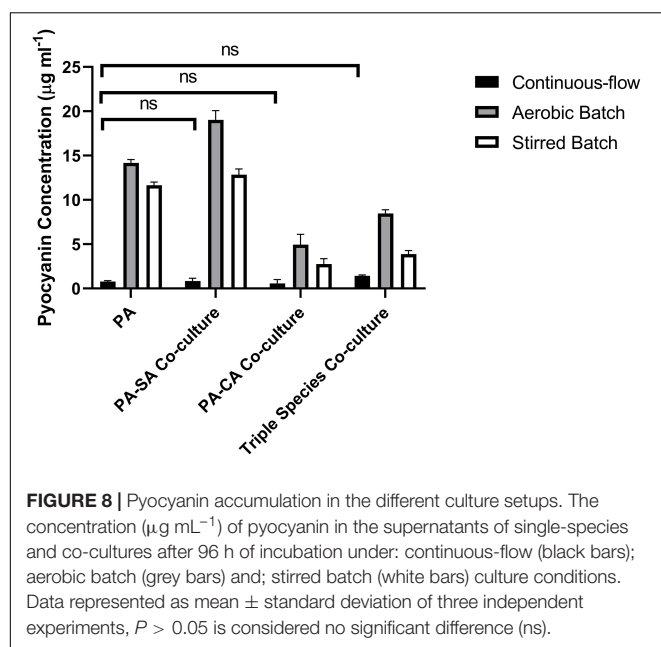


FIGURE 7 | Quorum sensing molecule accumulation in the different culture setups. Concentration of the indicated *P. aeruginosa* quorum sensing molecules in the supernatant of single-species or multi-species co-cultures after 24 and 96 h incubation (as indicated). **(A)** *Pseudomonas* quinolone signal (PQS); **(B)** *N*-(3-oxododecanoyl)-L-homoserine lactone (OdDHL); **(C)** *N*-butanoyl-L-homoserine lactone (BHL). Data represented as mean \pm standard deviation of three independent experiments.

maintain species diversity when patient-derived CF sputum is being used to inoculate the system, and our progress on that aspect of the model will be published presently. Fifth, the system is far more defined and controlled than an animal model, allowing facile experimental perturbation. This experimental tractability means that we can address biological questions in a way that is just not possible with, e.g., animal models. For example, new species or defined mutants can be readily introduced to examine their impact on succession dynamics, and the action of antibiotics on the entire community can be accessed. We have also been exploring ways of modifying the setup to promote biofilm growth in the culture vessel, and again, these findings will be published in the near future.

Our *in vitro* setup is also subject to a number of perceived disadvantages. Unlike an animal model, it does not incorporate any immune response. This may be significant since the immune response would be expected to play a major role in clearance of microbes from the airways, and therefore exerts

a selective pressure on the microbial community. Also, our model does not incorporate other types of host cell. This may be significant because in some circumstances (e.g., in patients carrying the DF508 CFTR mutation) the altered cell surface on the epithelia lining the airways has been implicated in promoting microbial colonisation (Campodónico et al., 2008). Mitigating these features, we note that few animal models accurately recapitulate the human CF airway environment, and aside from the difficulties associated with controlling and sampling such models, as far as we are aware, none of these models have yet been developed for maintaining a polymicrobial community of CF pathogens (O'Brien and Welch, 2019). One other potential disadvantage of our model is the requirement for continual flow. On the one hand, this is a feature that does allow maintenance of a stable steady-state community of microbes. On the other hand, even at low Q values, "washout" may prevent slow-growing species/variants from thriving, or key molecules from accumulating. For example, we noted that QS



molecules (and pyocyanin) fail to accumulate in the continuous-flow system, whereas these compounds reached high levels in batch culture. The most likely explanation for this is simple washout (through continual dilution) of the QS signals. However, it should be noted that with $Q = 170 \mu\text{L min}^{-1}$, it would take > 6 h to dilute the vessel contents by 50%, and all the while, the contained culture continues to grow and elaborate more QS molecules. To put this into context, previous work has shown that QS molecules more than double their concentration in batch cultures in a 2 h period (Davenport et al., 2015),

so assuming similar kinetics in ASM, these molecules should accumulate faster than they are diluted. If so, this suggests that QS plays a less important role in continuous-flow cultures than it does in batch cultures. The low steady-state concentrations of QS molecules documented here may also be advantageous (for the experimenter). First of all, the metabolic physiology of the community is defined and stable over the experiment's time course and we would not expect to see the bursts of metabolic activity which would normally accompany the accumulation of QS molecules in the post-quorate period (Davenport et al., 2015). Second, and if the effect(s) of QS molecules on community interactions does need to be examined, this can be easily be done through the addition of defined concentrations of exogenous QS molecules.

We conclude that the setup described here enables facile maintenance of PA, SA and CA (a Gram-negative bacterial species, a Gram-positive bacterial species and dimorphic fungus, respectively). Our approach provides a framework for potentially recapitulating the entire polymicrobial community associated with CF airway infections. The setup will provide leverage to access to key biological problems regarding inter-species interactions, the impact of antibiotics, and the impact that newly-introduced species may have on the community trajectory.

DATA AVAILABILITY STATEMENT

The raw data supporting the conclusions of this manuscript will be made available by the authors, without undue reservation, to any qualified researcher.

AUTHOR CONTRIBUTIONS

TO'B and MW conceived and designed the work and revised the manuscript. TO'B executed the experiments, analysed the data, and drafted the manuscript.

FUNDING

This work was supported by a studentship (NC/P001564/1) from the NC3Rs to support TO'B, and consumables support from the UK Cystic Fibrosis Trust and British Lung Foundation.

ACKNOWLEDGMENTS

Andres Floto is acknowledged for helpful discussions and for providing the *C. albicans*.

SUPPLEMENTARY MATERIAL

The Supplementary Material for this article can be found online at: <https://www.frontiersin.org/articles/10.3389/fmicb.2019.02713/full#supplementary-material>

REFERENCES

- Antunes, L. C., Ferreira, R. B., Buckner, M. M., and Finlay, B. B. (2010). Quorum sensing in bacterial virulence. *Microbiology* 156(Pt 8), 2271–2282. doi: 10.1099/mic.0.038794-0
- Baldan, R., Cigana, C., Testa, F., Bianconi, I., De Simone, M., and Pellin, D. (2014). Adaptation of *Pseudomonas aeruginosa* in cystic fibrosis airways influences virulence of *Staphylococcus aureus* in vitro and murine models of co-infection. *PLoS One* 9:e89614. doi: 10.1371/journal.pone.0089614
- Barnabe, P. M., and Whiteley, M. (2015). Iron-mediated control of *Pseudomonas aeruginosa*-*Staphylococcus aureus* interactions in the cystic fibrosis lung. *J. Bacteriol.* 197, 2250–2251. doi: 10.1128/JB.00303-15
- Biswas, L., Biswas, R., Schlag, M., Bertram, R., and Götz, F. (2009). Small-colony variant selection as a survival strategy for *Staphylococcus aureus* in the presence of *Pseudomonas aeruginosa*. *Appl. Environ. Microbiol.* 75, 6910–6912. doi: 10.1128/AEM.01211-09
- Bobadilla, J. L., Macek, M., Fine, J. P., and Farrell, P. M. (2002). Cystic fibrosis: a worldwide analysis of CFTR mutations—correlation with incidence data and application to screening. *Hum. Mutat.* 19, 575–606. doi: 10.1002/humu.10041
- Bouchara, J. P., Symoens, F., Schwarz, C., and Chaturvedi, V. (2018). Fungal respiratory infections in cystic fibrosis (cf): recent progress and future research agenda. *Mycopathologia* 183, 1–5. doi: 10.1007/s11046-017-0241-6
- Boucher, R. C. (2002). An overview of the pathogenesis of cystic fibrosis lung disease. *Adv. Drug Delivery Rev.* 54, 1359–1371. doi: 10.1016/S0169-409X(02)00144-8
- Boutin, S., Graeber, S. Y., Weitnauer, M., Panitz, J., Stahl, M., and Clausnitzer, D. (2015). Comparison of microbiomes from different niches of upper and lower airways in children and adolescents with cystic fibrosis. *PLoS One* 10:e0116029. doi: 10.1371/journal.pone.0116029
- Bragonzi, A., Farulla, I., Paroni, M., Twomey, K. B., Pirone, L., and Lorè, N. I. (2012). Modelling co-infection of the cystic fibrosis lung by *Pseudomonas aeruginosa* and *Burkholderia cenocepacia* reveals influences on biofilm formation and host response. *PLoS One* 7:e52330. doi: 10.1371/journal.pone.0052330
- Campodónico, V. L., Gadjeva, M., Paradis-Bleau, C., Uluer, A., and Pier, G. B. (2008). Airway epithelial control of *Pseudomonas aeruginosa* infection in cystic fibrosis. *Trends Mol. Med.* 14, 120–133. doi: 10.1016/j.molmed.2008.01.002
- Carmody, L. A., Zhao, J., Kalikin, L. M., LeBar, W., Simon, R. H., and Venkataraman, A. (2015). The daily dynamics of cystic fibrosis airway microbiota during clinical stability and at exacerbation. *Microbiome* 3:12. doi: 10.1186/s40168-015-0074-9
- Carmody, L. A., Zhao, J., Schloss, P. D., Petrosino, J. F., Murray, S., and Young, V. B. (2013). Changes in cystic fibrosis airway microbiota at pulmonary exacerbation. *Ann. Am. Thorac Soc.* 10, 179–187. doi: 10.1513/AnnalsATS.201211-107OC
- Castric, P. A. (1975). Hydrogen cyanide, a secondary metabolite of *Pseudomonas aeruginosa*. *Can. J. Microbiol.* 21, 613–618. doi: 10.1139/m75-088
- Conrad, D., Haynes, M., Salamon, P., Rainey, P. B., Youle, M., and Rohwer, F. (2013). Cystic fibrosis therapy: a community ecology perspective. *Am. J. Respir. Cell Mol. Biol.* 48, 150–156. doi: 10.1165/rcmb.2012-0059PS
- Cugini, C., Morales, D. K., and Hogan, D. A. (2010). Candida albicans-produced farnesol stimulates *Pseudomonas* quinolone signal production in LasR-defective *Pseudomonas aeruginosa* strains. *Microbiology* 156(Pt 10), 3096–3107. doi: 10.1099/mic.0.037911-0
- Cystic Fibrosis Foundation (2019). *Cystic Fibrosis Foundation* (<http://www.cff.org>). Bethesda: Cystic Fibrosis Foundation
- Cystic Fibrosis Mutation Database (2019). *Cystic Fibrosis Mutation Database*. Cystic Fibrosis Mutation Database: Bethesda.
- Davenport, P. W., Griffin, J. L., and Welch, M. (2015). Quorum sensing is accompanied by global metabolic changes in the opportunistic human pathogen *Pseudomonas aeruginosa*. *J. Bacteriol.* 197, 2072–2082. doi: 10.1128/JB.02557-14
- Dekimpe, V., and Déziel, E. (2009). Revisiting the quorum-sensing hierarchy in *Pseudomonas aeruginosa*: the transcriptional regulator RhlR regulates LasR-specific factors. *Microbiology* 155(Pt 3), 712–723. doi: 10.1099/mic.0.022764-0
- Dettman, J. R., Sztepanacz, J. L., and Kassen, R. (2016). The properties of spontaneous mutations in the opportunistic pathogen *Pseudomonas aeruginosa*. *BMC Genomics* 17:27. doi: 10.1186/s12864-015-2244-3
- Duan, K., Dammel, C., Stein, J., Rabin, H., and Surette, M. G. (2003). Modulation of *Pseudomonas aeruginosa* gene expression by host microflora through interspecies communication. *Mol. Microbiol.* 50, 1477–1491. doi: 10.1046/j.1365-2958.2003.03803.x
- Elborn, J. S. (2016). Cystic fibrosis. *Lancet* 388, 2519–2531. doi: 10.1016/S0140-6736(16)00576-6
- Elias, S., and Banin, E. (2012). Multi-species biofilms: living with friendly neighbors. *FEMS Microbiol. Rev.* 36, 990–1004. doi: 10.1111/j.1574-6976.2012.00325.x
- Filkins, L. M., Graber, J. A., Olson, D. G., Dolben, E. L., Lynd, L. R., and Bhujra, S. (2015). Coculture of *Staphylococcus aureus* with *Pseudomonas aeruginosa* Drives *S. aureus* towards fermentative metabolism and reduced viability in a cystic fibrosis model. *J. Bacteriol.* 197, 2252–2264. doi: 10.1128/JB.00059-15
- Fletcher, M. P., Diggle, S. P., Cámara, M., and Williams, P. (2007). Biosensor-based assays for PQS, HHQ and related 2-alkyl-4-quinolone quorum sensing signal molecules. *Nat. Protoc.* 2, 1254–1262. doi: 10.1038/nprot.2007.158
- Foster, P. L. (2006). Methods for determining spontaneous mutation rates. *Methods Enzymol.* 409, 195–213. doi: 10.1016/S0076-6879(05)09012-9
- Fugère, A., Lalonde Séguin, D., Mitchell, G., Déziel, E., Dekimpe, V., and Cantin, A. M. (2014). Interspecific small molecule interactions between clinical isolates of *Pseudomonas aeruginosa* and *Staphylococcus aureus* from adult cystic fibrosis patients. *PLoS One* 9:e86705. doi: 10.1371/journal.pone.0086705
- Gambello, M. J., Kaye, S., and Iglewski, B. H. (1993). LasR of *Pseudomonas aeruginosa* is a transcriptional activator of the alkaline protease gene (apr) and an enhancer of exotoxin A expression. *Infect Immun.* 61, 1180–1184.
- Ghio, A. J., Roggli, V. L., Soukup, J. M., Richards, J. H., Randall, S. H., and Muhlebach, M. S. (2013). Iron accumulates in the lavage and explanted lungs of cystic fibrosis patients. *J. Cyst. Fibros* 12, 390–398. doi: 10.1016/j.jcf.2012.10.010
- Gillum, A. M., Tsay, E. Y., and Kirsch, D. R. (1984). Isolation of the Candida albicans gene for orotidine-5'-phosphate decarboxylase by complementation of *S. cerevisiae* *ura3* and *E. coli* *pyrF* mutations. *Mol. Gen. Genet.* 198, 179–182. doi: 10.1007/bf00328721
- Goss, C. H., and Muhlebach, M. S. (2011). Review: *Staphylococcus aureus* and MRSA in cystic fibrosis. *J. Cyst. Fibros* 10, 298–306. doi: 10.1016/j.jcf.2011.06.002
- Grasemann, H., Ioannidis, I., Tomkiewicz, R. P., de Groot, H., Rubin, B. K., and Ratjen, F. (1998). Nitric oxide metabolites in cystic fibrosis lung disease. *Arch. Dis. Child* 78, 49–53. doi: 10.1136/adc.78.1.49
- Hibbing, M. E., Fuqua, C., Parsek, M. R., and Peterson, S. B. (2010). Bacterial competition: surviving and thriving in the microbial jungle. *Nat. Rev. Microbiol.* 8, 15–25. doi: 10.1038/nrmicro2259
- Hoffman, L. R., Déziel, E., D'Argenio, D. A., Lépine, F., Emerson, J., and McNamara, S. (2006). Selection for *Staphylococcus aureus* small-colony variants due to growth in the presence of *Pseudomonas aeruginosa*. *Proc. Natl. Acad. Sci. U.S.A.* 103, 19890–19895. doi: 10.1073/pnas.0606756104
- Hogan, D. A., Vik, A., and Kolter, R. (2004). A *Pseudomonas aeruginosa* quorum-sensing molecule influences *Candida albicans* morphology. *Mol. Microbiol.* 54, 1212–1223. doi: 10.1111/j.1365-2958.2004.04349.x
- Holcombe, L. J., McAlester, G., Munro, C. A., Enjalbert, B., Brown, A., and Gow, J. P. (2010). *Pseudomonas aeruginosa* secreted factors impair biofilm development in *Candida albicans*. *Microbiology* 156(Pt 5), 1476–1486. doi: 10.1099/mic.0.037549-0
- Holloway, B. W. (1955). Genetic recombination in *Pseudomonas aeruginosa*. *J. Gen. Microbiol.* 13, 572–581. doi: 10.1099/00221287-13-3-572
- Ibberson, C. B., Stacy, A., Fleming, D., Dees, J. L., Rumbaugh, K., and Gilmore, M. S. (2017). Co-infecting microorganisms dramatically alter pathogen gene essentiality during polymicrobial infection. *Nat. Microbiol.* 2:17079. doi: 10.1038/nmicrobiol.2017.79
- Jones, K. L., Hegab, A. H., Hillman, B. C., Simpson, K. L., Jinkins, P. A., and Grisham, M. B. (2000). Robbins: elevation of nitrotyrosine and nitrate concentrations in cystic fibrosis sputum. *Pediatr. Pulmonol.* 30, 79–85. doi: 10.1002/1099-0496(200008)30:2<79::aid-ppul1>3.0.co;2-1
- Jorth, P., Ehsan, Z., Rezayat, A., Caldwell, E., Pope, C., and Brewington, J. J. (2019). Direct lung sampling indicates that established pathogens dominate

- early infections in children with cystic fibrosis. *Cell Rep.* 27:1190–1204.e3. doi: 10.1016/j.celrep.2019.03.086
- Kirchner, S., Fothergill, J. L., Wright, E. A., James, C. E., Mowat, E., and Winstanley, C. (2012). Use of artificial sputum medium to test antibiotic efficacy against *Pseudomonas aeruginosa* in conditions more relevant to the cystic fibrosis lung. *J. Vis. Exp.* 5:e3857. doi: 10.3791/3857
- Knight, M., Hartman, P. E., Hartman, Z., and Young, V. M. (1979). A new method of preparation of pyocyanin and demonstration of an unusual bacterial sensitivity. *Anal. Biochem.* 95, 19–23. doi: 10.1016/0003-2697(79)90179-9
- Korgaonkar, A., Trivedi, U., Rumbaugh, K. P., and Whiteley, M. (2013). Community surveillance enhances *Pseudomonas aeruginosa* virulence during polymicrobial infection. *Proc. Natl. Acad. Sci. U.S.A.* 110, 1059–1064. doi: 10.1073/pnas.1214550110
- Lau, G. W., Hassett, D. J., Ran, H., and Kong, F. (2004). The role of pyocyanin in *Pseudomonas aeruginosa* infection. *Trends Mol. Med.* 10, 599–606. doi: 10.1016/j.molmed.2004.10.002
- Leekha, S., Terrell, C. L., and Edson, R. S. (2011). General principles of antimicrobial therapy. *Mayo Clin. Proc.* 86, 156–167. doi: 10.4065/mcp.2010.0639
- Limoli, D. H., Yang, J., Khansaheb, M. K., Helfman, B., Peng, L., and Stecenko, A. A. (2016). *Staphylococcus aureus* and *Pseudomonas aeruginosa* co-infection is associated with cystic fibrosis-related diabetes and poor clinical outcomes. *Eur. J. Clin. Microbiol. Infect. Dis.* 35, 947–953. doi: 10.1007/s10096-016-2621-0
- Lopes, S. P., Azevedo, N. F., and Pereira, M. O. (2017). Developing a model for cystic fibrosis sociomicrobiology based on antibiotic and environmental stress. *Int. J. Med. Microbiol.* 307, 460–470. doi: 10.1016/j.ijmm.2017.09.018
- Lopes, S. P., Ceri, H., Azevedo, N. F., and Pereira, M. O. (2012). Antibiotic resistance of mixed biofilms in cystic fibrosis: impact of emerging microorganisms on treatment of infection. *Int. J. Antimicrob. Agents* 40, 260–263. doi: 10.1016/j.ijantimicag.2012.04.020
- Lyczak, J. B., Cannon, C. L., and Pier, G. B. (2002). Lung infections associated with cystic fibrosis. *Clin. Microbiol. Rev.* 15, 194–222. doi: 10.1128/cmr.15.2.194-222.2002
- Machan, Z. A., Taylor, G. W., Pitt, T. L., Cole, P. J., and Wilson, R. (1992). 2-Heptyl-4-hydroxyquinoline N-oxide, an antistaphylococcal agent produced by *Pseudomonas aeruginosa*. *J. Antimicrob. Chemother.* 30, 615–623. doi: 10.1093/jac/30.5.615
- Magalhães, A. P., Lopes, S. P., and Pereira, M. O. (2016). Insights into cystic fibrosis polymicrobial consortia: the role of species interactions in biofilm development, phenotype, and response to in-use antibiotics. *Front. Microbiol.* 7:2146. doi: 10.3389/fmicb.2016.02146
- Makovcova, J., Babak, V., Kulich, P., Masek, J., Slany, M., and Cincaro, L. (2017). Dynamics of mono- and dual-species biofilm formation and interactions between *Staphylococcus aureus* and Gram-negative bacteria. *Microb. Biotechnol.* 10, 819–832. doi: 10.1111/1751-7915.12705
- Mashburn, L. M., Jett, A. M., Akins, D. R., and Whiteley, M. (2005). *Staphylococcus aureus* serves as an iron source for *Pseudomonas aeruginosa* during *in vivo* coculture. *J. Bacteriol.* 187, 554–566. doi: 10.1128/JB.187.2.554-566.2005
- McAlester, G., O'Gara, F., and Morrissey, J. P. (2008). Signal-mediated interactions between *Pseudomonas aeruginosa* and *Candida albicans*. *J. Med. Microbiol.* 57(Pt 5), 563–569. doi: 10.1099/jmm.0.47705-0
- Morales, D. K., Jacobs, N. J., Rajamani, S., Krishnamurthy, M., Cubillos-Ruiz, J. R., and Hogan, D. A. (2010). Antifungal mechanisms by which a novel *Pseudomonas aeruginosa* phenazine toxin kills *Candida albicans* in biofilms. *Mol. Microbiol.* 78, 1379–1392. doi: 10.1111/j.1365-2958.2010.07414.x
- Nguyen, A. T., Jones, J. W., Ruge, M. A., Kane, M. A., and Oglesby-Sherrouse, A. G. (2015). Iron depletion enhances production of antimicrobials by *Pseudomonas aeruginosa*. *J. Bacteriol.* 197, 2265–2275. doi: 10.1128/JB.00072-15
- Nguyen, A. T., and Oglesby-Sherrouse, A. G. (2016). Interactions between *Pseudomonas aeruginosa* and *Staphylococcus aureus* during co-cultivations and polymicrobial infections. *Appl. Microbiol. Biotechnol.* 100, 6141–6148. doi: 10.1007/s00253-016-7596-3
- Noto, M. J., Burns, W. J., Beavers, W. N., and Skaar, E. P. (2017). Mechanisms of pyocyanin toxicity and genetic determinants of resistance in *Staphylococcus aureus*. *J. Bacteriol.* 199:e221-17. doi: 10.1128/JB.00221-17
- O'Brien, T. J., and Welch, M. (2019). Recapitulation of polymicrobial communities associated with cystic fibrosis airway infections: a perspective. *Future Microbiol.* (in press). doi: 10.2217/fmb-2019-0200
- Palmer, K. L., Aye, L. M., and Whiteley, M. (2007). Nutritional cues control *Pseudomonas aeruginosa* multicellular behavior in cystic fibrosis sputum. *J. Bacteriol.* 189, 8079–8087. doi: 10.1128/JB.01138-07
- Park, J. H., Lee, J. H., Cho, M. H., Herzberg, M., and Lee, J. (2012). Acceleration of protease effect on *Staphylococcus aureus* biofilm dispersal. *FEMS Microbiol. Lett.* 335, 31–38. doi: 10.1111/j.1574-6968.2012.02635.x
- Peters, B. M., Jabra-Rizk, M. A. O., May, G. A., Costerton, J. W., and Shirliff, M. E. (2012). Polymicrobial interactions: impact on pathogenesis and human disease. *Clin. Microbiol. Rev.* 25, 193–213. doi: 10.1128/CMR.00013-11
- Quinn, R. A., Lim, Y. W., Maughan, H., Conrad, D., Rohwer, F., and Whiteson, K. L. (2014). Biogeochemical forces shape the composition and physiology of polymicrobial communities in the cystic fibrosis lung. *MBio* 5:e956-13. doi: 10.1128/mBio.00956-13
- Rajan, S., and Saiman, L. (2002). Pulmonary infections in patients with cystic fibrosis. *Semin Respir Infect* 17, 47–56. doi: 10.1053/srin.2002.31690
- Rogers, G. B., Carroll, M. P., and Bruce, K. D. (2009). Studying bacterial infections through culture-independent approaches. *J. Med. Microbiol.* 58(Pt 11), 1401–1418. doi: 10.1099/jmm.0.013334-0
- Rogers, G. B., Hoffman, L. R., Whiteley, M., Daniels, T. W., Carroll, M. P., and Bruce, K. D. (2010a). Revealing the dynamics of polymicrobial infections: implications for antibiotic therapy. *Trends Microbiol.* 18, 357–364. doi: 10.1016/j.tim.2010.04.005
- Rogers, G. B., Stressmann, F. A., Walker, A. W., Carroll, M. P., and Bruce, K. D. (2010b). Lung infections in cystic fibrosis: deriving clinical insight from microbial complexity. *Expert Rev. Mol. Diagn.* 10, 187–196. doi: 10.1586/erm.09.81
- Rüger, M., Ackermann, M., and Reichl, U. (2014). Species-specific viability analysis of *Pseudomonas aeruginosa*, *Burkholderia cepacia* and *Staphylococcus aureus* in mixed culture by flow cytometry. *BMC Microbiol.* 14:56. doi: 10.1186/1471-2180-14-56
- Schaaff, F., Reipert, A., and Bierbaum, G. (2002). An elevated mutation frequency favors development of vancomycin resistance in *Staphylococcus aureus*. *Antimicrob. Agents Chemother.* 46, 3540–3548. doi: 10.1128/aac.46.11.3540-3548.2002
- Schuster, M., and Greenberg, E. P. (2006). A network of networks: quorum-sensing gene regulation in *Pseudomonas aeruginosa*. *Int. J. Med. Microbiol.* 296, 73–81. doi: 10.1016/j.ijmm.2006.01.036
- Short, F. L., Murdoch, S. L., and Ryan, R. P. (2014). Polybacterial human disease: the ills of social networking. *Trends Microbiol.* 22, 508–516. doi: 10.1016/j.tim.2014.05.007
- Sibley, C. D., Parkins, M. D., Rabin, H. R., Duan, K., Norgaard, J. C., and Surette, M. G. (2008). A polymicrobial perspective of pulmonary infections exposes an enigmatic pathogen in cystic fibrosis patients. *Proc. Natl. Acad. Sci. U.S.A.* 105, 15070–15075. doi: 10.1073/pnas.0804326105
- Sibley, C. D., Rabin, H., and Surette, M. G. (2006). Cystic fibrosis: a polymicrobial infectious disease. *Future Microbiol.* 1, 53–61. doi: 10.2217/17460913.1.1.53
- Smith, R. S., and Iglewski, B. H. (2003). *P. aeruginosa* quorum-sensing systems and virulence. *Curr. Opin. Microbiol.* 6, 56–60. doi: 10.1016/s1369-5274(03)00008-0
- Spasnovski, T., Carroll, M. P., Lilley, A. K., Payne, M. S., and Bruce, K. D. (2010). Modelling the bacterial communities associated with cystic fibrosis lung infections. *Eur. J. Clin. Microbiol. Infect. Dis.* 29, 319–328. doi: 10.1007/s10096-009-0861-y
- Tate, S., MacGregor, G., Davis, M., Innes, J. A., and Greening, A. P. (2002). Airways in cystic fibrosis are acidified: detection by exhaled breath condensate. *Thorax* 57, 926–929. doi: 10.1136/thorax.57.11.926
- Thomas, P., Sekhar, A. C., Upreti, R., Mujawar, M. M., and Pasha, S. S. (2015). Optimization of single plate-serial dilution spotting (SP-SDS) with sample anchoring as an assured method for bacterial and yeast cfu enumeration and single colony isolation from diverse samples. *Biotechnol. Rep.* 8, 45–55. doi: 10.1016/j.btre.2015.08.003
- Treangen, T. J., Maybank, R. A., Enke, S., Friss, M. B., Diviak, L. F., and Karaolis, D. K. (2014). Complete genome sequence of the quality control strain *Staphylococcus aureus* subsp. *aureus* ATCC 25923. *Genome Announc.* 2:e1110-14. doi: 10.1128/genomeA.01110-14
- Turner, K. H., Wessel, A. K., Palmer, G. C., Murray, J. L., and Whiteley, M. (2015). Essential genome of *Pseudomonas aeruginosa* in cystic fibrosis sputum. *Proc. Natl. Acad. Sci. U.S.A.* 112, 4110–4115. doi: 10.1073/pnas.1419677112

- Voggu, L., Schlag, S., Biswas, R., Rosenstein, R., Rausch, C., and Götz, F. (2006). Microevolution of cytochrome bd oxidase in *Staphylococci* and its implication in resistance to respiratory toxins released by *Pseudomonas*. *J. Bacteriol.* 188, 8079–8086. doi: 10.1128/JB.00858-06
- Williams, C., Ranjendran, R., and Ramage, G. (2016). Pathogenesis of fungal infections in cystic fibrosis. *Curr. Fungal Infect. Rep.* 10, 163–169. doi: 10.1007/s12281-016-0268-z
- Winston, M. K., Swift, S., Fish, L., Throup, J. P., Jørgensen, F., and Chhabra, S. R. (1998). Construction and analysis of luxCDABE-based plasmid sensors for investigating N-acyl homoserine lactone-mediated quorum sensing. *FEMS Microbiol. Lett.* 163, 185–192. doi: 10.1111/j.1574-6968.1998.tb13044.x
- Worlitzsch, D., Tarran, R., Ulrich, M., Schwab, U., Cekici, A., and Meyer, K. C. (2002). Effects of reduced mucus oxygen concentration in airway *Pseudomonas* infections of cystic fibrosis patients. *J. Clin. Invest.* 109, 317–325. doi: 10.1172/JCI13870
- Zago, C. E., Silva, S., Sanitá, P. V., Barbugli, P. A., Dias, C. M., and Lordello, V. B. (2015). Dynamics of biofilm formation and the interaction between *Candida albicans* and methicillin-susceptible (MSSA) and -resistant *Staphylococcus aureus* (MRSA). *PLoS One* 10:e0123206. doi: 10.1371/journal.pone.0123206
- Zhao, J., Schloss, P. D., Kalikin, L. M., Carmody, L. A., Foster, B. K., and Petrosino, J. F. (2012). Decade-long bacterial community dynamics in cystic fibrosis airways. *Proc. Natl. Acad. Sci. U.S.A.* 109, 5809–5814. doi: 10.1073/pnas.1120577109
- Conflict of Interest:** The authors declare that the research was conducted in the absence of any commercial or financial relationships that could be construed as a potential conflict of interest.
- Copyright © 2019 O'Brien and Welch. This is an open-access article distributed under the terms of the Creative Commons Attribution License (CC BY). The use, distribution or reproduction in other forums is permitted, provided the original author(s) and the copyright owner(s) are credited and that the original publication in this journal is cited, in accordance with accepted academic practice. No use, distribution or reproduction is permitted which does not comply with these terms.

Recapitulation of polymicrobial communities associated with cystic fibrosis airway infections: a perspective

Thomas J O'Brien¹ & Martin Welch^{*,1}

¹Department of Biochemistry, University of Cambridge, Cambridge, CB2 1QW, UK

*Author for correspondence: mw240@cam.ac.uk

The airways of persons with cystic fibrosis are prone to infection by a diverse and dynamic polymicrobial consortium. Currently, no models exist that permit recapitulation of this consortium within the laboratory. Such microbial ecosystems likely have a network of interspecies interactions, serving to modulate metabolic pathways and impact upon disease severity. The contribution of less abundant/fastidious microbial species on this cross-talk has often been neglected due to lack of experimental tractability. Here, we critically assess the existing models for studying polymicrobial infections. Particular attention is paid to 3Rs-compliant *in vitro* and *in silico* infection models, offering significant advantages over mammalian infection models. We outline why these models will likely become the 'go to' approaches when recapitulating polymicrobial cystic fibrosis infection.

First draft submitted: 28 June 2019; Accepted for publication: 29 October 2019; Published online: 28 November 2019

Keywords: coculture • cystic fibrosis • *in silico* • *in vitro* • *in vivo* • infection model • interspecies interactions • microbiology • polymicrobial

Cystic fibrosis (CF) is the most common life-limiting genetic disease within the Caucasian population and is estimated to affect 70,000 people worldwide [1]. It results from an autosomal recessive defect within the cystic fibrosis transmembrane conductance regulator (CFTR) gene [2] and a myriad of different mutations have been described that bring about the onset of CF [3]. Dysfunctional CFTR activity leads to complications in multiple organs, but perhaps the most striking presentation of CF is the overproduction of a nutrient rich, viscous mucus in the CF-airways [4]. Defective mucociliary clearance mechanisms further contribute toward airway obstruction which results in the CF airways being a highly heterogeneous environment, typically characterized by steep oxygen gradients, lowered pH and an abundance of mucin, amino acids, nitrate and iron [5–10]. This unique environmental niche is prone to chronic microbial colonization, and such infections contribute toward the death of 80–95% of CF patients [11–15] through triggering bouts of excessive inflammation, termed acute pulmonary exacerbations (APEs). Cumulatively, these lead to tissue destruction and a steady decline in lung function [14,15].

Traditionally, culture-based microbiological investigation of sputum samples expectorated from CF-patients have been used to establish which microbial species are associated with chronic infection of the CF airways. It was suggested, in line with Koch's postulates, that single-microbial species were the primary cause of infection [16], with *Staphylococcus aureus* being prevalent in the early stages of life, before being outcompeted as *Pseudomonas aeruginosa* (PA) becomes the dominant pathogen alongside occasional co-infections from other 'keystone' respiratory pathogens [17–19]. More recently, culture-independent molecular profiling techniques, for example, sequencing of the hypervariable bacterial 16S rDNA and fungal ITS regions, suggest that a previously unanticipated diverse polymicrobial population of both bacteria and fungi are associated with CF-airway infections [14,15,18–22]. However, this notion has been strongly contended by the recent work of Jorth *et al.*, who sampled lavage fluid directly from the lungs of CF-children displaying stable lung function. These authors suggest that the previously reported diversity of the CF-associated microbiome may arise from the sampling of oral contaminants. This notwithstanding, Jorth *et al.* did suggest that a core population of 'nonconventional' bacterial species are found alongside the traditional CF-pathogens [23].

With the CF airways containing a polymicrobial ecosystem, it could be hypothesised that members of this community interact with one another either through quorum sensing, the recognition of cell surface proteins and the secretion of other small metabolites. Indeed, it has been demonstrated that the co-culture of different bacterial species leads to large alterations in their gene expression profile, both *in vivo* and *in vitro* [24]. Such changes can be synergistic or antagonistic in nature [25,26] and may cause members of the community to adopt different lifestyles and activate distinct metabolic pathways. These changes could alter the expression of virulence factors and influence the chemical environment, causing deviations from behaviors observed when studying single species in isolation [21,25,27–30]. For example PA is able to sense the presence of peptidoglycan shed from Gram-positive bacteria. This stimulates the production of extracellular factors that are lytic against both prokaryotic and eukaryotic cells [31]. Ultimately, polymicrobial infections display altered responses to therapeutic interventions. Such interventions are often aimed at decreasing the microbial load of a principal pathogen, and differentially impact disease severity between patients [32].

The microbial consortium present within the CF airway is thought to consist of both stable and disturbed states [25], yet little is known about what triggers the switch between the two. A better understanding of the extent of interactions occurring within the CF airway, and of how the architecture of polymicrobial communities adapts over time and responds to clinical intervention, may lead to the identification of novel therapeutic targets. It is possible that less abundant and poorly characterized species, typically viewed as avirulent when studied in isolation, could trigger the adoption of a more pathogenic lifestyle by known pathogens or in species classically thought to be nonpathogenic or nonconventional. Through targeting the pathways involved, and the chemical changes inducing the onset of a decline in lung function, it may be possible to delay or prevent key CF pathogens from dominating the patient's airways.

Despite the likely role played by interspecies interactions on the severity of disease within CF and other polymicrobial infections, relatively little is understood about this, or about how interspecies interactions impinge upon adaptation in the airways. This lack of understanding is, at least partially, attributable to the complexity of mixed-species interactions, and the paucity of polymicrobial models available for studying such interactions. Although research focus is now gradually moving away from studying single species in isolation, and moving more toward cocultivating the major members of mixed populations, these studies often ignore the presence of less abundant and hard-to-cultivate members of the community, thereby neglecting their impact as drivers of population change.

It would be of enormous benefit for models to be developed within the laboratory that enable the stable recapitulation of the whole polymicrobial community derived from the airways of CF-patients, in other words, those associated with sputum or bronchoalveolar lavage fluid (BALF) samples. These models would better represent the nature of the CF airway community and shed light on how both key pathogens and less represented species might be influenced by external perturbations. Such a model system would allow for a multitude of biological questions to be addressed relating to interspecies interactions and evolution within mixed microbial populations. The community-wide impact of external perturbations, either through antimicrobial treatment or through the introduction of new species/strain variants, could all be studied in a robust and reproducible manner.

This commentary aims to provide a critical overview of the existing models used to study microbial infection in relation to CF, and we hope to clarify how such approaches might be utilized to develop true polymicrobial infection models utilizing the microbial communities derived from CF sputum. Close attention is paid to the development of *in vitro* and *in silico* infection models that comply with the 3Rs guidelines for the reduction, replacement and refinement for the more humane use of animal models within research. Additionally, we highlight the need to consider CF as a mixed-species infection scenario, in order to identify novel targets for therapeutic intervention and understand the progression of disease within a more physiologically relevant context.

Mammalian CF infection models

Animals have long served in the field of comparative biology as a proxy for studying human genetic disease, and CF is no exception to this trend. In 1992, just 3 years after the identification and initial characterization of the CFTR gene, the first CF-mouse model was generated through gene targeting of embryonic stem cells to abolish CFTR activity [33]. In recent years, countless advances in gene editing techniques have led to the generation of a wealth of CF-animal models aimed at mimicking the mutations associated with the disease in humans, with varying success. However, some of these CF-animal models have been pivotal in furthering our understanding of the underlying mechanisms of CF pathology and the development of therapeutics now approved for the treatment of patients

carrying a distinct subset of CFTR mutations. This notwithstanding, our aim here is to provide an overview into how models can be used to study CF-associated infections, and as such we will not review further the utility of animal models for developing gene therapy treatments [34–36].

The comparatively low cost, rapid reproduction rate and ease of genetic manipulation ensure that mice are usually the first point of call when developing transgenic mammalian models. To date at least 14 different CF-mouse models have been reported, with differing CFTR mutations and genetic backgrounds available [37]. Despite this impressive selection of models at hand, numerous issues have plagued the use of mice for studying CF-associated microbial infections. The biggest issue seems to arise from differences in the spatial structure of murine airways and an inability to spontaneously develop airway infection [33], even with CF-mice demonstrating impaired mucociliary clearance. The CFTR protein is known to play a key role in innate lung immunity and several studies have since been undertaken to determine why even the ‘ β -NaEC’ mouse [38] and other backgrounds lacking residual CFTR expression fail to develop infection [39,40].

Lack of an existing microbial community could be considered a ‘clean-slate’ for inoculating CF-mice with polymicrobial communities derived from patients. However, the introduction of pathogens into these mice leads to rapid microbial clearance [41], and repeat infections cause death [42]. Infection timescales using murine hosts can be considered semi-chronic at best, with successful infection (when achieved) typically lasting no more than a few days and reliant upon immobilizing the bacteria (PA) within agarose/alginate/agar beads that are directly instilled into the lung [41–50]. Using specific hypermucoid strains (e.g., NH57388A) it has been possible to maintain strain specific PA infections of up to 3 months within a host that bears the hallmarks of chronic CF infection [44,50]. An alternative inoculation approach that avoids the mechanical immobilization of microbial species and attempts to better represent a natural route of infection is the intranasal inoculation of mouse models. A persistent infection lasting 28 days could be established in non-CF mice following the respiratory inhalation of the transmissible Liverpool epidemic strain (LES) of PA [51]. Bacteria were found to be harbored in the nasopharynx throughout the experiment, and no PA could be detected in the lungs even by day 14. However, on day 28, PA could once again be isolated at low levels from the lung (26 CF per lung). These findings demonstrate that persistence in the nasopharynx allows reseeded of the lower airways and support the hypothesis that the upper respiratory tract provides a ‘silent reservoir’ able to harbor CF-associated species that can then be aspirated in to the lungs of CF patients. It would certainly be interesting to compare how a CF-mouse model responds to the respiratory inhalation route of infection and if multiple microbial species could be maintained within the nasopharynx. The intranasal inoculation of PA isolates recovered longitudinally over the course of a patient’s life into CF-mice revealed that only late-stage ‘CF-adapted’ isolates could establish persistent infection [45,49]. It has also been suggested that older CF-mice may be more predisposed to microbial infection, but little work has been carried out to determine if such mice have an expanded range of infective capabilities [47,52].

Co-infection studies have been trialed in recent years, but again these have been limited to an acute infection timescale (often just 18 h) until the clearance of non-PA species occurs. Importantly, these studies have revealed that co-infection of PA with *S. aureus* or *Burkholderia cenocepacia* enhances the murine immune response and upregulates virulence factor production in the lungs [43,48,53]. Furthermore, *in vivo* coinfection studies of PA and *S. aureus* found that ‘late-stage’ PA isolates had undergone phenotypic adaptation associated with enhanced persistence in the CF lung, and demonstrated a reduced capacity to outcompete *S. aureus* during co-culture [48]. Interestingly, immobilizing *B. cenocepacia* in PA-derived alginate caused increased microbial persistence, inflammation and mortality rates [46]. Such studies provide clear evidence that interspecies interactions drive modulations in microbial lifestyles, and that these changes have a major impact upon disease severity.

Mouse infection models aim to provide an insight into the mechanisms underlying host-responses to infection but are severely limited by the small subset of PA isolates proven to be able to establish an infection once physically immobilized. Further research is required into how CF mice rapidly clear airway infections; this may lead to the generation of novel transgenic models with an improved propensity for sustaining mixed species infections. Until this is achieved, CF mice need to be considered with caution as models for polymicrobial CF infection. The impact of this is that researchers need to consider critically the impact that other members within a mixed community have on driving PA adaptation and host-immune responses in these systems, due to concerns regarding the physiological relevance of the model.

The inability of CF mice to spontaneously develop lung disease comparable to that observed in human patients led researchers to develop CF models within larger mammals that share a higher degree of airway similarity with humans. CF models have now been reported in ferrets [54–56], pigs [57–60] and more recently sheep [61], all with

higher levels of CFTR homology with the human gene (92, 91 and 91% respectively, and in contrast to just 78% in mice). Crucially, these larger mammals do develop spontaneous airway infections, demonstrating a reliance on functioning CFTR protein for effective airway clearance. Despite their apparent predisposition for microbial infection, these models are not without limitations and multiple issues hamper their use in studying polymicrobial CF-associated infections.

Soon after birth, CF ferrets develop spontaneous bacterial infection and severe lung pathologies mirroring those observed in humans. Examination of BALF established that members of the *Streptococcus*, *Staphylococcus*, *Enterococcus* and *Pseudomonas* genera were present at low levels and could not be eradicated from the airways [53–55]. This presence of a diverse airway microbiota suggests CF ferrets are permissive for microbial colonization, yet they are limited in their suitability for the inoculation of human-derived polymicrobial communities. Abnormal inflammation is believed to begin *in utero*, before being excessively amplified upon bacterial exposure at birth [55]. Single-species intratracheal microbial challenges with PA and *B. cenocepacia* in CF ferrets led to a hyperinflammatory response from the host macrophages and increased mortality rates [40], supporting the notion of bacterially driven immune modulation. The extreme severity of bacteria-associated lung pathologies result in neonatal CF ferrets relying on antimicrobial therapy to survive weaning [62], limiting their use in studying chronic infection. No studies have challenged a ferret model with a microbial co-culture, although given the spontaneous development of neonatal infection, it may be possible to develop acute infection models with polymicrobial communities derived from CF patients. It would be interesting to compare whether there are any similarities between the hyperinflammatory response(s) observed in CF ferrets with those observed during APEs in CF patients. In this regard, the acute ferret infection model could potentially provide a physiologically relevant framework for understanding better the mechanisms of host-microbe responses leading up to APEs.

Gut-corrected, humanized CF pig models provide an *in vivo* system that parallels human CF lung pathophysiology remarkably well. CF pigs develop spontaneous airway infections with diverse and varied microbial populations a few months after birth, and fail to eradicate bacteria as effectively as wild-type pigs [57–60]. The microbiota of older CF pigs mostly resembles that of adolescent human patients, with *S. aureus* being the most commonly isolated pathogen [20,57,59]. Infection studies have not yet been carried out on CF pigs, although introducing PA isolates into the established microbial population *in vivo* would provide unique insight into how this key CF pathogen initially adapts within the CF airways. Alternatively, a polymicrobial community derived from CF patients could be introduced into CF pigs to examine the host-microbe response and interspecies interactions that occur within an environment that is close to being physiologically representative of the human CF lung. However, the high costs and requirement for specialized expertise and dedicated lab space for conducting research using porcine models has restricted experimental sample size, widespread uptake, and length of studies; more so than many other *in vivo* models.

Plant & invertebrate infection models

With key differences in physiology being apparent between plants/invertebrates and the human airways, the use of such hosts cannot (strictly speaking) be considered CF-infection models. However, their low cost, basic equipment requirements and minimal technical skill requirements, as well as a lack of ethical concerns, means such models provide a highly attractive, high-throughput approach to screen mutant libraries for genes essential for virulence and growth *in vivo*.

Limited similarities exist between the immune response of mammals and such simple host systems, yet they do enable some insights into the host-response to infection. How closely invertebrates approximate mammalian models is still cause for debate. These models are primarily limited by which microbial species have the capability to establish an infection, and there is little chemical or spatial similarity in the infection environment compared with human hosts. The small size of invertebrate models means very low microbial inoculums are rapidly fatal [63] and ensures that in general only acute, single-species infection studies can be readily undertaken. Mutant knockout libraries of 'rare' or less abundant CF-associated microbial species simply do not currently exist, and cannot be subject to systematic screens or included within co-infection studies, in spite of the likely role(s) played by these species in modulating pathogenesis during CF infection. The result of library screens using plant and insect hosts must be viewed with caution as essential genes for infection within mammalian models may have been missed, yet such high-throughput screens are certainly useful in the identification of potential virulence genes that can be further characterized *in vitro* or in larger *in vivo* model systems.

Multiple plant-based infection assays have been reported, including: *Arabidopsis thaliana* [63], lettuce stems [64] and mung bean seedlings [65]. With a limited range of human pathogens able to establish infections within these models, the majority of studies simply focus on PA isolates and mutants. Infection assays often compare the extent of destruction within stem or leaf infiltration assays or compare the growth of seedlings infected with wild-type or mutant strains, enabling a rough quantitative measure of the contribution that specific genes have toward causing virulence *in vivo*. However, as several mutants can be introduced into the same model, for example, multiple mutant strains inoculated within a single lettuce stem [64], plants provide an extremely rapid fitness screening system for a limited number of microbial species.

Caenorhabditis elegans is a very well-characterized, well-established laboratory model organism and is susceptible to infection by a range of both bacterial and fungal species [66,67], including some that have been isolated from the CF-lung and are associated with worsened patient prognosis. Microbial species are introduced as a top lawn or bacterial suspension containing the nematodes during feeding, limiting infection studies to species that can be successfully cultivated *in vitro*. In order to establish a co-culture within *C. elegans* both species must first be successfully grown together without one outcompeting the other and is something which may not be possible for the polymicrobial communities associated with CF. Vega and Gore (2017) describe the successful co-culture of two members of the Enterobacteriaceae in *C. elegans* [68]. However, they also report the dominance of one species over the other within the intestine during 'slow colonization' further demonstrating the limitation of nematodes as a vehicle for maintaining both the rare and the dominant microbial species associated with CF. When grown on nutrient-rich media, PA isolates cause 'fast-killing' of nematodes due to the production of hydrogen cyanide and phenazine compounds [69], yet when grown on minimal media PA replicated within the digestive tract to cause 'slow-killing' [70]. Such results demonstrate that nematodes are susceptible to death from secreted metabolites and that the growth media used in the screening of mutant libraries must be carefully considered.

Galleria mellonella (waxmoth larvae) are an alternative invertebrate model used for studying key CF-pathogens. Although waxmoths are infected by a limited range of pathogens, they are susceptible to infection from PA and some fungal species associated with the CF-airway [71]. Comparative studies have established that the waxmoth infection model shows good correlation of antimicrobial efficacy, pharmacokinetics [72] and essential virulence requirements with mouse models [70], suggesting this system is more representative of mammalian infection than the plant or nematode models. However, waxmoths are extremely susceptible to infection, with as little as ten bacterial cells being fatal, thus limiting use of this model to acute single-species infection only. This notwithstanding, serial passage of microbial populations through waxmoths could be used to represent a more chronic infection, and reports suggest the phenotypic adaptation of PA isolates does reflect limited elements of evolution within the CF airways [73].

Drosophila melanogaster presents the most plausible invertebrate model for studying polymicrobial infections. Not only are there a large number of genetic tools available for the generation of mutant flies (enabling detailed genetic dissection of host-microbe interactions occurring during infection), but successful *S. aureus*-PA coinfection models have been reported [31,74]. These studies build upon previously described single-species feeding models which demonstrate that bacteria replicate within the fly-crop and cause host mortality. Using this invertebrate co-infection model it was found that PA can sense peptidoglycan shed from the walls of Gram-positive species, triggering an enhancement in toxin and antimicrobial production [31]. This not only causes a 1000-fold decrease in the Gram-positive flora, it also enhanced host mortality. A mutant PA strain, PA601, which lacks the peptidoglycan receptor, did not increase mortality rates upon co-infection with *S. aureus*, and these results were verified using a murine infection model [75]. Such co-infection studies not only provide strong evidence for the need to understand interspecies interactions in a suitable host model, but also provide clear insights into the mechanisms underpinning these. The *Drosophila* model also relies on feeding bacteria to the host, again severely limiting which species can be studied and preventing this model from being utilized for inoculation with patient-derived polymicrobial samples.

As with all infection studies, it can be difficult to pinpoint which of the multifarious biological interactions that occur within a host model are crucial for driving changes in human disease severity. A reductionist approach could be taken to systematically screen mutant libraries within an invertebrate co-infection model to identify key genes for subsequent study in more advanced model systems. *In vivo* models provide a system for studying host-microbe interactions, but they are ill-suited to analyse interspecies microbe-microbe interactions. This is because the added complexity of an immune response strongly limits the likelihood of sustaining a polymicrobial model mimicking the chronic infections often associated with CF patients. With emerging evidence suggesting that co-infection

drives changes in microbial lifestyles, that in turn impact upon disease severity, models that enable the real-time tracking of microbial populations are urgently required.

***In vitro* & ex vivo models of CF-infection**

Emerging evidence suggests that chemical, not spatio-temporal, challenges have the greatest impact on driving changes in microbial lifestyles [76,77]. Inherent natural variation between *in vivo* models leads to local variations in the chemical environment and immune responses, adding an additional layer of variability. There is clear need for a robust and reproducible model recapitulating a physiologically relevant environment that allows the chemical and genetic changes within a mixed population to be dissected. *In vitro* models present a defined and easily perturbable environment, that can potentially provide simple, tractable and high-throughput systems for studying mixed species populations derived from CF patient sputa. The real-time tracking of a model microbial population would allow a number of fundamental biological questions to be addressed, making it possible to identify novel therapeutic avenues that might be missed in *in vivo* infection models.

A number of microbial species associated with CF-airway infections are known to have a narrow host-range of infection, for example, *Haemophilus influenza* does not infect nonhuman hosts. Therefore, it may be impossible to develop certain *in vivo* polymicrobial infection models. Conversely, several species have been identified in *in vivo* CF-models that are not known to infect humans, adding an extra layer of complexity when trying to recapitulate human infection-associated microbial consortia *in vivo*. Rearing animal models under gnotobiotic conditions can potentially reduce the presence of animal-specific species, although this does add significantly to the cost of maintaining the model.

A combination of targeted and untargeted culture-independent molecular approaches can be used to follow the composition of a polymicrobial community over time in an *in vitro* infection model. Culture-independent molecular analyses allow the influence of less abundant and hard-to-isolate species to be tracked effectively within models representative of chronic infections. The utility of untargeted molecular approaches, such as sequencing the hypervariable 16S rDNA and ITS regions of bacteria and fungi (respectively), has been reviewed by Rogers *et al.* [21]. Moreover, the development of revolutionary, high-throughput and sensitive targeted gene assays such as the NanoString nCounter system allows the expression of up to 800 different genes to be studied in a single reaction [78]. Utilizing probes designed against known 16S rDNA and ITS regions alongside key virulence genes has allowed accurate determination of the microbial consortium associated with CF-sputum samples [79], alongside tracking the composition and transcriptome profiles of complex, mock microbial communities [80]. Probes targeting mRNA molecules provide a more sensitive indication of the metabolically active members of a community, identifying the key drivers that potentially influence community adaptation and responses to environmental challenges.

Artificial sputum medium (ASM) or synthetic cystic fibrosis sputum (SCFM), is a highly defined synthetic growth medium that closely mimics the nutritional composition of sputum found in the CF-airway [76,81–85]. Comparison of the essential genome of PA isolates following growth in patient-derived sputum or ASM found virtually no difference between the two [83], providing compelling evidence that ASM is a physiologically relevant *in vitro* culture medium to support the growth of CF isolates. This notwithstanding, Cornforth *et al.* recently showed that machine learning approaches can discriminate PA grown *in vivo* from PA grown *in vitro* in ASM based on transcriptional profiling. However, little account was taken in that study of possible differences in the *in vivo/in vitro* transcriptome data arising from the presence of less abundant non-PA species in the human samples [86].

ASM induces PA to grow as microcolonies closely associated with the mucin, strongly resembling the growth observed in CF-sputum [81]. However, numerous modified recipes for ASM have been proposed, each of which is associated with distinct changes in microbial growth phenotype [82,87], thus demonstrating the need to standardise this complex media to ensure reliability and reproducibility between *in vitro* experiments. *In vitro* models allow facile experimental tuning of growth conditions to mimic different disease states; something that is simply not possible using *in vivo* models. Using ASM, the long-term maintenance of both PA and *S. aureus* in mixed species biofilms has been made possible [84], something previously not attainable using conventional laboratory media [88] despite the co-isolation of both species from the airways of ~31% of CF-patients [89]. Although no published studies have yet attempted the cultivation of a CF-associated polymicrobial community within ASM, similarities in nutrient availability allow us to postulate that in these conditions, the microbiota might be experimentally maintained *in vitro*. Direct inoculation of the 'complete' microbial community contained within sputum samples would permit inter-species cross-feeding to occur between cohabiting organisms. This may permit the growth of fastidious and auxotrophic strains known to be associated with the CF-airways [90].

In addition to the ease with which *in vitro* models can be experimentally perturbed, such systems are free from the temporal limitations imposed by animal infection studies. Longitudinal sampling of an *in vitro* model inoculated with a diverse polymicrobial community would reveal the chain of evolutionary events preceding the latest sampling point, essentially allowing a direct experimental analysis of Gould's speculations about 'rewinding the tape of evolution'. Whether parallel, identically inoculated multi-species populations that are subject to the same (intensely competitive) selection pressures can demonstrably follow the same independent evolutionary trajectory becomes an experimentally tractable problem. Such studies that examine compositional and genetic changes within communities can also be supported with chemical analyses to link how these changes affect the chemical environment of the airways. A novel Winogradsky-based culture model (WinCF) using a number of different chemical indicators has been used to monitor the growth of sputum samples in ASM. The study revealed a 2 unit reduction in the pH and 30% increase in gas production due to the increased abundance of fermentative anaerobes present in the sputum prior to the onset of APEs [76]. We also note that sequential sampling the secretome of a polymicrobial community is possible within an *in vitro* model, allowing a direct analysis of the impact of inter-species interactions on virulence factor secretion.

Introducing sputum samples taken from disease states within the same CF patient, in other words, before, during and after APEs, into an *in vitro* system would allow differences in the polymicrobial composition to be studied and could shed light into how subtle differences within these complex communities contribute to a decline in lung function. Sousa *et al.* utilized ASM to develop a long-term (10 days) *in vitro* culture system mimicking the physiological conditions of the airways to determine how clinically used antibiotics affected the phenotypic diversification of PA isolates [85]. That study found that sub-inhibitory concentrations of ciprofloxacin drove diversification in CF isolates but not in laboratory reference strains. Similar studies using polymicrobial cocultures could be undertaken to examine how therapeutic intervention drives phenotypic changes within the total microbial consortium associated with CF airways.

New species or strain variants, including 'keystone' CF pathogens such as PA, could be introduced into an established steady-state *in vitro* polymicrobial community to simulate the events following initial introduction of such variants in the patient airways. Such events are very difficult indeed to capture through direct analysis of patient sputa. Furthermore, such an *in vitro* model provides the unparalleled opportunity to study the genetic and phenotypic changes that occur in both the 'invading' species and in the endogenous polymicrobial population. Similarly, hypermutator strains, for example, *mutS* mutants [91], could be introduced into CF derived polymicrobial populations to examine the impact of what happens to all the species present when one of them is allowed to 'step on the evolutionary gas pedal'. A knowledge of the order of succession of major CF pathogens in a polymicrobial community may reveal clinically relevant insights into the types of interspecies signaling pathways involved in maintaining stable community architectures [92].

Biofilm formation may be the biggest contributor toward enhancing infection persistence, decreasing antimicrobial susceptibility, and elevating mutation rates within the CF airways [26,29,84,93–96]. Unsurprisingly the formation of biofilms has been extensively studied *in vitro*, with a focus in recent years on moving away from mono-species biofilms in favor of co-cultures more representative of real infection scenarios [53,77,84,94–98]. Using mixed-species biofilm models it has been found that species co-isolated from the CF lung can either increase or decrease the antimicrobial susceptibility [77,95] and the production of biomass [52,84,95] by other species present, and that strain variants provide cross-protection against different host-generated antimicrobials [98]. Furthermore, *in vitro* co-cultures of PA–*S. aureus* biofilms show that the mutation rates within these species can be increased up to 500-fold, and that *S. aureus* adopts a drastically different growth phenotype reminiscent of isolates recovered directly from the CF lung. To date, there is only one report in which a polymicrobial biofilm derived from CF sputum has been reconstituted *in vitro* [99]. That study focused on how antimicrobials affect the population, and growth conditions were not optimized to represent the physiology in the CF airway. By more closely recapitulating the CF-associated chemical environment, it may be possible to maintain polymicrobial biofilms more representative of those residing in the airways of CF patients.

One major limitation of *in vitro* models is the lack of spatial organization closely resembling that of a host, and which is provided to some degree in *in vivo* infection models. To overcome this deficiency of *in vitro* model systems, an *ex vivo* infection model has recently been developed [100] to provide a tractable and high-throughput system that can be easily used to mimic the airway architecture within a laboratory environment. Using porcine lungs, a waste by-product of the food industry, and ASM, this *ex vivo* model provides an effective and ethical solution to introducing spatial organization into longitudinal culture studies. Furthermore, different sections of lung tissue can

be used to mimic either upper or lower respiratory tract infections [101]. So far only PA isolates have been cultured within this model and these results demonstrate that *ex vivo* models are an effective experimental approach to study CF infection. It would be fascinating to introduce the polymicrobial community derived from CF sputum into an *ex vivo* model and assess how this shapes the trajectory of, for example, PA evolution.

Perhaps the largest barrier to the use of *in vitro* polymicrobial infection models is a lack of host cells that likely play a role in influencing the composition and behavior of the microbial consortium. *In vitro* models will prove crucial for the study of microbe-microbe interactions and will effectively reveal information about how species are able to interact with one another. *In vivo* models on the other hand are not as well suited to study interspecies interactions, nor are they as experimentally reproducible or tractable. They do (however) allow a more direct insight into how hosts respond to infection. A combination of both *in vitro* and *in vivo* polymicrobial models would allow for changes in microbial populations and in the chemical environment to be correlated with host responses.

Human cell-culture infection models provide an alternative approach to introduce elements of the host response into *in vitro* studies, and in the future, may allow more direct investigation of human-microbe interactions. Such *in vitro* cell culture infection models have already been successfully used to study a monolayer of human bronchiole epithelial cells homozygous for the $\Delta F508$ CFTR mutation infected with a co-culture of *S. aureus* and PA [102]. It was found that PA decreases the viability of *S. aureus* and causes the species to adopt fermentative metabolic pathways. These results strongly correlate with changes reported to occur prior to the onset of APEs, and provide clear evidence that this type of *in vitro* infection model may effectively represent the CF airway environment. Advances in cell culture procedures and gene editing tools mean that it may soon be feasible to routinely culture cell lines derived directly from individual CF patients [103], which could, in turn, be infected with polymicrobial populations gathered from the sputum of the same patient. The generation of such 'personalized infection models' would allow an unparalleled advantage over the use of 'generic' cell-lines and *in vitro* models to study microbial populations, allowing a more efficacious testing of antimicrobial action prior to treatment, bridging the 'bench-to-bedside' gap.

***In silico* polymicrobial models**

The study of polymicrobial communities is not simply confined to 'the wet lab'. With our understanding of microbial metabolic pathways being continually refined, new, more accurate *in silico* modeling of polymicrobial communities is becoming readily available. Advancements in the semi-curation of complex microbial communities, using software such as ModelSeed and AGORA, have led to the metabolic modeling of CF-associated bacterial communities from published 16S rDNA data [104]. With better formulation for ensuring host-derived metabolite balance across the community (through use of SteadyCom software), sample-specific heterogeneous communities can be generated that accurately predict which CF-pathogens come to dominate a polymicrobial community. *In silico* models are becoming a highly valued tool to derive metabolic inferences that may be difficult to obtain or observe experimentally and provide a theoretical framework for interpreting *in vitro* studies.

Computational predictive models are limited by the type and quality of data gathered from experimental studies. This means that they poorly predict the rare and hard to cultivate microbial species present within CF-associated microbial communities. Additionally, strain variants and evolutionary 'cheats' cannot yet be accounted for within *in silico* models, meaning that these models do not predict or incorporate phenotypic adaptation among the species present. Similarly, the striking spatial heterogeneity reported within the airways of CF patients is not easily captured in *in silico* models. Despite these limitations, *in silico* models do provide a useful framework for further experimental analyses, informing on experimental design and interpretation.

Conclusion & future perspective

Culture-independent examination of sputum samples expectorated from CF patients have revealed that a diverse and varied microbial population (including bacteria and fungi) is associated with the airways of CF patients [14,15,18–22]. Increasing evidence suggests that interspecies interactions between members of this microbial consortium elicit mutual influence on the gene expression profile and metabolic pathways adopted by both pathogenic and typically nonpathogenic species. It is now clear that CF-associated infections must be considered as polymicrobial in nature, and that a better understanding of how microbial cross talk impacts upon the expression of virulence factors will be essential if we are to develop improved therapeutic interventions.

A lack of models enabling the stable, long-term cultivation of polymicrobial communities derived from CF patients, as well as some historical bias, has meant that until recently, most researchers focused their studies on the primary CF-associated pathogens, for example, PA and *S. aureus*, neglecting the impact of less abundant or more

fastidious species. The generation of such polymicrobial-infection models would be of enormous benefit to the research community, allowing the physiologically representative response(s) of the whole microbial community to common therapeutic interventions to be more effectively monitored. Furthermore, the phenotypic adaptation and evolutionary events leading to dominance of key pathogens, or the onset of a decline in lung function could be picked apart and better understood. Through understanding how interspecies interactions and changes within a microbial population lead to a worsened disease status, it may be possible to identify novel or improved therapeutic interventions to help alleviate disease symptoms and improve the quality of life for CF patients.

Animal models of CF are paramount for studying the pathophysiological progression of the disease within mammalian systems. However, as discussed earlier, the closer these models come to mimicking the human disease, the more complex and experimentally costly they become. Improvements in CF pigs and the development of CF sheep likely present the best chance for the development of an effective animal-based infection model, yet a lack of experimental evidence within the literature makes it difficult to conclude whether this will ever be realized. The introduction of PA to the existing microbiota of CF pigs would certainly help to reveal if an *in vivo* polymicrobial infection model could be attained in principle.

In vitro models provide a feasible approach for the recapitulation of sputum-derived polymicrobial communities within the laboratory, especially given the development of ASM and *ex vivo* porcine lung models. *In vitro* models are cost-effective, lack ethical concerns (i.e., are 3Rs-compliant) and hopefully will allow for high-throughput, chronic models of infection to be easily set up without the need for specialized animal handling facilities. A highly defined, experimentally tuneable chemical environment and lack of host-to-host variability means *in vitro* models would provide the perfect system to identify subtle, but key, changes occurring in the community.

Over the course of the next decade we predict that a viable and physiologically representative *in vitro* polymicrobial models will be developed and see widespread uptake. Such models will hopefully allow the economical recapitulation of an entire CF-associated polymicrobial community in the laboratory environment. Key areas to be examined using such an experimental model would include: understanding how the introduction of PA to an established polymicrobial population influences changes in community architecture and the chemical environment (secretome, nutrient availability etc), how the microbial population responds to external stressors such as antimicrobial agents, identification of the signaling pathways driving key phenotypic adaptations, and so on. Following their successful development and implementation, such *in vitro* models may allow novel therapeutic avenues to be explored, potentially leading to an improvement in quality of life for CF patients and possibly other chronic respiratory diseases involving polymicrobial infection.

Financial & competing interests disclosure

We thank the National Centre for the Replacement, Refinement and Reduction of Animals in Research (NC3Rs) for funding this work (grant NC/P001564/1 to MW). Article processing charges were paid from the Medical Research Council contribution to the RCUK block grant to The University of Cambridge. This work was also supported by a Venture and Innovation Award (VIA) from the UK Cystic Fibrosis Trust and by the BLF Pump Primer Award from The British Lung Foundation. The authors have no other relevant affiliations or financial involvement with any organization or entity with a financial interest in or financial conflict with the subject matter or materials discussed in the manuscript apart from those disclosed.

No writing assistance was utilized in the production of this manuscript.

Executive summary

Cystic fibrosis is a polymicrobial disease

- Culture-independent profiling has revealed a diverse and varied polymicrobial community is associated with the cystic fibrosis (CF) airways.
- Members of this community interact with one another, causing modulations in gene expression that potentially impact upon disease severity.
- No models currently exist that permit the recapitulation of a true CF-associated polymicrobial community in the laboratory.

Murine models of CF

- CF mice are incapable of developing spontaneous airway infections and microbial challenges are rapidly cleared.
- Only *Pseudomonas aeruginosa* isolates immobilized within beads that are instilled into the lung allow a semi-chronic infection scenario to be established.
- Although mice provide limited insights into the host-response to infection, murine models are not suited for the development of polymicrobial infection models.

Ferret & pig models of CF

- Both CF ferrets and CF pigs develop spontaneous airway infection with a range of microbial species soon after birth.
- Infections in CF ferrets induce fatal, hyperinflammatory immune responses that severely limit their use for development as polymicrobial models.
- The airway microbiota of CF pigs most closely resembles that of adolescent human patients, although infection with *P. aeruginosa* has not been examined.
- Costs and complexity hinder the uptake of CF pig models, and as a result, little research has been undertaken into airway infections using this model.

Plant & invertebrate models of CF

- Plant and invertebrate models provide high-throughput platforms to screen mutant libraries for a limited range of genes required for *in vivo* growth and virulence.
- Plant and invertebrate models support the growth of only a limited spectrum of CF-associated microbial species.

In vitro polymicrobial models

- The development of *in vitro* polymicrobial models provides a cost-effective, tractable and robust system for studying subtle interspecies interactions.
- *In vitro* models potentially allow long-term, 'chronic infection' to be recapitulated.
- Artificial sputum media is a defined synthetic medium closely mimicking the nutritional composition of CF-derived sputum. artificial sputum media provides a physiologically relevant *in vitro* culture medium to permit the growth of CF-associated species.
- Using sections of porcine lungs, an *ex vivo* culture system has been developed that introduces a spatial structure similar to that of the CF-airway into *in vitro* models.

In silico polymicrobial models

- *In silico* models can be used to accurately recapitulate polymicrobial communities from published experimental data inputs, and can yield information that may be difficult to obtain experimentally, but can help to guide experimental design in *in vitro* and *in vivo* models.
- Such models are limited by the quality and quantity of data gathered from experimental studies and so poorly represent hard-to-cultivate microbial species. However, as more (and better) input data is gathered, *in silico* models will inevitably improve.

References

Papers of special note have been highlighted as: • of interest; •• of considerable interest

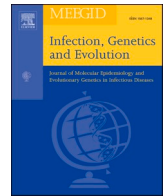
1. Cystic Fibrosis Foundation. www.cff.org
2. Knowles MR, Durie PR. What is cystic fibrosis? *N. Engl. J. Med.* 347(6), 439–442 (2002).
3. Cystic fibrosis mutation database. <http://www.genet.sickkids.on.20ca/cftr/>
4. Boucher RC. An overview of the pathogenesis of cystic fibrosis lung disease. *Adv. Drug. Deliv. Rev.* 54(11), 1359–1371 (2002).
5. Grasemann H, Ioannidis I, Tomkiewicz RP, de Groot H, Rubin BK, Ratjen F. Nitric oxide metabolites in cystic fibrosis lung disease. *Arch. Dis. Child.* 78(1), 49–53 (1998).
6. Jones KL, Hegab AH, Hillman BC *et al.* Elevation of nitrotyrosine and nitrate concentrations in cystic fibrosis sputum. *Pediatr. Pulmonol.* 30(2), 79–85 (2000).
7. Tate S, MacGregor G, Davis M, Innes JA, Greening AP. Airways in cystic fibrosis are acidified: detection by exhaled breath condensate. *Thorax* 57(11), 926–929 (2002).

8. Worlitzsch D, Tarran R, Ulrich M *et al.* Effects of reduced mucus oxygen concentration in airway *Pseudomonas* infections of cystic fibrosis patients. *J. Clin. Invest.* 109(3), 317–325 (2002).
9. Palmer KL, Aye LM, Whiteley M. Nutritional cues control *Pseudomonas aeruginosa* multicellular behavior in cystic fibrosis sputum. *J. Bacteriol.* 189(8), 8079–8087 (2007).
10. Ghio AJ, Roggli VL, Soukup JM, Richards JH, Randell SH, Muhlebach MS. Iron accumulates in the lavage and explanted lungs of cystic fibrosis patients. *J. Cyst. Fibros.* 12(4), 390–398 (2012).
11. Lyczak JB, Cannon CL, Pier GB. Lung infections associated with cystic fibrosis. *Clin. Microbiol. Rev.* 15(2), 194–222 (2002).
12. Rajan S, Saiman L. Pulmonary infections in patients with cystic fibrosis. *Semin. Respir. Infect.* 17(1), 47–56 (2002).
13. Elborn JS. Cystic fibrosis. *Lancet* 388(10059), 2519–2531 (2016).
14. Carmody LA, Zhao J, Schloss PD *et al.* Changes in cystic fibrosis airway microbiota at pulmonary exacerbation. *Ann. Am. Thorac. Soc.* 10(3), 179–187 (2013).
15. Carmody LA, Zhao J, Kalikin LM *et al.* The daily dynamics of cystic fibrosis airway microbiota during clinical stability and at exacerbation. *Microbiome* 3(12), doi:10.1186/s40168-015-0074-9 (2015).
16. Govan J, Nelson J. Microbiology of cystic fibrosis lung infections: themes and issues. *J. R. Soc. Med.* 86(Suppl. 20), 11–18 (1993).
17. Conrad D, Haynes M, Salamon P, Rainey PB, Youle M, Rohwer F. Cystic fibrosis therapy: a community ecology perspective. *Am. J. Respir. Cell. Mol. Biol.* 48(2), 105–156 (2012).
18. Zhao J, Schloss PD, Kalikin LM *et al.* Decade-long bacterial community dynamics in cystic fibrosis airways. *Proc. Natl Acad. Sci USA* 109(15), 5089–5814 (2012).
19. Boutin S, Graeber SY, Weitnauer M *et al.* Comparison of microbiomes from different niches of upper and lower airways in children and adolescents with cystic fibrosis. *PLoS ONE* 10(1), doi:10.1371/journal.pone.0116029 (2015).
20. Sibley CD, Parkins MD, Rabin HR, Duan K, Norgaard JC, Surette MG. A polymicrobial perspective of pulmonary infections exposes an enigmatic pathogen in cystic fibrosis patients. *Proc. Natl Acad. Sci. USA* 105(39), 15070–15075 (2008).
21. Rogers GB, Hoffman LR, Whiteley M, Daniels TW, Carroll MP, Bruce KD. Revealing the dynamics of polymicrobial infections: implications for antibiotic therapy. *Trends Microbiol.* 18(8), 357–364 (2010).
- **Reviews the utility of next-generation sequencing approaches for discerning the complexity of polymicrobial communities, using cystic fibrosis (CF) as a case study.**
22. Short FL, Murdoch SL, Ryan RP. Polymicrobial human disease: the ills of social networking. *Trends Microbiol.* 22(9), 508–516 (2014).
23. Jorth P, Ehsan Z, Rezayat A *et al.* Direct lung sampling indicates that established pathogens dominate early infections in children with cystic fibrosis. *Cell Press* 27(4), 1190–1204 (2019).
- **Provides direct counter evidence against the notion that the CF-airways contain a vastly diverse and dynamic array of microorganisms.**
24. Ibberson CB, Stacy A, Fleming D *et al.* Co-infecting microorganisms dramatically alter pathogen gene essentiality during polymicrobial infection. *Nat. Microbiol.* 2, 17079 (2017).
- **A paper crucial to demonstrating that a change in gene expression occurs when species are co-cultured together, here through coculturing *Pseudomonas aeruginosa* (PA) and *S. aureus* ~25% of the essential genome in *S. aureus* is converted to 'nonessential' when compared with a mono-culture.**
25. Hibbing ME, Fuqua C, Parsek MR, Peterson SB. Bacterial competition: surviving and thriving in the microbial jungle. *Nat. Rev. Microbiol.* 8(1), 15–25 (2010).
26. Elias S, Banin E. Multi-species biofilms: living with friendly neighbors. *FEMS. Microbiol. Rev.* 36(5), 990–1004 (2012).
27. Rogers GB, Carroll MP, Bruce KD. Studying bacterial infections through culture-independent approaches. *J. Med. Microbiol.* 58(11), 1401–1418 (2009).
28. Rogers GB, Stressmann FA, Walker AW, Carroll MP, Bruce KD. Lung infections in cystic fibrosis; deriving clinical insight from microbial complexity. *Exp. Rev. Mol. Diag.* 10(2), 187–196 (2010).
29. Leekha S, Terrell CL, Edson RS. General principles of antimicrobial therapy. *Mayo Clin. Proc.* 86(2), 156–167 (2011).
30. Quinn RA, Lim YW, Maughan H, Conrad D, Rohwer F, Whiteson KL. Biogeochemical forces shape the composition and physiology of polymicrobial communities in the cystic fibrosis lung. *MBio.* 5(2), e00956–13 (2014).
31. Korgaonkar A, Trivedi U, Rumbaugh KP, Whiteley M. Community surveillance enhances *Pseudomonas aeruginosa* virulence during polymicrobial infection. *Proc. Natl Acad. Sci. USA* 110(3), 1059–1064 (2013).
- **Demonstrates that PA is able to interact with other species present within the environment, in this case Gram-positive bacteria, this interaction then leads to alterations in the production of virulence factors thought to be active against both prokaryotic and eukaryotic organisms.**
32. Peters BM, Jabra-Rizk MA, O'May GA, Costerton JW, Shirtliff ME. Polymicrobial interactions: impact on pathogenesis and human disease. *Clin. Microbiol. Rev.* 25(1), 193–213 (2012).

33. Snouwaert JN, Brigman KK, Latour AM *et al.* An animal model for cystic fibrosis made by gene targeting. *Science*. 257(5073), 1083–1088 (1992).
34. Fisher JT, Zhang Y, Engelhardt JF. Comparative biology of cystic fibrosis animal models. *Meth. Mol. Biol.* 742, 311–334 (2011).
35. Rosen BH, Chanson M, Gawenis LR *et al.* Animal and model systems for studying cystic fibrosis. *J. Cyst. Fibros.* 17(2S), S28–S34 (2017).
36. Semaniakou A, Croll RP, Chappe V. Animal models in the pathophysiology of cystic fibrosis. *Front. Pharm.* 9(1475), doi:10.3389/fphar.2018.01475 (2019).
37. Guilbault C, Saeed Z, Downey GP, Radzioch D. Cystic fibrosis mouse models. *Am. J. Respir. Cell. Mol. Biol.* 36(1), 1–7 (2007).
38. Zhou Z, Duerr J, Johannesson B *et al.* The ENaC-overexpressing mouse as a model of cystic fibrosis lung disease. *J. Cyst. Fibros.* 10(S2), S172–S182 (2011).
39. Durie PR, Kent G, Phillips MJ, Ackerley CA. Characteristic multiorgan pathology of cystic fibrosis in a long-living cystic fibrosis transmembrane regulator knockout murine model. *Am. J. Pathol.* 164(4), 1481–14938 (2004).
40. Bruscia EM, Bonfield TL. Cystic fibrosis lung immunity: the role of the macrophage. *J. Innate. Immun.* 8(6), 550–563 (2016).
41. Cash HA, Woods DE, McCullough B, Johanson WG Jr, Bass JA. A rat model of chronic respiratory infection with *Pseudomonas aeruginosa*. *Am. Rev. Respir. Dis.* 119(3), 453–9 (1979).
42. Van Heeckeren AM, Schluchter MD, Xue W, Davis PB. Response to acute lung infection with mucoid *Pseudomonas aeruginosa* in cystic fibrosis. *Am. J. Respir. Crit. Care. Med.* 173(3), 288–96 (2006).
43. Duan K, Dammal C, Stein J, Rabin H, Surette MG. Modulation of *Pseudomonas aeruginosa* gene expression by host microflora through interspecies communication. *Mol. Microbiol.* 50(5), 1477–1491 (2003).
44. Hoffman N, Rasmussen TB, Jensen PØ *et al.* Novel mouse model of chronic *Pseudomonas aeruginosa* lung infection mimicking cystic fibrosis. *Infect. Imm.* 73(4), 2504–2514 (2005).
45. Moser C, Van Gennip M, Bjarnsholt T *et al.* Novel experimental *Pseudomonas aeruginosa* lung infection model mimicking long-term host-pathogen interactions in cystic fibrosis. *APMIS*. 117(2), 95–107 (2009).
46. Chattoraj SS, Murthy R, Ganesan S *et al.* *Pseudomonas aeruginosa* alginate promotes *Burkholderia cenocepacia* persistence in cystic fibrosis transmembrane conductance regulator knockout mice. *Infect. Immun.* 78(3), 984–993 (2010).
47. Munder A, Wölbeling F, Kerber-Momot T *et al.* Acute intratracheal *Pseudomonas aeruginosa* infection in cystic fibrosis mice is age dependent. *Respir. Res.* 12(148), doi:10.1186/1465-9921-12-148 (2011).
48. Baldan R, Cigana C, Testa F *et al.* Adaptation of *Pseudomonas aeruginosa* in cystic fibrosis airways influences virulence of *Staphylococcus aureus* *In vitro* and murine models of co-infection. *PLoS ONE* 9(3), e89614 (2014).
49. Cigana C, Loré NI, Riva C *et al.* Tracking the immunopathological response to *Pseudomonas aeruginosa* during respiratory infections. *Sci. Rep.* 6, 21465 (2015).
50. Bayes H, Ritchie N, Irvine S, Evans TJ. A murine model of early *Pseudomonas aeruginosa* lung disease with transition to chronic infection. *Sci. Rep.* 6, 35838 (2016).
51. Fothergill JL, Neill DR, Loman N, Winstanley C, Kadioglu A. *Pseudomonas aeruginosa* adaptation in the nasopharyngeal reservoir leads to migration and persistence in the lungs. *Nat Commun.* 5, 4780 (2014).
52. Teichgräber V, Ulrich M, Endlich N *et al.* Ceramide accumulation mediates inflammation, cell death and infection susceptibility in cystic fibrosis. *Nat Med.* 14(4), 382–391 (2008).
53. Bragonzi A, Farulla I, Paroni M *et al.* Modelling co-infection of the cystic fibrosis lung by *Pseudomonas aeruginosa* and *Burkholderia cenocepacia* reveals influences on biofilm formation and host response. *PLoS ONE* 7(12), e52330 (2012).
54. Sun X, Sui H, Fisher JT *et al.* Disease phenotype of a ferret CFTR-knockout model of cystic fibrosis. *J. Clin. Invest.* 120(9), 3149–3160 (2010).
55. Sun X, Olivier AK, Liang B *et al.* Lung phenotype of juvenile and adult cystic-fibrosis transmembrane conductance regulator-knockout ferrets. *Am. J. Respir. Cell. Mol. Biol.* 50(3), 502–512 (2014).
56. Keiser NW, Birket SE, Evans IA *et al.* Defective innate immunity and hyperinflammation in newborn cystic fibrosis transmembrane conductance regulator-knockout ferret lungs. *Am. J. Respir. Cell. Mol. Biol.* 52(6), 683–694 (2015).
57. Rogers CS, Stoltz DA, Meyerholz DK *et al.* Disruption of the CFTR gene produces a model of cystic fibrosis in newborn pigs. *Science*. 321(5897), 1837–1841 (2008).
58. Welsh MJ, Rogers CS, Stoltz DA, Meyerholz DK, Prather RS. Development of a porcine model of cystic fibrosis. *Trans. Am. Clin. Climatol. Assoc.* 120, 149–162 (2009).
59. Stoltz DA, Meyerholz DK, Pezzulo AA *et al.* Cystic fibrosis pigs develop lung disease and exhibit defective bacterial eradication at birth. *Sci. Transl. Med.* 2(29), 29ra31 (2010).
60. Wine JJ. The development of lung disease in cystic fibrosis pigs. *Sci. Transl. Med.* 2(29), 29s20 (2010).
61. Fan Z, Perisse IV, Cotton CU *et al.* A sheep model of cystic fibrosis generated by CRISPR/Cas9 disruption of the CFTR gene. *JCI insight*. 3(19), e123529 (2018).

62. Hoffman LR, Hajjar AM. Ferreting out the role of infection in cystic fibrosis lung disease. *Am. J. Respir. Crit. Care. Med.* 197(10), 1243–1244 (2018).
63. Rahme LG, Stevens EJ, Wolford SF, Shao J, Tompkins RG, Ausubel FM. Common virulence factors for bacterial pathogenicity in plants and animals. *Science*. 268(5219), 1899–1902 (1995).
64. Rahme LG, Tan MW, Le L *et al.* Use of plant hosts to identify *Pseudomonas aeruginosa* virulence factors. *Proc. Natl Acad. Sci. USA* 94(24), 13245–13250 (1997).
65. Garge S, Azimi S, Diggle SP. A simple mung bean infection model for studying the virulence of *Pseudomonas aeruginosa*. *Microbiology*. 164(5), 765–768 (2018).
66. Powell JR, Ausubel FM. Models of *Caenorhabditis elegans* infection by bacterial and fungal pathogens. *Meth. Mol. Biol.* 415, 403–427 (2008).
67. Marsh EK, May RC. *Caenorhabditis elegans* a model organism for investigating immunity. *Appl. Environ. Bio.* 78(7), 2075–2081 (2007).
68. Vega NM, Gore J. Stochastic assembly produces heterogenous communities in the *Caenorhabditis elegans* intestine. *PLoS Biol.* 15(3), e2000633 (2017).
69. Cezairliyan BO, Vinayavekhin N, Grenfell-Lee D, Yuen GJ, Saghatelian A, Ausubel FM. Identification of *Pseudomonas aeruginosa* phenazines that kill *Caenorhabditis elegans*. *PLoS Pathog.* 9, e1003101 (2013).
70. Tan MW, Mahajan-Miklos S, Ausubel FM. Killing of *Caenorhabditis elegans* by *Pseudomonas aeruginosa* used to model mammalian bacterial pathogenesis. *Proc. Natl Acad. Sci. USA* 96(2), 715–720 (1999).
71. Jander G, Rahme LG, Ausubel FM. Positive correlation between virulence of *Pseudomonas aeruginosa* mutants in mice and insects. *J. Bacteriol.* 182(13), 3843–3845 (2000).
72. Hill L. Evaluation of *Galleria mellonella* larvae for measuring efficacy and pharmacokinetics of antibiotic therapies against *Pseudomonas aeruginosa* infection. *Int. J. Antimicrob. Agents*. 43(3), 254–261 (2014).
73. Racey D, Inglis RF, Harrison F, Oliver A, Buckling A. The effect of elevated mutation rates on the evolution of cooperation and virulence of *Pseudomonas aeruginosa*. *Evolution* 64(2), 515–521 (2010).
74. Sibley CD, Duan K, Fischer C *et al.* Discerning the complexity of community interactions using a *Drosophila* model of polymicrobial infections. *PLoS Pathog.* 4(10), e1000184 (2008).
75. Lemaitre B. The road to Toll. *Nat Revs Immunol.* 4(7), 521–527 (2004).
76. Quinn RA, Whiteson K, Lim YW *et al.* A Winogradsky-based culture system shows an association between microbial fermentation and cystic fibrosis exacerbation. *ISME J.* 9(4), 1024–1038 (2015).
- **Provides experimental *in vitro* evidence that significant chemical changes may be occurring at the onset of acute pulmonary exacerbations and suggests that these events are driven by changes in the composition of the microbial population.**
77. Lopes SP, Azevedo NF, Pereira MO. Developing a model for cystic fibrosis sociomicrobiology based on antibiotic and environmental stress. *J. Med. Micro.* 307(8), 460–470 (2017).
78. Kulkarni MM. Digital multiplexed gene expression analysis using the NanoString nCounter system. *Curr. Protoc. Mol. Biol.* Chapter 25(Unit 25B.10), doi:10.1002/0471142727.mb25b10s94 (2011).
79. Grahl N, Dolben EL, Filkins LM *et al.* Profiling of bacterial and fungal microbial communities in cystic fibrosis sputum using RNA. *mSphere*. 3(4), e00292–18 (2018).
80. Cheng Y, Yam JKH, Cai Z. Population dynamics and transcriptomic responses of *Pseudomonas aeruginosa* in a complex laboratory microbial community. *NPJ Biofilms. Microbiomes* 5(1), doi:10.1038/s41522-018-0076-z (2019).
81. Sriramulu DD, Lünsdorf H, Lam JS, Römling U. Microcolony formation: a novel biofilm model of *Pseudomonas aeruginosa* for the cystic fibrosis lung. *J. Med. Microbiol.* 54(7), 667–676 (2005).
82. Haley CL, Colmer-Hamood JA, Hamood AN. Characterisation of biofilm-like structures formed by *Pseudomonas aeruginosa* in a synthetic mucus medium. *BMC. Microbiol.* 12(181), doi:10.1186/1471-2180-12-181. (2012).
83. Turner KH, Wessel AK, Palmer GC, Murray JL, Whiteley M. Essential genome of *Pseudomonas aeruginosa* in cystic fibrosis sputum. *Proc. Natl Acad. Sci. USA*. 12(13), 4110–4115 (2015).
- **The composition of a highly defined artificial sputum media (ASM) recipe is described, comparing the essential transcriptome of PA cultured within human derived sputum compared with this ASM found little difference in the essential gene expression-highlighting that this ASM may be particularly useful for culturing CF associated communities.**
84. Frapwell CJ, Howlin RP, Soren O *et al.* Increased rates of genomic mutation in a biofilm co-culture model of *P. aeruginosa* and *S. aureus*. *BioRxiv* doi:10.1101/387233 (2018).
85. Sousa AM, Monteiro R, Pereira MO. Unveiling the early events of *Pseudomonas aeruginosa* adaptation in cystic fibrosis airway environment using a long-term *in vitro* maintenance. *J. Med. Microbio.* 308(8), 1053–1064 (2018).
86. Cornforth DM, Dees JL, Ibberson CB *et al.* *Pseudomonas aeruginosa* transcriptome during human infection. *Proc. Natl Acad. Sci. USA* 115(22), E5125–E5134 (2018).

87. Tata M, Wolfinger TM, Amman F *et al.* RNASeq based transcriptional profiling of *Pseudomonas aeruginosa* PA14 after short- and long-term anoxic cultivation in synthetic cystic fibrosis sputum medium. *PLoS ONE* 11(1), e0147811 (2016).
88. Nguyen AT, Oglesby-Sherrouse AG. Interactions between *Pseudomonas aeruginosa* and *Staphylococcus aureus* during co-cultivations and polymicrobial infections. *Appl. Microbiol. Biotechnol.* 100(14), 6141–6148 (2016).
89. Limoli DH, Yang J, Khansaheb MK *et al.* *Staphylococcus aureus* and *Pseudomonas aeruginosa* co-infection is associated with cystic fibrosis related diabetes and poor clinical outcomes. *Eur. J. Clin. Microbiol. Infect. Dis.* 35(6), 947–953 (2016).
90. Barth AL, Pitt TL. Auxotrophic Variants of *Pseudomonas aeruginosa* are selected from prototrophic wild-type strains in respiratory infections in patients with cystic fibrosis. *J. Clin. Microbiol.* 33(1), 37–40 (1995).
91. Weigand MR, Sundin GW. General and inducible hypermutation facilitate parallel adaptation in *Pseudomonas aeruginosa* despite divergent mutation spectra. *Proc. Natl Acad. Sci. USA* 109(34), 13680–13685 (2012).
92. Defoirdt T, Brackman G, Coenye T. Quorum sensing inhibitors: how strong is the evidence? *Trends. Microbiol.* 21(12), 619–624 (2013).
93. Bjarnsholt T, Jensen PØ, Fiandaca MJ *et al.* *Pseudomonas aeruginosa* biofilms in the respiratory tract of cystic fibrosis patients. *Pediatr. Pulmonol.* 44(6), 547–558 (2009).
94. Lopes SP, Ceri H, Azevedo NF, Pereira MO. Antibiotic resistance of mixed biofilms in cystic fibrosis: impact of emerging microorganisms on treatment of infection. *Int. J. Antimicrob. Agents.* 40(3), 260–263 (2012).
95. Magalhães AP, Lopes SP, Pereira MO. Insights into cystic fibrosis polymicrobial consortia: the role of species interactions in biofilm development, phenotype, and response to in-use antibiotics. *Front Microbiol.* 7(2146), doi:10.3389/fmicb.2016.02146 (2017).
96. Makovcova J, Babak V, Kulich P, Masek J, Slany M, Cincaro L. Dynamics of mono- and dual-species biofilm formation and interactions between *Staphylococcus aureus* and Gram-negative bacteria. *Microb. Biotechnol.* 10(4), 819–832 (2017).
97. Malhotra S, Limoli DH, English AE, Parsek MR, Wozniak DJ. Mixed communities of mucoid and non-mucoid *Pseudomonas aeruginosa* exhibit enhanced resistance to host antimicrobials. *MBio* 9(2), e00275–18 (2018).
98. Woods PW, Haynes ZM, Mina EG, Marques CNH. Maintenance of *S. aureus* in co-culture with *P. aeruginosa* while growing as biofilms. *Front. Microbiol.* 9(3291), doi:10.3389/fmicb.2018.03291 (2019).
99. Spasenovski T, Carroll MP, Lilley AK, Payne MS, Bruce KD. Modelling the bacterial community associated with cystic fibrosis lung infections. *Eur. J. Clin. Microbiol. Infect. Dis.* 29(3), 319–328 (2010).
100. Harrison F, Muruli A, Higgins S, Diggle SP. Development of an ex vivo porcine lung model for studying growth, virulence, and signalling of *Pseudomonas aeruginosa*. *Infect. Immun.* 82(8), 3312–3323 (2014).
101. Harrison F, Diggle SP. An ex vivo lung model to study bronchioles infected with *Pseudomonas aeruginosa* biofilms. *Microbiology* 162(10), 1755–1760 (2016).
102. Filkins LM, Graber JA, Olson DG *et al.* Coculture of *Staphylococcus aureus* with *Pseudomonas aeruginosa* drives *S. aureus* towards fermentative metabolism and reduced viability in a cystic fibrosis model. *J. Bacteriol.* 197(14), 2252–2264 (2015).
103. Mou H, Brazauskas K, Rajagopal J. Personalized medicine for cystic fibrosis: establishing human model systems. *Pediatr. Pulmonol.* 50(S40), S14–23 (2015).
104. Henson MA, Orazi G, Phalak P, O'Toole GA. Metabolic modeling of cystic fibrosis airway communities predicts mechanisms of pathogen dominance. *mSystems*. 4(2), e00026–e00019 (2019).



Research paper

Virulence and antimicrobial resistance genes are enriched in the plasmidome of clinical *Escherichia coli* isolates compared with wastewater isolates from western Kenya

Sifuna Anthony Wawire^a, Oleg N. Reva^b, Thomas J. O'Brien^c, Wendy Figueroa^c, Victor Dinda^d, William A. Shivoga^e, Martin Welch^{c,*}

^a Department of Biochemistry, Masinde Muliro University of Science and Technology, P.O. Box 190, 50100 Kakamega, Kenya

^b Centre for Bioinformatics and Computational Biology, Dep. of Biochemistry, Genetics and Microbiology, University of Pretoria, Lynnwood Rd, Hillcrest, Pretoria 0002, South Africa

^c Department of Biochemistry, University of Cambridge, Hopkins Building, Tennis Court Road, Cambridge CB21QW, United Kingdom

^d Department of Medical Laboratory Science, Masinde Muliro University of Science and Technology, P.O. Box 190, 50100 Kakamega, Kenya

^e Department of Biological Sciences, Masinde Muliro University of Science and Technology, P.O. Box 190, 50100 Kakamega, Kenya

ARTICLE INFO

Keywords:

Escherichia coli

Genomics

Antimicrobial resistance

Virulence

Plasmid

Genomic islands

ABSTRACT

Many low-middle income countries in Africa have poorly-developed infectious disease monitoring systems. Here, we employed whole genome sequencing (WGS) to investigate the presence/absence of antimicrobial resistance (AMR) and virulence-associated (VA) genes in a collection of clinical and municipal wastewater *Escherichia coli* isolates from Kakamega, west Kenya. We were particularly interested to see whether, given the association between infection and water quality, the isolates from these geographically-linked environments might display similar genomic signatures. Phylogenetic analysis based on the core genes common to all of the isolates revealed two broad divisions, corresponding to the commensal/enterotoxigenic *E. coli* on the one hand, and uropathogenic *E. coli* on the other. Although the clinical and wastewater isolates each contained a very similar mean number of antibiotic resistance-encoding genes, the clinical isolates were enriched in genes required for in-host survival. Furthermore, and although the chromosomally encoded repertoire of these genes was similar in all sequenced isolates, the genetic composition of the plasmids from clinical and wastewater *E. coli* was more habitat-specific, with the clinical isolate plasmidome enriched in AMR and VA genes. Intriguingly, the plasmid-borne VA genes were often duplicates of genes already present on the chromosome, whereas the plasmid-borne AMR determinants were more specific. This reinforces the notion that plasmids are a primary means by which infection-related AMR and VA-associated genes are acquired and disseminated among these strains.

1. Introduction

Intestinal pathogenic *Escherichia coli* are the leading bacterial cause of diarrheal infection in low-middle income countries (LMICs) (Jafari et al., 2012). This situation is complicated by poorly-developed infectious disease monitoring programs, especially with regards to antimicrobial resistance (AMR) and pathogen surveillance (Vernet et al., 2014). In many LMICs, the lack of high-quality data frequently leads to inadequate treatment guidelines and poor infection management. One potentially transformative technology that could help improve pathogen surveillance programs in developing countries is whole genome sequencing (WGS) achieved through next generation sequencing (NGS)

technologies. When coupled with epidemiological and environmental investigations, WGS can deliver ultimate resolution for detecting and analysing transmission routes and in tracing the source(s) of epidemics and outbreaks (Cao et al., 2017; Besser et al., 2018; Rantsiou et al., 2018). In addition, WGS offers the unrivalled opportunity to monitor the gene content of microbial virulence determinants in isolates, and to map the spread of antimicrobial drug resistance determinants (European Centre for Disease Prevention and Control, 2018). The technology is also particularly good at identifying mobile genetic elements such as plasmids, transposons and integrons, which are increasingly recognized as playing a key role in disseminating AMR and virulence determinants (Bezuidt et al., 2009).

* Corresponding author at: Department of Biochemistry, University of Cambridge, Hopkins Building, Tennis Court Road, Cambridge CB21QW, United Kingdom.
E-mail address: mw240@cam.ac.uk (M. Welch).

<https://doi.org/10.1016/j.meegid.2021.104784>

Received 1 October 2020; Received in revised form 23 February 2021; Accepted 24 February 2021

Available online 27 February 2021

1567-1348/© 2021 Published by Elsevier B.V.

In the current study, we employed WGS to monitor the genetic structure of *E. coli* recovered from patients visiting a referral health facility and from a nearby wastewater treatment plant in Kakamega, western Kenya. Previous studies have shown that the wastewater treatment sites in Kakamega are inefficient in controlling or removing pathogens from the water-supply system (Malaho et al., 2018). This inefficient wastewater treatment may therefore plausibly provide means by which multi-drug resistant and/or pathogenic *E. coli* are disseminated among the local populace. Phylogenetic relationships between the *E. coli* isolates associated with nosocomial infections and wastewater treatment sites were inferred, and multilocus sequence typing of the isolates was performed. This revealed over-representation of one particular sequence type (ST 43) in the wastewater and clinical isolates. We also paid particular attention to the relative distribution of virulence-associated (VA) genes and antimicrobial resistance (AMR) genes on mobile genetic elements. Various VA and AMR genes were found in genomic islands (GIs) and plasmids of the sequenced strains. However, whereas VA and AMR genes were distributed among the GIs in both clinical and wastewater isolates, there was a marked enrichment of these genes in the plasmid DNA borne by the clinical isolates. This suggests that plasmid-mediated horizontal gene transfer may play a key role in defining the pathogenicity of these geographically linked *E. coli* isolates.

2. Materials and methods

2.1. Strains, isolation, and culture conditions

The *E. coli* strains from human were recovered from patients being treated at the Kakamega County Teaching and Referral Hospital, in western Kenya. Briefly, midstream urine specimens were cultured on cystine–lactose–electrolyte-deficient (CLED) medium (Hi-Media, India). The wound sample was collected from an abdominal surgical wound. Wastewater isolates were recovered from the Masinde Muliro University of Science and Technology (MMUST) wastewater treatment plant during the period March – June 2016. The wastewater and wound-derived samples were cultured on MacConkey agar (Hi-Media, India).

All cultures were incubated overnight at 37 °C. Pure (single colony) isolates were confirmed as *E. coli* using API20E biochemical test strips (Biomérieux) following the manufacturer's instructions. The isolates were further subjected to antibiotic susceptibility profiling using the Kirby Bauer disc diffusion method against the following panel of antibiotics: trimethoprim/sulfamethoxazole, amoxicillin/clavulanate, tetracycline, gentamicin, ceftazidime, cefuroxime, cefotaxime, ceftriaxone, meropenem, amikacin/cefepime, piperacillin/tazobactam, ampicillin, sulbactam, nitrofurantoin, imipenem, and ciprofloxacin. *Escherichia coli* ATCC 25922 was used as a reference for interpretation of the data based on the guidelines from the Clinical and Laboratory Standards Institute (CLSI) (2017). Cultures of the *E. coli* isolates were stored at –80 °C in trypticase soy broth supplemented with 15% v/v glycerol.

2.2. DNA sequencing

Whole genome sequencing was carried out by MicrobesNG (Birmingham, UK) using an Illumina HiSeq 2500 platform. Briefly, a single colony of each strain was picked and suspended in 100 µL of sterile 1 × phosphate-buffered saline (PBS) (Oxoid, UK). The suspension was spread thickly (using a sterile loop) onto a fresh LB-agar plate and incubated at 37 °C overnight. Dense colony growth was then scraped off and sent to MicrobesNG in supplied bar-coded bead tubes. Sequencing was carried out using an Illumina HiSeq 2500 platform, with 2 × 250 bp paired-end reads. The reads were trimmed using Trimmomatic v0.30 with a sliding window quality cut-off of Q15. Taxonomic classification of the sequences and assessment of sequence contamination was done using Kraken (Wood and Salzberg, 2014). The de novo assembly of contigs was done using SPAdes version 3.14.0 with default settings.

2.3. Annotation of contigs and prediction of chromosomal or plasmid affiliation

Automated annotation of the contigs was performed using Prokka v1.12. Antibiotic resistance genes were predicted using an internet-based algorithm, RGI (<https://card.mcmaster.ca/analyze>) implemented in the Web-service CARD (Alcock et al., 2020). Putative virulence-associated genes were identified via BLASTP alignment of all translated open reading frames (ORFs) against the sequences of known virulence associated proteins (Sarowska et al., 2019). Reference protein sequences were obtained from the NCBI GenBank database. To predict the putative plasmid affiliation of the assembled contigs, an internet-based program, mlplasmids - version 1.0.0 (<https://sarredondo.shinyapps.io/mlplasmids/>) was used (Arredondo-Alonso et al., 2018) with default parameters. All other contigs were considered as being chromosomal in origin. Genomic islands were identified using SeqWord Gene Island Sniffer (<http://seqword.bi.up.ac.za/sniffer/index.html>) (Bezuidt et al., 2009).

2.4. Multi-locus sequence typing

MLST was carried out using the interactive batch sequence query available at the Institute Pasteur *E. coli* MLST database (<https://bigsd.b.pasteur.fr/ecoli/>) and using the automated interactive MLST CGE Server (<https://cge.cbs.dtu.dk/services/MLST/>) (Larsen et al., 2012). Concatenated chromosomal contigs in FASTA format were queried against the MLSTwithMissingData database to predict sequence types based on the sequences of eight diagnostic genes: *dinB*, *icdA*, *pabB*, *polB*, *trpA*, *trpB* and *uidA*, which are defined as *E. coli* MLST marker loci in the EnterBase database (Zhou et al., 2020). Sequence types (ST) unambiguously predicted by at least one of the servers were recorded.

2.5. Gene ortholog prediction

Clusters of orthologous genes (COGs) in sequenced genomes were predicted using the program OrthoFinder (Emms and Kelly, 2015) with default parameters. Sequences of every COG were aligned using the MUSCLE algorithm (Edgar, 2004). Alignments were quality-controlled and ambiguous parts of the alignments were removed using the program Gblocks (Talavera and Castresana, 2007) with the default parameter settings. COG alignments were concatenated using BioPython scripts into a superstring alignment for further phylogenetic inferences.

2.6. Phylogenetic inferencing and clustering

Concatenated alignments of COGs were used to infer phylogenetic relations between the genome sequences. This was done using a Neighbor-Joining (NJ) algorithm with MEGA X and a bootstrap value of 100 (Kumar et al., 2018). For clustering of genomic islands (GIs), a distance matrix was built for all GIs, where the distance between two GIs, *i* and *j*, was calculated according to Eq. (1):

$$D_{ij} = 1 - \#shared_genes / \min(\#GI_i\ genes, \#GI_j\ genes) \quad (1)$$

where, *#shared_genes* is the number of orthologous genes shared by two GIs, and *#GI_i genes* and *#GI_j genes*, respectively, are the total numbers of genes in the first and second GIs. A dendrogram of GI clusters was then generated based on the distance matrix using the program *neighbor.exe* (NJ algorithm) of the PHYLIP 3.69 package (<http://evolution.genetics.washington.edu/phylip.html>).

The phylogenetic clustering approach outlined above tends to artificially group long plasmids around the root of the dendrogram, as they have a higher chance of sharing multiple genes. To circumvent this, phylogenetic clustering of the plasmids was done using a binary parsimony algorithm. A table of COGs shared by at least two plasmids was generated, with the absence and presence of orthologous genes in each

plasmid designated by 0 and 1, respectively. This binary table was formatted as an input file for the dollo parsimony algorithm (Huson and Steel, 2004) implemented in the program *dollop.exe* of the PHYLIP 3.69 package. Dendrograms were visualized using Dendroscope 3 (Huson and Scornavacca, 2012). It should be noted that in both aforementioned cases, the dendrograms should not (in *stricto sensu*) be considered as phylogenetic trees but as cladograms.

3. Results

3.1. Antibiotic resistance of *E. coli* environmental and clinical isolates

In total, 23 strains of *E. coli* were recovered from a referral hospital and a nearby municipal wastewater processing plant in western Kenya. The source and pattern of antibiotic resistance in each of the strains are shown in Table 1. Nine isolates (denoted A, F, H, K, L, N, O, P, Q) were derived from the wastewater source (located ca. 1.5 km from the referral hospital) and 14 isolates were obtained from the clinic (denoted E2, E4, E7, E8, E10-E15, and E17-E20). Of the clinical isolates, 13 were obtained from patients with urinary tract infections, and one (E10) was from a wound. Almost all isolates from both the clinical and wastewater sources were resistant to trimethoprim- sulfamethoxazole and amoxicillin, and the clinical isolates showed generally greater resistance (compared with the wastewater isolates) to co-amoxiclav (amoxicillin/clavulanate), ampicillin-sulbactam, tetracycline, gentamicin, amikacin, cefuroxime, cephalixin, ceftazidime, and ciprofloxacin. The majority of isolates from both environments remained resistant to nitrofurantoin and

chloramphenicol.

3.2. Phylogenetic relationships between the isolates and MLST assignment

To study phylogenetic relationships between the *E. coli* isolates, 2637 orthologous genes shared by all the genomes were identified and aligned using MUSCLE. We also included a selection of reference strains (as “signposts”) deposited in the NCBI. Alignments of the encoded protein sequences were concatenated into a “superstring alignment” comprised of 805,265 amino acid residues, and an NJ phylogenetic tree was constructed (Fig. 1).

The strains segregated in the tree into two broad clades, corresponding to commensal/enterotoxigenic *E. coli* variants (red shading in Fig. 1), and uropathogenic isolates (blue shading). Although the clinical isolates were roughly equally distributed between these two clusters, most of the wastewater isolates fell into the commensal/enterotoxigenic variant grouping (red shading). The isolates were associated with a diverse range of known MLSTs. Indeed, the only ST represented by more than a single isolate was ST 43, which was associated with a phylogenetic cluster comprising three clinical isolates and two wastewater isolates, as well as the uropathogenic *E. coli* strain NA114. ST 43 is widely distributed around the world, and of the 91 recorded ST 43 strains in the Institute Pasteur *E. coli* MLST database, 9 are clinical uropathogenic isolates. It is also noteworthy that although ST 131 is widely reported as one of the most common clinical *E. coli* isolates worldwide (Pitout and Laupland, 2008; Nicolas-Chanoine et al., 2014), there were no representatives of this ST among the *E. coli* strains we examined. Conversely,

Table 1

Antibiotic resistance profile and origin of the *E. coli* strains selected for WGS analysis in this study.

Isolate	Origin	ST	A	AM	S	T	N	G	AK	C	CX	CN	CA	CP
E2	Urine													
E4	Urine													
E7	Urine													
E8	Urine													
E10	Pus swab													
E11	Urine													
E12	Urine													
E13	Urine													
E14	Urine													
E15	Urine													
E17	Urine													
E18	Urine													
E19	Urine													
E20	Urine													
A	WW													
F	WW													
H	WW													
K	WW													
L	WW													
N	WW													
O	WW													
P	WW													
Q	WW													
Cutoff Point		≤10	≤13	≤13	≤11	≤11	≤14	≤12	≤14	≤12	≤14	≤14	≤17	≤15

Key: WW = wastewater; ST = trimethoprim-sulfamethoxazole; A = amoxicillin; AM = amoxicillin clavulanate; S = ampicillin-sulbactam; T = tetracycline; N = nitrofurantoin; G = gentamicin; AK = amikacin; C = chloramphenicol; CX = cefuroxime; CN = cephalixin; CA = ceftazidime; CP = ciprofloxacin; Red = resistant; Green = intermediate or sensitive.

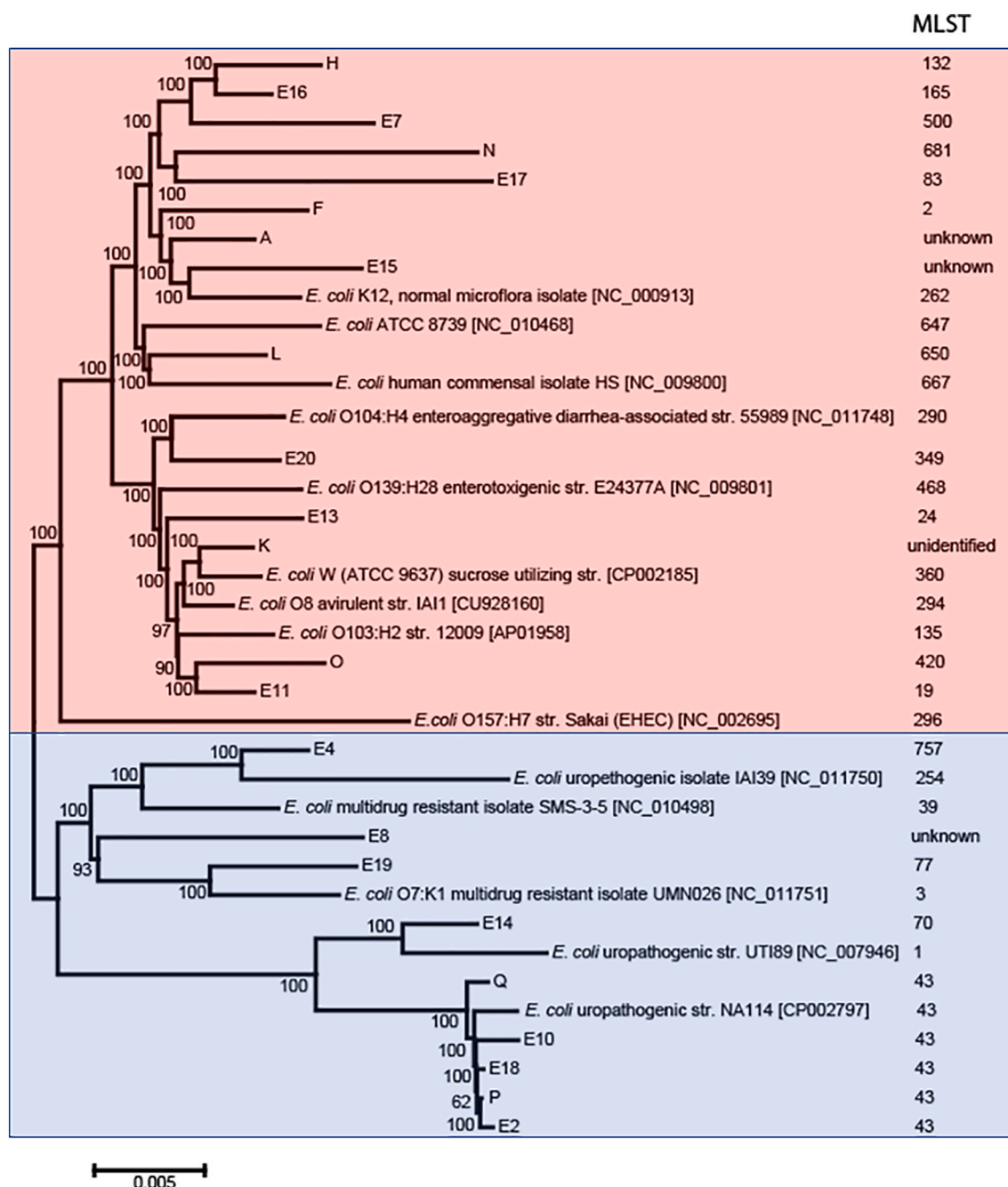


Fig. 1. An NJ phylogenetic tree of clinical and wastewater *E. coli* isolates (sequenced in this study) compared with a selection of NCBI reference strains. Bootstrap numbers are shown at each intermediate split in the tree. The identified MLST of the strains is shown in the corresponding column. The tree divided early on into two broad branches, enriched in either commensal/enterotoxigenic *E. coli* variants (red shading), or uropathogenic isolates (blue shading). [Note that in the wastewater isolate K, the *icdA* was fragmented in the contig preventing definitive assignment of a ST for this strain. However, based on the sequence profile of the other marker genes in isolate K, it may belong either to ST 735, or ST 910.]

our collection also included several strains with STs not yet recorded in the *E. coli* MLST database. For example, the uropathogenic isolate, E8, possessed unique combinations of variants in the sequences of all marker genes except *uidA*, indicating that E8 likely represents a completely new ST of *E. coli*.

3.3. Distribution of antibiotic resistance and virulence-associated genes

The WGS data for all of the isolates indicated that they encode numerous multidrug efflux pumps (including *mdlAB*, *mdtABCD*, *mdtIJ*, *mdtK*, *mdtEF*, *acrAB*-*acrD*-*acrEF*, *cmr*, *yddA*, *yojI*, *yjiO*, *emrAB*, *emrD*,

emrKY, and *hsrA*) and a selection of known antibiotic resistance genes, including *rarD* and *cmlA* for chloramphenicol resistance, and the β -lactamases, *ampH*, *ampC*, *bla*. AMR-genes were searched by the program CARD_RGI looking for similarities of protein sequences with records of its own comprehensive database of AMR-proteins (Alcock et al., 2020). A summary of the antibiotic resistance genes identified by CARD-RGI in each isolate is shown in Table 2. Interestingly, the mean number of all classes of AMR-associated genes was similar in both the wastewater and clinical isolates.

The genome sequences of the isolates also contained multiple genes known to be associated with virulence. Sarowska et al. (2019) listed

Table 2

Antibiotic resistance gene distribution in the chromosomal DNA of the indicated sequenced isolates. The numbers in each column represent the number of genes encoding the indicated antibiotic resistance mechanism identified in each isolate.

Isolate	β -lactamases	Efflux pump components	Drug resistance genes of other categories ^a
Wastewater isolates			
A	2	30	23
F	2	30	23
H	2	30	22
K	2	30	22
L	2	30	22
N	2	30	22
O	2	29	22
P	1	30	22
Q	1	30	22
Clinical isolates			
E2	1	30	22
E4	2	28	23
E7	2	28	22
E8	2	30	22
E10	1	30	22
E11	2	30	22
E13	2	30	22
E14	1	30	22
E15	2	29	22
E16	2	30	22
E17	1	28	22
E18	1	30	22
E19	2	30	23
E20	2	30	22

^a This column combines all other types of AMR genes including known transcriptional regulators of drug resistance response, antibiotic-modifying enzymes and uncharacterized drug resistance proteins.

several key groups of virulence factors frequently found in pathogenic *E. coli* isolates, including several classes of adhesins, siderophores, toxins and proteins important for intracellular survival of pathogens, colonization of non-GI tract tissues, and immune system avoidance. A summary of distribution of virulence-associated determinants in the isolates studied here is shown in Table 3. The data indicate an enrichment of genes associated with survival in the host among the clinical isolates including virulence-associated siderophores of five classes, *aer*, *iuc*, *irp*, *iron* and *sit*, which were present on the chromosomes of all the sequenced isolates. In several cases, additional copies of these siderophore genes were also found on plasmids (see Fig. 3 and discussion below).

3.4. Genomic islands and the distribution of drug resistance and virulence-associated genes

We next examined the genomic context of the AMR and virulence-associated (VA) genes i.e., are these genes located in the conserved “core chromosome”, or are they associated with the variable “accessory” genome (GIs and plasmids)? The genome sequences of all the isolates contained multiple horizontally-acquired GIs, including prophages, transposable elements and integrons. The GIs were clustered based on the “shared gene” algorithm in Eq. 1. We then further interrogated each resulting GI cluster for its AMR and VA gene content (Fig. 2).

Although the gene content of GIs was generally highly variable, this clustering approach revealed some intriguing genetic conservation. In the left-top corner of the cladogram (Fig. 2), there is a clutch of individual GIs bearing several VA genes. For example, the small multidrug resistance efflux transporter *emrE* is located on a GI found only in environmental isolate F, whereas the cell invasion gene *ibeB*, along with several genes conferring resistance to copper (collectively named “*copR*” in the figure) and a multidrug resistance gene (*emrK*) were found in two GIs from isolate E19. Clockwise from these, there is a cluster of five

highly similar GIs found in isolates F, K, L, E17 and E20, which bear genes for arsenate resistance (collectively named *arsR* in the figure) and the *mdtEF* multidrug efflux operon. Another individual GI found in isolate E9 contains the multiple stress resistance gene, *bhsA*. A large group of 13 GIs from both clinical and environmental isolates contains an operon encoding fimbria-like genes (*yadCKLMN* and *ecpD*), which are known to function as virulence-associated adhesins in enterohaemorrhagic and uropathogenic *E. coli* (Spurbeck et al., 2011; Chingcuanco et al., 2012; Stacy et al., 2014). Within this group, seven GIs from isolates N, E7, E9, E13, E14, E16 and E19 form a distinct sub-cluster possessing the daunorubicin/ doxorubicin resistance-associated gene, *draA*. Four GIs from the genome sequences of isolates P, Q, E2 and E10 contain virulence-associated toxin-encoding genes, including *sat*, *vat* and *pic*, together with a virulence regulon transcriptional activator-encoding gene, *virF*. Eight GIs from isolates K, L, E4, E7, E11, E16 and E20 contain the *ygiLGHJJK* operon, which encodes another set of virulence-associated fimbria-like proteins (Spurbeck et al., 2011). A very large group of 23 GIs, which were shared many of the sequenced isolates, comprises additional fimbria-encoding genes, *afa*, *fim* and *pap*. The *E. coli* fimbrial protein YehB is responsible for adhesion to abiotic surfaces (Ravan and Amandadi, 2015) and as such may contribute to the dissemination of nosocomial infections in hospitals, and possibly, also survival in the environment. This gene was found in eight GIs from isolates F, K, O, E4, E11, E13, E19 and E20. Another adhesion gene, *flu* (*agn43*), in combination with a persistence and stress-resistance toxin-antitoxin system, *pasTI*, was present in seven GIs from isolates H, E7, E11, E14, E16, E19 and E20. Twelve GIs from isolates H, O, K, E7, E8, E11, E13, E14, E15, E16, E17 and E20 carry the multidrug resistance operon, *emrYK*, and six GIs from environmental isolates A, H, N, O, P and Q encode a colanic acid biosynthetic pathway. Colanic acid is a capsular carbohydrate of uropathogenic bacteria and is known to be important for biofilm formation (Prigent-Combaret et al., 2000; Hanna et al., 2003). A short operon, *rfaPY*, which encodes a pair of lipopolysaccharide core heptose kinases (I and II), was found in 21 GIs. These genes may encode potential virulence factors, since the activation of heptose precursors is used in the biosynthesis of lipopolysaccharides (LPS), and LPS is known to contribute towards the pathogenicity of enterotoxigenic *E. coli* (Maigaard Hermansen et al., 2018). Interestingly, orthologues of the *sat* and *vat* toxins mentioned above are encoded on another group of four GIs from isolates E10, E11, E14 and E18. We note that isolate E10 also encodes *sat* and *vat* on a different GI. An increased copy number of these genes may influence the virulence of this strain (Elliott et al., 2013; Slager and Veening, 2016). Similarly, we also noted that the invasins, *ipaB*, was distributed between nine GIs which segregated into two distinct clusters (Venkatesan et al., 1988). The smaller of these clusters contains GIs from isolates E4, E8 and E19, whereas the larger one comprises GIs from E2, E8, E10, E14, E18 and E19. Once again, we noted that two of the isolates (E8 and E19) carried paralogous copies of *ipaB* in two separate GIs. Nine GIs from isolates H, K, L, E7, E8, E13, E16, E19 and E20 carry a large operon encoding a type III secretion system (Tree et al., 2009). The anti-phagocytosis factor-encoding gene, *neuA*, was found in three related GIs from isolates P, Q and E17. Three GIs from isolates E4, E8 and E19 carried a multidrug resistance gene, *mdtL*, and a chloramphenicol resistance gene *cmlA*. A group of 12 large GIs contained a polypeptide synthase gene (*irp*) encoding the siderophore, yersiniabactin. Host organisms often sequester iron to inhibit the growth of pathogens. Consequently, iron acquisition systems are often considered to be virulence factor/ survival mechanisms associated with pathogenicity (Skaar, 2010). Several other virulence-associated siderophores are involved in iron scavenging and transportation. The genes encoding the synthesis and transport of these siderophores were abundant in the isolates (Table 2). Orthologues of the multidrug resistance-associated gene, *mdtN*, were also found in two loosely clustered GIs from isolates E8 and E9. The same GI from E9 carries also another siderophore (aerobactin) encoding gene, *aer*. Finally, a group of 16 GIs contains several regulatory genes including the blue light- and temperature-regulated

Table 3

Known virulence determinants in the sequenced isolates. Black cells = presence of gene, white cells = absence of gene. BLASTP cutoff values for assignment of gene presence/absence were 0.0001.

Strains	Adhesins								Siderophores					Survival factors					Toxins							
	<i>afa</i>	<i>fim</i>	<i>dra</i>	<i>pap</i>	<i>sfa/foc</i>	<i>iha</i>	<i>mat/es</i>	<i>crl/cgs</i>	<i>flu</i>	<i>aer</i>	<i>iuc</i>	<i>irp</i>	<i>iron</i>	<i>sit</i>	<i>ibe</i>	<i>traT</i>	<i>neuA</i>	<i>Omp</i>	<i>iss</i>	<i>cvaC</i>	<i>pilC</i>	<i>sat</i>	<i>vat</i>	<i>hlyA</i>	<i>cnf</i>	
Commensal <i>E. coli</i>																										
K12																										
Wastewater isolates																										
A																										
F																										
H																										
K																										
L																										
N																										
O																										
P																										
Q																										
Clinical isolates																										
E2																										
E4																										
E7																										
E8																										
E10																										
E11																										
E13																										
E14																										
E15																										
E16																										
E17																										
E18																										
E19																										
E20																										

anti-repressor *bluF*. *BluF* is light and temperature sensing protein, which regulates biofilm formation (Tschowri et al., 2009). While it is not considered as a virulence factor, it may influence the survival of bacteria in the environment. These GIs were found in both the environmental and clinical samples (specifically, isolates A, F, L, P, Q, E2, E4, E7, E10, E11, E14, E16, E17, E19 and E20). Notably, in the genome of isolate E2, this GI was duplicated.

Not all virulence genes were associated with specific clusters of GIs. For example, the major fimbrial subunit gene *lpfA*, which influences epithelial cell invasion by mastitis-associated *E. coli* (Dogan et al., 2012), was found in seven unrelated GIs from clinical isolates E4, E9, E11, E13, E14, E15 and E20. We also noted that many GIs were enriched in genes encoding phage-related proteins and integrases (suggesting the likely mode of horizontal transmission), and many others also encoded metabolic enzymes and transmembrane transporters. It is possible that these cargo genes are involved in adaptation to specific environments, and may indirectly impact on virulence, AMR or survival in the face of

environmental challenges.

3.5. Role of plasmids in distribution of drug resistance and virulence associated genes

Predicted plasmid-borne contigs were identified in the assemblies from all of the isolates. These contigs contained between 4 coding sequences (CDS) in E8 up to 288 CDS in E11. It should be noted that assembly of plasmid contigs is problematic due to a higher level of sequence variability in these regions. Therefore, we note that the obtained contigs may not represent whole sequences of the plasmids in the studied isolates. Grouping of concatenated plasmid-borne contigs from different isolates based on shared homologous genes is shown in Fig. 3. This figure also summarizes the numbers of AMR and VA genes found in these contigs.

It is immediately clear from inspection of the data in Fig. 3 that the plasmid-borne DNA from clinical isolates is enriched in AMR and VA

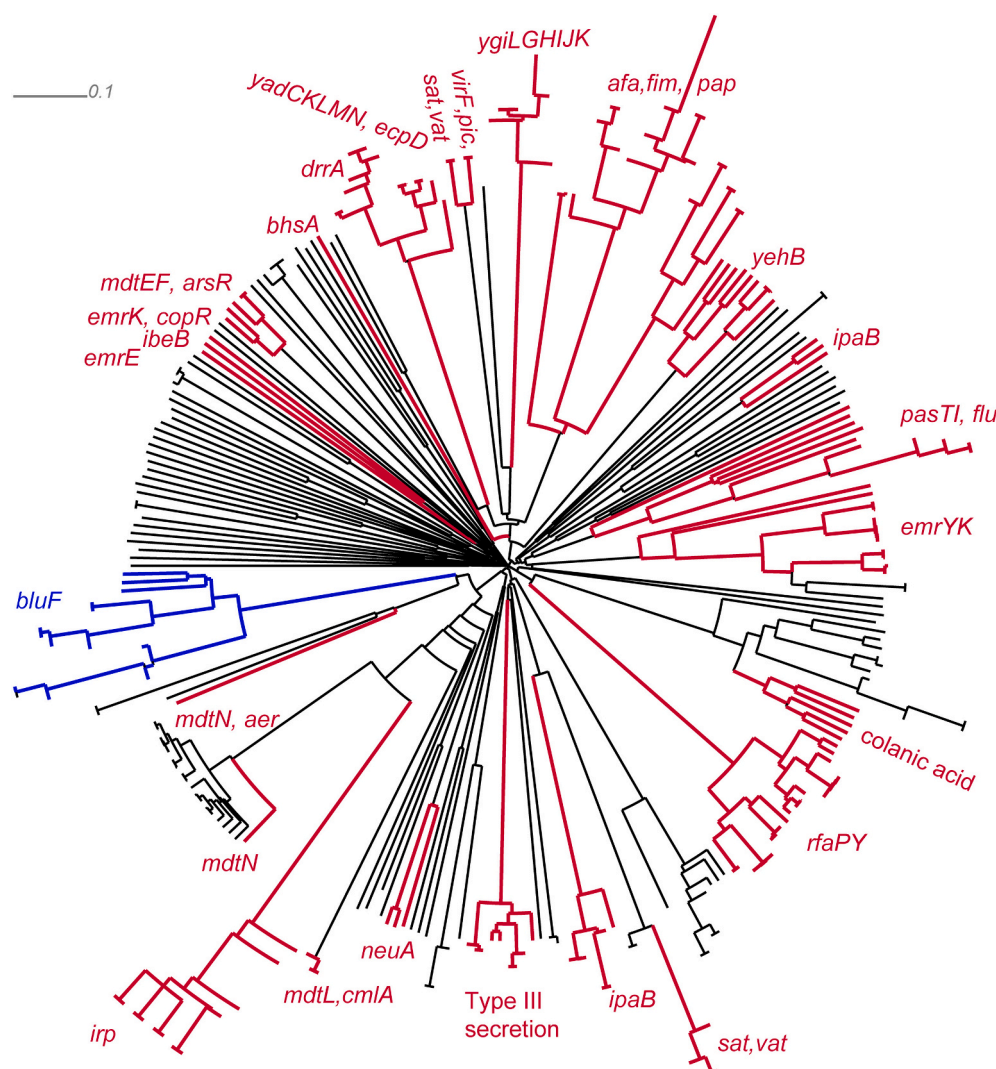


Fig. 2. Clustering of GIs based on gene content using an NJ algorithm (in turn, based on the distance matrix given in Eq. 1). A single line radiating from the center to the edge of the cladogram indicates a GI in a specific isolate. Branched radiating lines indicate diversification of a GI present in multiple isolates. The clustered GIs were further interrogated to identify AMR and virulence-associated genes using BLASTP. Groups of GIs containing known AMR and virulence-associated genes are shown red. GIs with the blue light- and temperature-regulated genes are shown blue.

genes compared with the wastewater isolates. Indeed, the plasmids from environmental isolates A, H, K, F, and L encoded no virulence-associated genes and only one or no AMR determinants. Exceptions to this trend included plasmids from the environmental isolates P and Q, which contained multiple AMR and VA genes, whereas the largest plasmid-associated contig in the dataset (from clinical isolate E8) contained no AMR or virulence determinants. The largest number of AMR determinants was identified in the plasmid DNA from E17, E18, E11 and E9, with the highest number of virulence-associated genes found in the plasmid from isolate E14. Interestingly, the plasmid-borne virulence-associated genes were often duplicates of genes already present on the chromosome, whereas the plasmid-borne AMR determinants were more specific.

4. Discussion

In this study, we found that clinical and wastewater isolates possessed similar overall numbers of chromosomally encoded AMR and VA genes, irrespective of their origin (Tables 2 and 3). However, the clinical isolates displayed an enrichment of AMR and VA genes in their plasmidome. Of note, a number of these genes were present in multiple paralogous copies (either on the chromosome, in GIs, or on plasmids). Gene duplication is a key driver of functional diversification and is also a facile means of increasing gene expression through increased copy number (Elliott et al., 2013; Slager and Veening, 2016). In bacteria,

there are several examples of genes encoding basic metabolic functions being present in two copies, with one copy on the chromosome and the other on a plasmid (Zheng et al., 2015). Our observation, that plasmids from the clinical isolates were enriched in AMR and VA genes indicates that these mobile elements may play a key role in pathogenicity. The plasmids associated with environmental isolates P and Q were exceptions to this general trend, since these were enriched with AMR and virulence-associated genes. Isolates P and Q are notable since they are phylogenetically related to the clinical isolates E2, E10 and E18, and all five isolates belonging to the uropathogenic ST 43 (Fig. 1). There may be two non-exclusive explanations for this observation. First, P and Q may be disseminated “clinical isolates” that just happen to have been captured in the local watershed following e.g., human discharge activities. Alternatively, these particular plasmids may confer a fitness advantage in the wastewater environment. The factors increasing the survival of these uropathogenic strains may include the presence of colanic acid biosynthetic genes and the light- and temperature-sensing anti-repressor, *bluF*. These genes have been shown to play an important role in the modulation of biofilm formation (Prigent-Combaret et al., 2000; Hanna et al., 2003; Tschowri et al., 2009) and therefore confer a potential advantage to ST 43 for survival in both non-host and host environments.

Collectively, our data suggest that plasmid-borne functions confer an advantage to *E. coli* in terms of infection and/or withstanding exposure to the antimicrobials commonly used to treat these infections. At the

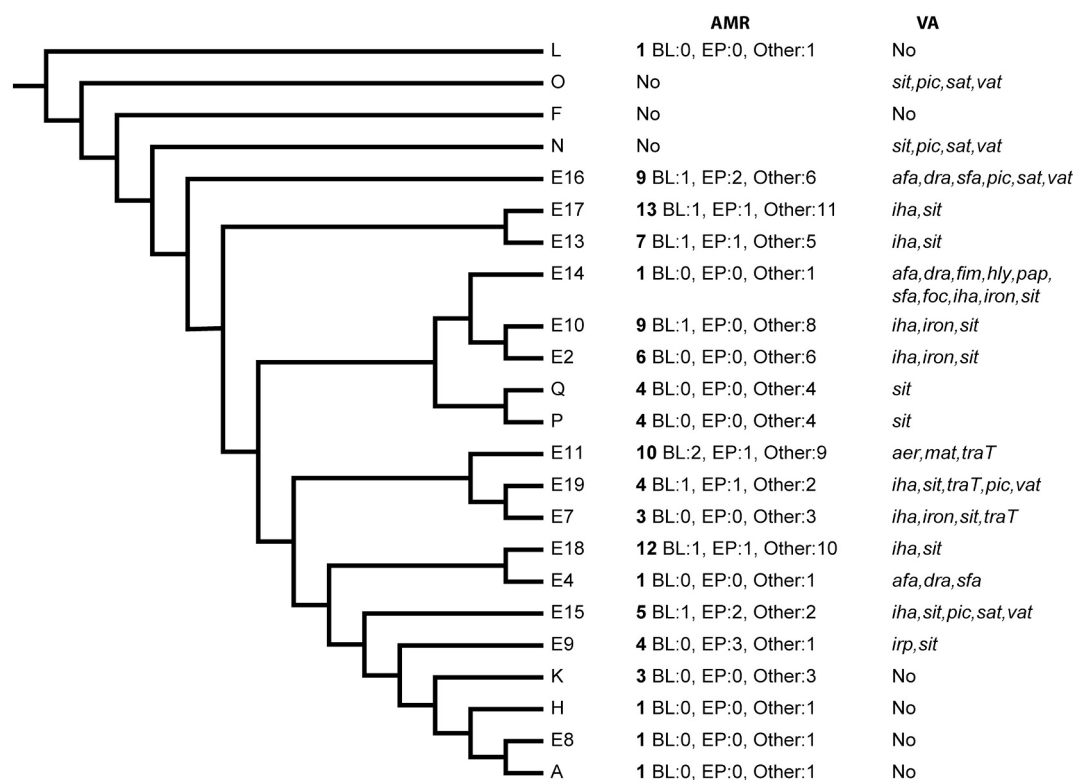


Fig. 3. Dollo parsimony clustering of plasmid contigs by presence/absence of shared homologous genes identified by a reciprocal BLASTP alignment. In line with the end-node titles, total numbers of antimicrobial resistance (AMR) genes are shown in bold followed by numbers per categories of β -lactamases (BL), efflux pumps (EP) and other categories of drug resistance genes. A list of the encoded virulence-associated (VA) genes is shown in the adjacent column. VA genes found on the plasmid-born contigs are: *aer* – siderophore; *afa* – Afa-like afimbrial adhesins; *dra* – Dra-like surface-exposed fimbria associated proteins common in uropathogenic *E. coli*; *fim* – type I fimbria proteins; *foc* – Foc-like adhesins to intestinal epithelial cells; *hly* – hemolysin transport protein creating pores in host cell membranes; *iha* – iron-regulated adhesin; *iron* – siderophore receptor; *irp* – yersiniabactin siderophore synthesis protein; *mat* – meningitis associated and temperature regulated fimbriae; *pap* – pilin, colonization factor in extraintestinal infections stimulating the production of cytokines by T lymphocytes; *pic* – mucin degrading serine protease; *sat* – serine protease autotransporter toxin; *sfa* – Sfa-like adhesins to intestinal epithelial cells; *sit* – Sit-like iron transmembrane transporters; *traT* – phagocytosis inhibitor; *vat* – vacuolating autotransporter toxin.

same time, these genes presumably confer a significant burden on bacterial growth and replicative potential during transit through the environment. Consequently, when not infecting a host, there is likely a selection pressure on bacterial populations to lose these plasmid-borne genes. This presumably generates a drive towards redistributing the encoded functions from the plasmid to the chromosome, which may be another reason why we see apparently multiple paralogous copies of some genes (Andersson and Hughes, 2010; Kussell, 2013; Melnyk et al., 2015).

In conclusion, our data confirm and extend previous reports indicating the high genomic diversity of *E. coli* in humans from tropical areas (Escobar-Páramo et al., 2004; Richter et al., 2018), and furthermore, implicate plasmids as a key driver of AMR and VA gene dissemination, especially among clinical isolates. Although plasmids come with an intrinsic fitness cost associated with their replication, we noted that in some circumstances (e.g., the isolates of ST 43) plasmid-borne AMR and VA genes were also associated with the environmental isolates. This ability to maintain plasmid-borne functions outside the host may contribute towards the global success of this sequence type.

Research data access

All sequence data generated in this study have been submitted to the NCBI BioProject database (BioProject: <https://www.ncbi.nlm.nih.gov/>) under accession numbers: PRJNA606749; PRJNA630767; PRJNA630874; PRJNA606697.

Author contributions

SAW, WAS, conceptualization, investigation and original draft; TJO, WF, VD investigation and methodology; OR bioinformatics analysis and original draft; MW supervision, draft review, funding procurement and editing.

Funding and acknowledgements

This work was supported by the Cambridge – Africa ALBORADA Research Fund and the Academy of Medical Sciences GCRF networking grant reference GCRFNG/100095. TJO was supported by a studentship (NC/P001564/1) from the NC3Rs awarded to MW. WF was supported by a studentship from the Cambridge Trust-CONACyT. This study was approved by Jaramogi Oginga Odinga Referral & Teaching Hospital IREC; reference number ERC.IB/VOL.1/141.

Declaration of Competing Interest

The authors declare that there are no conflicts of interest.

References

- Alcock, B.P., Raphenya, A.R., Lau, T.T.Y., Tsang, K.K., Bouchard, M., Edalatmand, A., Huynh, W., Nguyen, A.V., Cheng, A.A., Liu, S., Min, S.Y., Miroshnichenko, A., Tran, H.K., Werfalli, R.E., Nasir, J.A., Oloni, M., Speicher, D.J., Florescu, A., Singh, B., Faltyn, M., Hernandez-Koutoucheva, A., Sharma, A.N., Bordeleau, E., Pawlowski, A.C., Zubyk, H.L., Dooley, D., Griffiths, E., Maguire, F., Winsor, G.L., Beiko, R.G., Brinkman, F.S.L., Hsiao, W.W.L., Domselaar, G.V., McArthur, A.G.,

2020. CARD 2020: antibiotic resistome surveillance with the comprehensive antibiotic resistance database. *Nucleic Acids Res.* 48 (D1), D517–D525. <https://doi.org/10.1093/nar/gkz935>.
- Andersson, D.I., Hughes, D., 2010. Antibiotic resistance and its cost: is it possible to reverse resistance? *Nat. Rev. Microbiol.* 8, 260–271. <https://doi.org/10.1038/nrmicro2319>.
- Arredondo-Alonso, S., Rogers, M.R.C., Braat, J.C., Verschuuren, T.D., Top, J., Corander, J., Willems, R.J.L., Schürch, A.C., 2018. Miplasmids: a user-friendly tool to predict plasmid- and chromosome-derived sequences for single species. *Microb. Genom.* 4 (11) <https://doi.org/10.1099/mgen.0.000224>.
- Besser, J., Carleton, H.A., Gerner-Smidt, P., Lindsey, R.L., Trees, E., 2018. Next-generation sequencing technologies and their application to the study and control of bacterial infections. *Clin. Microbiol. Infect.* 24, 335–341. <https://doi.org/10.1016/j.cmi.2017.10.013>.
- Bezuidt, O., Lima-Mendez, G., Reva, O.N., 2009. SEQWord Gene Island sniffer: a program to study the lateral genetic exchange among bacteria. *World Acad. Sci. Eng. Technol.* 58, 1169–1174.
- Cao, Y., Fanning, S., Proos, S., Jordan, K., Srikumar, S., 2017. A review on the applications of next generation sequencing technologies as applied to food-related microbiome studies. *Front. Microbiol.* 8, 1829. <https://doi.org/10.3389/fmicb.2017.01829>.
- Chingcuano, F., Yu, Y., Kus, J.V., Que, L., Lackraj, T., Lévesque, C.M., Foster, B.D., 2012. Identification of a novel adhesin involved in acid-induced adhesion of enterohaemorrhagic *Escherichia coli* O157:H7. *Microbiol.* 158, 2399–2407. <https://doi.org/10.1099/mic.0.056374-0>.
- Performance standard for antimicrobial susceptibility testing 27th ed. In: CLSI (Ed.), 2017. CLSI supplement M100 Wayne. Clinical and Laboratory Standards Institutes, PA.
- Dogan, B., Rishniw, M., Bruant, G., Harel, J., Schukken, Y.H., Simpson, K.W., 2012. Phylogroup and *lpfA* influence epithelial invasion by mastitis associated *Escherichia coli*. *Vet. Microbiol.* 159 (1–2), 163–170. <https://doi.org/10.1016/j.vetmic.2012.03.033>.
- Edgar, R.C., 2004. MUSCLE: multiple sequence alignment with high accuracy and high throughput. *Nucleic Acids Res.* 32 (5), 1792–1797. <https://doi.org/10.1093/nar/gkh340>.
- Elliott, K.T., Cuff, L.E., Neidle, E.L., 2013. Copy number change: evolving views on gene amplification. *Future Microbiol.* 8 (7), 887–899. <https://doi.org/10.2217/fmb.13.53>.
- Emms, D.M., Kelly, S., 2015. OrthoFinder: solving fundamental biases in whole genome comparisons dramatically improves orthogroup inference accuracy. *Genome Biol.* 16, 157. <https://doi.org/10.1186/s13059-015-0721-2>.
- Escobar-Páramo, P., Grenet, K., Le Menac'h, A., Rode, L., Salgado, E., Amorin, C., Gouriou, S., Picard, B., Rahimy, M.C., Andremont, A., Denamur, E., Ruimy, R., 2004. Large-scale population structure of human commensal *Escherichia coli* isolates. *Appl. Environ. Microbiol.* 70 (9), 5698–5700. <https://doi.org/10.1128/AEM.70.9.5698-5700.2004>.
- European Centre for Disease Prevention and Control, 2018. Monitoring the Use of Whole-Genome Sequencing in Infectious Disease Surveillance in Europe. ECDC, Stockholm.
- Hanna, A., Berg, M., Stout, V., Razatos, A., 2003. Role of capsular colanic acid in adhesion of uropathogenic *Escherichia coli*. *Appl. Environ. Microbiol.* 69 (8), 4474–4481. <https://doi.org/10.1128/AEM.69.8.4474-4481.2003>.
- Huson, D.H., Scornavacca, C., 2012. Dendroscope 3: an interactive tool for rooted phylogenetic trees and networks. *Syst. Biol.* 61 (6), 1061–1067. <https://doi.org/10.1093/sysbio/sys062>.
- Huson, D.H., Steel, M., 2004. Phylogenetic trees based on gene content. *Bioinformatics.* 20 (13), 2044–2049. <https://doi.org/10.1093/bioinformatics/bth198>.
- Jafari, A., Aslani, M.M., Bouzari, S., 2012. *Escherichia coli*: a brief review of diarrheagenic pathotypes and their role in diarrheal diseases in Iran. *Iran. J. Microbiol.* 4 (3), 102–117. PMID: PMC3465535.
- Kumar, S., Stecher, G., Li, M., Nkay, C., Tamura, K., 2018. MEGA X: molecular evolutionary genetics analysis across computing platforms. *Mol. Biol. Evol.* 35 (6), 1547–1549. <https://doi.org/10.1093/molbev/msy096>.
- Kussell, E., 2013. Evolution in microbes. *Annu. Rev. Biophys.* 42, 493–514. <https://doi.org/10.1146/annurev-biophys-083012-130320>.
- Larsen, M.V., Cosentino, S., Rasmussen, S., Friis, C., Hasman, H., Marvig, R.L., Jelsbak, L., Sicheritz-Pontén, T., Ussery, D.W., Aarestrup, F.M., Lund, O., 2012. Multilocus sequence typing of total-genome-sequenced bacteria. *J. Clin. Microbiol.* 50 (4), 1355–1361. <https://doi.org/10.1128/JCM.06094-11>.
- Maigaard Hermansen, G.M., Boysen, A., Krogh, T.J., Nawrocki, A., Jelsbak, L., Møller-Jensen, J., 2018. HldE is important for virulence phenotypes in enterotoxigenic *Escherichia coli*. *Front. Cell. Infect. Microbiol.* 8, 253. <https://doi.org/10.3389/fcimb.2018.00253>.
- Malaho, C., Sifuna, A.W., Shivoga, A.W., 2018. Antimicrobial resistance patterns of *Enterobacteriaceae* recovered from wastewater, sludge and dumpsite environments in Kakamega town, Kenya; *Afr. J. Microbiol. Res.* 12 (28), 673–680. <https://doi.org/10.5897/AJMR2017.8656>.
- Melnik, A.H., Wong, A., Kassen, R., 2015. The fitness costs of antibiotic resistance mutations. *Evol. Appl.* 8, 273–283. <https://doi.org/10.1111/eva.12196>.
- Nicolas-Chanoine, M.H., Bertrand, X., Madec, J.Y., 2014. *Escherichia coli* ST131, an intriguing clonal group. *Clin. Microbiol. Rev.* 27 (3), 543–574. <https://doi.org/10.1128/CMR.00125-13>.
- Pitout, J.D., Laupland, K.B., 2008. Extended-spectrum beta-lactamase-producing *Enterobacteriaceae*: an emerging public-health concern. *Lancet Infect. Dis.* 8 (3), 159–166. [https://doi.org/10.1016/S1473-3099\(08\)70041-0](https://doi.org/10.1016/S1473-3099(08)70041-0).
- Prigent-Combaret, C., Prensier, G., Le Thi, T.T., Vidal, O., Lejeune, P., Dorel, C., 2000. Developmental pathway for biofilm formation in curli-producing *Escherichia coli* strains: role of flagella, curli and colanic acid. *Environ. Microbiol.* 2 (4), 450–464. <https://doi.org/10.1046/j.1462-2920.2000.00128.x>.
- Rantsiou, K., Kathariou, S., Winkler, A., Skandamis, P., Saint-Cyr, M.J., Rouzeau-Szynalski, K., Amézquita, A., 2018. Next generation microbiological risk assessment: opportunities of whole genome sequencing (WGS) for foodborne pathogen surveillance, source tracking and risk assessment. *Int. J. Food Microbiol.* 287, 3–9. <https://doi.org/10.1016/j.ijfoodmicro.2017.11.007>.
- Ravan, H., Amandadi, M., 2015. Analysis of *yeh* fimbrial gene cluster in *Escherichia coli* O157:H7 in order to find a genetic marker for this serotype. *Curr. Microbiol.* 71 (2), 274–282. <https://doi.org/10.1016/j.jfoodmicro.2017.11.007>.
- Richter, T.K.S., Hazen, T.H., Lam, D., Coles, C.L., Seidman, J.C., You, Y., Silbergeld, E.K., Fraser, C.M., Rasko, D.A., 2018. Temporal variability of *Escherichia coli* diversity in the gastrointestinal tracts of Tanzanian children with and without exposure to antibiotics. *mSphere* 3 (6), 3. <https://doi.org/10.1128/mSphere.00558-18.e00558-18>.
- Sarowska, J., Futoma-Koloch, B., Jama-Kmiecik, A., Frej-Madrzak, M., Ksiazczyk, M., Bugla-Ploskonska, G., Choroszy-Krol, I., 2019. Virulence factors, prevalence and potential transmission of extraintestinal pathogenic *Escherichia coli* isolated from different sources: recent reports. *Gut Pathog.* 11, 10. <https://doi.org/10.1186/s13099-019-0290-0>.
- Skaar, E.P., 2010. The battle for iron between bacterial pathogens and their vertebrate hosts. *PLoS Pathog.* 6 (8), e1000949. <https://doi.org/10.1371/journal.ppat.1000949>.
- Slager, J., Veening, J.W., 2016. Hard-wired control of bacterial processes by chromosomal gene location. *Trends Microbiol.* 24 (10), 788–800. <https://doi.org/10.1016/j.tim.2016.06.003>.
- Spurbeck, R.R., Stapleton, A.E., Johnson, J.R., Walk, S.T., Hooton, T.M., Mobley, H.L., 2011. Fimbrial profiles predict virulence of uropathogenic *Escherichia coli* strains: contribution of *ygi* and *yad* fimbriae. *Infect. Immun.* 79 (12), 4753–4763. <https://doi.org/10.1128/IAI.05621-11>.
- Stacy, A.K., Mitchell, N.M., Maddux, J.T., De la Cruz, M.A., Durán, L., Giron, J.A., Curtiss 3rd, R., Mellata, M., 2014. Evaluation of the prevalence and production of *Escherichia coli* common pilus among avian pathogenic *E. coli* and its role in virulence. *PLoS One* 9 (1). <https://doi.org/10.1371/journal.pone.0086565> e86565.
- Talavera, G., Castresana, J., 2007. Improvement of phylogenies after removing divergent and ambiguously aligned blocks from protein sequence alignments. *Syst. Biol.* 56, 564–577. <https://doi.org/10.1080/10635150701472164>.
- Tree, J.J., Wolfson, E.B., Wang, D., Roe, A.J., Gally, D.L., 2009. Controlling injection: regulation of type III secretion in enterohaemorrhagic *Escherichia coli*. *Trends Microbiol.* 17 (8), 361–370. <https://doi.org/10.1016/j.tim.2009.06.001>.
- Tschowri, N., Busse, S., Hengge, R., 2009. The BLUF-EAL protein YcgF acts as a direct anti-repressor in a blue-light response of *Escherichia coli*. *Genes Dev.* 23 (4), 522–534. <https://doi.org/10.1101/gad.499409>.
- Venkatesan, M., Buysse, J.M., Vandendries, E., Kopeck, D.J., 1988. Development and testing of invasion-associated DNA probes for detection of *Shigella* spp. and enteroinvasive *Escherichia coli*. *J. Clin. Microbiol.* 26 (2), 261–266. PMID: PMC266263.
- Vernet, G., Mary, C., Altmann, D.M., Doumbo, O., Morpeth, S., Bhutta, Z.A., Klugman, K.P., 2014. Surveillance for antimicrobial drug resistance in under-resourced countries. *Emerg. Infect. Dis.* 20 (3), 434–441. <https://doi.org/10.3201/eid2003.121157>.
- Wood, D.E., Salzberg, S.L., 2014. Kraken: ultrafast metagenomic sequence classification using exact alignments. *Genome Biol.* 15, R46. <https://doi.org/10.1186/gb-2014-15-3-r46>.
- Zheng, J., Guan, Z., Cao, S., Peng, D., Ruan, L., Jiang, D., Sun, M., 2015. Plasmids are vectors for redundant chromosomal genes in the *Bacillus cereus* group. *BMC Genomics* 16 (1), 6. <https://doi.org/10.1186/s12864-014-1206-5>.
- Zhou, Z., Alikhan, N.F., Mohamed, K., Fan, Y., Brown, D., Chattaway, M., Dallman, T., Delahay, R., Kornschöber, C., Pietzka, A., Malorny, B., Petrovska, L., Davies, R., Robertson, A., Tyne, W., Weill, F.X., Accou-Demartin, N., Williams, N., Achtman, M., 2020. The Enterobase user's guide, with case studies on *Salmonella* transmissions, *Yersinia pestis* phylogeny, and *Escherichia coli* core genomic diversity. *Genome Res.* 30 (1), 138–152. <https://doi.org/10.1101/gr.251678.119>.